CANCER ECOSYSTEMS

EDITED BY: Ubaldo E. Martinez-Outschoorn and Ramon Bartrons
PUBLISHED IN: Frontiers in Oncology and
Frontiers in Cell and Developmental Biology

frontiers Research Topics

ISSN 1664-8714
ISBN 978-2-88963-175-9
DOI 10.3389/978-2-88963-175-9

About Frontiers

Frontiers is more than just an open-access publisher of scholarly articles: it is a pioneering approach to the world of academia, radically improving the way scholarly research is managed. The grand vision of Frontiers is a world where all people have an equal opportunity to seek, share and generate knowledge. Frontiers provides immediate and permanent online open access to all its publications, but this alone is not enough to realize our grand goals.

Frontiers Journal Series

The Frontiers Journal Series is a multi-tier and interdisciplinary set of open-access, online journals, promising a paradigm shift from the current review, selection and dissemination processes in academic publishing. All Frontiers journals are driven by researchers for researchers; therefore, they constitute a service to the scholarly community. At the same time, the Frontiers Journal Series operates on a revolutionary invention, the tiered publishing system, initially addressing specific communities of scholars, and gradually climbing up to broader public understanding, thus serving the interests of the lay society, too.

Dedication to Quality

Each Frontiers article is a landmark of the highest quality, thanks to genuinely collaborative interactions between authors and review editors, who include some of the world's best academicians. Research must be certified by peers before entering a stream of knowledge that may eventually reach the public - and shape society; therefore, Frontiers only applies the most rigorous and unbiased reviews.
Frontiers revolutionizes research publishing by freely delivering the most outstanding research, evaluated with no bias from both the academic and social point of view. By applying the most advanced information technologies, Frontiers is catapulting scholarly publishing into a new generation.

What are Frontiers Research Topics?

Frontiers Research Topics are very popular trademarks of the Frontiers Journals Series: they are collections of at least ten articles, all centered on a particular subject. With their unique mix of varied contributions from Original Research to Review Articles, Frontiers Research Topics unify the most influential researchers, the latest key findings and historical advances in a hot research area! Find out more on how to host your own Frontiers Research Topic or contribute to one as an author by contacting the Frontiers Editorial Office: researchtopics@frontiersin.org

CANCER ECOSYSTEMS

Topic Editors:
Ubaldo E. Martinez-Outschoorn, Thomas Jefferson University, United States
Ramon Bartrons, Universitat de Barcelona, Spain

Citation: Martinez-Outschoorn, U. E., Bartrons, R., eds. (2019). Cancer Ecosystems. Lausanne: Frontiers Media SA. doi: 10.3389/978-2-88963-175-9

Table of Contents

frontiers in Oncology

EDITORIAL
published: 20 August 2019
doi: 10.3389/fonc.2019.00718

Editorial: Cancer Ecosystems

Ubaldo E. Martinez-Outschoorn[1], *Mireia Bartrons*[2] *and Ramon Bartrons*[3*]

[1] Department of Medical Oncology, Sidney Kimmel Cancer Center, Thomas Jefferson University, Philadelphia, PA, United States, [2] Aquatic Ecology Group, University of Vic - Central University of Catalonia, Vic, Spain, [3] Unitat de Bioquímica, Departament de Ciències Fisiològiques, Universitat de Barcelona, Barcelona, Spain

Keywords: cancer ecosystem, transforming growth factor-β, mitochondrial transfer, tunneling nanotubes, fructose 2, 6-bisphosphate, monocarboxylate transporter 4

Editorial on the Research Topic

Cancer Ecosystems

Oncology research pioneers such as Stephen Paget focused on how cancer cells favor particular environments (1) and Judah Folkman on how nutrients are provided to these harsh environments (2). The tumors consist of a heterogeneous population of cancer cells and a stroma with different cell types that define a specific microenvironment and form a tumoral ecosystem. The evolution of the tumors depends on the interactions of the cancer cells with their tumor microenvironment (TME), determining the progression, eradication, or tumor metastasis. A coral ecosystem is similar to tumors in that it is highly complex and energetically productive (3, 4) (**Table 1**). A tropical reef-building coral holobiont is composed of the coral metazoan host (the polyp), its endosymbiotic photosynthetic dinoflagellates (Symbiodiniaceae) and other microorganisms, including protozoans, fungi, bacteria, and archaea (5). Despite their complexity and very high productivity, corals commonly thrive in nutrient-poor environments (14), which are similar to what is observed in tumors. The contradiction of high coral productivity and limited nutrient availability has been named as the "Darwin Paradox," in reference to its first discoverer (19). This paradox can be explained by the high uptake and efficient recycling of nutrients by coral reef organisms. A similar paradox has been observed in tumors since it is unclear how this complex ecosystem thrives in such nutrient deprived conditions (4).

Scientists have debated how the extremely high productivity and diversity of coral reefs can thrive while living in such an oligotrophic environment, equivalent to a marine desert (13, 20). The answer relies on coral mutualistic relationships that allow the retention of resources and avoid their drift away in ocean currents. Sponges have been found to be the basis of this recycling of nutrients and energy back into the ecosystem (13). The largest resource produced on reefs are dissolved in organic matter (DOM), and sponges allow DOM to be transferred to higher trophic levels (13). In tumors, Otto Warburg focused on the idea that the key organic matter is glucose. He postulated that tumor cells maintain high glycolytic rates even with adequate oxygen supply, although he did not address how glucose becomes available to cancer cells (21). Compared to differentiated cells, many tumor cells have an altered energy metabolism. In particular, a change in metabolism based on respiration to one which is predominantly glycolytic (22, 23). Many glycolytic-related genes are systematically overexpressed in different types of cancer cells, have diagnostic utility, and may help predict therapeutic response (24). These data situate the glycolytic phenotype as a distinctive sign of tumor cells (22, 23, 25), providing advantages for proliferation.

Phosphofructokinase 1 (PFK1) and monocarboxylate transporter 4 (MCT4) are rate limiting steps in glycolysis (26). In this e-book collection, the role of one of the main glycolytic regulators, fructose 2,6-bisphosphate (Fru-2,6-P_2), in cancer cells is reviewed by Bartrons et al. Fru-2,6-P_2 allosterically induces PFK1 activity. TP53 Induced Glycolysis and Apoptosis Regulator (TIGAR) also regulates glycolysis via Fru-2,6-P_2 and

OPEN ACCESS

Edited and reviewed by:
Paolo Pinton,
University of Ferrara, Italy

***Correspondence:**
Ramon Bartrons
rbartrons@ub.edu

Specialty section:
This article was submitted to Molecular and Cellular Oncology, a section of the journal Frontiers in Oncology

Received: *15 May 2019*
Accepted: *19 July 2019*
Published: *20 August 2019*

Citation:
Martinez-Outschoorn UE, Bartrons M and Bartrons R (2019) Editorial: Cancer Ecosystems. Front. Oncol. 9:718. doi: 10.3389/fonc.2019.00718

TABLE 1 | Examples of similarities between Tumor and Coral Reef Ecosystems.

Tumor	Coral reef
Highly complex ecosystems with high nutrient utilization rates (4)	Highly complex ecosystems with high nutrient utilization rates (3)
Nutrient deprivation: Compromised blood supply (Zuazo-Gaztelu and Casanovas)	Nutrient deprivation: Nitrogen and Phosphorus deprivation (5–7) Compromised water flow (8)
Metabolic coupling: Between cancer and stromal cells (9) Between cancer cells (10) Between cancer cell organelles (Herst et al.)	Metabolic coupling: Between coral and fish (11, 12) Between coral and sponges (13) Between coral and symbiodiniaceae (14)
Importance of mitochondria-endosymbiont in metabolic coupling (4)	Importance of photosynthetic bacteria in metabolic coupling (15)
Anticancer immunity (Fox et al.)	Immunity to maintain homeostasis (16)
Apoptosis (Leverson and Cojocari)	Apoptosis (17)
TGF-Beta (Fabregat and Caballero-Diaz)	TGF-Beta (18)

drives metabolic symbiosis between cancer cells and cancer-associated fibroblasts (27). Another key regulator of glycolysis: monocarboxylate transporter 4 (MCT4) is also studied by Bisetto et al. and found to induce tumor aggressiveness. MCT4 is the main exporter of lactate from cells, a marker of glycolysis and is regulated by HIF-1α. Conversely, MCT1 is the main importer of lactate into cells, a marker of mitochondrial oxidative phosphorylation and is regulated by c-MYC (4). Most complex ecosystems such as coral reefs and tumors have heterogeneous metabolic activity. Only some cells have high activity of a particular metabolic pathway. As an example, MCT1 is highly expressed in cancer cells while MCT1 expression is low or absent in tumor-associated macrophages (28).

Cancer cells and corals do not exist in isolation. In fact, all living entities host diverse symbionts that contribute to their associated functions. Most studies on the metabolism of cancer cells have focused on the investigation of a single type of intra-tumoral cell, although recent studies have described a more complex scene, where the tumor ecosystem via metabolic symbiosis plays a critical role in cancer progression (9, 10, 29). Similar metabolic interactions to those observed in tumors occur in corals. The "coral probiotic hypothesis" states that corals have a dynamic relationship with their symbiotic microorganisms. By altering the population of symbionts, the coral host adapts to a changing environment. This adjustment of a time span of days to weeks is faster than if it were via mutation and selection that would take many years (30). In sum, it is the combined holobiont that exerts the unit of natural selection as opposed to its individual members and it has been named the hologenome theory of evolution (31).

Cancer cells have a great capacity to adapt to changes in the conditions of their TME, developing survival strategies (Leverson and Cojocari). Similar plasticity has been observed in coral reefs (17). The tumor and stromal cells establish a powerful relationship that determines the initiation and progression of the disease, as well as the patient's prognosis (32). Physiologically, the stroma is a physical barrier against tumorigenesis; however, cancer cells elicit changes to convert the adjacent TME into a pathological entity, favoring nutrient exchange, migration of stromal cells, matrix remodeling, and expansion of the vasculature. In addition to malignant cells, the TME contains stromal cells that have been implicated in tumor promotion, such as endothelial cells of the blood and lymphatic circulatory system, pericytes, fibroblasts, and various bone marrow derived cells, including macrophages, neutrophils, mast cells, myeloid cell-derived suppressor cells, and mesenchymal stem cells, and sometimes even adipocytes (33). The Coral–Symbiodiniaceae relationship depends on nutrient interactions and metabolism between the coral host and the microbial symbionts in response to environmental conditions (34), sharing features with intercellular relationships in tumors. In fact, species richness is a key driver of community biomass production and ecosystem function across a range of ecosystems (35).

Fibroblasts in the TME can be activated. Here they are referred to as cancer-associated fibroblasts (CAFs), and they can be recruited to the tumor by different cytokines and growth factors released by cancer and infiltrated cells. Activation into CAFs is accomplished through genetic modifications and altered activation of different signaling pathways, such as NFκB, IL-6/STAT3, FGF-2/FGFR1, and TGF-β/SMAD (Herst et al.). Recent research, reviewed by Herst et al., shows that stromal cells have the ability to transfer mitochondria to tumor cells deficient in respiration, thus restoring mitochondrial respiratory capacity. Alterations in nuclear and mitochondrial DNA can affect mitochondrial respiration, forcing the cells to search for anaerobic pathways for obtaining energy. These cells with a predominantly glycolytic metabolism tend to have rapid growth, are resistant to hypoxia and can produce metastasis. In contrast, cells lacking mitochondrial DNA cannot form tumors unless they incorporate mitochondrial DNA from neighboring cells. These data suggest that mitochondrial exchange between cells could be used as an additional target in the treatment of cancer. In addition, cancer cells as well as different stromal cells can modify their metabolism in response to different signaling pathways, which can affect the therapeutic response. The resilience of coral reefs to global warming is also dependent on the crosstalk between different cells in this ecosystem (36). In this sense, the NFκB transcription factor, important in regulating cellular responses, is activated when elevated water temperature or other environmental perturbations induce the loss of the algal symbiont Symbiodinium (37) (**Table 1**).

The crosstalk between cancer cells and macrophages in the TME is investigated by Li et al., with the aim of study the intercellular communication in the tumor ecosystem. Identification of the different mechanisms of transport between the cells of the TME is essential to understand the mechanisms of tumor growth and is herein reviewed by Lou et al. These authors demonstrate that the intercellular exchange of microRNAs, mitochondria and other components is carried out through

tunneling nanotubes (TNTs), cytoplasmic extensions based on actin. This transport through TNTs between malignant and stromal cells can modify the gene regulation and metabolism of TME cells, playing a critical role in tumor growth and metastasis, as well as in resistance to different treatments. Similarly, species particular trait values, such as fast growth rates and unique feeding strategies, can strongly affect ecosystem functions, such as coral reef productivity and nutrient cycling (38, 39). Alternatively, biodiversity can enhance ecosystem efficiency with a more complete utilization of resources (40–42). Such synergies are common in ecosystems like coral reefs, often occurring when functionally distinctive taxa increase the performance of other members of the ecosystem (43, 44) (**Table 1**).

The growth of tumor cells requires the supply of nutrients and oxygen. Therefore, the angiogenic program driven by TME cells is one of the first requirements in the tumoral ecosystem (2) and it is explored by Zuazo-Gaztelu and Casanovas. Angiogenesis, in addition to providing nutrients and oxygen, also facilitates the spread of tumor cells. Therefore, the blockade of this process has been proposed in the treatment of different types of cancer [(2); Zuazo-Gaztelu and Casanovas]. In this review, special emphasis is done on the interaction between tumor and stromal cells, suggesting that the molecular mechanisms of these interactions may be used for the development of new antiangiogenic agents. Coral reefs are also subjected to nutrient deprivation on the basis of changes in water flow (**Table 1**).

The protection offered by TME to tumor growth can be diminished by conditions such as chronic inflammation, with the subsequent release of cytokines and growth factors (45). In this way, chronic inflammation can trigger a response in which the proliferative signals induced by stromal cells are gradually enlarged. Fabregat and Caballero-Díaz review the role of TGF-β in hepatocarcinogenesis, considering that when chronic inflammation is established, inflammatory cells produce mediators, such as TGF-β, responsible for the activation of quiescent hepatic stellate cells to myofibroblasts (MFB), which mediate the synthesis of extracellular matrix proteins and are responsible of fibrogenesis. In parallel, TGF-β induces also changes in tumor cell characteristics, conferring migratory properties (Fabregat and Caballero-Díaz), as well as a glycolytic phenotype (46). TGF-β can also play important roles in the symbiotic or mutualistic relationships within coral reefs (**Table 1**).

Cancer cells near blood vessels grow at a higher rate, due to the high availability of nutrients and oxygen. Their energetic needs are supported by glycolysis and mitochondrial oxidative phosphorylation. In contrast, cells exposed to a microenvironment where nutrient and oxygen supplies are reduced, depend more on glycolysis which requires novel strategies to survive and proliferate. Thus, it is not surprising that these cells display higher grades of malignancy and chemo-resistance. Metabolic synergy between cancer and stroma cells is a driver of cancer aggressiveness and it has been shown that lactate is an essential metabolic intermediate between TME cells, fueling the oxidative metabolism of oxygenated tumor cells. In this way, a tumor symbiosis is produced by which the glycolytic and oxidative cells exchange metabolic substrates (4, 10). This metabolic compartmentalization allows for the exchange of metabolites between stroma and cancer cells, and this synergy is a result of differential expression of transporters and isoenzymes (10, 29). The article by Bisetto et al. studies the role of MCT4, an exporter of lactate, in head and neck squamous cell carcinoma (HNSCC) aggressiveness. It is demonstrated that MCT4 is a driver of aggressive cancer, it may be used as a diagnostic marker and its inhibitors could have therapeutic utility to prevent invasive HNSCC (Bisetto et al.).

We are beginning to understand the factors and pathways driving the glycolytic phenotype and metabolic reprogramming of tumor cells. Many genes are involved in this transformation, including RAS, TP53, HIF-1, and c-MYC. Although the change to the glycolytic phenotype is not an indispensable requirement for malignant transformation, the majority of studies indicate that it is an important phenomenon associated with survival advantage for the cells in the TME. In the review by Vaziri-Gohar et al., mutant KRAS is analyzed as an important player in the metabolic reprogramming of the pancreatic ductal adenocarcinoma cells (PDA). There is growing interest in the therapeutic exploitation of new metabolic inhibitors and in this review several clinical trials currently underway in patients with PDA are discussed.

A new and promising strategy for the cancer treatment uses mitochondria, since they are important in the regulation of metabolism and apoptosis. Cancer cell mitochondria exhibit multiple differential features with respect to that of normal cells. Among them, a stronger mitochondrial membrane potential that can allow the accumulation of cytotoxic cationic molecules within the cancer cells. González-Rubio et al. investigate the selective cytotoxic effect of cationic 10-N-nonyl acridine orange (NAO) on human lung carcinoma H520 cells. This compound is able to interfere with mitochondrial function and is a promising antitumor agent. In a similar way, mitochondrial anti-apoptotic proteins like BCL-2, BCL-XL, and MCL-1 are overexpressed in cancer cells (47) and offer a mechanism of survival and selective advantage in the nutrient deprived environment of tumors and are therefore attractive drug targets. Leverson and Cojocari review the literature on the BCL-2-inhibitor Venetoclax, approved for use in chronic lymphocytic leukemia and now being studied in a number of other hematologic malignancies. The results presented suggest that lymphoid microenvironments have a preponderant role in the sensitivity of cancer cells to Venetoclax (48). Scatena et al. identified new therapeutic targets that are relatively unique to cancer stem cells (CSCs). CSCs overexpress regulatory proteins of mitochondrial activity and their inhibition may represent a potentially new approach to eradicating CSCs. Different FDA-approved antibiotics, including Doxycycline, target mitochondria and the results obtained with this drug clearly show that it can selectively eradicate CSCs in breast cancer patients *in vivo* (Scatena et al.). Applying translational research, a clinical trial performed by Curry et al. used Metformin, an oral anti-diabetic drug that inhibits mitochondrial complex I, in patients with head and neck squamous cell carcinoma (HNSCC). Metformin resulted in an increase in cancer cell apoptosis and altered the cellular TME with an increased infiltrate of CD8+ Teff and FoxP3 Tregs at the invasive tumor margin of lymph nodes, suggesting an immunomodulatory effect in HNSCC.

Furthermore, a review of Lee et al. on Metformin, as a treatment for endometrial cancer, presents the available clinical data and the molecular mechanisms by which it exerts its effects, focusing on how it may modify the TME. The multiple effects of metformin on the regulation of metabolism, as well as the changes produced in intercellular communication, make it a promising drug for the treatment of different types of cancer.

One of the important challenges in the treatment of cancer is the persistence of drug-resistant cell populations. Resistant subpopulations arise, among other factors, through modifications in the TME. The accumulation of extracellular fibrous proteins and the modification of the extracellular matrix are associated with tumor progression. Joyce et al. have studied how this TME affects the sensitivity of breast cancer cells to chemotherapeutic treatment. The cultured breast carcinoma cells showed a stromal-dependent response to Doxorubicin, suggesting that the conditions of the tumor microenvironment largely govern the response to drugs.

A study by Mojena et al. investigated the effect of a series of compounds derived from benzylamine/2-thiophenomethylamine (ethylamine) that showed antitumor activity on different melanoma tumor cell lines. These compounds develop a potent cytotoxic/antiproliferative activity in cells *in vitro* and in animal models of melanoma tumors, enhancing animal survival.

Rappaport and Waldman explore the cGMP signaling in the intestinal epithelium and the mechanisms by which it opposes intestinal injury. In colorectal tumors, the expression of the endogenous ligand of Guanylate cyclase C (GUCY2C) is lost and the reconstitution of GUCY2C signaling through the genetic or oral replacement of the ligand opposes tumorigenesis in mice. These results suggest that colorectal cancer may arise in a tumor microenvironment with a functional inactivation of GUCY2C.

In recent years we have seen the progress of immunological therapy against different types of cancers. A crucial aspect for its development has been its ability to reverse the immunosuppression induced by tumors. In this sense, the catabolic enzyme of tryptophan indoleamine 2,3-dioxygenase-1 (IDO1) has received great attention as a driver of tumor-mediated suppression. It has been shown that IDO1 is overexpressed in different human cancers and associated with an unfavorable prognosis. Fox et al. review the action of an inhibitor of IDO1, Indoximod, as a co-adjuvant of treatment in several types of tumors.

In conclusion, the current collection gathers researchers studying disparate fields of the cancer ecosystem to better understand how to target it. One must consider historically how only limited efforts have been devoted to study cancer ecosystems, which provide additional information to that obtained when one component is studied in isolation. Tumor ecosystems share productivity features and vulnerabilities not only with coral reefs but also with swamps (36, 49) and future studies will need to determine their similarities and differences with other physiological and pathological ecosystems. The analysis and understanding of natural ecosystems can facilitate new ways of cancer treatment. It may be that, as in the Indian proverb of blind men encountering different parts of an elephant, specialized researchers have seen only one aspect of tumor aggressiveness and determined its mechanisms accordingly.

AUTHOR CONTRIBUTIONS

This invited editorial was conceived by UM-O and RB, contributing equally to the writing. MB provided information in her areas of expertise.

FUNDING

This work was supported by National Institutes of Health Grants NCI K08-CA175193 and NCI 5 P30 CA 56036 to UM-O and by Instituto de Salud Carlos III—FIS [PI17/00412]—and Fondo Europeo de Desarrollo Regional (FEDER) to RB.

REFERENCES

1. Paget S. The distribution of secondary growths in cancer of the breast. *Cancer Metastasis Rev.* (1989) 8, 98–101.
2. Folkman J. Angiogenesis. *Annu Rev Med.* (2006) 57:1–18. doi: 10.1146/annurev.med.57.121304.131306
3. McWilliam M, Chase TJ, Hoogenboom MO. Neighbor diversity regulates the productivity of coral assemblages. *Curr Biol.* (2018) 28:3634–9.e3633. doi: 10.1016/j.cub.2018.09.025
4. Martinez-Outschoorn UE, Peiris-Pages M, Pestell RG, Sotgia F, Lisanti MP. Cancer metabolism: a therapeutic perspective. *Nat Rev Clin Oncol.* (2017) 14:113. doi: 10.1038/nrclinonc.2017.1
5. Rädecker N, Pogoreutz C, Voolstra CR, Wiedenmann J, Wild C. Nitrogen cycling in corals: the key to understanding holobiont functioning? *Trends Microbiol.* (2015) 23:490–7. doi: 10.1016/j.tim.2015.03.008
6. Wiebe WJ, Johannes RE, Webb KL. Nitrogen fixation in a coral reef community. *Science.* (1975) 188:257–9. doi: 10.1126/science.188.4185.257
7. Ferrier-Pagès C, Godinot C, D'Angelo C, Wiedenmann J, Grover R. Phosphorus metabolism of reef organisms with algal symbionts. *Ecol Monograph.* (2016) 86:262–77. doi: 10.1002/ecm.1217
8. Comeau S, Edmunds PJ, Lantz CA, Carpenter RC. Water flow modulates the response of coral reef communities to ocean acidification. *Scient Rep.* (2014) 4:6681. doi: 10.1038/srep06681
9. Pavlides S, Whitaker-Menezes D, Castello-Cros R, Flomenberg N, Witkiewicz AK, Frank PG, et al. The reverse Warburg effect: aerobic glycolysis in cancer associated fibroblasts and the tumor stroma. *Cell Cycle.* (2009) 8:3984–4001. doi: 10.4161/cc.8.23.10238
10. Sonveaux P, Vegran F, Schroeder T, Wergin MC, Verrax J, Rabbani ZN, et al. Targeting lactate-fueled respiration selectively kills hypoxic tumor cells in mice. *J Clin Invest.* (2008) 118:3930–42. doi: 10.1172/JCI36843
11. Garcia-Herrera N, Ferse SCA, Kunzmann A, Genin A. Mutualistic damselfish induce higher photosynthetic rates in their host coral. *J Exp Biol.* (2017) 220:1803–11. doi: 10.1242/jeb.152462
12. Chase TJ, Pratchett MS, Frank GE, Hoogenboom MO. Coral-dwelling fish moderate bleaching susceptibility of coral hosts. *PLoS ONE.* (2018) 13:e0208545. doi: 10.1371/journal.pone.0208545
13. De Goeij JM, Van Oevelen D, Vermeij MJA, Osinga R, Middelburg JJ, De Goeij AFPM, et al. Surviving in a marine desert: the sponge loop retains resources within coral reefs. *Science.* (2013) 342:108–10. doi: 10.1126/science.1241981

14. Morris LA, Voolstra CR, Quigley KM, Bourne DG, Bay LK. Nutrient availability and metabolism affect the stability of coral–symbiodiniaceae symbioses. *Trends Microbiol.* (2019) 27:678–89. doi: 10.1016/j.tim.2019.03.004
15. Barott KL, Venn AA, Perez SO, Tambutteeé S, Tresguerres M, Somero GN. Coral host cells acidify symbiotic algal microenvironment to promote photosynthesis. *Proc Natl Acad Sci USA.* (2015) 112:607–12. doi: 10.1073/pnas.1413483112
16. Fuess LE, Mann WT, Jinks LR, Brinkhuis V, Mydlarz LD. Transcriptional analyses provide new insight into the late-stage immune response of a diseased caribbean coral. *Roy Soc Open Sci.* (2018) 5:172062. doi: 10.1098/rsos.172062
17. Libro S, Vollmer SV. Genetic signature of resistance to white band disease in the caribbean staghorn coral acropora cervicornis. *PLoS ONE.* (2016) 11:e0146636. doi: 10.1371/journal.pone.0146636
18. Detournay O, Schnitzler CE, Poole A, Weis VM. Regulation of cnidarian-dinoflagellate mutualisms: evidence that activation of a host TGFbeta innate immune pathway promotes tolerance of the symbiont. *Dev Comp Immunol.* (2012) 38:525–37. doi: 10.1016/j.dci.2012.08.008
19. Darwin C. *The Structure and Distribution of Coral Reefs.* 2nd ed. London: Smith Elder and Co. (1974).
20. Hatcher BG. Coral reef primary productivity. A hierarchy of pattern and process. *Trends Ecol Evol.* (1990) 5:149–55. doi: 10.1016/0169-5347(90)90221-X
21. Warburg O. On the origin of cancer cells. *Science.* (1956) 123:309–14. doi: 10.1126/science.123.3191.309
22. Bartrons R, Caro J. Hypoxia, glucose metabolism and the Warburg's effect. *J Bioenerg Biomembr.* (2007) 39:223–9. doi: 10.1007/s10863-007-9080-3
23. DeBerardinis RJ, Lum JJ, Hatzivassiliou G, Thompson CB. The biology of cancer: metabolic reprogramming fuels cell growth and proliferation. *Cell Metab.* (2008) 7:11–20. doi: 10.1016/j.cmet.2007.10.002
24. Cuezva JM, Krajewska M, de Heredia ML, Krajewski S, Santamaria G, Kim H, et al. The bioenergetic signature of cancer: a marker of tumor progression. *Cancer Res.* (2002) 62:6674–81.
25. Vander Heiden MG, Cantley LC, Thompson CB. Understanding the Warburg effect: the metabolic requirements of cell proliferation. *Science.* (2009) 324:1029–33. doi: 10.1126/science.1160809
26. Tanner LB, Goglia AG, Wei MH, Sehgal T, Parsons LR, Park JO, et al. Four key steps control glycolytic flux in mammalian cells. *Cell Syst.* (2018) 7:49–62 e48. doi: 10.1016/j.cels.2018.06.003
27. Ko YH, Domingo-Vidal M, Roche M, Lin Z, Whitaker-Menezes D, Seifert E, et al. TP53-inducible Glycolysis and Apoptosis Regulator (TIGAR) metabolically reprograms carcinoma and stromal cells in breast cancer. *J Biol Chem.* (2016) 291:26291–303. doi: 10.1074/jbc.M116.740209
28. Gooptu M, Whitaker-Menezes D, Sprandio J, Domingo-Vidal M, Lin Z, Uppal G, et al. Mitochondrial and glycolytic metabolic compartmentalization in diffuse large B-cell lymphoma. *Semin Oncol.* (2017) 44:204–17. doi: 10.1053/j.seminoncol.2017.10.002
29. Martinez-Outschoorn UE, Lisanti MP, Sotgia F. Catabolic cancer-associated fibroblasts transfer energy and biomass to anabolic cancer cells, fueling tumor growth. *Semin Cancer Biol.* (2014) 25:47–60. doi: 10.1016/j.semcancer.2014.01.005
30. Reshef L, Koren O, Loya Y, Zilber-Rosenberg I, Rosenberg E. The coral probiotic hypothesis. *Environ Microbiol.* (2006) 8:2068–73. doi: 10.1111/j.1462-2920.2006.01148.x
31. Rosenberg E, Koren O, Reshef L, Efrony R, Zilber-Rosenberg I. The role of microorganisms in coral health, disease and evolution. *Nat Rev Microbiol.* (2007) 5:355–62. doi: 10.1038/nrmicro1635
32. Quail DF, Joyce JA. Microenvironmental regulation of tumor progression and metastasis. *Nat Med.* (2013) 19:1423–37. doi: 10.1038/nm.3394
33. Balkwill FR, Capasso M, Hagemann T. The tumor microenvironment at a glance. *J Cell Sci.* (2012) 125:5591–6. doi: 10.1242/jcs.116392
34. Lin S, Cheng S, Song B, Zhong X, Lin X, Li W, et al. The Symbiodinium kawagutii genome illuminates dinoflagellate gene expression and coral symbiosis. *Science.* (2015) 350:691–4. doi: 10.1126/science.aad0408
35. Duffy JE, Godwin CM, Cardinale BJ. Biodiversity effects in the wild are common and as strong as key drivers of productivity. *Nature.* (2017) 549:261–4. doi: 10.1038/nature23886
36. Hughes TP, Kerry JT, Álvarez-Noriega M, Álvarez-Romero JG, Anderson KD, Baird AH, et al. Global warming and recurrent mass bleaching of corals. *Nature.* (2017) 543:373–7. doi: 10.1038/nature21707
37. Mansfield KM, Carter NM, Nguyen L, Cleves PA, Alshanbayeva A, Williams LM, et al. Transcription factor NF-κB is modulated by symbiotic status in a sea anemone model of cnidarian bleaching. *Scient Rep.* (2017) 7:16025. doi: 10.1038/s41598-017-16168-w
38. Vile D, Shipley B, Garnier E. Ecosystem productivity can be predicted from potential relative growth rate and species abundance. *Ecol Lett.* (2006) 9:1061–7. doi: 10.1111/j.1461-0248.2006.00958.x
39. Bellwood DR, Hughes TP, Hoey AS. Sleeping functional group drives coral-reef recovery. *Curr Biol.* (2006) 16:2434–9. doi: 10.1016/j.cub.2006.10.030
40. Tilman D, Knops J, Wedin D, Reich P, Ritchie M, Siemann E. The influence of functional diversity and composition on ecosystem processes. *Science.* (1997) 277:1300–2. doi: 10.1126/science.277.5330.1300
41. Cox E, Bonner J. Ecology. The advantages of togetherness. *Science.* (2001) 292:448–9. doi: 10.1126/science.1060456
42. Naeem S, Duffy JE, Zavaleta E. The functions of biological diversity in an age of extinction. *Science.* (2012) 336:1401–6. doi: 10.1126/science.1215855
43. Heemsbergen DA, Berg MP, Loreau M, van Hal JR, Faber JH, Verhoef HA. Biodiversity effects on soil processes explained by interspecific functional dissimilarity. *Science.* (2004) 306:1019–20. doi: 10.1126/science.1101865
44. Cardinale BJ, Palmer MA, Collins SL. Species diversity enhances ecosystem functioning through interspecific facilitation. *Nature.* (2002) 415:426–9. doi: 10.1038/415426a
45. Joyce JA, Pollard JW. Microenvironmental regulation of metastasis. *Nat Rev Cancer.* (2009) 9:239–52. doi: 10.1038/nrc2618
46. Rodriguez-Garcia A, Samso P, Fontova P, Simon-Molas H, Manzano A, Castano E, et al. TGF-beta1 targets Smad, p38 MAPK, and PI3K/Akt signaling pathways to induce PFKFB3 gene expression and glycolysis in glioblastoma cells. *FEBS J.* (2017) 284:3437–54. doi: 10.1111/febs.14201
47. Certo M, Del Gaizo Moore V, Nishino M, Wei G, Korsmeyer S, Armstrong SA, et al. Mitochondria primed by death signals determine cellular addiction to antiapoptotic BCL-2 family members. *Cancer Cell.* (2006) 9:351–65. doi: 10.1016/j.ccr.2006.03.027
48. Scott DW, Gascoyne RD. The tumour microenvironment in B cell lymphomas. *Nat Rev Cancer.* (2014) 14:517–34. doi: 10.1038/nrc3774
49. Amend SR, Pienta KJ. Ecology meets cancer biology: the cancer swamp promotes the lethal cancer phenotype. *Oncotarget.* (2015) 6:9669–78. doi: 10.18632/oncotarget.3430

Conflict of Interest Statement: The authors declare that the research was conducted in the absence of any commercial or financial relationships that could be construed as a potential conflict of interest.

frontiers in Oncology

ORIGINAL RESEARCH
published: 23 January 2019
doi: 10.3389/fonc.2019.00010

Computational Modeling of the Crosstalk Between Macrophage Polarization and Tumor Cell Plasticity in the Tumor Microenvironment

Xuefei Li[1†], *Mohit Kumar Jolly*[1†‡], *Jason T. George*[1,2,3], *Kenneth J. Pienta*[4] *and Herbert Levine*[1,2,5,6*]

[1] Center for Theoretical Biological Physics, Rice University, Houston, TX, United States, [2] Department of Bioengineering, Rice University, Houston, TX, United States, [3] Medical Scientist Training Program, Baylor College of Medicine, Houston, TX, United States, [4] The James Buchanan Brady Urological Institute, Johns Hopkins University School of Medicine, Baltimore, MD, United States, [5] Department of Physics and Astronomy, Rice University, Houston, TX, United States, [6] Department of Physics, Northeastern University, Boston, MA, United States

OPEN ACCESS

Edited by:
Ubaldo Emilio Martinez-Outschoorn, Thomas Jefferson University, United States

Reviewed by:
Rafael Coelho Lopes De Sa, University of Massachusetts Amherst, United States
Virendra K. Chaudhri, Cincinnati Children's Hospital Medical Center, United States

***Correspondence:**
Herbert Levine
herbert.levine@rice.edu

[†] These authors have contributed equally to this work

[‡]Present Address:
Mohit Kumar Jolly, Centre for BioSystems Science and Engineering, Indian Institute of Science, Bangalore, India

Specialty section:
This article was submitted to Molecular and Cellular Oncology, a section of the journal Frontiers in Oncology

Received: 03 October 2018
Accepted: 03 January 2019
Published: 23 January 2019

Citation:
Li X, Jolly MK, George JT, Pienta KJ and Levine H (2019) Computational Modeling of the Crosstalk Between Macrophage Polarization and Tumor Cell Plasticity in the Tumor Microenvironment. Front. Oncol. 9:10. doi: 10.3389/fonc.2019.00010

Tumor microenvironments contain multiple cell types interacting among one another via different signaling pathways. Furthermore, both cancer cells and different immune cells can display phenotypic plasticity in response to these communicating signals, thereby leading to complex spatiotemporal patterns that can impact therapeutic response. Here, we investigate the crosstalk between cancer cells and macrophages in a tumor microenvironment through *in silico* (computational) co-culture models. In particular, we investigate how macrophages of different polarization (M_1 vs. M_2) can interact with epithelial-mesenchymal plasticity of cancer cells, and conversely, how cancer cells exhibiting different phenotypes (epithelial vs. mesenchymal) can influence the polarization of macrophages. Based on interactions documented in the literature, an interaction network of cancer cells and macrophages is constructed. The steady states of the network are then analyzed. Various interactions were removed or added into the constructed-network to test the functions of those interactions. Also, parameters in the mathematical models were varied to explore their effects on the steady states of the network. In general, the interactions between cancer cells and macrophages can give rise to multiple stable steady-states for a given set of parameters and each steady state is stable against perturbations. Importantly, we show that the system can often reach one type of stable steady states where cancer cells go extinct. Our results may help inform efficient therapeutic strategies.

Keywords: MET–mesenchymal-to-epithelial transition, EMT–epithelial-to-mesenchymal transition, M1-/M2-polarized macrophages, interaction network, multi-stability

INTRODUCTION

Cancer has been largely considered as a cell-autonomous disease, but recent investigations have highlighted the crucial role of the tumor microenvironment in determining cancer progression (1). Cancer cells can communicate bi-directionally through various mechanical and/or chemical ways with their neighboring cancer cells (2, 3), and/or with other components of the tumor microenvironment such as macrophages and fibroblasts, driving aggressive malignancy (4–6). The

interconnected feedback loops formed by these interactions can often generate many emergent outcomes for the tumor. Interestingly, many of the latest therapeutic innovations such as immunotherapy are aimed at targeting aspects of the tumor microenvironment instead of the cancer cells (7).

Tumor-associated macrophages (TAMs) are one of the most abundant immune cell populations in the microenvironment (8, 9). They have been shown to promote cancer progression in many ways, such as promoting angiogenesis, suppressing function of cytotoxic T lymphocytes, and assisting extravasation of cancer cells (8–12). Generally, the secretome and functions of TAMs have been shown to be close to that of the so-called alternatively activated macrophages (M_2) (13). In the case of pathogen infections, macrophages that can engulf the pathogen and present processed antigens to adaptive immune cells, are generally characterized as the classically activated ones (M_1) (14). M_1 and M_2 macrophages have different roles during wound healing: while M_1 macrophages initiate inflammatory responses, M_2 macrophages contribute to tissue restoration (13). In the context of cancer, M_1 macrophages have been generally considered anti-tumor (15–17), whereas M_2 macrophages have been considered as pro-tumor (10).

However, macrophage polarization is not as rigid as the differentiation of T lymphocytes (18); instead, M_1, M_2, and any intermediate state(s) of macrophage polarization are quite plastic (13, 19, 20). Thus, the idea that reverting TAMs in the cancer microenvironment to its cancer-suppressing counterpart is tempting, the proof of principle of which has been demonstrated in mice models (21–25).

Not only TAMs, but also cancer cells themselves can be extremely plastic, a canonical example of which is epithelial-mesenchymal plasticity, i.e., cancer cells can undergo varying degrees of Epithelial-Mesenchymal Transition (EMT) and its reverse Mesenchymal-Epithelial Transition (MET) (26, 27). EMT/MET has been associated with metastasis (28), chemoresistance (29), tumor-initiation potential (30), resistance against cell death (31), and evading the immune system (32).

Importantly, macrophages and cancer cells can interact with and influence the behavior of one another, as shown by many *in vitro* experiments. Specifically, some epithelial cancer cells are capable of polarizing monocytes into M_1-like macrophages (33). Forming a negative feedback loop, these M_1-like macrophages can decrease the confluency of the cancer cells that polarized them (33). Moreover, pre-polarized M_1 macrophages can induce senescence and apoptosis in human cancer cell lines A549 (34) and MCF-7 (35). Intriguingly, factors released by apoptosis of cancer cells can convert M_1 macrophages into M_2-like macrophages (35), thus switching macrophage population from being tumor-suppressive to being tumor-promoting. On the other hand, mesenchymal cancer cells can polarize monocytes into M_2-like macrophages (33, 36, 37), that can in turn assist EMT (37, 38). Thus, the interaction network among macrophages and cancer cells is formidably complex, and the emergent dynamics of these interactions can be non-intuitive (39) yet are often crucial in deciding the success of therapeutic strategies targeting cancer and/or immune cells. For example, even if TAMs at some time can be converted exogenously to M_1-like macrophages, if most cancer cells still tend to polarize monocytes to TAMs, other coordinated perturbations may be needed at different time-points to restrict the aggressiveness of the disease.

Here, we develop mathematical models to capture the abovementioned set of interactions among cancer cells in varying phenotypes (epithelial and mesenchymal) and macrophages of different polarizations (M_1-like and M_2-like). We characterize the multiple steady states of the network that can be obtained as a function of different initial conditions and key parameters, and thus analyze various potential compositions of cellular populations in the tumor microenvironment. This *in silico* co-culture system can not only help explain *in vitro* multiple experimental observations and clinical data, but also help acquire novel insights into designing effective therapeutic strategies aimed at cancer cells and/or macrophages.

RESULTS

Crosstalk Among Cancer Cells and Macrophages Can Lead to Two Distinct Categories of Steady States

We first considered the following interactions in setting up our mathematical model: (a) proliferation of epithelial and mesenchymal cells (but not that of monocytes M_0, or macrophages M_1 and M_2), (b) EMT promoted by M_2-like macrophages and MET promoted by M_1-like macrophages, (c) polarization of monocytes (M_0) to M_1-like cells aided by epithelial cells, and that to M_2-like cells aided by mesenchymal cells, (d) induction of senescence in epithelial cells by M_1-like macrophages (**Figure 1A**). No inter-conversion among M_1-like and M_2-like macrophages or cell-death of macrophages is considered here in this model (hereafter referred to as "Model I"; see section Methods).

Furthermore, this model also considers that mesenchymal cells can secrete soluble factors, such as TGFβ, that can induce or maintain the mesenchymal state in autocrine or paracrine manners (40, 41). Therefore, we hypothesized that mesenchymal cells can resist M_1-promoted MET. However, this resistance might not fully suppress MET, as MET still happens in the presence of M_1 macrophages (38). Therefore, in Equation (1), we assume a Hill-like function to represent the resistance to M_1-promoted MET and the resistance term saturates to a finite value as a function of mesenchymal population M. And the corresponding half-saturation constant is K_M^0. Similarly, epithelial cells adhere to each other via E-cadherin, sequestering β-catenin on the membrane, thus interfering with the induction of EMT (42). Thus, we hypothesized that the M_2-promoted EMT can be inhibited by epithelial cells in a cooperative manner, because this inhibition of EMT requires direct physical cell-cell contact and hence involves multiple epithelial cells. Therefore, in Equation (1), we assume a Hill-like function to represent this resistance to M_2-dependent EMT and the resistance term saturates to a finite value as a function of epithelial population E. And the corresponding half-saturation

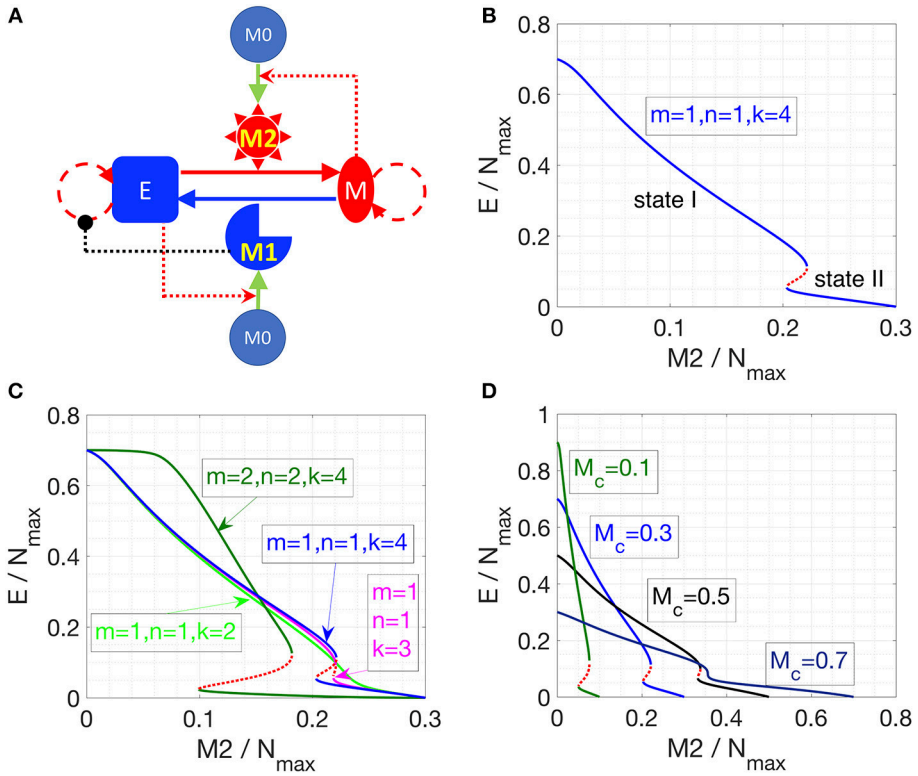

FIGURE 1 | Cancer-immune interplay can give rise to the co-existence of two types of steady states. **(A)** Interaction network for Model I. Conversions between cells are indicated by solid lines. Cell proliferation is indicated by dashed lines. Inhibition (in black) and activation (in red) is indicated by dotted lines. **(B)** Steady states of the epithelial population are plotted as a function of M_2-like macrophage population. Stable steady states are plotted in solid blue lines and unstable steady states are plotted in dotted red line. The key parameters are as indicated. **(C)** As the cooperativity of epithelial cancer cells in their resistance of M_2-promoted EMT is reduced, i.e., $k = 4, 3, 2$ (blue, cyan, and light-green line), the overlapped region between state I and II shrinks and then disappears. Increasing the cooperativity of M_2-promoted EMT or M_1-promoted MET, i.e., m and n increase from 1 to 2, can expand the overlapped region (between state I and II) of the system (dark-green lines). Stable steady states are plotted in solid lines and unstable steady states are plotted in dotted lines. **(D)** As the total number of macrophages (M_c) increases, the overlapped region (between state I and II) of the system shrinks and then disappears.

constant is K_E^0. Furthermore, the epithelial-cell-dependent term has a cooperativity parameter k to represent the effects of E-cadherin-β-catenin interaction between multiple epithelial cells.

Note that in all of our calculations, we assumed that there is a carrying-capacity of cells (N_{max}, including both cancer cells and macrophages) in the co-culture system *in vitro*. We vary the initial number of different cells while keeping the total number of macrophages (M_1+M_2+M_0) to be a constant (M_c). Therefore, the maximum number of cancer cells will be N_{max} -M_c.

In Model I, the final populations of E, M, M_1, and M_2 cells are simply determined by the following equations:

$$\eta_{me} M \frac{M_1^n}{M_1^n + \frac{M}{M+K_M^0}} = \eta_{em} E \frac{M_2^m}{M_2^m + \frac{E^k}{E^k + (K_E^0)^k}},$$
$$M_1 + M_2 = M_c, \qquad E + M = N_{\max} - M_c$$

where η_{em} and η_{me} are the EMT and MET rate constants, respectively. The above equations give two categories of stable steady states: (a) state I, dominated by epithelial cancer cells, and (b) state II, dominated by mesenchymal cancer cells. The final steady state of the system depends on the number of M_2 macrophages in that state; since there are only three equations for four unknowns, M_2 can be used as a parameter specifying (possibly discrete set of) solutions. As soon as M_2/N_{max} crosses a threshold, the system switches from state I to state II (**Figure 1B**). This prediction is largely robust to parameter variation (**Figure S1**).

Next, we explored what factors could change the qualitative behavior of the model, i.e., enable a smoother and continuous transition of epithelial and mesenchymal percentages as a function of the M_2-macrophage population. We identified that reducing the cooperativity of epithelial cancer cells in their resistance of M_2-promoted EMT can lead to a loss of the feature with two-types of steady states (**Figure 1C**, blue, cyan, and light-green lines). Conversely, increasing the cooperativity of M_2-promoted EMT or M_1-promoted MET can expand the region of overlapping between state I and II of the system (**Figure 1C**, green lines). Another factor that can alter the behavior of the model is the initial number of monocytes in the system. At high enough number of monocytes, the absolute number of cancer cells will be small, thus the effect of the

cooperativity between epithelial cancer cells will be reduced, and consequently, as discussed above, the overlap of the two types of steady states of the system will disappear (**Figure 1D**). Together, this increased propensity of multi-stability in the system upon including cooperative effects in the interactions among different species (or variables) is reminiscent of observations in models of biochemical networks (43).

Note that using the M_2/N_{max} as the "control variable" is specific for Model I, because there is no interconversion between M_1 and M_2 macrophages. For a given set of parameters, the steady state level of M_2 can vary continuously from 0 to M_c (**Figures 1B–D**), and in practice is determined by the initial conditions (initial number of E, M, M_1, M_2, and M_0). For models in the following sections, M_2/N_{max} will be shown to be fixed to discrete allowed values (instead of continuously varying) for a given set of parameters. For example, if we add a very small conversion rate between M_1 and M_2, the steady state of the system will collapse to only one steady state (**Figure S2**): on the shorter time scale, the trajectory of the system (on the phase plane of E and M_2) will first converge to one steady state in Model I (with the same M_2/N_{max}); on the longer time scale, as determined by the value of inter-conversion rate between M_1 and M_2, the system will slowly evolve to the steady state (blue dot in **Figure S2**), following along the now-approximate steady states in Model I.

Cancer-Cell Enhanced Interconversion Between M_1- and M_2-Like Macrophages Lead to Bi-Stability

In the next iteration of our model (hereafter referred to as "Model II"), we included the possibility of interconversion between M_1-like and M_2-like macrophages, as reported in the literature (13, 35, 44, 45) (**Figure 2A**, see section Methods). We first assume constant interconversion between M_1 and M_2 (with rates denoted as η_{21}^0 and η_{12}^0) and investigate the effects of varying the rate of conversion of mesenchymal cells to epithelial cells (η_{me}). At small values of η_{me}, the system has small number of epithelial cells, which is equivalent to state II in Model I; with increasing η_{me}, a threshold is crossed, and the system can switch to states with larger number of epithelial cells, which is equivalent to state I in Model I (solid black lines, **Figure 2B**). Thus, we can observe bi-stability of cancer cell population in this system. However, the populations of macrophages stay constant as a function of η_{me}, since the M_1/M_2 ratio is simply determined by η_{21}^0/η_{12}^0 according to Equation (2) when $\eta_{12} = \eta_{21} = 0$). In this model, we focused on increased cooperativity of M_2-assisted EMT and M_1-assisted MET (i.e., $m = n = 2$), because the interconversion between M_1 and M_2, in absence of such cooperativity (as considered in model I with $m = n = 1$; **Figure 1B**), gives rise to a narrower bi-stable region (**Figure S3**). Note again that in our calculations, we assumed that there is a carrying-capacity of cells (N_{max}, including both cancer cells and macrophages) in the co-culture system *in vitro*. Again, the total number of macrophages is constant, since no cell death or cell division of macrophages is considered.

We chose η_{me} as a control parameter, because it can act as a bottleneck for the transition between the two types of stable steady states of the system. Lowering the transition threshold of η_{me} can be helpful in a sense that the system can potentially stay at state I (high epithelial state, supposed to be less aggressive) only. Due to the inherent symmetry in the network, the effect of lowering the threshold of η_{me} can be recapitulated via other perturbations, such as a smaller rate of M_1-assisted MET (η_{em}), lower M_1 to M_2 conversion rate (η_{12}), or higher M_2 to M_1 conversion rate (η_{21}) (**Figure S4**).

We next consider the case where interconversion between M_1-like and M_2-like macrophages is enhanced by cancer cells, i.e., mesenchymal cells enhance the M_1-to-M_2 transition, while epithelial cells enhance M_2-to-M_1 transition. In this case, we observe the existence of a bi-stable region, and the range of the epithelial-cell-low solution (equivalent to state II) is wider than that for the previous case without any effects of epithelial (E) and mesenchymal (M) cancer cells on M_1-M_2 interconversion (**Figures 2B,C**, solid blue lines). The reason for the expanded epithelial-cell-low region is that the positive feedback loop between mesenchymal and M_2 cells makes the mesenchymal- and M_2-dominated state more stable. Therefore, a higher η_{me} is required to compensate for the effects of low M_1 population. For therapeutic purposes, state I is favored, for it is believed that epithelial cells are typically less aggressive than mesenchymal ones. Therefore, symmetrical mutual enhancement might not be helpful for the therapy because of the expanded epithelial-low (mesenchymal-high) region. For the same reason, the lower threshold of η_{me} to switch from state II to state I also shift to a higher value, which means that for a small η_{me}, the system will only have one stable steady state, i.e., state II with high number of mesenchymal cells.

In order to drive the system to be bi-stable at a smaller η_{me}, we tested the case with asymmetrical interconversion rates between M_1 and M_2, i.e., higher conversion rate from M_2 to M_1 enhanced by epithelial cells (η_{21}). In this case, the lower threshold of η_{me} can indeed shift to a smaller value (**Figure 2D**), which makes it theoretically possible to switch the system from state II (low epithelial cells) to state I (high epithelial cells) at a fairly small η_{me} value.

In summary, our results for Model II suggest that one can switch the system from state II (low epithelial cells) to state I (high epithelial cells) by increasing both η_{me} and the effective conversion from M_2 to M_1. Note that the interactions in Model 2 are rather symmetric: the interconversion rates between M_1 and M_2 are either constants or enhanced by the corresponding cancer-cells. In the following section, we will consider the asymmetric case where only the M_1 to M_2 conversion is enhanced by factors released by apoptotic epithelial cancer cells.

Cell Apoptosis-Induced M1-to-M2 Conversion Leads to Symmetry Breaking in the Cancer-Immune Interaction Network

Finally, we incorporated one other set of experimentally documented interactions, i.e., M_1 macrophages can drive the apoptosis of epithelial cells, and factors released during cancer cell apoptosis can drive M_1-to-M_2 conversion (referred as Model III, see section Methods) (35). The newly introduced interactions are highlighted in thick lines in **Figure 3A**. This interaction induces "symmetry breaking" (46) in the system, as previously

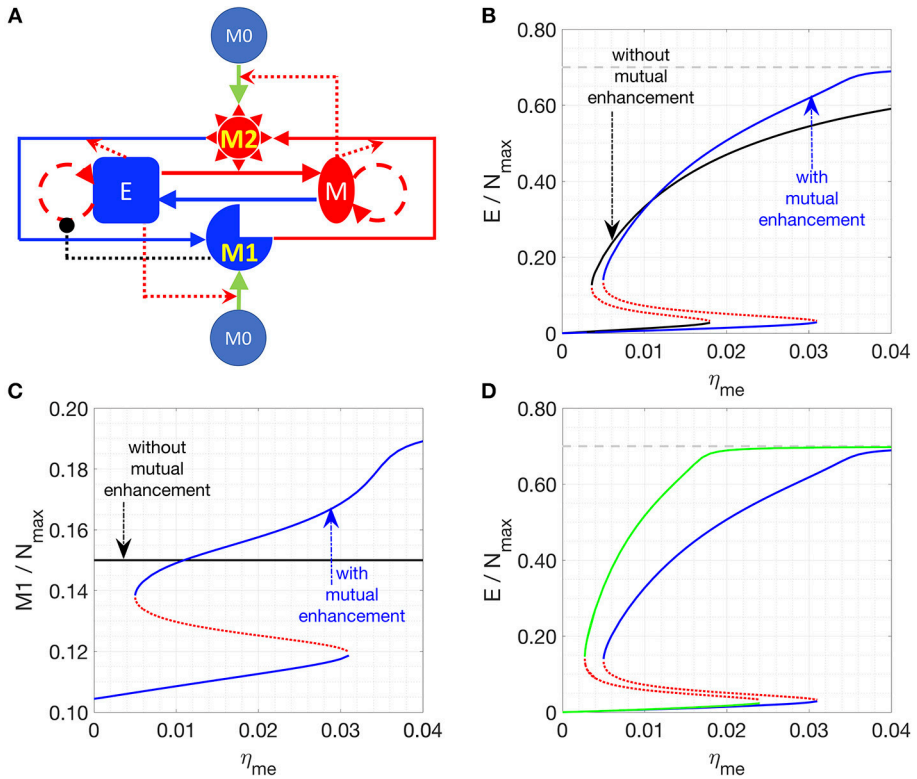

FIGURE 2 | Effects of interconversion between M_1 and M_2 cells, mediated by cancer cells. **(A)** Network of Model II. **(B,C)** Steady states of the epithelial **(B)** or M_1 **(C)** populations are plotted as a function of η_{me}. Stable steady states are plotted in solid lines and unstable steady states are plotted in dotted lines. The key parameters in **(B,C)** are: $\eta_{12} = \eta_{21} = 0$ (for black lines) or 1/72 h^{-1} (for blue lines), $m = 2$, $n = 2$, $k = 4$, $\eta_{21}^0 = \eta_{12}^0 = 1/72$ h^{-1}. **(D)** In this plot, the key parameters are: $\eta_{21} = 1/72$ h^{-1} (for blue lines) or 1/36 h^{-1} (for green lines), $m = 2$, $n = 2$, $k = 4$, $\eta_{21}^0 = \eta_{12}^0 = 1/72$ h^{-1}, and $\eta_{12} = 1/72$ h^{-1}. In **(B,D)**, the gray line is the maximum fraction of cancer cells (=0.7) as M_C is set as 0.3.

most of the interactions considered were of a "symmetric" nature, i.e., M_1 cells driving MET and M_2 cells driving EMT, and epithelial cells driving M_1 maturation while mesenchymal cells driving M_2 maturation. With this new interaction, the system is now biased against epithelial cells, because (a) epithelial but not mesenchymal cells, are killed by M_1-macrophages, and (b) their dead counterparts may convert M_1 to M_2 cells that can, in turn, convert some epithelial cells to mesenchymal ones (EMT). In addition, the conversion from M_2 to M_1 is essential to bring the system back from the mesenchymal-cancer-cell biased state and it can be enhanced by introducing IL-12 (45) or Type 1 T helper cells (44).

Thus, in the parameter region investigated, there are 3 types of stable steady states, which are represented by solid blue, red and black lines, respectively. At small values of the control parameter η_{me} (rate of M_1 macrophage assisted MET), there is only one type of stable steady state: the system is biased toward the mesenchymal-dominated state (solid blue curves in **Figures 3B–E**), whereas the cancer-extinction state (E = M = 0, dashed black curves in **Figures 3B–E**) is unstable. As η_{me} increases and goes across a critical value η_{me}^a =0.0626 h^{-1}), the extinction state (E = M = 0) becomes stable as well as a new set of steady states emerges (red lines in **Figures 3B–E**). Between η_{me} =0.0663 h^{-1} and η_{me} =0.0747 h^{-1}, the steady states depicted as a solid red line (**Figures 3B–E**) are stable; here both populations of epithelial and mesenchymal cancer cells are at a low level. This phenomenon can be understood in the following sense: at higher η_{me}, proliferating mesenchymal cells are continuously being converted to epithelial cells, which will be killed by M_1 macrophages. This effect brings down the overall fraction of cancer cells. Note that in this region, three types of stable steady states co-exist in the system for a given set of parameters. As η_{me} increases and goes across η_{me}^b =0.0747 h^{-1}, the stable steady states in solid red lines disappears and the other two types of stable steady states co-existed (solid blue and black lines in **Figures 3B–E**). As η_{me} further increases and goes across η_{me}^c =0.1532 h^{-1}, there is only one stable steady state: cancer cells are necessarily eliminated from the system. We note in passing that the instability that drives the red solution unstable as η_{me} is lowered past 0.0663 h^{-1} is a Hopf bifurcation to an unstable limit cycle.

Furthermore, for the breast cancer cell line MDA-MB-231 used in Yang et al. (38), η_{me} is estimated to be around 1/120 h^{-1} (~0.0083 h^{-1}). In order to explore the conditions for the absolute extinction of cancer cells around the estimated η_{me}, we

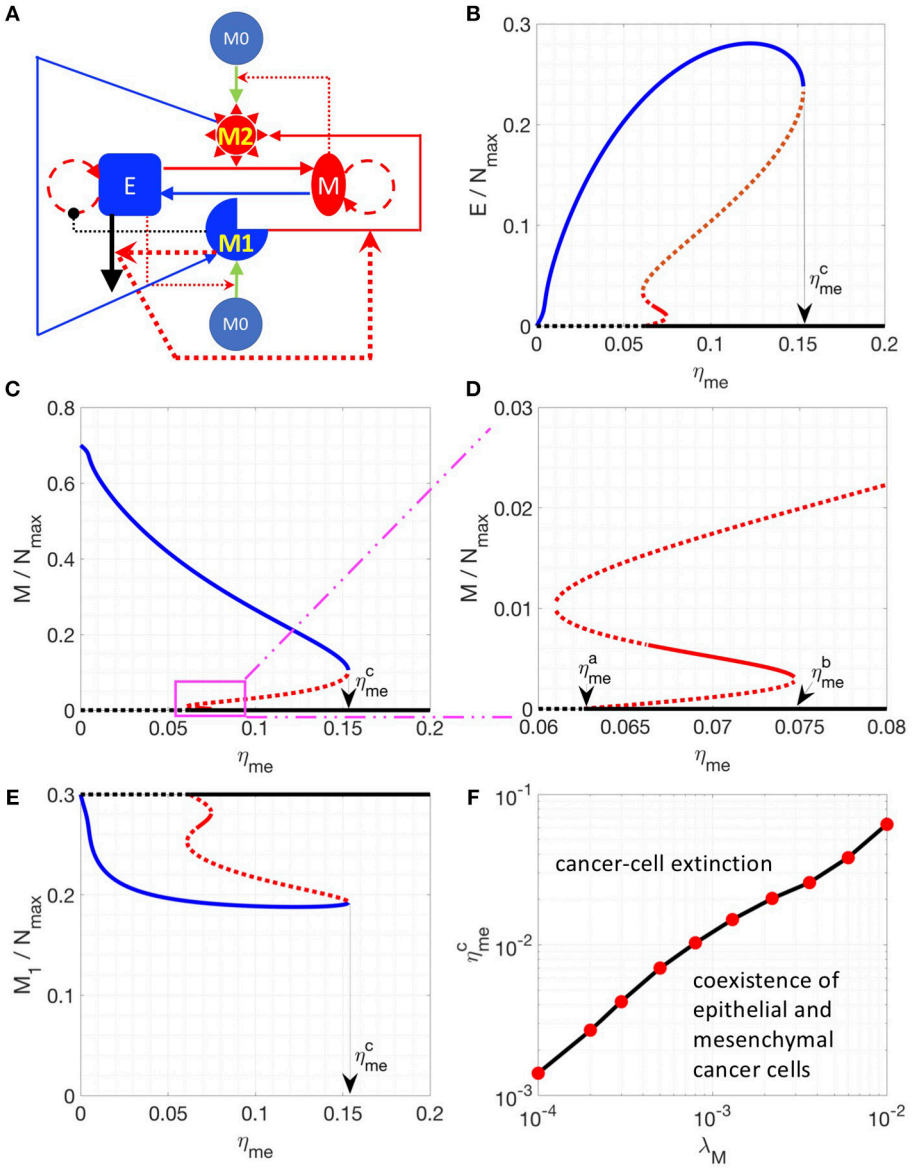

FIGURE 3 | Steady state solutions for a model including the M_1 to M_2 conversion assisted by apoptotic epithelial cancer cells**. (A)** Network of Model III. In this network, M_1 induces the apoptosis of epithelial cancer cells. And the factors released by apoptotic cancer cells enhance the M_1 to M_2 conversion. These interactions are highlighted by thicker lines. **(B–E)** Steady states of the epithelial **(B)**, mesenchymal **(C,D)** and M_1 **(E)** populations are plotted as a function of η_{me}. **(D)** is a zoomed-in version of **(C)**. Stable steady states are plotted in solid lines and unstable steady states are plotted in dotted lines. The model-specific parameters are: $\beta = 1/36\ h^{-1}$, $\beta_c = 1/1200\ h^{-1}$, $\eta_{12} = \eta_{21} = 1/72\ h^{-1}$. When η_{me} is higher than a critical value η^a_{me}, the steady state E = M = 0 becomes stable **(D)**. When η_{me} is higher than a critical value η^c_{me}, the steady state E = M = 0 is the only stable steady state of the system. **(F)** For a given λ_M, the critical value η^c_{me} is plotted.

varied different parameters (such as λ_M, η_{em}, and η_{21}) to get the corresponding η^c_{me} where the extinction state is the only stable steady state of the system. We found that lowering the growth rate of mesenchymal cells (λ_M) can reduce η^c_{me} to the nominal experimental value $1/120\ h^{-1}$ (**Figure 3F**) whereas lowering down η_{em} or increasing η_{21} might not (**Figure S5**). Therefore, for therapeutic purposes, increasing η_{me} and decreasing λ_M can be a promising combination to help to eliminate cancer cell populations. In addition, increasing the number of macrophages in the co-culture system can also shift η^c_{me} to a lower value (**Figure S6**) because of a potentially higher level of cancer-killing M_1-like macrophages.

EMT Scores Correlate With Multiple Genes Upregulated in M2 Macrophages

As a proof of principle for the predictions of our model, we investigated multiple TCGA datasets (see section Methods for the source of datasets), using our previously developed EMT scoring metric (47). This metric quantifies the extent of EMT in a particular sample, and correspondingly assigns a score between

TABLE 1 | Correlation coefficients of expression levels of specific genes with EMT scores, across many TCGA datasets.

Gene	FC (M_1/M_0)	FC (M_2/M_0)	Correlation Colorectal ($n = 286$)	Correlation Lung ($n = 515$)	Correlation Prostate ($n = 497$)	Correlation Breast ($n = 1097$)
ACTN1	0.46	2.37	0.32	0.41	0.32	0.13
FLRT2	0.47	7.29	0.33	0.36	0.33	0.40
MRC1 (CD206)	0.02	2.82	0.21	0.31	0.21	0.28
PTGS1	0.44	11.02	0.28	0.47	0.28	0.18
RHOJ	0.21	2.96	0.36	0.30	0.36	0.35
TMEM158	0.37	2.99	0.24	0.31	0.24	0.14
ARHGAP24	2.38	0.36	0.29	0.24	0.29	0.37
FIIR	3.43	0.41	-0.12	-0.44	-0.12	-0.19
STAT1	2.27	0.27	-0.02	0.29	-0.02	0.04
RSAD2	3.03	0.09	0.08	0.27	0.08	0.02
TUBA4A	2.18	0.33	0.11	-0.12	0.11	-0.01
XAF1	2.09	0.25	0.05	0.27	0.05	0.05

FC is the fold-change of gene expression levels in M_1 or M_2 macrophages relative to M_0, which is measured in Jablonski et al. (48) for murine bone marrow derived macrophages polarized in vitro. Those shown in red indicated upregulated in M_2, those in blue indicate upregulated in M_1. In all cases, the Pearson's correlation coefficient (r) is calculated and the corresponding p-values of those correlation coefficients are <0.05.

0 (fully epithelial) and 2 (fully mesenchymal). We calculated the correlation coefficients for EMT scores with various genes reported to be differently regulated in M_1 or M_2 macrophages relative to M_0 macrophages. The list of those genes is taken from Jablonski et al. (48). Out of 52 genes investigated, we observed that many genes upregulated in M2 and downregulated in M_1 macrophages–ACTN1, FLRT2, MRC1, PTGS1, RHOJ, TMEM158–correlated positively with the EMT scores (**Table 1,** first 6 rows) across multiple cancer types. The higher the EMT scores, the higher the levels of those genes, including the canonical M_2 macrophage marker CD206 (MRC1). On the other hand, out of the 52 genes investigated, many genes upregulated in M_1 macrophages but downregulated in M_2 macrophages–FIIR, STAT1, RSAD2, TUBA4A, and XAF1–showed either a negative or an overall weak positive correlation with EMT scores (**Table 1**, last 5 rows). The only exception observed in this trend was that for ARHGP24 which correlated positively with EMT scores across cancer types. Together, these correlation results in multiple TCGA datasets offer a promising initial validation of our model predictions that a state dominated by epithelial cells typically has higher number of M_1 macrophages, while the other state dominated by mesenchymal cells typically has higher number of M_2 macrophages.

Furthermore, to go beyond the correlation analysis between a single gene and the EMT-score, we investigated whether genes that are expressed higher in M_2-like macrophages will be enriched in EMT-score-high tumors and whether genes that are expressed higher in M_1-like macrophages will be enriched in EMT-score-low tumors. Again, the lists of genes that are expressed higher in M_1- or M_2-like macrophages are from Jablonski et al. (48) and the EMT-scores were calculated for each sample of the four TCGA dataset investigated in this work. We define a tumor to be EMT-score-high if its EMT-score is higher than the median score of the specific dataset and vice versa. Then, the expressions of a gene in EMT-score-high and low tumors in each dataset are used to determine whether this gene has a significantly high/low expression in EMT-score-high/low tumors. As expected, the genes that are expressed higher in M_2-like macrophages (but lower in M_1-like macrophages) are enriched in EMT-score-high tumors across the 4 types of cancers investigated (**Table 2**). This result is consistent with our model predictions: M_2-like macrophages and mesenchymal cancer cells tend to stably co-exist. However, somewhat to our surprise, the genes that expressed higher in M_1-like macrophages (but lower in M_2-like macrophages) are also enriched in EMT-score high tumors across the 4 types of cancers investigated (**Table S1**). This result is not in line with our model prediction where M_1-like macrophages are expected to stably co-exist with epithelial cancer cells. Possible reasons for this inconsistency will be discussed later. Nevertheless, the gene enrichment analysis in multiple TCGA datasets offer a promising initial validation of (most of) our model predictions.

DISCUSSION

The tumor microenvironment involves multiple cell types that interact among each other in diverse ways, thus giving rise to a complex adaptive ecological system (49–51). For such a system, mathematical models can help reveal the mechanisms underlying the emergent behavior and eventually aid in designing effective therapeutic strategies to modulate those aspects of the microenvironment that fuel disease aggressiveness (52–58).

Here, we focused on the interactions among macrophages of different polarizations (M_1 and M_2) and cancer cells with different phenotypes (epithelial and mesenchymal). Based on the literature, we focused on two types of models: with (Model II and III) or without (Model I) interconversion between M_1 and M_2 macrophages. All three models share a common feature: with a given set of parameters, multiple types of stable steady states can co-exist. More specifically, in Model I (without M_1-M_2 interconversion), with a given set of parameters, the system

TABLE 2 | M_2-associated gene set enrichment: Reported are all genes (out of 31 total) having statistically significant differential expression (samples segregated based on median EMT score) across TCGA colorectal adenocarcinoma (Adeno COL; $n = 286$), prostate adenocarcinoma (Adeno PCA; $n = 497$), invasive breast cancer (BCA invasive; $n = 1097$), and lung adenocarcinoma (Lung Adeno; $n = 515$).

	Adeno COL		Adeno PCA		BCA Invasive		Lung Adeno	
M_2 Gene	***p*-value**	**95% CI**	***p*-value**	**95% CI**	***p*-value**	**95% CI**	***p*-value**	**95% CI**
ACTN1	4.36E−05	(0.14 0.39)	1.61E−17	(0.41 0.65)	1.52E−05	(0.11 0.28)	3.65E−13	(0.36 0.61)
AMZ1	4.75E−06	(0.23 0.55)	ns	(−0.03 0.14)	2.50E−02	(0.03 0.28)	4.92E−06	(0.35 0.87)
ATP6V0A1	ns	(−0.03 0.16)	2.89E−02	(−0.16 −0.01)	4.22E−03	(−0.16 −0.03)	1.20E−03	(0.07 0.28)
BCAR3	ns	(−0.17 0.13)	3.83E−07	(0.19 0.43)	1.37E−02	(0.03 0.28)	1.95E−03	(0.10 0.44)
CCL22	ns	(−0.07 0.56)	1.13E−03	(0.13 0.53)	7.21E−06	(0.22 0.56)	5.58E−06	(0.36 0.90)
CD300LD	ns	(−0.03 0.08)	ns	(0.00 0.01)	ns	(−0.01 0.00)	ns	(−0.02 0.03)
CD83	2.08E−08	(0.33 0.67)	1.94E−05	(0.15 0.40)	1.86E−14	(0.33 0.55)	5.03E−12	(0.43 0.76)
CDH1	ns	(−0.15 0.10)	2.10E−03	(−0.34 −0.08)	1.13E−28	(−1.25 −0.88)	2.59E−02	(−0.33 −0.02)
CHST7	7.71E−04	(0.13 0.49)	ns	(−0.06 0.13)	8.64E−08	(0.15 0.32)	1.44E−06	(0.20 0.46)
CLEC10A	2.55E−03	(0.19 0.89)	7.33E−05	(0.22 0.64)	7.52E−15	(0.63 1.05)	1.21E−08	(0.52 1.06)
CLEC7A	1.35E−05	(0.38 0.98)	9.67E−07	(0.24 0.56)	6.03E−10	(0.32 0.62)	4.63E−16	(0.67 1.07)
EGR2	1.21E−13	(0.88 1.47)	2.16E−04	(0.24 0.77)	5.27E−27	(0.71 1.02)	4.60E−11	(0.48 0.87)
EMP2	1.38E−03	(−0.39 −0.09)	2.97E−04	(0.09 0.30)	9.75E−03	(−0.25 −0.03)	ns	(−0.23 0.11)
FLRT2	1.63E−10	(0.78 1.44)	2.25E−23	(0.86 1.25)	3.14E−42	(0.95 1.25)	5.17E−09	(0.48 0.95)
IL6ST	3.97E−03	(0.12 0.60)	4.50E−07	(0.52 1.16)	1.69E−04	(0.24 0.76)	2.09E−08	(0.40 0.83)
LMNA	2.50E−02	(−0.27 −0.02)	3.51E−02	(0.01 0.26)	1.29E−02	(−0.22 −0.03)	1.73E−05	(−0.38 −0.14)
MATK	2.53E−05	(0.37 0.99)	ns	(−0.33 0.22)	8.10E−03	(0.06 0.43)	5.33E−05	(0.24 0.69)
MMP12	ns	(−0.34 0.53)	ns	(−0.29 0.17)	ns	(−0.01 0.52)	1.22E−05	(0.53 1.39)
MMP9	1.75E−04	(0.39 1.23)	ns	(−0.31 0.27)	ns	(−0.11 0.36)	9.30E−08	(0.50 1.07)
MRC1	8.03E−08	(0.71 1.51)	3.75E−08	(0.35 0.73)	6.62E−19	(0.66 1.03)	2.54E−10	(0.67 1.20)
MYC	3.50E−02	(0.02 0.41)	ns	(−0.15 0.18)	ns	(−0.04 0.26)	ns	(−0.16 0.23)
OLFM1	3.64E−06	(0.44 1.06)	7.57E−03	(0.06 0.37)	ns	(−0.03 0.38)	7.80E−05	(0.31 0.91)
P2RY1	ns	(−0.47 0.06)	ns	(−0.34 0.19	4.96E−16)	(0.35 0.56)	1.57E−12	(0.53 0.92)
PLK2	ns	(−0.06 0.43)	1.18E−04	(0.15 0.47)	ns	(−0.03 0.22)	ns	(−0.02 0.33)
PTGS1	6.95E−03	(0.11 0.68)	8.55E−11	(0.50 0.93)	1.72E−12	(0.29 0.52)	3.61E−17	(0.61 0.97)
RHOJ	2.08E−09	(0.51 0.99)	2.83E−20	(0.53 0.80)	7.62E−32	(0.55 0.77)	2.23E−09	(0.31 0.61)
SOCS6	1.24E−03	(−0.36 −0.09)	4.95E−04	(0.07 0.25)	1.07E−03	(0.06 0.23)	1.43E−02	(−0.22 −0.02)
TANC2	ns	(−0.08 0.53)	ns	(−0.13 0.10)	ns	(−0.05 0.23)	9.54E−03	(0.05 0.35)
TIAM1	1.22E−04	(0.31 0.93)	2.06E−06	(0.22 0.53)	6.42E−05	(0.13 0.39)	6.75E−24	(0.83 1.21)
TMEM158	ns	(−0.11 0.40)	2.49E−07	(0.32 0.72)	1.68E−03	(0.12 0.51)	3.35E−05	(0.30 0.83)
VWF	4.88E−06	(0.38 0.94)	2.78E−04	(0.13 0.42)	2.00E−17	(0.39 0.62)	4.89E−07	(0.33 0.74)

For each gene, an unpaired t-test at significance level $\alpha = 0.05$ was performed under the null hypothesis that EMT-high and EMT-low mean gene expression signatures are equal. Red p-values correspond to the M_2-associated genes that are enriched in EMT-score-high tumors, whereas blue p-values correspond to the M_2-associated genes that are enriched in EMT-score-low tumors. "ns" stands for non-significant.

can converge to continuous range of states depending on the initial condition. However, these steady states belong to two categories: state I with a higher epithelial population and state II with a lower epithelial population. After the system reaches a steady state, perturbations applied only to cancer cell populations cannot drive the system out of the original steady state whereas perturbations on macrophage populations will drive the system out of the original steady state. However, the perturbation on macrophage populations might not drive the system out of the original category of steady states unless the perturbation is sufficiently strong. In Model II and III, with a given set of parameters, the system can again converge to two types of steady states depending on the initial condition: state I with a higher epithelial population and state II with a lower (or even zero for Model III) epithelial population. Now, however, the states are discrete. After the system reaches a steady state, perturbations of any single cell population might not drive the system out of the original steady state. Therefore, in general, it is not easy to switch the cancer-macrophage system from a mesenchymal- and M_2-dominated state to an epithelial- and M_1-dominated state.

Mathematical approaches similar to ours may be useful in explaining, and even predicting, the efficacy of different therapeutic intervention(s) and their combinations. For example, various efforts have been made to switch populations of macrophages from M_2- into M_1-like (25), such as depletion of TAMs, reprogramming of TAMs toward M_1-Like macrophages, inhibition of circulating monocyte recruitment into tumor, etc. The polarization of M_2 macrophages can also be altered via

inhibiting the endothelial-mesenchymal transition (EndMT), a process similar to EMT (59). However, it is unclear that how effective these types of strategies would be. Our modeling studies suggest that when we consider the interactions in Model III, the efforts on manipulating the M_1-M_2 interconversion might not be effective to eliminate cancer cells; whereas in Model II increasing the M_2-to-M_1 conversion rate can help the system to switch to the epithelial cancer cell and M_1 macrophage dominated state, which is believed to be less aggressive. Therefore, the effective therapeutic strategies strongly depend on the type of interactions present between cancer cells and macrophages.

Furthermore, we attempted to investigate whether the model-predicted stable co-existence of M_1-like macrophages and epithelial cancer cells (and likewise M_2-like macrophages and mesenchymal cancer cells) can be seen in the TCGA dataset. Indeed, we can observe the enrichment of many genes that are expressed higher in M_2-like macrophages in more mesenchymal tumors. This observation is consistent with our mathematical modeling analysis. However, we also detected the enrichment of genes that are expressed higher in M_1-like macrophages in more mesenchymal tumors. There can be several reasons for the enrichment of M_1 genes in mesenchymal tumors: (i) the list of genes used here to identify the ones preferentially expressed in M_1-like macrophages is from a study of mouse macrophages (48). For human macrophages, not as many markers have been validated as those in mice; future experiments can help characterize these better; (ii) for the TCGA sample used, the gene expression data that are used to calculate the EMT-score could be not exclusively that of cancer cells but may incorporate other types of cells, such as fibroblasts. Future experiments that can separate and measure gene expression of cancer cells separately, through techniques such as laser microdissection, will be more precise in quantifying the EMT status of cancer cells.

In addition, it is also important to recognize that our model suffers from limitations. For instance: (a) it does not consider spatial aspects of these interactions, for instance, mesenchymal cells may migrate and invade through the matrix, thus changing the interactions among the cells considered in our framework; (b) it does not consider the effects of senescence on epithelial cell growth (60); and (c) it considers EMT and macrophages polarization as a binary process, whereas emerging reports support the notion that in both cases there is likely to exist a spectrum of states/ phenotypes (61, 62). A more realistic model that can overcome the abovementioned assumptions and thus reflect the dynamics of tumor microenvironment more accurately can be used to help designing a more effective way to switch and stably maintain the system into a less aggressive state.

Despite the abovementioned limitations, our model can contribute to identifying key parameters of the system. For example, it suggests that to design an effective therapy to maintain the system in a M_1-dominated and cancer-free steady state, not only the conversion rate from mesenchymal to epithelial cells should be significant, but also the growth rate of mesenchymal cells should be low enough. In other words, MET-inducing and cell-growth-suppressing mechanisms can together synergistically restrict disease aggressiveness.

In summary, our results show that the interaction network between tumor cells and macrophages may lead to multi-stability in the network: one state dominated by epithelial and M_1-like cells, the other dominated by mesenchymal and M_2-like cells. We also identify that inducing MET and inhibiting cancer-cell growth might be much more efficient in "normalizing" (1) the tumor microenvironment that can otherwise be engineered by cancer cells to support their growth (63).

METHODS

Computational Models

According to *in vitro* experiments in literature, we construct three mathematical models. In Model I, factors secreted by epithelial (mesenchymal) cancer cells will polarize monocytes into M_1-like (M_2-like) macrophages. M_1-like macrophages will induce senescence of epithelial cancer cells and convert mesenchymal cancer cells to epithelial ones. On the other hand, M_2-like macrophages will convert epithelial cancer cells to mesenchymal ones. In addition, a mesenchymal cancer cell can secrete soluble factors to help maintain the mesenchymal state of itself and its neighbors, whereas an epithelial cancer cell can maintain the epithelial state through being in contact with its neighboring epithelial cancer cells. There is assumed to be no cell growth or death for macrophages and there is a maximum "carrying capacity" of cells in the system. The figure that illustrate this

TABLE 3 | Parameters used in our models.

Parameters	Values	References
N_{max}	1	Normalization factor
λ_E	1/72 h^{-1}	Estimated from (33)
λ_M	1/72 h^{-1}	Estimated from (33)
α	100	Estimated from (34)
K_1	0.1 N_{max}	Estimated (varied)
η_{me}	1/120 h^{-1}	Estimated from (38)
η_{em}	1/72 h^{-1}	Estimated from (38)
K_M^0	0.1 N_{max}	Estimated
K_E^0	0.1 N_{max}	Estimated
k	4	Estimated
β	0 or 1/36 h^{-1}	Estimated from (35)
K_2	1 N_{max}	Estimated
n	1 or 2	Estimated (varied)
m	1 or 2	Estimated (varied)
β_c	1/1200 h^{-1}	Estimated
η_1	1/24 h^{-1}	Estimated from (35)
K_E	0.1 N_{max}	Estimated
η_2	1/24 h^{-1}	Symmetric assumption
K_M	0.1 N_{max}	Estimated
K_C	1	Estimated
η_{12}^0	1/72 h^{-1}	Estimated (varied)
η_{21}^0	1/72 h^{-1}	Symmetric assumption (varied)
η_{12}	1/72 h^{-1}	Estimated from (35) (varied)
η_{21}	1/72 h^{-1}	Symmetric assumption (varied)

model is in **Figure 1A**. The equations to describe this system is as follows:

$$\begin{aligned}
\frac{dE}{dt} &= \lambda_E E\left(1-\frac{E+M+M_1+M_2+M_0}{N_{max}}\right)\frac{1}{1+\alpha\frac{M_1}{M_1+K_1}} \\
&\quad +\eta_{me}M\frac{M_1^n}{M_1^n+\frac{M}{M+K_M^0}}-\eta_{em}E\frac{M_2^m}{M_2^m+\frac{E^k}{E^k+(K_E^0)^k}} \\
\frac{dM}{dt} &= \lambda_M M\left(1-\frac{E+M+M_1+M_2+M_0}{N_{max}}\right) \\
&\quad -\eta_{me}M\frac{M_1^n}{M_1^n+\frac{M}{M+K_M^0}}+\eta_{em}E\frac{M_2^m}{M_2^m+\frac{E^k}{E^k+(K_E^0)^k}} \qquad (1) \\
\frac{dM_1}{dt} &= \eta_1\frac{E}{E+K_E}M_0 \\
\frac{dM_2}{dt} &= \eta_2\frac{M}{M+K_M}M_0 \\
\frac{dM_0}{dt} &= -\eta_1\frac{E}{E+K_E}M_0-\eta_2\frac{M}{M+K_M}M_0
\end{aligned}$$

The description and the value of each parameter are given in **Table 3**.

In Model II, interconversions between M_1 and M_2 macrophages are included. Furthermore, the interconversions can be enhanced by corresponding cancer cells. The figure that illustrate this model is in **Figure 2A**. The equation to describe this system is as follows:

$$\begin{aligned}
\frac{dE}{dt} &= \lambda_E E\left(1-\frac{E+M+M_1+M_2+M_0}{N_{max}}\right)\frac{1}{1+\alpha\frac{M_1}{M_1+K_1}} \\
&\quad +\eta_{me}M\frac{M_1^n}{M_1^n+\frac{M}{M+K_M^0}}-\eta_{em}E\frac{M_2^m}{M_2^m+\frac{E^k}{E^k+(K_E^0)^k}} \\
\frac{dM}{dt} &= \lambda_M M\left(1-\frac{E+M+M_1+M_2+M_0}{N_{max}}\right) \\
&\quad -\eta_{me}M\frac{M_1^n}{M_1^n+\frac{M}{M+K_M^0}}+\eta_{em}E\frac{M_2^m}{M_2^m+\frac{E^k}{E^k+(K_E^0)^k}} \qquad (2) \\
\frac{dM_1}{dt} &= \eta_1\frac{E}{E+K_E}M_0-\left(\eta_{12}^0+\eta_{12}\frac{M}{M+K_M}\right)M_1 \\
&\quad +\left(\eta_{21}^0+\eta_{21}\frac{E}{E+K_E}\right)M_2 \\
\frac{dM_2}{dt} &= \eta_2\frac{M}{M+K_M}M_0+\left(\eta_{12}^0+\eta_{12}\frac{M}{M+K_M}\right)M_1 \\
&\quad -\left(\eta_{21}^0+\eta_{21}\frac{E}{E+K_E}\right)M_2 \\
\frac{dM_0}{dt} &= -\eta_1\frac{E}{E+K_E}M_0-\eta_2\frac{M}{M+K_M}M_0
\end{aligned}$$

In the third model, additional interactions were introduced as illustrated in **Figure 3A**. M_1-like macrophages can induce apoptosis of epithelial cancer cells and factors released by apoptotic cancer cells can convert M_1-like macrophages into M_2-like macrophages. In order to restore the symmetry of the system, we further consider the therapeutic interaction: M_2-like macrophages can be re-polarized back to M_1-like macrophage by Type 1 T helper cells or IL-12. The equation to describe this system is as follows:

$$\begin{aligned}
\frac{dE}{dt} &= \lambda_E E\left(1-\frac{E+M+M_1+M_2+M_0}{N_{max}}\right)\frac{1}{1+\alpha\frac{M_1}{M_1+K_1}} \\
&\quad +\eta_{me}M\frac{M_1^n}{M_1^n+\frac{M}{M+K_M^0}}-\eta_{em}E\frac{M_2^m}{M_2^m+\frac{E^k}{E^k+(K_E^0)^k}} \\
&\quad -\beta E\frac{M_1}{M_1+K_2} \\
\frac{dM}{dt} &= \lambda_M M\left(1-\frac{E+M+M_1+M_2+M_0}{N_{max}}\right) \\
&\quad -\eta_{me}M\frac{M_1^n}{M_1^n+\frac{M}{M+K_M^0}}+\eta_{em}E\frac{M_2^m}{M_2^m+\frac{E^k}{E^k+(K_E^0)^k}} \qquad (3) \\
\frac{dC}{dt} &= \beta E\frac{M_1}{M_1+K_2}-\beta_c C \\
\frac{dM_1}{dt} &= \eta_1\frac{E}{E+K_E}M_0-\eta_{12}\frac{C}{C+K_C}M_1+\eta_{21}M_2 \\
\frac{dM_2}{dt} &= \eta_2\frac{M}{M+K_M}M_0+\eta_{12}\frac{C}{C+K_C}M_1-\eta_{21}M_2 \\
\frac{dM_0}{dt} &= -\eta_1\frac{E}{E+K_E}M_0-\eta_2\frac{M}{M+K_M}M_0
\end{aligned}$$

The description and the corresponding values of additional parameters are given in **Table 3**.

Correlation Analysis

For a fixed dataset, linear regression was performed for each gene of interest against the predicted EMT score (47). In each case samples were discretized into EMT-high or EMT-low based on median EMT score for hypothesis testing. The linear correlation coefficient was recorded in each case. We performed statistical analysis under the null hypothesis of zero correlation between gene expression fold-change and EMT score and recorded the corresponding p-values at significance level $\alpha = 0.05$ using unpaired t-test. All datasets (colon adenocarcinoma, $n = 286$; lung adenocarcinoma, $n = 525$; prostate adenocarcinoma, $n = 497$; breast invasive carcinoma, $n = 1{,}097$) were obtained from the R2: Genomics Analysis and Visualization Platform (http://r2.amc.nl).

AUTHOR CONTRIBUTIONS

XL, MKJ, KJP, and HL designed research. XL, MKJ, and JTG performed research. MKJ and JTG analyzed data. XL, MKJ, KJP, and HL wrote the paper.

FUNDING

This work was sponsored by the National Science Foundation NSF grant PHY-1427654 (Center for Theoretical Biological Physics). XL was supported by Stand Up to Cancer and The V Foundation. MKJ was also supported by a training fellowship from Gulf Coast Consortium as computational cancer biology training grant (CPRIT RP1705593). JTG was supported by National Cancer Institute of NIH (F30CA213878). KJP is supported by National Cancer Institute NCI grant CA093900. HL is also a Cancer Prevention and Research Institute of Texas Scholar in Cancer Research of the State of Texas at Rice University.

SUPPLEMENTARY MATERIAL

The Supplementary Material for this article can be found online at: https://www.frontiersin.org/articles/10.3389/fonc.2019.00010/full#supplementary-material

REFERENCES

1. Jain RK. Normalizing tumor microenvironment to treat cancer: bench to bedside to biomarkers. *J Clin Oncol*. (2013) 31:2205–18. doi: 10.1200/JCO.2012.46.3653
2. Bocci F, Jolly MK, Tripathi SC, Aguilar M, Hanash SM, Levine H, et al. Numb prevents a complete epithelial-mesenchymal transition by modulating Notch signaling. *J R Soc Interface* (2017) 14:20170512. doi: 10.1098/rsif.2017.0512
3. Peng DH, Ungewiss C, Tong P, Byers LA, Wang J, Canales JR, et al. ZEB1 induces LOXL2-mediated collagen stabilization and deposition in the extracellular matrix to drive lung cancer invasion and metastasis. *Oncogene* (2016) 36:1925–38. doi: 10.1038/onc.2016.358
4. Wang T, Liu G, Wang R. The intercellular metabolic interplay between tumor and immune cells. *Front Immunol*. (2014) 5:358. doi: 10.3389/fimmu.2014.00358
5. del Pozo Martin Y, Park D, Ramachandran A, Ombrato L, Calvo F, Chakravarty P, et al. Mesenchymal cancer cell-stroma crosstalk promotes niche activation, epithelial reversion, and metastatic colonization. *Cell Rep*. (2015) 13:2456–69. doi: 10.1016/j.celrep.2015.11.025
6. Nagarsheth N, Wicha MS, Zou W. Chemokines in the cancer microenvironment and their relevance in cancer immunotherapy. *Nat Rev Immunol*. (2017) 17:559–72. doi: 10.1038/nri.2017.49
7. Pitt JM, Marabelle A, Eggermont A, Soria JC, Kroemer G, Zitvogel L. Targeting the tumor microenvironment: removing obstruction to anticancer immune responses and immunotherapy. *Ann Oncol*. (2016) 27:1482–92. doi: 10.1093/annonc/mdw168
8. Mantovani A, Bottazzi B, Colotta F, Sozzani S, Ruco L. The origin and function of tumor-associated macrophages. *Immunol Today* (1992) 13:265–70. doi: 10.1016/0167-5699(92)90008-U
9. Noy R, Pollard JW. Tumor-associated macrophages: from mechanisms to therapy. *Immunity* (2014) 41:49–61. doi: 10.1016/j.immuni.2014.06.010
10. Mantovani A, Schioppa T, Porta C, Allavena P, Sica A. Role of tumor-associated macrophages in tumor progression and invasion. *Cancer Metastasis Rev*. (2006) 25:315–22. doi: 10.1007/s10555-006-9001-7
11. Allavena P, Sica A, Solinas G, Porta C, Mantovani A. The inflammatory micro-environment in tumor progression: The role of tumor-associated macrophages. *Crit Rev Oncol Hematol*. (2008) 66:1–9. doi: 10.1016/j.critrevonc.2007.07.004
12. Solinas G, Germano G, Mantovani A, Allavena P. Tumor-associated macrophages (TAM) as major players of the cancer-related inflammation. *J Leukoc Biol*. (2009) 86:1065–73. doi: 10.1189/jlb.0609385
13. Sica A, Mantovani A. Macrophage plasticity and polarization: *in vivo* veritas. *J Clin Invest*. (2012) 122:787–95. doi: 10.1172/JCI 59643
14. Mantovani A, Sozzani S, Locati M, Allavena P, Sica A. Macrophage polarization: tumor-associated macrophages as a paradigm for polarized M2 mononuclear phagocytes. *Trends Immunol*. (2002) 23:549–55. doi: 10.1016/S1471-4906(02)02302-5
15. Edin S, Wikberg ML, Dahlin AM, Rutegård J, Öberg Å, Oldenborg PA, et al. The Distribution of macrophages with a M1 or M2 phenotype in relation to prognosis and the molecular characteristics of colorectal cancer. *PLoS ONE* (2012) 7:e47045. doi: 10.1371/journal.pone.0047045
16. Ohri CM, Shikotra A, Green RH, Waller DA, Bradding P. Macrophages within NSCLC tumour islets are predominantly of a cytotoxic M1 phenotype associated with extended survival. *Eur Respir J*. (2009) 33:118–26. doi: 10.1183/09031936.00065708
17. Ma J, Liu L, Che G, Yu N, Dai F, You Z. The M1 form of tumor-associated macrophages in non-small cell lung cancer is positively associated with survival time. *BMC Cancer* (2010) 10:112. doi: 10.1186/1471-2407-10-112
18. Murphy KM, Stockinger B. Effector T cell plasticity: flexibility in the face of changing circumstances. *Nat Immunol*. (2010) 11:674–80. doi: 10.1038/ni.1899
19. Das A, Sinha M, Datta S, Abas M, Chaffee S, Sen CK, et al. Monocyte and macrophage plasticity in tissue repair and regeneration. *Am J Pathol*. (2015) 185:2596–606. doi: 10.1016/j.ajpath.2015.06.001
20. Moghaddam AS, Mohammadian S, Vazini H, Taghadosi M, Esmaeili S-A, Mardani F, et al. Macrophage plasticity, polarization and function in health and disease. *J Cell Physiol*. (2018) 233:6425–40. doi: 10.1002/jcp.26429
21. Guiducci C, Vicari AP, Sangaletti S, Trinchieri G, Colombo MP. Redirecting *in vivo* elicited tumor infiltrating macrophages and dendritic cells towards tumor rejection. *Cancer Res*. (2005) 65:3437–46. doi: 10.1158/0008-5472.CAN-04-4262
22. Rolny C, Mazzone M, Tugues S, Laoui D, Johansson I, Coulon C, et al. HRG inhibits tumor growth and metastasis by inducing macrophage polarization and vessel normalization through downregulation of PlGF. *Cancer Cell* (2011) 19:31–44. doi: 10.1016/j.ccr.2010.11.009
23. Xu M, Liu M, Du X, Li S, Li H, Li X, et al. Intratumoral delivery of IL-21 overcomes anti-Her2/Neu resistance through shifting tumor-associated macrophages from M2 to M1 phenotype. *J Immunol*. (2015) 194:4997–5006. doi: 10.4049/jimmunol.1402603
24. Geeraerts X, Bolli E, Fendt SM, Van Ginderachter JA. Macrophage metabolism as therapeutic target for cancer, atherosclerosis, and obesity. *Front Immunol*. (2017) 8:289. doi: 10.3389/fimmu.2017.00289
25. Genard G, Lucas S, Michiels C. Reprogramming of tumor-associated macrophages with anticancer therapies: radiotherapy versus chemo- and immunotherapies. *Front Immunol*. (2017) 8:828. doi: 10.3389/fimmu.2017.00828
26. Nieto MA, Huang RY, Jackson RA, Thiery JP. EMT: 2016. *Cell* (2016) 166:21–45. doi: 10.1016/j.cell.2016.06.028
27. Jolly MK, Ware KE, Gilja S, Somarelli JA, Levine H. EMT and MET: necessary or permissive for metastasis? *Mol Oncol*. (2017) 11:755–69. doi: 10.1002/1878-0261.12083
28. Krebs AM, Mitschke J, Losada ML, Schmalhofer O, Boerries M, Busch H, et al. The EMT-activator Zeb1 is a key factor for cell plasticity and promotes metastasis in pancreatic cancer. *Nat Cell Biol*. (2017) 19:518–29. doi: 10.1038/ncb3513
29. Siebzehnrubl FA, Silver DJ, Tugertimur B, Deleyrolle LP, Siebzehnrubl D, Sarkisian MR, et al. The ZEB1 pathway links glioblastoma initiation, invasion and chemoresistance. *EMBO Mol Med*. (2013) 5:1196–212. doi: 10.1002/emmm.201302827
30. Jolly MK, Jia D, Boareto M, Mani SA, Pienta KJ, Ben-Jacob E, et al. Coupling the modules of EMT and stemness: A tunable "stemness window" model. *Oncotarget* (2015) 6:25161–74. doi: 10.18632/oncotarget.4629
31. Huang RYJ, Wong MK, Tan TZ, Kuay KT, Ng AHC, Chung VY, et al. An EMT spectrum defines an anoikis-resistant and spheroidogenic intermediate

mesenchymal state that is sensitive to e-cadherin restoration by a src-kinase inhibitor, saracatinib (AZD0530). *Cell Death Dis*. (2013) 4:e915. doi: 10.1038/cddis.2013.442
32. Tripathi SC, Peters HL, Taguchi A, Katayama H, Wang H, Momin A, et al. Immunoproteasome deficiency is a feature of non-small cell lung cancer with a mesenchymal phenotype and is associated with a poor outcome. *Proc Natl Acad Sci USA*. (2016) 113:E1555–64. doi: 10.1073/pnas.1521812113
33. Hollmén M, Roudnicky F, Karaman S, Detmar M. Characterization of macrophage–cancer cell crosstalk in estrogen receptor positive and triple-negative breast cancer. *Sci Rep*. (2015) 5:9188. doi: 10.1038/srep09188
34. Yuan A, Hsiao YJ, Chen HY, Chen HW, Ho CC, Chen YY, et al. Opposite effects of M1 and M2 macrophage subtypes on lung cancer progression. *Sci Rep*. (2015) 5:14273. doi: 10.1038/srep14273
35. Weigert A, Tzieply N, von Knethen A, Johann AM, Schmidt H, Geisslinger G, et al. Tumor cell apoptosis polarizes macrophages role of sphingosine-1-phosphate. *Mol Biol Cell* (2007) 18:3810–9. doi: 10.1091/mbc.E06-12-1096
36. Sousa S, Brion R, Lintunen M, Kronqvist P, Sandholm J, Mönkkönen J, et al. Human breast cancer cells educate macrophages toward the M2 activation status. *Breast Cancer Res*. (2015) 17:101. doi: 10.1186/s13058-015-0621-0
37. Su S, Liu Q, Chen J, Chen J, Chen F, He C, et al. A Positive feedback loop between mesenchymal-like cancer cells and macrophages is essential to breast cancer metastasis. *Cancer Cell* (2014) 25:605–20. doi: 10.1016/j.ccr.2014.03.021
38. Yang M, Ma B, Shao H, Clark AM, Wells A. Macrophage phenotypic subtypes diametrically regulate epithelial-mesenchymal plasticity in breast cancer cells. *BMC Cancer* (2016) 16:419. doi: 10.1186/s12885-016-2411-1
39. Mobius W, Laan L. Physical and mathematical modeling in experimental papers. *Cell* (2015) 163:1577–83. doi: 10.1016/j.cell.2015.12.006
40. Gregory PA, Bracken CP, Smith E, Bert AG, Wright JA, Roslan S, et al. An autocrine TGF-beta/ZEB/miR-200 signaling network regulates establishment and maintenance of epithelial-mesenchymal transition. *Mol Biol Cell* (2011) 22:1686–98. doi: 10.1091/mbc.E11-02-0103
41. Scheel C, Eaton EN, Li SHJ, Chaffer CL, Reinhardt F, Kah KJ, et al. Paracrine and autocrine signals induce and maintain mesenchymal and stem cell states in the breast. *Cell* (2011) 145:926–40. doi: 10.1016/j.cell.2011.04.029
42. Schmalhofer O, Brabletz S, Brabletz T. E-cadherin, beta-catenin, and ZEB1 in malignant progression of cancer. *Cancer Metastasis Rev*. (2009) 28:151–66. doi: 10.1007/s10555-008-9179-y
43. Jia D, Jolly MK, Harrison W, Boareto M, Ben-Jacob E, Levine H. Operating principles of tristable circuits regulating cellular differentiation. *Phys Biol*. (2017) 14:035007. doi: 10.1088/1478-3975/aa6f90
44. Heusinkveld M, de Vos van Steenwijk PJ, Goedemans R, Ramwadhdoebe TH, Gorter A, Welters MJ, et al. M2 macrophages induced by prostaglandin E2 and IL-6 from cervical carcinoma are switched to activated M1 macrophages by CD4+ Th1 cells. *J Immunol*. (2011) 187:1157–65. doi: 10.4049/jimmunol.1100889
45. Wang Y, Lin Y-X, Qiao S-L, An H-W, Ma Y, Qiao Z-Y, et al. Polymeric nanoparticles promote macrophage reversal from M2 to M1 phenotypes in the tumor microenvironment. *Biomaterials* (2017) 112:153–63. doi: 10.1016/J.BIOMATERIALS.2016.09.034
46. Frost JJ, Pienta KJ, Coffey DS. Symmetry and symmetry breaking in cancer: a foundational approach to the cancer problem. *Oncotarget* (2017) 9:11429–40doi: 10.18632/oncotarget.22939
47. George JT, Jolly MK, Xu S, Somarelli JA, Levine H. Survival outcomes in cancer patients predicted by a partial EMT gene expression scoring metric. *Cancer Res*. (2017) 77:6415–28. doi: 10.1158/0008-5472.CAN-16-3521
48. Jablonski KA, Amici SA, Webb LM, Ruiz-Rosado JDD, Popovich PG, Partida-Sanchez S, et al. Novel markers to delineate murine M1 and M2 macrophages. *PLoS ONE* (2015) 10:e0145342. doi: 10.1371/journal.pone.0145342
49. Whiteside TL. The tumor microenvironment and its role in promoting tumor growth. *Oncogene* (2008) 27:5904–12. doi: 10.1038/onc.2008.271
50. Gajewski TF, Schreiber H, Fu YX. Innate and adaptive immune cells in the tumor microenvironment. *Nat Immunol*. (2013) 14:1014–22. doi: 10.1038/ni.2703
51. Augsten M. Cancer-associated fibroblasts as another polarized cell type of the tumor microenvironment. *Front Oncol*. (2014) 4:62. doi: 10.3389/fonc.2014.00062
52. Kuznetsov VA, Knott GD. Modeling tumor regrowth and immunotherapy. *Math Comput Model* (2001) 33:1275–87. doi: 10.1016/S0895-7177(00)00314-9
53. Knútsdóttir H, Pálsson E, Edelstein-Keshet L. Mathematical model of macrophage-facilitated breast cancer cells invasion. *J Theor Biol*. (2014) 357:184–99. doi: 10.1016/j.jtbi.2014.04.031
54. Knutsdottir H, Condeelis JS, Palsson E. 3-D individual cell based computational modeling of tumor cell–macrophage paracrine signaling mediated by EGF and CSF-1 gradients. *Integr Biol.* (2016) 8:104–19. doi: 10.1039/C5IB00201J
55. Serre R, Benzekry S, Padovani L, Meille C, Andre N, Ciccolini J, et al. Mathematical modeling of cancer immunotherapy and its synergy with radiotherapy. *Cancer Res.* (2016) 76:4931–40. doi: 10.1158/0008-5472.CAN-15-3567
56. Guo Y, Nie Q, MacLean AL, Li Y, Lei J, Li S. Multiscale modeling of inflammation-induced tumorigenesis reveals competing oncogenic and oncoprotective roles for inflammation. *Cancer Res*. (2017) 77:6429–41. doi: 10.1158/0008-5472.CAN-17-1662
57. Mahlbacher G, Curtis LT, Lowengrub J, Frieboes HB. Mathematical modeling of tumor-associated macrophage interactions with the cancer microenvironment. *J Immunother Cancer* (2018) 6:10. doi: 10.1186/s40425-017-0313-7
58. Michor F, Beal K. Improving cancer treatment via mathematical modeling: surmounting the challenges is worth the effort. *Cell* (2015) 163:1059–63. doi: 10.1016/j.cell.2015.11.002
59. Choi SH, Kim AR, Nam JK, Kim JM, Kim J-Y, Seo HR, et al. Tumour-vasculature development via endothelial-to-mesenchymal transition after radiotherapy controls CD44v6+ cancer cell and macrophage polarization. *Nat Commun*. (2018) 9:5108. doi: 10.1038/s41467-018-07470-w
60. Storer M, Mas A, Robert-Moreno A, Pecoraro M, Ortells MC, Di Giacomo V, et al. Senescence is a developmental mechanism that contributes to embryonic growth and patterning. *Cell* (2013) 155:1119–30. doi: 10.1016/j.cell.2013.10.041
61. Jolly MK, Ward C, Eapen MS, Myers S, Hallgren O, Levine H, et al. Epithelial–mesenchymal transition, a spectrum of states: Role in lung development, homeostasis, and disease. *Dev Dyn* (2018) 247:346–58. doi: 10.1002/dvdy.24541
62. Aras S, Raza Zaidi M. TAMeless traitors: macrophages in cancer progression and metastasis. *Br J Cancer* (2017) 117:1583–91. doi: 10.1038/bjc.2017.356
63. Amend SR, Roy S, Brown JS, Pienta KJ. Ecological paradigms to understand the dynamics of metastasis. *Cancer Lett*. (2016) 380:237–42. doi: 10.1016/j.canlet.2015.10.005

Conflict of Interest Statement: The authors declare that the research was conducted in the absence of any commercial or financial relationships that could be construed as a potential conflict of interest.

frontiers in Oncology

REVIEW
published: 12 December 2018
doi: 10.3389/fonc.2018.00617

Metabolic Dependencies in Pancreatic Cancer

*Ali Vaziri-Gohar[1], Mahsa Zarei[2,3], Jonathan R. Brody[4] and Jordan M. Winter[1,5]**

[1] School of Medicine, Case Western Reserve University, Cleveland, OH, United States, [2] Department of Veterinary Physiology and Pharmacology, Texas A&M University, College Station, TX, United States, [3] Department of Medicine, Brigham and Women's Hospital and Harvard Medical School, Boston, MA, United States, [4] Division of Surgical Research, Department of Surgery, Jefferson Pancreas, Biliary and Related Cancer Center, Jefferson Medical College, Thomas Jefferson University, Philadelphia, PA, United States, [5] Department of Surgery and Division of Surgical Oncology, University Hospitals Cleveland Medical Center, Cleveland, OH, United States

Pancreatic ductal adenocarcinoma (PDA) is a highly lethal cancer with a long-term survival rate under 10%. Available cytotoxic chemotherapies have significant side effects, and only marginal therapeutic efficacy. FDA approved drugs currently used against PDA target DNA metabolism and DNA integrity. However, alternative metabolic targets beyond DNA may prove to be much more effective. PDA cells are forced to live within a particularly severe microenvironment characterized by relative hypovascularity, hypoxia, and nutrient deprivation. Thus, PDA cells must possess biochemical flexibility in order to adapt to austere conditions. A better understanding of the metabolic dependencies required by PDA to survive and thrive within a harsh metabolic milieu could reveal specific metabolic vulnerabilities. These molecular requirements can then be targeted therapeutically, and would likely be associated with a clinically significant therapeutic window since the normal tissue is so well-perfused with an abundant nutrient supply. Recent work has uncovered a number of promising therapeutic targets in the metabolic domain, and clinicians are already translating some of these discoveries to the clinic. In this review, we highlight mitochondria metabolism, non-canonical nutrient acquisition pathways (macropinocytosis and use of pancreatic stellate cell-derived alanine), and redox homeostasis as compelling therapeutic opportunities in the metabolic domain.

Keywords: pancreatic cancer, metabolism, redox homeostasis, metabolic dependencies, targeting metabolism

OPEN ACCESS

Edited by:
Ramon Bartrons, University of Barcelona, Spain

Reviewed by:
Vincenzo Ciminale, Università degli Studi di Padova, Italy
Mohamed Jemaà, Lund University, Sweden

***Correspondence:**
Jordan M. Winter
jordan.winter@UHhospitals.org

Specialty section:
This article was submitted to Molecular and Cellular Oncology, a section of the journal Frontiers in Oncology

Received: *11 October 2018*
Accepted: *29 November 2018*
Published: *12 December 2018*

Citation:
Vaziri-Gohar A, Zarei M, Brody JR and Winter JM (2018) Metabolic Dependencies in Pancreatic Cancer. Front. Oncol. 8:617. doi: 10.3389/fonc.2018.00617

OVERVIEW OF PANCREATIC CANCER TREATMENT AND BIOLOGY

Pancreatic cancer is the third leading cause of cancer-related death in the United States (1). The disease is predicted to be the second leading cause within the next decade (2). Cures are exceedingly rare, and the 5-years survival for patients with metastatic disease is just 3%. Even patients with localized PDA who undergo resection with curative intent have a 5-years survival of only 30% (1). This survival rate is by far the lowest of the common cancers, and is attributable in large part to PDAs uniquely aggressive behavior and resistance to conventional therapy (3, 4).

The majority of pancreatic cancer patients already have experienced macroscopic or microscopic spread at the time of diagnosis (5–7). Cytotoxic chemotherapeutic agents are the only approved systemic treatments for these patients, and are grouped into two separate multi-agent regimens used as standard-of-care: (1) gemcitabine and nab-paclitaxel (albumin-bound paclitaxel or

Abraxane) or (2) 5-fluorouracil, leucovorin, irinotecan, and oxaliplatin (FOLFIRINOX). Unless researchers discover effective strategies to detect PDA earlier or preventative tactics, new ways to treat invasive PDA are desperately needed (8, 9).

Pancreatic cancer develops over many years due to the additive effects of numerous genetic changes (10). Gain-of-function mutations in KRAS at codons 12, 13, and 61 are observed in over 90% of PDAs. Loss-of-function mutations in three specific tumor suppressor genes occur in the majority of PDAs: TP53, CDKN2A, and SMAD4 (11–14). These oncogenic changes occur early in the adenoma to carcinoma progression (15, 16). The vast majority of pancreatic cancers are sporadic. Approximately 10% of patients have one or more immediate family members with a history of PDA. Germline culprits include genes that are important for DNA repair, such as BRCA2, PALB2, ATM, FANCC, and FANCG genes (11, 17).

Histologically, pancreatic tumorigenesis passes through three non-invasive, pre-malignant stages before acquiring an invasive phenotype. The premalignant stages are referred to as pancreatic intraepithelial neoplasia (PanIN 1, 2, and 3). More detailed descriptions of the genetics and pathobiology of pancreatic cancer appear elsewhere (18–20). In addition to well-characterized genetic mutations, there other molecular abnormalities common to PDA including hyperactivated growth factor signaling, epigenetic changes, dysregulated gene expression (transcriptional or post-transcriptional), and abnormal post-translational modifications (18, 21–23).

THE TUMOR MICROENVIRONMENT AND IMPLICATIONS FOR AN AGGRESSIVE PDA PHENOTYPE

The PDA tumor microenvironment is characterized by one of the most abundant stromal compartments of any tumor type, and this feature is the principal biologic driver of the PDA metabolic program. Neoplastic epithelial cells account for roughly 10–15% of the tumor mass, while non-neoplastic elements comprise the remainder of the tumor. The stroma, or desmoplastic response, consists of an extracellular matrix and diverse cellular elements including fibroblasts, myofibroblasts, lymphatic vessels, blood vessels, pancreatic stellate cells, and immune cells (24, 25). As a result of these elements, the stroma is extremely dense, with a high interstitial fluid pressure (26). Consequently, blood vessels are compressed by biochemical forces and microscopic arteriolar-venular shunts are common events (27, 28). Compounding this significant biologically relevant perfusion challenge, microscopic vessel density is markedly reduced in PDA stroma as compared to normal pancreata (26).

PDA hypovascularity is easy to appreciate macroscopically. Transected PDAs are pale gray and necrotic (**Figure 1A**). On imaging, PDA appears as a hypodense tumor, easily distinguished by the well-perfused and contrast-enhancing normal pancreatic parenchyma (**Figure 1B**). This biologic reality accounts for the harsh, nutrient deprived, and hypoxic conditions that are hallmarks of the PDA microenvironment. Indeed, PDA survives, and thrives, in a desert!

Studies implicate mutant KRAS as a key driver of the desmoplastic response. Temporally, this genetic model fits since KRAS mutations arise in PanIN1 lesions when the stroma first develops. As evidence, withdrawal of mutant KRAS expression using shRNAs in genetically engineered KPC mice (autochthonous PDA mice with conditional expression of oncogenic KRAS and TP53 mutations) (16) resulted in the disappearance of the stromal compartment (29).

GLUCOSE METABOLISM

Oxidative phosphorylation is an energy extracting process where pyruvate enters the mitochondria matrix via pyruvate translocase and is oxidized to generate ATP, H_2O, and CO_2. Oxygen acts as a final electron acceptor in the electron transport chain. As a result of the associated redox reactions, an electrochemical potential is generated across the inner mitochondrial membrane, which drives a proton-motive force across the membrane, and directly results in the formation of ATP. Thus, carbon flows through the tricarboxylic acid (TCA) cycle and is oxidized to its simplest form, creating basic energy subunits with high energy phosphate bonds that drive other chemical reactions required for cell viability. Well-perfused and differentiated normal cells generate the bulk of their cellular energy through oxidative phosphorylation in the mitochondria (30). Cancer cells, on the other hand, are often oxygen-poor. This scenario theoretically poses an obstacle for effective oxidative phosphorylation. Even in the presence of sufficient oxygen, however, scientists believed for decades that cancer cells were reprogrammed.

Scientists posited that cancer cells relied on cytosolic glycolysis to produce ATP instead of oxidative phosphorylation, even though the energy yield was far less efficient (2 ATP vs. 36 ATP). A preference for aerobic glycolysis is eponymously referred to as the "Warburg's effect" (31), and there have been numerous lines of evidence that in fact reveal robust glycolytic activity in pancreatic cancer cells in certain experimental models, including patient samples. For instance, endogenous expression of many glycolytic enzymes is increased, including hexokinase 2, enolase 2, and lactate dehydrogenases (both LDHA and LDHB isoforms) (32–35). Consequently, glycolytic metabolites, including lactate, are also elevated in pancreatic cancer cells (32, 33, 36).

Generally speaking, a biochemical penchant for glycolysis can serve cancer cells in multiple ways. First, Lactic acid build-up reduces cellular and extracellular pH. This contributes to invasiveness by promoting genetic changes in PDA cells

Abbreviations: ALDH3A1, aldehyde dehydrogenases; ASCT2, alanine-serine-cysteine transporter 2; dCTP, deoxycytidine triphosphate; Drp1, dynamin-related protein 1; EIPA, 5-(*N*-ethyl-*N*-isopropyl)amiloride; G6PD, glucose-6-phosphate dehydrogenase; GLUD, glutamate dehydrogenase; GLUT1, glucose transporter 1; HIF-1α, hypoxia-inducible factor-1a; IDH, isocitrate dehydrogenase; LDH, lactate dehydrogenase; ME, malic enzyme; MTHFD, methylenetetrahydrofolate dehydrogenase; NAD^+, oxidized nicotinamide adenine dinucleotide; NADK, NAD^+ kinase; $NADP^+$, oxidized nicotinamide adenine dinucleotide phosphate; NADPH, reduced nicotinamide adenine dinucleotide phosphate; NAMPT, nicotinamide phosphoribosyltransferase; NMN, nicotinamide mononucleotide; NNT, nicotinamide nucleotide transhydrogenase; NRF2, nuclear factor erythroid 2 related factor 2; OAA, oxaloacetate; OXPHOS, oxidative phosphorylation; PanIN, pancreatic intraepithelial neoplasia; PDA, pancreatic ductal adenocarcinoma; PDHK1, pyruvate dehydrogenase kinase 1; PGD, phosphogluconate dehydrogenase; PPP, pentose phosphate pathway; ROS, reactive oxygen species; shRNA, short hairpin RNA; TCA, tricarboxylic acid.

(spurring on genetic selection), impairing the anti-tumor immune response (protecting cancer cells from immune patrol), reducing adherens junctions on cancer cell membranes (facilitating detachment and metastases), and hydrolysis of extracellular proteins to encourage cell invasion (37). Just as important, enhanced glycolytic activity minimizes combustion of carbon from glucose to CO_2. Instead, organic carbon is preserved, and diverted into cellular building blocks through biosynthetic pathways, such as lipid synthesis, the hexosamine biosynthesis pathway, and the pentose phosphate pathway. This reprogramming effort promotes the macromolecular synthesis needed for cell proliferation (i.e., anabolism) (30, 38, 39). As stated above for desmoplasia (and a common theme for many of the adaptive reprogramming responses described below), oncogenic KRAS drives glycolytic activity in PDA. For instance, KRAS activation leads to increased glucose uptake and elevated levels of glycolysis-associated metabolites (40, 41). *In vivo* models modified by an inducible KRAS extinction mechanism in pancreatic tumors corroborate these findings (29).

Additional studies show that oncogenic KRAS activity supports glycolysis by replenishing the supply of NAD^+, via upregulation of NAD(P)H oxidase (42). At a regulatory level, the Pasteur effect (an increase in glucose consumption and lactic acid fermentation under low oxygen conditions) is also encouraged by certain transcription factors and related proteins (34, 43). As examples, HIF-1α and MUC1 upregulate glucose transporter 1 (GLUT1) and aldolase A, which leads to increased glucose uptake and glycolysis. MUC1 collaborates with HIF-1α for this purpose. Additionally, under hypoxic conditions, pyruvate dehydrogenase kinase 1 (PDHK1) protein expression is increased, leading to a reduction in pyruvate dehydrogenase (32, 44, 45) activity, and consequently a reduction in oxidative phosphorylation (46).

THE IMPORTANCE OF MITOCHONDRIAL FUNCTION IN PDA

As it turns out, the classic Warburg model misses a large part of the story. Current perspectives maintain that a balance between aerobic glycolysis and oxidative phosphorylation is much more complex, and seems to be highly variable between different tumor types. Moreover, the balance is not fixed in a given tumor. Rather, the metabolic program is dynamic, and responds to ambient conditions (47). Contrary to Warburg's teachings, mitochondria in cancer are often highly functional, and aerobic respiration is even critical for cancer cell survival (48). A preponderance of new evidence shows that pancreatic cancer cells are especially dependent on mitochondrial oxidative phosphorylation under low nutrient conditions, and that mitochondrial metabolism represents a key metabolic vulnerability (47–51).

Diverse macromolecular substrates are utilized by pancreatic cancer cells for catabolic and anabolic purposes, but glucose is consistently viewed as the most important nutrient. Glucose is even likely more limiting in the microenvironment than oxygen, especially in poorly perfused PDA. Oxygen levels exist in the microenvironment around 1.5% (compared to 21% in the atmosphere and 5% in normal tissues (52). At these low levels, mitochondria still function relatively well. In fact, mitochondria perform sufficiently at oxygen levels as low as 0.5% (53, 54). Glucose concentrations frequently dip below 1 mM in poorly perfused tumors, and these levels are profoundly deleterious. Cell necrosis is the outcome at these levels, even when sufficient oxygen is present (55).

An siRNA screen of 2,752 metabolic genes revealed that mitochondrial genes encoding electron transport chain components were functionally the most important genes in cancer cell survival under low glucose conditions (51). Moreover, when 28 cell lines were evaluated for their ability to withstand low glucose conditions, resistant cell lines consistently increased oxygen consumption on demand, as compared to the most vulnerable cell lines. Further, the vulnerable cell lines exhibited higher rates of genetic mutations in mitochondria-encoded electron transport genes (51). Studies revealed that under low glucose, cell proliferation markedly decreases (49, 56, 57). All of these findings suggest a model where cancer cells that are well-adapted to harsh and unfavorable metabolic conditions prioritize the conservation of glucose, and reprogram their biology to maximize energy yields through enhanced mitochondrial respiration. This metabolic shift ensures the production of sufficient ATP to power critical cellular processes. Under austere conditions, cancer cells choose to divert carbon away from biosynthetic pathways, which minimizes unnecessary ATP utilization. Cell proliferation is deferred for a later time when energy supplies become more available, or the cells become even more adept at scavenging nutrients from a deprived microenvironment (**Figure 2**).

A number of bioenergetic observations support this model. As glucose levels decline, cellular respiration markedly increases. The mitochondrial matrix becomes more acidic as protons return to the matrix through ATP synthase, and hydroxide anions are expelled in phosphate/OH^- exchangers. This supports ATP production. A burst of oxidative activity is usually observed (49). Morphologically, the matrix condenses, and cristae expand in functional and working mitochondria. Mitochondrial fusion and elongation are favored over fission events (58–60). Inhibition of an important fission-related protein, dynamin-related protein 1 (Drp1), has been shown to shift the balance from mitochondrial fission to fusion under low nutrient conditions (61).

We have recently found that an RNA-binding protein and regulator of acute survival processes, HuR (ELAVL1), plays an important role in increasing mitochondrial performance in stressed PDA cells. This occurs over a very short timescale. We observed that HuR-proficient PDA cells cultured under low glucose conditions exhibited higher rates of oxygen consumption and ATP production, as compared to isogenic HuR-deficient cancer cells (50). Additionally, HuR expression promoted mitochondrial biogenesis (Vaziri-Gohar, unpublished). Consequently, HuR-deficient PDA cells were unable to ramp up mitochondrial activity under metabolic stress, and were especially vulnerable under low glucose conditions *in vitro*.

Thus, it stands to reason that mitochondrial biology represents a promising therapeutic target in nutrient-deprived cancers (e.g., PDA). There are some clinical studies that support

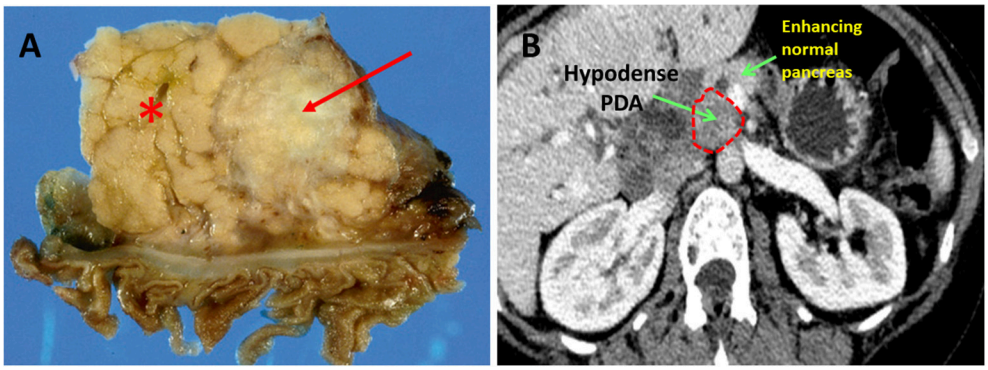

FIGURE 1 | Pancreatic ductal adenocarcinoma. **(A)** Resected human PDA. The arrow identifies the characteristically pale, gray, and hypovascular pancreatic ductal adenocarcinoma. The asterisk marks pancreatic parenchyma. **(B)** On CT scan imaging with intravenous contrast, PDA appears hypodense (dark gray), while well-perfused normal pancreatic parenchyma shows bright enhancement due to penetration by the contrast.

this idea in pancreatic cancer patients. A common diabetic drug, metformin, inhibits complex 1 of the electron transport chain. A meta-analysis of nine retrospective studies and two randomized studies in patients with pancreatic cancer revealed that metformin use was associated with prolonged survival (62–64). Notably, however, the two randomized, phase II studies included in the meta-analysis (both in patients with advanced PDA) were negative studies (63, 64). Prolonged survival was only observed in patients with localized PDA, suggesting that the drug may not be effective in patients with macroscopic distant disease (62). The strategy may be correct, but for improved efficacy, a more potent drug may be required.

More recently, a novel mitochondrial inhibitor was tested in a phase I study of patients with advanced pancreatic cancer. The results were extremely promising. CPI-613 is a lipoic acid analog that disrupts the activity of two mitochondrial enzymes: pyruvate dehydrogenase and α-ketoglutarate dehydrogenase (65, 66). The drug was given to 18 patients at a maximum tolerated dose of 500 mg/m^2 on days 1 and 3, of a 2-weeks cycle, and in combination with modified FOLFIRINOX (67). The disease control rate, response rate, and complete response rate were 89, 61, and 17%, respectively. In contrast, the rates for FOLFIRINOX alone in a prior phase III study are 71, 32, and 0.6%, respectively (68). A registration phase III trial is planned to begin shortly as of this manuscript writing, and we are poised to test the same combination in a phase II trial of patients with locally advanced PDA at our institution. These studies are expected to be actively accruing by the start of 2019.

NUTRIENT ACQUISITION PATHWAYS

PDA cells also adapt to low nutrient conditions by recruiting unconventional nutrient sources or biochemical salvage pathways to meet bioenergetic demands in a nutrient-deprived microenvironment. There is a small, but important body of literature that highlights some of these biologic processes. Like mitochondrial biology, these non-canonical metabolic pathways represent novel therapeutic opportunities. We have categorized them as intracellular processes (*intrinsic*) or those dependent on the microenvironment (*extrinsic*). While some salvage pathways, like nucleotide salvage, are not directly addressed here, we have focused on ones that have received attention in the recent pancreatic cancer literature.

INTRINSIC NUTRIENT ACQUISITION MECHANISMS

Autophagy

Autophagy is a cytoplasmic recycling process that breaks down dysfunctional organelles and unfolded proteins into their basic components for reuse by cells. Mechanistically, unwanted structures are enwrapped by a double-membrane structure called a phagophore to produce an autophagosome. When the vesicle fuses with a lysosome, the contents are enzymatically digested. Autophagy is driven by starvation-induced activation of AMPK, and is suppressed by mTORC1 in normal cells (69, 70). However, oncogenic KRAS signaling appears to regulate or induce autophagy in PDA cells (71, 72). Conceptually, autophagy functions as an effective nutrient salvage pathway for KRAS-driven PDA, especially when extrinsic nutrient sources are deficient. Cleaved LC3 is an indicator of active autophagy (70, 73) and is increased in late PanIN lesions, as well as in PDA (74). Increased autophagy markers have also been associated with worse prognosis in patients with PDA (75). At the subcellular level, inhibiting autophagy in PDA cells disrupts mitochondrial oxidative phosphorylation and exacerbates oxidative damage (74). Autophagy inhibitors like chloroquine and Bafilomycin A1 have been shown to reduce PDA growth in cell culture and pre-clinical animal models (74, 76).

NAD$^+$ Salvage Pathway

NADH is an essential cofactor for enzymatic reactions in both glycolysis and respiration. The molecule provides reducing equivalents for the electron transport chain, which drives the proton-motive force to ultimately yield ATP for basic

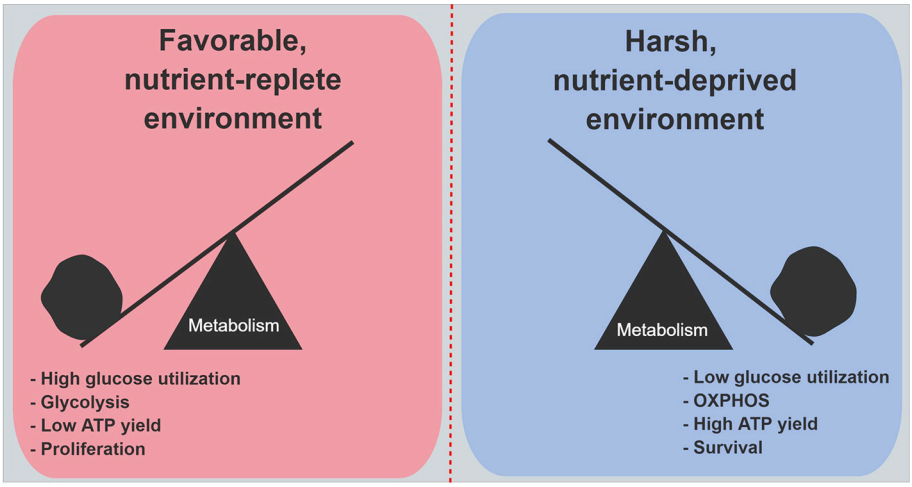

FIGURE 2 | Metabolic features in PDA cells under nutrient abundance and deprivation. Under nutrient abundance, PDA cells have a proliferative phenotype and macromolecular synthesis is prioritized over ATP generation. Under nutrient deprivation, PDA cells have a survival phenotype, and nutrient conservation with maximal ATP generation are prioritized. OXPHOS, oxidative phosphorylation.

cellular functions. The regeneration of NAD^+ as an upstream substrate of NADH production is, therefore, an absolute requirement PDA cell survival, particularly when mitochondrial demands escalate. Tryptophan is the principal source of NAD^+ production through canonical biochemical pathways (77). However, PDA cells show increased reliance on a separate NAD^+ salvage pathway. In the cancer-associated salvage pathway, nicotinamide phosphoribosyltransferase (NAMPT) is the rate-limiting step in the production of the NAD^+ precursor molecule nicotinamide mononucleotide (NMN). NAMPT expression was found to be elevated in PDA cell lines and tissues (78), and its expression was inversely linked to miR-206 activity (78). Based on these findings, NAMPT is recognized as another promising metabolic target against PDA. Inhibitors like FK866 and STF-118804 reduce NAD^+ levels, glycolytic activity, and mitochondrial function. Importantly, these drugs reduced PDA growth both *in vitro* and *in vivo* (78–80).

EXTRINSIC NUTRIENT ACQUISITION MECHANISMS

When glucose is scarce, amino acids are able to fuel the tricarboxylic acid cycle through various anaplerotic reactions that involve the conversion of aspartate to oxaloacetate (aspartate transaminase), glutamate to α-ketoglutarate (glutamate dehydrogenase), or alanine to pyruvate (alanine transaminase). Biologic processes exploited by PDA cells to extract these anaplerotic substrates from the microenvironment represent additional metabolic dependencies (81), and consequently are also metabolic vulnerabilities and therapeutic targets in the context of an austere PDA microenvironment.

Macropinocytosis

As with so many other adaptive responses used by PDA cells in the context of severe stress, macropinocytosis is enhanced by oncogenic KRAS (35, 82). In this cellular process, the plasma membrane envelops ambient polypeptides, such as albumin within a macropinosome. Like autophagy, the protein containing vesicle fuses with lysosomes, and proteins are proteolyzed into constituent amino acids (83). Glutamine is the most abundant amino acid released through this process. As a result of macropinocytosis, PDA cells are able to sustain the tricarboxylic acid cycle in the absence of glucose or free glutamine. Targeted inhibition of macropinocytosis with 5-(*N*-ethyl-*N*-isopropyl)amiloride (EIPA) in tissue culture models impaired PDA growth (35). *In vitro* studies revealed that PDA cells experienced sustained viability in the absence of essential amino acids, as long as albumin was present in the media (84). When resected PDA tissues were incubated with tetramethylrhodamine-conjugated dextran (TMR-dextran) for detection purposes, macropinosomes were clearly visualized by immunofluorescence microscopy (84).

Pancreatic Stellate-Derived Alanine

While PDA stroma has relatively low levels of free nutrients, the stroma is, in fact, replete with non-neoplastic cell types that are potential fuel sources. Pancreatic stellate cells appear important to PDA cells toward this end. These cells are myofibroblasts that generate the extracellular matrix in the exocrine pancreas and provide a scaffold for desmoplasia in PDA. Studies indicate that pancreatic stellate cells produce alanine by autophagy. Interestingly, PDA cells appear to stimulate this process, possibly through paracrine signaling, although the inducing factor remains unknown. Free alanine excreted by pancreatic stellate cells is imported into PDA cells and converted into pyruvate by alanine transaminase. Alanine anaplerosis than supplies the

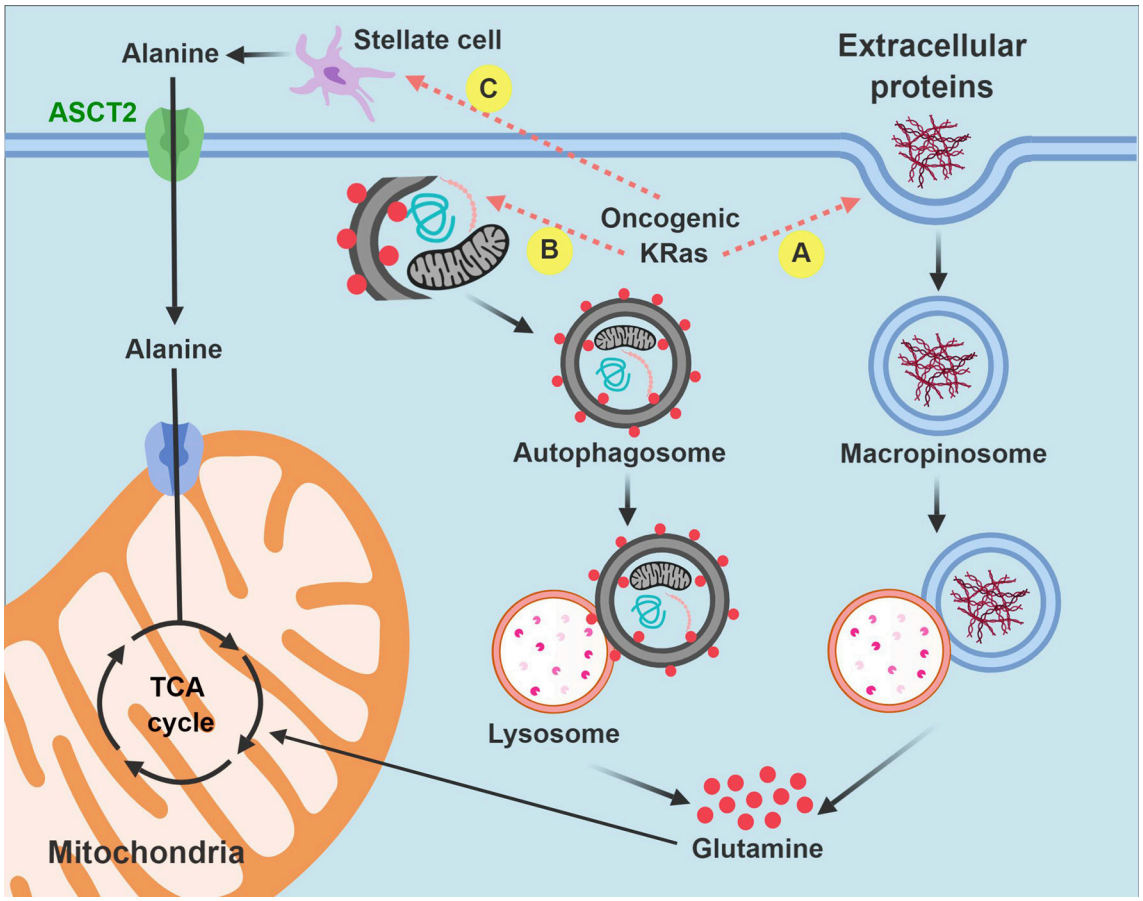

FIGURE 3 | Intrinsic and extrinsic nutrient acquisition pathways in PDA cells. PDA cells hijack stromal elements to fuel the tricarboxylic acid (anaplerosis) and other biochemical processes when nutrients are limited. Carbon is extracted by macropinocytosis **(A)** and autophagy **(B)** after auto-digestion by lysosomes. PDA cells also stimulate pancreatic stellate cells to produce and excrete free alanine **(C)**. Non-functional mitochondria are dark in the figure and are targeted for autophagy. Functional mitochondria are colored pink. TCA, tricarboxylic acid.

tricarboxylic acid cycle to sustain it under nutrient stress (85). The authors refer to the communication and interdependence between PDA cells and pancreatic stellate cells as an example of metabolic cross-talk. It is becoming increasingly clear that multi-lineage 3-D models to study metabolic cross-talk in PDA may yield new key insights into additional metabolic vulnerabilities.

In summary, macropinocytosis and metabolic cross-talk between PDA cells and pancreatic stellate cells offer two compelling examples of how PDA cells hijack existing biologic processes or resources from the microenvironment for their own survival advantage. By recruiting these pathways, PDA cells have discovered alternative strategies to fuel the tricarboxylic acid cycle and meet their bioenergetic when the pantry is otherwise bare (**Figure 3**).

Redox Homeostasis

PDA cells utilize a positive feedback loop between oncogenic KRAS signaling and reactive oxygen species (ROS) to sustain tumor growth (86, 87). This interplay seems to be especially important early in the adenoma-to-carcinoma progression sequence when ROS levels are manageable. ROS stimulates other pro-growth pathways early on in cancer progression as well, like PI3K signaling (88). The generation of genetic mutations by ROS may also play a tumor-promoting role in cancer development (89). The link between ROS and early cancer progression fits with the timing of KRAS mutations, which first appear in PanIN1 lesions. Along these lines, a reduction in mitochondrial ROS using a mitochondrial antioxidant, mitoQ, actually thwarted PanIN formation in an animal model (86).

However, as PDA precursor lesions advance, and invasive PDA matures, the stroma becomes more pronounced, conditions are more severe, and nutrients are in shorter supply. The nutrient-deprived stroma becomes more oxidative under these conditions. More specifically, low glucose conditions drive a surge in ROS levels (50, 90–92), principally because glucose is the main substrate for multiple NADPH-generating pathways. The pentose phosphate pathway and serine biosynthesis with one-carbon metabolism are perhaps the best-studied examples (90). Chemotherapy adds to ROS levels in the PDA microenvironment, which further compounds the oxidative

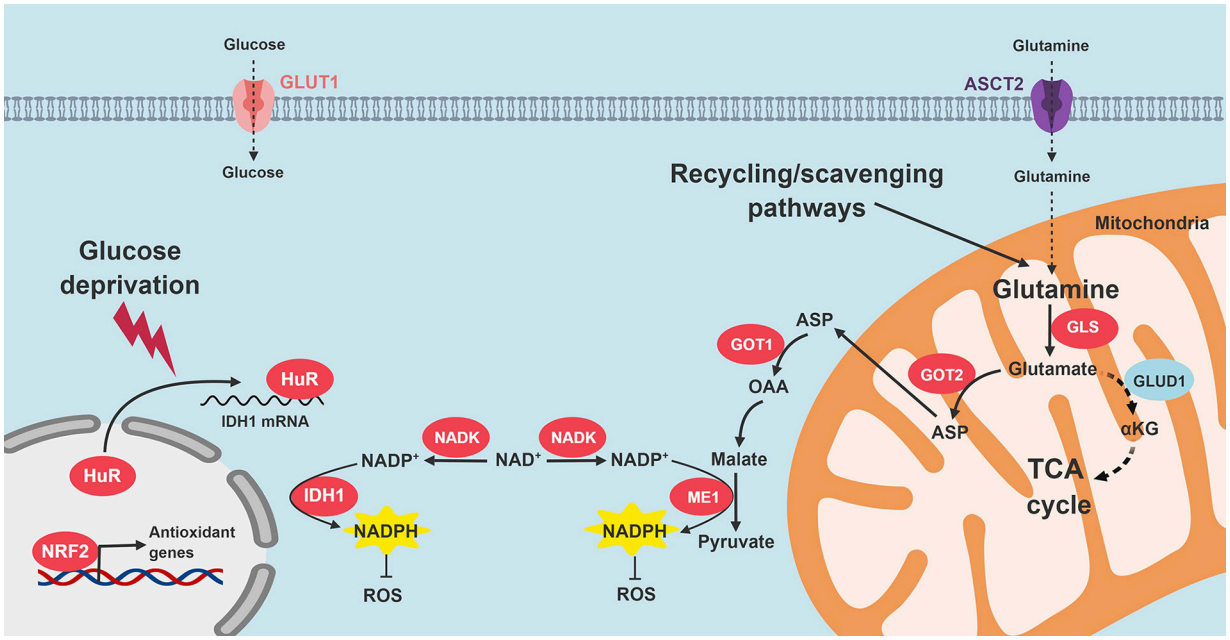

FIGURE 4 | Signaling pathways that restore redox homeostasis in PDA. Nutrient scarcity in the PDA microenvironment augments oxidative stress. Multiple adaptive strategies are recruited by PDA cells. KRAS signaling promotes NADPH production through glutamine catabolism, followed by ME1 activity. In addition, NRF2 and NADK are upregulated. HuR cytoplasmic translocation stabilizes IDH to enhance reductive power. GLS, glutaminase; GOT, aspartate transaminase; ME1, malic enzyme 1; IDH1, isocitrate dehydrogenase 1; TCA, tricarboxylic acid; ROS, reactive oxygen species; NADK, NAD^+ kinase.

TABLE 1 | Metabolic dependencies in PDA.

Event	Mediated by	References
MITOCHONDRIAL METABOLISM		
Increased oxidative phosphorylation	Down regulation of Drp1	(61)
	HuR	(50)
Increased biogenesis	HuR	Unpublished
NUTRIENT ACQUISITION		
Autophagy	Oncogenic KRAS	(74)
NAD^+ salvage pathway	miR-206	(78, 79)
Macropinocytosis	Oncogenic KRAS	(35)
Increased alanine uptake	Oncogenic KRAS	(85)
REDOX HOMEOSTASIS		
Upregulation of ME1	Oncogenic KRAS	(57)
Upregulation of NRF2	Oncogenic KRAS	(97)
Upregulation of IDH1	HuR	(50)

perils routinely faced by these malignant cells (93). Thus, as the dangers of ROS mount, adverse consequences and toxicities associated with ROS start to outstrip any pro-survival benefits favoring tumor growth. Enhanced antioxidant defense mechanisms become paramount to PDA cells for survival (94).

KRAS-driven pancreatic cancer cells bypass the oxidative phase of the pentose phosphate pathway (29). Therefore, alternative NADPH-generating pathways are likely to be important for maintenance of cellular reductive power. There are 13 different metabolic enzymes known to directly interconvert $NADP^+$ to NADPH, and augment the basic reducing currency in cells. These enzymes include: ME (1, 2, and 3), IDH (1 and 2), MTHFD (1 and 2), G6PD, PGD, NNT, GLUD (1 and 2), and ALDH3A1. Reducing equivalents from NADPH maintain glutathione in its reduced form. Glutathione and NADPH collaborate to biochemically prime the remainder of the antioxidant defense system, which consists of roughly 40 enzymes including superoxide dismutases, catalases, glutathione peroxidases, thioredoxins, peroxiredoxins, and glutaredoxins (95).

Son and colleagues demonstrate that malic enzyme 1 (ME1) plays an especially key role in augmenting NADPH levels in PDA. In this non-canonical NADPH biosynthesis pathway, glutamine is converted to glutamate by GLS1 in the mitochondria. Glutamate is generated and transports out of the mitochondria into the cytosol through the malate-aspartate shuttle, where it is converted to cytosolic oxaloacetate (OAA). Mitochondrial and cytosolic aspartate transaminase (GOT2 and GOT1, respectively) are required for this sequence (57). After additional oxidative reactions in the cytosol, ME1 finally yields NADPH. As seen before, oncogenic KRAS appears to influence this adaptive PDA redox program. The authors, and others identified GOT1 and GOT2 as promising therapeutic targets based on these biologic insights (57, 96).

Oncogenic KRAS also induces the transcription of the NRF2 transcription factor (97). NRF2 positively regulates antioxidant defense elements, such as genes that drive glutathione synthesis, glutathione peroxidase, glutathione reductase, glutathione transferases, thioredoxins, and several NADPH-generating enzymes (G6PD, GPD, IDH1, and ME1) (98, 99). Additionally,

TABLE 2 | Clinical trials targeting key steps of PDA metabolism.

Target	Agent	Phase and status	NCT no.	References
MITOCHONDRIAL OXPHOS				
ETC	Metformin + gemcitabine + ertotinib	II; Completed	NCT01210911	(63)
	Metformin + paclitaxel	II; Completed	NCT01971034	(103)
	Metformin + gemcitabine/nab-paclitaxel	I; Recruiting	NCT02336087	
	Metformin + mFOLFIRINOX	II; Active	NCT01666730	
	Metformin + rapamycin	Ib; Active	NCT02048384	
	Metformin + radiosurgery	I; Active	NCT02153450	
TCA cycle	CPI-613	I; Completed	NCT01839981	
	CPI-613 + mFOLFIRINOX	I; Active	NCT01835041	(67)
	CPI-613 + gemcitabine/nab-paclitaxel	I; Active	NCT03435289	
NUTRIENT ACQUISITION				
Autophagy	HCQ	II; Completed	NCT01273805	(104)
	HCQ + gemcitabine	I/II; Active	NCT01128296	
	HCQ + gemcitabine + abraxane	I/II; Active	NCT01506973	
	CQ + gemcitabine	I; Completed	NCT01777477	(105, 106)
REDOX HOMEOSTASIS				
Glutaminase	CB-839	I; Active	NCT02071862	

HCQ, hydroxychloroquine; CQ, chloroquine; mFOLFIRINOX, modified FOLFIRINOX.

NAD^+ kinase (NADK) was recently identified as an additional component of PDA antioxidant defense. The enzyme converts NAD^+ to $NADP^+$, and is upregulated in PDA cells, as compared to normal cells. Silencing NADK increased ROS levels, and also diminished PDA growth in cell lines and *in vivo* (100).

We recently reported that HuR enhances antioxidant defense through post-transcriptional stabilization of the NADPH-generating enzyme, IDH1 (50). When PDA cells are exposed to an acute oxidative stress, HuR rapidly binds to the 3′-untranslated regions of IDH1 transcripts, stabilizes the transcript, increases IDH1 protein expression and activity, augments NADPH levels, and reduces intracellular ROS (50). The whole process is executed in just a few hours, which enables PDA to respond to acute oxidative stress in short order. Genetic modulation of IDH1 with siRNAs reduced PDA survival under glucose withdrawal more than any other NADPH-generating enzyme (Vaziri-Gohar, unpublished). While IDH1 mutations are oncogenic in other cancer types, our work highlights the importance of wild-type IDH1 in PDA pathogenesis. Moreover, while IDH1 is cytosolic, enhanced reductive power related to this enzyme also appears to impact redox levels in the mitochondria [Vaziri-Gohar, unpublished, and also (101, 102)]. **Figure 4** summarizes PDA adaptations that restore redox balance.

CONCLUSION AND SUMMARY OF METABOLIC VULNERABILITIES IN PDA

While the molecular determinants of aggressive PDA biology have not been definitively determined, it seems plausible that the adaptive mechanisms used by PDA cells to overcome the harsh metabolic milieu also contribute to the aggressive and chemotherapy-resistant phenotype responsible for poor patient outcomes. PDA's transformation toward a seemingly invincible state is akin to a runner training at high altitudes or a cactus surviving in a desert. These performance enhanced cells simply cannot be eradicated by conventional DNA targeting agents (i.e., chemotherapy) currently in use. A better understanding of the metabolic dependencies needed to survive harsh conditions will likely uncover metabolic vulnerabilities, and these alternative therapeutic strategies are not likely to be as critical to well-perfused normal cells.

In this review, we highlighted mutant KRAS as an important player in adaptive metabolic reprogramming to the PDA microenvironment. However, new targets or strategies have also come to light, including NRF2, HuR, mitochondrial biology, non-canonical nutrient acquisition processes (autophagy, macropinocytosis, alanine uptake), and antioxidant defense (NADPH-generating enzymes like ME1 and IDH1) (**Table 1**). There is a growing interest in exploiting new insights into cancer metabolism with good reason. A number of clinical trials targeting metabolic pathways in patients with PDA have been completed or are underway (**Table 2**).

AUTHOR CONTRIBUTIONS

AV-G and JW wrote the manuscript and prepared the figures. MZ and JB critically reviewed the manuscript. AV-G and JW approved the final manuscript.

FUNDING

This work was supported by American Cancer Society Mentored Research Scholar Grant-14-019-01-CDD (JW), R01 CA212600 (JB and JW), and 1R37CA227865 (JW and JB).

REFERENCES

1. Siegel RL, Miller KD, Jemal A. Cancer statistics, 2018. *CA Cancer J Clin.* (2018) 68:7–30. doi: 10.3322/caac.21442
2. Rahib L, Smith BD, Aizenberg R, Rosenzweig AB, Fleshman JM, Matrisian LM. Projecting cancer incidence and deaths to 2030: the unexpected burden of thyroid, liver, and pancreas cancers in the United States. *Cancer Res.* (2014) 74:2913–21. doi: 10.1158/0008-5472.CAN-14-0155
3. Morgan G, Ward R, Barton M. The contribution of cytotoxic chemotherapy to 5-year survival in adult malignancies. *Clin Oncol (R Coll Radiol).* (2004) 16:549–60. doi: 10.1016/j.clon.2004.06.007
4. Van Cutsem E, Verslype C, Grusenmeyer PA. Lessons learned in the management of advanced pancreatic cancer. *J Clin Oncol.* (2007) 25:1949–52. doi: 10.1200/JCO.2006.09.4664
5. Ren C, Chen H, Han C, Jin G, Wang D, Tang D. Detection and molecular analysis of circulating tumor cells for early diagnosis of pancreatic cancer. *Med Hypotheses* (2013) 80:833–6. doi: 10.1016/j.mehy.2013.03.027
6. Hidalgo M. Pancreatic cancer. *N Engl J Med.* (2010) 362:1605–17. doi: 10.1056/NEJMra0901557
7. Vincent A, Herman J, Schulick R, Hruban RH, Goggins M. Pancreatic cancer. *Lancet* (2011) 378:607–20. doi: 10.1016/S0140-6736(10)62307-0
8. Li D, Xie K, Wolff R, Abbruzzese JL. Pancreatic cancer. *Lancet* (2004) 363:1049–57. doi: 10.1016/S0140-6736(04)15841-8
9. Von Hoff DD, Ervin T, Arena FP, Chiorean EG, Infante J, Moore M, et al. Increased survival in pancreatic cancer with nab-paclitaxel plus gemcitabine. *N Engl J Med.* (2013) 369:1691–703. doi: 10.1056/NEJMoa1304369
10. Yachida S, Iacobuzio-Donahue CA. Evolution and dynamics of pancreatic cancer progression. *Oncogene* (2013) 32:5253–60. doi: 10.1038/onc.2013.29
11. Roberts NJ, Norris AL, Petersen GM, Bondy ML, Brand R, Gallinger S, et al. Whole genome sequencing defines the genetic heterogeneity of familial pancreatic cancer. *Cancer Discov.* (2016) 6:166–75. doi: 10.1158/2159-8290.CD-15-0402
12. Hahn WC, Counter CM, Lundberg AS, Beijersbergen RL, Brooks MW, Weinberg RA. Creation of human tumour cells with defined genetic elements. *Nature* (1999) 400:464–8. doi: 10.1038/22780
13. Bardeesy N, Aguirre AJ, Chu GC, Cheng KH, Lopez LV, Hezel AF, et al. Both p16(Ink4a) and the p19(Arf)-p53 pathway constrain progression of pancreatic adenocarcinoma in the mouse. *Proc Natl Acad Sci USA.* (2006) 103:5947–52. doi: 10.1073/pnas.0601273103
14. Olivier M, Eeles R, Hollstein M, Khan MA, Harris CC, Hainaut P. The IARC TP53 database: new online mutation analysis and recommendations to users. *Hum Mutat.* (2002) 19:607–14. doi: 10.1002/humu.10081
15. Tuveson DA, Hingorani SR. Ductal pancreatic cancer in humans and mice. *Cold Spring Harb Symp Quant Biol.* (2005) 70:65–72. doi: 10.1101/sqb.2005.70.040
16. Hingorani SR, Wang L, Multani AS, Combs C, Deramaudt TB, Hruban RH, et al. Trp53R172H and KrasG12D cooperate to promote chromosomal instability and widely metastatic pancreatic ductal adenocarcinoma in mice. *Cancer Cell* (2005) 7:469–83. doi: 10.1016/j.ccr.2005.04.023
17. Jaffee EM, Hruban RH, Canto M, Kern SE. Focus on pancreas cancer. *Cancer Cell* (2002) 2:25–8. doi: 10.1016/S1535-6108(02)00093-4
18. Winter JM, Maitra A, Yeo CJ. Genetics and pathology of pancreatic cancer. *HPB* (2006) 8:324–36. doi: 10.1080/13651820600804203
19. Yabar CS, Winter JM. Pancreatic cancer: a review. *Gastroenterol Clin North Am.* (2016) 45:429–45. doi: 10.1016/j.gtc.2016.04.003
20. Hezel AF, Kimmelman AC, Stanger BZ, Bardeesy N, Depinho RA. Genetics and biology of pancreatic ductal adenocarcinoma. *Genes Dev.* (2006) 20:1218–49. doi: 10.1101/gad.1415606
21. Murthy D, Attri KS, Singh PK. Phosphoinositide 3-kinase signaling pathway in pancreatic ductal adenocarcinoma progression, pathogenesis, and therapeutics. *Front Physiol.* (2018) 9:335. doi: 10.3389/fphys.2018.00335
22. Ndlovu R, Deng LC, Wu J, Li XK, Zhang JS. Fibroblast growth factor 10 in pancreas development and pancreatic cancer. *Front Genet.* (2018) 9:482. doi: 10.3389/fgene.2018.00482
23. Sato N, Goggins M. The role of epigenetic alterations in pancreatic cancer. *J Hepatobiliary Pancreat Surg.* (2006) 13:286–95. doi: 10.1007/s00534-005-1057-1
24. Feig C, Gopinathan A, Neesse A, Chan DS, Cook N, Tuveson DA. The pancreas cancer microenvironment. *Clin Cancer Res.* (2012) 18:4266–76. doi: 10.1158/1078-0432.CCR-11-3114
25. Erkan M, Reiser-Erkan C, Michalski CW, Kleeff J. Tumor microenvironment and progression of pancreatic cancer. *Exp Oncol.* (2010) 32:128–31.
26. Provenzano PP, Cuevas C, Chang AE, Goel VK, Von Hoff DD, Hingorani SR. Enzymatic targeting of the stroma ablates physical barriers to treatment of pancreatic ductal adenocarcinoma. *Cancer Cell* (2012) 21:418–29. doi: 10.1016/j.ccr.2012.01.007
27. Xie K, Huang S. Regulation of cancer metastasis by stress pathways. *Clin Exp Metastasis* (2003) 20:31–43. doi: 10.1023/A:1022590402748
28. Sutherland RM. Cell and environment interactions in tumor microregions: the multicell spheroid model. *Science* (1988) 240:177–84.
29. Ying H, Kimmelman AC, Lyssiotis CA, Hua S, Chu GC, Fletcher-Sananikone E, et al. Oncogenic kras maintains pancreatic tumors through regulation of anabolic glucose metabolism. *Cell* (2012) 149:656–70. doi: 10.1016/j.cell.2012.01.058
30. Vander Heiden MG, Cantley LC, Thompson CB. Understanding the Warburg effect: the metabolic requirements of cell proliferation. *Science* (2009) 324:1029–33. doi: 10.1126/science.1160809
31. Warburg O, Wind F, Negelein E. The metabolism of tumors in the body. *J Gen Physiol.* (1927) 8:519–30.
32. Guillaumond F, Leca J, Olivares O, Lavaut MN, Vidal N, Berthezène P, et al. Strengthened glycolysis under hypoxia supports tumor symbiosis and hexosamine biosynthesis in pancreatic adenocarcinoma. *Proc Natl Acad Sci USA.* (2013) 110:3919–24. doi: 10.1073/pnas.1219555110
33. Mikuriya K, Kuramitsu Y, Ryozawa S, Fujimoto M, Mori S, Oka M, et al. Expression of glycolytic enzymes is increased in pancreatic cancerous tissues as evidenced by proteomic profiling by two-dimensional electrophoresis and liquid chromatography-mass spectrometry/mass spectrometry. *Int J Oncol.* (2007) 30:849–55. doi: 10.3892/ijo.30.4.849
34. Akakura N, Kobayashi M, Horiuchi I, Suzuki A, Wang J, Chen J, et al. Constitutive expression of hypoxia-inducible factor-1alpha renders pancreatic cancer cells resistant to apoptosis induced by hypoxia and nutrient deprivation. *Cancer Res.* (2001) 61:6548–54.
35. Commisso C, Davidson SM, Soydaner-Azeloglu RG, Parker SJ, Kamphorst JJ, Hackett S, et al. Macropinocytosis of protein is an amino acid supply route in Ras-transformed cells. *Nature* (2013) 497:633–7. doi: 10.1038/nature12138
36. Shi M, Cui J, Du J, Wei D, Jia Z, Zhang J, et al. A novel KLF4/LDHA signaling pathway regulates aerobic glycolysis in and progression of pancreatic cancer. *Clin Cancer Res.* (2014) 20:4370–80. doi: 10.1158/1078-0432.CCR-14-0186
37. Payen VL, Porporato PE, Baselet B, Sonveaux P. Metabolic changes associated with tumor metastasis, part 1: tumor pH, glycolysis and the pentose phosphate pathway. *Cell Mol Life Sci.* (2016) 73:1333–48. doi: 10.1007/s00018-015-2098-5
38. Hume DA, Weidemann MJ. Role and regulation of glucose metabolism in proliferating cells. *J Natl Cancer Inst.* (1979) 62:3–8.
39. Lunt SY, Vander Heiden MG. Aerobic glycolysis: meeting the metabolic requirements of cell proliferation. *Annu Rev Cell Dev Biol.* (2011) 27:441–64. doi: 10.1146/annurev-cellbio-092910-154237
40. Barthel A, Okino ST, Liao J, Nakatani K, Li J, Whitlock JP, et al. Regulation of GLUT1 gene transcription by the serine/threonine kinase Akt1. *J Biol Chem.* (1999) 274:20281–6.
41. Fan J, Kamphorst JJ, Mathew R, Chung MK, White E, Shlomi T, et al. Glutamine-driven oxidative phosphorylation is a major ATP source in transformed mammalian cells in both normoxia and hypoxia. *Mol Syst Biol.* (2013) 9:712. doi: 10.1038/msb.2013.65
42. Ju HQ, Ying H, Tian T, Ling J, Fu J, Lu Y, et al. Mutant Kras- and p16-regulated NOX4 activation overcomes metabolic checkpoints in development of pancreatic ductal adenocarcinoma. *Nat Commun.* (2017) 8:14437. doi: 10.1038/ncomms14437
43. Chaika NV, Gebregiworgis T, Lewallen ME, Purohit V, Radhakrishnan P, Liu X, et al. MUC1 mucin stabilizes and activates hypoxia-inducible factor 1 alpha to regulate metabolism in pancreatic cancer. *Proc Natl Acad Sci USA.* (2012) 109:13787–92. doi: 10.1073/pnas.1203339109
44. Brahimi-Horn MC, Chiche J, Pouysségur J. Hypoxia signalling controls metabolic demand. *Curr Opin Cell Biol.* (2007) 19:223–9. doi: 10.1016/j.ceb.2007.02.003

45. Kim JW, Tchernyshyov I, Semenza GL, Dang CV. HIF-1-mediated expression of pyruvate dehydrogenase kinase: a metabolic switch required for cellular adaptation to hypoxia. *Cell Metab.* (2006) 3:177–85. doi: 10.1016/j.cmet.2006.02.002
46. DeBerardinis RJ, Lum JJ, Hatzivassiliou G, Thompson CB. The biology of cancer: metabolic reprogramming fuels cell growth and proliferation. *Cell Metab.* (2008) 7:11–20. doi: 10.1016/j.cmet.2007.10.002
47. Jose C, Bellance N, Rossignol R. Choosing between glycolysis and oxidative phosphorylation: a tumor's dilemma? *Biochim Biophys Acta* (2011) 1807:552–61. doi: 10.1016/j.bbabio.2010.10.012
48. Zheng J. Energy metabolism of cancer: glycolysis versus oxidative phosphorylation (Review). *Oncol Lett.* (2012) 4:1151–7. doi: 10.3892/ol.2012.928
49. Rossignol R, Gilkerson R, Aggeler R, Yamagata K, Remington SJ, Capaldi RA. Energy substrate modulates mitochondrial structure and oxidative capacity in cancer cells. *Cancer Res.* (2004) 64:985–93. doi: 10.1158/0008-5472.CAN-03-1101
50. Zarei M, Lal S, Parker SJ, Nevler A, Vaziri-Gohar A, Dukleska K, et al. Posttranscriptional upregulation of IDH1 by HuR establishes a powerful survival phenotype in pancreatic cancer cells. *Cancer Res.* (2017) 77:4460–71. doi: 10.1158/0008-5472.CAN-17-0015
51. Birsoy K, Possemato R, Lorbeer FK, Bayraktar EC, Thiru P, Yucel B, et al. Metabolic determinants of cancer cell sensitivity to glucose limitation and biguanides. *Nature* (2014) 508:108–12. doi: 10.1038/nature13110
52. McKeown SR. Defining normoxia, physoxia and hypoxia in tumours-implications for treatment response. *Br J Radiol.* (2014) 87:20130676. doi: 10.1259/bjr.20130676
53. Rumsey WL, Schlosser C, Nuutinen EM, Robiolio M, Wilson DF. Cellular energetics and the oxygen dependence of respiration in cardiac myocytes isolated from adult rat. *J Biol Chem.* (1990) 265:15392–402.
54. Weinberg SE, Chandel NS. Targeting mitochondria metabolism for cancer therapy. *Nat Chem Biol.* (2015) 11:9–15. doi: 10.1038/nchembio.1712
55. Schroeder T, Yuan H, Viglianti BL, Peltz C, Asopa S, Vujaskovic Z, et al. Spatial heterogeneity and oxygen dependence of glucose consumption in R3230Ac and fibrosarcomas of the Fischer 344 rat. *Cancer Res.* (2005) 65:5163–71. doi: 10.1158/0008-5472.CAN-04-3900
56. Burkhart RA, Pineda DM, Chand SN, Romeo C, Londin ER, Karoly ED, et al. HuR is a post-transcriptional regulator of core metabolic enzymes in pancreatic cancer. *RNA Biol.* (2013) 10:1312–23. doi: 10.4161/rna.25274
57. Son J, Lyssiotis CA, Ying H, Wang X, Hua S, Ligorio M, et al. Glutamine supports pancreatic cancer growth through a KRAS-regulated metabolic pathway. *Nature* (2013) 496:101–5. doi: 10.1038/nature12040
58. Gao AW, Cantó C, Houtkooper RH. Mitochondrial response to nutrient availability and its role in metabolic disease. *EMBO Mol Med.* (2014) 6:580–9. doi: 10.1002/emmm.201303782
59. Liesa M, Shirihai OS. Mitochondrial dynamics in the regulation of nutrient utilization and energy expenditure. *Cell Metab.* (2013) 17:491–506. doi: 10.1016/j.cmet.2013.03.002
60. Molina AJ, Wikstrom JD, Stiles L, Las G, Mohamed H, Elorza A, et al. Mitochondrial networking protects beta-cells from nutrient-induced apoptosis. *Diabetes* (2009) 58:2303–15. doi: 10.2337/db07-1781
61. Rambold AS, Kostelecky B, Elia N, Lippincott-Schwartz J. Tubular network formation protects mitochondria from autophagosomal degradation during nutrient starvation. *Proc Natl Acad Sci USA.* (2011) 108:10190–5. doi: 10.1073/pnas.1107402108
62. Li X, Li T, Liu Z, Gou S, Wang C. The effect of metformin on survival of patients with pancreatic cancer: a meta-analysis. *Sci Rep.* (2017) 7:5825. doi: 10.1038/s41598-017-06207-x
63. Kordes S, Pollak MN, Zwinderman AH, Mathot RA, Weterman MJ, Beeker A, et al. Metformin in patients with advanced pancreatic cancer: a double-blind, randomised, placebo-controlled phase 2 trial. *Lancet Oncol.* (2015) 16:839–47. doi: 10.1016/S1470-2045(15)00027-3
64. Reni M, Dugnani E, Cereda S, Belli C, Balzano G, Nicoletti R, et al. (Ir)relevance of metformin treatment in patients with metastatic pancreatic cancer: an open-label, randomized phase II trial. *Clin Cancer Res.* (2016) 22:1076–85. doi: 10.1158/1078-0432.CCR-15-1722
65. Lycan TW, Pardee TS, Petty WJ, Bonomi M, Alistar A, Lamar ZS, et al. A phase II clinical trial of CPI-613 in patients with relapsed or refractory small cell lung carcinoma. *PLoS ONE* (2016) 11:e0164244. doi: 10.1371/journal.pone.0164244
66. Egawa Y, Saigo C, Kito Y, Moriki T, Takeuchi T. Therapeutic potential of CPI-613 for targeting tumorous mitochondrial energy metabolism and inhibiting autophagy in clear cell sarcoma. *PLoS ONE* (2018) 13:e0198940. doi: 10.1371/journal.pone.0198940
67. Alistar A, Morris BB, Desnoyer R, Klepin HD, Hosseinzadeh K, Clark C, et al. Safety and tolerability of the first-in-class agent CPI-613 in combination with modified FOLFIRINOX in patients with metastatic pancreatic cancer: a single-centre, open-label, dose-escalation, phase 1 trial. *Lancet Oncol.* (2017) 18:770–8. doi: 10.1016/S1470-2045(17)30314-5
68. Conroy T, Desseigne F, Ychou M, Bouché O, Guimbaud R, Bécouarn Y, et al. FOLFIRINOX versus gemcitabine for metastatic pancreatic cancer. *N Engl J Med.* (2011) 364:1817–25. doi: 10.1056/NEJMoa1011923
69. He C, Klionsky DJ. Regulation mechanisms and signaling pathways of autophagy. *Annu Rev Genet.* (2009) 43:67–93. doi: 10.1146/annurev-genet-102808-114910
70. Mizushima N, Yoshimori T, Levine B. Methods in mammalian autophagy research. *Cell* (2010) 140:313–26. doi: 10.1016/j.cell.2010.01.028
71. Yang Z, Klionsky DJ. Eaten alive: a history of macroautophagy. *Nat Cell Biol.* (2010) 12:814–22. doi: 10.1038/ncb0910-814
72. White E. Deconvoluting the context-dependent role for autophagy in cancer. *Nat Rev Cancer* (2012) 12:401–10. doi: 10.1038/nrc3262
73. Gohar AV, Cao R, Jenkins P, Li W, Houston JP, Houston KD. Subcellular localization-dependent changes in EGFP fluorescence lifetime measured by time-resolved flow cytometry. *Biomed Opt Express.* (2013) 4:1390–400. doi: 10.1364/BOE.4.001390
74. Yang S, Wang X, Contino G, Liesa M, Sahin E, Ying H, et al. Pancreatic cancers require autophagy for tumor growth. *Genes Dev.* (2011) 25:717–29. doi: 10.1101/gad.2016111
75. Fujii S, Mitsunaga S, Yamazaki M, Hasebe T, Ishii G, Kojima M, et al. Autophagy is activated in pancreatic cancer cells and correlates with poor patient outcome. *Cancer Sci.* (2008) 99:1813–9. doi: 10.1111/j.1349-7006.2008.00893.x
76. Guo JY, Chen HY, Mathew R, Fan J, Strohecker AM, Karsli-Uzunbas G, et al. Activated Ras requires autophagy to maintain oxidative metabolism and tumorigenesis. *Genes Dev.* (2011) 25:460–70. doi: 10.1101/gad.2016311
77. Magni G, Amici A, Emanuelli M, Raffaelli N, Ruggieri S. Enzymology of NAD^+ synthesis. *Adv Enzymol Relat Areas Mol Biol.* (1999) 73:135–82, xi.
78. Ju HQ, Zhuang ZN, Li H, Tian T, Lu YX, Fan XQ, et al. Regulation of the Nampt-mediated NAD salvage pathway and its therapeutic implications in pancreatic cancer. *Cancer Lett.* (2016) 379:1–11. doi: 10.1016/j.canlet.2016.05.024
79. Chini CC, Guerrico AM, Nin V, Camacho-Pereira J, Escande C, Barbosa MT, et al. Targeting of NAD metabolism in pancreatic cancer cells: potential novel therapy for pancreatic tumors. *Clin Cancer Res.* (2014) 20:120–30. doi: 10.1158/1078-0432.CCR-13-0150
80. Espindola-Netto JM, Chini CCS, Tarragó M, Wang E, Dutta S, Pal K, et al. Preclinical efficacy of the novel competitive NAMPT inhibitor STF-118804 in pancreatic cancer. *Oncotarget* (2017) 8:85054–67. doi: 10.18632/oncotarget.18841
81. Sidaway P. Pancreatic cancer: pancreatic cancer cells digest extracellular protein. *Nat Rev Clin Oncol.* (2017) 14:138. doi: 10.1038/nrclinonc.2017.3
82. Perera RM, Bardeesy N. Pancreatic cancer metabolism: breaking it down to build it back up. *Cancer Discov.* (2015) 5:1247–61. doi: 10.1158/2159-8290.CD-15-0671
83. Bar-Sagi D, Feramisco JR. Induction of membrane ruffling and fluid-phase pinocytosis in quiescent fibroblasts by ras proteins. *Science* (1986) 233:1061–8.
84. Kamphorst JJ, Nofal M, Commisso C, Hackett SR, Lu W, Grabocka E, et al. Human pancreatic cancer tumors are nutrient poor and tumor cells actively scavenge extracellular protein. *Cancer Res.* (2015) 75:544–53. doi: 10.1158/0008-5472.CAN-14-2211
85. Sousa CM, Biancur DE, Wang X, Halbrook CJ, Sherman MH, Zhang L, et al. Pancreatic stellate cells support tumour metabolism through autophagic alanine secretion. *Nature* (2016) 536:479–83. doi: 10.1038/nature19084

86. Liou GY, Döppler H, DelGiorno KE, Zhang L, Leitges M, Crawford HC, et al. Mutant KRas-induced mitochondrial oxidative stress in acinar cells upregulates EGFR signaling to drive formation of pancreatic precancerous lesions. *Cell Rep.* (2016) 14:2325–36. doi: 10.1016/j.celrep.2016.02.029
87. Weinberg F, Hamanaka R, Wheaton WW, Weinberg S, Joseph J, Lopez M, et al. Mitochondrial metabolism and ROS generation are essential for Kras-mediated tumorigenicity. *Proc Natl Acad Sci USA*. (2010) 107:8788–93. doi: 10.1073/pnas.1003428107
88. Sullivan LB, Chandel NS. Mitochondrial reactive oxygen species and cancer. *Cancer Metab.* (2014) 2:17. doi: 10.1186/2049-3002-2-17
89. Feig DI, Reid TM, Loeb LA. Reactive oxygen species in tumorigenesis. *Cancer Res.* (1994) 54(7 Suppl.):1890s—4s.
90. Khramtsov VV, Gillies RJ. Janus-faced tumor microenvironment and redox. *Antioxid Redox Signal.* (2014) 21:723–9. doi: 10.1089/ars.2014.5864
91. Ahmad IM, Aykin-Burns N, Sim JE, Walsh SA, Higashikubo R, Buettner GR, et al. Mitochondrial O_2^{*}- and H_2O_2 mediate glucose deprivation-induced stress in human cancer cells. *J Biol Chem.* (2005) 280:4254–63. doi: 10.1074/jbc.M411662200
92. Chio IIC, Tuveson DA. ROS in cancer: the burning question. *Trends Mol Med.* (2017) 23:411–29. doi: 10.1016/j.molmed.2017.03.004
93. Sangeetha P, Das UN, Koratkar R, Suryaprabha P. Increase in free radical generation and lipid peroxidation following chemotherapy in patients with cancer. *Free Rad Biol Med.* (1990) 8:15–9.
94. Izuishi K, Kato K, Ogura T, Kinoshita T, Esumi H. Remarkable tolerance of tumor cells to nutrient deprivation: possible new biochemical target for cancer therapy. *Cancer Res.* (2000) 60:6201–7.
95. Policastro LL, Ibanez IL, Notcovich C, Duran HA, Podhajcer OL. The tumor microenvironment: characterization, redox considerations, and novel approaches for reactive oxygen species-targeted gene therapy. *Antioxid Redox Signal.* (2013) 19:854–95. doi: 10.1089/ars.2011.4367
96. Yang S, Hwang S, Kim M, Seo SB, Lee JH, Jeong SM. Mitochondrial glutamine metabolism via GOT2 supports pancreatic cancer growth through senescence inhibition. *Cell Death Dis.* (2018) 9:55. doi: 10.1038/s41419-017-0089-1
97. DeNicola GM, Karreth FA, Humpton TJ, Gopinathan A, Wei C, Frese K, et al. Oncogene-induced Nrf2 transcription promotes ROS detoxification and tumorigenesis. *Nature* (2011) 475:106–9. doi: 10.1038/nature10189
98. Hayes JD, Dinkova-Kostova AT. The Nrf2 regulatory network provides an interface between redox and intermediary metabolism. *Trends Biochem Sci.* (2014) 39:199–218. doi: 10.1016/j.tibs.2014.02.002
99. Tonelli C, Chio IIC, Tuveson DA. Transcriptional regulation by Nrf2. *Antioxid Redox Signal.* (2017) 29:1727–45. doi: 10.1089/ars.2017.7342
100. Tsang YH, Dogruluk T, Tedeschi PM, Wardwell-Ozgo J, Lu H, Espitia M, et al. Functional annotation of rare gene aberration drivers of pancreatic cancer. *Nat Commun.* (2016) 7:10500. doi: 10.1038/ncomms10500
101. Sena LA, Chandel NS. Physiological roles of mitochondrial reactive oxygen species. *Mol Cell.* (2012) 48:158–67. doi: 10.1016/j.molcel.2012.09.025
102. Ciccarese F, Ciminale V. Escaping death: mitochondrial redox homeostasis in cancer cells. *Front Oncol.* (2017) 7:117. doi: 10.3389/fonc.2017.00117
103. Braghiroli MI, de Celis Ferrari AC, Pfiffer TE, Alex AK, Nebuloni D, Carneiro AS, et al. Phase II trial of metformin and paclitaxel for patients with gemcitabine-refractory advanced adenocarcinoma of the pancreas. *Ecancermedicalscience* (2015) 9:563. doi: 10.3332/ecancer.2015.563
104. Wolpin BM, Rubinson DA, Wang X, Chan JA, Cleary JM, Enzinger PC, et al. Phase II and pharmacodynamic study of autophagy inhibition using hydroxychloroquine in patients with metastatic pancreatic adenocarcinoma. *Oncologist* (2014) 19:637–8. doi: 10.1634/theoncologist.2014-0086
105. Balic A, Sørensen MD, Trabulo SM, Sainz B, Cioffi M, Vieira CR, et al. Chloroquine targets pancreatic cancer stem cells via inhibition of CXCR4 and hedgehog signaling. *Mol Cancer Ther.* (2014) 13:1758–71. doi: 10.1158/1535-7163.MCT-13-0948
106. Samaras P, Tusup M, Nguyen-Kim TDL, Seifert B, Bachmann H, von Moos R, et al. Phase I study of a chloroquine-gemcitabine combination in patients with metastatic or unresectable pancreatic cancer. *Cancer Chemother Pharmacol.* (2017) 80:1005–12. doi: 10.1007/s00280-0173446-y

Conflict of Interest Statement: The authors declare that the research was conducted in the absence of any commercial or financial relationships that could be construed as a potential conflict of interest.

frontiers in Oncology

CORRECTION
published: 31 January 2019
doi: 10.3389/fonc.2018.00672

Corrigendum: Metabolic Dependencies in Pancreatic Cancer

Ali Vaziri-Gohar[1], *Mahsa Zarei*[2,3], *Jonathan R. Brody*[4] *and Jordan M. Winter*[1,5]*

[1] School of Medicine, Case Western Reserve University, Cleveland, OH, United States, [2] Department of Veterinary Physiology and Pharmacology, Texas A&M University, College Station, TX, United States, [3] Department of Medicine, Brigham and Women's Hospital and Harvard Medical School, Boston, MA, United States, [4] Division of Surgical Research, Department of Surgery, Jefferson Pancreas, Biliary and Related Cancer Center, Jefferson Medical College, Thomas Jefferson University, Philadelphia, PA, United States, [5] Department of Surgery and Division of Surgical Oncology, University Hospitals Cleveland Medical Center, Cleveland, OH, United States

Keywords: pancreatic cancer, metabolism, redox homeostasis, metabolic dependencies, targeting metabolism

A Corrigendum on

Metabolic Dependencies in Pancreatic Cancer
by Vaziri-Gohar, A., Zarei, M., Brody, J. R., and Winter, J. M. (2018). Front. Oncol. 8:617. doi: 10.3389/fonc.2018.00617

In the original article, all references for in **Tables 1**, **2** were incorrectly listed. The corrected references for both **Table 1** and **Table 2** have been corrected and provided below.

In the original article, references in **Table 2** were not provided in the reference list. The references have now been inserted.

The authors apologize for these errors and state that they do not change the scientific conclusions of the article in any way. The original article has been updated.

OPEN ACCESS

Approved by:
Frontiers in Oncology Editorial Office, Frontiers Media SA, Switzerland

***Correspondence:**
Jordan M. Winter
jordan.winter@UHhospitals.org

Specialty section:
This article was submitted to Molecular and Cellular Oncology, a section of the journal Frontiers in Oncology

Received: *19 December 2018*
Accepted: *20 December 2018*
Published: *31 January 2019*

Citation:
Vaziri-Gohar A, Zarei M, Brody JR and Winter JM (2019) Corrigendum: Metabolic Dependencies in Pancreatic Cancer. Front. Oncol. 8:672. doi: 10.3389/fonc.2018.00672

TABLE 1 | Metabolic dependencies in PDA.

Event	Mediated by	References
MITOCHONDRIAL METABOLISM		
Increased oxidative phosphorylation	Down regulation of Drp1	(61)
	HuR	(50)
Increased biogenesis	HuR	Unpublished
NUTRIENT ACQUISITION		
Autophagy	Oncogenic KRAS	(74)
NAD^+ salvage pathway	miR-206	(78, 79)
Macropinocytosis	Oncogenic KRAS	(35)
Increased alanine uptake	Oncogenic KRAS	(85)
REDOX HOMEOSTASIS		
Upregulation of ME1	Oncogenic KRAS	(57)
Upregulation of NRF2	Oncogenic KRAS	(97)
Upregulation of IDH1	HuR	(50)

TABLE 2 | Clinical trials targeting key steps of PDA metabolism.

Target	Agent	Phase and status	NCT No.	References
MITOCHONDRIAL OXPHOS				
ETC	Metformin + gemcitabine + ertotinib	II; Completed	NCT01210911	(63)
	Metformin + paclitaxel	II; Completed	NCT01971034	(103)
	Metformin + gemcitabine/nab-paclitaxel	I; Recruiting	NCT02336087	
	Metformin + mFOLFIRINOX	II; Active	NCT01666730	
	Metformin + rapamycin	Ib; Active	NCT02048384	
	Metformin + radiosurgery	I; Active	NCT02153450	
TCA cycle	CPI-613	I; Completed	NCT01839981	
	CPI-613 + mFOLFIRINOX	I; Active	NCT01835041	(67)
	CPI-613 + gemcitabine/nab-paclitaxel	I; Active	NCT03435289	
NUTRIENT ACQUISITION				
Autophagy	HCQ	II; Completed	NCT01273805	(104)
	HCQ + gemcitabine	I/II; Active	NCT01128296	
	HCQ + gemcitabine + abraxane	I/II; Active	NCT01506973	
	CQ + gemcitabine	I; Completed	NCT01777477	(105, 106)
REDOX HOMEOSTASIS				
Glutaminase	CB-839	I; Active	NCT02071862	

HCQ, hydroxychloroquine; CQ, chloroquine; mFOLFIRINOX, modified FOLFIRINOX.

REFERENCES

35. Commisso C, Davidson SM, Soydaner-Azeloglu RG, Parker SJ, Kamphorst JJ, Hackett S, et al. Macropinocytosis of protein is an amino acid supply route in Ras-transformed cells. *Nature* (2013) 497:633–7. doi: 10.1038/nature12138
50. Zarei M, Lal S, Parker SJ, Nevler A, Vaziri-Gohar A, Dukleska K, et al. Posttranscriptional upregulation of IDH1 by HuR establishes a powerful survival phenotype in pancreatic cancer cells. *Cancer Res.* (2017) 77:4460–71. doi: 10.1158/0008-5472.CAN-17-0015
57. Son J, Lyssiotis CA, Ying H, Wang X, Hua S, Ligorio M, et al. Glutamine supports pancreatic cancer growth through a KRAS-regulated metabolic pathway. *Nature* (2013) 496:101–5. doi: 10.1038/nature12040
61. Rambold AS, Kostelecky B, Elia N, Lippincott-Schwartz J. Tubular network formation protects mitochondria from autophagosomal degradation during nutrient starvation. *Proc Natl Acad Sci USA.* (2011) 108:10190–5. doi: 10.1073/pnas.1107402108
63. Kordes S, Pollak MN, Zwinderman AH, Mathot RA, Weterman MJ, Beeker A, et al. Metformin in patients with advanced pancreatic cancer: a double-blind, randomised, placebo-controlled phase 2 trial. *Lancet Oncol.* (2015) 16:839–47. doi: 10.1016/S1470-2045(15)00027-3
67. Alistar A, Morris BB, Desnoyer R, Klepin HD, Hosseinzadeh K, Clark C, et al. Safety and tolerability of the first-in-class agent CPI-613 in combination with modified FOLFIRINOX in patients with metastatic pancreatic cancer: a single-centre, open-label, dose-escalation, phase 1 trial. *Lancet Oncol.* (2017) 18:770–8. doi: 10.1016/S1470-2045(17)30314-5
74. Yang S, Wang X, Contino G, Liesa M, Sahin E, Ying H, et al. Pancreatic cancers require autophagy for tumor growth. *Genes Dev.* (2011) 25:717–29. doi: 10.1101/gad.2016111
78. Ju HQ, Zhuang ZN, Li H, Tian T, Lu YX, Fan XQ, et al. Regulation of the Nampt-mediated NAD salvage pathway and its therapeutic implications in pancreatic cancer. *Cancer Lett.* (2016) 379:1–11. doi: 10.1016/j.canlet.2016.05.024
79. Chini CC, Guerrico AM, Nin V, Camacho-Pereira J, Escande C, Barbosa MT, et al. Targeting of NAD metabolism in pancreatic cancer cells: potential novel therapy for pancreatic tumors. *Clin Cancer Res.* (2014) 20:120–30. doi: 10.1158/1078-0432.CCR-13-0150
85. Sousa CM, Biancur DE, Wang X, Halbrook CJ, Sherman MH, Zhang L, et al. Pancreatic stellate cells support tumour metabolism through autophagic alanine secretion. *Nature* (2016) 536:479–83. doi: 10.1038/nature19084
97. DeNicola GM, Karreth FA, Humpton TJ, Gopinathan A, Wei C, Frese K, et al. Oncogene-induced Nrf2 transcription promotes ROS detoxification and tumorigenesis. *Nature* (2011) 475:106–9. doi: 10.1038/nature10189
103. Braghiroli MI, de Celis Ferrari AC, Pfiffer TE, Alex AK, Nebuloni D, Carneiro AS, et al. Phase II trial of metformin and paclitaxel for patients with gemcitabine-refractory advanced adenocarcinoma of the pancreas. *Ecancermedicalscience* (2015) 9:563. doi: 10.3332/ecancer.2015.563
104. Wolpin BM, Rubinson DA, Wang X, Chan JA, Cleary JM, Enzinger PC, et al. Phase II and pharmacodynamic study of autophagy inhibition using hydroxychloroquine in patients with metastatic pancreatic adenocarcinoma. *Oncologist* (2014) 19:637–8. doi: 10.1634/theoncologist.2014-0086
105. Balic A, Sørensen MD, Trabulo SM, Sainz B, Cioffi M, Vieira CR, et al. Chloroquine targets pancreatic cancer stem cells via inhibition of CXCR4 and hedgehog signaling. *Mol Cancer Ther.* (2014) 13:1758–71. doi: 10.1158/1535-7163.MCT-13-0948
106. Samaras P, Tusup M, Nguyen-Kim TDL, Seifert B, Bachmann H, von Moos R, et al. Phase I study of a chloroquine-gemcitabine combination in patients with metastatic or unresectable pancreatic cancer. *Cancer Chemother Pharmacol.* (2017) 80:1005–12. doi: 10.1007/s00280-0173446-y

frontiers in Oncology

ORIGINAL RESEARCH
published: 13 November 2018
doi: 10.3389/fonc.2018.00514

Enhanced Cytotoxic Activity of Mitochondrial Mechanical Effectors in Human Lung Carcinoma H520 Cells: Pharmaceutical Implications for Cancer Therapy

Sergio González Rubio[1,2†], *Nuria Montero Pastor*[1,2†], *Carolina García*[3], *Víctor G. Almendro-Vedia*[1,2], *Irene Ferrer*[2,4], *Paolo Natale*[1,2], *Luis Paz-Ares*[2,4,5,6], *M. Pilar Lillo*[3] *and Iván López-Montero*[1,2*]

[1] Departamento de Química Física, Universidad Complutense de Madrid, Madrid, Spain, [2] Instituto de Investigación Hospital 12 de Octubre (i+12), Madrid, Spain, [3] Departamento de Química Física Biológica, Instituto de Química-Física "Rocasolano" (CSIC), Madrid, Spain, [4] Centro Nacional de Investigaciones Oncológicas (CNIO), Madrid, Spain, [5] Departamento de Medicina, Universidad Complutense de Madrid, Madrid, Spain, [6] Ciberonc, Madrid, Spain

OPEN ACCESS

Edited by:
Ubaldo Emilio Martinez-Outschoorn, Thomas Jefferson University, United States

Reviewed by:
Nirmalya Chatterjee, Harvard Medical School, United States
Mohamed Jemaà, Lund University, Sweden

***Correspondence:**
Iván López-Montero
ivanlopez@quim.ucm.es

[†] *These authors have contributed equally to this work*

Specialty section:
This article was submitted to Molecular and Cellular Oncology, a section of the journal Frontiers in Oncology

Received: *03 July 2018*
Accepted: *22 October 2018*
Published: *13 November 2018*

Citation:
González Rubio S, Montero Pastor N, García C, Almendro-Vedia VG, Ferrer I, Natale P, Paz-Ares L, Lillo MP and López-Montero I (2018) Enhanced Cytotoxic Activity of Mitochondrial Mechanical Effectors in Human Lung Carcinoma H520 Cells: Pharmaceutical Implications for Cancer Therapy. Front. Oncol. 8:514. doi: 10.3389/fonc.2018.00514

Cancer cell mitochondria represent an attractive target for oncological treatment as they have unique hallmarks that differ from their healthy counterparts, as the presence of a stronger membrane potential that can be exploited to specifically accumulate cytotoxic cationic molecules. Here, we explore the selective cytotoxic effect of 10-*N*-nonyl acridine orange (NAO) on human lung carcinoma H520 cells and compare them with healthy human lung primary fibroblasts. NAO is a lipophilic and positively charged molecule that promotes mitochondrial membrane adhesion that eventually leads to apoptosis when incubated at high micromolar concentration. We found an enhanced cytotoxicity of NAO in H520 cancer cells. By means Fluorescence lifetime imaging microscopy (FLIM) we also confirmed the formation of H-dimeric aggregates originating from opposing adjacent membranes that interfere with the mitochondrial membrane structure. Based on our results, we suggest the mitochondrial membrane as a potential target in cancer therapy to mechanically control the cell proliferation of cancer cells.

Keywords: NAO, mitochondrial targeting, membrane adhesion, cancer therapy, NSCLC cells, FLIM, phasor analysis

INTRODUCTION

Cancer remains one of the most common causes of death worldwide. In particular, lung cancer is usually detected at later stages of development (1). Additionally, the appearance of drug resistance during the course of treatment often leads to unsatisfying outcomes and a poor prognosis of patients (2) limited to a 5 years survival rate (3).

Traditional chemotherapeutics interfere with replication or cell division to prevent cell growth, increase cell death and restrict the spreading of the cancer (4). Side effects of traditional cancer treatments as surgery, chemotherapy or radiation therapy are significant as many healthy cells are killed during the treatment, due to the lack of target specificity. With the aim to specifically target only cancer cells, a new generation of cancer treatment has been developed recently known as the targeted cancer therapy (5), where pharmacological agents (monoclonal antibodies, small

molecule inhibitors or immunotoxins) that interfere with specific signaling proteins involved in tumor genesis are used (5). For instance, the epidermal growth factor receptor (EGFR) represents currently a major target in lung cancer therapy. However, the development of acquired resistance is now well recognized for promising monoclonal antibodies acting as EGFR inhibitors (6, 7). A new promising strategy for cancer therapy focuses on mitochondria as they participate as key regulators in the apoptosis. Mitochondria of cancer cells exhibit unique and multiple characteristics that differ from their healthy counterparts. Among them, a stronger (more negative) mitochondrial membrane potential (8) that suggests an underlying increased accumulation of cytotoxic cationic molecules within cancer cells (9–13). The compounds directed to mitochondria and able to interfere with the mitochondrial function, become promising antitumor agents (4, 14–16) and may represent a more selective and effective option for therapy.

As a proof-of-concept, we explore here the selective cytotoxic effect of the compound 10-*N*-nonyl acridine orange (NAO) on human lung carcinoma H520 cells. NAO is a lipophilic fluorescent molecule used as a mitochondrial marker that stains the inner mitochondrial membrane (IMM) (11). NAO was previously shown to be cytotoxic when present at low milimolar concentrations (17) and we have recently shown the underlying molecular mechanisms of this cytotoxicity. The formation H-aggregates of NAO molecules originating from opposing adjacent membranes elicits interbilayer adhesion of mitochondria and interferes with mitochondrial dynamics leading to apoptosis (18).

We demonstrate the specific cytotoxic activity of NAO in H520 human lung carcinoma cells exposed at NAO concentration that are not harmful for healthy human lung primary fibroblast (HLPF). H520 cells represent a paradigmatic non-small cell lung cancer (NSCLC) cells and they have proven to be a powerful tool for cancer research. We also identify by means of Fluorescence life time imaging microscopy (FLIM) the presence of long-lifetime H-dimers of NAO, generally formed when present at high local concentration.

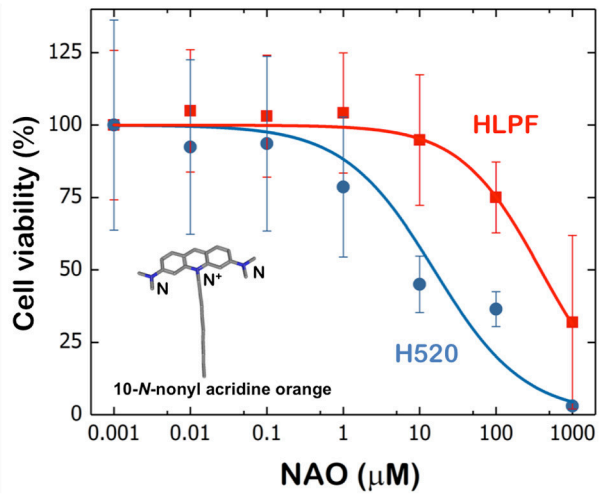

FIGURE 1 | Cell viability of HLPF and H520 cells upon NAO incubation. The experimental data were satisfactorily fitted by a classical sigmoidal curve that is obtained with the Hill model (19). The Hill model is based on the equation $C_{Hill} = C_0 + \frac{C_\infty - C_0}{1+\left(\frac{CC_{50}}{C}\right)^H}$, which describes the cytotoxic effect C_{Hill} obtained at a given concentration C; where CC_{50} is the relative 50% cytotoxic concentration reducing cell viability by 50%, H is the Hill exponent, C_∞ is the maximum cytotoxicity and C_0 is the viability in the absence of NAO. **Inset:** Chemical structure of 10-*N*-nonyl acridine orange (NAO).

RESULTS

NAO Exhibits a Strong Cytotoxic Activity in H520 Cancer Cells

To determine the enhanced cytotoxicity of NAO in cancer cells, H520 cancer cells and healthy HLPF (control) were exposed for 60 min to increasing amounts of NAO (1 nM−1 mM) and cell viability was determined by the MTT assay (**Figure 1**). The viability of H520 starts to be compromised in the presence of 0.1 μM and cells were severely killed in the presence of NAO at concentrations up to 1 mM. The cell viability of HLPF is not affected until the presence of 10 μM of NAO and shows a survival of approximately 30% in the presence of 1 mM of NAO. The calculated CC_{50} values vary 25 fold with ≈15 μM for H520 and ≈385 μM for HLPF (**Figure 1**). Alternative cationic dyes 1,1′-Dioctadecyl-3,3,3′,3′-Tetramethylindotricarbocyanine Iodide (DiR) and Tetramethyl rhodamine methyl ester (TMRM) were also tested for cell toxicity. DiR is long-chain lipophilic carbocyanine dye (20) and TMRM is a dye used for monitoring the mitocondrial membrane potential (21). The obtained CC_{50} values of these dyes vary from ≈3 × 10^2 μM for H520 cells to > mM for HLPF cells (**Figure S1**). The toxicity of DiR and TMRM were only observed in cancer cells and at one order of magnitude higher than observed for NAO. Hereinafter we focus on NAO because of its enhanced cytotoxicity.

Next, we measured the conformational arrangement of NAO in H520 and HLPF cells by means of fluorescence confocal microscopy. The incubation with high concentration of NAO leads to cell death accompanied with a green-to-red emission shift where the maximum emission wavelength at λ_{em} = 525 nm shifts to 640 nm due to the formation of supramolecular aggregates (22) that result from the π-π interactions between the stacked acridine orange moieties (23, 24). In agreement with the previous literature and our own observations (11, 18) the incubation of NAO at low nM concentrations merely stains the mitochondrial network of both H520 and HLPF cells, but does not exhibit visual signs of cytotoxicity (**Figure S2**). The low red shift of NAO observed in HPLF cells did not induced apoptosis, even for long incubation times (up to 48 h). In contrast, at high μM concentrations, the mitochondria of H520 immediately stained and cells entered apoptosis that can be appreciated by the global morphological changes as membrane blebbing or cell shrinkage (**Figure 2**). As previously shown, this morphological remodeling of the mitochondrial network into spherical liposomal appearance is simultaneously accompanied by the red shift of NAO and a direct consequence of the formation of supramolecular NAO zippers among adjacent mitochondrial

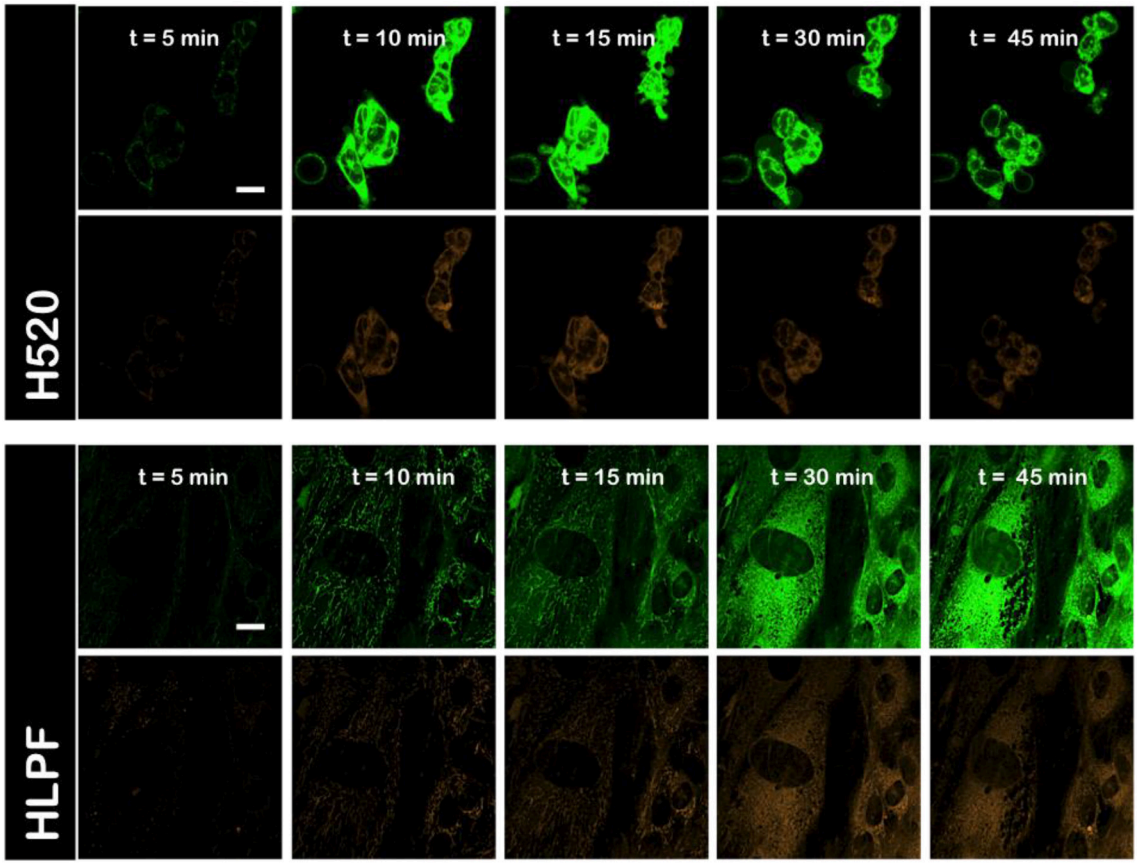

FIGURE 2 | Interbilayer NAO dimers elicit cytotoxicity in HLPF and H520 cells. Confocal fluorescence micrographs (green channel, $\lambda_{exc} = 488$ nm and red channel, $\lambda_{exc} = 561$nm) of HLPF and H520 mitochondria in the presence of 5 μM of NAO. NAO induces apoptosis and the spectral shift from green to red, indicative for the formation of interbilayer NAO dimers (See main text for details). Scale bars are 10 μm.

membranes (**Figure 2**) (18). At high concentrations, also HLPF control cells were compromised and both the red shift and the morphological changes of mitochondria were appreciated at longer incubation times (**Figure 2**).

The Cytotoxic Effect of NAO in H520 and HLPF Cells Originates From the Supramolecular Assembly of NAO Dimers in Mitochondrial Membranes

Time-resolved fluorescence imaging allowed us to characterize the molecular basis of the NAO induced cytotoxicity. Within eukaryotic cells and depending on the administered concentration of NAO, three spectroscopic molecular species of NAO can be observed in the mitochondrial membranes. The molecular species are characterized by different excited-state lifetimes of 0.2 ns (very short excited-state species), 2.0 ns (intermediate excited-state species), and 10 ns (long excited-state species). The very short species corresponds to the self-quenched clustered form of NAO, the intermediate species to the monomeric form and the long excited-state species to the red-shifted dimeric form (18). Note that, the 10-ns lifetime NAO species was only detected in the red channel #1; whereas the 2.0-ns and 0.2-ns NAO species were detected in both emission channels, but mainly in the green channel #2.

Two-photon FLIM-phasor images of a representative group of H520 and HLPF cells incubated for 60 min with 10 nM NAO show the presence and the quantification of the three species. All three lifetimes (10, 2.0, and 0.2 ns) lie on the universal phasor circle (black cursors) (25). In the low nM concentration regime (**Figure 3**), the phasor clusters determined for the channel #1 and #2 FLIM images correspond to nearly pure NAO monomer molecules for both cell lines. Note that the lower accumulation of NAO in HLPF cells leads the phasor cluster of the channel #1 to overlap the phasor cluster corresponding to autofluorescence. When both H520 and HLPF cells are incubated for short times (up to 60 min) with NAO at high μM concentrations the phasor cluster correspond to a mixture of the three species as indicated by the localization of the phasor cluster inside the three species triangle in channel #1 and #2 (**Figure 4**).

Though the population of NAO (2.0 ns) monomers species predominates (blue cursor and blue color in the phasor color map) in the early stages of the interaction, the (10 ns) long excited-state NAO species becomes predominant (in red channel

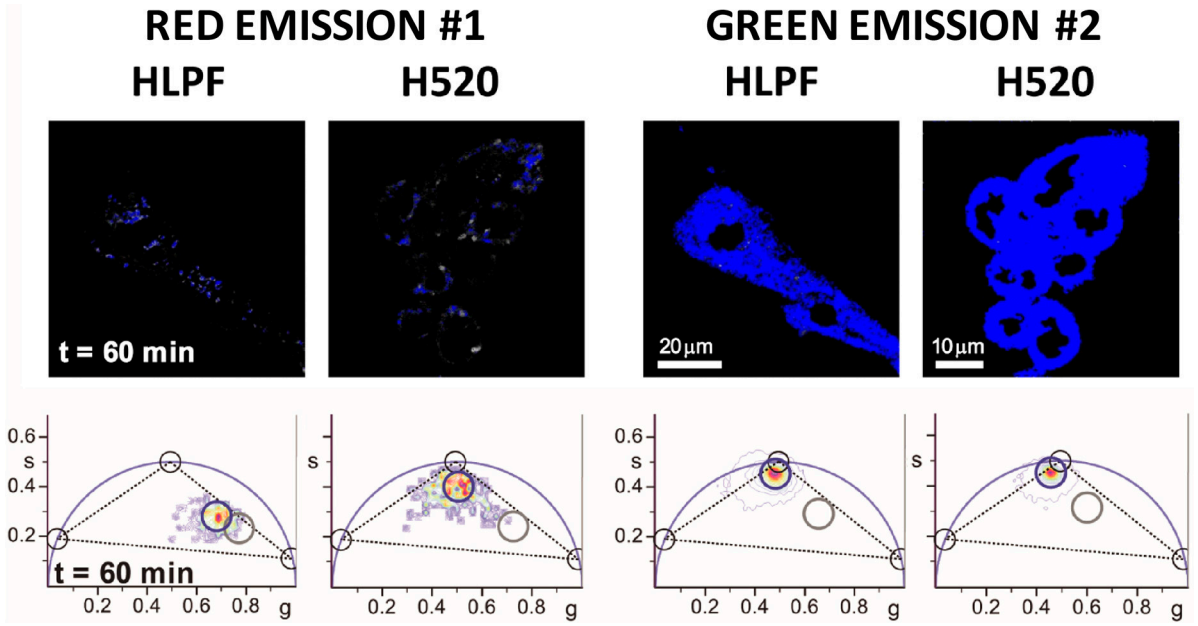

FIGURE 3 | Spatial distribution of NAO molecular species in HLPF and H520 cells. Basal *XY* sections of representative groups of cells treated with 10 nM NAO for 60 min and their corresponding phasor plots showing regions enriched in intermediate-lifetime NAO monomers (blue cursor; as detected in channel #1 and channel #2). Gray cursors show cell autofluorescence. Black cursors on the phasor plot represent 100% pure NAO species: NAO antiparallel H-dimers (τ = 10 ns), monomeric NAO (τ = 2.0 ns), and self-quenched NAO aggregates (τ = 0.2 ns). Black dashed lines joining the three pure species phasors form a triangle that would contain phasors from all possible intensity-weighted combinations of the three NAO molecular species. Pixels corresponding to the cluster of phasors enclosed by the colored circles are highlighted on the intensity image using the same color. λ_{exc} = 850 nm, red channel (#1) FF01 685/40, green channel (#2) FF02 520/35, dichroic filter FF560-Di01 (Semrock, Germany), 1.2 ms/pixel.

#1; red cursor and red color in the phasor color map) and the (0.2 ns) self-quenched population species emerges (blue channel #2; light blue cursor and light blue color in the phasor color map) during the progress of NAO accumulation. As previously shown (18) the formation of red-shifted NAO-dimers indicates the supramolecular assembly of molecular zippers between stacked NAO from opposing bilayers producing membrane remodeling in mitochondria that compromise the survival of the cell (**Figure 2**). This molecular mechanism by which the widely used mitochondrial dye NAO exhibits cytotoxicity is enhanced in NSCLC H520 cells as compared to HLPF cells (**Figure 1**).

DISCUSSION

The primary function of mitochondria is to provide the chemical energy to eukaryotic cells in the form of adenosine triphosphate (ATP). As this function is essential for cell viability, mitochondria are being explored as a promising target for therapeutic purposes. The fact that mitochondria of cancer cells exhibit characteristics different from healthy cells, allow the design of new strategies focusing on enhanced selectivity and reduced acquired drug resistance. Beyond its well-established role in cellular energetics, mitochondria are key controllers of apoptosis (26). Pro-apoptotic factors, such as cytochrome c, reside in the mitochondrial intermembrane space and are liberated to the cytoplasm during apoptosis. This activates caspase proteases and the subsequent cleavage of structural and regulatory proteins in the cytoplasm and the nucleus (27). New cancer therapies aim to specifically induce apoptosis through pharmacological agents acting on mitochondria and promoting mitochondrial failure or damage (14). Cancer cells exhibit a stronger (more negative) mitochondrial membrane potential, a particular feature that opens the way to control of cell proliferation and survival by means of regulation of the mechanical properties of mitochondrial membranes. This strong membrane potential of mitochondria allows the accumulation of cationic lipophilic molecules within the mitochondrial matrix at non-effective concentrations of normal cells. This rational leads to the design and synthesis of mitochondrial dyes (18, 28), such as NAO, a lipophilic and positively charged fluorescent dye able to diffuse spontaneously into membrane environments (17). The incubation with concentrations in the µM range of NAO induces cytotoxicity (26). In contrast to other cationic dyes that accumulate in mitochondria (DiR and TMRM), it is only required a lower concentration of NAO to produce fatal consequences for cell viability (17). The ability of NAO to form supramolecular stacks is provided by the acridine orange moiety (23), but the presence of the aliphatic chain enhances the partitioning of NAO into the membrane and promotes its cytotoxic mechanism (18). NAO dimers from opposite membranes trigger their adhesion and cause severe mechanical alterations of mitochondrial dynamics, promoting mitochondrial

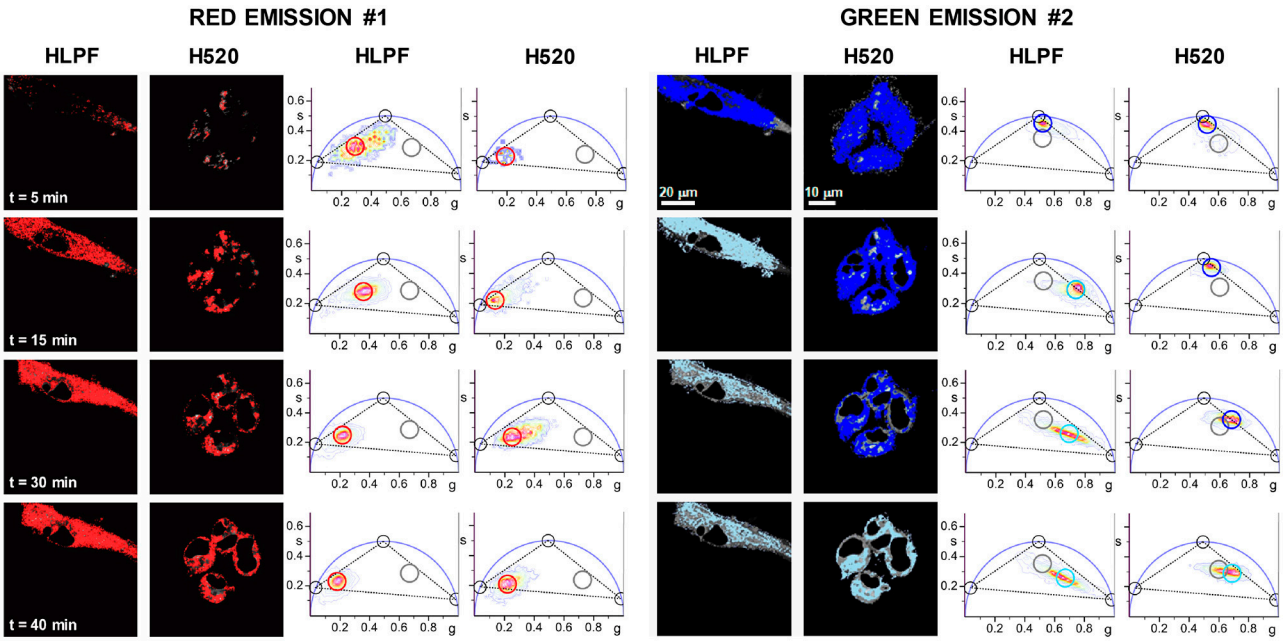

FIGURE 4 | Spatial distribution of H-dimers in HLPF and H520 cells. Basal *XY* sections of representative groups of cells treated with 5 μM NAO at different times. Their corresponding phasor plots show regions enriched in long-lifetime NAO antiparallel H-dimers (red cursor; as detected in channel #1), intermediate-lifetime NAO monomers (blue cursor; as detected in channel #2) and the short-lifetime NAO self-quenched clusters (light blue cursor; as detected in channel #2). Gray cursors show cell autofluorescence. Black cursors on the phasor plot represent again 100% pure NAO species: NAO antiparallel H-dimers (τ = 10 ns), monomeric NAO (τ = 2.0 ns), and self-quenched NAO aggregates (τ = 0.2 ns). Black dashed lines joining the three pure species phasors form a triangle that would contain phasors from all possible intensity-weighted combinations of the three NAO molecular species. Pixels corresponding to the cluster of phasors enclosed by the colored circles are highlighted on the intensity image using the same color. λ_{exc} = 850 nm, red channel (#1) FF01 685/40, green channel (#2) FF02 520/35, dichroic filter FF560-Di01 (Semrock, Germany), 1.2 ms/pixel.

membrane remodeling. As a result, mitochondria lose their characteristic ultrastructure and form double-membrane vesicles comprising the outer and inner membranes (18, 29). The stronger cytotoxicity of NAO on carcinoma H520 cells is compatible with a higher accumulation of NAO into cancer mitochondria producing cell death at lower effective dose compared to non-cancerous cells (**Figure 1**). We also show a similar accumulating effect in cancer cells for the other cationic dyes tested (**Figure S1**).

Note that the mitochondrial membrane potential established by the Nernst equation:

$$E = 2.3\frac{RT}{zF}\,log\left[\frac{[NAO]_o}{[NAO]_i}\right]$$

where E is the membrane potential, $[NAO]_o$ is the cytosolic concentration of NAO, $[NAO]_i$ is the mitochondrial concentration of NAO, R is the ideal gas constant, T is the temperature, z is the charge of the dye and F is the Faraday's constant. Thus, a stronger (e.g., two-fold) mitochondrial potential in cancer cells (21, 29) will result in a ten-fold accumulation of the cationic probe within the cancer cell (**Figure 5**). Additional factors as an increased mitochondrial mass (30) or a different composition of negatively charged lipids as cardiolipin (31) can also control the enhanced selectivity of lipophilic and positively charged molecules. To reliably ground the physico-chemical mechanisms that drive the enhanced NAO accumulation in cancer mitochondria the direct measurement of both the membrane potential and the absolute concentration of NAO in living cells is required (32).

Anticancer drugs that directly target mitochondria might have the potential to bypass the drug-resistance acquired by cancer cells during chemotherapy treatment. In particular, novel targeted therapies must be based on physical mechanisms at the mesoscale, the adhesion of mitochondrial membranes in our case, instead of interfering with the molecular biochemical signals that can be easily reprogrammed by the cell. The mechanical targeting proposed here may provide a unique tool to circumvent the acquired survival mechanisms and may be effective in otherwise resistant forms of cancer. The proof-of-concept still needs to explore the therapeutic window with more NSCLC cell lines including those that acquired resistance during chemotherapy and more important with other kind of healthy cells, in particular for those more susceptible to mitochondrial functioning. Also, *in vivo* experiments with murine models are essential for a complete validation of the approach.

MATERIALS AND METHODS

Chemicals

10-*N*-nonyl acridine orange (NAO), 1,1′-Dioctadecyl-3,3,3′,3′-Tetramethylindotricarbocyanine Iodide (DiR) and

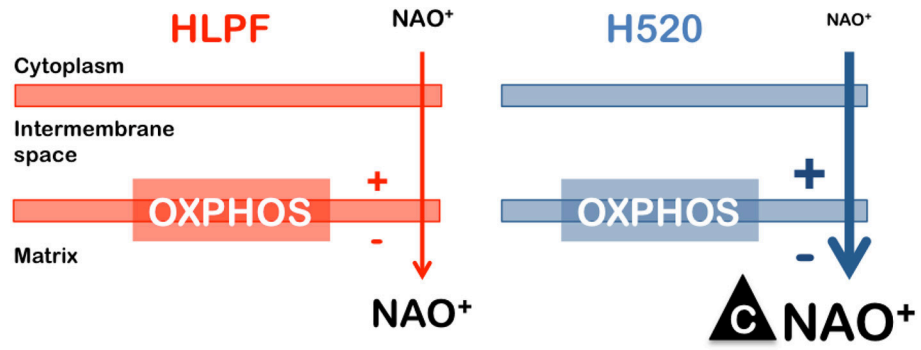

FIGURE 5 | Strategy focusing on enhanced selectivity for cancer cells. The negative membrane potential of healthy mitochondria (HLPF cells) enables lipophilic and positively charged molecules (NAO) to accumulate in the inner membrane. A more negative membrane potential in cancer cells (H520 cells) triggers an enhanced accumulation of NAO leading to cytotoxicity.

Tetramethyl rhodamine methyl ester (TMRM) were supplied by Thermofisher. Ultrapure water was produced from a Milli-Q unit (Millipore, conductivity below 18 MΩ cm).

Cell Culture

The cell line of human lung primary fibroblast (HLPF) was provided by Pr. Alejandro Sweet-Cordero from University of California San Francisco (UCSF) under the terms of a Material Transfer Agreement; and no ethical approvals were required for their use in this study as per local legislation and national guidelines. HLPF cells were maintained in DMEM + GlutaMax-I, supplemented with 10% fetal bovine serum (FBS), penicillin (50 U/mL) and streptomycin (50 μg/mL) (Thermofisher) and human lung tumor cells (H520) were maintained in RPMI-1640 medium, supplemented with 10% fetal bovine serum (FBS), penicillin (50 U/mL) and streptomycin (50 μg/mL) (Thermofisher). All cells were maintained in a humidified incubator at 37°C and 5% CO_2 atmosphere (Forma Steri-Cycle Themofisher; 5% CO_2). Cells were plated in 75 cm^2 flasks (Thermofisher) and were passaged when reaching 95% confluence, by gentle trypsinization 0.05% trypsin/0.53 mM EDTA; Invitrogen Life Technologies).

Cell Viability

Cell viability was evaluated by using the methylthiazoletetrazolium assay (MTT; Sigma-Aldrich). All experimental conditions were performed in quadruplicate. Cells were seeded in 96-well flat-bottom plates at 5,000 cells/well. After 24 h, the medium was replaced with 100 μl medium with different concentrations of NAO, DiR and TMRM (1 nM−1 mM). After 60, 90, 120, and 150 min, each well was replaced with 100 μl MTT solution (5 mg/ml). After 2 h incubation at 37°C, 5% CO_2, each well was replaced with 100 μl DMSO (Sigma-Aldrich). The cell viability was determined by measuring the absorbance at 570 nm using a spectrophotometer (Multiskan^{TM} FC, Thermofisher). Results are presented as the percentage survival in relation to untreated control cells.

Confocal Microcopy

Confocal microscopy images of cells were collected at 37°C with a Nikon Ti-E inverted microscope equipped with a Nikon C2 confocal scanning confocal module, 488 and 561 nm continuous lasers, emission bandpass filters, and a Nikon Plan Apo 100 × NA 1.45 oil immersion objective. Both H520 and HLPF cells were seeded at 3 × 10^4 cells per cm^2 in a four-chamber Lab-Tek® slide (Thermofisher) and incubated with complete DMEM for HLPF cells and RPMI for H520 cells, both for 24 h at 37°C. Prior to confocal fluorescence imaging, cells were supplemented with NAO (5 nM or 5 μM).

Two-Photon Fluorescence Lifetime Imaging

Two-photon, two-color (red channel #1 and green channel #2) fluorescence-lifetime imaging (2P-FLIM) of XY sections of cells was carried out on a MicroTime200 system (PicoQuant, Germany) equipped with a mode-locked, femtosecond-pulsed Ti:Sapphire laser (Mai-Tai, Spectra Physics, CA) operating at a repetition rate of 80 MHz, horizontally polarized, and tuned to 850 nm; an Olympus IX71 inverted microscope mounted with a 60X water-immersion objective NA1.2; a piezo XY-scanning table and two single-photon counting avalanche diodes (τ-SPAD, PicoQuant, Germany), and a PicoHarp 300 PC-board (PicoQuant, Germany), synchronized with the excitation laser pulses using the Time-Tagged Time-Resolved (TTTR) detection mode at 23°C. The TTTR mode allows the recording of every individual fluorescence photon from each pixel, together with its timing and emission color (channel #1, channel #2). The acquisition time per pixel accounted for 1.2 ms, resulting in an image overall acquisition time of 180 s. Once the acquisition of the image was finished, all the detected photons per pixel were used to build steady-state fluorescence intensity images or to produce Fast FLIM (**Figure S3**) and FLIM phasor images using the ps-temporal resolution of the system, SymphoTime 64 software (Fast FLIM; PicoQuant, Germany), and SimFCS software (Phasor Analysis) developed at the Laboratory of Fluorescence Dynamics (LFD, UC Irvine). The filters used in this study were all from Semrock (Germany). Red channel (#1):

FF01-685/40; green channel (#2): FF01-520/35; with a dichroic beam splitter FF560-Di01. Although in the red channel #1 we mostly select red NAO aggregates, a non-negligible bleed through from NAO monomers may exist, particularly when the monomer NAO population is the majority. The excitation power was lower than 1 mW at the sample, and it was adjusted using a variable optical attenuator LS-107AT (Lasing, S.A. Spain) to achieve counting rates below 10^6 photons/s. Both H520 and HLPF cells were seeded at 2×10^4 cells per cm^2 in an 8-chamber Lab-Tek® slide (Thermofisher) and incubated with complete RPMI 1640 or DMEM for 24/36 h at 37°C. Prior to FLIM imaging at the micro-spectrometer, cells were washed with Tyrode-glucose buffer (NaCl 145 mM, KCl 4 mM, $MgCl_2$ 1 mM, $CaCl_2$ 1.8 mM, HEPES-Na 10 mM, glucose 10 mM, pH 7.4) and supplemented with NAO (10 nM or 5 μM).

AUTHOR CONTRIBUTIONS

IL-M designed research. SGR, NM, CG, VA-V, and MPL performed research. IF and LP-A contributed new reagents. SGR, NM, CG, MPL, and IL-M analyzed data. PN, LP-A, MPL, and IL-M wrote the paper.

ACKNOWLEDGEMENTS

The authors wish to thank Pr. Alejandro Sweet-Cordero from University of California San Francisco (UCSF) for providing HLPF cells. This work was supported by the ERC Starting Grant MITOCHON (ERC-StG-2013-338133), ERC Proof of Concept mitozippers (ERC-PoC-2017-780440) and FIS2015-70339-C2-1-R from the Spanish Ministry of Economy MINECO (IL-M); and FIS2015-70339-C2-2-R (MPL and CG).

SUPPLEMENTARY MATERIAL

The Supplementary Material for this article can be found online at: https://www.frontiersin.org/articles/10.3389/fonc.2018.00514/full#supplementary-material

REFERENCES

1. Siegel RL, Miller KD, Jemal A. Cancer statistics, 2018. *CA Cancer J Clin.* (2018) 68:7–30. doi: 10.3322/caac.21442
2. Askoxylakis V, Thieke C, Pleger ST, Most P, Tanner J, Lindel K, et al. Long-term survival of cancer patients compared to heart failure and stroke: a systematic review. *BMC Cancer* (2010) 10:105. doi: 10.1186/1471-2407-10-105
3. Vilmar AC, Sorensen JB. Customising chemotherapy in advanced nonsmall cell lung cancer: daily practice and perspectives. *Eur Respir Rev.* (2011) 20:45–52. doi: 10.1183/09059180.00007310
4. Hanahan D, Weinberg RA. The hallmarks of cancer. *Cell* (2000) 100:57–70. doi: 10.1016/S0092-8674(00)81683-9
5. Baudino TA. Targeted cancer therapy: the next generation of cancer treatment. *Curr Drug Discov Technol.* (2015) 12:3–20. doi: 10.2174/1570163812666150602144310
6. Brand TM, Iida M, Wheeler DL. Molecular mechanisms of resistance to the EGFR monoclonal antibody cetuximab. *Cancer Biol Ther.* (2011) 11:777–92. doi: 10.4161/cbt.11.9.15050
7. Westover D, Zugazagoitia J, Cho BC, Lovly CM, Paz-Ares L. Mechanisms of acquired resistance to first- and second-generation EGFR tyrosine kinase inhibitors. *Ann Oncol.* (2018) 29:i10–9. doi: 10.1093/annonc/mdx703
8. Forrest MD. Why cancer cells have a more hyperpolarised mitochondrial membrane potential and emergent prospects for therapy. *bioRxiv* (2015). doi: 10.1101/025197
9. Summerhayes IC, Lampidis TJ, Bernal SD, Nadakavukaren JJ, Nadakavukaren KK, Shepherd EL, et al. Unusual retention of rhodamine 123 by mitochondria in muscle and carcinoma cells. *Proc Natl Acad Sci USA.* (1982) 79:5292–6. doi: 10.1073/pnas.79.17.5292
10. Nadakavukaren KK, Nadakavukaren JJ, Chen LB. Increased rhodamine 123 uptake by carcinoma cells. *Cancer Res.* (1985) 45:6093–9.
11. Septinus M, Berthold T, Naujok A, Zimmermann HW. Hydrophobic acridine dyes for fluorescent staining of mitochondria in living cells. 3. Specific accumulation of the fluorescent dye NAO on the mitochondrial membranes in HeLa cells by hydrophobic interaction. Depression of respiratory activity, changes in the ultrastructure of mitochondria due to NAO. Increase of fluorescence in vital stained mitochondria *in situ* by irradiation. *Histochemistry* (1985) 82:51–66.
12. Modica-Napolitano JS, Aprille JR. Delocalized lipophilic cations selectively target the mitochondria of carcinoma cells. *Adv Drug Deliv Rev.* (2001) 49:63–70. doi: 10.1016/S0169-409X(01)00125-9
13. Fantin VR, Berardi MJ, Scorrano L, Korsmeyer SJ, Leder P. A novel mitochondriotoxic small molecule that selectively inhibits tumor cell growth. *Cancer Cell* (2002) 2:29–42. doi: 10.1016/S1535-6108(02)00082-X
14. Fulda S, Galluzzi L, Kroemer G. Targeting mitochondria for cancer therapy. *Nature Reviews Drug Discovery* (2010) 9:447–64. doi: 10.1038/nrd3137
15. D'souza GGM, Wagle MA, Saxena V, Shah, A. Approaches for targeting mitochondria in cancer therapy. *Biochim Biophys Acta* (2011) 1807:689–96. doi: 10.1016/j.bbabio.2010.08.008
16. Wen S, Zhu D, Huang P. Targeting cancer cell mitochondria as a therapeutic approach. *Future Med Chem.* (2013) 5:53–67. doi: 10.4155/fmc.12.190
17. Septinus M, Berthold T, Naujok A, Zimmermann HW. Über hydrophobe Acridinfarbstoffe zur Fluorochromierung von Mitochondrien in lebenden Zellen. *Histochemistry* (1985) 82:51–66.
18. Almendro-Vedia VG, Garcia C, Ahijado-Guzman R, De La Fuente-Herreruela D, Muñoz-Ubeda M, Natale P, et al. Supramolecular zippers elicit interbilayer adhesion of membranes producing cell death. *Biochim Biophys Acta Gen Subj.* (2018) 1862:2824–34. doi: 10.1016/j.bbagen.2018.08.018
19. Prentice RL. A generalization of the probit and logit methods for dose response curves. *Biometrics* (1976) 32:761–8. doi: 10.2307/2529262
20. Texier I, Goutayer M, Da Silva A, Guyon L, Djaker N, Josserand V, et al. Cyanine-loaded lipid nanoparticles for improved *in vivo* fluorescence imaging. *J Biomed Opt.* (2009) 14:054005. doi: 10.1117/1.3213606
21. Ehrenberg B, Montana V, Wei MD, Wuskell JP, Loew LM. Membrane potential can be determined in individual cells from the nernstian distribution of cationic dyes. *Biophys J.* (1988) 53:785–94. doi: 10.1016/S0006-3495(88)83158-8
22. Mileykovskaya E, Dowhan W, Birke RL, Zheng D, Lutterodt L, Haines TH. Cardiolipin binds nonyl acridine orange by aggregating the dye at exposed hydrophobic domains on bilayer surfaces. *FEBS Lett.* (2001) 507:187–90. doi: 10.1016/S0014-5793(01)02948-9
23. Kapuscinski J, Darzynkiewicz Z. Interactions of acridine orange with double stranded nucleic acids. Spectral and affinity studies *J Biomol Struct Dyn.* (1987) 5:127–43. doi: 10.1080/07391102.1987.10506381
24. Thomé MP, Filippi-Chiela EC, Villodre ES, Migliavaca CB, Onzi GR, Felipe KB, et al. Ratiometric analysis of Acridine Orange staining in the study of acidic organelles and autophagy. *J Cell Sci.* (2016) 129:4622–32. doi: 10.1242/jcs.195057
25. Stringari C, Cinquin A, Cinquin O, Digman MA, Donovan PJ, Gratton E. Phasor approach to fluorescence lifetime microscopy distinguishes different

metabolic states of germ cells in a live tissue. *Proc Natl Acad Sci USA*. (2011) 108:13582–7. doi: 10.1073/pnas.1108161108
26. Tait SW, Green DR. Mitochondria and cell death: outer membrane permeabilization and beyond. *Nat Rev Mol Cell Biol.* (2010) 11:621–32. doi: 10.1038/nrm2952
27. Philchenkov A. Caspases: potential targets for regulating cell death. *J Cell Mol Med.* (2004) 8:432–44. doi: 10.1111/j.1582-4934.2004.tb00468.x
28. Maftah A, Petit JM, Julien R. Specific interaction of the new fluorescent dye 10-*N*-nonyl acridine orange with inner mitochondrial membrane. *A lipid-mediated inhibition of oxidative phosphorylation FEBS Lett.* (1990) 260:236–40. doi: 10.1016/0014-5793(90)80112-V
29. Yousif LF, Stewart KM, Kelley SO. Targeting mitochondria with organelle-specific compounds: strategies and applications. *Chembiochem* (2009) 10:1939–50. doi: 10.1002/cbic.200900185
30. Lamb R, Bonuccelli G, Ozsvari B, Peiris-Pages M, Fiorillo M, Smith DL, et al. Mitochondrial mass, a new metabolic biomarker for stem-like cancer cells: Understanding WNT/FGF-driven anabolic signaling. *Oncotarget* (2015) 6:30453–71. doi: 10.18632/oncotarget.5852
31. Sapandowski A, Stope M, Evert K, Evert M, Zimmermann U, Peter D, et al. Cardiolipin composition correlates with prostate cancer cell proliferation. *Mol Cell Biochem.* (2015) 410:175–85. doi: 10.1007/s11010-015-2549-1
32. Ma N, Digman MA, Malacrida L, Gratton E. Measurements of absolute concentrations of NADH in cells using the phasor FLIM method. *Biomed Opt Express* (2016) 7:2441–52. doi: 10.1364/BOE.7.002441

Conflict of Interest Statement: The authors declare that the research was conducted in the absence of any commercial or financial relationships that could be construed as a potential conflict of interest.

frontiers in Oncology

REVIEW
published: 22 October 2018
doi: 10.3389/fonc.2018.00458

Hematologic Tumor Cell Resistance to the BCL-2 Inhibitor Venetoclax: A Product of Its Microenvironment?

Joel D. Leverson[1]* *and Dan Cojocari*[2]

[1] Oncology Development, AbbVie, Inc., North Chicago, IL, United States, [2] Oncology Discovery, AbbVie, Inc., North Chicago, IL, United States

BCL-2 family proteins regulate the intrinsic pathway of programmed cell death (apoptosis) and play a key role in the development and health of multicellular organisms. The dynamics of these proteins' expression and interactions determine the survival of all cells in an organism, whether the healthy cells of a fully competent immune system or the diseased cells of an individual with cancer. Anti-apoptotic proteins like BCL-2, BCL-X_L, and MCL-1 are well-known for maintaining tumor cell survival and are therefore attractive drug targets. The BCL-2-selective inhibitor venetoclax has been approved for use in chronic lymphocytic leukemia and is now being studied in a number of other hematologic malignancies. As clinical data mature, hypotheses have begun to emerge regarding potential mechanisms of venetoclax resistance. Here, we review accumulating evidence that lymphoid microenvironments play a key role in determining hematologic tumor cell sensitivity to venetoclax.

Keywords: venetoclax, BCL-2, microenvironment, resistance, tumor

OPEN ACCESS

Edited by:
Saverio Marchi,
University of Ferrara, Italy

Reviewed by:
Junxian Lim,
The University of Queensland, Australia
Afshin Samali,
National University of Ireland Galway, Ireland

***Correspondence:**
Joel D. Leverson
joel.leverson@abbvie.com

Specialty section:
This article was submitted to Molecular and Cellular Oncology, a section of the journal Frontiers in Oncology

Received: *03 July 2018*
Accepted: *01 October 2018*
Published: *22 October 2018*

Citation:
Leverson JD and Cojocari D (2018) Hematologic Tumor Cell Resistance to the BCL-2 Inhibitor Venetoclax: A Product of Its Microenvironment? Front. Oncol. 8:458. doi: 10.3389/fonc.2018.00458

INTRODUCTION

The BCL-2 Family: Arbiters of Cell Survival and Programmed Cell Death

The *BCL2* gene was discovered as part of the *t*(14;18) translocation associated with follicular lymphoma (1) and was later characterized as the first oncogene to work by maintaining tumor cell survival (2–5). Scientists went on to discover a host of related proteins that now comprise the BCL-2 family (**Figure 1A**) [see (6) for review]. These proteins are characterized by closely related structural units known as BCL-2 homology (BH) motifs—a collection of alpha-helices that assemble to form surfaces that mediate interactions amongst family members. The BH1-BH4 motifs of anti-apoptotic proteins such as BCL-2, BCL-X_L and MCL-1 form a shallow, hydrophobic groove that accommodates binding of the amphipathic BH3 motif of certain pro-apoptotic family members like the multi-domain "effector" proteins BAK and BAX. Each BCL-2 family member exhibits a binding selectivity profile reflecting its tendencies to interact more avidly with certain counterparts (**Figure 1B**). For example, the effector protein BAK tends to be sequestered by BCL-X_L, MCL-1, or A1, whereas BAX exhibits binding to all the anti-apoptotic proteins. Likewise, all anti-apoptotic proteins are thought to be capable of sequestering the so-called "BH3-only" protein BIM, a pro-apoptotic "activator" that can promote the insertion of BAX into the mitochondrial outer membrane. Thus activated, BAX can oligomerize and form complexes with BAK to form pores in the mitochondrial outer membrane (**Figure 1C**). When so-called "sensitizer" proteins bind to anti-apoptotic counterparts, they can preclude sequestration

of activators and effectors, thereby promoting apoptosis. For example, the pro-apoptotic protein BAD binds to BCL-2, BCL-X_L, and BCL-W but not to MCL-1, whereas NOXA binds preferentially to MCL-1 and A1 (**Figure 1B**). Certain cellular stresses can lead to elevations in pro-apoptotic proteins, which can then overwhelm the anti-apoptotic proteins and go on to trigger the key events of intrinsic apoptosis, including mitochondrial outer membrane permeabilization (MOMP) by BAK-BAX oligomers, the release of mitochondrial cytochrome *c* into the cytosol, the proteolytic activation of caspases, and the eventual dismantling of the cell and its engulfment by macrophages (**Figure 1C**).

For cancer cells, which often must evolve to survive in harsh environments, the overexpression of anti-apoptotic proteins allows increased numbers of pro-apoptotic proteins to be sequestered, offering a mechanism of survival, and a selective advantage. However, because they carry such high levels of these complexes, these cells essentially exist on the brink of initiating apoptosis, a state which has been referred to as "primed for death" (7). In an attempt to exploit this therapeutically, small-molecule BH3 mimetics have been designed to bind competitively to anti-apoptotic proteins and liberate pro-apoptotic proteins in the hopes of triggering apoptosis in primed cancer cells (**Figure 1C**) [see (8) for review]. Decades of intense drug discovery efforts have recently borne fruit with regulatory agency approvals of venetoclax, a selective BCL-2 inhibitor.

The BCL-2-Selective Inhibitor Venetoclax

The first BH3 mimetics, such as ABT-737 and ABT-263 (navitoclax), exhibited the same binding profile as the BH3-only protein BAD, inhibiting BCL-2, BCL-X_L, and BCL-W (9, 10). This profile accounted for both the early anti-tumor activity that was observed in CLL (11) and the dose-limiting toxicity of thrombocytopenia, with BCL-2 inhibition driving the former and BCL-X_L inhibition the latter (12, 13). Based on these findings, drug discovery scientists designed BCL-2-selective agents, such as ABT-199/venetoclax and S55746/BCL201, which maintain killing activity against CLL cells while sparing platelets (8, 14). Venetoclax was the first BCL-2-selective agent to enter the clinic and quickly showed signs of anti-tumor activity. Tumor lysis syndrome (TLS) was observed in two of the first three CLL patients to receive a dose (14) and objective response rates nearing 80% were reported for relapsed/refractory patients, including those with high-risk forms of the disease (15). Based on these and other data, venetoclax was approved by the FDA for use in relapsed/refractory CLL with 17p deletion. A host of other clinical trials are now under way, including combination studies in CLL, acute lymphocytic leukemias, myeloid leukemias, non-Hodgkin lymphomas, and breast cancer [see (16) for review].

PREDICTING MECHANISMS OF RESISTANCE TO VENETOCLAX

As the first encouraging signs of venetoclax activity were being observed in the clinic, translational scientists were already at work, hoping to anticipate mechanisms of resistance that might emerge. Early efforts focused on cancer cell lines that acquired resistance after prolonged culture with venetoclax. By comparing the parental cells to the resistant populations that emerged, a variety of potential resistance mechanisms were identified. Unlike the very specific "gatekeeper" mutations that primarily account for tyrosine kinase inhibitor resistance in CML, a more diverse array of alterations were observed in the cell lines exhibiting venetoclax resistance. Not surprisingly, resistance in some cell lines was associated with elevations in anti-apoptotic proteins such as BCL-X_L or MCL-1 (17), which can serve to back up BCL-2. Conversely, pro-apoptotic proteins like BIM and BAX were seen to be mutated, reduced or even lost in resistant populations (17, 18). There were also some surprising cases, analogous to gatekeeper mutations, in which BH3-binding pocket mutations in BCL-2 reduced venetoclax binding while apparently retaining affinity for endogenous pro-apoptotic ligands. Mutations in phenylalanine 101 (F101C, F101L) of murine Bcl-2 were identified in venetoclax-resistant murine cell lines (18) while, in a separate lab, the corresponding mutation (F103) was observed in a resistant population of the human cancer cell line SC-1 (17). Taken as a whole, these findings indicate that numerous, distinct mechanisms could account for resistance to venetoclax when given as monotherapy.

VENETOCLAX RESISTANCE AND THE TUMOR MICROENVIRONMENT

While these first clues about cancer cell-intrinsic mechanisms of venetoclax resistance were emerging, other labs began to explore the role of extrinsic factors found in the tumor microenvironment. Like normal hematopoietic cells, which rely on interactions with stromal cells and certain immune cells as they develop and differentiate, cancer cells retain a dependence on supportive cells in lymphoid organs such as the bone marrow, spleen and lymph nodes. Within these organs stromal cells and immune cells deposit extracellular matrix and secrete growth factors, chemokines, and interleukins that provide tumor cells with homing, adhesion, growth, proliferation and survival signals [see (19) for an excellent review]. For example, malignant B-cells receive survival signals from supporting T follicular helper (T_{FH}) cells expressing the CD40 ligand (CD40L), which drives NFκB signaling downstream of CD40 engagement. B-cell receptor (BCR) signaling, crucial to normal B-cell survival and development, also remains active in most lymphomas and certain leukemias, either as a function of self-antigen engagement in the tumor microenvironment or through mechanisms that leave the BCR constitutively activated and antigen-independent. Toll-like receptors (TLR) like TLR9 have also shown a role in mediating tumor cell survival signals originating in lymphoid organs.

VENETOCLAX RESISTANCE IN CHRONIC LYMPHOCYTIC LEUKEMIA

Researchers exploring these concepts and their potential impact on venetoclax resistance began to recognize some familiar themes. Just as previous work had demonstrated that kinase

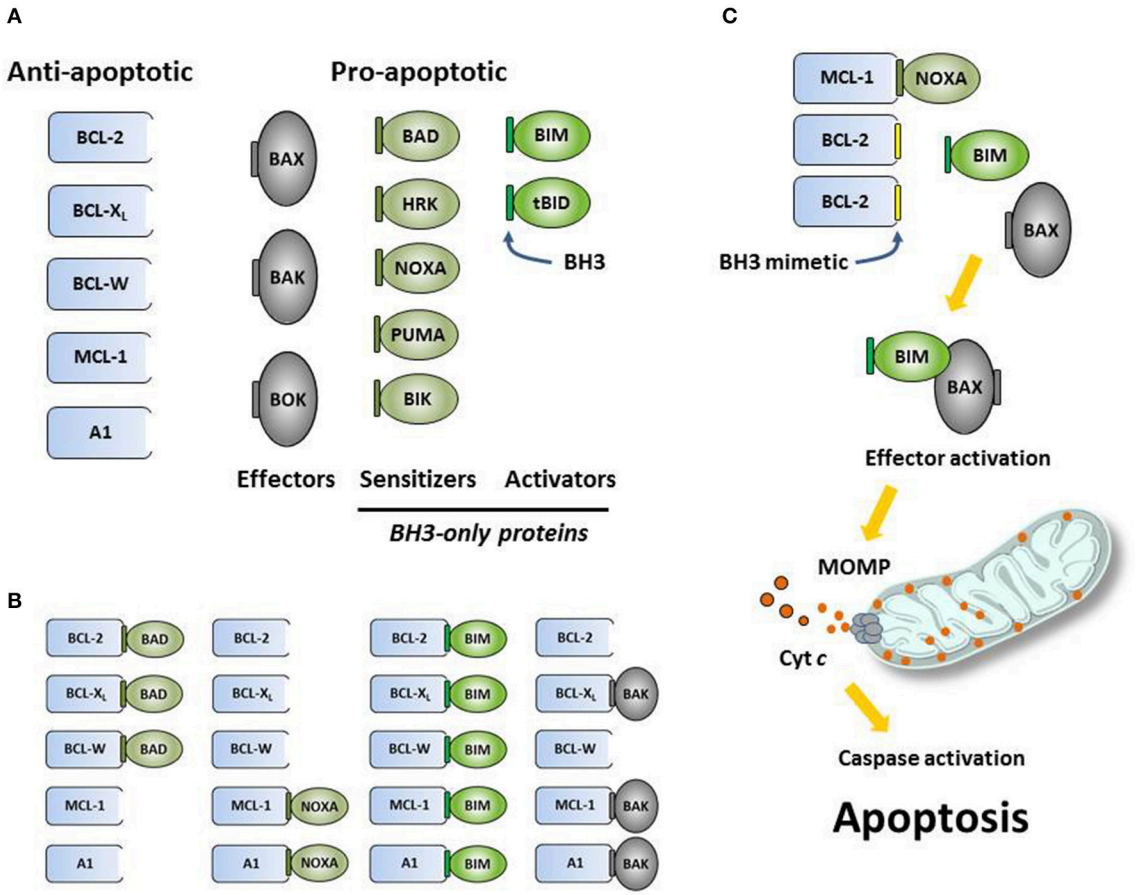

FIGURE 1 | (A) The intrinsic (mitochondrial) pathway of apoptosis is regulated by structurally related proteins in the BCL-2 family, which share from one to four BCL-2 homology (BH1-BH4) motifs. These proteins can be sub-classified as anti-apoptotic (pro-survival) or pro-apoptotic (pro-death). Pro-apoptotic proteins can be further sub-divided into multi-BH effector proteins (BAX, BAK, BOK) and so-called BH3-only proteins. Certain BH3-only proteins like BIM can bind and allosterically activate effector proteins, promoting their insertion into mitochondrial membranes and subsequent oligomerization. Other BH3-only proteins, such as NOXA, can act as sensitizers of apoptosis by binding to anti-apoptotic proteins and precluding their sequestration of pro-apoptotic effectors and activators. **(B)** Anti-apoptotic proteins bind the BH3 motifs (depicted as small, green rectangles) of specific pro-apoptotic proteins, thereby sequestering them and preventing the initiation of apoptosis. Each pro-apoptotic protein demonstrates its own selectivity profile regarding which anti-apoptotic protein(s) it tends to associate with. **(C)** Synthetic small-molecule "BH3 mimetics" (depicted as small, yellow rectangles) like venetoclax are designed to bind certain anti-apoptotic proteins and compete for binding with pro-apoptotic proteins. Pro-apoptotic proteins liberated by BH3 mimetics are free to initiate the key molecular events of programmed cell death, including effector activation, mitochondrial outer membrane permeabilization (MOMP), the release of apoptogenic factors like cytochrome *c* (depicted as small red circles) into the cytosol, the proteolytic activation of caspases and the dismantling of the cell.

signaling cascades downstream of CD40 engagement signal the upregulation of anti-apoptotic proteins like BCL-X_L, MCL-1 and BFL-1/A1 in B-cells (20–24), so CLL cells co-cultured with CD40L-expressing fibroblasts were found to upregulate BCL-X_L, MCL-1 and BFL-1 (25)—changes that rendered these cells essentially insensitive to venetoclax. Consistent with other reports (26), BCL-X_L seemed to play the most prominent role in this resistance, as its siRNA-mediated silencing, but not that of MCL-1, led to some re-sensitization of these cells to venetoclax. Based on the elucidation of signaling pathways known to function downstream of CD40, these teams began to assess kinase inhibitors that might resensitize tumor cells to venetoclax. ABL tyrosine kinase inhibitors like imatinib and dasatinib were able to prevent CD40L-dependent upregulation of BCL-X_L, MCL-1, and BFL-1 and reverse resistance to venetoclax, whereas BCR signaling inhibitors like the BTK inhibitor ibrutinib and the PI3Kδ inhibitor idelalisib had little effect. Similarly, in another study of venetoclax resistance mediated by BCR pathway stimulation, ibrutinib and idelalisib were less effective than the SYK tyrosine kinase inhibitors R406 and entospletinib at reducing MCL-1 levels and sensitizing CLL cells to venetoclax (27). The SYK/JAK inhibitor cerdulatinib has also been shown to synergize with venetoclax by inhibiting the upregulation of BCL-X_L and MCL-1 in CLL cells treated with CD40L and IL-4 or co-cultured with nurse-like cells (28). Significant resistance to the BCL-2/BCL-X_L inhibitor ABT-737 was also observed in CLL cells cultured in the presence of IL-4 and CD115-expressing fibroblasts, which induced the expression of BCL-X_L and BCL2A1 (22). A phase 1 study is currently under way to explore the combination of venetoclax and the SYK

inhibitor TAK-659 for patients with relapsed/refractory NHL (NCT03357627). The cytoplasmic tyrosine kinase LYN has also been implicated as a mediator of microenvironment-mediated CLL cell survival (29) and may play crucial roles in the supporting stromal cells themselves.

Although these studies suggested that BTK inhibitors and PI3K inhibitors may not be ideally suited for counteracting venetoclax resistance when tumor cells are residing in protective niches, it is important to note that these inhibitors are highly effective at mobilizing tumor cells out of those niches into peripheral circulation. In fact, it is common to observe large elevations in circulating lymphocytes (lymphocytosis) in the first 1–2 months of ibrutinib treatment, as abnormal B-cells migrate out of lymphoid organs upon disruption of BCR signaling (30). Based on the co-culture experiments described above, the prediction would be that these cells should be particularly susceptible to venetoclax-mediated killing while in circulation. Indeed, residual tumor cells isolated from the blood of CLL patients taking BTK inhibitors such as ibrutinib or acalabrutinib have been shown to be highly sensitive to venetoclax (31, 32). Similar results were observed when venetoclax was added to mantle cell lymphoma (MCL) cells isolated from circulation after ibrutinib treatment (33). Moreover, early data from clinical studies exploring the combination of venetoclax and ibrutinib have shown impressive objective response rates, including high rates of minimal residual disease (MRD)-negativity (see section below).

Other kinase signaling pathways have also been implicated in stroma-mediated venetoclax resistance. CLL cells collected from peripheral blood were shown to upregulate MCL-1 when co-cultured with NK-tert bone marrow stromal cells (34). Although cyto-protective, the interaction with stromal cells did not induce proliferation of the CLL cells. Stroma-mediated elevations in MCL-1 were associated with increased AKT and MAPK/ERK signaling, which may reduce MCL-1 proteolysis, as well as increased phosphorylation of serine 5 of the RNA polymerase-II C-terminal domain, which is mediated by CDK9 and known to support the elongation of *MCL1* transcripts. Other studies support the idea that combinations with MEK (35) or CDK9 (36–38) inhibitors could enhance venetoclax activity and circumvent resistance, and ongoing clinical studies in acute myeloid leukemia (AML) may soon provide clinical data (see below).

While most early resistance studies focused specifically on alterations in BCL-2 family members (a rational starting point), more recent work has begun to explore venetoclax resistance in an unbiased fashion. For example, Herling et al. performed whole-exome sequencing of samples from CLL patients before receiving venetoclax and after developing resistance (39). Similar to the work done *in vitro*, these studies identified a number of potential resistance-associated alterations, including mutations in *BTG1* or *BRAF*, homozygous deletion of *CDKN2A/B* and high-level focal amplification of *CD274*, the gene encoding the immune checkpoint protein PD-L1. Although the sample size of this study was small ($n = 8$) and the causative role of these potential resistance mutations remain to be confirmed, it is anticipated that data accrued from this and similar unbiased analyses will continue to define novel venetoclax resistance mechanisms.

VENETOCLAX RESISTANCE IN NON-HODGKIN LYMPHOMAS

Although the early results from venetoclax studies in CLL were highly encouraging, data from studies in follicular lymphoma (FL) and diffuse large B-cell lymphomas (DLBCL) have been less compelling. In a monotherapy study, objective response rates of 38 and 18% were reported for FL and DLBCL, respectively (40). These results were somewhat perplexing, given the fact that these tumors are often defined by the *t*(14;18) translocation, which drives high-level expression of BCL-2 in most cases. Although preclinical studies using FL and DLBCL cell lines had suggested a strong correlation between *t*(14;18)-positivity or *BCL2* gene amplification and sensitivity to venetoclax *in vitro* (14), the link does not seem as strong in the clinic. While disappointing, this may not be surprising given the potential intratumoral heterogeneity of BCL-2 expression in follicular lymphomas (41). One possibility is that the *t*(14;18) translocation is a crucial driver of tumor initiation but, as the cancer evolves, becomes dispensable for survival and tumor maintenance.

In a recent study, *t*(14;18)-positive lymphoma cells were treated with venetoclax for an extended period to induce resistance (42). Comparing the venetoclax-resistant and parental cell lines, the resistant FL cells had significantly higher levels of ERK1/2 and BIM phosphorylation at serine 69. Phosphorylation of BIM at serine 69 has been shown to target BIM for proteasomal degradation, thus reducing the pro-apoptotic priming of the cells (43). Targeting the cell surface protein CD20 with the chimeric monoclonal antibody rituximab prevented the phosphorylation of ERK1/2 and BIM, and improved the activity of venetoclax in xenograft models of these FL cells (42). Similar findings were reported in MCL (44).

The influence of the tumor microenvironment in lymphomas (19) could also account for the weaker-than-expected efficacy signals. FL cells are known to split time between peripheral circulation and germinal centers, where processes like activation-induced cytidine deaminase (AID)-mediated mutagenesis could drive clonal evolution and acquired dependencies on other anti-apoptotic proteins (45). Similarly, lymphoma cells may simply upregulate other BCL-2 family survival proteins while residing in lymph nodes, making them distinct from cell lines that are cultured in monolayers *in vitro*. Indeed, MCL cells co-cultured with CD40L-expressing fibroblasts were shown to express elevated levels of BCL-X_L downstream of NFκB signaling (33, 44). Jayappa et al. described a similar mechanism in response to CD40, IL-10 or TLR9 agonists that can account for the resistance of MCL cells to venetoclax-ibrutinib combinations (46).

VENETOCLAX RESISTANCE IN MYELOID MALIGNANCIES AND MULTIPLE MYELOMA

Although most of its early clinical trials were focused on B-cell malignancies like CLL and NHLs, venetoclax has also begun to show activity in myeloid malignancies. For example, a Phase 2 study exploring venetoclax as monotherapy in patients with relapsed/refractory AML reported a 19% objective response rate

(47), though the durability of responses was limited. Sequencing of paired patient samples from that study indicated that FMS-like tyrosine kinase (FLT3) mutations are associated with basal and acquired resistance (48), and so combinations with FLT3 inhibitors like quizartinib or gilteritinib would therefore represent rational combinations. Venetoclax combinations with standard-of-care agents such as hympomethylating agents (HMAs) and low-dose cytarabine (LoDAC) are already being explored in elderly, treatment-naïve populations who are unfit for high-intensity induction regimens. Objective response rates (ORR), which include complete responses (CR), complete responses with incomplete bone marrow recovery (CRi) and partial responses (PR), have been reported as 62% for combination with LoDAC (49) and 61–67% for combinations with HMAs (50, 51)—well above historical values reported for those agents on their own. Based on these data, the FDA granted breakthrough therapy designation for both combinations. Venetoclax combinations with CDK9 inhibitors like alvocidib (NCT03441555) or dinaciclib (NCT03484520) are also being pursued, with the hypothesis that these agents will synergize with venetoclax based on their ability to inhibit MCL-1 expression [see (36–38)]. There is also optimism that BH3 mimetics such as AMG176, which can inhibit MCL-1 directly [see (8) for review], will prove safe enough in ongoing AML and multiple myeloma studies (NCT02675452) to combine with venetoclax.

Plasma cells are known to depend on MCL-1 for survival and, following malignant transformation, multiple myeloma cells appear to preserve this dependency. However, studies using cell lines or *ex vivo* cultures of patient cells treated with venetoclax or ABT-737 have shown that there are also subsets of myeloma cells that are primarily BCL-2-dependent (52, 53). A Phase 1 trial of venetoclax monotherapy showed that myeloma patients with *t*(11;14)-positive tumors, which tend to express high levels of BCL-2 and low levels of BCL-X_L and MCL-1, showed an objective response rate of 40% (54). In the non-*t*(11;14) population, BCL-X_L and/or MCL-1 are likely to play a larger role in maintaining myeloma cell survival, and the tumor microenvironment likely plays a role in driving their expression. Some studies have indicated that bone marrow stromal cell-derived cytokine Interleukin-6 (IL-6) can upregulate MCL-1 and BCL-X_L expression in myeloma cells, thus providing a possible mechanism of resistance to venetoclax (55). More recent studies have revealed that IL-6 may also influence sensitivity to venetoclax through mechanisms other than regulating the expression of BCL-2 family proteins (56). Using an immortalized bone marrow stromal cell line or conditioned media from these cells, the authors induced resistance to either venetoclax or ABT-737 in myeloma cell lines, and this resistance was reversed by a neutralizing IL-6 antibody. Interestingly, IL-6 did not alter the expression of BCL-2 family member proteins but instead shifted BIM binding from BCL-2/BCL-X_L to MCL-1. This shift in priming occurred through the ERK1/2-mediated phosphorylation of serines 69 and 77 on BIM, similar to an acquired resistance mechanism observed with venetoclax in FL (42). As a result, the shift to MCL-1:BIM priming, and thus MCL-1 dependence, was prevented by inhibitors of either JAK1/2 or MEK signaling pathways.

Despite the observed synergy between JAK and BCL-2/BCL-X_L inhibition in myeloma it was unclear whether the tumor microenvironment plays a similar role in other malignancies, and whether JAK inhibitors might combine with venetoclax to counteract bone marrow stroma-mediated resistance in those diseases. One team screening a panel of 304 inhibitors against AML patient samples identified bone marrow stromal cell conditions that significantly reduced responses to around 10% of the molecules (57). In the presence of cytokines from stromal cell-conditioned media, AML cell killing mediated by venetoclax was significantly lower. The cytokines activated JAK/STAT signaling to support AML cell proliferation and survival and decreased the expression of BCL-2 relative to BCL-X_L. Unlike multiple myeloma, where IL-6 was found to be crucial, GM-CSF was the essential stroma-derived factor for AML cell survival. The JAK2 inhibitor ruxolitinib was more active in the presence of the cytokine-rich media and, when combined with venetoclax, demonstrated synergistic killing activity. This result was recapitulated in a systemic xenograft model of AML. Another team employing an *ex vivo* drug sensitivity profiling screen using freshly isolated patient samples identified the venetoclax-ruxolitinib combination as the most active in killing malignant myeloid cells (58). Despite the lack of stromal cell culture media in these screens, drug sensitivity was evaluated *ex vivo* within 24 h of sample collection, which may have preserved the bone marrow stromal effects.

Most of the tumor cell resistance mechanisms described here have focused on the modulation of BCL-2 family proteins that can occur downstream of stromal cell engagement. However, the interplay between tumor cells and cells in their microenvironment may be even more complex. Intriguing new work has begun to show that metabolites and organelles, including some as large as mitochondria, can be transferred between cells, including cancer cells and their "normal" neighbors in tumor microenvironments. One study recently described how AML cells, which are thought to be reliant on oxidative phosphorylation (OxPhos) to generate energy, can (mis)appropriate the mitochondria of stromal cells in the bone marrow, with the apparent survival benefit of enhanced OxPhos capacity. In an elegant series of experiments, Marlein et al. showed that AML cells can accomplish this mitochondrial pilfering through the use of tunneling nanotubes (TNTs), filamentous actin-based structures that may exceed 200 nm in diameter (59). In order to visualize this process, the plasma membranes of AML cells were labeled with a red dye to distinguish them from co-cultured bone marrow stromal cells. The latter were labeled with green Mito tracker, making it possible to track the localization and any inter-cellular migrations of stromal cell mitochondria. Intriguingly, red-labeled TNTs could be observed extending out from AML cells to contact neighboring stromal cells. In addition, speckles of red dye could be observed pock-marking the surface of stromal cells that had thus been probed. These TNT access points, or "TAPs," seemed to be concentrated on specific stromal cells, which the investigators took as a clue that some form of active signaling

might be involved. The group went on to show that NADPH oxidase-2 (NOX2) on the surface of AML cells may produce concentrated zones of superoxide, which stromal cells read as a signal to increase production of mitochondria. Indeed, proliferator-activated receptor gamma coactivator 1-alpha (PGC-1α) signaling was found to be upregulated in the stromal cells, and drove the increased expression of genes encoding mitochondrial components (60). Once this crop of mitochondria has been produced, the AML cells begin TAPping these cells to harvest the mitochondria and reap the benefit of their enhanced OxPhos capacity.

It is tempting to speculate that AML cells thus acquiring "foreign" mitochondria, could acquire a new BCL-2 family dependence profile based on the complement of anti-apoptotic proteins populating those mitochondria. While these mitochondrial profiles would not be inherited permanently (BCL-2 family proteins are not encoded by mitochondrial genes), it is conceivable that such a mechanism could provide enough survival advantage to promote the outgrowth of certain sub-clones. It will be interesting to see how this nascent field matures and whether therapeutic strategies to target these microenvironment-driven mechanisms prove effective.

OVERCOMING TUMOR MICROENVIRONMENT-MEDIATED VENETOCLAX RESISTANCE

Based on the mechanisms of venetoclax resistance that have been observed preclinically, a number of rational combination hypotheses have emerged. For example, CD20 antibodies such as rituximab and obinutuzumab were shown to reverse venetoclax resistance that occurred when CLL cells were co-cultured with stromal cells (25). Because these agents are standards-of-care for many B-cell malignancies, their combination with venetoclax was already being explored clinically. Strong activity in a single-arm Phase 1b study of relapsed/refractory CLL combining venetoclax with rituximab (ORR: 86%, CR: 51%, MRD-negativity in bone marrow: 57%; $n = 49$) (61) led to the granting of breakthrough therapy designation by the FDA, and data were recently reported for the randomized Phase 3 study MURANO (62), which compared venetoclax-rituximab to the combination of rituxumab and the alkylating agent bendamustine in patients with relapsed/refractory CLL. That study reported an ORR of 93.3% and a CR/CRi rate of 26.8% for the venetoclax-rituximab arm, per investigator assessments (ORR: 92.3%, CR/CRi: 8.2% by independent review committee). The median progression-free survival (mPFS) of patients receiving venetoclax-rituximab ($n = 194$) had not been reached after a median follow-up of 24.8 months, compared to a median PFS (investigator-assessed) of 17 months for the bendamustine-rituximab arm ($n = 195$) (hazard ratio: 0.17, 95% confidence interval: 0.11–0.25, $p = 0.0001$). Independent review committee assessments were similar, with mPFS for the venetoclax-rituximab arm not reached, vs. 18.1 months for patients receiving bendamustine-rituximab (hazard ratio: 0.19, 95% confidence interval: 0.13–0.28, $p = 0.0001$). These data led the FDA to grant full approval of venetoclax in combination with rituximab for patients with CLL having received at least one prior therapy. A Phase 1b study of venetoclax plus obinutuzumab in previously untreated CLL reported an ORR of 100% and a CR/CRi rate of 72% ($n = 32$) (63). Similarly, the CLL14 Phase 3 study (venetoclax plus obinutuzumab in previously untreated CLL patients with coexisting medical conditions) reported an ORR of 100% and a CR rate of 58%, with MRD-negativity in peripheral blood of 92% ($n = 12$) (64).

Based on their ability to mobilize leukemia cells out of protective lymphoid niches, BCR pathway inhibitors are also being explored in combination with venetoclax. An initial period of tumor debulking is typically implemented with the mobilizing agent alone to mitigate the risk of tumor lysis syndrome associated with venetoclax. Results from ongoing studies of venetoclax and ibrutinib have been particularly promising. In the CLARITY study, an objective response rate of 100% was reported, with 60% CR/CRi ($n = 25$) (65). When assessed in bone marrow, an MRD-negativity rate of 28% was observed. A separate Phase 2 study of venetoclax combined with ibrutinib includes a cohort of treatment-naïve CLL patients and has reported an overall response rate of 100%, with CR/CRi and MRD-negativity rates increasing over time (CR/CRi: 61%, MRD-negativity: 21% after 3 months of combination, $n = 33$; CR/CRi: 75%, MRD-negativity: 45% after 6 months of combination, $n = 20$; CR/CRi: 80%, MRD-negativity: 80% after 9 months of combination, $n = 10$) (66). There are also preclinical data demonstrating synergy between venetoclax and PI3K inhibitors like the PI3Kδ inhibitor idelalisib and the dual PI3Kδ/PI3Kγ inhibitor duvelisib (67). SYK inhibitors like entospletinib (27) or cerdulatinib (28) have also shown promise preclinically. The cytoplasmic tyrosine kinase LYN may also be a good target, having roles in BCR signaling as well as in cells of the tumor microenvironment (29).

CONCLUSION AND FUTURE DIRECTIONS

The studies described here are excellent examples of how preclinical data can inform improved clinical strategies. With the identification of potential mechanisms of venetoclax resistance mechanisms have come clear hypotheses for combination strategies to avert or reverse it. Some of these hypotheses are already being tested clinically and are showing signs of promise. Venetoclax combinations with CD20 antibodies or BCR pathway inhibitors have shown clear improvements in efficacy relative to the respective monotherapies. Moreover, improved depth-of-response and increased rates of MRD-negativity have also been observed, raising hopes that some CLL patients could discontinue treatment and experience extended treatment-free periods. However, some questions still remain about how the tumor microenvironment influences venetoclax sensitivity, even in CLL.

According to the 2008 International Workshop for CLL response criteria, a patient's disease must show not only a major reduction in circulating tumor burden (blood lymphocytes <4,000/μL), but also a reduction in the size of all affected lymph nodes (with none measuring >15 mm), an elimination

of any splenomegaly or hepatomegaly, and a clearance of the bone marrow (normocellular, with <30% lymphocytes and no B lymphoid nodules) to qualify as a complete response. Therefore, the CRs described in studies to-date indicate that, at least in some CLL patients, venetoclax is able to significantly reduce tumor burden not only in the periphery, but also in primary and secondary lymphatic sites. Although these data seem inconsistent with factors in the lymph nodes and bone marrow mediating resistance to venetoclax, it is not clear whether venetoclax is actually killing tumor cells *in situ* (within these compartments) or simply triggering apoptosis of cells that have temporarily migrated away from their protective niches. It is possible that, when compared to the rapid clearance of circulating tumor cells, the extended amount of time required for venetoclax to clear lymph nodes and bone marrow reflects the protective impact of the microenvironment and the kinetics of tumor cell migration into and out of those niches. The kinetics of venetoclax-mediated reductions in lymphadenopathy and the clearance of disease from bone marrow have not been examined exhaustively, and so it is possible that these effects are actually occurring more rapidly than the current schedule of assessments would indicate. It would be interesting to assess the kinetics and localization of apoptosis by real-time live imaging or other approaches that could shed light on the drug's mechanisms of action.

Because BCL-2 plays such an important role in the development and shaping of the immune system it will also be interesting to explore how venetoclax may impact tumor microenvironments. Might potent BCL-2 inhibition lead to reductions or enrichments in tumor-infiltrating immune cells such as dendritic cells, natural killer cells, myeloid derived suppressor cells, and various B- and T-cell populations? If so, what might be the impact of venetoclax on the efficacy of other immune-modulators? Such combination trials have recently been initiated, and so answers will likely be forthcoming.

These are only a few examples of questions that remain and, clearly, much work remains to be done as we continue to explore ways to harness the activity of BCL-2-selective inhibitors for cancer therapy. As clinical data mature, the oncology community will doubtless continue to refine treatment approaches. At the same time, the hope is that ongoing work in the research community will continue to enhance our understanding of resistance and point the way toward improved therapies for people with cancer.

AUTHOR CONTRIBUTIONS

JL and DC participated in the conception and writing of this review.

REFERENCES

1. Tsujimoto Y, Finger LR, Yunis J, Nowell PC, Croce CM. Cloning of the chromosome breakpoint of neoplastic B cells with the t(14;18) chromosome translocation. *Science* (1984) 226:1097–9. doi: 10.1126/science.6093263
2. Vaux DL, Cory S, Adams JM. Bcl-2 gene promotes haemopoietic cell survival and cooperates with c-myc to immortalize pre-B cells. *Nature* (1988) 335:440–2. doi: 10.1038/335440a0
3. Reed JC, Cuddy M, Slabiak T, Croce CM, Nowell PC. Oncogenic potential of bcl-2 demonstrated by gene transfer. *Nature* (1988) 336:259–61. doi: 10.1038/336259a0
4. Hockenberry D, Nunez G, Milliman C, Schreiber RD, Korsmeyer SJ. Bcl-2 is an inner mitochondrial membrane protein that blocks programmed cell death. *Nature* (1990) 348:334–6. doi: 10.1038/348334a0
5. McDonnell TJ, Deane N, Platt FM, Nunez G, Jaeger U, McKearn JP, et al. Bcl-2-immunoglobulin transgenic mice demonstrate extended B cell survival and follicular lymphoproliferation. *Cell* (1989) 57:79–88.
6. Czabotar PE, Lessene G, Strasser A, Adams JM. Control of apoptosis by the BCL-2 protein family: implications for physiology and therapy. *Nat Rev Mol Cell Biol*. (2014) 15:49–63. doi: 10.1038/nrm3722
7. Certo M, Del Gaizo Moore V, Nishino M, Wei G, Korsmeyer S, Armstrong SA, et al. Mitochondria primed by death signals determine cellular addiction to antiapoptotic BCL-2 family members. *Cancer Cell* (2006) 9:351–65. doi: 10.1016/j.ccr.2006.03.027
8. Ashkenazi A, Fairbrother WJ, Leverson JD, Souers AJ. From basic apoptosis discoveries to advanced selective BCL-2 family inhibitors. *Nat Rev Drug Discov*. (2017) 16:273–84. doi: 10.1038/nrd.2016.253
9. Oltersdorf T, Elmore SW, Shoemaker AR, Armstrong RC, Augeri DJ, Belli BA, et al. An inhibitor of Bcl-2 family proteins induces regression of solid tumors. *Nature* (2005) 435:677–81. doi: 10.1038/nature03579
10. Tse C, Shoemaker AR, Adickes J, Anderson MG, Chen J, Jin S, et al. ABT-263: A Potent and orally bioavailable Bcl-2 family inhibitor. *Cancer Res*. (2008) 68:3421–8. doi: 10.1158/0008-5472.CAN-07-5836
11. Roberts AW, Seymour JF, Brown JR, Wierda WG, Kipps TJ, Khaw SL, et al. Substantial susceptibility of chronic lymphocytic leukemia to BCL2 inhibition: results of a phase I study of navitoclax in patients with relapsed or refractory disease. *J Clin Oncol*. (2012) 30:488–96. doi: 10.1200/JCO.2011.34.7898
12. Zhang H, Nimmer PM, Tahir SK, Chen J, Fryer RM, Hahn KR, et al. Bcl-2 family proteins are essential for platelet survival. *Cell Death Differ*. (2007) 14:943–51. doi: 10.1038/sj.cdd.4402081
13. Mason KD, Carpinelli MR, Fletcher JI, Collinge JE, Hilton AA, Ellis S, et al. Programmed anuclear cell death delimits platelet life span. *Cell* (2007) 128:1173–86. doi: 10.1016/j.cell.2007.01.037
14. Souers AJ, Leverson JD, Boghaert ER, Ackler SL, Catron ND, Chen J, et al. ABT-199, a potent and selective BCL-2 inhibitor, achieves antitumor activity while sparing platelets. *Nat Med*. (2013) 19:202–8. doi: 10.1038/nm.3048
15. Roberts AW, Davids MS, Pagel JM, Kahl BS, Puvvada SD, Gerecitano JF, et al. Targeting BCL2 with venetoclax in relapsed chronic lymphocytic leukemia. *N Engl J Med*. (2016) 374:311–22. doi: 10.1056/NEJMoa1513257
16. Leverson JD, Sampath D, Souers AJ, Rosenberg SH, Fairbrother WJ, Amiot M, et al. Found in translation: how preclinical research is guiding the clinical development of the BCL-2 selective inhibitor venetoclax. *Cancer* Discov. (2017) 7:1376–93. doi: 10.1158/2159-8290.CD-17-0797
17. Tahir SK, Smith M, Hessler P, Roberts-Rapp L, Idler KP, Park CH, et al. Potential mechanisms of resistance to venetoclax and strategies to circumvent it. *BMC Cancer* (2017) 17:399. doi: 10.1186/s12885-017-3383-5
18. Fresquet V, Rieger M, Carolis C, García-Barchino MJ, Martinez-Climent JA. Acquired mutations in BCL2 family proteins conferring resistance to the BH3 mimetic ABT-199 in lymphoma. *Blood* (2014) 123:4111–9. doi: 10.1182/blood-2014-03-560284
19. Scott DW, Gascoyne RD. The tumour microenvironment in B cell lymphomas. *Nat Rev Cancer* (2014) 14:517–34. doi: 10.1038/nrc3774
20. Lee HH, Dadgostar H, Cheng Q, Shu J, Cheng G. NF-kappaB-mediated up-regulation of Bcl-x and Bfl-1/A1 is required for CD40 survival signaling in B lymphocytes. *Proc Natl Acad Sci USA*. (1999) 96:9136–41. doi: 10.1073/pnas.96.16.9136
21. Pedersen IM, Kitada S, Leoni LM, Zapata JM, Karras JG, Tsukada N, et al. Protection of CLL B cells by a follicular dendritic cell line is dependent on induction of Mcl-1. *Blood* (2002) 100:1795–801.
22. Vogler M, Butterworth M, Majid A, Walewska RJ, Sun XM, Dyer MJ, et al. Concurrent up-regulation of BCL-XL and BCL2A1 induces approximately

1000-fold resistance to ABT-737 in chronic lymphocytic leukemia. *Blood* (2009) 113:4403–13. doi: 10.1182/blood-2008-08-173310
23. Tromp JM, Tonino SH, Elias JA, Jaspers A, Luijks DM, Kater AP, et al. Dichotomy in NF-kappaB signaling and chemoresistance in immunoglobulin variable heavy-chain-mutated versus unmutated CLL cells upon CD40/TLR9 triggering. *Oncogene* (2010) 29:5071–82. doi: 10.1038/onc.2010.248
24. Tromp JM, Geest CR, Breij EC, Elias JA, van Laar J, Luijks DM, et al. Tipping the Noxa/Mcl-1 balance overcomes ABT-737 resistance in chronic lymphocytic leukemia. *Clin Cancer Res*. (2012) 18:487–98. doi: 10.1158/1078-0432.CCR-11-1440
25. Thijssen R, Slinger E, Weller K, Geest CR, Beaumont T, van Oers MH, et al. Resistance to ABT-199 induced by microenvironmental signals in chronic lymphocytic leukemia can be counteracted by CD20 antibodies or kinase inhibitors. *Haematologica* (2015) 100:e302–6. doi: 10.3324/haematol.2015.124560
26. Oppermann S, Ylanko J, Shi Y, Hariharan S, Oakes CC, Brauer PM, et al. High-content screening identifies kinase inhibitors that overcome venetoclax resistance in activated CLL cells. *Blood* (2016) 128:934–47. doi: 10.1182/blood-2015-12-687814
27. Bojarczuk K, Sasi BK, Gobessi S, Innocenti I, Pozzato G, Laurenti L, et al. BCR signaling inhibitors differ in their ability to overcome Mcl-1-mediated resistance of CLL B cells to ABT-199. *Blood* (2016) 127:3192–201. doi: 10.1182/blood-2015-10-675009
28. Blunt MD, Koehrer S, Dobson RC, Larrayoz M, Wilmore S, Hayman A, et al. The dual SYK/JAK inhibitor cerdulatinib antagonizes B-cell receptor and microenvironmental signaling in chronic lymphocytic leukemia. *Clin Cancer Res*. (2017) 23:2313–24. doi: 10.1158/1078-0432.CCR-16-1662
29. Nguyen PH, Fedorchenko O, Rosen N, Koch M, Barthel R, Winarski T, et al. LYN kinase in the tumor microenvironment is essential for the progression of chronic lymphocytic leukemia. *Cancer Cell* (2016) 30:610–22. doi: 10.1016/j.ccell.2016.09.007
30. Byrd JC, Furman RR, Coutre SE, Flinn IW, Burger JA, Blum KA, et al. Targeting BTK with ibrutinib in relapsed chronic lymphocytic leukemia. *N Engl J Med*. (2013) 369:32–42. doi: 10.1056/NEJMoa1215637
31. Cervantes-Gomez F, Lamothe B, Woyach JA, Wierda WG, Keating MJ, Balakrishnan K, et al. Pharmacological and protein profiling suggests venetoclax (ABT-199) as optimal partner with ibrutinib in chronic lymphocytic leukemia. *Clin Cancer Res*. (2015) 21:3705–15. doi: 10.1158/1078-0432.CCR-14-2809
32. Deng J, Isik E, Fernandes SM, Brown JR, Letai A, Davids MS. Bruton's tyrosine kinase inhibition increases BCL-2 dependence and enhances sensitivity to venetoclax in chronic lymphocytic leukemia. *Leukemia* (2017) 31:2075–84. doi: 10.1038/leu.2017.32
33. Chiron D, Dousset C, Brosseau C, Touzeau C, Maïga S, Moreau P, et al. Biological rationale for sequential targeting of Bruton tyrosine kinase and Bcl-2 to overcome CD40-induced ABT-199 resistance in mantle cell lymphoma. *Oncotarget* (2015) 6:8750–9. doi: 10.18632/oncotarget.3275
34. Balakrishnan K, Burger JA, Fu M, Doifode T, Wierda WG, Gandhi V. Regulation of Mcl-1 expression in context to bone marrow stromal microenvironment in chronic lymphocytic leukemia. *Neoplasia* (2014) 116:1036–46. doi: 10.1016/j.neo.2014.10.002
35. Crassini K, Shen Y, Stevenson WS, Christopherson R, Ward C, Mulligan SP, et al. MEK1/2 inhibition by binimetinib is effective as a single agent and potentiates the actions of Venetoclax and ABT-737 under conditions that mimic the chronic lymphocytic leukaemia (CLL) tumour microenvironment. *Br J Haematol*. (2018). doi: 10.1111/bjh.15282. [Epub ahead of print].
36. Li L, Pongtornpipat P, Tiutan T, Kendrick SL, Park S, Persky DO, et al. Synergistic induction of apoptosis in high-risk DLBCL by BCL2 inhibition with ABT-199 combined with pharmacologic loss of MCL1. *Leukemia* (2015) 29:1702–12. doi: 10.1038/leu.2015.99
37. Phillips DC, Xiao Y, Lam LT, Litvinovich E, Roberts-Rapp L, Souers AJ, et al. Loss in MCL-1 function sensitizes non-Hodgkin's lymphoma cell lines to the BCL-2-selective inhibitor venetoclax (ABT-199). *Blood Cancer J*. (2016) 6:e403. doi: 10.1038/bcj.2016.12
38. Zhou L, Zhang Y, Sampath D, Leverson J, Dai Y, Kmieciak M. Flavopiridol enhances ABT-199 sensitivity in unfavourable-risk multiple myeloma cells *in vitro* and *in vivo*. *Br J Cancer* (2018) 118:388–97. doi: 10.1038/bjc.2017.432
39. Herling CD, Abedpour N, Weiss J, Schmitt A, Jachimowicz RD, Merkel O, et al. Clonal dynamics towards the development of venetoclax resistance in chronic lymphocytic leukemia. *Nat Commun*. (2018) 9:727. doi: 10.1038/s41467-018-03170-7
40. Davids MS, Roberts AW, Seymour JF, Pagel JM, Kahl BS, Wierda WG, et al. Phase I first-in-human study of venetoclax in patients with relapsed or refractory non-Hodgkin lymphoma. *J Clin Oncol*. (2017) 35:826–33. doi: 10.1200/JCO.2016.70.4320
41. Barreca A, Martinengo C, Annaratone L, Righi L, Chiappella A, Ladetto M, et al. Inter- and intratumoral heterogeneity of BCL2 correlates with IgH expression and prognosis in follicular lymphoma. *Blood Cancer J*. (2014) 4:e249. doi: 10.1038/bcj.2014.67
42. Bodo J, Zhao X, Durkin L, Souers AJ, Phillips DC, Smith MR, et al. Acquired resistance to venetoclax (ABT-199) in t(14;18) positive lymphoma cells. *Oncotarget* (2016) 7:70000–10. doi: 10.18632/oncotarget.12132
43. Luciano F, Jacquel A, Colosetti P, Herrant M, Cagnol S, Pages G, et al. Phosphorylation of Bim-EL by Erk1/2 on serine 69 promotes its degradation via the proteasome pathway and regulates its proapoptotic function. *Oncogene* (2003) 22:6785–93. doi: 10.1038/sj.onc.1206792
44. Chiron D, Bellanger C, Papin A, Tessoulin B, Dousset C, Maiga S, et al. Rational targeted therapies to overcome microenvironment-dependent expansion of mantle cell lymphoma. *Blood* (2016) 128:2808–18. doi: 10.1182/blood-2016-06-720490
45. Sungalee S, Mamessier E, Morgado E, Grégoire E, Brohawn PZ, Morehouse CA, et al. Germinal center reentries of BCL2-overexpressing B cells drive follicular lymphoma progression. *J Clin Invest*. (2014) 124:5337–51. doi: 10.1172/JCI72415
46. Jayappa KD, Portell CA, Gordon VL, Capaldo BJ, Bekiranov S, Axelrod MJ, et al. Microenvironmental agonists generate de novo phenotypic resistance to combined ibrutinib plus venetoclax in CLL and MCL. *Blood Adv*. (2017) 1:933–46. doi: 10.1182/bloodadvances.2016004176
47. Konopleva M, Pollyea DA, Potluri J, Chyla B, Hogdal L, Busman T, et al. Efficacy and biological correlates of response in a phase II study of venetoclax monotherapy in patients with acute myelogenous leukemia. *Cancer Discov*. (2016) 6:1106–17. doi: 10.1158/2159-8290.CD-16-0313
48. Chyla B, Daver N, Doyle K, McKeegan E, Huang X, Ruvolo V, et al. Genetic biomarkers of sensitivity and resistance to venetoclax monotherapy in patients with relapsed acute myeloid leukemia. *Am. J. Hematol.* (2018). doi: 10.1002/ajh.25146. [Epub ahead of print].
49. Wei A, Strickland SA, Roboz GJ, Hou J-Z, Fiedler W, Lin TL, et al. Phase 1/2 study of venetoclax with low-dose cytarabine in treatment-naive, elderly patients with acute myeloid leukemia unfit for intensive chemotherapy: 1-year outcomes. *Blood* (2017) 130:890.
50. DiNardo CD, Pollyea DA, Jonas BA, Konopleva M, Pullarkat V, Wei A, et al. Updated safety and efficacy of venetoclax with decitabine or azacitidine in treatment-naive, elderly patients with acute myeloid leukemia. *Blood* (2017) 130:2628.
51. DiNardo CD, Pratz KW, Letai A, Jonas BA, Wei AH, Thirman M, et al. Safety and preliminary efficacy of venetoclax with decitabine or azacitidine in elderly patients with previously untreated acute myeloid leukaemia: a non-randomised, open-label, phase 1b study. *Lancet Oncol*. (2018) 19:216–28. doi: 10.1016/S1470-2045(18)30010-X
52. Bodet L, Gomez-Bougie P, Touzeau C, Dousset C, Descamps G, Maiga S, et al. ABT-737 is highly effective against molecular subgroups of multiple myeloma. *Blood* (2011) 118:3901–10. doi: 10.1182/blood-2010-11-317438
53. Touzeau C, Dousset C, Le Gouill S, Sampath D, Leverson JD, Souers AJ, et al. The Bcl-2 specific BH3 mimetic ABT-199: a promising targeted therapy for t(11;14) multiple myeloma. *Leukemia* (2014) 28:210–2. doi: 10.1038/leu.2013.216
54. Kumar S, Kaufman JL, Gasparetto C, Mikhael J, Vij R, Pegourie B, et al. Efficacy of venetoclax as targeted therapy for relapsed/refractory t(11;14) multiple myeloma. *Blood* (2017) 130:2401–9. doi: 10.1182/blood-2017-06-788786
55. Puthier D, Derenne S, Barillé S, Moreau P, Harousseau JL, Bataille R, et al. Mcl-1 and Bcl-xL are co-regulated by IL-6 in human myeloma cells. *Br. J. Haematol*. (1999) 107:392–5. doi: 10.1046/j.1365-2141.1999.01705.x
56. Gupta VA, Matulis SM, Conage-Pough JE, Nooka AK, Kaufman JL, Lonial S, et al. Bone marrow microenvironment-derived signals induce

Mcl-1 dependence in multiple myeloma. *Blood* (2017) 129:1969–79. doi: 10.1182/blood-2016-10-745059
57. Karjalainen R, Pemovska T, Popa M, Liu M, Javarappa KK, Majumder MM, et al. JAK1/2 and BCL2 inhibitors synergize to counteract bone marrow stromal cell-induced protection of AML. *Blood* (2017) 130:789–802. doi: 10.1182/blood-2016-02-699363
58. Kurtz SE, Eide CA, Kaempf A, Khanna V, Savage SL, Rofelty A, et al. Molecularly targeted drug combinations demonstrate selective effectiveness for myeloid- and lymphoid-derived hematologic malignancies. *Proc Natl Acad Sci USA*. (2017) 114:E7554–63. doi: 10.1073/pnas.1703094114
59. Marlein CR, Zaitseva L, Piddock RE, Robinson SD, Edwards DR, Shafat MS, et al. NADPH oxidase-2 derived superoxide drives mitochondrial transfer from bone marrow stromal cells to leukemic blasts. *Blood* (2017) 130:1649–60. doi: 10.1182/blood-2017-03-772939
60. Marlein C, Zaitseva L, Piddock RE, Shafat MS, Collins A, Bowles KM, et al. PGC1α-driven mitochondrial biogenesis within the bone marrow stromal cells of the AML micro-environment is a pre-requisite for mitochondrial transfer to leukemic blasts. *Blood* (2017) 130:3927.
61. Seymour JF, Ma S, Brander DM, Choi MY, Barrientos J, Davids MS, et al. Venetoclax plus rituximab in relapsed or refractory chronic lymphocytic leukaemia: a phase 1b study. *Lancet Oncol*. (2017) 18:230–40. doi: 10.1016/S1470-2045(17)30012-8
62. Seymour JH, Kipps TJ, Eichhorst BF, Hillmen P, D'Rozario JM, Assouline S, et al. Venetoclax plus rituximab is superior to bendamustine plus rituximab in patients with relapsed/refractory chronic lymphocytic leukemia - Results from pre-planned interim analysis of the randomized phase 3 MURANO study. *Blood* (2017) 130:LBA-2.
63. Flinn IW, Gribben J, Dyer MJS, Wierda W, Maris MB, Furman RR, et al. Safety, efficacy and MRD negativity of a combination of venetoclax and obinutuzumab in patients with previously untreated chronic lymphocytic leukemia: results from a phase Ib study (GP28331). *Blood* (2017) 130:430.
64. Fischer K, Al-Sawaf O, Fink AM, Dixon M, Bahlo J, Warburton S, et al. Venetoclax and obinutuzumab in chronic lymphocytic leukemia. *Blood* (2017) 129:2702–5. doi: 10.1182/blood-2017-01-761973
65. Hillmen P, Munir T, Rawstron A, Brock K, Munoz Vicente S, Yates F, et al. Initial results of ibrutinib plus venetoclax in relapsed, refractory CLL (*Blood*wise TAP CLARITY Study): high rates of overall response, complete remission and MRD eradication after 6 months of combination therapy. *Blood* (2017) 130:428.
66. Jain N, Thompson P, Ferrajoli A, Burger J, Borthakur G, Takahashi K, et al. Combined venetoclax and ibrutinib for patients with previously untreated high-risk CLL, and relapsed/refractory CLL: A phase II trial. *Blood* (2017) 130:429.
67. Patel VM, Balakrishnan K, Douglas M, Tibbitts T, Xu EY, Kutok JL, et al. Duvelisib treatment is associated with altered expression of apoptotic regulators that helps in sensitization of chronic lymphocytic leukemia cells to venetoclax (ABT-199). *Leukemia* (2017) 31:1872–81. doi: 10.1038/leu.2016.382

Conflict of Interest Statement: JL and DC are employees and shareholders of AbbVie, Inc.

frontiers in Oncology

ORIGINAL RESEARCH
published: 12 October 2018
doi: 10.3389/fonc.2018.00452

Doxycycline, an Inhibitor of Mitochondrial Biogenesis, Effectively Reduces Cancer Stem Cells (CSCs) in Early Breast Cancer Patients: A Clinical Pilot Study

Cristian Scatena[1], Manuela Roncella[1,2], Antonello Di Paolo[3], Paolo Aretini[4], Michele Menicagli[4], Giovanni Fanelli[5], Carolina Marini[6], Chiara Maria Mazzanti[4], Matteo Ghilli[2], Federica Sotgia[7], Michael P. Lisanti[7] and Antonio Giuseppe Naccarato[1]**

[1] Department of Translational Research and New Technologies in Medicine and Surgery, University of Pisa, Pisa, Italy, [2] Breast Surgery Unit, Azienda Ospedaliero-Universitaria Pisana, Pisa, Italy, [3] Department of Clinical and Experimental Medicine, University of Pisa, Pisa, Italy, [4] Fondazione Pisana per la Scienza, Pisa, Italy, [5] Department of Laboratory Medicine, Azienda Ospedaliero-Universitaria Pisana, Pisa, Italy, [6] Division of Breast Radiology, Azienda Ospedaliero-Universitaria Pisana, Pisa, Italy, [7] Translational Medicine, University of Salford, Greater Manchester, Manchester, United Kingdom

OPEN ACCESS

Edited by:
Ramon Bartrons,
University of Barcelona, Spain

Reviewed by:
Gyorgy Szabadkai,
University College London, United Kingdom
Francesco De Francesco,
Azienda Ospedaliero Universitaria Ospedali Riuniti, Italy

***Correspondence:**
Michael P. Lisanti
michaelp.lisanti@gmail.com
Antonio Giuseppe Naccarato
giuseppe.naccarato@med.unipi.it

Specialty section:
This article was submitted to Molecular and Cellular Oncology, a section of the journal Frontiers in Oncology

Received: 02 July 2018
Accepted: 26 September 2018
Published: 12 October 2018

Citation:
Scatena C, Roncella M, Di Paolo A, Aretini P, Menicagli M, Fanelli G, Marini C, Mazzanti CM, Ghilli M, Sotgia F, Lisanti MP and Naccarato AG (2018) Doxycycline, an Inhibitor of Mitochondrial Biogenesis, Effectively Reduces Cancer Stem Cells (CSCs) in Early Breast Cancer Patients: A Clinical Pilot Study. Front. Oncol. 8:452. doi: 10.3389/fonc.2018.00452

Background and objectives: Cancer stem cells (CSCs) have been implicated in tumor initiation, recurrence, metastatic spread and poor survival in multiple tumor types, breast cancers included. CSCs selectively overexpress key mitochondrial-related proteins and inhibition of mitochondrial function may represent a new potential approach for the eradication of CSCs. Because mitochondria evolved from bacteria, many classes of FDA-approved antibiotics, including doxycycline, actually target mitochondria. Our clinical pilot study aimed to determine whether short-term pre-operative treatment with oral doxycycline results in reduction of CSCs in early breast cancer patients.

Methods: Doxycycline was administered orally for 14 days before surgery for a daily dose of 200 mg. Immuno-histochemical analysis of formalin-fixed paraffin-embedded (FFPE) samples from 15 patients, of which 9 were treated with doxycycline and 6 were controls (no treatment), was performed with known biomarkers of "stemness" (CD44, ALDH1), mitochondria (TOMM20), cell proliferation (Ki67, p27), apoptosis (cleaved caspase-3), and neo-angiogenesis (CD31). For each patient, the analysis was performed both on pre-operative specimens (core-biopsies) and surgical specimens. Changes from baseline to post-treatment were assessed with MedCalc 12 (unpaired *t*-test) and ANOVA.

Results: Post-doxycycline tumor samples demonstrated a statistically significant decrease in the stemness marker CD44 (p-value < 0.005), when compared to pre-doxycycline tumor samples. More specifically, CD44 levels were reduced between 17.65 and 66.67%, in 8 out of 9 patients treated with doxycycline. In contrast, only one patient showed a rise in CD44, by 15%. Overall, this represents a positive response rate of nearly 90%. Similar results were also obtained with ALDH1, another marker of stemness. In contrast, markers of mitochondria, proliferation, apoptosis, and neo-angiogenesis, were all similar between the two groups.

Conclusions: Quantitative decreases in CD44 and ALDH1 expression are consistent with pre-clinical experiments and suggest that doxycycline can selectively eradicate CSCs in breast cancer patients *in vivo*. Future studies (with larger numbers of patients) will be conducted to validate these promising pilot studies.

Keywords: doxycycline, mitochondria, cancer stem cells, translational study, mitochondrial biogenesis

INTRODUCTION

Tumor-initiating cells (TICs) share many functional characteristics with normal stem cells and are important drivers of tumor initiation and cancer progression (1–7). As such, new therapies for targeting TICs [a.k.a., cancer stem cells (CSCs)] could be used for cancer prevention. Interestingly, circulating tumor cells (CTCs) can also functionally behave as initiators of tumor formation.

Because of their resistance to conventional anti-cancer treatments (i.e., chemo-therapy and radio-therapy), CSCs are also thought to underpin the cellular and molecular basis of tumor recurrence, distant metastasis and ultimately treatment failure, in most cancer types (1–6). Thus, new treatment strategies are urgently needed to help remedy this unmet clinical need (1–4).

One simplistic idea is to identify novel therapeutic targets that are relatively unique to CSCs, which can be then be inhibited with FDA-approved drugs that show few side effects and have excellent safety profiles (1–3). We recently used this promising approach to identify mitochondria in CSCs as a conserved therapeutic target (7). In this context, the antibiotic doxycycline emerged as an excellent candidate for drug repurposing (8, 9). In 1967, Doxycycline was first approved by the FDA, more than 50 years ago. It shows minimal side effects and is currently used world-wide as a broad-spectrum antibiotic, mainly for the treatment of acne and acne rosacea. Doxycycline has excellent pharmaco-kinetics, with very good oral absorption (∼100%) and a long serum half-life (18–22 h), at the standard dose of 200 mg per day.

Doxycycline functionally behaves as a non-toxic inhibitor of mitochondrial biogenesis, because of the evolutionarily conserved similarities between bacterial ribosomes and mitochondrial ribosomes (10–12). Therefore, this "manageable side-effect" of doxycycline could be repurposed as a "therapeutic effect," to target and inhibit mitochondrial biogenesis in CSCs (13, 14).

Previously, doxycycline has been used clinically to target cancer-associated infections, with promising results, leading to a complete pathological response (CPR) or "remission" in patients with MALT lymphoma (15, 16). Interestingly, this CPR did not correlate with the presence of micro-organisms, possibly suggesting that doxycycline might be acting on the tumor cells themselves.

In 2015, the Sotgia/Lisanti laboratory first demonstrated that doxycycline treatment was sufficient to successfully halt the propagation of CSCs *in vitro* (13, 14). For this purpose, we tested 12 different human tumor cell lines, representing eight different cancer types, such as DCIS, breast [ER(+) and ER(-)], lung, ovarian, pancreatic, and prostate carcinomas, as well as glioblastoma (GBM) and melanoma (13). Remarkably, doxycycline inhibited CSC propagation across this entire panel of diverse cell lines (13).

Further mechanistic studies, using luciferase based assays in MCF7 cells (a human breast cancer cell line) revealed that doxycycline treatment effectively inhibits CSC signaling, across multiple pathways, including Wnt, Notch, Hedgehog and STAT1/3-signaling (14). Therefore, doxycycline is an excellent candidate for drug repurposing, in clinical pilot studies aimed at validating its ability to target CSCs in cancer patients. As such, here we evaluated the ability of doxycycline to target CSCs in breast cancer patients *in vivo*, using well-established CSC markers (CD44 and ALDH1) as a read-out.

The ability of doxycycline to target breast CSCs *in vitro* has already been confirmed independently (17, 18) and extended to several other classes of antibiotics and mitochondrial OXPHOS inhibitors (19–24). Consistent with these findings, mitochondrial mass is increased in CSCs (25, 26) and high expression levels of mitochondrial markers directly correlates with poor clinical outcome in ovarian (27) and breast cancer patients (28).

Finally, as early as 2002, it was first reported that doxycycline effectively reduces bone metastasis, by up to ∼60–80%, in an *in vivo* pre-clinical murine model of human breast cancer (29). Mechanistically, these findings may be due to the ability of doxycycline to eradicate CSCs, although this hypothesis was not tested at that time.

RESULTS

Description of the Breast Cancer Patient Population

A summary diagram highlighting the organizational structure of this doxycycline "window-of-opportunity" study (Phase II) is shown in **Figure 1**.

A total of 15 female patients with early breast cancer participated in the current pilot study. Nine patients received doxycycline (200 mg per day) for a 14-day period, while six patients remained untreated. A summary of the clinical characteristics of the patient population are shown in **Table 1**.

Briefly, in the doxycycline treatment group, patient age at diagnosis ranged between 42 and 65 years of age, tumor size was between 10 and 30 mm, and 6 out of 9 patients were grade 2. In addition, 7 out of 9 patients were ER(+), with 6 being of the luminal A sub-type and one of the luminal B sub-type. In addition, two patients were of the HER2(+) sub-type.

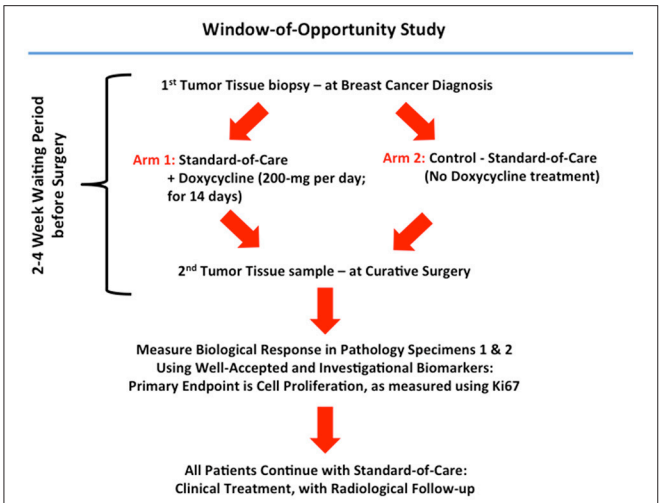

FIGURE 1 | Schematic diagram summarizing the organizational structure of the Doxycycline clinical pilot study. Note that this Phase II "Window-of-Opportunity" format provides an excellent clinical mechanism for evaluating FDA-approved antibiotics, as potential candidates for drug repurposing.

TABLE 1 | Clinical characteristics of the patient population.

Treated patients	Age	Tumor size (mm)	Grade	Molecular subtype
Case 1	42	12	2	Luminal A
Case 2	57	15	3	HER2pos
Case 4	65	23	3	HER2pos
Case 5	52	10	2	Luminal A
Case 7	46	12	2	Luminal A
Case 8	46	27	2	Luminal B
Case 13	50	10	2	Luminal A
Case 14	52	13	1	Luminal A
Case 15	44	30	2	Luminal A
Untreated patients				
Case 3	71	25	3	Luminal B
Case 6	50	15	2	Luminal A
Case 9	51	12	2	Luminal A
Case 10	48	25	3	Luminal B
Case 11	41	21	2	Luminal A
Case 12	69	16	3	Luminal/HER2pos

In the untreated control group, patient age ranged between 41 and 71 years of age, and tumor size was between 12 to 25 mm; 3 patients were grade 2 and 3 patients were grade 3. All 6 patients were ER(+), with 3 of the luminal A sub-type, 2 of the luminal B sub-type and one showing characteristics of both luminal/HER2(+) sub-types.

Thus, both groups were well-matched for age and clinical characteristics.

Status of Biomarkers in Tumor Tissue Sections, Before and After Receiving Oral Doxycycline

We quantitatively assessed the expression of several diverse biomarkers in paraffin-embedded tumor tissue sections. These included markers of "stemness" (CD44, ALDH1), mitochondria (TOMM20), cell proliferation (Ki67, p27), apoptosis (cleaved caspase-3), and neo-angiogenesis (CD31).

Figure 2 highlights that most of the tumor markers remained unchanged before and after receiving oral doxycycline, with the exception of CD44—a marker of "stemness." More specifically, CD44 was reduced on average by ∼40% ($p < 0.005$), in the patients examined. Note that 4 out of 9 patients showed reductions of 50% or greater in CD44.

The results of multi-variate analysis are included as Supplemental Information and demonstrated that CD44 reductions remained significant (ANOVA; $p < 0.0007$) and were independent of all the other variables tested [including histological grade (1, 2, 3), tumor diameter type (small, large) and molecular subtype] (see **Tables S1–S15**). In contrast, cleaved caspase-3 levels appeared to be elevated after receiving oral doxycycline; however, this did not reach statistical significance, except in the case of low histological grade (See **Table S4**).

Figure 3 shows a waterfall plot of CD44 expression in the 9 individual breast cancer patients. Remarkably, CD44 levels were reduced between 17.65 and 66.67%, in 8 out of 9 patients treated with doxycycline. Representative images of this reduction in CD44 immuno-staining are illustrated in **Figure 4** for two patients. In contrast, only one patient showed a rise in CD44, by 15%. Overall, this represents a positive response rate approaching 90%. It is worth noting that the levels of cleaved caspase-3 were most strikingly elevated in the two patients (Cases 8 & 14) that showed the largest reductions in CD44 expression (**Figure 5**). Therefore, a certain threshold level may need to be reached to augment the activation of caspase-3.

The two patients of the HER2(+) sub-type, also showed positivity for another stem cell marker, namely ALDH1. Interestingly, ALDH1 levels were reduced by nearly 60% in one patient (Case 2), while ALDH1 levels were reduced by ∼90% in the other patient (Case 4) (**Figure 6**), all in response to doxycycline. These results are also consistent with reductions in CD44; in these same two HER2(+) patients, CD44 levels were reduced by nearly 40% (Case 2) and 60% (Case 4), respectively (**Figure 3**).

Status of Biomarkers in Tumor Tissue Sections From the Untreated Control Group, Before and After Surgery

In contrast to our results with the doxycycline treated patient population, patients in the untreated control group did not show any statistically significant changes in the expression of CD44, when tumor tissue sections were compared before and after surgery (**Figure S1**). The results of multi-variate analysis are included as Supplemental Information (**Tables S11–S15**) and showed that CD44 remained unchanged (see **Table S13**; ANOVA; $P < 0.7707$).

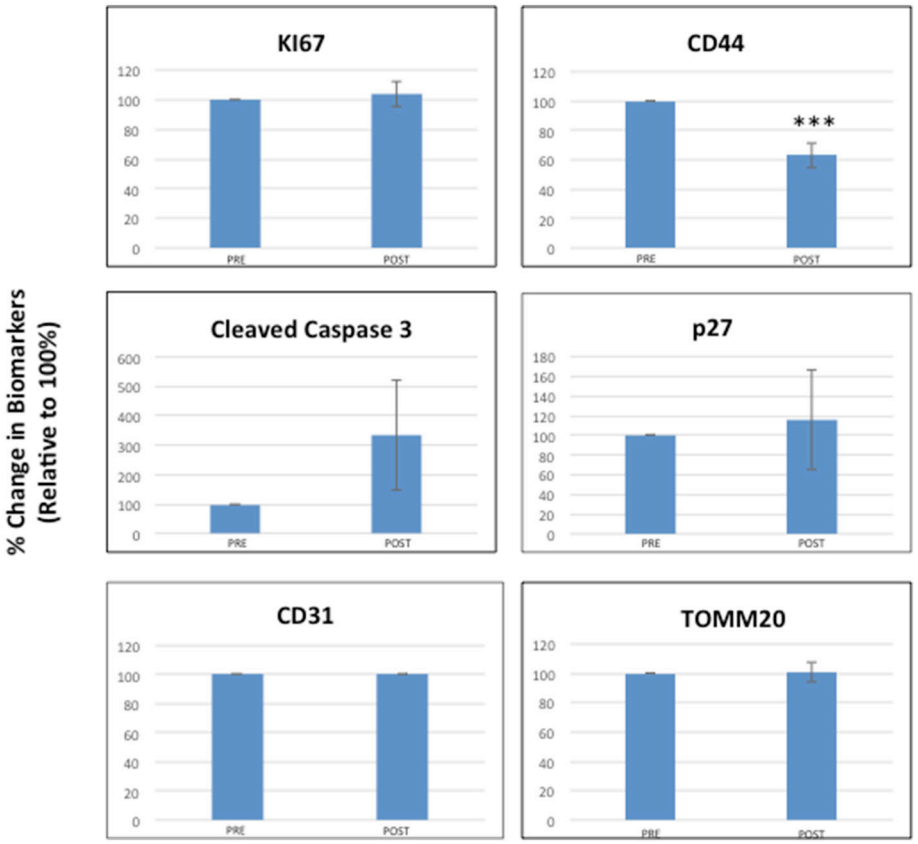

FIGURE 2 | Effects of doxycycline administration on the expression of six different classes of biomarkers in early breast cancer patients (Ki67, Cleaved Caspase-3, CD31, CD44, p27, and TOMM20). Note that only CD44 levels were significantly reduced on average by nearly 40% (***; $p < 0.005$), while the levels of other markers remained unchanged. The results of multi-variate analysis are included as Supplemental Information and show that CD44 remained significant (ANOVA; $p < 0.0007$) and was independent of all the other variables tested [histological grade (1, 2, 3), diameter type (small, large) and molecular subtype] (see **Tables S1–S15**).

Therefore, surgery itself was not sufficient to significantly change the expression levels of the tumor markers examined, including CD44.

DISCUSSION

Here, we conducted a clinical pilot study with doxycycline, to assess its effects in early breast cancer patients. Importantly, most biomarkers tested remained unchanged, with the exception of CD44, which was reduced on average by nearly 40%, in a period of only two weeks of treatment. Analysis of waterfall plot data revealed that in 8 out of 9 patients treated with doxycycline, CD44 levels were reduced between 17.65 and 66.67%. In contrast, only one patient showed a rise in CD44, by 15%. Two patients of the HER2(+) sub-type, also showed positivity for another stem cell marker, namely ALDH1. In these HER2(+) patients, ALDH1 levels were reduced by nearly 60% in one patient, while ALDH1 levels were reduced by 90% in the other patient, in response to doxycycline. Thus, oral doxycycline treatment effectively reduced the expression of two CSC markers, in early breast cancer patients.

Our current *in vivo* results are consistent with recent findings in MCF7 and MDA-MB-468 cells, two human breast cancer cell lines in culture, which showed significant reductions in the CD44(+)/CD24(-/low) CSC population, after treatment with doxycycline (17). In addition, the expression levels of other "stemness" markers (Oct4, Sox2, Nanog and CD44) were also reduced by >50%, in response to doxycycline, as assessed by mRNA levels and independently confirmed by immuno-blot analysis (17).

Similarly, doxycycline has been shown to reduce ALDH(+) breast CSCs in HER2(+) and triple-negative human breast cancer cell lines *in vitro* (18). As such, doxycycline may be useful for targeting both the CD44(+) and ALDH(+) sub-populations of human breast CSCs (17, 18).

The levels of cleaved caspase-3 appeared to be elevated after treatment with Doxycycline; however, this did not reach statistical significance in all the tumor grades. Nevertheless, Doxycycline has been shown to induce apoptosis in human breast cancer cell lines *in vitro* (17).

CONCLUSIONS

Pre-operative treatment with oral doxycycline (200 mg per day) for 2 weeks is sufficient to reduce both CD44 and ALDH1 expression in tumor tissue from early breast cancer

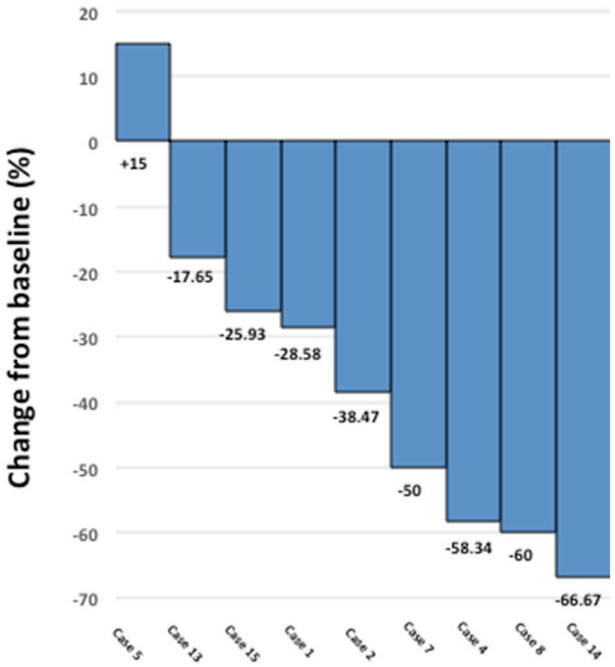

FIGURE 3 | Effect of doxycycline administration on the expression of CD44 in early breast cancer patients: Waterfall plot. Note that CD44 levels were reduced between 17.65 and 66.67%, in 8 out of 9 patients treated. In contrast, only one patient showed a rise in CD44, by 15%. Overall, this represents a positive response rate of nearly 90%. Also, note that 4 out of 9 patients showed reductions of 50% or greater in CD44.

patients. However, additional clinical studies (with larger patient numbers) will be required to further validate these promising clinical pilot studies.

MATERIALS AND METHODS

Trial Construction, Ethical Review and EU Clinical Trial Registration

A Phase II clinical trial (pre-operative "window" study; **Figure 1**) for the use of oral doxycycline in early breast cancer patients was submitted, reviewed, and approved by the local and national ethics committees at the Pisa University Hospital and the Italian Ministry of Health (Rome, Italy). All patients underwent informed written consent, prior to their inclusion in the study. Doxycycline was administered during the "window-of-opportunity," after diagnosis and exactly 14 days before the date of surgery, while the patient was waiting for tumor excision at surgery. The acronym for the trial is ABC (Antibiotics for Breast Cancer) and the EudraCT registration number is 2016-000871-26. EudraCT is the European Clinical Trials Database (European Union Drug Regulating Authorities Clinical Trials). The full title of the study is: "A Phase II Open-Label Randomized Controlled Pre-Surgical Feasibility Study of Doxycycline in Early Breast Cancer." The objective and primary goal of the trial is: To determine whether short-term (2-weeks) pre-operative treatment with oral doxycycline of stage I-to-III early breast cancer patients results in inhibition of tumor proliferation markers, as determined by a reduction in tumor Ki67 from baseline (pre-treatment) to post-treatment (at time of surgical excision). Doxycycline (Bassado-brand) was administered orally, 100-mg twice a day for a total of 200-mg per day, for a period of 14-days. During this period, the control group received no medical therapy (i.e., standard of care: waiting for surgery). Information about study subjects is kept confidential and managed according to the requirements of the EU and Italian regulations. All of our breast cancer cases were NST (No Special Type, invasive carcinomas), previously known as "ductal" carcinomas.

Plasma Doxycycline Levels

Doxycycline oral intake was validated by measuring the concentrations in plasma samples, obtained immediately prior to surgery [mean +/− SD, 0.76 ± 0.41 mg/L, range 0.25–1.57 mg/L]. Doxycycline levels were determined by mass spectrometry analysis. This precise monitoring confirmed the compliance of patients to the planned treatment regimen, proposed to them at the time of enrollment.

Immuno-Staining Reagents

Antibodies for immuno-staining were purchased from commercial sources, as briefly summarized in **Table S16**.

Immuno-Staining and Quantitation

Tumor expression of Ki67, p27, cleaved caspase 3, CD31, CSC markers (CD44, ALDH1), and mitochondria (TOMM20) was performed on formalin-fixed paraffin-embedded tumor tissues. Tissue sections (4 micron) were de-paraffinized with xylene and rehydrated through a graded alcohol series. After rinsing with phosphate buffer saline (PBS) sample were immersed in sodium citrate buffer (pH 6) for p27 and cleaved caspase 3 and in UNMASKER buffer (pH 7,8) for CD44, TOMM20, ADLH1, and heated in a microwave oven at 100°C. The endogenous peroxidase was blocked by 10 min incubation in 3% H_2O_2. After blocking with normal goat serum for 10 min at room temperature, the slides were further incubated overnight at 4°C with the following primary antibodies: mouse anti CD44 (1:1000, clone 156-3C11), mouse anti-ALDH1A1, (1:500, clone 703410), rabbit anti cleaved caspase 3 (Asp175; 1:150), rabbit anti-p27 (1:250) and mouse anti TOMM20 (1:250, clone F-10). A biotin conjugated goat derived secondary antibody was applied followed by the enzyme-labeled streptavidin and substrate chromogen (Rabbit/Mouse specific HRP/DAB-ABC detection IHC kit, Abcam). Slides were counterstained with hematoxylin. The immunostaining for Ki67 (ready to use, clone MIB-1, Dako) and CD31 (ready to use, clone JC70, Ventana Medical Systems) instead was performed in an automated immunostainer (BenchMark Ultra, Ventana Medical Systems). Staining intensity and percentage of positive tumor cells was measured. Ki67 is a nuclear marker expressed in all phases of the cell cycle except G_0. The "Ki67 index" (percentage of nuclei showing nuclear immuno-reactivity of any intensity) was determined as per

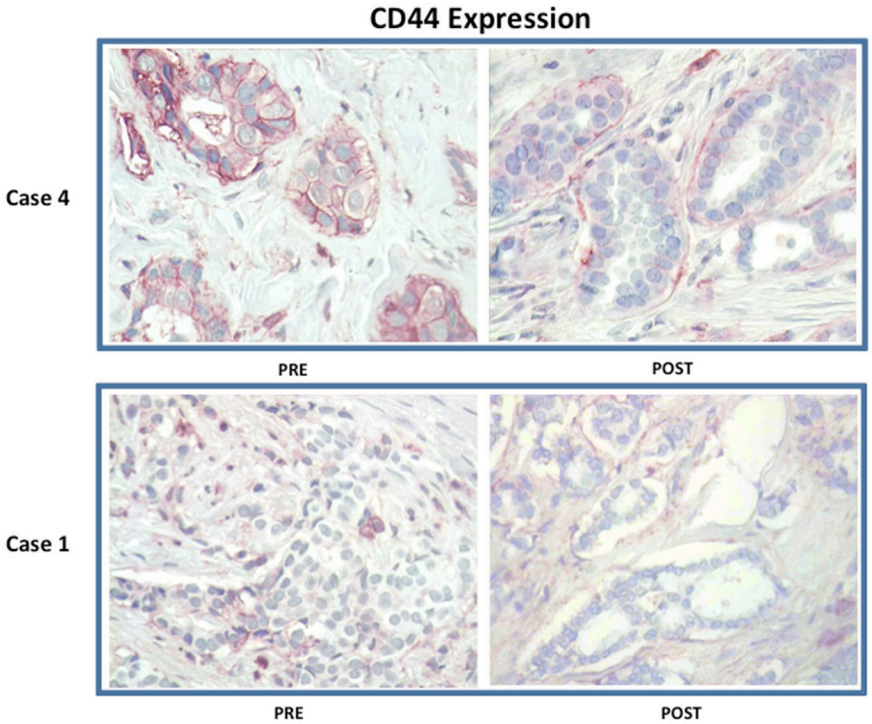

FIGURE 4 | Effect of doxycycline administration on the expression of CD44 in early breast cancer patients: Representative images are shown. Note that treatment with doxycycline reduces the expression of CD44, as seen by immuno-histochemical staining. Representative images from two case are shown. Magnification, 40X.

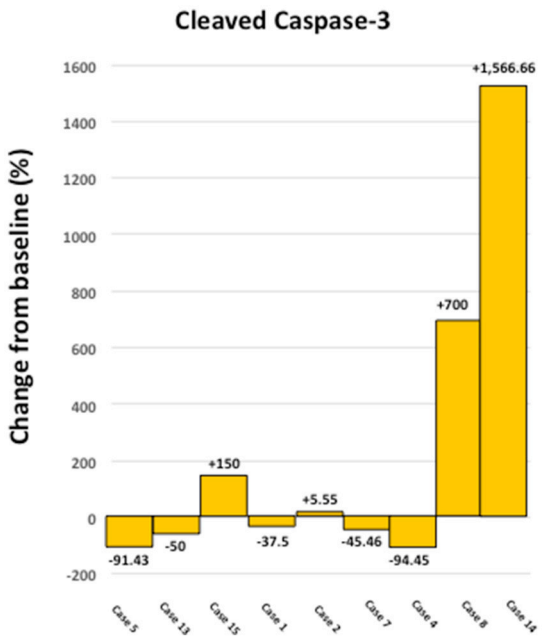

FIGURE 5 | Effect of doxycycline administration on the levels of cleaved caspase 3 in early breast cancer patients. Note that the levels of cleaved caspase 3 showed the largest increases in two patients, which demonstrated the highest reductions in CD44 levels (Cases 8 and14); compare with **Figure 3**. In addition, the levels of cleaved caspase 3 were increased in 4 out of 9 patients studied (~44 %).

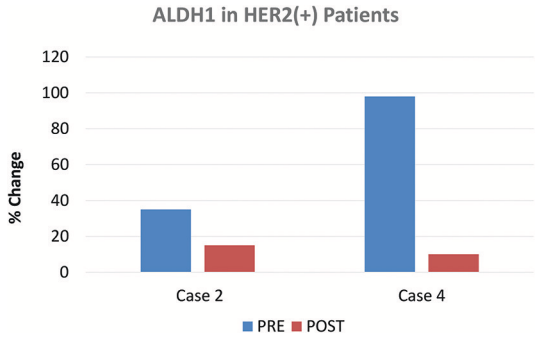

FIGURE 6 | Effect of doxycycline administration on the expression of ALDH1 in HER2(+) early breast cancer patients. The two patients of the HER2(+) sub-type, also showed positivity for another stem cell marker, namely ALDH1. Note that ALDH1 levels were reduced by nearly 60% in one patient (Case 2), while ALDH1 levels were reduced by 90% in the other patient (Case 4), in response to doxycycline.

routine protocols. p27 (nuclear staining) is a cell cycle inhibitor that negatively correlates with Ki67. Caspase-3 (cytoplasmic and/or nuclear staining) is synthesized as an inactive pro-enzyme which is activated by cleavage in cells undergoing apoptosis. CD31 (membranous staining) is expressed by endothelial cells and is used as a marker of angiogenesis. CD44 (membranous staining: complete or incomplete, of any intensity) and ALDH1 (cytoplasmic staining) are well-established markers that are

elevated in cells with "stem-like" characteristics. TOMM20 (cytoplasmic staining), a central component of the receptor complex responsible for the recognition and translocation of cytosolically synthesized mitochondrial preproteins, is used as a marker of mitochondria. Staining percentage of positive tumor cells was measured independently by two blinded-pathologists. Discrepancies in interpretation or scoring (<5% of cases) were resolved by consensus conference at a double-headed microscope. All changes in tumor markers were analyzed as a percentage (pre-post/pre x 100) and an absolute (pre-post) change from baseline.

Statistical Analysis

The values of the markers before the treatment were our reference (100%), and all the other values measured after the treatment are presented as a post/pre ratio, to point out any increases or decreases from the reference value. The values in the graphs are represented by the average value of each endpoint, with relative standard error of the mean (SEM). The significant differences were assessed with MedCalc 12 (unpaired *t*-test). Values of $p < 0.05$ were considered statistically significant. Multi-variate analysis with ANOVA was also carried out and the results of this analysis are included as Supplementary Information (see **Tables S1–S15**).

AUTHOR CONTRIBUTIONS

The ABC trial is being carried out at the Breast Care Center at the Pisa University Hospital. Patient recruitment is led by the surgeons (MR and MG). FS and ML initially conceived the idea of a doxycycline-based breast cancer clinical trial and wrote a first draft of the clinical trial. CS, MR, AD, GF, CM, MG, CMM, and AN edited and implemented the clinical trial. CS processed the tissue samples and generated the final figures. MM performed immuno-staining on the tissue sections. AD performed the analysis of the doxycycline blood dosages. PA performed the statistical analyses. FS and ML wrote the first draft of the paper, which was edited and approved by all the co-authors.

FUNDING

This work was supported by generous donations from the Healthy Life Foundation (HLF) and the Foxpoint Foundation (to FS and MPL), as well as The Pisa Science Foundation (to the University Hospital of Pisa). The authors also wish to thank Katia De Ieso from the Immunohistochemistry Laboratory, Department of Laboratory Medicine, Azienda Ospedaliero-Universitaria Pisana, Pisa, Italy.

SUPPLEMENTARY MATERIAL

The Supplementary Material for this article can be found online at: https://www.frontiersin.org/articles/10.3389/fonc.2018.00452/full#supplementary-material

Figure S1 | Expression of six different classes of biomarkers in early breast cancer patients. In contrast to our results with the doxycycline treated patient population, patients in the untreated control group did not show any significant changes in the expression of tumor markers, when tumor sections were compared, before and after surgery.

REFERENCES

1. Martinez-Outschoorn UE, Peiris-Pagés M, Pestell RG, Sotgia F, Lisanti MP. Cancer metabolism: a therapeutic perspective. *Nat Rev Clin Oncol.* (2017) 14:11–31. doi: 10.1038/nrclinonc.2016.60
2. Martinez-Outschoorn UE, Sotgia F, Lisanti MP. Caveolae and signalling in cancer. *Nat Rev Cancer* (2015) 15:225–37. doi: 10.1038/nrc3915
3. De Francesco EM, Sotgia F, Lisanti MP. Cancer stem cells (CSCs): metabolic strategies for their identification and eradication. *Biochem J.* (2018) 475:1611–34. doi: 10.1042/BCJ20170164
4. Peiris-Pagès M, Martinez-Outschoorn UE, Pestell RG, Sotgia F, Lisanti MP. Cancer stem cell metabolism. *Breast Cancer Res.* (2016) 18:55. doi: 10.1186/s13058-016-0712-6
5. Luo M, Clouthier SG, Deol Y, Liu S, Nagrath S, Azizi E, Wicha MS. Breast cancer stem cells: current advances and clinical implications. *Methods Mol Biol.* (2015) 1293:1–49. doi: 10.1007/978-1-4939-2519-3_1
6. Brooks MD, Burness ML, Wicha MS. Therapeutic Implications of Cellular Heterogeneity and Plasticity in Breast Cancer. *Cell Stem Cell* (2015) 17:260–71. doi: 10.1016/j.stem.2015.08.014
7. Lamb R, Harrison H, Hulit J, Smith DL, Lisanti MP, Sotgia F. Mitochondria as new therapeutic targets for eradicating cancer stem cells: quantitative proteomics and functional validation via MCT1/2 inhibition. *Oncotarget* (2014) 5:11029–37. doi: 10.18632/oncotarget.2789
8. Peiris-Pagès M, Sotgia F, Lisanti MP. Doxycycline and therapeutic targeting of the DNA damage response in cancer cells: old drug, new purpose. *Oncoscience* (2015) 2:696–9. doi: 10.18632/oncoscience.215
9. Ozsvári B, Lamb R, Lisanti MP. Repurposing of FDA-approved drugs against cancer - focus on metastasis. *Aging* (2016) 8:567–8. doi: 10.18632/aging.100941
10. Ozsvari B, Sotgia F, Lisanti MP. A new mutation-independent approach to cancer therapy: Inhibiting oncogenic RAS and MYC, by targeting mitochondrial biogenesis. *Aging* (2017) 9:2098–116. doi: 10.18632/aging.101304
11. Ozsvari B, Fiorillo M, Bonuccelli G, Cappello AR, Frattaruolo L, Sotgia F, et al. Mitoriboscins: Mitochondrial-based therapeutics targeting cancer stem cells (CSCs), bacteria and pathogenic yeast. *Oncotarget* (2017) 8:67457–72. doi: 10.18632/oncotarget.19084
12. De Francesco EM, Bonuccelli G, Maggiolini M, Sotgia F, Lisanti MP. Vitamin C and Doxycycline: a synthetic lethal combination therapy targeting metabolic flexibility in cancer stem cells (CSCs). *Oncotarget* (2017) 8:67269–86. doi: 10.18632/oncotarget.18428
13. Lamb R, Ozsvari B, Lisanti CL, Tanowitz HB, Howell A, Martinez-Outschoorn UE, et al. Antibiotics that target mitochondria effectively eradicate cancer stem cells, across multiple tumor types: Treating cancer like an infectious disease. *Oncotarget* (2015) 6:4569–84. doi: 10.18632/oncotarget.3174
14. Lamb R, Fiorillo M, Chadwick A, Ozsvari B, Reeves KJ, Smith DL, et al. Doxycycline down-regulates DNA-PK and radiosensitizes tumor initiating cells: Implications for more effective radiation therapy. *Oncotarget* (2015) 6:14005–25. doi: 10.18632/oncotarget.4159
15. Han JJ, Kim TM, Jeon YK, Kim MK, Khwarg SI, Kim CW, et al. Long-term outcomes of first-line treatment with doxycycline in patients with previously untreated ocular adnexal marginal zone B cell lymphoma. *Ann Hematol.* (2015) 94:575–81. doi: 10.1007/s00277-014-2240-8
16. Ferreri AJ, Govi S, Pasini E, Mappa S, Bertoni F, Zaja F, et al. Chlamydophila psittaci eradication with doxycycline as first-line targeted therapy for ocular adnexae lymphoma: final results of an international phase II trial. *J Clin Oncol.* (2012) 30:2988–94. doi: 10.1200/JCO.2011.41.4466

17. Zhang L, Xu L, Zhang F, Vlashi E. Doxycycline inhibits the cancer stem cell phenotype and epithelial-to-mesenchymal transition in breast cancer. *Cell Cycle* (2017) 16:737–45. doi: 10.1080/15384101.2016.1241929
18. Lin CC, Lo MC, Moody RR, Stevers NO, Tinsley SL, Sun D. Doxycycline targets aldehyde dehydrogenase-positive breast cancer stem cells. *Oncol Rep*. (2018) 39:3041–7. doi: 10.3892/or.2018.6337
19. Fiorillo M, Lamb R, Tanowitz HB, Mutti L, Krstic-Demonacos M, Cappello AR, et al. Repurposing atovaquone: Targeting mitochondrial complex III and OXPHOS to eradicate cancer stem cells. *Oncotarget* (2016) 7:34084–99. doi: 10.18632/oncotarget.9122
20. Fiorillo M, Lamb R, Tanowitz HB, Cappello AR, Martinez-Outschoorn UE, Sotgia F, et al. Bedaquiline, an FDA-approved antibiotic, inhibits mitochondrial function and potently blocks the proliferative expansion of stem-like cancer cells (CSCs). *Aging* (2016) 8:1593–607. doi: 10.18632/aging.100983
21. Fiorillo M, Peiris-Pagès M, Sanchez-Alvarez R, Bartella L, Di Donna L, Dolce V, et al. Bergamot natural products eradicate cancer stem cells (CSCs) by targeting mevalonate, Rho-GDI-signalling and mitochondrial metabolism. *BBA Bioenerget.* (2018) 1859:984–96. doi: 10.1016/j.bbabio.2018.03.018
22. Bonuccelli G, De Francesco EM, de Boer R, Tanowitz HB, Lisanti MP. NADH autofluorescence, a new metabolic biomarker for cancer stem cells: Identification of Vitamin C and CAPE as natural products targeting "stemness". *Oncotarget* (2017) 8:20667–78. doi: 10.18632/oncotarget.15400
23. De Luca A, Fiorillo M, Peiris-Pagès M, Ozsvari B, Smith DL, Sanchez-Alvarez R, et al. Mitochondrial biogenesis is required for the anchorage-independent survival and propagation of stem-like cancer cells. *Oncotarget* (2015) 6:14777–95. doi: 10.18632/oncotarget.4401
24. Ozsvari B, Sotgia F, Simmons K, Trowbridge R, Foster R, Lisanti MP. Mitoketoscins: Novel mitochondrial inhibitors for targeting ketone metabolism in cancer stem cells (CSCs). *Oncotarget* (2017) 8:78340–50. doi: 10.18632/oncotarget.21259
25. Lamb R, Bonuccelli G, Ozsvári B, Peiris-Pagès M, Fiorillo M, Smith DL, et al. Mitochondrial mass, a new metabolic biomarker for stem-like cancer cells: Understanding WNT/FGF-driven anabolic signaling. *Oncotarget* (2015) 6:30453–71. doi: 10.18632/oncotarget.5852
26. Farnie G, Sotgia F, Lisanti MP. High mitochondrial mass identifies a sub-population of stem-like cancer cells that are chemo-resistant. *Oncotarget* (2015) 6:30472–86. doi: 10.18632/oncotarget.5401
27. Sotgia F, Lisanti MP. Mitochondrial mRNA transcripts predict overall survival, tumor recurrence and progression in serous ovarian cancer: companion diagnostics for cancer therapy. *Oncotarget* (2017) 8:66925–39. doi: 10.18632/oncotarget.19963
28. Sotgia F, Fiorillo M, Lisanti MP. Mitochondrial markers predict recurrence, metastasis and tamoxifen-resistance in breast cancer patients: Early detection of treatment failure with companion diagnostics. *Oncotarget* (2017) 8:68730–45. doi: 10.18632/oncotarget.19612
29. Duivenvoorden WC, Popović SV, Lhoták S, Seidlitz E, Hirte HW, Tozer RG, Singh G. Doxycycline decreases tumor burden in a bone metastasis model of human breast cancer. *Cancer Res*. (2002) 62:1588–91.

Conflict of Interest Statement: The authors declare that the research was conducted in the absence of any commercial or financial relationships that could be construed as a potential conflict of interest.

frontiers in Oncology

CLINICAL TRIAL
published: 11 October 2018
doi: 10.3389/fonc.2018.00436

Metformin Clinical Trial in HPV+ and HPV– Head and Neck Squamous Cell Carcinoma: Impact on Cancer Cell Apoptosis and Immune Infiltrate

Joseph M. Curry[1], Jennifer Johnson[2], Mehri Mollaee[3], Patrick Tassone[1], Dev Amin[1], Alexander Knops[1], Diana Whitaker-Menezes[2], My G. Mahoney[4], Andrew South[4], Ulrich Rodeck[4], Tingting Zhan[5], Larry Harshyne[6], Nancy Philp[3], Adam Luginbuhl[1], David Cognetti[1], Madalina Tuluc[3] and Ubaldo Martinez-Outschoorn[2]*

[1] Department of Otolaryngology Head and Neck Surgery, Thomas Jefferson University Philadelphia, Philadelphia, PA, United States, [2] Department of Medical Oncology, Thomas Jefferson University Philadelphia, Philadelphia, PA, United States, [3] Department of Pathology, Anatomy and Cell biology, Thomas Jefferson University Philadelphia, Philadelphia, PA, United States, [4] Department of Dermatology and Cutaneous Biology, Thomas Jefferson University Philadelphia, Philadelphia, PA, United States, [5] Department of Pharmacology and Experimental Therapeutics, Thomas Jefferson University Philadelphia, Philadelphia, PA, United States, [6] Department of Neurological Surgery, Thomas Jefferson University Philadelphia, Philadelphia, PA, United States

OPEN ACCESS

Edited by:
Paolo Pinton,
University of Ferrara, Italy

Reviewed by:
Anca Maria Cimpean,
University of Medicine and Pharmacy, Timisoara, Romania
Mauro G. Tognon,
University of Ferrara, Italy

***Correspondence:**
Joseph M. Curry
joseph.curry@jefferson.edu

Specialty section:
This article was submitted to Molecular and Cellular Oncology, a section of the journal Frontiers in Oncology

Received: *22 June 2018*
Accepted: *19 September 2018*
Published: *11 October 2018*

Citation:
Curry JM, Johnson J, Mollaee M, Tassone P, Amin D, Knops A, Whitaker-Menezes D, Mahoney MG, South A, Rodeck U, Zhan T, Harshyne L, Philp N, Luginbuhl A, Cognetti D, Tuluc M and Martinez-Outschoorn U (2018) Metformin Clinical Trial in HPV+ and HPV– Head and Neck Squamous Cell Carcinoma: Impact on Cancer Cell Apoptosis and Immune Infiltrate. Front. Oncol. 8:436. doi: 10.3389/fonc.2018.00436

Background: Metformin, an oral anti-hyperglycemic drug which inhibits mitochondrial complex I and oxidative phosphorylation has been reported to correlate with improved outcomes in head and neck squamous cell carcinoma (HNSCC) and other cancers. This effect is postulated to occur through disruption of tumor-driven metabolic and immune dysregulation in the tumor microenvironment (TME). We report new findings on the impact of metformin on the tumor and immune elements of the TME from a clinical trial of metformin in HNSCC.

Methods: Human papilloma virus—(HPV–) tobacco+ mucosal HNSCC samples ($n = 12$) were compared to HPV+ oropharyngeal squamous cell carcinoma (OPSCC) samples ($n = 17$) from patients enrolled in a clinical trial. Apoptosis in tumor samples pre- and post-treatment with metformin was compared by deoxynucleotidyl transferase dUTP nick end labeling (TUNEL) assay. Metastatic lymph nodes with extra-capsular extension (ECE) in metformin-treated patients ($n = 7$) were compared to archival lymph node samples with ECE ($n = 11$) for differences in immune markers quantified by digital image analysis using co-localization and nuclear algorithms (PD-L1, FoxP3, CD163, CD8).

Results: HPV–, tobacco + HNSCC (mean Δ 13.7/high power field) specimens had a significantly higher increase in apoptosis compared to HPV+ OPSCC specimens (mean Δ 5.7/high power field) ($p < 0.001$). Analysis of the stroma at the invasive front in ECE nodal specimens from both HPV—HNSCC and HPV+ OPSCC metformin treated specimens showed increased CD8+ effector T cell infiltrate (mean 22.8%) compared to archival specimens (mean 10.7%) ($p = 0.006$). Similarly, metformin treated specimens showed an increased FoxP3+ regulatory T cell infiltrate (mean 9%) compared to non-treated archival specimens (mean 5%) ($p = 0.019$).

Conclusions: This study presents novel data demonstrating that metformin differentially impacts HNSCC subtypes with greater apoptosis in HPV−HNSCC compared to HPV+ OPSCC. Moreover, we present the first *in vivo* human evidence that metformin may also trigger increased CD8+ Teff and FoxP3+ Tregs in the TME, suggesting an immunomodulatory effect in HNSCC. Further research is necessary to assess the effect of metformin on the TME of HNSCC.

Keywords: head and neck cancer, squamous cell carcinoma, metformin, tumor microenvironment, immune infiltrate, HPV, tumor metabolism

INTRODUCTION

Metformin is an oral biguanide anti-hyperglycemic and the most commonly prescribed medication for type 2 diabetes mellitus. Interestingly, data suggests that metformin may have antineoplastic properties as well. Retrospective epidemiologic analyses, while limited due to the number of confounders, have also shown a decreased incidence of HNSCC in patients taking metformin (1, 2). Diabetics treated with metformin have a cancer risk reduction of approximately 40% compared to diabetics not treated with metformin (3, 4). Other studies have also shown a reduction in the frequency of cancer with metformin use (5). Evans et al. reported that the risk of subsequent cancer diagnosis was reduced in patients with type 2 diabetes who received metformin (with an odds ratio of 0.85 for any metformin exposure versus no metformin exposure) (6).

Extensive preclinical data support the effectiveness of metformin as an antineoplastic agent (7–10). In HNSCC specifically, metformin inhibits proliferation of carcinoma cells and induces apoptosis *in vitro* and *in vivo*, in addition to reducing colony formation with cell cycle arrest *in vitro* (7). *In vitro* and *in vivo* animal models have also shown that metformin can prevent the conversion of premalignant oral lesions to squamous cell carcinoma. Metformin has been shown to reduce the size and numbers of oral tumors in mouse models treated with 4NQO and halt the progression of potential premalignant lesions (11). This study, by Vitale-Cross et al. not only showed a decrease in the total number of oral lesions in animals treated with metformin compared to control, but also showed almost complete absence of transformation to squamous cell carcinoma.

Additional preclinical data was recently published suggesting that there may be a synergy between immune-oncology agents and metformin. Scharping et al. demonstrated a substantial increase in response rate in the murine B16 melanoma model and MC38 colon adenocarcinoma model with combination therapy utilizing PD-1 axis inhibition in combination with metformin (12). PD-1 blockade alone in B16 resulted in no reduction of tumor burden and 20% reduction of tumor burden in MC38 mice. Metformin alone demonstrated no reduction in tumor burden. However, combination therapy of PD-1 blockade and metformin resulted in tumor regression in 70% of B16 mice and 80% of MC38 mice. Moreover, CD8+ effector T cells (Teff) showed increased production of effector cytokines in the combination therapy group, suggesting a direct impact on the immune TME. The interplay of the immune antitumor response and metabolism in the TME is an area of active investigation, as dysregulated metabolism in immune cells critically alters effector function. Immune cell metabolic exhaustion is believed to be one of the key factors contributing to suppressed cytotoxic CD8 effector function in the TME (13). Further, T cells undergo reversible anergy when they are placed in a low pH environment, characteristic of many cancers and particularly HNSCC (14, 15).

To further explore the impact of metformin in HNSCC, we performed a window of opportunity trial using metformin alone prior to definitive surgical resection in HNSCC patients. This study showed increase in the percent of samples showing caveolin1 (CAV1) expression in cancer associated fibroblasts (CAFs) from an average of 17–65% of the samples tested (16). This "rescue" of CAV1, a key regulator of mitochondrial metabolism, in CAFs suggests that metformin may induce a partial reversal of the metabolic phenotype of CAFs (17). We demonstrated a significant increase in tumor cell apoptosis in tumor cells after treatment with metformin by TUNEL (terminal deoxyribonucleotidyl transferase mediated dUTP-digoxigenin nick end labeling) assay ($p < 0.001$). Here we report results of novel sub-analyses on cancer cell apoptosis in HPV+ and HPV– groups and alterations in the immune TME mediated by metformin and an exploration of the impact of metformin treatment on the immune TME of involved lymph nodes.

MATERIALS AND METHODS

Subjects

The metformin clinical trial specimens were primary tumor and lymph node samples obtained from a surgical trial in HNSCC patients. This study was carried out in accordance with the recommendations of Internal Review Board (IRB) of Thomas Jefferson University with written informed consent from all subjects. All subjects gave written informed consent in accordance with the Declaration of Helsinki. The protocol was approved by the Internal Review Board of Thomas Jefferson University. The trial was conducted with IRB approval and design, enrollment, and demographics are as described in detail elsewhere (16). (https://www.clinicaltrials.gov/ct2/show/NCT02083692). The flow for the trial is shown in **Figure 1**. Briefly, paired pre- and post-operative primary tumor tissue samples were compared for each patient. Patients included had a new, pathologically-confirmed diagnosis of HNSCC.

Demographics are shown in **Table 1**. Enrolled patients received metformin titrated up every 3 days up to a standard anti-diabetic dose of 1000mg twice daily for up to 28 days prior to surgery with only specimens from patients with ≥9 days (range 9–24, mean 13.6 days) of therapy being analyzed. Patients received no additional cancer treatment while metformin was being administered. Of the 50 HNSCC patients enrolled, 39 completed the course of at least 9 days and had evaluable data and pre and post treatment specimens; of these 17 were HPV+ oropharyngeal squamous cell carcinoma (OPSCC) and 22 were HPV– HNSCC. Primary tumor samples were categorized according to HPV and smoking status. HPV status was demonstrated by p16 staining and subsequent *in situ* hybridization for HPV16 and 18. The pre-treatment and post-treatment specimens were compared by terminal deoxynucleotidyl transferase dUTP nick end labeling (TUNEL) assay for tumor cell apoptosis. For the current TUNEL comparison, HPV+ OPSCC samples ($n = 17$) were compared to HPV–, tobacco + HNSCC samples ($n = 12$). To assess immune elements of the TME, analysis of CD8, FoxP3, PD-L1, and CD163 staining intensity was carried out via digital image analysis using Aperio (Leica Biosystems, Wetzlar, Germany) co-localization and nuclear algorithms for assessment of intensity and quantification. FFPE lymph node specimens from patients on the trial with nodal metastasis demonstrating ECE ($n = 7$) were compared to archival FFPE ECE lymph node specimens ($n = 11$) from patients not receiving metformin either on trial or as a part of their medical record prior to surgery. Archival specimens were obtained with IRB approval.

TABLE 1 | Demographics for clinical trial patients.

Demographics			
Age	61.7 (35–80)		
Gender	28 m/11 f		
Days on metformin	13.56 (9–24)		
Anatomic subsite			
Oral cavity	13 (33.3%)	**Oropharynx**	21 (53.8%)
Skin	1 (2.6%)	HPV+ OPSCC	17/21 (81.0%)
Larynx	3 (7.7%)	**Hypopharynx**	1 (2.6%)
Staging (AJCC 2017)			
***T* stage**		***N* stage**	
Tis	1 (2.6%)	N0	16 (41.0%)
T1	8 (20.5%)	N1	3 (7.7%)
T2	19 (48.7%)	N2a	5 (12.8%)
T3	3 (7.7%)	N2b	12 (30.8%)
T4a	8 (20.5%)	N2c	0 (0%)
T4b	0 (0%)	N3	3 (7.7%)
Pathologic markers		**Differentiation**	
ECE	10 (25.6%)	*in situ*	1 (2.6%)
Positive margins	4 (10.3%)	Well	3 (7.7%)
PNI	16 (41.0%)	Moderate	18 (46.2%)
LVI	14 (35.9%)	Poor	16 (41.0%)

HPV, human papilloma virus; OPSCC, oropharyngeal squamous cell carcinoma; AJCC, American Joint Commission on Cancer; Tis, tumor stage in situ; ECE, extracapsular extension; PNI, perineural invasion; LVI, lymphovascular invasion.

Immunohistochemistry

Tissue sections (4 μm) for IHC analysis were dewaxed, rehydrated through graded ethanols, and antigen retrieval was performed on the Ventana Discovery ULTRA staining platform using Discovery CCI (Ventana cat#950-500) for a total application time of 64 min. Secondary immunostaining used a Horseradish Peroxidase (HRP) multimer cocktail (Ventana cat#760-500) and immune complexes were visualized using the ultraView Universal DAB (diaminobenzidine tetrahydrochloride) Detection Kit (Ventana cat#760-500). Slides were then washed with a Tris based reaction buffer (Ventana cat#950-300) and stained with Hematoxylin II (Ventana cat #790-2208) for 8 min. The CD8 antibody (CONFIRM Anti-CD8 SP57 Rabbit Monoclonal Primary antibody) and PD-L1 antibody (VENTANA PD-L1 (SP263) Rabbit Monoclonal Primary Antibody were obtained from Roche-Ventana, Tucson,AZ, USA). The FoxP3 (SP97) antibody was obtained from Spring Biosciences (Pleasanton, CA). The CD163 antibody (MRQ-26 mouse monoclonal antibody) was obtained from Cell Marque (Rocklin, CA, USA). Sections were counterstained with hematoxylin.

For quantification of apoptotic cells the TUNEL-based ApopTag Peroxidase *in situ* Apoptosis Detection Kit (Millipore Sigma Lifesciences, Burlington, MA) was used. The number of nuclei with TUNEL staining per high power field (hpf) was averaged over five HPFs in each specimen, and the mean was reported. For each sample, scores from two pathologists were averaged to yield a final score for statistical analysis.

Digital image analysis of CD8, FoxP3, CD163, and PD-L1 IHC was performed employing digital pathology with Aperio software as previously described (18). CD8 was utilized as a marker for Teff cells. FoxP3 was utilized as a marker for regulatory T cells (Tregs). CD163 was utilized as a marker for suppressive (M2) tumor associated macrophages (TAM). Programmed death ligand 1 (PD-L1) is highly expressed on cancer cells and some immune cells in the TME, such as TAMs. Briefly, tissue sections were scanned on a ScanScope™ XT at 40x, with an average scan time of 120 s (compression quality 70). Images were analyzed using the Color Deconvolution and the Colocalization Aperio Image Analysis tool. Areas of staining were color separated from hematoxylin counter-stained sections and the intensity of the staining was measured on a continuous 0 (bright white) to 255 (black) scale. For each marker, only the cells of highest intensity staining (digitally scored on a scale of 0–3+) were counted in the region of interest. Measurements from 5 hpf were taken and averaged to score each sample. The results are reported as % of nuclei/cells in a given region of interest with high intensity (3+) staining.

Statistical Analysis

Linear regression to assess strength of associations between continuous variables was performed. Significant *p*-values were

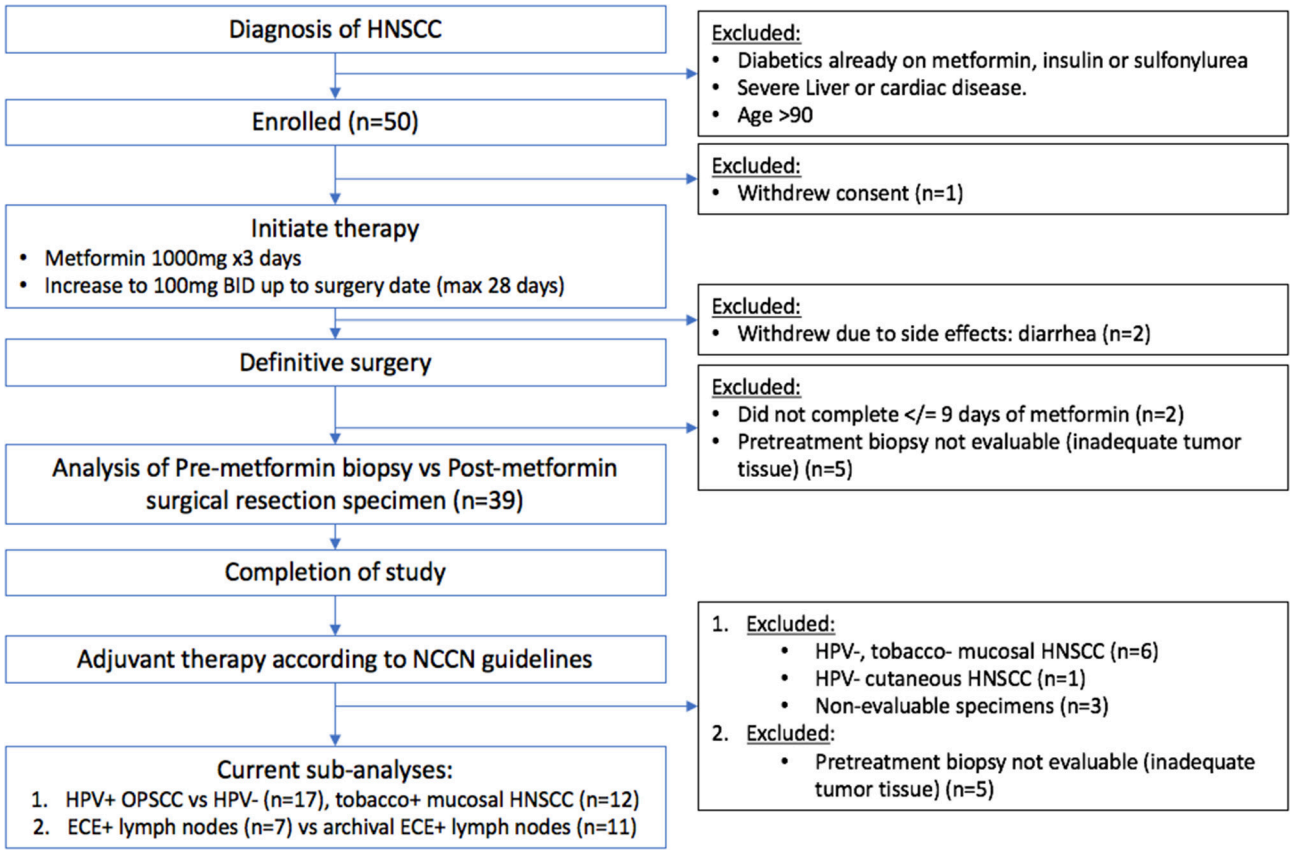

FIGURE 1 | Consort flow chart for the clinical trial.

considered < 0.05. TUNEL assay results were compared by multivariable robust linear mixed model with predictors (pre- vs. post-treatment) and HPV status as well as their interaction. CD8, FoxP3, CD-163, and PD-L1 IHC intensity was analyzed using Aperio as described above using a membrane staining algorithm using linear regression as above. Data were analyzed with R v3.5.0 (R-project.org).

RESULTS

TUNEL Apoptosis Assay

The metformin pre- and post-treatment groups were stratified and compared by tobacco and HPV status for analysis of tumor cell apoptosis in the primary tumor samples. Among these patients, there was a significantly greater increase in apoptosis with metformin treatment in HPV–, tobacco+ mucosal HNSCC ($n = 12$, mean Δ 13.7/hpf) compared to HPV+ OPSCC ($n = 17$, mean Δ 5.7/hpf) ($p < 0.001$) (**Figures 1–3**). Number of days treated with metformin for the two groups was similar ($p = 0.92$, t-test), with a mean 13.58 days for the HPV-tobacco+ group (range: 10–16 days) and a mean 13.71 days for the HPV+ group (range: 9–24).

Immune Infiltrate in Node Specimens

To analyze the immune TME of the invasive tumor front, post-treatment lymph node specimens showing ECE were also compared to archival specimens with ECE. In a previous study, we demonstrated that the invasive front of lymph nodes with ECE is histologically similar to the invasive primary tumor front (19). The nodal samples were used to preserve limited pre-treatment primary tumor biopsy tissue for possible future analysis. Using the Aperio digital image analysis software, comparisons of staining intensity for CD8, FoxP3, CD163, and PD-L1 was made to quantify percentage of cells staining positive for each marker in the various compartments in the TME. In both groups, the CD163, FOXP3, and PD-L1 expression in the perinodal stroma at the site of invasion were significantly higher compared to regions with an intact lymph node capsule ($p < 0.001$) (**Figures 4**, **5**). Further, these areas were similar at the invasive front between the metformin and non-metformin groups with respect to CD163 and PD-L1 suggesting that there was no significant change related to metformin treatment. Most interestingly, CD8 infiltrates were significantly greater in the tumor stroma at the invasive front of the metformin group (mean 22.8%) compared to the control (mean 10.7%) ($p = 0.006$). Moreover, FoxP3+ Tregs were also greater in metformin treated group (mean 9%) compared to the non-metformin treated group (mean 5%) ($p = 0.019$).

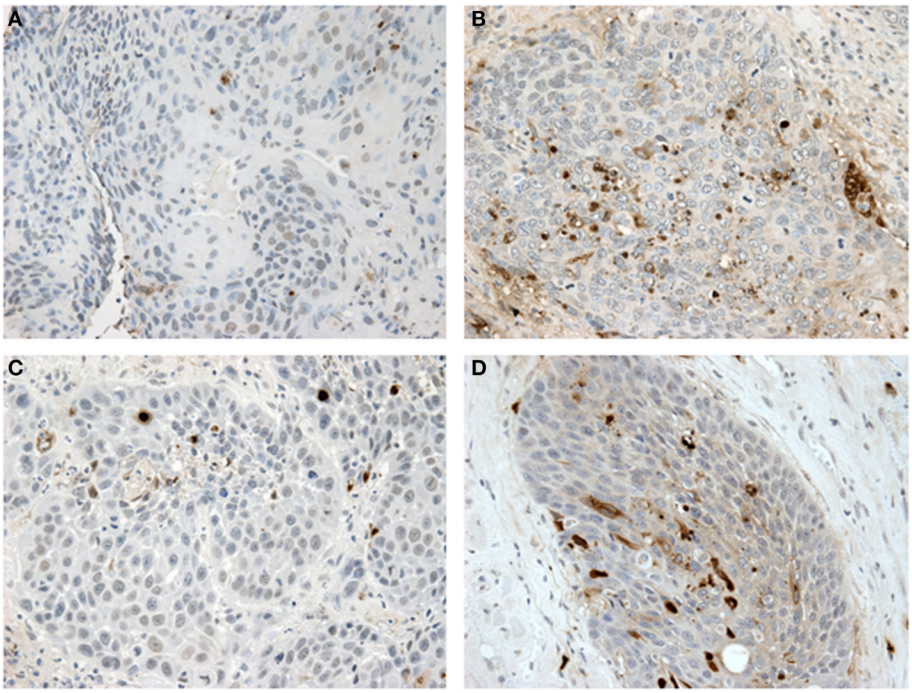

FIGURE 2 | Tunel assay results: **(A,B)** show paired samples from an HPV—HNSCC specimen pre- and post-treatment with metformin showing a significant increase in apoptosis after metformin treatment. **(C,D)** show paired samples from an HPV+ OPSCC specimen also showing an increase in apoptosis after metformin treatment.

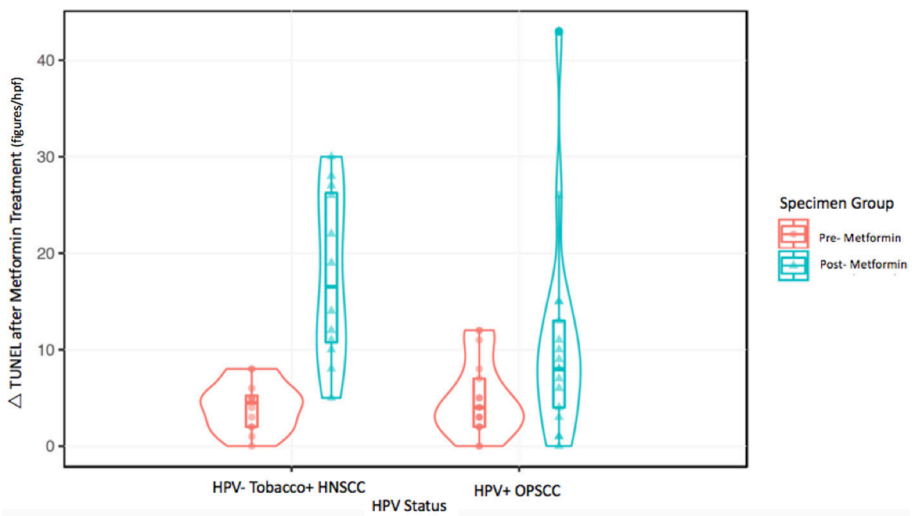

FIGURE 3 | Violin plot for regression analysis of TUNEL data.

DISCUSSION

Here we present novel data on analysis of specimens from a clinical trial of metformin in HNSCC demonstrating a significantly increased cancer cell apoptosis in HPV– tobacco+ mucosal HNSCC compared to HPV+ OPSCC tumor samples after metformin treatment ($p < 0.001$, **Figures 1**, **2**). This differential effect on the two tumor types is intriguing, but of unclear etiology. The mechanism by which metformin may exert its anticancer effects is not entirely understood, but it is known to impact cellular metabolism by multiple mechanisms, including inhibition of mitochondrial complex I, upregulation of AMP kinase and subsequent regulation of mTOR (20). Thus the effect on cancers may be attributed to the metabolic impact on the TME by metformin. In one study, HPV– HNSCC has been shown to be highly glycolytic, generate large amounts

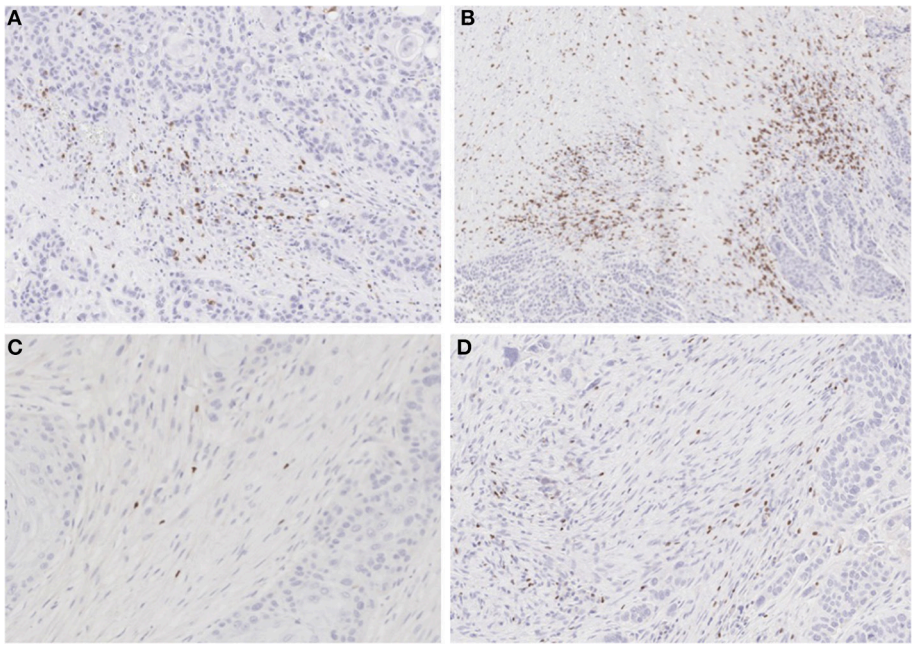

FIGURE 4 | IHC for CD8 and FoxP3: **(A)** non-treated and **(B)** metformin treated samples stained for CD8 showing higher Teff cell count in the metformin treated specimens. **(C)** non-treated and **(D)** metformin treated specimens stained for FoxP3, showing a higher Treg count in metformin treated specimens.

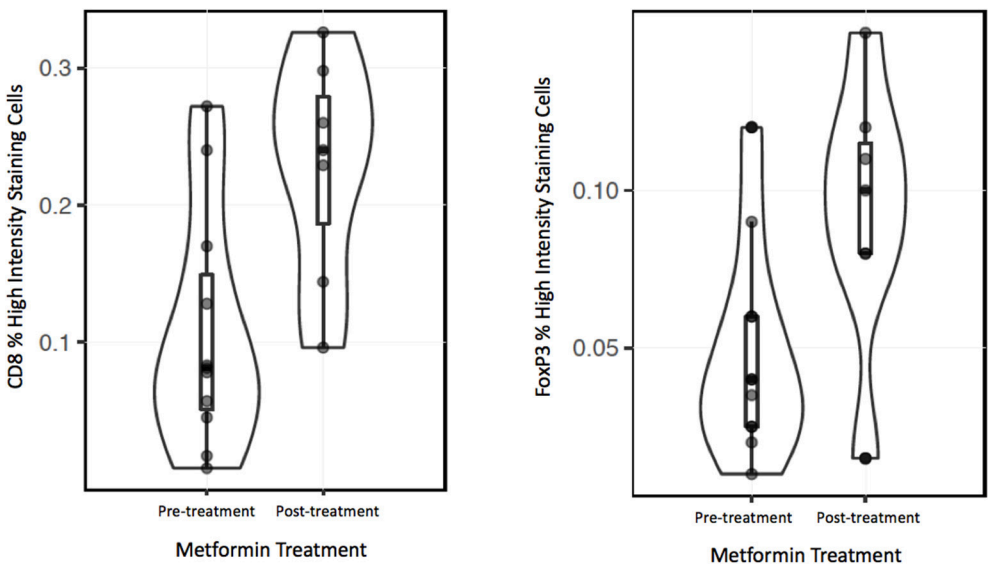

FIGURE 5 | Violin plot for regression analysis of CD8 and FoxP3 IHC data.

of lactate and have high levels of hypoxia, while HPV+ tumors demonstrated that effective utilization of glycolysis and oxidative phosphorylation (21). We previously demonstrated that HNSCC samples with high expression of the lactate exporter, monocarboxylate transporter 4 (MCT4), staining have a worse prognosis; high expression of MCT4 correlates with high glycolysis (22). Taken together, these data suggest differing metabolism between the two tumor types with higher reliance on glycolytic metabolism in HPV–, tobacco+ HNSCC. It is possible that metformin exerts a metabolic strain that is beyond the tolerance of the already highly glycolytic HPV– tumors. Yet, further research is required to test this hypothesis. Alternatively, the anticancer effects of metformin may be indirectly mediated through effects on other elements of the TME such as enhanced immune activity as seen in animal models of other tumor types (12).

Therefore, we hypothesized that the anticancer effects of metformin may also be due to an increased anti-tumor immune response. Dysregulated metabolism in the TME contributes to immune evasion through various mechanisms including impairment of tumor infiltrating T cell function, TAM function and checkpoint inhibition among other mechanisms (23, 24). Mitigation of this dysregulation in cancer may result in enhanced immune function. We analyzed specimens for alterations in key immune elements, including CD8, FoxP3, CD163, and PD-L1. For this exploratory analysis, we utilized lymph nodes with ECE as the invasive front at the site of ECE is a point of direct interaction with the surrounding tissue and stroma (19). We compared metformin treated specimens to matched archival specimens without metformin exposure. This group of ECE+ nodal specimens consisted of both HPV+ and HPV– lymph nodes from the trial, as the individual groups from the trial were too small to analyze separately. The archival samples were matched HPV+ and HPV– samples. No significant difference in PD-L1 or CD163 staining was noted in the cancer or tumor stroma of samples from patients that had received metformin or the controls.

However, there was a significant increase in the CD8+ T cell infiltrate in the tumor stroma at the invasive front in metformin treated patients compared to archival specimens. (**Figures 4**, **5**) This finding represents the first clinical data to point to a link between a metabolic and immune altering mechanism for metformin. As described above, preclinical data in an immunocompetent C57BL/6 murine model with syngeneic MC-38 colon adenocarcinoma and B16 melanoma cancer cells demonstrates that metformin synergizes with PD-1 inhibition to substantially increase the antitumor effect of immunotherapy (12). Metformin inhibited oxygen consumption within the tumor, resulting in mitigation of hypoxia mediating enhanced effect of PD-1 inhibition. This preclinical data combined with evidence of clinical efficacy provides support to explore the combination of metformin with anticancer immunotherapy in clinical trials. Further, there is currently a clinical trial underway in HNSCC to study the impact of metformin on tissue hypoxia (NCT03510390).

Interestingly, we also identified an increase in FoxP3+ Tregs in the metformin treated group. This finding was unexpected in light of the increased CD8+ T cells, as typically Tregs are thought to be suppressive and thought to inhibit an effective anti-tumor response (25). However, a recent meta-analysis suggests that in HPV– HNSCC a higher infiltration of FoxP3+ Tregs correlated with an improved prognosis (26). There is little data on the effects of FoxP3+ Tregs in HPV+ OPSCC but there is a trend toward improved survival with higher infiltrate, and one study showed evidence that the patients with higher peripheral Treg counts had a better prognosis (27–29). Recent data based on analysis of The Cancer Genome Atlas (TCGA) showed that HPV– tumors are characterized by an immune-poor TME with lower overall infiltrate and that this finding correlates with a worse prognosis (30). In contrast HPV+ OPSCC is characterized by an immune rich TME, which has a better prognosis. An increase in immune infiltrate may correlate with improved anti-tumor response.

This study has several limitations, including sample size is limited for both the apoptosis assay and the immune IHC studies, although statistical significance was reached. The sample size in this study was too small to determine whether HPV+ OPSCC or HPV– HNSCC had differential changes in immune infiltrates for CD8+ Teff or FoxP3+ Tregs. Additionally, we studied lymph node specimens from subjects receiving metformin and controls for analysis of the immune markers but the status of these immune markers is unknown in the primary tumor specimens. The immune status of the TME of the lymph node or surrounding soft tissue may differ from that of the primary tumor; however, we would argue that the data regarding the immune TME of lymph nodes is also important. Further, studies must be undertaken to validate these results and to obtain mechanistic data on how metformin causes increased cancer cell apoptosis and the increased immune infiltrate and also whether these two effects are directly linked. Nevertheless, this study does present intriguing preliminary data directly from HNSCC clinical trial samples.

CONCLUSION

Metformin resulted in a greater increase in apoptosis in HPV– tobacco+ HNSCC than occurred in HPV+ OPSCC. While the mechanism has yet to be clarified, metformin also appears to alter the immune TME with an increased infiltrate of CD8+ Teff and FoxP3 Tregs at the invasive tumor margin of lymph nodes with ECE.

AUTHOR CONTRIBUTIONS

JC design of study, data accrual, and manuscript preparation. JJ, DW-M, MGM, AS, UR, LH, NP, AL, DC, UM-O design of study, manuscript prep and editing. MM, PT, DA, AK, DW-M data accrual and management. MT pathology oversight, manuscript preparation, and editing. TZ biostatistics oversight.

REFERENCES

1. Becker C, Jick SS, Meier CR, Bodmer M. Metformin and the risk of head and neck cancer: a case-control analysis. *Diabetes Obes Metab*. (2014) 16:1148–54. doi: 10.1111/dom.12351
2. Yen YC, Lin C, Lin SW, Lin YS, Weng SF. Effect of metformin on the incidence of head and neck cancer in diabetics. *Head Neck* (2014) 37:1268–73. doi: 10.1002/hed.23743
3. Giovannucci E, Harlan DM, Archer MC, Bergenstal RM, Gapstur SM, Habel LA, et al. Diabetes and cancer: a consensus report. *Diabetes Care* (2010) 33:1674–85. doi: 10.2337/dc10-0666
4. Johnson JA, Pollak M. Insulin, glucose and the increased risk of cancer in patients with type 2 diabetes. *Diabetologia* (2010) 53:2086–8. doi: 10.1007/s00125-010-1855-0
5. Libby G, Donnelly LA, Donnan PT, Alessi DR, Morris AD, Evans JM. New users of metformin are at low risk of incident cancer: a cohort

study among people with type 2 diabetes. *Diabetes Care* (2009) 32:1620–5. doi: 10.2337/dc08-2175
6. Evans JM, Donnelly LA, Emslie-Smith AM, Alessi DR, Morris AD. Metformin and reduced risk of cancer in diabetic patients. *BMJ* (2005) 330:1304–5. doi: 10.1136/bmj.38415.708634.F7
7. Luo Q, Hu D, Hu S, Yan M, Sun Z, Chen F. *In vitro* and *in vivo* anti-tumor effect of metformin as a novel therapeutic agent in human oral squamous cell carcinoma. *BMC Cancer* (2012) 12:1. doi: 10.1186/1471-2407-12-517
8. Patrick T, Domingo-Vidal M, Whitaker-Menezes D, Lin Z, Roche M, Tuluc M. Metformin effects on metabolic coupling and tumor growth in oral cavity squamous cell carcinoma coinjection xenografts. *Otolaryngol Head Neck Surg.* (2018) 158:1–11. doi: 10.1177/0194599817746934
9. Rizos CV, Elisaf MS. Metformin and cancer. *Eur J Pharmacol.* (2013) 705:96–108. doi: 10.1016/j.ejphar.2013.02.038
10. Verma A, Rich LJ, Vincent-Chong VK, Seshadri M. Visualizing the effects of metformin on tumor growth, vascularity, and metabolism in head and neck cancer. *J Oral Pathol Med.* (2018) 47:484–91. doi: 10.1111/jop.12705
11. Vitale-Cross L, Molinolo AA, Martin D, Younis RH, Maruyama T, Patel V, et al. Metformin prevents the development of oral squamous cell carcinomas from carcinogen-induced premalignant lesions. *Cancer Prevent Res.* (2012) 5:562–73. doi: 10.1158/1940-6207.CAPR-11-0502
12. Scharping NE, Menk AV, Whetstone RD, Zeng X, Delgoffe GM. Efficacy of PD-1 blockade is potentiated by metformin-induced reduction of tumor hypoxia. *Cancer Immunol Res.* (2017) 5:9–16. doi: 10.1158/2326-6066.CIR-16-0103
13. Kouidhi S, Ben Ayed F, Benammar Elgaaied A. Targeting tumor metabolism: a new challenge to improve immunotherapy. *Front Immunol.* (2018) 9:353. doi: 10.3389/fimmu.2018.00353
14. Leung E, Cairns RA, Chaudary N, Vellanki RN, Kalliomaki T, Moriyama EH, et al. Metabolic targeting of HIF-dependent glycolysis reduces lactate, increases oxygen consumption and enhances response to high-dose single-fraction radiotherapy in hypoxic solid tumors. *BMC Cancer* (2017) 17:418. doi: 10.1186/s12885-017-3402-6
15. Romero-Garcia S, Moreno-Altamirano MM, Prado-Garcia H, Sánchez-García FJ. Lactate contribution to the tumor microenvironment: mechanisms, effects on immune cells and therapeutic relevance. *Front Immunol.* (2016) 7:52. doi: 10.3389/fimmu.2016.00052
16. Curry J, Johnson J, Tassone P, Vidal MD, Menezes DW, Sprandio J, et al. Metformin effects on head and neck squamous carcinoma microenvironment: window of opportunity trial. *Laryngoscope* (2017) 127:1808–15. doi: 10.1002/lary.26489
17. Asterholm IW, Mundy DI, Weng J, Anderson RGW, Scherer PE. Altered mitochondrial function and metabolic inflexibility associated with loss of caveolin-1. (2018) 5:171–85. doi: 10.1016/j.cmet.2012.01.004
18. Johnson JM, Lai SY, Cotzia P, Cognetti D, Luginbuhl A, Pribitkin EA, et al. Mitochondrial metabolism as a treatment target in anaplastic thyroid cancer. *Sem Oncol.* (2015) 42:915–22. doi: 10.1053/j.seminoncol.2015.09.025
19. Curry J, Tassone P, Gill K, Tuluc M, BarAd V, Mollaee M, et al. Tumor metabolism in the microenvironment of nodal metastasis in oral squamous cell carcinoma. *YMHN* (2017) 157:798–807. doi: 10.1177/0194599817709224
20. Mallik R, Chowdhury TA. Metformin in cancer. *Diabetes Res Clin Pract.* (2018) 2:57. doi: 10.1016/j.diabres.2018.05.023
21. Jung YS, Najy AJ, Huang W, Sethi S, Snyder M, Sakr W, et al. HPV-associated differential regulation of tumor metabolism in oropharyngeal head and neck cancer. *Oncotarget* (2017) 8:51530–41. doi: 10.18632/oncotarget.17887
22. Curry JM, Tuluc M, Whitaker-Menezes D, Ames JA, Anantharaman A, Butera A, et al. Cancer metabolism, stemness and tumor recurrence. *Cell Cycle* (2014) 12:1371–84. doi: 10.4161/cc.24092
23. Colegio OR, Chu NQ, Szabo AL, Chu T, Rhebergen AM, Jairam V, et al. Functional polarization of tumour-associated macrophages by tumour-derived lactic acid. *Nature* (2014) 513:559–63. doi: 10.1038/nature13490
24. Siska PJ, Rathmell JC. T cell metabolic fitness in antitumor immunity. *Trends Immunol.* (2015) 36:257–64. doi: 10.1016/j.it.2015.02.007
25. Sakaguchi S, Yamaguchi T, Nomura T, Ono M. Regulatory T cells and immune tolerance. *Cell* (2008) 133:775–87. doi: 10.1016/j.cell.2008.05.009
26. de Ruiter EJ, Ooft ML, Devriese LA, Willems SM. The prognostic role of tumor infiltrating T-lymphocytes in squamous cell carcinoma of the head and neck: a systematic review and meta-analysis. *OncoImmunology* (2017) 6:1–10. doi: 10.1080/2162402X.2017.1356148
27. Näsman A, Romanitan M, Nordfors C, Grün N, Johansson H, Hammarstedt L, et al. Tumor infiltrating CD8+ and Foxp3+ lymphocytes correlate to clinical outcome and human papillomavirus (HPV) status in tonsillar cancer. *PLoS ONE* (2012) 7:e38711. doi: 10.1371/journal.pone.0038711
28. Oguejiofor K, Hall J, Slater C, Betts G, Hall G, Slevin N, et al. Stromal infiltration of CD8 T cells is associated with improved clinical outcome in HPV-positive oropharyngeal squamous carcinoma. *Br J Cancer* (2015) 113:886–93. doi: 10.1038/bjc.2015.277
29. Punt S, Dronkers EAC, Welters MJP, Goedemans R, Koljenović S, Bloemena E, et al. A beneficial tumor microenvironment in oropharyngeal squamous cell carcinoma is characterized by a high T cell and low IL-17(+) cell frequency. *Cancer Immunol Immunother.* (2016) 65:393–403. doi: 10.1007/s00262-016-1805-x
30. Mandal R, Senbabaoglu Y, Desrichard A, Havel JJ, Dalin MG, Riaz N., et al. The head and neck cancer immune landscape and its immunotherapeutic implications. *JCI Insight* (2016) 1:1–19. doi: 10.1172/jci.insight.89829

Conflict of Interest Statement: The authors declare that the research was conducted in the absence of any commercial or financial relationships that could be construed as a potential conflict of interest.

frontiers in Cell and Developmental Biology

HYPOTHESIS AND THEORY
published: 02 October 2018
doi: 10.3389/fcell.2018.00095

Cellular and Molecular Networking Within the Ecosystem of Cancer Cell Communication via Tunneling Nanotubes

Emil Lou[1], Edward Zhai[1†], Akshat Sarkari[1†], Snider Desir[1,2], Phillip Wong[1,3], Yoshie Iizuka[4], Jianbo Yang[5], Subbaya Subramanian[6], James McCarthy[5], Martina Bazzaro[4] and Clifford J. Steer[3]*

[1] Division of Hematology, Oncology and Transplantation, Department of Medicine, University of Minnesota, Minneapolis, MN, United States, [2] Department of Integrative Biology and Physiology, University of Minnesota, Minneapolis, MN, United States, [3] Division of Gastroenterology, Hepatology and Nutrition, Department of Medicine, University of Minnesota, Minneapolis, MN, United States, [4] Division of Gynecologic Oncology and Women's Health, Department of Obstetrics and Gynecology, Masonic Cancer Center, University of Minnesota, Minneapolis, MN, United States, [5] Department of Laboratory Medicine and Pathology, University of Minnesota, Minneapolis, MN, United States, [6] Department of Surgery, University of Minnesota, Minneapolis, MN, United States

OPEN ACCESS

Edited by:
Ubaldo Emilio Martinez-Outschoorn, Thomas Jefferson University, United States

Reviewed by:
Eliseo A. Eugenin, The University of Texas Medical Branch at Galveston, United States
Robbie B. Mailliard, University of Pittsburgh, United States

***Correspondence:**
Emil Lou
emil-lou@umn.edu

[†]These authors have contributed equally to this work

Specialty section:
This article was submitted to Molecular and Cellular Oncology, a section of the journal Frontiers in Cell and Developmental Biology

Received: *07 June 2018*
Accepted: *02 August 2018*
Published: *02 October 2018*

Citation:
Lou E, Zhai E, Sarkari A, Desir S, Wong P, Iizuka Y, Yang J, Subramanian S, McCarthy J, Bazzaro M and Steer CJ (2018) Cellular and Molecular Networking Within the Ecosystem of Cancer Cell Communication via Tunneling Nanotubes. Front. Cell Dev. Biol. 6:95. doi: 10.3389/fcell.2018.00095

Intercellular communication is vital to the ecosystem of cancer cell organization and invasion. Identification of key cellular cargo and their varied modes of transport are important considerations in understanding the basic mechanisms of cancer cell growth. Gap junctions, exosomes, and apoptotic bodies play key roles as physical modalities in mediating intercellular transport. Tunneling nanotubes (TNTs)—narrow actin-based cytoplasmic extensions—are unique structures that facilitate direct, long distance cell-to-cell transport of cargo, including microRNAs, mitochondria, and a variety of other sub cellular components. The transport of cargo via TNTs occurs between malignant and stromal cells and can lead to changes in gene regulation that propagate the cancer phenotype. More notably, the transfer of these varied molecules almost invariably plays a critical role in the communication between cancer cells themselves in an effort to resist death by chemotherapy and promote the growth and metastases of the primary oncogenic cell. The more traditional definition of "Systems Biology" is the computational and mathematical modeling of complex biological systems. The concept, however, is now used more widely in biology for a variety of contexts, including interdisciplinary fields of study that focus on complex interactions within biological systems and how these interactions give rise to the function and behavior of such systems. In fact, it is imperative to understand and reconstruct components in their native context rather than examining them separately. The long-term objective of evaluating cancer ecosystems in their proper context is to better diagnose, classify, and more accurately predict the outcome of cancer treatment. Communication is essential for the advancement and evolution of the tumor ecosystem. This interplay results in cancer progression. As key mediators of intercellular communication within the tumor ecosystem, TNTs are the central topic of this article.

Keywords: angiogenesis, cancer ecosystems, cancer pathophysiology, intercellular communication, intercellular transfer, tumor microenvironment, tumor microtubes, tunneling nanotubes

INTRODUCTION

Malignant tumors are heterogeneous and highly dynamic ecosystems. Cellular communication is a critical component of heterotypic and homotypic interactions in the complex, ever-changing tumor microenvironment. Tunneling nanotubes (TNTs) are long filamentous actin-based cellular protrusions that contribute to these interactions, with a special role in long-range communication (Rustom et al., 2004; Onfelt et al., 2005; Eugenin et al., 2009; Gousset et al., 2009, 2013; Chauveau et al., 2010; Plotnikov et al., 2010; Lou et al., 2012; Pasquier et al., 2013; Zhang and Zhang, 2015). While substantial progress has been made in understanding the function of TNTs over the past 5 years, there remain many unknowns, such as whether or not there exist a single or multiple sets of structural or other biomarkers that are characteristic of and specific to TNTs across cell types. In addition, many of their behavioral characteristics remain unclear.

By using a systems biology approach to characterize TNTs, we can further shed light on the interactions that are mediated within the tumor microenvironment. These interactions include not only cell-to-cell communication among malignant cells, but also interactions between malignant and stromal cells within the extracellular matrix, including vascular endothelial cells and cancer-associated fibroblasts. These are just two examples of stromatous cell types that are susceptible to potential reprogramming. Downstream effects of cellular reprogramming that result from indirect or direct cell communication have strong implications in altering not only the growth of tumor but also its metastatic potential.

Here, we discuss our theory that investigating the tumor ecosystem by focusing on long-range communication via TNTs will yield novel perspectives on their role in the evolution of cancer. There is strong interest in the identification of stimulatory factors and molecular machinery of TNT formation and maintenance as potential biomarkers of the disease. We follow up on our previous report that hypoxia—a physiologic condition that is characteristic of the tumor microenvironment and one that is heavily associated with metabolic dysfunction and tumor invasiveness—induces TNTs in ovarian cancer cells (Desir et al., 2016), by confirming this in another model system (colon cancer). Taking this a step further, we hypothesize that the conditions of hypoxia are not only favorable for the formation of TNTs but also that these TNTs in turn are capable of propagating hypoxia-inducible factor-1α (HIF-1α) and vascular endothelial growth factor (VEGF) between connected cells to stimulate angiogenesis. Another form of heterotypic interaction occurs between malignant cells and the hematologic system, including red blood cells (RBCs) and platelets, which themselves have been found to form pseudopodia-like protrusions that may in fact signify TNTs. We also examine other potential candidate components of the plasma membrane (proteoglycan chondroitin sulfate proteoglycan 4, or CSPG4) and cellular machinery of motility (UNC-45A) in relation to cancer cell TNTs. Another form of transmembrane protein, the nucleoside transporter human equilibrative nucleoside transporter 1 (hENT1), whose expression is associated with more efficient cell-to-cell diffusion of fluoropyrimidine chemotherapeutic drugs, is also of interest; we examine whether this protein varies with TNT formation. The growing body of evidence that TNTs play a role in connecting cells within the cancer ecosystem provides a basis for expanding potential applications of TNTs to explain fundamental processes in cancer as well as in normal cell function. The clinical relevance of this field is focused on TNTs as structural components of cells that are potential targets for drug therapy or for other targeting strategies.

TNT FORMATION IS UPREGULATED BY HYPOXIC CONDITIONS IN MULTIPLE FORMS OF CANCER, INCLUDING COLON CANCER

Tunneling nanotubes are a form of cellular stress response to conditions that favor physiologic and metabolic dysregulation (Lou et al., 2012; Wang and Gerdes, 2012). In 2016, we reported that hypoxia, a state that is characteristic of invasive malignancies and the solid tumor microenvironment, induced a higher rate of TNT formation in ovarian cancer cells (Desir et al., 2016). Moreover, the effect was most pronounced in chemoresistant ovarian cancer cells even after treatment with a compound that effectively suppressed TNTs in sensitive cells. To provide further confirmation that this observation could be applied to other cancer cell types, we compared TNT formation under conditions identical to colon cancer cells subjected to hypoxia vs. normoxia. We used three different cell lines (SW480, HCT-116, and DLD-1), in addition to two non malignant cell types, the colon adenoma (premalignant)-derived cell line AAC1 and fibroblasts (NIH 3T3 cell line). Following the same experimental approach that previously showed upregulated HIF-1α expression (Desir et al., 2016), we detected TNT formation when all three of the colon cancer cell lines were cultured in hypoxic conditions (**Figure 1**). The AAC1 cells failed to form TNTs under normoxic conditions, and this lack of TNT formation was again observed even under hypoxic conditions. We also confirmed that NIH 3T3 fibroblasts readily formed TNTs under both conditions. Upon analysis of absolute numbers of TNTs it was found that SW480 and HCT-116 carcinoma cells and NIH 3T3 cells formed more TNTs under hypoxic than normoxic conditions, but DLD-1 cells demonstrated no difference. To account for alterations in cell metabolism and cell viability, we again used absorbance as a surrogate for the direct quantification of cells using the Cell Counting Kit (see Methods section for details); this procedure ensured that differences in numbers of TNTs could not be attributed to changes in cell proliferation under differing conditions. After accounting for altered cell metabolism from hypoxia, the differences in TNT formation were most profound for the HCT-116 and NIH 3T3 cells by 72 h. Conversely, TNT formation was negligible for SW480 cells. In contrast, DLD-1 cells were less responsive to hypoxia; overall, the TNT/absorbance ratio was actually lower for these cells after hypoxic exposure at all three time points (24, 48, and 72 h).

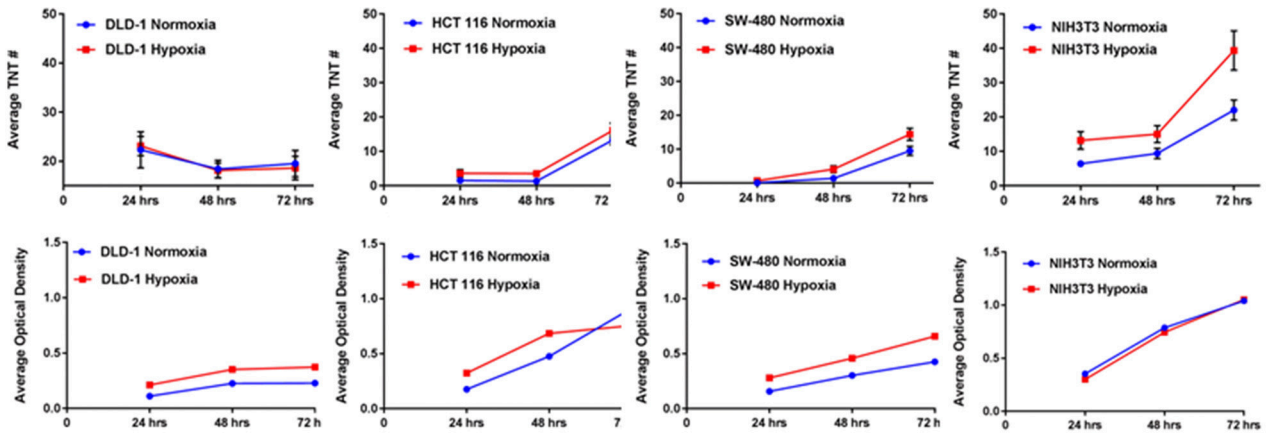

FIGURE 1 | Hypoxia induces TNT formation in colon cancer cells, independent of alterations in cell proliferation. Graphs demonstrate changes in average number of TNTs at 24 h, 48 h, and 72 h (top row) under normoxic vs. hypoxic conditions and average optical density as a surrogate for cell proliferation at the same time points (bottom row) for the colon cancer cell lines DLD-1, HCT-116, and SW-480 and for the comparison of the fibroblast cell line NIH 3T3. Materials and Methods section for experiments shown in the figure is available in the **Supplementary Material**.

HETEROTYPIC INTERACTIONS BETWEEN MALIGNANT CELLS AND STROMA MEDIATED BY TNTs: DECIPHERING COMMUNICATION BETWEEN VASCULAR, HEMATOLOGIC, AND IMMUNE CELLS

Overall, these results provided confirmation and support for our prior work demonstrating that hypoxic conditions induce metabolic stress that results in upregulated TNT formation in some invasive cancer cells but not in others. Nonetheless, the confirmation of the hypoxic effects of TNTs on both malignant and stromal (fibroblast) cells provides further support for an important spatial and developmental timing niche for TNTs in the process of tumor growth. This prospect opens the door to deciphering the potential role of these TNTs in mediating heterotypic matrix-cancer cellular interactions in invasive, hypoxic tumors. A prime translational example of this context is angiogenesis, the process of vascular tube formation that arises in reaction to hypoxia that stems from diminished diffusion of oxygen that usually permeates toward the central portions of tumors. Angiogenesis is central to vascular interactions within the cancer ecosystem. As tumors grow and oxygen levels decrease, malignant cells secrete soluble VEGF that diffuses across the intercellular space and is taken up by the vascular endothelium via its corresponding receptor. This process results in angiogenesis, in which malignant cells essentially direct the construction of their own stromal matrix and mediate a new form of enriched oxygenation through increased blood flow. To date, the secretion and downstream effects of VEGF have been assumed to occur solely by diffusion through the microenvironment. However, it is also conceivable that TNTs can form between malignant and vascular endothelial cells and act as conduits for VEGF transfer. If true, this concept would expand our view of stromal-cancer cell interactions and the understanding of this stage of cancer pathophysiology. The images and schematic in the accompanying figure (**Figure 2**) provide a glimpse of this potential, as we have observed and confirmed intercellular connection via TNTs that form between malignant and human vascular endothelial cells (HUVEC); furthermore, it was confirmed via time-lapse imaging that these TNTs transfer VEGF and even HIF-1α. This provides a prime example of how malignant cells contained within the extracellular matrix can not only contact but also potentially reprogram other cells, thereby, leading to invasion and metastasis. As a whole, this collective set of interactions would effectively serve as a mammalian and cancer version of quorum sensing (Schertzer and Whiteley, 2011; Doganer et al., 2016) but with the significant addition of TNTs as a more intimate and direct mode of interaction and exchange of information. While the term "quorum sensing" is usually reserved for bacteria, it should also be used to effectively describe the choreography of complex and dynamic interactions and exchange of "social information" among cancer cells by TNTs and other means.

A natural clinical extension of angiogenesis is the fact that cancer provides not just a pro-inflammatory state but also one that is prothrombotic. The transmembrane receptor tissue factor (TF) is known to bind plasma factors that initiate the cascade of events leading to hypercoagulation, and this process is expedited by TF-positive microparticles released by cancer cells (Geddings and Mackman, 2013). For this reason, the risk of venous thromboembolism (VTE) is significantly increased in the presence of cancer, and the development of VTE can potentially be fatal when not diagnosed and treated with anticoagulation therapy in a timely fashion. Part of the biochemical cascade that results in VTE includes activation of thrombin, a serine protease that converts fibrinogen to fibrin. A recent elegant study demonstrated the ability of thrombin to induce TNTs in endothelial cells (Pedicini et al., 2018), providing further support to the notion that TNTs play a previously uncovered role in this cancer-related process.

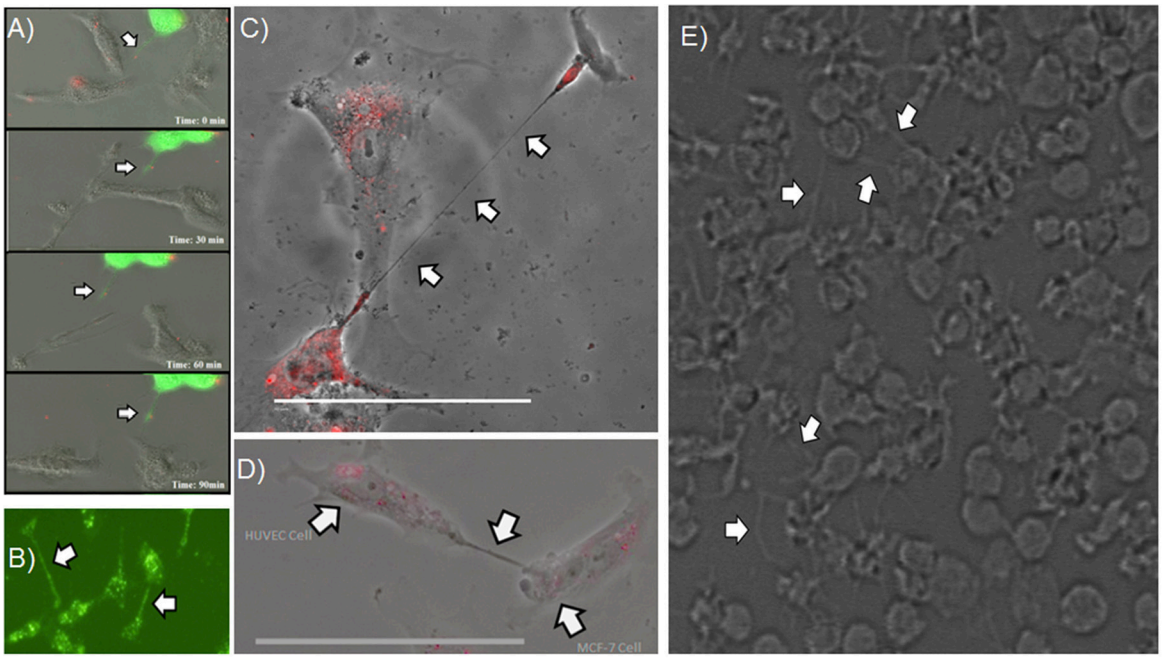

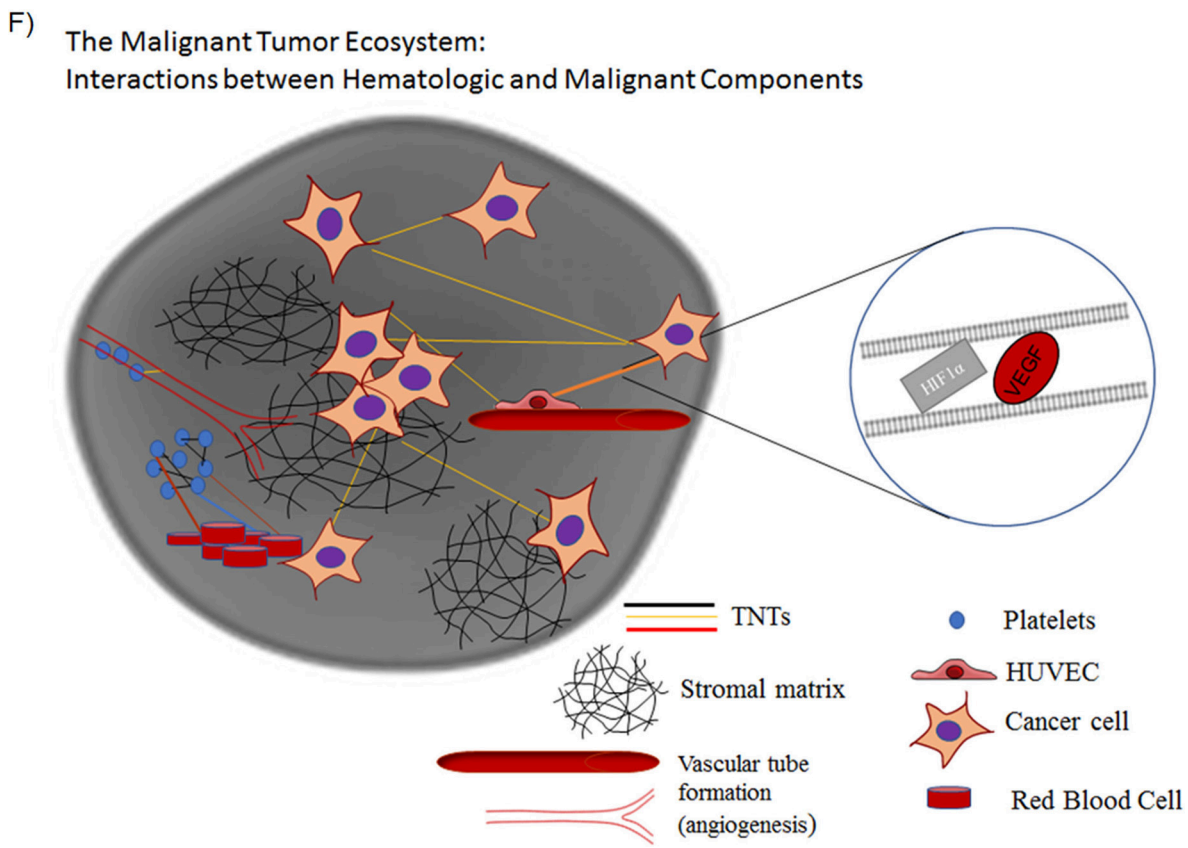

FIGURE 2 | TNTs induced by hypoxia stimulate a potential positive feedback loop by mediating intercellular transfer of HIF-1α and VEGF. Heterotypic forms of TNTs include malignant cell-endothelial cell TNT formation, as well as potential TNT formation among clusters of platelets. **(A)** Composite of images from a time-lapse series demonstrating intercellular transfer of GFP-tagged HIF-1α via a TNT that connects SKOV3 ovarian cancer cells. **(B)** SKOV3 cells expressing GFP-VEGF form TNTs that transfer VEGF. **(C)** HUVECs stained with DiI connected via a long TNT. **(D)** Heterotypic TNT formation between a HUVEC (left) and a breast cancer cell (MCF-7, on the right). **(E)** A cluster of platelets cultured *in vitro* forming many fine pseudopodia-like protrusions representing potential TNTs. **(F)** Schematic demonstrating potential interplay among microthrombi formed by platelets and/or RBCs communicating via TNTs, in the same ecosystem as malignant cells communicating with TNTs. Scale bars = 100 μm. Materials and Methods section for experiments shown in the figure is available in the **Supplementary Material**.

In addition to heterotypic TNT connections between hematologic, malignant, and vascular endothelial cells, there is also potential for TNTs to connect cell bodies and factors that comprise thromboemboli, including platelets. There are emerging data to support this concept. Platelet aggregation has a strong association with advanced malignancy; the resulting VTE or microthrombi are not just by-products of this cancer-induced inflammatory state. Paraneoplastic thrombocytosis is a known phenomenon in which inflammatory cytokines, such as interleukin-6 (IL-6), released by malignant cells lead to increased synthesis of thrombopoietin and platelet number, which in turn further stimulate tumor growth (Stone et al., 2012). If platelet-tumor cell interactions are direct, rather than dependent on diffusible soluble factors, this form of communication would be highly effective in the relatively enclosed space of the tumor-hematologic interface within the cancer microenvironment. Studies that employ electron microscopy (EM) to examine platelets have led to visualization of podosome-like structures that are composed of actin nodules (Poulter et al., 2015). Moreover, longer slender actin-based protrusions that connect platelets, containing bead-like bulges that may represent transported cargo, have been identified and labeled as pseudopodia or other types of cell protrusions (Junt et al., 2007; Schwertz et al., 2010; van Rooy and Pretorius, 2016). However, in hindsight, some or all of the above forms of protrusions may in fact have been TNTs. In culturing human platelets *in vitro*, we too have identified similar pseudopodia connecting platelets in a fashion identical to TNTs connecting cancer cells (**Figure 2**). We speculate that TNTs may form and play a role in communication not just between cells but also between anucleate structures, such as RBCs and platelets (Swanepoel and Pretorius, 2013; Olumuyiwa-Akeredolu and Pretorius, 2015).

Platelets and RBCs can interact, and the membrane structure of both of these hematologic components is dictated by lipid content, which includes the formation and maintenance of lipid rafts. In fact, over a decade ago it was reported that tubular budding of RBCs led to the formation of TNTs and that these TNTs function by permitting vesicular transfer between connected erythrocytes (Iglic et al., 2007). Furthermore, our group has previously reported that cells that form TNTs are enriched in lipid rafts, and this finding includes localization of these raft complexes at the base of TNTs (Thayanithy et al., 2014a); a finding that is consistent with the report of tubular budding as an early precursor of TNT formation. The observations and background findings summarized above open new avenues to a potential role of TNTs in benign hematologic studies as well as in malignancy by providing a direct link between intercellular communication and the pro-inflammatory state that induces a higher degree of tumor aggressiveness.

There is a growing body of evidence that TNTs also mediate cellular interactions between malignant cells and immune cells that infiltrate the tumor microenvironment. Correlation of immune infiltration of tumors with patient prognosis and risk of recurrence following definitive treatment is now better recognized. For example, in patients with stages I-III colon carcinoma, the extent of tumor-infiltrating T cells is inversely correlated with risk of recurrence (Pagès et al., 2018). It is, therefore, conceivable that T cells infiltrating the tumor matrix are communicating with each other, with other immune-type cells, vascular endothelium, hematologic cells, and even with the malignant cells themselves via TNTs to enact an antitumor response (Lachambre et al., 2014; Al Heialy et al., 2015). Another example of immune cell TNT formation has been identified in macrophages (Hanna et al., 2017). Tumor-associated macrophages (TAMs) present in colon tumor stroma are associated with more invasive forms of this disease (Zhang et al., 2013). Intercellular cross talk between malignant colon cells and the M2 phenotype of macrophages induces a faster migration of the malignant cells, which in turn secrete cytokines such as IL-10 that promote further differentiation of the macrophages (Zhang et al., 2013). It is conceivable that this form of cross talk could also be mediated by TNTs, which in this scenario are promoting a more aggressive phenotype within the tumor ecosystem. The above represents just two of the many potential possibilities for immune-cancer interactions that are facilitated by TNTs. Whether TNT-mediated interplay between immune cells and other heterogeneous components of the tumor matrix results in a net increase or decrease in metastatic potential is a possibility that needs to be explored.

TUNNELING NANOTUBES AND THE DUNBAR NUMBER: UNCOVERING THE EXTENT AND LIMITATIONS OF INTERCELLULAR CONVERSATIONS

There is potential merit in learning from and borrowing concepts of social interactions in society to behavior at the cellular level. This approach is compatible with the cancer systems biology approach of examining cells—which themselves are small components of an ever-changing, dynamic, and heterogenous tumor microenvironment—in their greater context rather than in isolation.

A unique concept from the field of anthropology and mathematics has emerged in which the number of potential social interactions by a human being is defined and limited. Richard Dunbar, an anthropologist, proposed a very specific and finite number for the potential social interactions by a human: 150 (Dossey, 2017). We found the hypothesis and his rationale to be intriguing and considered that TNTs—the purveyors of connections and communication at the cellular level—might also have a finite number in any given cell system. In our previously reported work, we gained insight into the heterogeneity of intercellular interactions and communication via TNTs that formed between chemoresistant and chemosensitive ovarian cells as well as between malignant and benign ovarian-derived cells (Desir et al., 2016). To further investigate the notion that there might be an equivalent Dunbar's number for TNTs that are formed *in vitro*, we reanalyzed the time-lapse imaging we had produced that documented TNT formation between cancer cells. As an example, we conducted a frame-by-frame examination of one of our time-lapse videos of malignant (Mg63.2-GFP-expressing osteosarcoma cell line) cells cocultured

with osteoblast (the hFOB cell line stained with red DiI lipophilic dye) cells characteristic of the bone matrix (**Figure 3**, **Supplementary Video 1**). Each image represented a time frame of 30 min, over a total time of 40 h of cell culture. There was a range of average duration of TNTs—the time length of the intercellular "conversations" taking place—of 30 min to 2 h, but the vast majority of TNTs lasted no longer than 30 min (136/168 or >80%). The total percentage of TNTs that lasted 1–2 h was cumulatively small, at ∼19% (32/168), and none lasted longer than 2 h. Interestingly, the overall proportion of cells that developed intercellular interactions with TNTs was small (7%) within the first 10 h in culture. However, between 10 h and 40 h, while there was a wide fluctuation between frames in some periods (range of TNTs = 0–8; range of ratio of cells with TNTs = 0–0.266), the average percentage of cells with TNTs tended to equilibrate despite this range of fluctuation throughout this period. The mean percentage of cells that formed TNTs was 3.5% within the first 10 h but 9.1% during the remainder of the 40-h period. In terms of the absolute numbers of TNTs, the mean was 1.05 TNTs within the first 10 h and 2.75 during the remainder of the 40-h period.

This preliminary analysis supports the notion that while TNTs are finite and dynamic structures, the overall ecosystem of semi-confluent cells in culture generally equilibrates to an overall stable number of TNTs at any given time. Whether this number is the "cellular equivalent" of a Dunbar's number is speculative, it underscores the role of systems biology as a key element in the development and survival of the overall tumor ecosystem. While it is likely that the actual number and percentages will vary from cell type to cell type, the concept that TNTs—as conduits of intercellular interactions and communication—may actually follow similar rate-limiting steps as social interactions is fascinating and further open the door to viewing the function and mechanisms that support TNTs in a new light.

ULTRASTRUCTURE OF TNTs: ARE THEY SINGLE OR MULTI-LANE CELLULAR HIGHWAYS OR CAN THEY ALSO ACT AS INTERCELLULAR BRIDGE TRACKS FOR CARGO SURFING?

An ongoing debate that is central to the function, mechanism, and structural biology of TNTs is whether they are open-ended or closed structures. It is clear that TNTs are conduits that are capable of mediating cell-to-cell spread of cargo. Whether they are truly "tunneled" at both ends, remains a matter of debate. For that reason, in some studies the term "membrane nanotubes" or the equivalent is the preferred nomenclature. Advances in high-resolution microscopy are beginning to address these questions and will be crucial in the accurate evaluation of TNTs in the *in vivo* setting (Lou et al., 2017). In our initial studies, using malignant pleural mesothelioma as a model system, we reported from electron microscopic imaging that some TNTs had multiple insertion points in the cell membrane (Lou et al., 2012). By EM, we also identified single or multiple cable-like insertions that stem from the cell membrane (**Figure 4A**). Although we assumed that these short strands form the base of TNTs and merge into a single thicker TNT, we also considered that each of these strands represent independent TNTs that ultimately run parallel to each other on their way to connecting distant cells.

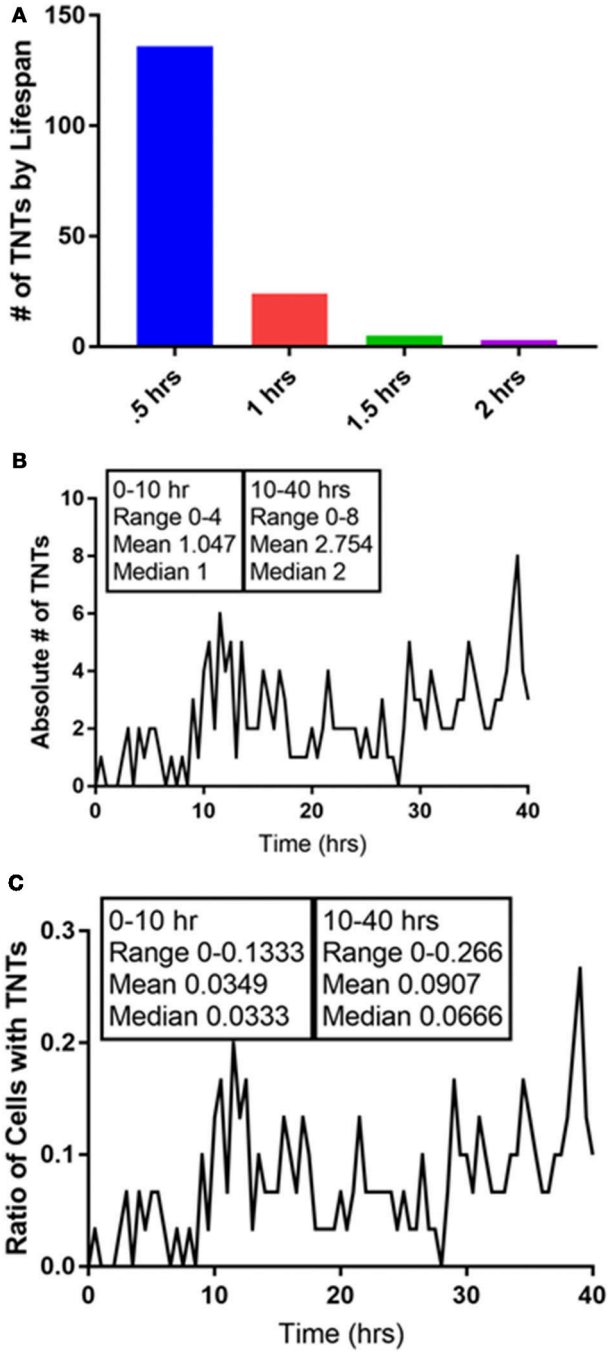

FIGURE 3 | Quantification of the intercellular interactions that occur via TNTs: in search of a Dunbar's number for TNTs. We analyzed a 40-h time-lapse set of images of a coculture of Mg63.2 osteosarcoma cells with hFOB osteoblast cells. **(A)** The duration of TNTs is relatively short, as nearly all of the TNTs that were formed lasted for 1 hour or less. **(B)** The absolute number of TNTs increases after 10 h in culture, as does the ratio of number of cells with TNTs **(C)**. All of these images are presented in video form in **Supplementary Video 1**. Materials and Methods section for experiments shown in the figure is available in the **Supplementary Material**.

Such a scenario might explain the heterogeneity of widths seen in TNTs across different cell types (across cancers and between cancer and non-cancer cells) as well as differences seen between nanotubes *in vitro* and tumor microtubes seen in *in vivo* tumor models (Osswald et al., 2015; Jung et al., 2017; Weil et al., 2017). A recent preprint article presented strong evidence supporting this concept using cryo-correlative light- and electron microscopy (CLEM) (Sartori-Rupp et al., 2018). The definition of what is and what is not a TNT continues to remain a bit of a controversy.

There is also precedence for the notion that if some nanotubes are indeed membranous but not necessarily tunneled, then cargo can still be transported by utilizing the tubes as "tracks" to guide the way to recipient cells. A prime example is retroviral virion particles "surfing" along the outer surface of TNT-like filopodial bridges as a means for intercellular transport (Sherer et al., 2007). Our work on TNTs in malignant mesothelioma showed that tumor cell-derived exosomes stimulated formation of more TNTs in this cell type; furthermore, using time-lapse fluorescence microscopy, we visualized exosomes tracking along and/or within these TNTs to connecting cells (Thayanithy et al., 2014a). The concept of exosomal/extracellular vesicles (ECVs) transferring within TNTs is not entirely new and is supported by work from other labs as well (Hood et al., 2009; Mineo et al., 2012). By scanning EM, we have captured at least one instance that further distinguished TNTs at their insertion/extrusion point in the membrane. What was most noticeable, however, was an adjoining TNT-like protrusion that appeared to be "carrying" an ECV (or microvesicle) that adhered to this protrusion by two short cable-like structures (**Figure 4B**). We speculated that this finding represents a form by which ECV cargo tracks along TNTs or similar cell extensions to more efficiently move from cell-to-cell. Overall, the refined use of EM and other high-resolution microscopic techniques will better elucidate the topography, landscape and interaction of cells, TNTs, and ECVs within the tumor ecosystem.

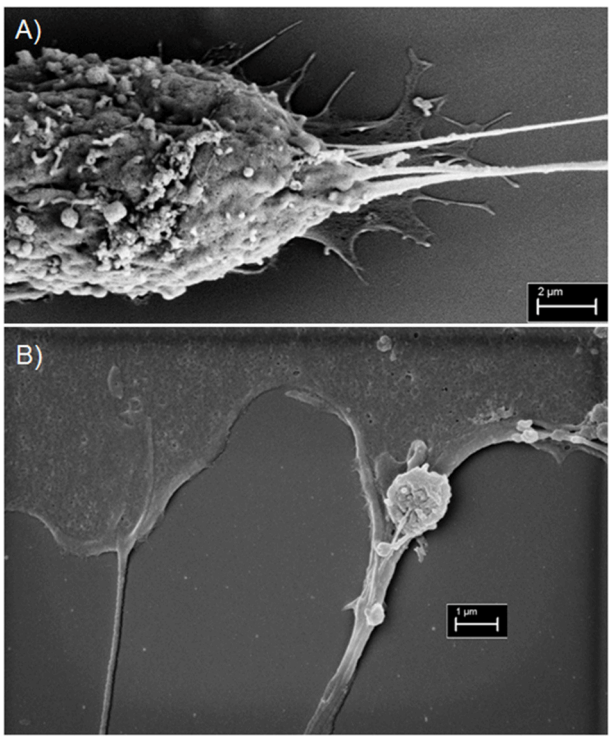

FIGURE 4 | Scanning electron microscopy imaging of TNTs in MSTO-211H malignant mesothelioma cells. **(A)** Electron micrograph revealing multiple insertion points vs. points of extrusion of TNTs in the membrane of a MSTO cell (Scale bar = 2 µm; Magnification 14.62 k X; width = 20.52 µm). **(B)** A TNT is seen on the left, and on the right is a TNT-like protrusion vs. filopodia/invadopodial extension. An extracellular vesicle is overlying the extension on the right (Scale bar = 1 µm; Magnification 24.69 k X; width = 12.15 µm). Materials and Methods section for experiments shown in the figure is available in the **Supplementary Material**.

OVEREXPRESSION OF CSPG4 IS ASSOCIATED WITH INCREASED RATE OF TNT FORMATION

The search for structural or functional markers of TNTs remains a significant challenge. We have theorized, based on our experience so far, that while there are commonalities between TNTs in different cell types, there may also be unique structural features of TNTs that are upregulated in specific disease states, including cancer. One of the best characterized potential biomarkers of TNTs, to date, is M-Sec (TNF-aip2), which has been examined primarily in macrophages and other immune cells (Hase et al., 2009; Ohno et al., 2010; Schiller et al., 2013). We found that M-Sec was also upregulated in malignant mesothelioma cells cultured in conditions conducive to upregulation of TNTs (Ady, 2014). Thus, this marker may be the closest universal candidate that has been characterized, to date, across multiple cell types. Other standard components of cellular actin-based machinery, such as Cdc42 and Rac1, have also been associated with TNT formation (Hanna et al., 2017).

We have reported that mesothelioma cells that form TNTs are enriched in lipid rafts as compared with cells in coculture that do not form TNTs (Thayanithy et al., 2014a). Lipid rafts are cholesterol microdomains that aggregate at the intracytoplasmic domain in regions on the invasive leading edge of cells and have, therefore, been implicated in malignant invasion. We hypothesized that similar cell surface markers involved in cell migration and invasion might also be associated with and possibly stimulated TNT formation. Thus, we selected CSPG4, also known as neuron-glial antigen 2 or NG2. A transmembrane proteoglycan, CSPG4 plays a key role in stabilizing cell-substratum interactions in early melanoma cell invasion. Most importantly, it is overexpressed in mesothelioma but not in normal mesothelium (Rivera et al., 2012) and plays a role in mediating pericyte interaction with endothelial cells. Ablation of CSPG4/NG2 in a breast cancer animal model resulted in decreased progression and development of vasculature (Gibby et al., 2012). Targeting CSPG4 using monoclonal antibodies decreases mesothelioma cell invasiveness as well, and it has been proposed as a potential target for the treatment of mesothelioma, breast cancer, and melanoma (Wang et al., 2010; Price et al., 2011; Yu et al., 2011; Rivera et al., 2012). On the basis of our findings

in mesothelioma, we concluded that the association of certain cellular markers such as lipid rafts with TNTs is an indicator of cell invasion (i.e., CSPG4) and that this leads to increased formation of TNTs.

To test this hypothesis, we used the melanocyte-derived radial growth phase melanoma cell line WM-1552, which was transfected to stably express CSPG4 (Yang et al., 2004) and was designated as WM1552-CSPG4. The expression of CSPG4 in WM1552 cells causes enhanced cell adhesion and spreading, increased motility, enhanced epithelial-to-mesenchymal transition (EMT), anchorage independent growth, and tumorigenic potential compared with the CSPG4 negative mock transfected counterparts (Yang et al., 2009; Price et al., 2011). In the current study, we compared TNT formation in WM1552c mock transfectants lacking CSPG4 with WM1552c CSPG4-expressing melanoma cell lines. We cultured WM1552 mock and CSPG4 cells separately in low-serum, hyperglycemic RPMI medium (2.5% FCS, 50 mM glucose) and counted TNTs manually at 24-h intervals for 96 h. To assess the rate of cellular proliferation, we also determined the relative absorbance of a surrogate measure of cell growth over time. We detected significantly higher numbers of TNTs at 96 h in WM1552-CSPG4 culture as compared with WM1552-mock cells (**Figure 5**). This increase in TNT formation was independent of two-dimensional cell growth. After accounting for a higher cellular absorbance rate for the former cell line as a measure of cell proliferation, TNT/absorbance remained significantly higher for WM1552-CSPG4 (1.2-fold higher or 21% higher, at 72 h), suggesting an association and potential stimulatory role of CSPG4 in the formation of TNTs. Functionally, CSPG4 is localized on the tips of filopodia and stimulates key oncogenic signaling pathways, including focal adhesion kinase, constitutively activated BRAF/Erk 1,2 and Rho family GTPases, all of which could be important for the stimulation of TNT formation (Price et al., 2011). Furthermore, the function of CSPG4 requires the cytoplasmic tail of the core protein. Thus, studies that interrogate CSPG4 may shed considerable insight into the molecular mechanisms that govern TNT formation (Price et al., 2011). Since CSPG4 is a potential target, studies that interrogate mechanisms of CSPG4 function may also positively identify the importance of TNTs as a clinical target in malignant progression.

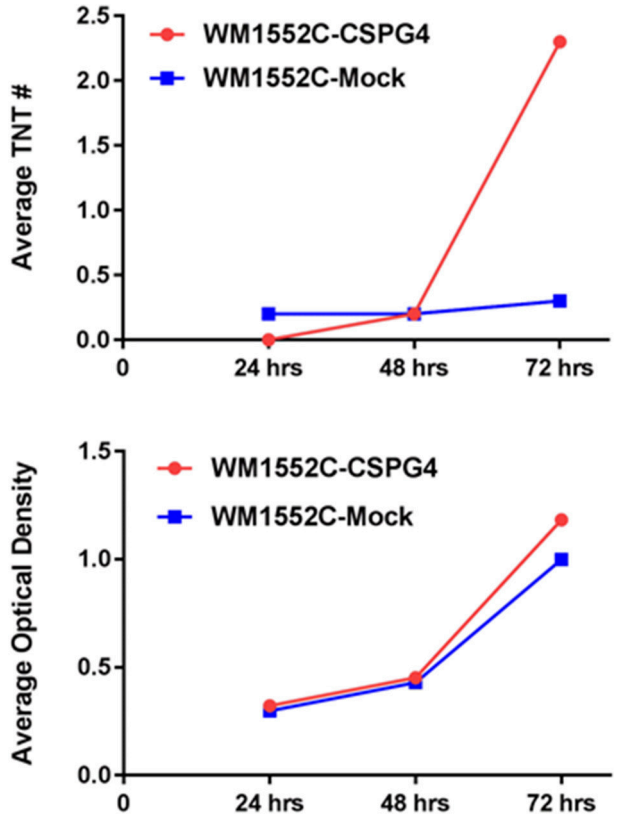

FIGURE 5 | Melanoma cells that overexpress CSPG4 form TNTs at a higher rate over time. We quantified TNTs between WM1552C-CSPG4 and WM1552C-mock cells at 24 h, 48 h, and 72 h. The average number of TNTs per time point is shown **(Top)** as well as cell proliferation measured as average optical density **(Bottom)**. Materials and Methods section for experiments shown in the figure is available in the **Supplementary Material**.

THE QUESTION OF ACTIVE vs. PASSIVE DIFFUSION: THE MYOSIN CHAPERONE UNC-45A CORRELATES WITH TNT FORMATION FOR A LIMITED TIME, BUT IS INVERSELY ASSOCIATED WITH TNT FORMATION AFTER 48 H IN CULTURE

There remain many questions regarding the active vs. passive nature of intercellular cargo transport that is mediated by TNTs. Discovery of a defining molecular component that is specific to TNTs remains elusive, and it is conceivable that a single one may not exist. The prevailing thought is that these filamentous actin-based cell protrusions employ the myosin motor complex in a fashion similar to other well-established modes of actin-based machinery.

UNC-45A is a chaperone protein that has been well characterized for its function in the assembly and maintenance of the myosin II motor complex. It has been shown to be overexpressed in serous ovarian carcinomas and is associated with significantly increased cancer cell proliferation as well as motility (Bazzaro et al., 2007). Furthermore, the UNC-45A protein tracks at the leading edge of cells and is known to accumulate at the cell furrow during cytokinesis. We postulated that as TNTs arise at the cell edge, they might utilize UNC-45 for formation and maintenance. Thus, we examined TNT formation in ovarian cancer cells with intact UNC-45A expression as compared with the same cell line (SKOV3) with shRNA knockdown of UNC-45A; a scramble version of the lentivirus offered an additional form of control. We quantified the number of TNTs and cells in 20X fields of view to establish the TNT index (number of TNTs/cell over time), a method we have described in detail in other publications (Ady, 2014). Interestingly, we found that while the average number of TNTs per cell was significantly lower in the UNC-45A-knockdown

group at 24 h and 48 h, by 72 h the reverse was seen, as on average there were more TNTs/cell among the cells in which ∼80% of UNC-45A had been suppressed via shRNA knockdown (**Figure 6**). This finding was initially unexpected, but, upon further analysis, it made sense in the overall context based on the known role of UNC-45A in modulating cellular motility and proliferation.

This finding provides stimulus for examining the time course of TNTs and better understanding their niche, not just spatially but also in time. Tunneling nanotubes are most prolific in subconfluent cell cultures. As cultures become increasingly confluent, the physical space between cells is diminished, and there is less need for TNTs to form bridges between these cells. Knockdown of UNC-45A continued to suppress cell proliferation by 72 h; in comparison with scramble and wild type, the ratio of the number of TNTs/cell was naturally higher (**Figure 6**). This observation provided potential insight into the notion that UNC-45A and other mediators of myosin motors might be essential to the early stages of TNT formation among non-crowded cell populations; however, its importance might diminish over time in more confluent or nearly-confluent cell populations and in terms of maintenance, rather than formation, of TNTs.

hENT1 EXPRESSION IS INVERSELY CORRELATED WITH TNTs IN PANCREATIC CANCER

The tumor microenvironment comprises a vast and complex set of players that mediate intracellular and intercellular discussion. Important players of intercellular communication include diffusible soluble hormone signals, exosomes and other ECVs, and connexin-based gap junctions for cells in immediate proximity. In certain cancers, there are other forms of transporters. One such example is hENT1. Human equilibrative nucleoside transporter 1 is highly expressed in malignant pancreatic tumors, has a life cycle of 14 h, and has been associated with improved prognosis in pancreatic cancer (Nivillac et al., 2011), although there is no apparent correlation of hENT1 expression to survival (Poplin et al., 2013).

The rationale for studying hENT is that it functions effectively as a transporter of nucleosides. More specifically, hENT1 permits intercellular transfer of chemotherapeutic agents such as the fluoropyrimidine gemcitabine, a standard of care drug that is potentially effective once it has successfully penetrated the dense stroma-rich microenvironment that is characteristic of this type of cancer. We recently reported that despite the especially dense

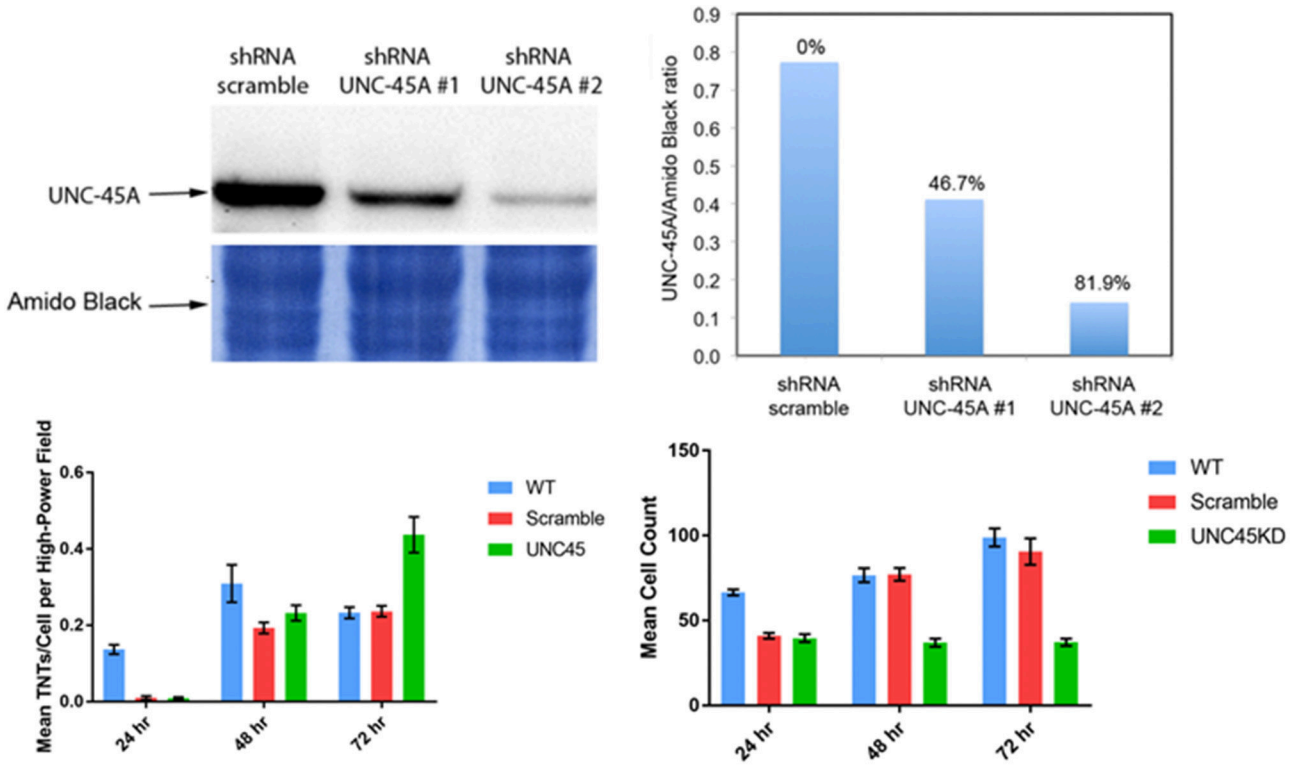

FIGURE 6 | Knockdown of the UNC-45A myosin motor protein chaperone diminishes TNT formation, but this finding is limited in duration. Upper left: western blot demonstrating effective knockdown of UNC-45A using shRNA. Based on these results, shRNA #2 was used in our study. Upper right: quantitation of effective UNC45-A knockdown by shRNA #1 and #2. Lower left: mean number of TNTs at 24 h, 48 h, and 72 h in wild type SKOV3 ovarian cancer cells compared with cells transfected with the scramble and UNC-45A shRNA #2. Lower right: mean cell count for the same conditions and time points. Materials and Methods section for experiments shown in the figure is available in the **Supplementary Material**.

nature of the pancreatic stromal reaction, TNTs could be detected in human pancreatic tumor tissue (Desir et al., 2018). We further postulated that if TNTs were the mediators of local and regional invasion and metastasis, then their presence would be inversely proportional to the expression of hENT1. As proof of concept, we examined a metastatic pancreatic carcinoma-derived cell line, S2013, for hENT1 expression using a fluorescent antibody. We detected focal expression of this transporter protein along the membrane, as expected. Quantifying its expression as arbitrary units (a.u.), and accounting for the area of each cell and the TNTs, we reported the expression in a fashion identical to our previously published study that examined lipid raft enrichment in TNT-forming cells (Thayanithy et al., 2014a). Consistent with our hypothesis, we found an inverse correlation between hENT1 expression and TNTs in these pancreatic cancer cells (**Figure 7**). In the S2013 cells, hENT1 expression was 1.8-fold higher in cells not forming TNTs than in cells in the same culture forming TNTs ($p = 0.0023$).

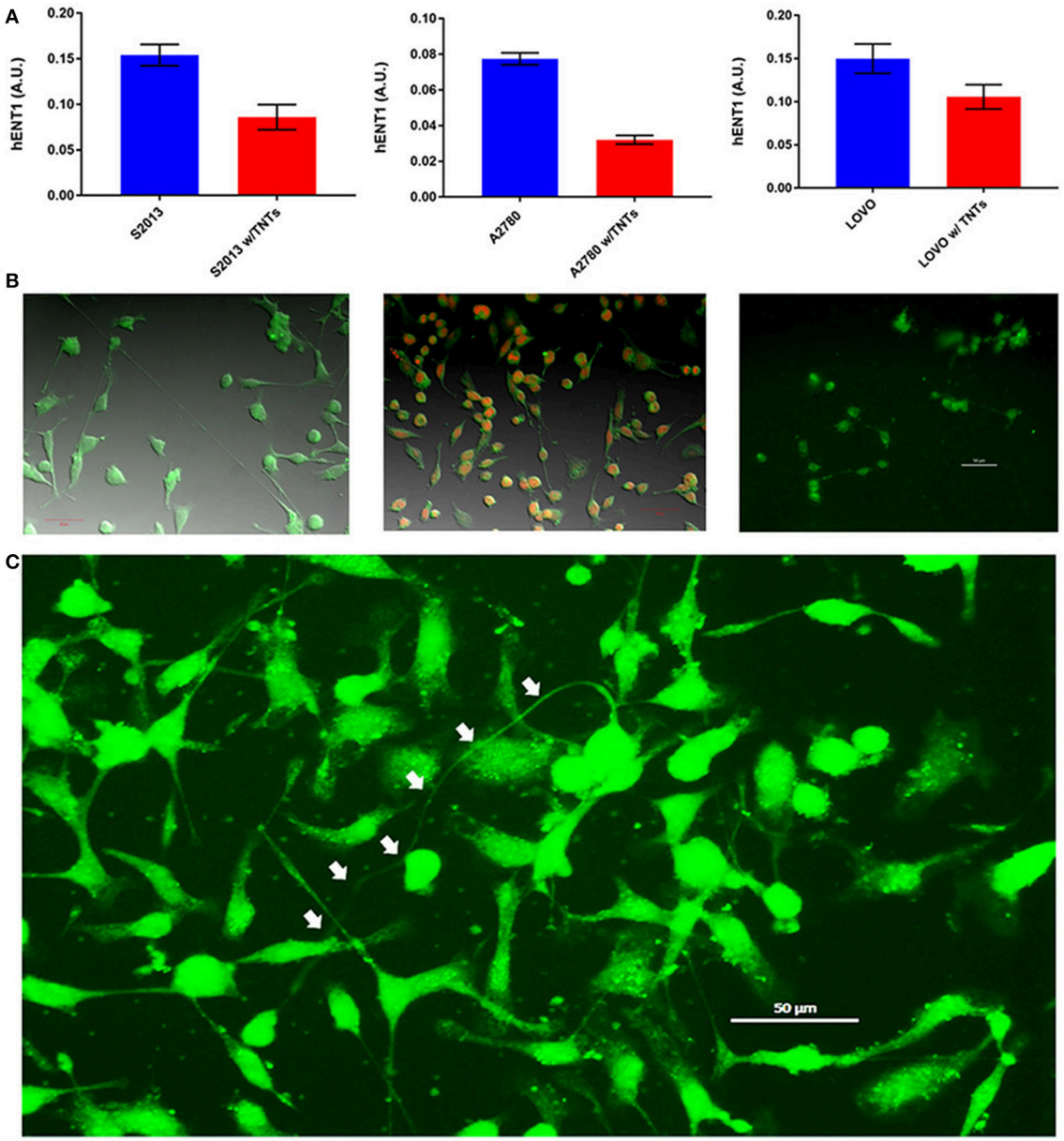

FIGURE 7 | Cancer cells forming more TNTs demonstrate lower expression of hENT1. **(A)** hENT1 expression in S2013 pancreatic cancer cells, A270 ovarian cancer cells, and LOVO colon cancer cells with and without TNTs. **(B)** Corresponding images for each cell line are located beneath each graph. Cells were stained with immunofluorescent antibody that marks the expression of hENT1, and the expression was quantified as described. Scale bars = 50 µm for each of these panels. **(C)** The larger image on the bottom demonstrates a particularly long and curved TNT (indicated by white arrows) connecting hENT1-expressing S2013 cells. Materials and Methods section for experiments shown in the figure is available in the **Supplementary Material**.

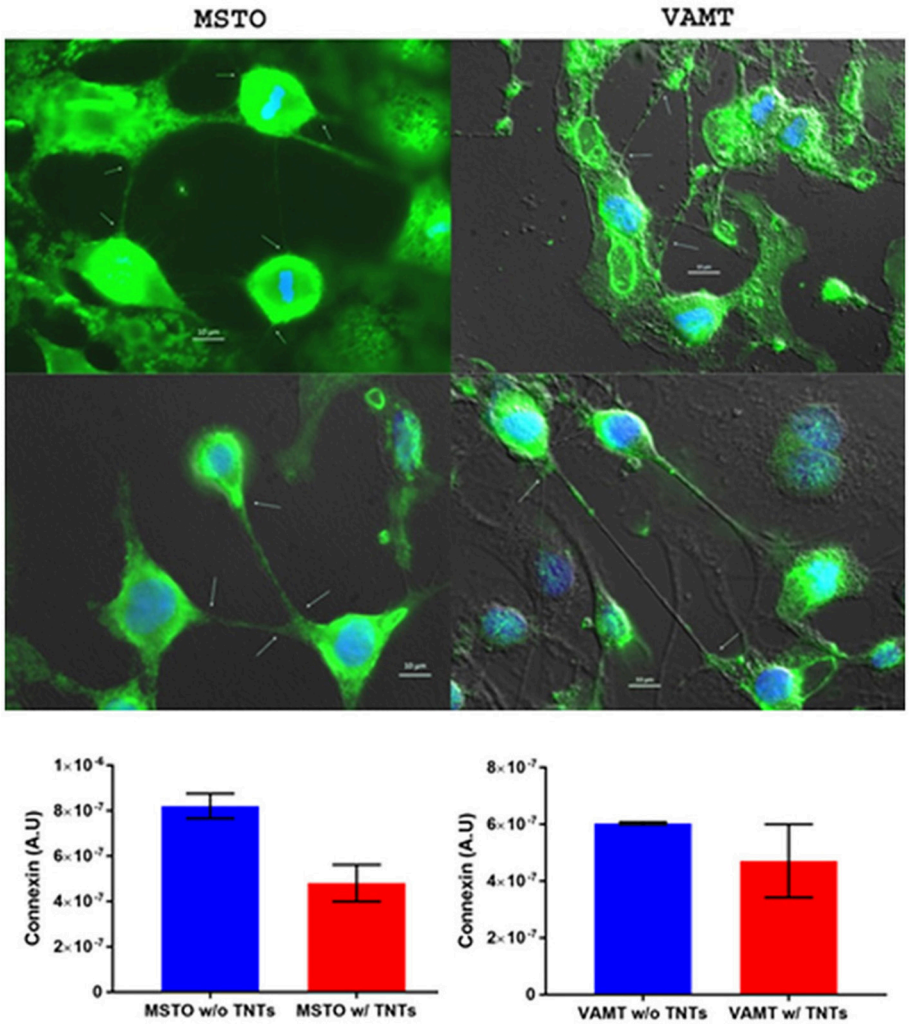

FIGURE 8 | Connexin expression may be inversely correlated with TNT formation, and its expression co-localizes most prominently at the base and/or tips of TNTs. This experiment was performed using malignant mesothelioma cell lines MSTO-211H and VAMT. The upper panel shows representative images following fluorophore-tagged connexin staining of both cells lines. The lower panels show graphs of connexin expression in cells forming no TNTs (blue column) compared with those forming TNTs (red column). MSTO cell data are in the lower left graph, and VAMT data are in the lower right. Scale bars = 10 μm. Materials and Methods section for experiments shown in the figure is available in the **Supplementary Material**.

Although hENT1 is most often associated with pancreatic carcinomas, it is also present in other forms of cancer, including ovarian cancer (>90% expression) (Farré et al., 2004) and colon cancer (Liu et al., 2017). Thus, for comparison, we performed the same analysis in representative cell lines from these cancers as well. The results in those cell lines were consistent with our findings of inverse correlations of hENT1 to TNTs, indicating that TNTs may be indicative of more chemoresistant and/or more invasive cells. The expression of hENT1 was 2.4-fold higher in A2780 cells not forming TNTs as compared with those forming TNTs ($p = 0.0126$); this difference was 1.4-fold in LOVO cells, respectively ($p = 0.0049$).

It will be important not only to substantiate but also reconcile this finding with some of our own recent findings that TNTs are also conduits for mediating intercellular efflux of chemotherapeutic drugs (Desir et al., 2018). In fact, it has been reported that TNT-like tumor microtubes (TMs) seen in gliomas correlate with a higher degree of cellular invasion and drug resistance (Osswald et al., 2015, 2016; Jung et al., 2017; Weil et al., 2017).

LOCALIZATION OF CONNEXIN PROTEINS IN RELATION TO TNTs

Connexin channels that compose gap junctions mediate intercellular transfer of calcium and other small soluble factors; they are also not inherently separate from TNTs. Tunneling nanotubes and TMs have also been shown to mediate intercellular calcium flux effectively between malignant cells (Osswald et al., 2015; Lock et al., 2016). In fact, in both

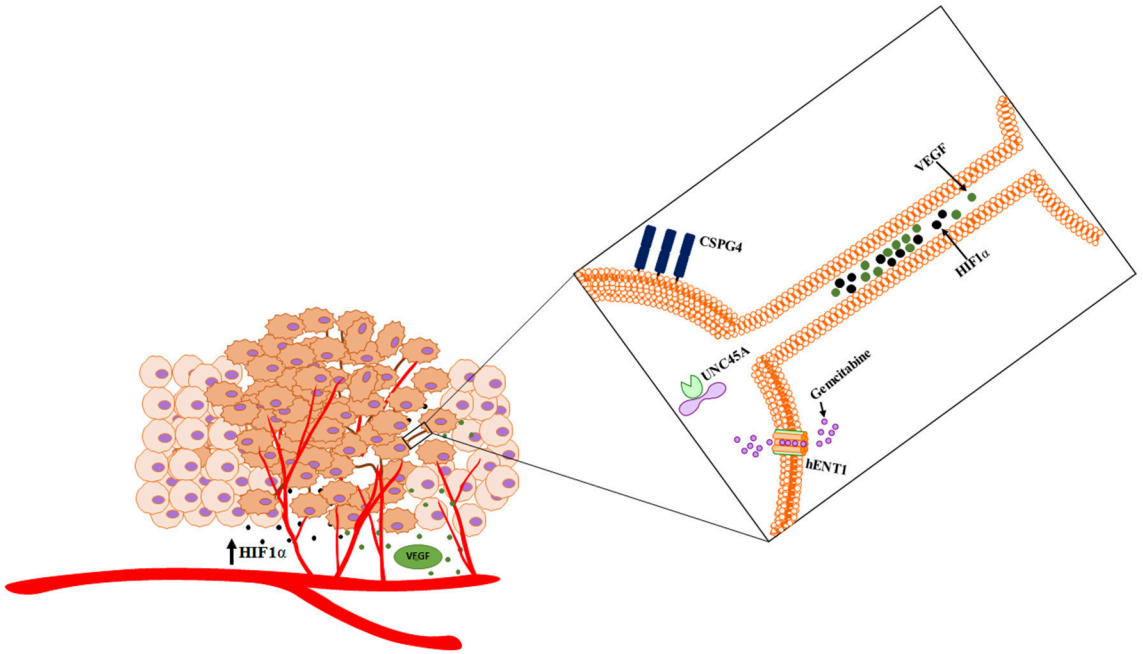

FIGURE 9 | Schematic of cross talk via hypoxia-induced TNTs that facilitate the intercellular transfer of cargo. TNTs facilitate dynamic interplay that has implications in angiogenesis and other processes that are critical to the ecosystem.

of these cited studies, the localization and attachment of connexins was found to be crucial to this TNT/TM-mediated process.

It is well established that gap junctions are downregulated in cancer cells undergoing EMT, a state that is strongly associated with stem cell-like properties and metastasis, which our own group showed was associated with significant upregulation in TNTs in malignant mesothelioma cells (Lou et al., 2012). Gap junctions have been reported to be localized at the tip of TNTs, for example in astrocytes (Wang and Gerdes, 2012), but reports, to date, have been inconsistent with this finding. The finding may be variable based on the timing of TNT formation, detection in its state at the time (e.g., in the midst of forming, transporting cargo, or disconnecting from recipient cells), the state of confluence of the cell culture being examined, and the cell type (malignant vs. non malignant or even heterogeneous between different cancer cell types). Furthermore, it is not yet firmly established whether gap junctions actually mediate the formation of TNTs from the plasma membrane and/or represent structural foundations of TNTs across all cell types. It remains to be determined whether connexins localize more at the base of TNTs where they emerge from the donor cell or at the point of entry into putative recipient cells.

The question remains as to whether connexin expression differs quantitatively between cancer cells with or without TNTs. The answer is likely time-dependent; that is, dependent on the extent of cell confluency, distance between cells, and number of TNTs. We have extensively characterized TNT formation, function, and characterization in several cell lines of malignant mesothelioma (Lou et al., 2012; Ady, 2014, 2016; Thayanithy et al., 2014a). To examine connexin localization in these cells, we stained MSTO-211H and VAMT cells with immunofluorescent markers and performed inverted microscopy. A preliminary analysis was performed to quantify differences in connexin expression relative to expression in non-TNT forming cells. We found a 1.7-fold increase in connexin expression in MSTO cells not forming TNTs, as compared with cells forming TNTs; for the VAMT cell line, the difference was 1.28-fold (**Figure 8**). In the scope of systems biology, no component of the tumor matrix works independently. Rather, all of the components are dynamic and function as a unified process. For example, it is now established that exosomes interact synergistically with TNTs in cancer (Thayanithy et al., 2014a); connexin channels associated with TNTs may play a role in their initial formation and/or maintenance. It will be important to determine the variability between cancer cell types based on tissue of origin, state of EMT, and molecular status and also between cancer and non-cancer cell types.

CONCLUSIONS

Cancer cells cannot be studied in isolation, as they interact in a complex biological system. With the improved and rapidly expanded understanding of the function and importance of intercellular communication in modulating the tumor microenvironment, it is critical to investigate malignancy as a unique and continuously evolving ecosystem. These interactions can take many forms. Homotypic interactions of malignant cells are mediated via TNTs, exosomes, gap junctions, and a

wide ranging list of diffusible and soluble factors. Heterotypic interactions include interactions of the extracellular matrix with malignant cells, vascular endothelium with cancer, immune cells with cancer, and hematologic components with cancer. Altogether, these events comprise a spectrum of intratumoral interactions that reprogram cells for invasion, metastasis, and emergence of resistance to treatment. The interplay and dynamics of the subtopics that we have begun to examine here are illustrated in the accompanying schematic (**Figure 9**). Perturbations to this complex ecosystem, such as those provided by drug- or radiation-induced injuries, can instead induce cellular stress responses that in turn increase the extent of any or all of these inflammatory interactions. Increased characterization of TNTs and their role in cancer cell invasion and chemoresistance over the past decade continues to provide novel mechanistic insights into how the heterogeneous tumor microenvironment adapts and evolves over time. Continued work in this exciting field, including concepts described here and elsewhere, will clarify to what extent TNTs play an important role in mediating the tumor ecosystem.

AUTHOR CONTRIBUTIONS

EL wrote the initial drafts of the manuscript. EL, EZ, AS, SD, PW, YI, JM, and MB provided initial analysis of the data and prepared the figures. EL, SS, JM, MB, and CS performed further analysis and interpretation of the data and wrote subsequent drafts of the manuscripts. All authors reviewed and approved the final submitted manuscript.

FUNDING

This research was supported by the Minnesota Masonic Charities; the Central Society for Clinical and Translational Research Early Career Development Award; the National Pancreas Foundation Research Grant (provided in partnership with the National Pancreas Foundation, several NPF Chapters and the Horvitz/Lebovitz Research Fund); University of Minnesota's Deborah E. Powell Centre for Women's Health Interdisciplinary Seed Grant support (Grant #PCWH-2013-002); the Institutional Research Grant #118198-IRG-58-001-52-IRG94 from the American Cancer Society; the Mezin-Koats Colon Cancer Research Award; the Randy Shaver Cancer Research and Community Fund; the Litman Family Fund for Cancer Research; family and friends of G. Huntington, G. Derfus, and A. Baffa; cancer research fundraisers by the Mu Sigma Chapter of the Phi Gamma Delta Fraternity, the University of Minnesota, and the Courage and a Cure Foundation, Goodyear, Arizona; the Minnesota Medical Foundation/University of Minnesota Foundation; the Masonic Cancer Center and the Department of Medicine, Division of Hematology, Oncology and Transplantation, University of Minnesota; and the NIH Clinical and Translational Science KL2 Scholar Award 8UL1TR000114. The content is solely the responsibility of the authors and does not represent the official views of the National Institutes of Health.

ACKNOWLEDGMENTS

We would like to thank Guillermo Marques, Ph.D. and Mark Sanders, Ph.D. of the University Imaging Centers (UIC) at the University of Minnesota for providing assistance with confocal microscopy; Zhilian Xia for providing support with the experiments; Nina Lampen, Electron Microscopy Core at the Memorial Sloan-Kettering Cancer Center, for preparation of cells and for providing assistance with imaging for electron microscopic evaluation; Timothy Starr, Ph.D. for helpful discussion and help with the use of equipment for hypoxic conditions; and Michael Franklin, M.S., for helpful critiques and editorial suggestions for this manuscript.

SUPPLEMENTARY MATERIAL

The Materials and Methods section for the experiments described in this paper is located in the Supplementary Material of this article, which can be found online at: https://www.frontiersin.org/articles/10.3389/fcell.2018.00095/full#supplementary-material

Supplementary Video 1 | Time-lapse video of a coculture of Mg63.2 osteosarcoma cells with hFOB osteoblast cells.

REFERENCES

Ady, J. (2016). Tunneling nanotubes: an alternate route for propagation of the bystander effect following oncolytic viral infection. *Mol. Ther. Oncolyt.* 3:16029. doi: 10.1038/mto.2016.29

Ady, J. W. (2014). Intercellular communication in malignant pleural mesothelioma: properties of tunneling nanotubes. *Front. Physiol.* 5:400. doi: 10.3389/fphys.2014.00400

Al Heialy, S., Zeroual, M., Farahnak, S., McGovern, T., Risse, P. A., and Novali M. et al. (2015). Nanotubes connect CD4+ T cells to airway smooth muscle cells: novel mechanism of T cell survival. *J. Immunol.* 194, 5626–5634. doi: 10.4049/jimmunol.1401718

Aravalli, R. N., Cressman, E. N., and Steer, C. J. (2012). Hepatic differentiation of porcine induced pluripotent stem cells *in vitro*. *Vet. J.* 194, 369–374. doi: 10.1016/j.tvjl.2012.05.013

Banerjee, S., Thayanithy, V., Sangwan, V., Mackenzie, T. N., Saluja, A. K., and Subramanian, S. (2013). Minnelide reduces tumor burden in preclinical models of osteosarcoma. *Cancer Lett.* 335, 412–420. doi: 10.1016/j.canlet.2013.02.050

Bazzaro, M., Santillan, A., Lin, Z., Tang, T., Lee, M. K., Bristow, R. E., et al. (2007). Myosin II co-chaperone general cell UNC-45 overexpression is associated with ovarian cancer, rapid proliferation, and motility. *Am. J. Pathol.* 171, 1640–1649. doi: 10.2353/ajpath.2007.070325

Chauveau, A., Aucher, A., Eissmann, P., Vivier, E., and Davis, D. M. (2010). Membrane nanotubes facilitate long-distance interactions between natural killer cells and target cells. *Proc. Natl. Acad. Sci. U.S.A.* 107, 5545–5550. doi: 10.1073/pnas.0910074107

Desir, S., Dickson, E. L., Vogel, R. I., Thayanithy, V., Wong, P., Teoh, D., et al. (2016). Tunneling nanotube formation is stimulated by hypoxia in ovarian cancer cells. *Oncotarget*. 7, 43150–43161. doi: 10.18632/oncotarget.9504

Desir, S., O'Hare, P., Vogel, R. I., Sperduto, W., Sarkari, A., Dickson, E., et al. (2018). Chemotherapy-Induced tunneling nanotubes mediate intercellular drug efflux in pancreatic cancer. *Sci. Rep.* 8:9484. doi: 10.1038/s41598-018-27649-x

Doganer, B. A., Yan, L. K. Q., and Youk, H. (2016). Autocrine signaling and quorum sensing: extreme ends of a common spectrum. *Trends Cell Biol.* 26, 262–271. doi: 10.1016/j.tcb.2015.11.002

Dossey, L. (2017). Is friendship limited? An inquiry into dunbars number. *Explore* 13, 1–5. doi: 10.1016/j.explore.2016.10.008

Eugenin, E. A., Gaskill, P. J., and Berman, J. W. (2009). Tunneling nanotubes (TNT) are induced by HIV-infection of macrophages: a potential mechanism for intercellular HIV trafficking. *Cell Immunol.* 254, 142–148 doi: 10.1016/j.cellimm.2008.08.005

Farré, X., Guillén-Gómez, E., Sánchez, L., Hardisson, D., Plaza, Y., Lloberas, J., et al. (2004). Expression of the nucleoside-derived drug transporters hCNT1, hENT1 and hENT2 in gynecologic tumors. *Int. J. Cancer* 112, 959–966. doi: 10.1002/ijc.20524

Geddings, J. E., and Mackman, N. (2013). Tumor-derived tissue factor-positive microparticles and venous thrombosis in cancer patients. *Blood* 122, 1873–1880. doi: 10.1182/blood-2013-04-460139

Gibby, K., You, W. K., Kadoya, K., Helgadottir, H., Young, L. J., Ellies, L. B., et al. (2012). Early vascular deficits are correlated with delayed mammary tumorigenesis in the MMTV-PyMT transgenic mouse following genetic ablation of the NG_2 proteoglycan. *Breast Cancer Res.* 14:R67. doi: 10.1186/bcr3174

Gousset, K., Marzo, L., Commere, P. H., and Zurzolo, C. (2013). Myo10 is a key regulator of TNT formation in neuronal cells. *J. Cell Sci.* 126(Pt 19), 4424–4435. doi: 10.1242/jcs.129239

Gousset, K., Schiff, E., Langevin, C., Marijanovic, Z., Caputo, A., Browman, D., et al. (2009). Prions hijack tunnelling nanotubes for intercellular spread. *Nat. Cell Biol.* 11, 328–336. doi: 10.1038/ncb1841

Hanna, S. J., McCoy-Simandle, K., Miskolci, V., Guo, P., Cammer, M., Hodgson, L., et al. (2017). The Role of Rho-GTPases and actin polymerization during macrophage tunneling nanotube biogenesis. *Sci. Rep*:7:8547. doi: 10.1038/s41598-017-08950-7

Hase, K., Kimura, S., Takatsu, H., Ohmae, M., Kawano, S., Kitamura, H., et al. (2009). M-Sec promotes membrane nanotube formation by interacting with Ral and the exocyst complex. *Nat. Cell Biol.* 11, 1427–1432. doi: 10.1038/ncb1990

Hood, J. L., Pan, H., Lanza, G. M., and Wickline, S. A. (2009). Paracrine induction of endothelium by tumor exosomes. *Lab Invest.* 89, 1317–1328. doi: 10.1038/labinvest.2009.94

Iglic, A., Lokar, M., Babnik, B., Slivnik, T., Veranic, P., Hägerstrand, H., et al. (2007). Possible role of flexible red blood cell membrane nanodomains in the growth and stability of membrane nanotubes. *Blood Cells Mol. Dis.* 39, 14–23. doi: 10.1016/j.bcmd.2007.02.013

Iizuka, Y., Cichocki, F., Sieben, A., Sforza, F., Karim, R., Coughlin, K., et al. (2015). UNC-45A is a nonmuscle myosin IIA chaperone required for NK cell cytotoxicity via control of lytic granule secretion. *J. Immunol.* 195, 4760–4770. doi: 10.4049/jimmunol.1500979

Iizuka, Y., Mooneyham, A., Sieben, A., Chen, K., Maile, M., Hellweg, R., et al. (2017). UNC-45A is required for neurite extension via controlling NMII activation. *Mol. Biol. Cell* 28, 1337–1346. doi: 10.1091/mbc.e16-06-0381

Jung, E., Osswald, M., Blaes, J., Wiestler, B., Sahm, F., Schmenger, T., et al. (2017). Tweety-homologue 1 drives brain colonization of gliomas. *J. Neurosci.* 37, 6837–6850. doi: 10.1523/JNEUROSCI.3532-16.2017

Junt, T., Schulze, H., Chen, Z., Massberg, S., Goerge, T., Krueger, A., et al. (2007). Dynamic visualization of thrombopoiesis within bone marrow. *Science* 317, 1767–1770. doi: 10.1126/science.1146304

Lachambre, S., Chopard, C., and Beaumelle, B. (2014). Preliminary characterisation of nanotubes connecting T-cells and their use by HIV-1. *Biol. Cell* 106, 394–404. doi: 10.1111/boc.201400037

Liu, Y., Zuo, T., Zhu, X., Ahuja, N., and Fu, T. (2017). Differential expression of hENT1 and hENT2 in colon cancer cell lines. *Genet. Mol. Res.* 16:gmr16019549. doi: 10.4238/gmr16019549

Lock, J. T., Parker, I., and Smith, I. F. (2016). Communication of Ca(2+) signals via tunneling membrane nanotubes is mediated by transmission of inositol trisphosphate through gap junctions. *Cell Calc.* 60, 266–272. doi: 10.1016/j.ceca.2016.06.004

Lou, E., Fujisawa, S., Morozov, A., Barlas, A., Romin, Y., Dogan, Y., et al. (2012). Tunneling nanotubes provide a unique conduit for intercellular transfer of cellular contents in human malignant pleural mesothelioma. *PLoS ONE* 7:e33093. doi: 10.1371/journal.pone.0033093

Lou, E., Gholami, S., Romin, Y., Thayanithy, V., Fujisawa, S., Desir, S., et al. (2017). Imaging tunneling membrane tubes elucidates cell communication in tumors. *Trends Cancer* 3, 678–685. doi: 10.1016/j.trecan.2017.08.001

Mineo, M., Garfield, S. H., Taverna, S., Flugy, A., De Leo, G., Alessandro, R., et al. (2012). Exosomes released by K562 chronic myeloid leukemia cells promote angiogenesis in a Src-dependent fashion. *Angiogenesis* 15, 33–45. doi: 10.1007/s10456-011-9241-1

Nivillac, N. M., Bacani, J., and Coe, I. R. (2011). The life cycle of human equilibrative nucleoside transporter 1: from ER export to degradation. *Exp. Cell Res.* 317, 1567–1579. doi: 10.1016/j.yexcr.2011.03.008

Ohno, H., Hase, K., and Kimura, S. (2010). M-Sec: emerging secrets of tunneling nanotube formation. *Commun. Integr. Biol.* 3, 231–233. doi: 10.4161/cib.3.3.11242

Olumuyiwa-Akeredolu, O. O., and Pretorius, E. (2015). Platelet and red blood cell interactions and their role in rheumatoid arthritis. *Rheumatol. Int.* 35, 1955–1964. doi: 10.1007/s00296-015-3300-7

Onfelt, B., Purbhoo, M. A., Nedvetzki, S., Sowinski, S., and Davis, D. M. (2005). Long-distance calls between cells connected by tunneling nanotubules. *Sci. STKE* 2005:pe55. doi: 10.1126/stke.3132005pe55

Osswald, M., Jung, E., Sahm, F., Solecki, G., Venkataramani, V., Blaes, J., et al. (2015). Brain tumour cells interconnect to a functional and resistant network. *Nature* 528, 93–98. doi: 10.1038/nature16071

Osswald, M., Solecki, G., Wick, W., and Winkler, F. (2016). A malignant cellular network in gliomas: potential clinical implications. *Neuro. Oncol.* 18, 479–485. doi: 10.1093/neuonc/now014

Pagès, F., Mlecnik, B., Marliot, F., Bindea, G., Ou, F. S., Bifulco, J., et al. (2018). International validation of the consensus Immunoscore for the classification of colon cancer: a prognostic and accuracy study. *Lancet* 391, 2128–2139. doi: 10.1016/S0140-6736(18)30789-X

Park, C. W., Zeng, Y., Zhang, X., Subramanian, S., and Steer, C. J. (2010). Mature microRNAs identified in highly purified nuclei from HCT116 colon cancer cells. *RNA Biol.* 7, 606–614. doi: 10.4161/rna.7.5.13215

Pasquier, J., Guerrouahen, B. S., Al Thawadi, H., Ghiabi, P., Maleki, M., Abu-Kaoud, N. et al. (2013). Preferential transfer of mitochondria from endothelial to cancer cells through tunneling nanotubes modulates chemoresistance. *J. Transl. Med.* 11:94. doi: 10.1186/1479-5876-11-94

Pedicini, L., Miteva, K. T., Hawley, V., Gaunt, H. J., Appleby, H. L. and Cubbon, R. M., et al. (2018). Homotypic endothelial nanotubes induced by wheat germ agglutinin and thrombin. *Sci Rep.* 8:7569. doi: 10.1038/s41598-018-25853-3

Plotnikov, E. Y., Khryapenkova, T. G., Galkina, S. I., Sukhikh, G. T., and Zorov, D. B. (2010). Cytoplasm and organelle transfer between mesenchymal multipotent stromal cells and renal tubular cells in co-culture. *Exp. Cell Res.* 316, 2447–2455. doi: 10.1016/j.yexcr.2010.06.009

Poplin, E., Wasan, H., Rolfe, L., Raponi, M., Ikdahl, T., Bondarenko, I., et al. (2013). Randomized, multicenter, phase II study of CO-101 versus gemcitabine in patients with metastatic pancreatic ductal adenocarcinoma: including a prospective evaluation of the role of hENT1 in gemcitabine or CO-101 sensitivity. *J. Clin. Oncol.* 31, 4453–4461. doi: 10.1200/JCO.2013.51.0826

Poulter, N. S., Pollitt, A. Y., Davies, A., Malinova, D., Nash, G. B., and Hannon, M. J. et al. (2015). Platelet actin nodules are podosome-like structures dependent on Wiskott-Aldrich syndrome protein and ARP2/3 complex. *Nat. Commun.* 6:7254. doi: 10.1038/ncomms8254

Price, M. A., Colvin Wanshura, L. E., Yang, J., Carlson, J., Xiang, B., and Li, G. et al. (2011). CSPG4, a potential therapeutic target, facilitates malignant progression of melanoma. *Pigment Cell Melanoma Res.* 24, 1148–1157. doi: 10.1111/j.1755-148X.2011.00929.x

Rivera, Z., Ferrone, S., Wang, X., Jube, S., Yang, H., Pass, H., et al. (2012). CSPG4 as a target of antibody-based immunotherapy for malignant mesothelioma. *Clin. Cancer Res.* 18, 5352–5363. doi: 10.1158/1078-0432.CCR-12-0628

Rustom, A., Saffrich, R., Markovic, I., Walther, P., and Gerdes, H. H. (2004). Nanotubular highways for intercellular organelle transport. *Science* 303, 1007–1010. doi: 10.1126/science.1093133

Sartori-Rupp, A., Cordero Cervantes, D., Pepe, A., Delage, E., Gousset, K., Corroyer-Dulmont, S., C., et al. (2018). Mapping of TNTs using correlative cryo-electron microscopy reveals a novel structure. bioRxiv. *[preprint]* doi: 10.1101/342469

Sarver, A. L., Li, L., and Subramanian, S. (2010). MicroRNA miR-183 functions as an oncogene by targeting the transcription factor EGR1 and promoting tumor cell migration. *Cancer Res.* 70, 9570–9580. doi: 10.1158/0008-5472.CAN-10-2074

Schertzer, J. W., and Whiteley, M. (2011). Microbial communication superhighways. *Cell* 144, 469–470. doi: 10.1016/j.cell.2011.02.001

Schiller, C., Diakopoulos, K. N., Rohwedder, I., Kremmer, E., von Toerne, C., Ueffing, M. et al. (2013). LST1 promotes the assembly of a molecular machinery responsible for tunneling nanotube formation. *J. Cell Sci.* 126(Pt 3), 767–777. doi: 10.1242/jcs.114033

Schwertz, H., Köster, S., Kahr, W. H., Michetti, N., Kraemer, B. F., Weitz, D. A., et al. (2010). Anucleate platelets generate progeny. *Blood* 115, 3801–3809. doi: 10.1182/blood-2009-08-239558

Sherer, N. M., Lehmann, M. J., Jimenez-Soto, L. F., Horensavitz, C., Pypaert, M., and Mothes, W. (2007). Retroviruses can establish filopodial bridges for efficient cell-to-cell transmission. *Nat. Cell Biol.* 9, 310–315. doi: 10.1038/ncb1544

Stone, R. L., Nick, A. M., McNeish, I. A., Balkwill, F., Han, H. D., Sood, A. K. et al. (2012). Paraneoplastic thrombocytosis in ovarian cancer. *N. Engl. J. Med.* 366, 610–618. doi: 10.1056/NEJMoa1110352

Swanepoel, A. C., and Pretorius, E. (2013). Red blood cell and platelet interactions in healthy females during early and late pregnancy, as well as postpartum. *Blood* 121:3788. doi: 10.1182/blood-2013-01-480053

Thayanithy, V., Babatunde, V., Dickson, E. L., Wong, P., Oh, S., Ke X., et al. (2014a). Tumor exosomes induce tunneling nanotubes in lipid raft-enriched regions of human mesothelioma cells. *Exp. Cell Res.* 323, 178–188. doi: 10.1016/j.yexcr.2014.01.014

Thayanithy, V., Dickson, E. L., Steer, C., Subramanian, S., and Lou, E. (2014b). Tumor-stromal cross talk: direct cell-to-cell transfer of oncogenic microRNAs via tunneling nanotubes. *Transl. Res.* 164, 359–365. doi: 10.1016/j.trsl.2014.05.011

Thayanithy, V., O'Hare, P., Wong, P., Zhao, X., Steer, C. J., Subramanian S., et al. (2017). A transwell assay that excludes exosomes for assessment of tunneling nanotube-mediated intercellular communication. *Cell Commun. Signal* 15:46. doi: 10.1186/s12964-017-0201-2

van Rooy, M. J., and Pretorius, E. (2016). Platelet interaction with erythrocytes and propensity to aggregation in essential thrombocythaemia. *Lancet* 387:1210. doi: 10.1016/S0140-6736(14)62293-5

Wang, X., and Gerdes, H. H. (2012). Long-distance electrical coupling via tunneling nanotubes. *Biochim. Biophys. Acta* 1818, 2082–2086. doi: 10.1016/j.bbamem.2011.09.002

Wang, X., Osada, T., Wang, Y., Yu, L., Sakakura, K., Katayama, A., et al. (2010). CSPG4 protein as a new target for the antibody-based immunotherapy of triple-negative breast cancer. *J. Natl. Cancer Inst.* 102, 1496–1512. doi: 10.1093/jnci/djq343

Weil, S., Osswald, M., Solecki, G., Grosch, J., Jung, E., Lemke, D., et al. (2017). Tumor microtubes convey resistance to surgical lesions and chemotherapy in gliomas. *Neuro. Oncol.* 19, 1316–1326. doi: 10.1093/neuonc/nox070

Yang, J., Price, M. A., Li, G. Y., Bar-Eli, M., Salgia, R., and Jagedeeswaran, R. et al. (2009). Melanoma proteoglycan modifies gene expression to stimulate tumor cell motility, growth, and epithelial-to-mesenchymal transition. *Cancer Res.* 69, 7538–7547. doi: 10.1158/0008-5472.CAN-08-4626

Yang, J., Price, M. A., Neudauer, C. L., Wilson, C., Ferrone, S., Xia H., et al. (2004). Melanoma chondroitin sulfate proteoglycan enhances FAK and ERK activation by distinct mechanisms. *J. Cell. Biol.* 165, 881–891. doi: 10.1083/jcb.200403174

Yu, L., Favoino, E., Wang, Y., Ma, Y., Deng, X., and Wang, X. (2011). The CSPG4-specific monoclonal antibody enhances and prolongs the effects of the BRAF inhibitor in melanoma cells. *Immunol. Res.* 50, 294–302. doi: 10.1007/s12026-011-8232-z

Zhang, L., and Zhang, Y. (2015). Tunneling nanotubes between rat primary astrocytes and C6 glioma cells alter proliferation potential of glioma cells. *Neurosci. Bull.* 31, 371–378. doi: 10.1007/s12264-014-1522-4

Zhang, Y., Sime, W., Juhas, M., and Sjölander, A. (2013). Crosstalk between colon cancer cells and macrophages via inflammatory mediators and CD47 promotes tumour cell migration. *Eur. J. Cancer* 49, 3320–3334. doi: 10.1016/j.ejca.2013.06.005

Conflict of Interest Statement: The authors declare that the research was conducted in the absence of any commercial or financial relationships that could be construed as a potential conflict of interest.

frontiers in Oncology

REVIEW
published: 11 September 2018
doi: 10.3389/fonc.2018.00370

Indoximod: An Immunometabolic Adjuvant That Empowers T Cell Activity in Cancer

*Eric Fox[1], Thomas Oliver[1], Melissa Rowe[1], Sunil Thomas[2], Yousef Zakharia[3], Paul B. Gilman[1,2], Alexander J. Muller[2,4] and George C. Prendergast[2,4]**

[1] Department of Hematology-Oncology, Lankenau Medical Center, Wynnewood, PA, United States, [2] Lankenau Institute for Medical Research, Wynnewood, PA, United States, [3] Holden Comprehensive Cancer Center, University of Iowa, Iowa City, IA, United States, [4] Sidney Kimmel Cancer Center, Thomas Jefferson University, Philadelphia, PA, United States

Exploding interest in immunometabolism as a source of new cancer therapeutics has been driven in large part by studies of tryptophan catabolism mediated by IDO/TDO enzymes. A chief focus in the field is IDO1, a pro-inflammatory modifier that is widely overexpressed in cancers where it blunts immunosurveillance and enables neovascularization and metastasis. The simple racemic compound 1-methyl-D,L-tryptophan (1MT) is an extensively used probe of IDO/TDO pathways that exerts a variety of complex inhibitory effects. The L isomer of 1MT is a weak substrate for IDO1 and is ascribed the weak inhibitory activity of the racemate on the enzyme. In contrast, the D isomer neither binds nor inhibits the purified IDO1 enzyme. However, clinical development focused on D-1MT (now termed indoximod) due to preclinical cues of its greater anticancer activity and its distinct mechanisms of action. In contrast to direct enzymatic inhibitors of IDO1, indoximod acts downstream of IDO1 to stimulate mTORC1, a convergent effector signaling molecule for all IDO/TDO enzymes, thus possibly lowering risks of drug resistance by IDO1 bypass. In this review, we survey the unique biological and mechanistic features of indoximod as an IDO/TDO pathway inhibitor, including recent clinical findings of its ability to safely enhance various types of cancer therapy, including chemotherapy, chemo-radiotherapy, vaccines, and immune checkpoint therapy. We also review the potential advantages indoximod offers compared to selective IDO1-specific blockade, which preclinical studies and the clinical study ECHO-301 suggest may be bypassed readily by tumors. Indoximod lies at a leading edge of broad-spectrum immunometabolic agents that may act to improve responses to many anticancer modalities, in a manner analogous to vaccine adjuvants that act to boost immunity in settings of infectious disease.

Keywords: immunometabolism, immune adjuvant, Immunotherapy, immuno-chemotherapy, immuno-radiotherapy

OPEN ACCESS

Edited by:
Ubaldo Emilio Martinez-Outschoorn, Thomas Jefferson University, United States

Reviewed by:
Paolo Puccetti, University of Perugia, Italy
Francesca Fallarino, University of Perugia, Italy

***Correspondence:**
George C. Prendergast
prendergast@limr.org

Specialty section:
This article was submitted to Molecular and Cellular Oncology, a section of the journal Frontiers in Oncology

Received: *11 July 2018*
Accepted: *21 August 2018*
Published: *11 September 2018*

Citation:
Fox E, Oliver T, Rowe M, Thomas S, Zakharia Y, Gilman PB, Muller AJ and Prendergast GC (2018) Indoximod: An Immunometabolic Adjuvant That Empowers T Cell Activity in Cancer. Front. Oncol. 8:370. doi: 10.3389/fonc.2018.00370

INTRODUCTION

Immune therapy has risen to the forefront of cancer therapy in recent years, providing a new approach to cancer therapy, and in some instances has begun to shift the paradigm of cancer care from chemotherapy to immunotherapy. One of the factors crucial to the success of immunotherapy is reversing tumor-mediated immunosuppression (1). The tryptophan catabolic enzyme indoleamine 2,3-dioxygenase-1 (IDO1) has received a great deal of attention as a driver of tumor-mediated suppression (2–4). IDO1 has been shown to be active in many human cancers and its expression has been associated widely with poor prognosis (5, 6). Accordingly, inhibitors of the enzymatic activity and effector functions of IDO1 have been developed as tools to leverage cancer therapy (7).

Elevated tryptophan catabolism as a characteristic of patients with cancer was initially reported over 60 years ago (8). The basis for this observation and later observations in various types of cancer patients was not clear until IDO1 was discovered in the 1960s. An association of elevated tryptophan cata olism with inflammation was established in the 1970s−1980s with demonstrations that IDO1 is induced strongly in the lungs by LPS, viral infection and interferon (9–12). In a seminal line of work in the late 1990s by Munn and Mellor and colleagues, tryptophan catabolism was implicated in immunosuppression during pregnancy, based on the preferential sensitivity of T cells to tryptophan deprivation leading to an impairment of antigen-dependent T cell activation (13–15). In these studies, the key probe in defining this mechanism of immune tolerance was the racemic compound 1-methyl-tryptophan (1MT), a tryptophan mimetic with complex IDO inhibitory effects discussed further below. Indeed, much of the huge amount of subsequent work on IDO and disease pathogenesis has relied on this compound, including most importantly cancer studies.

A causal relationship between IDO1 activity and cancer growth was founded by pivotal studies in the 2000s that have been reviewed in detail elsewhere (7). IDO1 was found to be overexpressed widely in human cancers and 1MT could slow the growth of murine tumors (6, 16, 17). IDO1 overexpression in cancer cells was linked genetically to inactivation of BIN1 (18), a tumor suppressor gene widely attenuated in human cancer (19). Loss of BIN1 empowers IFN/STAT and NFkB mediated IDO1 transcription and later studies also implicated the RAS/MAPK, COX2, and PI3K pathways in driving IDO1 expression (18, 20–22). Interestingly, drugs that target molecules relying on these pathways may act in part by indirectly blocking IDO1 expression, such as the case with imatinib (Gleevec) (23). Pharmacological blockade with 1MT or true catalytic inhibitors of IDO1 enzyme were found to display unimpressive efficacy unless combined with DNA damaging therapies, which led to regression of otherwise unstoppable tumors (18, 24, 25). Preclinical genetic proofs of IDO1 as a valid therapeutic target in cancer were enabled in IDO1-deficient mice, where fundamental connections between IDO1 expression and cancerous inflammatory programs were also established (21, 26, 27).

In the tumor microenvironment or draining lymph nodes, IDO1 activity suppresses the function of T effector cells (Teff) and natural killer (NK) cells and promotes the induction and activation of T regulatory cells (Treg) and the activation, recruitment and expansion of myeloid-derived suppressor cells (MDSC) (**Figure 1**) [Fallarino(21, 29–36)]. IDO1 effector functions are mediated by the tryptophan catabolite kynurenine (Kyn) and by two stress signals generated by locoregional deprivation of tryptophan (7), as discussed further below. Investigations of IDO1 in immune tolerance have focused heavily on antigen-presenting dendritic cells where IDO1 is upregulated by interferons, TLR ligands and other immune signals (37). Beyond its roles in provoking Treg development, IDO1 also acts in certain dendritic cells to directly suppress effector T cell responses (38, 39).

BIOLOGICAL ROOTS OF INDOXIMOD AS AN IMMUNOMETABOLIC ADJUVANT FOR CANCER THERAPY

The racemic compound 1-methyl-D,L-tryptophan (1MT) was first described as a competitive inhibitor of the IDO1 enzyme by Cady and Sono in the early 1990s (40). After the seminal demonstration that 1MT could elicit allogeneic conceptus rejection by ablating T cell tolerance to paternal fetal antigens (13), 1MT was shown to weakly retard the growth of cancer cells in mouse tumor graft or spontaneous transgenic models of cancer (16, 17). While the anticancer effects of 1MT were unremarkable as monotherapy, its striking therapeutic power was revealed in combinations with DNA damaging chemotherapy which elicit regressions of otherwise recalcitrant tumors (18). This discovery was an important advance in providing the first indication of how to use an IDO inhibitor to improve cancer therapy. The regressions achieved by 1MT in combination therapy did not appear to reflect drug-drug interactions that raised the cytotoxicity of the chemotherapies tested, as the efficacy was increased without increasing the known side-effects of the chemotherapies tested (18). Further, T cell depletion in subjects nullified the therapeutic benefits of 1MT administration, establishing that its action was based in provoking T cell attacks in the presence of chemotherapy (18). Overall, these observations challenged the paradigm at the time that active immunotherapy and chemotherapy are fundamentally incompatible by offering one of the first demonstrations of a productive immunochemotherapy regimen based exclusively on small molecule drugs (41).

Careful biochemical studies with purified IDO1 enzyme revealed that only the L racemer of 1MT exerted any catalytic inhibitory activity (42), and it became apparent that L-1MT is actually a weak substrate rather than a true catalytic inhibitor of IDO1 as discussed in detail elsewhere (43). Unexpectedly, the D racemer lacking enzyme inhibitory activity was actually more potent in empowering chemotherapy as well as relieving T cell suppression by IDO1-positive dendritic cells from mouse or human sources (42), although there are conflicting data on T cell suppression (44, 45). Mouse genetic studies were consistent with IDO1 pathway targeting in showing that the anticancer efficacy of D-1MT relied genetically on the presence of a functionally intact

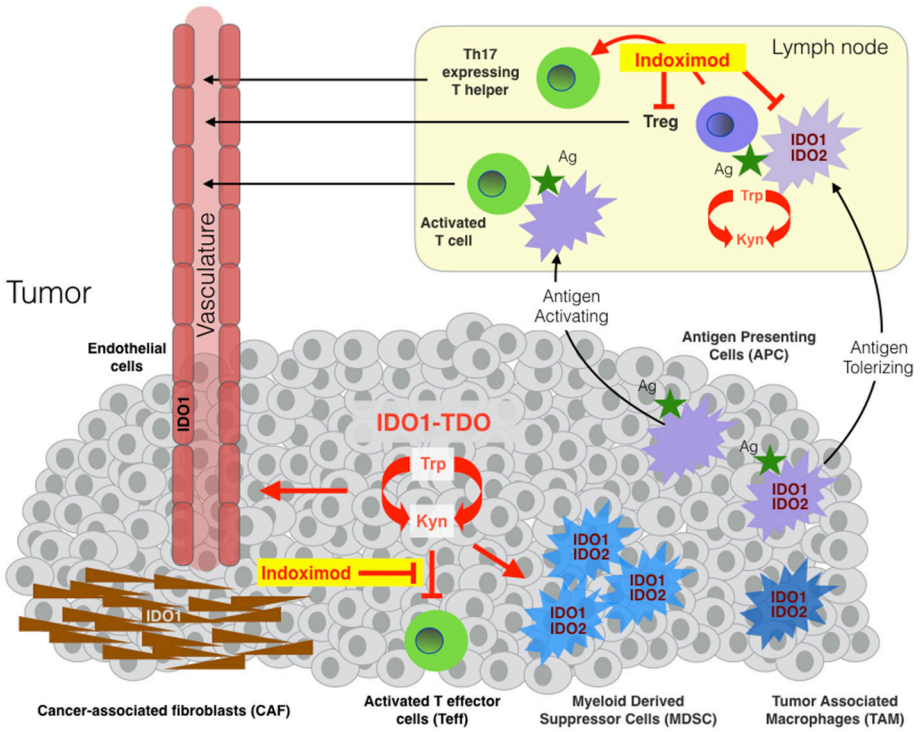

FIGURE 1 | Sites of indoximod action in cancer**.** IDO1, TDO, and IDO2 are expressed variously in malignant, immune, stromal and vascular cells in the tumor microenvironment and in antigen-presenting cells (APC) of tumor-draining lymph nodes. TDO and IDO2 are relatively more narrowly expressed than IDO1 in human cancers, with TDO overexpressed in some tumors independently or in parallel with IDO1 and IDO2 expressed in antigen-presenting cells including B cells where it may influence IDO1 function (28). Tryptophan catabolism in tumor cells leads to locoregional generation of kynurenine at the cost of tryptophan, enabling suppression of local T effector cells (Teff), licensing and recruitment of myeloid-derived suppressor cells (MDSC) and support of a tumor-enabling vasculature. The tumor microenvironment variously recruits cancer-associated fibroblasts, vascular endothelial and inflammatory myeloid cells that express IDO1 and/or IDO2. Tumor antigens absorbed by IDO1/IDO2-expressing antigen-presenting cells (APC) rove to draining lymph nodes where they promote the formation and activation of T regulatory cells (Tregs). Studies suggest that indoximod enables Teff in tumors and attenuate in draining lymph nodes, in the latter case by acting on dendritic cells leading to suppression and/or reprogramming of Tregs and the formation of Th17-expressing T helper cells.

IDO1 gene (42), similar to *bona fide* IDO1 enzyme inhibitors (24, 25). However, subsequent studies of D-1MT make it clear that its antitumor effects in cells and in animals is likely to be complex (7, 43). Indeed, mechanistic studies have made it clear that neither racemer of 1MT is a valid probe of IDO1 enzyme activity, a question ultimately addressed by isolation of several unique structural classes of true enzymatic inhibitors with related antitumor properties, as reviewed elsewhere (7). Cellular mechanisms of action for indoximod have been defined which involve relief of suppression of Teff cells in tumors, limitations on the generation of Tregs, and re-programming of Tregs to Th17 helper cells in draining lymph nodes (**Figure 1**) (2, 46, 47). The robust preclinical efficacy of D-1MT/indoximod in combination with DNA damaging chemotherapy led to its inclusion on a list of 'top ten' agents for clinical evaluation by an NCI immunotherapy workshop (48, 49). In 2008, a decision was made to advance D-1MT/indoximod (NLG-8189) to first-in-man trials as a single molecular species through an FDA investigational new drug application by a collaborative team of investigators from the Medical College of Georgia, Lankenau Institute for Medical Research, National Cancer Institute and NewLink Genetics Corporation as corporate sponsor.

CLINICAL EVALUATION OF INDOXIMOD

Phase 1 studies of indoximod as a monotherapy or in combination with chemotherapy showed it to be well-tolerated in patients with advanced breast cancers or other solid tumors (50, 51). In a first-in-man dose escalation study conducted in advanced breast cancer patients receiving standard of care taxane therapy, the administration of indoximod was well-tolerated to a maximum delivered dose of 1,200 mg twice daily. Four partial responses were observed in the patients studied ($n = 22$) in the absence of any apparent drug-drug interactions (50). In a larger dose escalation study of advanced cancer patients with various solid tumors, the maximum tolerated dose was not reached until 2,000 mg twice daily (51). Notably, several patients on the indoximod trial who had been treated previously with ipilimumab developed hypophysitis, an autoimmune reaction to the pituitary gland which had been documented in patients treated with ipilimumab. In these patients, stable disease >6 months was observed, encouraging the notion that indoximod can reactivate latent T cell immunity in cancer patients. In the initial trials of indoximod, its relative apparent safety is notable given comparisons to the acute side-effects of immune

checkpoint therapy, however, a case of Parkinsonism was reported recently in a patient receiving indoximod treatment (52). While safety studies were not able to identify a maximum tolerated dose (MTD) for indoximod, pharmacokinetic analysis indicated that 1,200 mg twice daily (BID) was the maximum exposure that could be achieved in a patient based on a plateau that occurred in plasma AUC and Cmax beyond this dose. Oral dosing generated a Cmax at 2.9 h with a serum halflife of 10.5 h. Interestingly, there was evidence in indoximod-treated patients of increased levels of both C reactive protein (CRP) and autoantibodies to tumor antigens, consistent with an increased inflammatory response to the chemotherapy onboard (51). Based on these initial studies, multiple Phase 2 studies of indoximod in continuous oral cycles have been conducted at a dose of 1,200 mg twice daily.

Phase 2 data from several trials of indoximod in different types of cancer has been provocative but not uniformly positive in all disease settings examined so far (**Table 1**). All trials have been conducted in combination with standard of care treatments, including in metastatic cutaneous, mucosal, or uveal melanoma with immune checkpoint therapy; advanced breast cancer (BRCA), acute myeloid leukemia (AML), and pancreatic ductal adenocarcinoma (PDAC) with chemotherapy; and advanced prostate carcinoma (PC) with sipuleucel-T (Provenge®), an approved dendritic cell vaccine. In particular, the melanoma and prostate trials have illustrated significant therapeutic activity of indoximod in empowering anti-PD1 treatment (pembrolizumab) and sipuleucel-T vaccine treatment (Provenge® autologous dendritic cells), respectively.

Metastatic Melanoma

The initial phase 1b study in melanoma illustrated the safety of indoximod in combination with the anti-CTLA4 antibody ipilimumab, the standard of care treatment for metastatic melanoma at the time of testing. Nine patients with unresectable stage 3 or 4 melanoma patients were treated with escalating doses of indoximod (600 mg BID, then 1,200 mg BID). Unlike an IDO1 enzyme inhibitor (epacadostat) which yields dose-limiting toxicity (DLT) in combination with ipilimumab, no DLT was encountered with indoximod. Thus, the pre-specified highest dose of indoximod (1,200 mg BID) was deemed tolerable and used as the recommended phase 2 dose (RP2D) in combination with checkpoint inhibitors (59).

The phase 2 melanoma study enrolled over 100 patients in a single-arm trial of indoximod plus provider choice of immune checkpoint antibodies (ipilimumab or the anti-PD1 antibodies nivolimumab or pembrolizumab) (NCT03301636). A preclinical treatment rationale was provided by a study showing that indoximod could improve the response of B16 murine melanoma tumors to immune checkpoint therapy (60). In this single-arm trial (53), 85 patients were treated with pembrolizumab plus indoximod with on-treatment imaging to meet a pre-specified definition of evaluable for efficacy. Overall response rate (ORR) was 53% with a rate of complete response (CR) of 18% and disease control rate (DCR) of 73%. Median progression-free survival (PFS) was 12.4 months (95% confidence interval: 7.1, 24.9). Notably, these efficacy data paralleled those achieved by the approved combination of nivolumab and ipilimumab, but without the elevated rate of severe autoimmune side-effects experienced by patients treated with these agents (61). Stratifying the data by PD-L1 expression status, the ORR in PD-L1 positive (+) patients was 77% vs. 37% in PD-L1 negative (-) patients. Some responses seen in uveal melanomas were encouraging given its extremely aggressive nature and complete lack of response to immune checkpoint therapy (62). Overall, these data suggest the ability of indoximod to safely augment anti-PD1 antibody responses, strongly encouraging a randomized Phase 3 trial in this disease setting. These data are striking in light of the failure of epacadastat, a direct IDO1 enzyme inhibitor, to show any benefit to melanoma patients in the phase 3 ECHO-301 study when administered in combination with pembrolizumab. Given the different mechanism of action of indoximod, its independent evaluation must not be dismissed out of hand.

Metastatic Castrate-Resistant Prostate Cancer

Further significant evidence of the efficacy of indoximod as an immunometabolic adjuvant has been documented in advanced prostate cancer. In a randomized study of metastatic castrate-resistant disease (NCT01560923), 46 patients treated with the dendritic cell vaccine sipuleucel-T (Provenge®) received placebo ($n = 24$) or indoximod ($n = 22$) with the latter cohort displaying a >2-fold increase in overall survival (OS) (54). Indoximod was administered for 10 weeks with 3 additional months in cases where an absence of radiographic or clinical progression was documented. Immune monitoring of patients was the same as performed for the IMPACT study which led to approval of sipuleucel-T (63). Indoximod was well tolerated with no significant difference in adverse events between the two study arms. Median OS had not yet been achieved at the time of report, but median radiographic PFS was 10.3 months in the treatment arm vs. 4.1 months in placebo arm ($p = 0.011$). Notably, the PFS on the placebo arm was identical to that reported in the pivotal IMPACT study for sipuleucel-T. These positive data align with recent evidence that epithelial-mesenchyme transition (EMT) drives IDO1 expression as part of this key step in metastatic progression of prostate cancer to its deadly castrate-resistant form (64). Overall, the findings of this randomized phase 2 trial with a placebo control arm strongly encourages further study of indoximod as an immunometabolic adjuvant for prostate cancer treatment.

Acute Myelogenous Leukemia (AML)

In a Phase 1b trial that includes a randomized Phase 2a component to treat AML, patients with newly diagnosed disease received remission-induction chemotherapy (cytarabine plus idarubicin) plus consolidation chemotherapy (high dose cytarabine), a standard of care regimen, with the addition of indoximod or placebo as maintenance therapy (55) (NCT02835729). The dose escalation was a standard 3+3 design for the phase 1 portion aimed at gauging toxicities in combination with the chemotherapy regimen [400, 600, 1,000, 1,200 mg indoximod]. A different schedule was used in this trial, with indoximod provided every 8 h starting on day 8 of induction

TABLE 1 | Overview of indoximod clinical data (phase 1b/2, phase 2 trials).

Disease	Design	Combination	Number of Patients Evaluated	Evidence of Efficacy?	NCT Reference Number	References
Melanoma *cutaneous, mucosal, uveal*	Phase 2, single arm, 1200 mg bid	SOC Pembrolizumab (evaluated), Nivolimumab or Ipilimumab (non-evaluated)	85	Yes ORR 53% (PD-L1+ 77%, PD-L1− 37%) CR 18%	03301636	(53)
Prostate *metastatic CRPC*	Phase 2, dual arm, randomized 1200 mg bid or placebo	SOC sipuleucel-T vaccine	46 (24 placebo, 22 indoximod)	Yes 10.3 mos treatment vs 4.1 mos placebo (p=0.011)	0156092	(54)
Acute Myeloid Leukemia	Phase 1b/2 dual arm (var. doses ± placebo in Phase 2)	SOC Induction + Maintenance Chemotherapy	6	High occurrence of MRD after one cycle of induction therapy in 5/6 patients	02835729	(55)
Brain *Adult glioma*	Phase 1b/2a single arm (var. doses)	SOC Temozolomide + Bevacizumab + Radiotherapy	12	SD (5-10 mos) 3/12 patients previously refractory to SOC; near PR, 1/12 pts with progressive ongoing reduction in tumor size	02052648	(56)
Brain *Pediatric*	Phase 1b/2 single arm (var. doses)	SOC Temozolomide ± Radiotherapy	29 (12 chemo, 17 chemo+radio)	Yes TTRF=12 mos vs. 3.2 mos chemo+radio vs. chemo-only	02502708	(57)
Pancreas *PDAC*	Phase 2 single arm 1200 bid	SOC Gemcitabine or Nab-Paclitaxel	104	Some, but did not meet pre-specifed goal 30% reduction in HR. Median OS = 10.9 ORR = 46.2%	02077881	(58)
Breast *Stage IV (naïve)*	Phase 2 single arm 1200 bid	SOC Taxotere	169	No No difference in ORR, PFS, or OS	01191216	NA

SOC, standard of care; SD, stable disease; PR, partial response; CR, complete response; HR, hazard ratio; MRD, minimal residual disease; PFS, progression-free survival; TTRF, time to regimen failure.

therapy, avoiding administration on days that patients received consolidation chemotherapy, and then stopping it 4 weeks prior to hematopoietic stem cell allo-transplanation. At the time of the report, the evidence presented indicated that indoximod did not add significant toxicity to standard of care treatment, and early response data suggested a high occurrence of minimal residual disease after one cycle of induction chemotherapy.

Brain Cancer

Phase 1b/2 single-arm trials in adult and pediatric brain cancers are being conducted in which indoximod is combined with chemotherapy or chemo-radiotherapy, with some early but intriguing efficacy data being reported. A preclinical treatment rationale was established in a robust orthotopic model of malignant brain cancer (glioblastoma), where the synergistic effects of indoximod were demonstrated in combination with temozolomide (TMZ) and radiation as a cooperative DNA damaging modality (65). In the latest report from the adult trial (NCT02052648) (56), 12 patients who had progressed on standard of care therapy with TMZ were enrolled in a traditional 3+3 dose escalation study of indoximod (600, 1,000, or 1,200 mg twice daily). No dose-limiting toxicity was encountered nor did indoximod cause a delay or reduction in TMZ dosing in any patient. The best responses documented were 1 patient with partial response per Response Assessment in Neuro-Oncology (RANO) criteria at 15 months and 4 patients with stable disease lasting between 4 and 11 months (66). A phase 2 expansion of the study is ongoing at the 1,200 mg twice daily dose in combination with TMZ, bevacizumab and ateriotactic radiation (SRS) (NCT02052648).

In the pediatric brain cancer trial (NCT02502708) (57), the first trial to evaluate indoximod both in children and in the context of radiotherapy, 17 patients from an original cohort of 29 heavily pretreated patients in the dose escalation phase 1b study who were eligible to receive further treatment were administered indoximod and radiotherapy followed by standard of care cycles of TMZ with indoximod as maintenance therapy. The other 12 patients received only indoximod and TMZ. Both treatments were well tolerated with minimal toxicity attributed to indoximod. Overall, at the time of the report, 29 patients in the dose-escalation phase of the study exhibited a median PFS of 6.2 months and median time to regimen failure (TTRF) of 11.7 months, which compares favorably with historical controls. Notably, patients receiving radiotherapy appeared to benefit significantly when indoximod was added, with a median TTRF of 12 months observed vs. 3.2 months without radiotherapy ($p = 0.04$). These data suggested a dose-sparing effect of indoximod on conventional chemo-radiotherapy, potentially extending efficacious responses. The notion that targeting the IDO pathway may improve chemo-radiotherapy is supported a recent study in lung cancer (67). Encouraged by these response data, the same regimen is now being tested in patients with diffuse intrinsic pontine glioma (DIPG), a dismal disease with no effective treatment option. Thus far, 3/6 patients enrolled are reported to have achieved good symptomatic and radiographic response.

Pancreatic Ductal Adenocarcinoma (PDAC) and Breast Cancer (BRCA)

In contrast to the trials above, two phase 2 studies of >100 patients in pancreatic or breast cancer have shown little to no evidence of efficacy. In a single-arm study of metastatic PDAC (NCT02077881), 104 of 135 patients enrolled to receive a standard of care regimen of gemcidabine or nab-paclitaxel plus indoximod were judged evaluable for efficacy by a pre-specified definition (58). Patients were enrolled with treatment-naïve disease or first line therapy following earlier resection and adjuvant therapy. Treatment was administered until disease progression or toxicity occurred. Median OS was 10.9 months with an ORR of 46.2%. Notably, responding patients exhibited an increased density of intratumoral CD8+ T cells. This study did not meet its pre-specified goal of a hazard ratio (HR) = 0.70, but the increased ORR that was observed correlated with a positive immunological response. In contrast, a study of metastatic BRCA patients failed to produce any evidence of efficacy. In this study of 169 newly diagnosed patients treated with taxotere and indoximod (NCT01191216), no statistically significant difference in PFS, OS, or ORR was observed. While these two types of aggressive cancer set a high bar for improvements in efficacy, the selection of subjects who were not heavily pre-treated opened a window of opportunity for indoximod. Taken together, clinical findings clearly encourage further study of indoximod as an immunometabolic adjuvant for immunotherapy in treatment of melanoma and prostate cancer, and possibly for DNA damaging modalities in treatment brain cancer and AML, a diverse set of diseases and combinations that illustrate the potentially broad uses indoximod may realize in the clinical setting.

MECHANISMS OF ACTION OF INDOXIMOD

Relieving Suppression of mTORC1 Activity in T Cells Due To Tryptophan Starvation

The molecular mechanisms of action of indoximod as an inhibitor of the IDO pathway are a subject of continued study. However, only one mechanism of action has been described that is consistent with pharmacokinetic analyses of the blood serum levels of indoximod that are actually achieved in human subjects (68). Specifically, in cells subjected to IDO/TDO-mediated tryptophan depletion, indoximod has been shown to relieve suppression of the master metabolic kinase mTORC1 that occurs in tryptophan-depleted cells, with an IC50 (∼70 nM) that is more potent than L-tryptophan itself (68). mTORC1 controls protein synthesis, coordinating nutrient levels to different cellular physiological responses of autophagy vs. growth. In T cells, mTORC1 is pivotal in determining autophagy/tolerance vs. growth/activation. mTORC1 is downregulated by depletion of essential amino acids like tryptophan, to which it responds by activating autophagy as an attempt to access tryptophan from intracellular stores. Accordingly, depletion of tryptophan by IDO/TDO activation downregulates mTORC1 and promotes autophagy which indoximod reverses as a tryptophan mimetic (**Figure 2**). Although the precise connections between IDO/TDO-mediated downregulation of mTORC1 in T cells

are not well understood, there is evidence of an intermediate role for the amino acid sensing kinase GLK1 which acts upstream to regulate not only mTORC1 but also PKC-θ, a T cell receptor regulatory kinase (69). Thus, GLK1 may be a linchpin between tryptophan catabolism by IDO/TDO enzymes and mTORC1 downregulation in T cells (7).

By restoring mTORC1 activity, indoximod acts to reverse mTORC1-activated autophagy triggered by tryptophan depletion (68). Since indoximod is a D-tryptophan analog, it cannot support protein translation, but nevertheless it is interpreted by the mTORC1 kinase as a high-potency L-tryptophan mimetic. Why this is the case is unclear, but a mammalian capability to recognize (if not use) D-amino acids might reflect immune crosstalk with the microbiome given their use in bacteria (70). In any case, mTORC1 has a critical role in human Teff cell activity and indoximod acts directly in human T cells where it exerts a direct effect, unlike IDO1 enzyme inhibitors (71).

There are at least three implications of this mechanism of action. First, by targeting a downstream effector molecule, indoximod differs from IDO1 enzyme inhibitors in being agnostic to the IDO/TDO enzyme(s) contributing to cancer pathogenesis. Thus, indoximod is rationalized to treat tumor cells overexpressing IDO1, IDO2 or TDO (or any combination thereof), which is not the case for an enzyme-selective inhibitor. This is a useful feature in heterogenous plastic tumors which represent the norm in advanced cancer patients. Second, by targeting a convergent effector mechanism used by all IDO/TDO enzymes, indoximod may prove less sensitive to inherent or acquired resistance that may arise in patients due to IDO1 mutation, IDO1 overexpression or other target bypass mechanisms that heterogeneous cancers evolve. On this point, preclinical genetic studies illustrate clearly how tumoral bypass of an IDO1-specific blockade is associated with IDO1-independent elevation of regional kynurenine levels (21), suggesting the availability of resistance pathways via TDO2 or IDO2 activation. The critical question of inherent and acquired resistance to IDO1 selective blockade is discussed in greater depth in a separate review of the failed ECHO-301 phase 3 clinical trial in melanoma patients of pembrolizumab with epacadastat, a direct IDO1 enzyme inhibitor that added no benefit to the immune checkpoint therapy under the conditions of study (72). Lastly, mTORC1 is implicated in tumor cell growth and proliferation as well as in T cell activation. Thus, if indoximod also provokes mTORC1 activation in tumor cells, the drug may also empower tumor cell killing when combined with chemotherapeutic drugs, which generally exhibit greater cytotoxicity against growing cells.

Overall, the evidence that indoximod may broaden the efficacy of pembrolizumab (53) suggests that restoring mTORC1 in effector T cells might be sufficient to improve therapeutic responses with reduced risks of resistance due to IDO1 bypass. On this point, it is known that mTORC1 drives expression of ICOS, a positive-acting T cell co-regulatory receptor, and that elevated expression of ICOS in melanoma patients receiving immune checkpoint therapy correlates with the most favorable outcomes (73). In efforts to further leverage its features as an IDO/TDO effector pathway inhibitor, novel salts of indoximod and a pro-drug form of the drug (NLG-802) with superior pharmacokinetic properties have recently been described which have entered clinical testing (71).

Other Mechanisms of Action

Indoximod clearly has complex immunomodulatory properties, as illustrated, for example, by its ability to act on B cells to relieve inflammation in a murine model of autoimmune rheumatoid arthritis (74, 75). Thus, other mechanisms of action that have been described for indoximod are likely to illuminate its therapeutic properties.

Indirect Blockade of IDO2 Which Is Implicated in IDO1-Mediated Treg Activation

The catalytic activity of IDO2 has been shown to be inhibited indirectly by indoximod in human kidney cells where the IDO2 gene is expressed normally (76). There is conflicting data in dendritic cells, which express IDO2 as well as IDO1, on the ability of indoximod in this setting to block T cell suppression (42, 77, 78). However, mouse genetic studies support a link between indoximod action and IDO2 function, for example, in demonstrating that the therapeutic benefits of indoximod administration in a model of rheumatoid arthritis that relies on the presence of the *Ido2* gene (74), which interacts genetically with IDO1 in IDO1-mediated activation of Treg cells in the mouse (28). Here we note that the ability of indoximod to limit rheumatoid arthritis is highly relevant to combination treatments with immune checkpoint antibodies, which often cause autoimmune side-effect in patients. In this sense, indoximod co-administration with immune checkpoint antibodies may widen the therapeutic window at both ends, by extending efficacy and reducing side-effects, unlike IDO1-selective enzyme inhibitors.

AHR Modulation

At high concentrations in cell culture (1 mM), evidence has been presented that D-1MT/indoximod can elevate transcription of IDO1 leading to increased production of kynurenine in cancer cells (79), but the concentrations used in this study, which exceed by ∼100-fold the serum levels of indoximod achieved in patients in clinical trials (50), cast doubt on the physiological relevance of this observation. However, a very recent report offers additional support for the related idea that indoximod may somehow affect IDO1 expression in cell-specific ways via AHR (80), a transcription factor that binds and is activated by kynurenine (81) as a convergent effector pathway downstream of all IDO/TDO enzymes (7). Indeed, other evidence has been presented for an autocrine feedback pathway involving IDO1, AHR, and IL-6 that controls IDO1 expression in cancer cells (82).

The AHR connection for indoximod is complex. There are binding sites for AHR in the IDO1 gene and other genes that influence the differentiation of dendritic cells, T helper cells and Tregs and the proliferation of Teffs and Tregs where AHR has influence (83). In a recent study reported at the 2018 AACR conference (80), indoximod was reported to modulate AHR-dependent transcriptional activity in human liver and primary T cells, in the latter case altering the transcription of genes

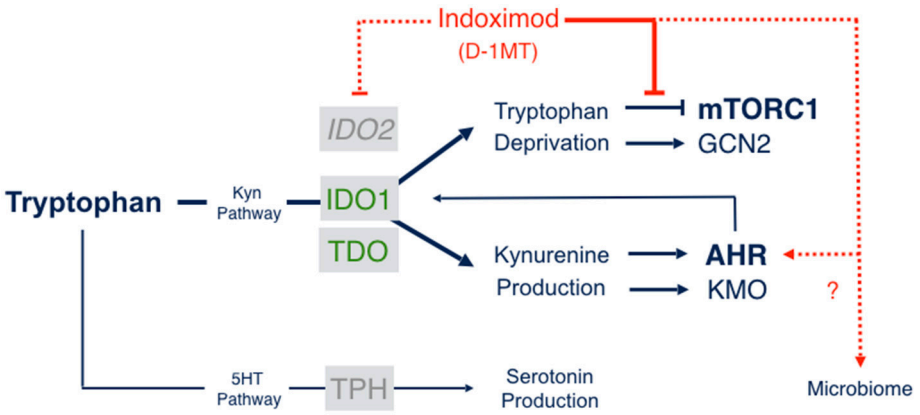

FIGURE 2 | Indoximod mechanisms of action**.** Tryptophan catabolism proceeds through pathways leading to serotonin or NAD production, the latter through the kynurenine pathway which handles ~95% of Trp catabolism in mammals. Indoximod is a Trp mimetic which mTORC1 interprets as L-Trp under conditions of high Trp catabolism and autophagy. Thus, the drug acts to block the suppressive signal on mTORC1 function generated by IDO/TDO activity. Other suggested mechanisms of action include an indirect suppression of IDO2 activity; a modulation of kynurenine-regulated AHR function, which may also influence feedback on IDO1 expression and activity; and an influence on gut microbial physiology influencing systemic immunity (see the text).

associated with T helper and Treg phenotypes. These effects were reversed by an AHR inhibitor, suggesting that indoximod acts upstream of AHR (80). In plasmacytoid dendritic cells *in vitro* and *in vivo* (in tumor-draining lymph nodes), indoximod was found to downregulate IDO1 expression and function, decrease kynurenine production and increase T cell proliferation, while promoting a phenotypic shift in T cells from Treg to Th17-producing T helper cells (80). Thus, in addition to resuscitating Teff cells in tumors, indoximod may also act in draining lymph nodes to reprogram the AHR effector pathway to shift Tregs to Th17 cells.

Perspectives of Indoximod on IDO/TDO/AHR Signaling to the Gut Microbiome

Immune homeostasis involves a dynamic balance between tolerance of commensals and suitable immune responses to eradicate or otherwise control pathogens (84, 85). Tolerance is important to avoid tissue injury but at the potential costs of chronic infections and inflammation which in the long term become factors in metabolic diseases, autoimmunity, and, in certain settings, cancer (85). Regarding indoximod mechanisms this is an important area to survey given evidence that the therapeutic impact of anti-PD1 therapy is determined by microbiome character, in both preclinical models (86, 87) and clinical settings (88–90).

Cross-regulatory circuitry between IDO1 and AHR is a key factor in mediating disease tolerance (91). For example, exposure to bacterial lipopolysaccharide will program a state of refractoriness to further LPS challenge (endotoxin tolerance), a phenomenon reflecting the engagment of AHR in long-term control of systemic inflammation only when IDO1 is active, which responds late upon initial stimulation but earlier upon subsequent challenge. Mechanistic studies have revealed a feedback control cycle, with SRC kinase as an intermediate between kynurenine-activated AHR and IDO1 expression in regulating tolerance to bacterial endotoxins, a state that protects against immunopathology in Gram-negative and Gram-positive infections. In this fundamental way, IDO1 and especially AHR contribute to immunologic host fitness (91).

IDO1 and AHR are highly expressed in the small and large intestine (92). IDO1 expression increases further during aging, a key factor in the likelihood of a positive therapeutic response to anti-PD1 treatment (93). In the intestine of adult germ-free mice, IDO1 levels are reduced suggesting that commensal microorganisms mediate the age-dependent increase in IDO1. Supporting the likelihood that it modulates mucosal immunity to intestinal microbiota, IDO1-deficient mice exhibit resistance to enteric pathogens, for example, to *Citrobacter rodentium* (94). Tryptophan catabolites produced by microbiota such as gut *Lactobacillus* can also act as AHR ligands, confounding a clear interpretation of the link between IDO1 and cancer that may involve microbiota-mediated tryptophan catabolism (85).

In melanoma studies of anti-PD-1/PD-L1 it appears that gut commensals of *Bifidobacteria* can enhance therapeutic efficacy (86, 88–90). Given evidence that indoximod can heighten the benefit of anti-PD1 therapy, it will be important to evaluate *Bifidobacteria* as a potential mediator in this effects, which raises the possibility of conceptualizing indoximod as a prebiotic substance. In one clue that this may be the case, indoximod was able to reverse the effects of IDO1 activity in models of colitis that are quieted by *Bifidobacteria* (95). While still in their infancy, studies of the effects on indoximod and the IDO/TDO/AHR pathways on gut microbial physiology and cancer immunity is a rich area for exploration.

POTENTIAL BENEFITS OF INDOXIMOD TREATMENT TO QUALITY OF LIFE IN CANCER PATIENTS

Recent studies suggest that indoximod may exert a variety of benefits as an immunometabolic adjuvant on the quality of

life of cancer patients and survivors. The conditions that are improved are not critical to overall survival, but are of major importance to affected individuals and their oncologists and caregivers. As noted above, one interesting feature of indoximod is its ability to limit autoimmune arthritis in preclinical models, possibly by limiting IDO2 function implicated in this condition (96). Autoimmune joint inflammation is a common short and long term side effect of immune checkpoint therapy in cancer patients which indoximod may limit. This potential may be confirmed through long-term follow up of melanoma patients receiving combinations of indoximod and pembrolizumab in the phase 2 trial discussed above. Other beneficial effects of indoximod that have been described are behavioral, as evaluated in preclinical models of depression, anhedonia, anxiety or pain (97–100), one or more of which occur commonly in cancer patients and survivors. Given its relative safety in trials to date, it may be possible to consider uses in these settings, not only during cancer therapy but as a palliative adjunctive therapy. In summary, indoximod is a unique immunometabolic adjuvant with a wide potential range of uses to improve cancer therapy in adults and children, not only safely but with possible collateral benefits to quality of life.

AUTHOR CONTRIBUTIONS

All authors contributed to composing the text. GP composed the figures. YZ, PG, AM, and GP made final edits to the text and figures.

ACKNOWLEDGMENTS

We thank our many colleagues and collaborators and apologize for omitting citations to many primary research reports cited through reviews due to space limitations. GP and AM acknowledge grant support from the NCI (R01 CA191119) and The W.W. Smith Trust, with additional support from the Lankenau Medical Center Foundation and the Main Line Health System. GP holds The Havens Chair for Biomedical Research at the Lankenau Institute for Medical Research.

REFERENCES

1. Prendergast GC, Jaffee EM. Cancer immunologists and cancer biologists: why we didn't talk then but need to now. *Cancer Res.* (2007) 67:3500–4. doi: 10.1158/0008-5472.CAN-06-4626
2. Munn DH, Mellor AL. IDO in the tumor microenvironment: inflammation, counter-regulation, and tolerance. *Trends Immunol.* (2016) 37:193–207. doi: 10.1016/j.it.2016.01.002
3. Amobi A, Qian F, Lugade AA, Odunsi K. Tryptophan catabolism and cancer immunotherapy targeting IDO mediated immune suppression. *Adv Exp Med Biol.* (2017) 1036:129–44. doi: 10.1007/978-3-319-67577-0_9
4. Prendergast GC, Malachowski WJ, Mondal A, Scherle P, Muller AJ. Indoleamine 2,3-dioxygenase and its therapeutic inhibition in cancer. *Int Rev Cell Mol Biol.* (2018) 336:175–203. doi: 10.1016/bs.ircmb.2017.07.004
5. Godin-Ethier J, Hanafi LA, Piccirillo CA, Lapointe R. Indoleamine 2,3-dioxygenase expression in human cancers: clinical and immunologic perspectives. *Clin Cancer Res.* (2011) 17:6985–91. doi: 10.1158/1078-0432.CCR-11-1331
6. Theate I, Van Baren N, Pilotte L, Moulin P, Larrieu P, Renauld JC, et al. Extensive profiling of the expression of the indoleamine 2,3-dioxygenase 1 protein in normal and tumoral human tissues. *Cancer Immunol Res.* (2015) 3:161–72. doi: 10.1158/2326-6066.CIR-14-0137
7. Prendergast GC, Malachowski WP, Duhadaway JB, Muller AJ. Discovery of IDO1 inhibitors: from bench to bedside. *Cancer Res.* (2017) 77:6795–811. doi: 10.1158/0008-5472.CAN-17-2285
8. Boyland E, Williams DC. The metabolism of tryptophan. 2. the metabolism of tryptophan in patients suffering from cancer of the bladder. *Biochem J.* (1956) 64:578–82. doi: 10.1042/bj0640578
9. Yoshida R, Hayaishi O. Induction of pulmonary indoleamine 2,3-dioxygenase by intraperitoneal injection of bacterial lipopolysaccharide. *Proc Natl Acad Sci USA.* (1978) 75:3998–4000. doi: 10.1073/pnas.75.8.3998
10. Yoshida R, Urade Y, Tokuda M, Hayaishi O. Induction of indoleamine 2,3-dioxygenase in mouse lung during virus infection. *Proc Natl Acad Sci USA.* (1979) 76:4084–6. doi: 10.1073/pnas.76.8.4084
11. Yoshida R, Imanishi J, Oku T, Kishida T, Hayaishi O. Induction of pulmonary indoleamine 2,3-dioxygenase by interferon. *Proc Natl Acad Sci USA.* (1981) 78:129–32. doi: 10.1073/pnas.78.1.129
12. Yasui H, Takai K, Yoshida R, Hayaishi O. Interferon enhances tryptophan metabolism by inducing pulmonary indoleamine 2,3-dioxygenase: its possible occurence in cancer patients. *Proc Natl Acad Sci USA.* (1986) 83:6622–6. doi: 10.1073/pnas.83.17.6622
13. Munn DH, Zhou M, Attwood JT, Bondarev I, Conway SJ, Marshall B, et al. Prevention of allogeneic fetal rejection by tryptophan catabolism. *Science* (1998) 281:1191–3. doi: 10.1126/science.281.5380.1191
14. Munn DH, Shafizadeh E, Attwood JT, Bondarev I, Pashine A, Mellor AL. Inhibition of T cell proliferation by macrophage tryptophan catabolism. *J Exp Med.* (1999) 189:1363–72. doi: 10.1084/jem.189.9.1363
15. Mellor AL, Sivakumar J, Chandler PKS, Molina H, Mao D, Munn DH. Prevention of T cell-driven complement activation and inflammation by tryptophan catabolism during pregnancy. *Nat. Immunol.* (2001) 2:64–8. doi: 10.1038/83183
16. Friberg M, Jennings R, Alsarraj M, Dessureault S, Cantor A, Extermann M, et al. Indoleamine 2,3-dioxygenase contributes to tumor cell evasion of T cell-mediated rejection. *Int J Cancer* (2002) 101:151–5. doi: 10.1002/ijc.10645
17. Uyttenhove C, Pilotte L, Theate I, Stroobant V, Colau D, Parmentier N, et al. Evidence for a tumoral immune resistance mechanism based on tryptophan degradation by indoleamine 2,3-dioxygenase. *Nat Med.* (2003) 9:1269–74. doi: 10.1038/nm934
18. Muller AJ, Duhadaway JB, Sutanto-Ward E, Donover PS, Prendergast GC. Inhibition of indoleamine 2,3-dioxygenase, an immunomodulatory target of the tumor suppressor gene Bin1, potentiates cancer chemotherapy. *Nat Med.* (2005) 11:312–9. doi: 10.1038/nm1196
19. Prendergast GC, Muller AJ, Ramalingam A, Chang MY. BAR the door: cancer suppression by amphiphysin-like genes. *Biochim Biophys Acta* (2009) 1795:25–36. doi: 10.1016/j.bbcan.2008.09.001
20. Basu GD, Tinder TL, Bradley JM, Tu T, Hattrup CL, Pockaj BA, et al. Cyclooxygenase-2 inhibitor enhances the efficacy of a breast cancer vaccine: role of IDO. *J Immunol.* (2006) 177:2391–402. doi: 10.4049/jimmunol.177.4.2391
21. Smith C, Chang MY, Parker KH, Beury DW, Duhadaway JB, Flick HE, et al. IDO Is a nodal pathogenic driver of lung cancer and metastasis development. *Cancer Discov.* (2012) 2:722–35. doi: 10.1158/2159-8290.CD-12-0014
22. Hennequart M, Pilotte L, Cane S, Hoffmann D, Stroobant V, De Plaen E, et al. Constitutive IDO1 expression in human tumors is driven by Cyclooxygenase-2 and mediates intrinsic immune resistance. *Cancer Immunol Res.* (2017). 5:695–709. doi: 10.1158/2326-6066.CIR-16-0400
23. Balachandran VP, Cavnar MJ, Zeng S, Bamboat ZM, Ocuin LM, Obaid H, et al. Imatinib potentiates antitumor T cell responses in gastrointestinal stromal tumor through the inhibition of Ido. *Nat Med.* (2011) 17:1094–100. doi: 10.1038/nm.2438

24. Banerjee T, Duhadaway JB, Gaspari P, Sutanto-Ward E, Munn DH, Mellor AL, et al. A key *in vivo* antitumor mechanism of action of natural product-based brassinins is inhibition of indoleamine 2,3-dioxygenase. *Oncogene* (2008) 27:2851–7. doi: 10.1038/sj.onc.1210939
25. Kumar S, Jaller D, Patel B, Lalonde JM, Duhadaway JB, Malachowski WP, et al. Structure based development of phenylimidazole-derived inhibitors of indoleamine 2,3-dioxygenase. *J Med Chem.* (2008) 51:4968–77. doi: 10.1021/jm800512z
26. Muller AJ, Sharma MD, Chandler PR, Duhadaway JB, Everhart ME, Johnson BA. III et al. Chronic inflammation that facilitates tumor progression creates local immune suppression by inducing indoleamine 2,3 dioxygenase. *Proc Natl Acad Sci USA*. (2008) 105:17073–78. doi: 10.1073/pnas.0806173105
27. Muller AJ, Duhadaway JB, Chang MY, Ramalingam A, Sutanto-Ward E, Boulden J, et al. Non-hematopoietic expression of IDO is integrally required for inflammatory tumor promotion. *Cancer Immunol Immunother.* (2010) 59:1655–63. doi: 10.1007/s00262-010-0891-4
28. Metz R, Smith C, Duhadaway JB, Chandler P, Baban B, Merlo LM, et al. IDO2 is critical for IDO1-mediated T cell regulation and exerts a non-redundant function in inflammation. *Int Immunol.* (2014) 26:357–67. doi: 10.1093/intimm/dxt073
29. Fallarino F, Grohmann U, Vacca C, Bianchi R, Orabona C, Spreca A, et al. T cell apoptosis by tryptophan catabolism. *Cell Death Diff.* (2002) 9:1069–77. doi: 10.1038/sj.cdd.4401073
30. Frumento G, Rotondo R, Tonetti M, Damonte G, Benatti U, Ferrara GB. Tryptophan-derived catabolites are responsible for inhibition of T and natural killer cell proliferation induced by indoleamine 2,3-dioxygenase. *J Exp Med.* (2002) 196:459–68. doi: 10.1084/jem.20020121
31. Munn DH, Sharma MD, Lee JR, Jhaver KG, Johnson TS, Keskin DB, et al. Potential regulatory function of human dendritic cells expressing indoleamine 2,3-dioxygenase. *Science* (2002) 297:1867–70. doi: 10.1126/science.1073514
32. Terness P, Bauer TM, Rose L, Dufter C, Watzlik A, Simon H, et al. Inhibition of allogeneic T cell proliferation by indoleamine 2,3-dioxygenase-expressing dendritic cells: mediation of suppression by tryptophan metabolites. *J Exp Med.* (2002) 196:447–57. doi: 10.1084/jem.20020052
33. Mellor AL, Chandler P, Baban B, Hansen AM, Marshall B, Pihkala J, et al. Specific subsets of murine dendritic cells acquire potent T cell regulatory functions following CTLA4-mediated induction of indoleamine 2,3 dioxygenase. *Int Immunol.* (2004) 16:1391–401. doi: 10.1093/intimm/dxh140
34. Munn DH, Sharma MD, Baban B, Harding HP, Zhang Y, Ron D, et al. GCN2 kinase in T cells mediates proliferative arrest and anergy induction in response to indoleamine 2,3-dioxygenase. *Immunity* (2005) 22:633–42. doi: 10.1016/j.immuni.2005.03.013
35. Della Chiesa M, Carlomagno S, Frumento G, Balsamo M, Cantoni C, Conte R, et al. The tryptophan catabolite L-kynurenine inhibits the surface expression of NKp46- and NKG2D-activating receptors and regulates NK-cell function. *Blood* (2006) 108:4118–25. doi: 10.1182/blood-2006-03-006700
36. Holmgaard RB, Zamarin D, Li Y, Gasmi B, Munn DH, Allison JP. et al. Tumor-expressed IDO recruits and activates MDSCs in a Treg-dependent manner. *Cell Rep.* (2015) 13:412–24. doi: 10.1016/j.celrep.2015.08.077
37. Mellor AL, Munn DH. Creating immune privilege: active local suppression that benefits friends, but protects foes. *Nat Rev Immunol.* (2008) 8:74–80. doi: 10.1038/nri2233
38. Grohmann U, Fallarino F, Puccetti P. Tolerance, DCs and tryptophan: much ado about IDO. *Trends Immunol.* (2003) 24:242–8. doi: 10.1016/S1471-4906(03)00072-3
39. Mellor AL, Munn DH. IDO expression by dendritic cells: tolerance and tryptophan catabolism. *Nat Rev Immunol.* (2004) 4:762–74. doi: 10.1038/nri1457
40. Cady SG, Sono M. 1-methyl-DL-tryptophan, beta-(3-benzofuranyl)-DL-alanine (the oxygen analog of tryptophan), and beta-[3-benzo(b)thienyl]-DL-alanine (the sulfur analog of tryptophan) are competitive inhibitors for indoleamine 2,3-dioxygenase. *Arch Biochem Biophys.* (1991) 291:326–33. doi: 10.1016/0003-9861(91)90142-6
41. Muller AJ, Prendergast GC. Marrying immunotherapy with chemotherapy: why say IDO? *Cancer Res.* (2005) 65:8065–8. doi: 10.1158/0008-5472.CAN-05-2213
42. Hou DY, Muller AJ, Sharma MD, Duhadaway J, Banerjee T, Johnson M, et al. Inhibition of indoleamine 2,3-dioxygenase in dendritic cells by stereoisomers of 1-methyl-tryptophan correlates with antitumor responses. *Cancer Res.* (2007) 67:792–801. doi: 10.1158/0008-5472.CAN-06-2925
43. Prendergast GC, Smith C, Thomas S, Mandik-Nayak L, Laury-Kleintop L, Metz R, et al. Indoleamine 2,3-dioxygenase pathways of pathogenic inflammation and immune escape in cancer. *Cancer Immunol Immunother.* (2014) 63:721–35. doi: 10.1007/s00262-014-1549-4
44. Lob S, Konigsrainer A, Schafer R, Rammensee HG, Opelz G, Terness P. Levo- but not dextro-1-methyl tryptophan abrogates the IDO activity of human dendritic cells. *Blood* (2008) 111:2152–4. doi: 10.1182/blood-2007-10-116111
45. Qian F, Villella J, Wallace PK, Mhawech-Fauceglia P, Tario JD Jr, Andrews C, et al. Efficacy of levo-1-methyl tryptophan and dextro-1-methyl tryptophan in reversing indoleamine-2,3-dioxygenase-mediated arrest of T-cell proliferation in human epithelial ovarian cancer. *Cancer Res.* (2009) 69:5498–504. doi: 10.1158/0008-5472.CAN-08-2106
46. Munn DH, Bronte V. Immune suppressive mechanisms in the tumor microenvironment. *Curr Opin Immunol.* (2016) 39:1–6. doi: 10.1016/j.coi.2015.10.009
47. Munn DH, Sharma MD, Johnson TS, Rodriguez P. IDO, PTEN-expressing tregs and control of antigen-presentation in the murine tumor microenvironment. *Cancer Immunol Immunother.* (2017) 66:1049–58. doi: 10.1007/s00262-017-2010-2
48. Cheever MA. Twelve immunotherapy drugs that could cure cancers. *Immunol Rev.* (2008) 222:357–68. doi: 10.1111/j.1600-065X.2008.00604.x
49. Cheever MA, Allison JP, Ferris AS, Finn OJ, Hastings BM, Hecht TT, et al. The prioritization of cancer antigens: a national cancer institute pilot project for the acceleration of translational research. *Clin Cancer Res.* (2009) 15:5323–37. doi: 10.1158/1078-0432.CCR-09-0737
50. Soliman HH, Jackson E, Neuger T, Dees EC, Harvey RD, Han H, et al. A first in man phase I trial of the oral immunomodulator, indoximod, combined with docetaxel in patients with metastatic solid tumors. *Oncotarget* (2014) 5:8136–46. doi: 10.18632/oncotarget.2357
51. Soliman HH, Minton SE, Han HS, Ismail-Khan R, Neuger A, Khambati F, et al. A phase I study of indoximod in patients with advanced malignancies. *Oncotarget* (2016) 7:22928–38. doi: 10.18632/oncotarget.8216
52. Floyd M, Osta BE, Tang SC. First report of parkinsonism associated with indoximod, an immune-modulating agent. *J Global Oncol.* (2018) 4:1–2. doi: 10.1200/JGO.2016.007492
53. Zakharia Y, Rixe O, Ward JH, Drabick JJ, Shaheen MF, Milhem MM, et al. Phase 2 trial of the IDO pathway inhibitor indoximod plus checkpoint inhibition for the treatment of patients with advanced melanoma. *J Clin Oncol.* (2018) 36:9512.
54. Jha GG, Gupta S, Tagawa ST, Koopmeiners JS, Vivek S, Dudek AZ, et al. A phase II randomized, double-blind study of sipuleucel-T followed by IDO pathway inhibitor, indoximod, or placebo in the treatment of patients with metastatic castration resistant prostate cancer (mCRPC). *J Clin Oncol.* (2017) 35:3066. doi: 10.1200/JCO.2017.35.15
55. Emadi A, Holtzman NG, Imran M, El-Chaer F, Koka M, Singh Z, et al. *Indoximod in Combination with Idarubicin and Cytarabine for Upfront Treatment of Patients with Newly Diagnosed Acute Myeloid Leukemia (AML): Phase 1 Report.* II Congress of the European Hematology Association. (2017).
56. Colman H, Mott F, Spira AI, Johnson TS, Zakharia Y, Vahanian NN, et al. A phase 1b/2 study of the combination of the IDO pathway inhibitor indoximod and temozolomide for adult patients with temozolomide-refractory primary malignant brain tumors: Safety analysis and preliminary efficacy of the phase 1b component. *J Clin Oncol.* (2015) 33:2070. doi: 10.1200/jco.2015.33.15
57. Johnson TS. Radio-chemo-immunotherapy using the IDO-inhibitor indoximod for childhood brain cancer. In: *2017 International Pediatric Neuro-oncology Conference*. (Houston TX, Texas Children's Hospital) (2017).
58. Bahary N, Wang-Gillam A, Haraldsdottir S, Somer BG, Lee JS, O'rourke MA, et al. Phase 2 trial of the IDO pathway inhibitor indoximod plus gemcitabine/nab-paclitaxel for the treatment of patients with metastatic pancreas cancer. *J Clin Oncol.* (2018) 36:4015. doi: 10.1200/JCO.2018.36.15
59. Zakharia Y, Drabick JJ, Khleif SN, Munn DH, Link CJ, Vahanian NN, et al. Results of a Phase 1b trial of the indoleamine 2,3-dioxygenase (IDO) pathway

inhibitor indoximod plus ipilimumab for the treatment of unresectable stage 3 or 4 melanoma. In: *European Cancer Congress 2015 (18th ECCO/40th ESMO)*, Vienna. abstract #514 (2015).
60. Holmgaard RB, Zamarin D, Munn DH, Wolchok JD, Allison JP. Indoleamine 2,3-dioxygenase is a critical resistance mechanism in antitumor T cell immunotherapy targeting CTLA-4. *J Exp Med.* (2013) 210:1389–402. doi: 10.1084/jem.20130066
61. Postow MA, Chesney J, Pavlick AC, Robert C, Grossmann K, Mcdermott D, et al. Nivolumab and ipilimumab versus ipilimumab in untreated melanoma. *N Engl J Med.* (2015) 372:2006–17. doi: 10.1056/NEJMoa1414428
62. Zakharia Y, Mcwilliams R, Shaheen M, Grossman K, Drabick J, Milhem M, et al. Interim analysis of the Phase 2 clinical trial of the IDO pathway inhibitor indoximod in combination with pembrolizumab for patients with advanced melanoma. *Cancer Res.* (2017) 77:CT117. doi: 10.1158/1538-7445.AM2017-CT117
63. Kantoff PW, Higano CS, Shore ND, Berger ER, Small EJ, Penson DF, et al. Sipuleucel-T immunotherapy for castration-resistant prostate cancer. *N Engl J Med.* (2010) 363:411–22. doi: 10.1056/NEJMoa1001294
64. Kolijn K, Verhoef EI, Smid M, Bottcher R, Jenster GW, Debets R, et al. Epithelial-mesenchymal transition in human prostate cancer demonstrates enhanced immune evasion marked by IDO1 expression. *Cancer Res.* (2018) 78:4671–9. doi: 10.1158/0008-5472.CAN-17-3752
65. Li M, Bolduc AR, Hoda MN, Gamble DN, Dolisca S-B, Bolduc AK, et al. The indoleamine 2,3-dioxygenase pathway controls complement-dependent enhancement of chemo-radiation therapy against murine glioblastoma. *J Immunother Cancer* (2014) 2:21. doi: 10.1186/2051-1426-2-21
66. Zakharia Y, Colman H, Mott F, Lukas R, Vahanian N, Link C, et al. IMCT-21 updates on phase 1b/2 combination study of the IDO pathway inhibitor indoximod with temozolomide for adult patients with temozolomide-refractory primary malignant brain tumors. *Neuro-Oncology* (2015) 17:v112. doi: 10.1093/neuonc/nov218.21
67. Wang W, Huang L, Jin JY, Jolly S, Zang Y, Wu H, et al. IDO immune status after chemoradiation may predict survival in lung cancer patients. *Cancer Res.* (2018) 78:809–16. doi: 10.1158/0008-5472.CAN-17-2995
68. Metz R, Rust S, Duhadaway JB, Mautino MR, Munn DH, Vahanian NN, et al. IDO inhibits a tryptophan sufficiency signal that stimulates mTOR: a novel IDO effector pathway targeted by D-1-methyl-tryptophan. *Oncoimmunology* (2012) 1:1460–8. doi: 10.4161/onci.21716
69. Chuang HC, Lan JL, Chen DY, Yang CY, Chen YM, Li JP, et al. The kinase GLK controls autoimmunity and NF-kappaB signaling by activating the kinase PKC-theta in T cells. *Nat Immunol.* (2011) 12:1113–8. doi: 10.1038/ni.2121
70. Thomas S, Izard J, Walsh E, Batich K, Chongsathidkiet P, Clarke G, et al. The host microbiome regulates and maintains human health: a primer and perspective for non-microbiologists. *Cancer Res.* (2017) 77:1783–812. doi: 10.1158/0008-5472.CAN-16-2929
71. Mautino MR, Kumar S, Zhuang H, Waldo J, Jaipuri F, Potturi H, et al. a novel prodrug of indoximod with enhanced pharmacokinetic properties. *Cancer Res.* (2017) 77:4076. doi: 10.1158/1538-7445.AM2017-4076
72. Muller A, Manfredi M, Zakharia Y, Prendergast GC. Inhibiting IDO pathways to treat cancer: lessons from the ECHO-301 trial and beyond. *Semin Immunopathol.* (in press).
73. Fu T, He Q, Sharma P. The ICOS/ICOSL pathway is required for optimal antitumor responses mediated by anti-CTLA-4 therapy. *Cancer Res.* (2011) 71:5445–54. doi: 10.1158/0008-5472.CAN-11-1138
74. Merlo LM, Pigott E, Duhadaway JB, Grabler S, Metz R, Prendergast GC, et al. IDO2 Is a critical mediator of autoantibody production and inflammatory pathogenesis in a mouse model of autoimmune arthritis. *J Immunol.* (2014) 92:2082–90. doi: 10.4049/jimmunol.1303012
75. Merlo LM, Duhadaway JB, Grabler S, Prendergast GC, Muller AJ, Mandik-Nayak L. IDO2 modulates T Cell-dependent autoimmune responses through a B Cell-intrinsic mechanism. *J Immunol.* (2016) 196:4487–97. doi: 10.4049/jimmunol.1600141
76. Metz R, Duhadaway JB, Kamasani U, Laury-Kleintop L, Muller AJ, Prendergast GC. Novel tryptophan catabolic enzyme IDO2 is the preferred biochemical target of the antitumor indoleamine 2,3-dioxygenase inhibitory compound D-1-methyl-tryptophan. *Cancer Res.* (2007) 67:7082–7. doi: 10.1158/0008-5472.CAN-07-1872
77. Lob S, Konigsrainer A, Zieker D, Brucher BL, Rammensee HG, Opelz G, et al. IDO1 and IDO2 are expressed in human tumors: levo- but not dextro-1-methyl tryptophan inhibits tryptophan catabolism. *Cancer Immunol Immunother.* (2009) 58:153–7. doi: 10.1007/s00262-008-0513-6
78. Qian F, Liao J, Villella J, Edwards R, Kalinski P, Lele S, et al. Effects of 1-methyltryptophan stereoisomers on IDO2 enzyme activity and IDO2-mediated arrest of human T cell proliferation. *Cancer Immunol Immunother.* (2012) 61:2013–20. doi: 10.1007/s00262-012-1265-x
79. Opitz CA, Litzenburger UM, Opitz U, Sahm F, Ochs K, Lutz C, et al. The indoleamine-2,3-dioxygenase (IDO) inhibitor 1-methyl-D-tryptophan upregulates IDO1 in human cancer cells. *PLoS ONE* (2011) 6:e19823. doi: 10.1371/journal.pone.0019823
80. Brincks EL, Adams J, Essmann M, Turner BA, Wang L, Ke J, et al. Indoximod modulates AhR-driven transcription of genes that control immune function. *Cancer Res.* (2018) 78. doi: 10.1158/1538-7445.AM2018-3753
81. Opitz CA, Litzenburger UM, Sahm F, Ott M, Tritschler I, Trump S, et al. An endogenous tumour-promoting ligand of the human aryl hydrocarbon receptor. *Nature* (2011) 478:197–203. doi: 10.1038/nature10491
82. Litzenburger UM, Opitz CA, Sahm F, Rauschenbach KJ, Trump S, Winter M, et al. Constitutive IDO expression in human cancer is sustained by an autocrine signaling loop involving IL-6, STAT3 and the AHR. *Oncotarget* (2014) 5:1038–51. doi: 10.18632/oncotarget.1637
83. Zhou L. AHR Function in Lymphocytes: emerging Concepts. *Trends Immunol.* (2016) 37:17–31. doi: 10.1016/j.it.2015.11.007
84. Raberg L, Sim D, Read AF. Disentangling genetic variation for resistance and tolerance to infectious diseases in animals. *Science* (2007) 318:812–4. doi: 10.1126/science.1148526
85. Zelante T, Iannitti RG, Fallarino F, Gargaro M, De Luca A, Moretti S, et al. Tryptophan Feeding of the IDO1-AhR Axis in Host-Microbial Symbiosis. *Front Immunol.* (2014) 5:640. doi: 10.3389/fimmu.2014.00640
86. Sivan A, Corrales L, Hubert N, Williams JB, Aquino-Michaels K, Earley ZM, et al. Commensal Bifidobacterium promotes antitumor immunity and facilitates anti-PD-L1 efficacy. *Science* (2015) 350:1084–9. doi: 10.1126/science.aac4255
87. Vetizou M, Pitt JM, Daillere R, Lepage P, Waldschmitt N, Flament C, et al. Anticancer immunotherapy by CTLA-4 blockade relies on the gut microbiota. *Science* (2015) 350:1079–84. doi: 10.1126/science.aad1329
88. Gopalakrishnan V, Spencer CN, Nezi L, Reuben A, Andrews MC, Karpinets TV, et al. Gut microbiome modulates response to anti-PD-1 immunotherapy in melanoma patients. *Science* (2018) 359:97–103. doi: 10.1126/science.aan4236
89. Matson V, Fessler J, Bao R, Chongsuwat T, Zha Y, Alegre ML, et al. The commensal microbiome is associated with anti-PD-1 efficacy in metastatic melanoma patients. *Science* (2018) 359:104–8. doi: 10.1126/science.aao3290
90. Routy B, Le Chatelier E, Derosa L, Duong CPM, Alou MT, Daillere R, et al. Gut microbiome influences efficacy of PD-1-based immunotherapy against epithelial tumors. *Science* (2018) 359:91–7. doi: 10.1126/science.aan3706
91. Bessede A, Gargaro M, Pallotta MT, Matino D, Servillo G, Brunacci C, et al. Aryl hydrocarbon receptor control of a disease tolerance defence pathway. *Nature* (2014) 511:184–90. doi: 10.1038/nature13323
92. Rhee SJ, Walker WA, Cherayil BJ. Developmentally regulated intestinal expression of IFN-gamma and its target genes and the age-specific response to enteric Salmonella infection. *J Immunol.* (2005) 175:1127–36. doi: 10.4049/jimmunol.175.2.1127
93. Kugel CH III, Douglass SM, Webster MR, Kaur A, Liu Q, Yin X, et al. Age correlates with response to Anti-PD1, reflecting age-related differences in intratumoral effector and Regulatory T-Cell populations. *Clin Cancer Res.* (in press). doi: 10.1158/1078-0432.CCR-18-1116
94. Harrington L, Srikanth CV, Antony R, Rhee SJ, Mellor AL, Shi HN, et al. Deficiency of indoleamine 2,3-dioxygenase enhances commensal-induced antibody responses and protects against Citrobacter rodentium-induced colitis. *Infect Immun.* (2008) 76:3045–53. doi: 10.1128/IAI.00193-08
95. Zhao L, Suolang Y, Zhou D, Tang Y, Zhang Y. Bifidobacteria alleviate experimentally induced colitis by upregulating indoleamine

2, 3-dioxygenase expression. *Microbiol Immunol.* (2018) 62:71–9. doi: 10.1111/1348-0421.12562
96. Prendergast GC, Metz R, Muller AJ, Merlo LM, Mandik-Nayak L. IDO2 in immunomodulation and autoimmune disease. *Front Immunol.* (2014) 5:585. doi: 10.3389/fimmu.2014.00585
97. Salazar A, Gonzalez-Rivera BL, Redus L, Parrott JM, O'connor JC. Indoleamine 2,3-dioxygenase mediates anhedonia and anxiety-like behaviors caused by peripheral lipopolysaccharide immune challenge. *Horm Behav.* (2012) 62:202–9. doi: 10.1016/j.yhbeh.2012.03.010
98. Liu YN, Peng YL, Liu L, Wu TY, Zhang Y, Lian YJ, et al. TNFalpha mediates stress-induced depression by upregulating indoleamine 2,3-dioxygenase in a mouse model of unpredictable chronic mild stress. *Eur Cytokine Netw.* (2015) 26:15–25. doi: 10.1684/ecn.2015.0362
99. Huang L, Ou R, Rabelo De Souza G, Cunha TM, Lemos H, Mohamed E, et al. Virus Infections Incite Pain Hypersensitivity by Inducing Indoleamine 2,3 Dioxygenase. *PLoS Pathog.* (2016) 12:e1005615. doi: 10.1371/journal.ppat.1005615
100. Barreto FS, Chaves Filho AJM, De Araujo M, De Moraes MO, De Moraes MEA, Maes M, et al. Tryptophan catabolites along the indoleamine 2,3-dioxygenase pathway as a biological link between depression and cancer. *Behav Pharmacol.* (2018) 29:165–80. doi: 10.1097/FBP.0000000000000384

Conflict of Interest Statement: GP and AM disclose equity ownership in NewLink Genetics reflecting inventorship of licensed IDO intellectual property including indoximod and its uses in cancer treatment from the Lankenau Institute of Medical Research, as described in U.S. Patents Nos. 7705022, 7714139, 8008281, 8058416, 8383613, 8389568, 8436151, 8476454, and 8586636. GP additionally discloses equity ownership in Incyte and Merck; former and present advisory board roles for NewLink Genetics and Kyn Therapeutics, respectively; and a board director role for Meditope Biosciences. AM additionally discloses roles as an advisory board member and grant recipient for I-O Biotech AG, which is developing IDO vaccines for cancer treatment. YZ discloses research and travel support from NewLink Genetics and advisory board roles for Amgen, Roche Diagnostics, Novartis, Eisai, Castle Bioscience and Exelixis.

The remaining authors declare that the research was conducted in the absence of any commercial or financial relationships that could be construed as a potential conflict of interest.

frontiers in Oncology

REVIEW
published: 10 September 2018
doi: 10.3389/fonc.2018.00357

Transforming Growth Factor-β-Induced Cell Plasticity in Liver Fibrosis and Hepatocarcinogenesis

Isabel Fabregat[1,2,3]* *and Daniel Caballero-Díaz*[1,3]*

[1] TGF-β and Cancer Group, Oncobell Program, Bellvitge Biomedical Research Institute, Barcelona, Spain, [2] Department of Physiological Sciences, School of Medicine, University of Barcelona, Barcelona, Spain, [3] Oncology Program, CIBEREHD, National Biomedical Research Institute on Liver and Gastrointestinal Diseases, Instituto de Salud Carlos III, Barcelona, Spain

The Transforming Growth Factor-beta (TGF-β) family plays relevant roles in the regulation of different cellular processes that are essential for tissue and organ homeostasis. In the case of the liver, TGF-β signaling participates in different stages of disease progression, from initial liver injury toward fibrosis, cirrhosis and cancer. When a chronic injury takes place, mobilization of lymphocytes and other inflammatory cells occur, thus setting the stage for persistence of an inflammatory response. Macrophages produce profibrotic mediators, among them, TGF-β, which is responsible for activation -transdifferentiation- of quiescent hepatic stellate cells (HSC) to a myofibroblast (MFB) phenotype. MFBs are the principal source of extracellular matrix protein (ECM) accumulation and prominent mediators of fibrogenesis. TGF-β also mediates an epithelial-mesenchymal transition (EMT) process in hepatocytes that may contribute, directly or indirectly, to increase the MFB population. In hepatocarcinogenesis, TGF-β plays a dual role, behaving as a suppressor factor at early stages, but contributing to later tumor progression, once cells escape from its cytostatic effects. As part of its potential pro-tumorigenic actions, TGF-β induces EMT in liver tumor cells, which increases its pro-migratory and invasive potential. In parallel, TGF-β also induces changes in tumor cell plasticity, conferring properties of a migratory tumor initiating cell (TIC). The main aim of this review is to shed light about the pleiotropic actions of TGF-β that explain its effects on the different liver cell populations. The cross-talk with other signaling pathways that contribute to TGF-β effects, in particular the Epidermal Growth Factor Receptor (EGFR), will be presented. Finally, we will discuss the rationale for targeting the TGF-β pathway in liver pathologies.

Keywords: TGF-β, plasticity, liver, cancer biology, fibrosis, HCC, EMT, hepatic stellate cell

OPEN ACCESS

Edited by:
Ubaldo Emilio Martinez-Outschoorn, Thomas Jefferson University, United States

Reviewed by:
Przemyslaw Blyszczuk, Universität Zürich, Switzerland
Anna Laurenzana, Università degli Studi di Firenze, Italy

***Correspondence:**
Isabel Fabregat
ifabregat@idibell.cat
Daniel Caballero-Díaz
dcaballero@idibell.cat

Specialty section:
This article was submitted to Molecular and Cellular Oncology, a section of the journal Frontiers in Oncology

Received: *22 June 2018*
Accepted: *13 August 2018*
Published: *10 September 2018*

Citation:
Fabregat I and Caballero-Díaz D (2018) Transforming Growth Factor-β-Induced Cell Plasticity in Liver Fibrosis and Hepatocarcinogenesis. Front. Oncol. 8:357. doi: 10.3389/fonc.2018.00357

INTRODUCTION

The liver shows an unique regenerative response to injuries produced by physical or toxic treatments, which induce tissue damage (1–3). Liver injuries can be classify depending on their persistence or duration and can develop acute and chronic liver diseases. Acute liver injuries can be completely restored, without any evidence of the injury, only withdrawing the damaging agent in a short period of time. In these cases, the liver architecture and function remain stable. However,

long-time exposure with the damaging agent generates progressive liver damage, parenchyma alterations and vascular architectural distortion, which eventually results in liver fibrosis, cirrhosis, and ultimately, hepatocellular carcinoma (HCC), which is the end-stage of most chronic liver diseases (4, 5).

Chronic liver diseases are characterized by a parenchyma damage with a continued wound healing response, tissue remodeling, inflammatory environment and an altered molecular signaling pathways. Strong evidences point out the relevant role of the Transforming Growth Factor beta (TGF-β) signaling during all phases of the development of liver fibrosis and hepatocarcinogenesis. Perturbation of signaling by TGF-β family members is often seen in different diseases, including malignancies, inflammatory and fibrotic conditions (6). Under physiological conditions, TGF-β has a cytostatic and pro-apoptotic role in adult hepatocytes, which is critical for the control of liver mass. Loss of these functions may result in hyperproliferative disorders and cancer (7–9). Indeed, in early-stage carcinomas, TGF-β exerts tumor-suppressing activities, inducing cell cycle arrest and apoptosis. However, in late-stage carcinomas, once cells acquire resistance to its suppressive effects, TGF-β actions switch to pro-oncogenic, conferring cell survival, inducing cell migration and invasion, mediating immune alterations and microenvironment modifications (10, 11).

Recent evidences suggest that many of the pathological TGF-β effects could be related with its capacity to regulate cell plasticity, contributing to modifications in the phenotype of different liver cell populations. Cell plasticity refers to the interconversion of different stem cell pools, activation of facultative stem cells, and dedifferentiation, transdifferentiation or phenotypic transition of differentiated cells within a tissue (12) and is related with the ability of cells to reversibly change their phenotype and to take on characteristics of other cell types (13). The most studied and classic event related with cell plasticity is the epithelial-mesenchymal transition (EMT) and the opposite mesenchymal-epithelial transition (MET) (14). After specific stimuli, the cells suffer genetic and epigenetic changes, as well as cytoskeleton remodeling, which alter their phenotype and functions. TGF-β induces EMT in hepatocytes (15) and it is responsible for activation of hepatic stellate cells (HSC) to myofibroblasts (MFB) (16), both effects contributing to liver fibrosis. Moreover, during hepatocarcinogenesis TGF-β could also mediate an EMT process in liver tumor cells. This review will update recent evidences indicating the relevance of TGF-β signaling pathway in the regulation of the cell plasticity during the progression and pathogenesis of liver chronic diseases, as well as the molecular mechanisms involved. Finally, we will discuss the rationale for targeting the TGF-β pathway in liver pathologies.

TGF-β SIGNALING PATHWAYS

In humans, the pleiotropic TGF-β cytokine superfamily includes different members, such as bone morphogenetic proteins (BMPs), growth and differentiation factors (GDFs) and TGF-β isoforms (TGF-β1, TGF-β2, and TGF-β3). TGF-β signaling pathways regulates different cellular processes playing essential roles in proliferation, migration, differentiation, or cell death. These processes are essential for the homeostasis of tissues and organs and TGF-β signaling deregulation contributes to human disease. TGF-β1 (TGF-β from now on) has essential roles in liver physiology and pathology and contribute to all stages of disease progression: from liver injury through inflammation, fibrosis, cirrhosis and HCC (7, 8).

Most of the functions of the cells involved in the fibrotic tissue and in the tumor microenvironment are under the control of TGF-β: promotes MFB differentiation, the recruitment of immune cells, affects epithelial and endothelial cell differentiation and inhibits the anti-tumor immune responses (17, 18). Besides TGF-β responses could be different depending on the cell type, its receptors are expressed on most of the cells and its signaling pathway is very similar in all of them (6). All TGF-β isoforms are synthesized within the cell as pro-peptide precursors containing a pro-domain, named Latency-Associated peptide (LAP), and the mature domain. This latent form is secreted to the extracellular matrix (ECM) and stored as a fast and available pool of TGF-β, without *a novo* synthesis (19). By different mechanisms, TGF-β is cleaved and the bioactive form signals via binding to its specific kinase receptor at the cell surface of target cells. Stored TGF-β could be activated by the cell contractile force, which is transmitted by integrins (20, 21). Specific integrins and matrix protein interactions could be required for activation of the latent form of TGF-β. Integrins αv are the major regulators of the local activation of latent TGF-β and in this activation it is required the RGD (Arg-Gly-Asp) sequence (21). Integrin αv deletion in HSC protected mice from CCl_4-induced hepatic fibrosis (22). A recent review summarized the crosstalk between TGF-β and tissue extracellular matrix components (23).

TGF-β binds to its receptors triggering the formation of a heterotetrameric complex of type I and type II serine/threonine kinase receptors, in which the constitutively active type II receptor phosphorylates and activates the type I receptor. There are several types of both type I and type II receptors, but TGF-β preferentially signals through activin receptor-like kinase 5 (ALK5) type I receptor (TβRI) and the TGF-β type II receptor (TβRII). In addition, endoglin and betaglican (TβRIII), also called accessory receptors, bind TGF-β with low affinity and present it to the TβRI and TβRII. Activated receptor complexes mediate canonical TGF-β signaling through phosphorylation of the Receptor Associated SMADs (R-SMADs) at their carboxy-terminal. Humans express eight SMAD proteins that can be classified into three groups: R-SMADs, Cooperating SMADs (Co-SMADs) and Inhibitory SMADs (I-SMADs: SMAD6 and SMAD7). Among the R-SMADs, SMAD2 and 3 mediate the TGF-β1 branch of signaling (6, 8). After phosphorylation, R-SMADs form a trimeric complex with SMAD4, which translocates to the nucleus and associates with other transcription factors in order to regulate gene expression (7, 8). In addition to the canonical SMAD pathway, TGF-β is able to use non-SMAD effectors to mediate some of its biological responses, including non-receptor tyrosine kinases proteins such as Src and FAK, mediators of cell survival (e.g., NF-kB, PI3K/Akt pathways), MAPK (ERK1/2, p38 MAPK, and JNK among others), and Rho

GTPases like Ras, RhoA, Cdc42, and Rac1. Interestingly, these pathways can also regulate the canonical SMAD pathway and are involved in TGF-β-mediated biological responses (**Figure 1**) (8, 24–26).

LIVER FIBROSIS

Liver fibrosis is a common pathological chronic liver disease, consequence of a continued injury with a huge accumulation of extracellular matrix proteins, mainly enriched in fibrillar collagens, due to a multiple reparative and regenerative processes (5, 27, 28). After liver damage, reparative mechanisms are triggered to replace necrotic and apoptotic hepatocytes, generating wound healing and inflammatory responses that are essential for liver regeneration (5). However, if the damage persists over a long time, the excessive accumulation of extracellular matrix proteins (collagens I, II, and III, undulin, fibronectin, laminin, elastin, proteoglycans and hyaluronan) could replace parenchymal areas leading fibrosis to a cirrhotic state. In advanced stages, it develops an abnormal liver architecture, altered vascularization and fibrotic septa surroundings with regenerative nodules. Liver systemic failure, portal hypertension, high susceptibility to infection and high risk to develop HCC are the main clinical consequences of cirrhosis (28, 29). Interestingly, multiple clinical reports have reported that liver insult eradication can regret liver fibrosis in huge number of patients, mostly during the first stages (29–32). In the development of liver fibrosis, TGF-β plays crucial roles regulating the different stages of the disease, among them, the control of cell plasticity of different liver cell populations, which is summarize in the **Figure 2** and we detail in the next chapters.

TGF-β REGULATES MACROPHAGE PLASTICITY DURING LIVER FIBROSIS

Inflammation plays a key role in liver fibrosis development. After injury takes place, infiltration of immune system cells -macrophages, lymphocytes, eosinophils, and plasma cells- arises to the damaged place. Lymphocytes produce cytokines

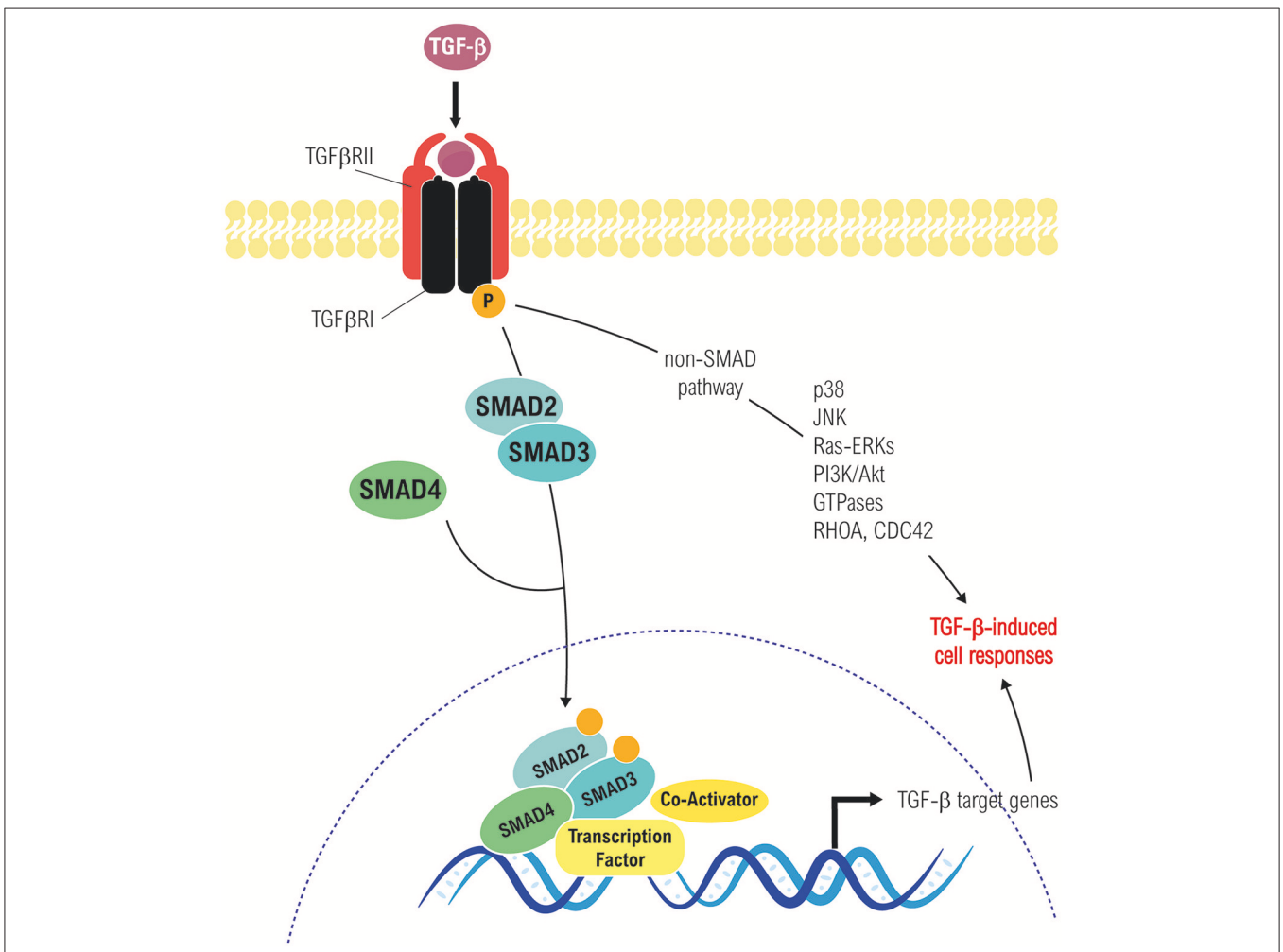

FIGURE 1 | Canonical (Smad-dependent) and non-canonical (Smad-independent) TGF-β signaling pathways. Both converge in transcriptional-dependent and independent effects on cell proliferation, differentiation, apoptosis/survival, migration, etc., in a cell and context-dependent manner.

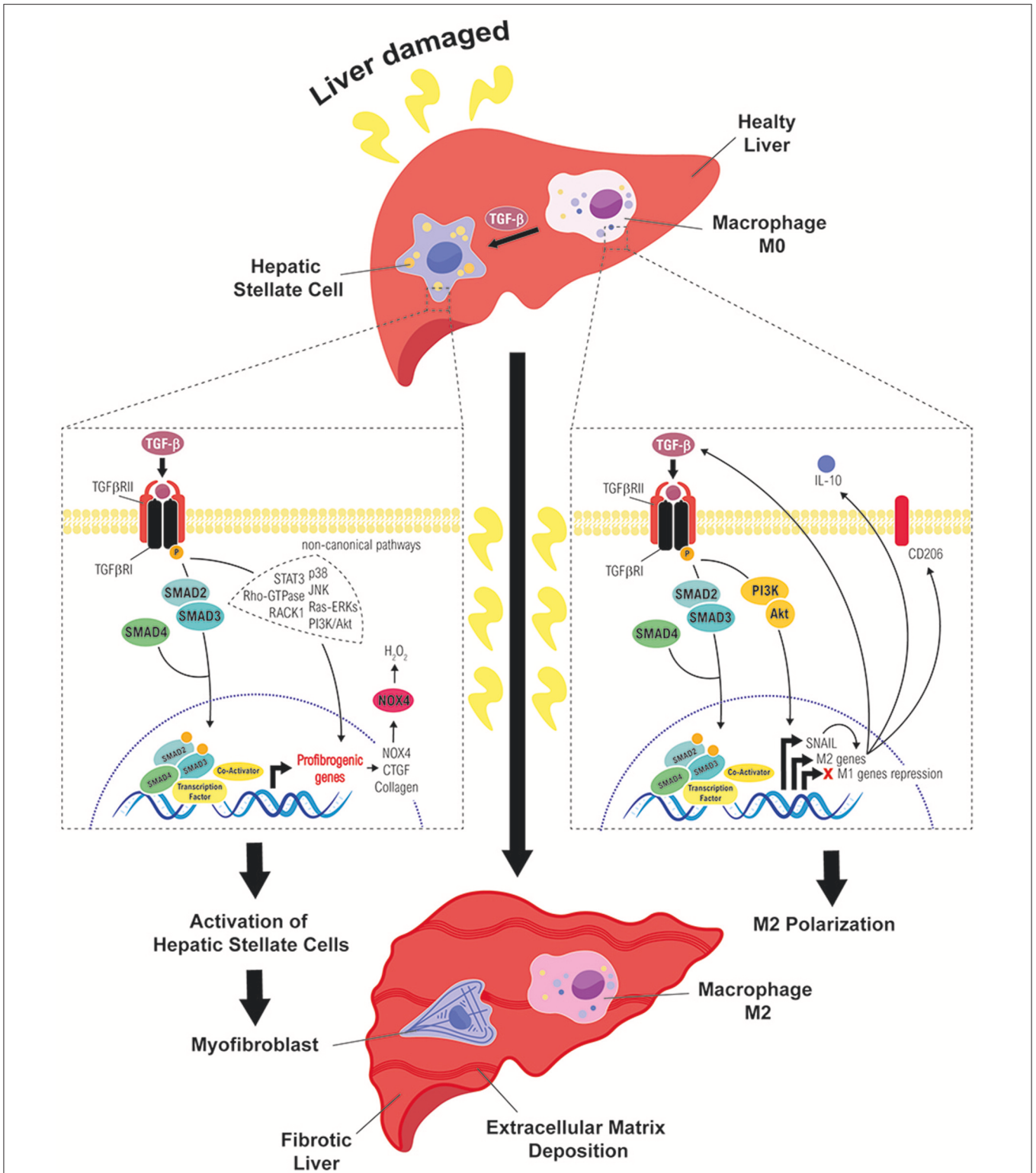

FIGURE 2 | Role of TGF-β in the cell plasticity of hepatic stellate cells and macrophages during liver fibrosis. Different routes followed by TGF-β signals to mediate activation of HSC into MFB (left) or polarization of macrophages to a M2 state (right), which contribute to sustain a fibrotic and immunosuppressive environment, favorable to the initiation of a hepatocarcinogenic process.

and chemokines, which activate macrophages. Activated macrophages stimulate inflammatory cells such as lymphocyte, among others, over-activating and maintaining the inflammatory environment (33). During fibrosis, macrophages produce pro-fibrotic factors such as TGF-β and platelet derived growth factor (PDGF), control ECM turnover by regulating the balance of various matrix metalloproteases and tissue inhibitors of metalloproteinases (TIMPs) (27, 34, 35) and are found very close to collagen-producing MFB (36–38) suggesting the macrophages relevance in the activation of MFB. In this sense, hepatic macrophages have been described as a potential targets against fibrosis (39, 40).

Macrophages represent a heterogeneous cell population with a huge cell plasticity, where diverse microenvironment stimuli polarize them into different phenotypes (41). There are mainly two sources of hepatic macrophages: liver resident macrophages, also called Kupffer cells (42), and circulating monocytes (inflammatory recruited macrophages) (43). Besides the origin, both could play significant roles in the development of fibrosis. *In vitro* and *in vivo* studies described that both Kupffer cells and monocyte-derived macrophages can activate HSC and induce their transdifferentiation by paracrine mechanisms, including TGF-β (44–47). Resident hepatic macrophages secrete the chemokine CCL2 (a potent chemoattractant) in order to recruit monocytes which could increase and promote fibrosis. Although, it was described that the pro-fibrotic functions of these resident macrophages remain functional even when recruited macrophages are pharmacologically inhibited using CCL2 antagonists (48). Transgenic rats that express a mutated form of the CCL2 (acting as a negative-mutant), and tail vein injection of adenovirus that overexpress a truncated form of TGF-β receptor II (acting as a negative-receptor mutant) attenuate liver fibrosis in a DEN-induced fibrosis model in rats (49), suggesting the relevance of inflammation and TGF-β pathway during this disease.

In the early stages, activated macrophages secrete pro-inflammatory cytokines and produce reactive oxygen species (ROS), while in late stages macrophages have been associated with release of anti-inflammatory factors, attenuating inflammation and promoting tissue regeneration (43, 50). Macrophages are classify into M1, also known as classical or pro-inflammatory; and M2, also known as alternative or anti-inflammatory macrophages (51, 52). It is not easy to strictly separate both liver macrophage populations, since they could show common gene expression, and even more M2 macrophages are classify also in different subclasses. For that reason, it has been proposed that could be more adequate to separate them according to their functions: defensive, restorative and regulatory macrophages (53). In the classical classification, M1 macrophages are associated with inflammatory diseases due to microbicidal activity (through their capacity to produce ROS and their phagocytic functions), antigen presentation and antitumor activity. M1 macrophages prevail during the onset of injury (54) and are related with the release of metalloproteinases that degrade ECM and promote EMT/Endothelial-to-mesenchymal transition (EndMT). On the other hand, M2 macrophages secrete anti-inflammatory factors such as IL-10, arginase, TGF-β, and HO-1. Their polarization is promoted by IL-4 and IL-13, and are characterized for the expression of Arg1, Ym1, and Fizz, secretion of angiogenic factors such as IL-8, VEGF, and EGF4 and increased mannose receptor (CD206), with lower ROS production (47, 50). M2 macrophages stimulate an anti-inflammatory environment and promote regeneration and wound healing. However, if injury becomes chronic, M2 macrophages take up a pro-fibrotic role secreting pro-fibrotic factors such as TGF-β, PDGF, among others (47).

Nowadays it is clear that macrophages are essential players in the regulation of liver fibrosis and they are an important source of TGF-β but, could this cytokine regulate the phenotype between M1 and M2 macrophages and their functions? Recent data described that TGF-β could induce M2-like macrophage polarization via SNAIL (55). SNAIL-overexpression in human THP-1 macrophages promotes M2 markers (such as CD206), induces the expression of the anti-inflammatory IL-10 and inhibits pro-inflammatory M1-related cytokines (TNF-α and IL-12). By contrast, SNAIL knockdown by siRNA technology abolishes TGF-β-M2-induced phenotype and partly restores M1 polarization through up-regulation of pro-inflammatory cytokines. The canonical SMAD2/3 and the non-canonical PI3K/AKT signaling pathways are crucial for TGF-β-induced SNAIL overexpression in THP-1 cells. The blockade of TGF-β/SNAIL signaling restores the production of pro-inflammatory cytokines. Likewise, TGF-β also stimulates murine BMDM macrophages to display an M2-like phenotype characterized by high levels of IL-10 and low levels of IL-12p70, and M1-specific markers. Macrophages isolated from fibrotic mouse livers show higher balance of M2/M1 macrophages in comparison to control mice (56). In other fibrotic animal models, such as lung fibrosis, TGF-β could modulate M2 responses (57); and in kidney, TGF-β/Smad3-dependt pathway could transdifferentiate M2-macrophages to myofibroblast favoring kidney fibrosis (58). Moreover, TβRII–/– mice show a defective polarization to M2-macrophages (59). Fibrosis-induced model in rats by thioacetamide show that both M1 and M2-macrophagues polarizations occur during development of the disease (60). Overall results show up that M2-activation/polarization has a relevant role in the development of fibrosis in mice and patients with liver fibrosis (61). However, due to the heterogenicity and higher plasticity of macrophages and the complexity of their study *in vivo* models in liver, further works are needed in order to clarify the molecular mechanisms whereby TGF-β pathway promote the polarization and the pro-fibrotic functions of macrophages *in vivo* models. Current data seems to indicate that both hepatic and recruited macrophages play relevant roles in the progression and reversion of liver fibrosis. Targeting both and the reorientation of their phenotypes are arising as attractive therapies (62).

TGF-β REGULATES LIVER EPITHELIAL CELLS PLASTICITY DURING LIVER FIBROSIS

"Activated" fibroblast or MFB are the main producing cells of fibrogenesis mediators and ECM components, participating actively in their accumulation (63). In the liver, the most

fibrogenic MFB are endogenous and their origin is controversial and still unclear, but nowadays there are accepted different sources (63–65), among them, portal and resident fibroblasts (66), activation and differentiation of HSC (more details in the next section) (16, 67), bone marrow-derived fibrocytes (68), liver epithelial cells (hepatocytes and cholangiocytes) that undergo EMT (69–71), endothelial cells that undergo EndMT (66, 72), vascular smooth muscle cells and pericytes (73).

EMT-clear example of cellular plasticity- is a process that drives a de-differentiation of epithelial cells to a mesenchymal-like phenotype increasing their migratory and invasive properties (13, 14, 74, 75). The reverse process is called as MET and allows cells to differentiate into different organs and tissues. In a tumorigenic context, mesenchymal migratory tumor cells undergo MET to metastasize (76). The EMT process includes loss of epithelial genes, such as E-cadherin and cytokeratins (8, 18 and 19), and up-regulation of mesenchymal genes, such as N-cadherin, alfa-Smooth Muscle Actin (α-SMA, *ACTA2* gene) which correlate with the expression of EMT transcription factors (EMT-TFs) Snail (*SNA1* gene), Slug (*SNA2* gene), Twist and ZEB (74, 75). Intermediates states are also found between EMT and MET (77). Partial EMT is described for cells that co-express both epithelial and mesenchymal markers. Even more, EMT is classified into different subclasses related with the biological context (78): Type 1 EMT is involved in development stages; type 2 EMT concerns regenerative process and organ fibrosis; and type 3 EMT is related with metastatic process.

During liver fibrosis, type 2 EMT plays a relevant role in the appearance of a pro-fibrotic fibroblast phenotype. Bipotent adult hepatic progenitor cells, which possess the cell plasticity to differentiate into hepatocytes and cholangiocytes after different stimuli (79), are able to undergo EMT in response to liver injury during cholestatic liver fibrosis. Hepatocyte plasticity could play relevant roles during the progression of chronic liver diseases. Mouse hepatocytes that survive to the apoptotic effects of TGF-β, could regulate -in a TGF-β dependent manner- the expression of fibrosis-related genes, such as Connective Tissue Growth Factor (*CTGF*) or fibronectin, and EMT-related genes, such as Snail, and β-catenin (15, 71, 80), with downregulation of epithelial markers (81). Even more, primary adult hepatocytes could transdifferentiate to a more fibroblastic-like phenotype with loss of cell–cell contacts and polarity, after TGF-β treatment (80). Indeed, hepatocyte-derived fibroblasts are an additional and significant lineage of mesenchymal cells that contribute to progression of liver fibrosis. Zeisberg and collaborators elegantly demonstrate that adult hepatocytes can undergo an EMT process after TGF-β stimuli, contributing to the *in vivo* pool of fibroblast during liver fibrosis (82). The role of hepatocytes during liver fibrosis *in vivo* related with TGF-β was also previously described in a transgenic animal model which overexpress SMAD7 (inhibitor of the pathway) specifically in hepatocytes. These transgenic animals have attenuated the TGF-β signaling and EMT, with less ECM depositions and improved CCl_4-dependent liver damage and fibrosis (83). Bone morphogenetic protein-7 (BMP-7), a member of the TGF-β family which plays opposite roles to TGF-β, induces MET. Primary rat hepatocytes treated with TGF-β upregulate the expression levels of fibrotic markers, whereas BMP-7 treatment upregulated E-cadherin and decreases SMAD2/3 phosphorylation levels. Even more, in CCl_4-treated rats treated with TGF-β, which show advanced fibrosis with higher expression of α-SMA and lower E-cadherin, the fibrotic situation was rescued after BMP-7 treatment (84). Moreover, cholangiocytes -another epithelial cell population- activate, proliferate and change into a more fibroblastic phenotype, increasing the expression of pro-fibrotic cytokines and factors such as TGF-β, PDGF and CTGF (85). These results open new ideas about how epithelial liver cells, through an EMT process, could generate mesenchymal/fibroblastic cells, which could be relevant in the progression of the fibrotic diseases.

RELEVANCE OF TGF-β AND HSC DIFFERENTIATION DURING LIVER FIBROGENESIS

In the normal liver, HSC (around 5–8% of the cells in the liver) are in a quiescent phenotype hosted in the space of Disse between hepatic epithelial and the sinusoidal endothelial cells (86). HSC are characterized by the store of vitamin A, lipid droplets and the expression of a large number of adipogenic genes and neural markers. After liver insults, different paracrine and autocrine signals are triggered promoting the HSC activation -transdifferentiation- from a quiescent state to an activated myofibroblastic phenotype. MFB are characterized by the expression of α-SMA, loss of retinoids and lipid droplets and *de novo* expression of receptors for mitogenic, fibrogenic and chemotactic factors, leading an increase in proliferation and survival, enhanced synthesis of matrix proteins (predominantly fibrillar collagens) and inhibitors of matrix degradation TIMPs, and secretion of pro-inflammatory cytokines and chemokines. This provokes the progressive scar formation and the development of liver fibrosis (29, 32).

HSC activation is one of the most important steps during liver fibrosis and is mediated by different signals, such as growth factors (PDGF and CTGF, among others), lipidic mediators, as well as ROS and cytokines produced by hepatocytes, cholangiocytes, endothelial cells, macrophages (Kupffer cells) and immune cells (67, 86). Among these cytokines, TGF-β plays a master role in the activation of the HSC to MFB (16). In fact, some of the previous factors stimulate the expression, production and activation of TGF-β, which at the end is responsible for the activation of HSC (87). Furthermore, MFB demonstrate a growth stimulatory effect in response to TGF-β (88), which also contributes to the maintenance of their myofibroblastic phenotype (89). SMAD3 has been identified as the main mediator of the TGF-β-induced fibrogenic transcriptional program, particularly the up-regulation of collagen expression (7, 8, 30, 31). HSC isolated from SMAD3 knock-out mice showed lower expression of *Collagen1A1* mRNA mediated by p38 MAPK (30). Interestingly, it has been proposed that TGF-β activates the p38 MAPK pathway, further leading to SMAD3 phosphorylation at the linker region in the cultured MFBs, which promoted hetero-complex formation and nuclear translocation of SMAD3 and

SMAD4 (31). These results would indicate that non-canonical activation of the SMAD3/SMAD4 transcriptional activity accounts for SMAD3-dependent extracellular matrix production in MFBs.

During liver fibrogenesis, activated HSC express CTGF, which acts downstream of TGF-β modulating the ECM production. *CTGF* mRNA expression is under the control of the canonical TGF-β/SMAD3 and non-canonical ERKs, JNK, p38, and STAT3 pathways (90, 91). Moreover, receptor for activated C-kinase 1 (RACK1), a scaffold protein involved in numerous cellular processes and signaling pathways, is another TGF-β downstream target involved in the HSC activation. RACK1 is able to induce pro-fibrogenic pathways in a TGF-β-dependent manner, contributing to differentiation, proliferation, and migration of HSC (92, 93). Indeed, in this migratory phenotype and in remodeling of the cytoskeleton in TGF-β-activated HSC is also involved the role of Rho guanosine triphosphatase (Rho GTPase) signaling (94). TGF-β also regulates the expression of TRPM7 (transient receptor potential melastatin 7) in a SMAD3-depend manner, which inhibition attenuates TGF-β-induced expression of MFB markers (95).

Mild to moderate liver fibrosis may be reversible. The reversion process is related with the elimination of the damaging stimuli. During liver fibrosis reversion, activated HSC (or myofibroblast) reverted to an inactivated phenotype. In this state, inactivated HSC decrease the expression of fibrogenic genes (including *COL1A1* and *ACTA2*) and up-regulate the expression of some quiescence-associated genes like *PPARγ* (96, 97). Furthermore, inactivating some of the TGF-β downstream signals, such as ROS production, allows the reversion of the myofibroblast phenotype (89).

ROLE OF ROS DURING HSC ACTIVATION BY TGF-β

Oxidative stress plays a relevant role in the sequence of events following TGF-β activation of HSC. Actually, antioxidants can inhibits HSC transdifferentiation into MFB (98, 99). In both normal physiological and pathological conditions, ROS are critical intermediates. Oxidative stress plays a role during both initial inflammatory phase and its progression to fibrosis (100). Oxidative stress markers have been detected in experimental liver fibrosis/cirrhosis animals and in the biopsy and serum samples from liver cirrhotic patients (101). It is well known that ROS may act upstream and downstream of the TGF-β pathway. Upstream, ROS, through LAP activation and subsequent TGF-β release, promote fibrosis activating latent TGF-β (102) and/or via matrix metalloproteinases activation (103). Indeed, LAP/TGF-β complex has been suggested to function as an oxidative stress sensor (104). Furthermore, in many cell types such as HSC and hepatocytes, ROS may up-regulate the expression and secretion of TGF-β in a positive feedback loop (105, 106). ROS may be generated in the liver by multiple sources, including the cytochrome p450 family members, peroxisomes, mitochondrial respiratory chain, xanthine oxidase, and nicotinamide adenine dinucleotide phosphate (NADPH) oxidases. Worthy to note, accumulating evidence indicates that NADPH oxidases (NOX)-mediated ROS have a critical role in HSC activation and hepatic fibrogenesis (101) mediating TGF-β actions.

NOX enzyme family generate ROS, either hydrogen peroxide or superoxide as the primary species, during oxygen catalytic metabolism for arrange of signaling functions and host defense. There are described seven NOX isoforms in mammalian cells (NOX1-5, DUOX1, and DUOX2). Liver cells (either parenchymal and non-parenchymal) express different members of the NOX family. Hepatocytes and HSC express NOX1, NOX2, NOX4, DUOX1, and DUOX2; endothelial cells express mainly NOX1, NOX2, and NOX4; and Kupffer cells express the phagocytic NOX2 (101, 107). NOXs proteins could be playing relevant roles during liver fibrosis development (101, 108). Both NOX1- and NOX2-deficient HSC had decreased ROS generation and failed to upregulate collagen and TGF-β in response to angiotensin II (109). Of relevance, NOXes mediate TGF-β activation of HSC to MFB process (89, 110). In different organs, such as heart, the main mediator for the activation of MFB is NOX4, downstream from TGF-β (111), lung (112) and kidney (113). In *in vivo* models of liver fibrosis, the levels of NOX4 are up-regulated, as well as in patients with chronic hepatitis C virus derived infection, increasing along the fibrosis degree. HSC respond to TGF-β inducing NOX4-derived ROS (105), which play a key role in hepatic MFB in both *in vivo* and *in vitro* (89, 114). In NOX4 knock-out animals and in NOX4 downregulated cells the TGF-β-transactivation of HSC is attenuated (89, 114), and even more, the myofibroblastic state could also be reversible (89). During liver fibrosis, NOX4 is required for both HSC activation and maintenance of the activated phenotype in MFB in a TGF-β-dependent manner and mediates the TGF-β pro-apoptotic response in hepatocytes, which might be relevant to blunt regeneration and create a pro-fibrogenic microenvironment. In this sense, apoptotic hepatocytes after liver injury generate apoptotic bodies which were described to promote HSC survival (115). HSC can engulf and clear apoptotic hepatocytes bodies inducing their activation in JAK1/STAT3-dependent pathway and a NOX-dependent PI3K/Akt/NF-κB induction pathway, concomitant with a production of ECM components (115). Recent evidences show up the dual role of NOX1/NOX4 pharmacological inhibitors in decreasing both the apparition of fibrogenic markers and hepatocyte apoptosis *in vivo* (114, 116), highlighting the relevance of NOX1 and NOX4 in liver fibrosis and opening new perspectives for its treatment. Actually, NOX1 and NOX4 signaling mediates hepatic fibrosis through activation of HSC (114, 117). Indeed, it was recently described that NOX4, downstream TGF-β, would play a role in the acquisition and maintenance of the MFB phenotype (89). Deficiency of NOX1 and NOX4 attenuates liver fibrosis in mice after CCl_4 treatment. Activated HSC and ROS generation are also attenuated in HSC lacking NOX1 and NOX4, suggesting NOX1 and NOX4 play important roles in liver fibrosis and injury through regulating inflammation, proliferation and fibrogenesis in HSC (117). Therefore, targeting NOX1/4 is emerging as a new and attractive therapy for liver fibrosis in order to impair the pathological effects of TGF-β over this disease.

HUMAN HEPATOCELLULAR CARCINOMA (HCC)

HCC is a major public health problem worldwide with almost 800,000 new cases each year and its incidence is increasing in Europe and worldwide. In 2015 reports from World Health Organization, liver cancer is the second leading cause of cancer-related deaths, following lung cancer (118). HCC is the most common primary liver malignancy in adults. Intriguingly, there are significant differences on the incidence when considering the gender, being the male to female ratio estimated to be 2.4. This difference is mainly attributed to the different exposition to risk factors, as well as the influence of androgens and oestrogens on HCC progression (119). Exposition to risk factors also determines the incidence of liver cancer regarding age or ethnicity and the highest incidence of HCC is found in Asia and sub-Saharian Africa (120–122). In most cases, HCC develops within an established background of chronic liver disease. Progressive hepatic fibrosis frequently evolves to cirrhosis, which is the largest risk factor for developing liver cancer. Up to 90% of cases of HCC arise in the setting of advanced fibrosis or cirrhosis regardless of etiology (121, 123–125).

During hepatocarcinogenesis, a complex multistep process, many signaling cascades are altered as a result of genetic and epigenetic changes that contribute to a heterogeneous molecular profile. Furthermore, cellular plasticity increases the complexity of the cellular heterogenicity. Indeed, tumor heterogeneity in HCC is impressive: it can be observed between patients, between nodules in the same patient (i.e., second primary tumors after curative treatment or synchronous multifocal tumors of different clonality) and even within a single tumor nodule (126). Many molecular mechanisms are known to be clearly involved in HCC (127). Signaling pathways are related mainly with cell proliferation, angiogenesis, invasion, and metastasis. IGF-1, Epidermal Growth Factor (EGF), PDGF, Hepatocyte Growth Factor (HGF), VEGF, as well as TGF-β, are the most frequent growth factors and cytokines involved in HCC development. (128). The role of the microenvironment in tumor initiation and progression in HCC is critical and HCC cells could acquire an abnormal phenotype due to tissue remodeling altering their biological behavior (129, 130).

ROLE OF TGF-β DURING HEPATOCARCINOGENESIS

As it was mentioned before, TGF-β signaling -in the liver- participates in all stages of disease progression, from initial liver injury through inflammation and fibrosis, to cirrhosis and cancer (7, 8). During early stages of tumorigenesis TGF-β acts as a tumor suppressor, while in late stages it acts with a pro-tumorigenic role, promoting invasiveness and metastasis once cells become resistant to its suppressor effects (8, 131). In non-transformed hepatocytes and HSC, the cytostatic effects of TGF-β are often dominant over the opposing mitogenic signals; however, carcinoma-derived cells are usually refractory to growth inhibition by this cytokine. Activation of the TGF-β pathway induces antiproliferative responses due to the regulation of the cell cycle at G1-S by inhibiting c-MYC and cyclin-dependent kinase complex (CDK)-1-6 and 7 and regulates cycling inhibitors such as p21 and p15 (132–134). Smad4 –/– mice could develop head and neck cancer demonstrating the role of the TGF-β pathway as cytostatic regulator (135). Other proteins involved in the regulation of the pathway, such as β-II spectrin, which plays a role as scaffold for SMAD3 and SMAD4 and their subsequent activation after TGF-β. *Sptbn2* heterozygote mutants develop HCC indicating that TGF-β signaling and β-II spectrin suppress hepatocarcinogenesis, potentially through cyclin D1 deregulation (136). TGF-β pathway also activates the NRF2 transcription factor which is involved in the expression of many cytoprotective genes which are relevant in the protection of the cells against toxic insults, and its depletion increases tumorigenic process (137). These data show up the relevance of the cytoprotective and suppressor role of TGF-β pathway, which could be altered during the carcinogenesis process. Malignant cells surpass the suppressive effects of TGF-β either through inactivation of core components of the pathway (such as TGF-β receptors and/or SMADs) or by downstream alterations repressing the tumor-suppressive arm. In late stages, liver cancer cells take advantages from the TGF-β-dependent pathways to acquire capabilities that contribute to tumor progression, such as production of autocrine mitogens, release of pro-metastatic cytokines and chemokines and up-regulation of receptors that mediate the response to them (10, 138–140). In this sense, different evidences suggest that TGF-β plays a dual role in hepatocarcinogenesis. On one side, as commented above, TGF-β inhibits proliferation and induces apoptosis in hepatocytes and liver tumor cells (141, 142), but simultaneously, it activates survival pathways, such as Akt, and induces an increase in the expression of anti-apoptotic BCL-2-related proteins (143–145), a process that is related to the capacity of TGF-β to transactivate c-Src and EGFR pathways, among others (146). Interestingly, the inhibition of the EGFR increases the apoptotic response to TGF-β (146, 147). In fact, in hepatocytes, TGF-β-induced apoptosis could be counteracted by EGF (an important survival signal) (141, 148) a process that requires activation of the PI3K/Akt axis to counteract TGF-β-induced upregulation of the NOX4, oxidative stress and mitochondrial-dependent apoptosis (149, 150). Another member of the NOX family, NOX1, is involved in this anti-apoptotic role. TGF-β-mediated activation of NOX1 promotes autocrine growth of liver tumor cells through the activation of the EGFR pathway, via upregulation of EGFR ligands expression through a c-Src (151) and NF-κB (152) dependent mechanism. The autocrine loop of EGFR activated by TGF-β in non-transformed hepatocytes and liver cancer cells requires the activity of the metalloprotease TACE/ADAM17 (142, 146) in a Caveolin-1/Src/NOX1 dependent manner (153, 154). This proliferation can be impaired by the addition of the NOX inhibitor VAS2870 (155). Moreover, TGF-β is able to mediate the production of EGFR ligands, which eventually confers resistance to its pro-apoptotic effects in hepatocytes (149, 152) and HCC cells (156). Importantly, the capacity of hepatocytes to survive to TGF-β is also dependent on their differentiation status (157). Thus, rat hepatoma cells respond to TGF-β inducing survival signals,

whereas adult hepatocytes do not (142). In the same way, different features of HCC cell lines, like the activation of the EGFR or MEK/ERK pathways, may provoke different outcomes after TGF-β exposure (156, 158).

Once cells overcome the cytostatic and apoptotic effects of TGF-β, this cytokine regulates cell plasticity, a fact that has been elegantly evidenced in a study by Coulouarn and col., where they proposed different liver TGF-β gene signatures, defining a cohort of genes related to its tumor suppressor capacity and another cohort of genes related with its tumor promoting effects: the early and the late TGF-β-signatures. The "early" TGF-β signature is associated to genes involved in growth inhibition and apoptosis, whereas the termed "late" TGF-β signature is associated to EMT, migration and invasion (159). Of relevance, this study also discriminated HCC cell lines by degree of invasiveness. Interestingly, the early response pattern is associated with longer, and the late response pattern with shorter, survival in human HCC patients. In addition, tumors expressing the late TGF-β-responsive genes displayed invasive phenotype, increased tumor recurrence and accurately predicted liver metastasis. In the development of liver hepatocarcinogenesis, TGF-β plays crucial roles regulating the different stages of the disease, some of these roles are summarize in the **Figure 3** and we detail in the next chapters.

TGF-β PROMOTES EMT IN HCC

Tumor cells that overcome the suppressor effects of TGF-β become ready to respond to this cytokine inducing other effects, such as EMT, processes that contribute to either fibrosis and/or tumor dissemination (160). Neoplastic transformation of hepatocytes and progenitor cells, which both are epithelial-like, to a mesenchymal-like phenotype boost heterogeneity in HCC (75).

TGF-β is one of the strongest inducers of EMT under both physiological and pathological context (161), regulating the expression and activity of EMT-TFs (14). Different *in vitro* studies support the idea that TGF-β induces EMT in non-tumorigenic epithelial cells, transforming them into a fibroblast-like phenotype. For example, alveolar epithelia cells via FoxM1/Snail1 can undergo EMT after TGF-β exposure (162, 163); mammary epithelial cells undergo EMT in a TGF-β/PI3K/mTOR pathway (164, 165). After liver insult, non-transformed hepatocytes can undergo EMT as an adaptative response to move and scape from damaged, inflammatory, hypoxic and redox-activated microenvironment allowing them to find better conditions (166). Moreover, TGF-β induces anti-apoptotic signals in transformed hepatocytes, through the activation of the EGFR pathway (143, 146), and liver cells that overcome TGF-β pro-apoptotic effects undergo EMT in a Snail1-dependent manner conferring resistance to apoptosis (15, 71, 142, 156). Besides apoptotic resistance, mesenchymal-like phenotype increases migratory properties in HCC cells through activation of the CXCR4/CXCL12 axis in TGF-β-dependent manner (139), a mechanism that would contribute to tumor progression in HCC patients (167). Interestingly, CXCR4 is localized in the migratory front of the tumors and is coincident with TGF-β signaling overactivation, suggesting this pathway as a future prognostic factor to predict patient response to TGF-β therapies. MicroRNAs (miRNA) are also involved in the regulation of EMT and in the progression and development of HCC. MiR-181, which is regulated by TGF-β, is overexpressed in HCC samples and is associated with and EMT phenotype (168–170). In hepatocytes, miR-181 induces an EMT-like response and mimics TGF-β-effects, upregulating MMP2, α-SMA and vimentin, downregulating E-cadherin and inducing morphological changes.

Upon HCC development, the excessive growth of transformed cells also generates hostile nodules for cancer cells due to oxygen depletion in internal areas (hypoxic environment) (171) as compared to tumor stroma borders, which induces tumor cell necrosis. Malignant hepatocytes or progenitor cells could undergo EMT as an option to escape from these places and to move toward a cytokine/chemokine better and enriched microenvironment, as well as a resistance mechanisms of survival to cell death stimuli (172, 173). In addition, hypoxic factors, such as HIF-1α, could stimulate EMT in hepatocytes in a TGF-β-dependent manner due to hypoxic hepatocytes secrete enzymes that activate latent TGF-β (174).

TGF-β REGULATES CANCER STEM CELL PLASTICITY

The variability in the prognosis of HCC patients suggests that it may comprise several distinct biological phenotypes, but individuals with HCC who shared a gene expression pattern with foetal hepatoblasts showed to have a poor prognosis (175). Several evidences provide insight into the role of TGF-β in regulating the cancer stem cell niche (176), much less is known about the potential crosstalk between TGF-β-induced EMT in the HCC cells and the acquisition of stem cell properties (74, 177). It is proved that liver epithelial cells that undergo a TGF-β-dependent EMT process show a less differentiated phenotype. Chronic TGF-β treatment in rat and human fetal hepatocytes, as well as in human HCC cells, promotes a mesenchymal-like phenotype concomitant with decreased expression of specific hepatic genes and the appearance of stem cell features, reminiscent of a progenitor-like phenotype (156, 177, 178). Cancer stem cells (CSC) or tumor-initiating cells (TICs) in the liver could derive from hepatic progenitor cells exposed to chronic TGF-β-exposure during hepatocarcinogenesis (179). TGF-β is involved in the neoplastic transformation of liver progenitor cells, through a miR-216a/PTEN/Akt-dependent pathway (179), concomitant with FOXO3a nuclear exportation. FOXO transcription factors are implicated in a huge cellular events and are also related with the neoplastic phenotypes linked to PI3K/Akt activation (180).

It is suggested that the expression of stem-related genes could also be mediating the acquisition of an EMT phenotype.

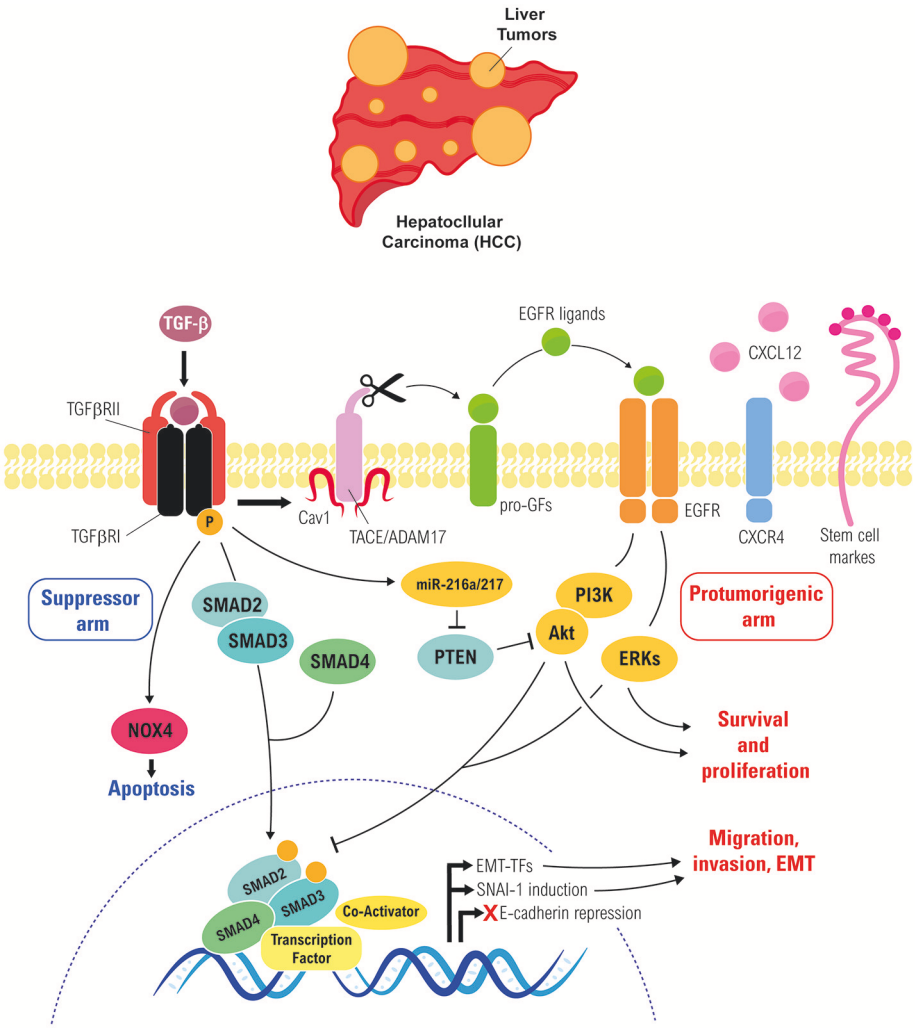

FIGURE 3 | Role of TGF-β in regulating EMT of liver tumor cells. Cross-talk between the TGF-β and the EGFR pathways in liver tumor cells, which rescues cells from TGF-β-induced apoptosis and allows them to respond to it undergoing a partial or full EMT, which increase their migratory/invasive and stemness properties.

In this sense, the stem-related CD44 or CD133 are not only involved in the acquisition of stem properties, but also in the switch to a more mesenchymal, migratory phenotype (181, 182). TGF-β-mediated mesenchymal-like phenotype is regulated by CD44, and its overexpression provokes down-regulation in E-cadherin expression and up-regulation of vimentin, which correlate with higher phospho-SMAD2-positive nuclei and poor prognosis in HCC patients (181, 183). Moreover, intermediate EMT states have recently been identified as crucial drivers of organ fibrosis and tumor progression (14). During partial-EMT stage, both epithelial and mesenchymal stem genes can be expressed. In this sense, it is worthy to mention that in certain HCC cell lines, TGF-β-treatment induces the expression of mesenchymal genes, such as *VIM* (vimentin), and the mesenchymal-related stem-related genes *CD44* and *CD90*, but simultaneously, they express *E-cadherin* and the epithelial-related stem genes *EPCAM* or *CD133* (177). Interestingly, this partial EMT phenotype confers to the HCC cells the highest stemness stage concomitant with an increased migratory/invasive capacity (177).

CSCs could contribute to the failure of therapies to abolish malignant tumors. In pre-clinical assays, cancer stem-like spheres from de-differentiated HCC-derived cell lines show increased expression of stemness markers (CD44), and higher resistance to anticancer drugs (184). Furthermore, the acquisition of some mesenchymal properties and the expression of CD44 impair the HCC cell response to sorafenib-induced apoptosis (183). For this, novel strategies are focused to target CSC development. It is interesting to mention that treatment with inhibitors of the TGF-β pathway, such as Galunisertib (LY2157299–a selective ATP-mimetic inhibitor of TGF-β receptor I) decreased the stemness related genes of mesenchymal HCC cells and their ability to form colonies, liver spheroids and invasive growth (185). Resminostat, a novel orally histone deacetylases inhibitor, has been demonstrated as a good therapy in the SHELTER study (a phase I/II clinical study) in mono and combination

therapy with sorafenib (186). The combination therapy revealed an advantage in terms of overall survival and time to progression. In HCC cells with a mesenchymal phenotype, caused by autocrine expression of TGF-β, resminostat sensitizes them to the apoptotic response induced by sorafenib (187). Mesenchymal-related gene expression was decreased in resminostat-treated HCC cells. This event is concomitant with an epithelial-related gene expression increase, more organized tight junctions and lower invasive growth. Indeed, resminostat down-regulated *CD44* expression is coincident with a decrease in the stemness properties. These results reinforce the strong impact of the TGF-β-induced mesenchymal/stemness phenotype on HCC drug resistance.

LIVER CANCER STROMA CELL PLASTICITY AND TGF-β

TGF-β display multiple effects on the microenvironment (188), which plays a relevant role in HCC development and progression. In the stroma, TGF-β induces microenvironment changes, including generation of cancer-associated fibroblasts (CAFs) (23) that play a relevant role in facilitating the production of growth factors and cytokines, which contribute to cell proliferation, invasion and neoangiogenesis, being related with poor prognosis (189–192). Different origins are described, but in the liver CAFs could be originated from epithelial cells–hepatocytes, cholangiocytes- and HSC that undergo an EMT process. To promote their tumoral functions, CAFs need the expression of EMT-TFs. Indeed, Snail expression in CAFs is necessary for their response to TGF-β, increased production of fibronectin and stiffness of the ECM (23). CAFs are also a potent source of TGF-β and are described to promote the migration and invasion of HCC cells *in vitro* and facilitate the HCC metastasis to the bone, brain and lung in NOD/SCID mice (193).

In HCC microenvironment anti-tumor response is impaired due to various immune suppressive elements, such as Tumor Associated Macrophages (TAMs) and regulatory T cells (Treg) (194–196). Similarly to that occurs with macrophages in fibrosis, during HCC progression, TAMs are mainly polarized toward an M2 phenotype, due to the higher levels of TGF-β (among others factors) (197). M2-like macrophages are major players in the connection between inflammation and cancer, involved in functions such as: promotion of tumor cell proliferation, ECM turnover, inhibition of adaptive immunity, among others (198, 199), TAMs are correlated with angiogenesis, metastasis, and poor prognosis (200, 201). Moreover, TAMs can promote cancer stem cell properties in a TGF-β-dependent manner (202). CAFs can also educate Natural Killer (NK) cells (203), dendritic cells (204) and upregulate the production of Treg in a TGF-β-dependent manner (205). CAFs promote Treg cell induction, through upregulation and activation of the human B7 homolog 1(B7-H1)/programmed death 1 (PD-1) signaling, which are involved in immunosuppressive functions in a mTOR/Akt dependent-manner (206). Accumulating evidence indicates that the immune system microenvironment plays key roles in the development of HCC (207, 208). CD4+ naïve T cells show an enormous cell plasticity and under TGF-β-treatment could differentiate into Treg cells (209). Poor prognosis in HCC patients is associated with infiltration liver tissue prognosis in HCC patients. Treg cells -Foxp3-positive cells- are involved in immune homeostasis, peripheral tolerance and prevention of autoimmunity (210, 211). TGF-β induces the expression of the transcriptional factor Foxp3 involved in the conversion of naïve CD4+CD25 T cells to CD4+CD25+ Treg cells with potent immunosuppressive potential (212). Blocking TGF-β signaling with SM-16 (TGF-β inhibitor) significant decreases the percentage of Treg cells in liver tissue concomitant with an attenuation of the hepatocarcinogenesis process in a DEN-model (213). Interestingly, addition of exogenous TGF-β restores the expression level of *Foxp3* and the presence of Treg cells. Exogenous addition of TGF-β normalizes Treg cell numbers and promoted their cell differentiation. Moreover, In HCC patient samples, the expression of both genes, *TGFB1* and *FOXP3*, correlate positively and are involved in tumoral progression. (213). On summary, TGF-β promotes tumor immune escape and survival by maintaining natural Treg levels, inducing Treg cell differentiation and TAMs polarization into M2-phenotype.

NEW THERAPIES TO INHIBIT THE TGF-β PATHWAY

Developing an effective therapy to target the TGF-β pathway in liver pathologies requires a better understanding of its complex role in this organ, considering its pleiotropic effects on cell proliferation, death and differentiation of different liver cell types, its ability to induce EMT in epithelial cells or EndEMT in the endothelial ones, as well as its capacity to act as an immune modulator. In spite of this, targeting TGF-β was proposed a good approach to delay the progression of liver diseases and, in particular, of HCC (9, 214, 215). Indeed, first experiments indicated that inhibiting the TGF-β pathway in HCC cell lines blocked migration and invasion of HCC cells by up-regulating E-cadherin and down-regulating CXCR4 (167, 188), as well as inhibiting the upregulated levels of CTGF induced by TGF-β, reducing the stromal component of the microtumoural environment and slowing the HCC growth *in vivo* (216). These data suggested that there could be a mechanistic use for targeting TGF-β in HCC clinical trials.

Several different strategies have been proposed to inhibit the TGF-β pathway in liver pathologies, including the use of chimeric proteins, monoclonal antibodies, peptide inhibitors, small molecules that inhibit the receptors' kinase activity and antisense oligonucleotides (217). First studies demonstrated the efficiency of potential peptide inhibitors of TGF-β1 (derived from TGF-β1 and from its type III receptor) *in vitro* and *in vivo* in reducing liver fibrosis (218, 219). These peptide inhibitors were proved to be also useful in enhancing the efficacy of antitumor immunotherapy (220). To increase the delivery efficiency, in a recent study, one of these peptides (P-17) was loaded separately into folic acid-functionalized nano-carriers

made of bovine serum albumin. Cellular studies demonstrated the targeting efficiency of the hybrid carriers (221).

In the last years the interest has been focused on the TβRI kinase inhibitor Galunisertib, developed by Lilly (LY2157299, a selective ATP-mimetic inhibitor of TβRI) that has proved more efficient than neutralizing humanized antibodies, such as D10 against TβRII, in blocking the canonical TGF-β signaling in HCC cells, experiments that supported the use of this drug in preclinical and clinical trials (9, 222). Despite limited antiproliferative effects, Galunisertib yielded potent anti-invasive properties in HCC models and in *ex vivo* tumor tissue samples from patients (223). Worthy to note, in combination, Galunisertib potentiated the effect of sorafenib efficiently by inhibiting proliferation and increasing apoptosis. Galunisertib also reduced the expression of stemness-related genes, such as *CD44* and *THY1*, *in vitro* and in *ex vivo* human HCC specimens, overcoming stemness-derived aggressiveness (185). Furthermore, it also showed antitumor activity through the activation of CD8+ T-cell antitumor responses (224). Recent studies have also suggested the potential efficiency of Galunisertib as antifibrotic drug. In *ex vivo* studies, using both healthy and cirrhotic human precision-cut liver slices, Galunisertib reduced fibrosis-related transcription, which correlated with a significant inhibition in the production and maturation of collagens (225). Furthermore, in an experimental preclinical model (Abcb4ko mice) the treatment with Galunisertib decreased the expression of several fibrogenic genes, such as collagens (*Col1a1* and *Col1a2*), *Tgfb1* and *Timp1*, and reduced the ECM/stromal components, fibronectin and laminin-332, as well as the carcinogenic β-catenin pathway (226).

A phase II clinical trial using Galunisertib in patients with advanced HCC to test safety, time to progression and overall survival (OS) is ongoing (NCT01246986 http://clinicaltrials.gov). Preliminary data show that patients with higher levels of circulating TGF-β1 are more likely to respond to therapy with Galunisertib. TGF-β1 reduction in response to the treatment is related to improvement in OS when compared to patients with non-TGF-β1 reduction. Some efforts are being made in optimizing the delivery of Galunisertib in form of novel polymeric nano-micelles, to avoid acidic pH of gastrointestinal tract, colon alkaline pH and anti-immune recognition (227).

Once it is proven the safety and the benefit of using Galunisertib in HCC, biomarkers will be extremely useful in the proper selection of patients who might benefit from receiving the drug. In this sense, high *TGFB1* expression in HCC patients, concomitant with high expression of the genes that mediate its invasive effects, such as *PDGF, CXCR4,* or *CD44*, (167, 177, 228) would anticipate a benefit for the use of Galunisertib. Furthermore, a recent study has proposed *SKIL* and *PMEPA1* as strongly downregulated by Galunisertib, correlating with endogenous TGFβ-1 (185, 229). These target genes identified may also serve as biomarkers for the stratification of HCC patients undergoing treatment with Galunisertib. Since biopsy is not frequent in HCC patients, new areas of research must be focused on the improvement of liquid biopsies in these patients to develop the possibility that this kind of analysis may be done in tumor circulating cells.

Finally, new approaches to interfere not only the TGF-β canonical, but also the non-canonical pathways must be developed in the next future, as previously mentioned, the switch from tumor-suppressive to pro-oncogenic TGF-β actions could be directed by its crosstalk with Receptor Tyrosine Kinases, in particular, EGFR. So, interference with EGFR signaling, by employing approved targeted drugs, in TGF-β/SMAD-positive HCC patients might be effective in improving the effectiveness of Galunisertib.

CONCLUDING REMARKS

TGF-β plays unique actions in modulating cell plasticity, and the liver reveals as a tissue where these actions would be very relevant during the response to injuries that cause chronic diseases. In general terms, TGF-β-induced changes in cell plasticity may converge in transdifferentiation toward a different phenotype, such as the case of activation of HSC to MFB or the dedifferentiation/acquisition of stem cell properties in hepatocytes and liver tumor cells. But it may also proportionate to the cells new capabilities, such as cell survival or increase in migratory/invasive properties that the liver tumor cells acquire when they undergo EMT in response to TGF-β. And, worthy to note the essential role that TGF-β plays inducing Treg cell differentiation and TAMs polarization into M2-phenotype, which promotes tumor immune escape and survival. Despite all current knowledge, there are still many gaps that need to be clarify. However, these evidences point toward the use of tools that target the TGF-β signaling pathway to counteract liver disease progression.

AUTHORS CONTRIBUTIONS

Both authors equally contribute to the writing and revision of this work. Figures were designed and elaborated by DC-D and supervised by IF.

FUNDING

Grants: Ministry of Science, Innovation and Universities, Spain (cofounded by FEDER funds/Development Fund—a way to build Europe): SAF2015-64149-R. DC-D was recipient of a fellowship from the FPI program, Ministry of Economy, Industry and Competitiveness, Spain: BES-2016 0077564. The CIBEREHD, National Biomedical Research Institute on Liver and Gastrointestinal Diseases, is funded by the Instituto de Salud Carlos III, Spain.

ACKNOWLEDGMENTS

We would like to give thanks to Esther Bertran and Judit López-Luque for all their support and advices.

REFERENCES

1. Rozga J. Hepatocyte proliferation in health and in liver failure. *Med Sci Monit*. (2002) 8:RA32–8.
2. Zhang DY, Friedman SL. Fibrosis-dependent mechanisms of hepatocarcinogenesis. *Hepatology* (2012) 56:769–75. doi: 10.1002/hep.25670
3. Michalopoulos GK. Advances in liver regeneration. *Expert Rev Gastroenterol Hepatol*. (2014) 8:897–907. doi: 10.1586/17474124.2014.934358
4. Malhi H, Gores GJ. Cellular and molecular mechanisms of liver injury. *Gastroenterology* (2008) 134:1641–54. doi: 10.1053/j.gastro.2008.03.002
5. Pellicoro A, Ramachandran P, Iredale JP, Fallowfield JA. Liver fibrosis and repair: immune regulation of wound healing in a solid organ. *Nat Rev Immunol*. (2014) 14:181–94. doi: 10.1038/nri3623
6. Heldin C-H, Moustakas A. Signaling receptors for TGF-β family members. *Cold Spring Harb Perspect Biol*. (2016) 8:a022053. doi: 10.1101/cshperspect.a022053
7. Dooley S, ten Dijke P. TGF-β in progression of liver disease. *Cell Tissue Res*. (2012) 347:245–56. doi: 10.1007/s00441-011-1246-y
8. Fabregat I, Moreno-Càceres J, Sánchez A, Dooley S, Dewidar B, Giannelli G., et al. TGF-β signalling and liver disease. *FEBS J*. (2016) 283:2219–32. doi: 10.1111/febs.13665
9. Giannelli G, Mikulits W, Dooley S, Fabregat I, Moustakas A, ten Dijke, P., et al. The rationale for targeting TGF-β in chronic liver diseases. *Eur J Clin Invest*. (2016) 46:349–61. doi: 10.1111/eci.12596
10. Massagué J. TGFbeta in cancer. *Cell* (2008) 134:215–30. doi: 10.1016/j.cell.2008.07.001
11. Giannelli G, Rani B, Dituri F, Cao Y, Palasciano G. Moving towards personalised therapy in patients with hepatocellular carcinoma: the role of the microenvironment. *Gut* (2014) 63:1668–76. doi: 10.1136/gutjnl-2014-307323
12. Varga J, Greten FR. Cell plasticity in epithelial homeostasis and tumorigenesis. *Nature Cell Biol*. (2017) 19:1133–41. doi: 10.1038/ncb3611
13. Nieto MA. Epithelial plasticity: a common theme in embryonic and cancer cells. *Science* (2013) 342:1234850. doi: 10.1126/science.1234850
14. Nieto MA, Huang RYJ, Jackson RA, Thiery JP. EMT: 2016. *Cell* (2016) 166:21–45. doi: 10.1016/j.cell.2016.06.028
15. Franco DL, Mainez J, Vega S, Sancho P, Murillo MM, de Frutos CA, et al. Snail1 suppresses TGF-beta-induced apoptosis and is sufficient to trigger EMT in hepatocytes. *J Cell Sci*. (2010) 123:3467–77. doi: 10.1242/jcs.068692
16. Dewidar B, Soukupova J, Fabregat I, Dooley S. TGF-β in hepatic stellate cell activation and liver fibrogenesis: updated. *Curr Pathobiol Rep*. (2015) 3:291–305. doi: 10.1007/s40139-015-0089-8
17. Kim KK, Sheppard D, Chapman HA. TGF-β1 signaling and tissue fibrosis. *Cold Spring Harb Perspect Biol*. (2017) 10:a022293. doi: 10.1101/cshperspect.a02229.
18. Pickup MW, Owens P, Moses HL. TGF-β, Bone morphogenetic protein, and activin signaling and the tumor microenvironment. *Cold Spring Harb Perspect Biol*. (2017) 9:a022285. doi: 10.1101/cshperspect.a022285
19. Robertson IB, Rifkin DB. Regulation of the bioavailability of TGF-β and TGF-β-related proteins. *Cold Spring Harb Perspect Biol*. (2016) 8:a021907. doi: 10.1101/cshperspect.a021907
20. Thomas GJ, Hart IR, Speight PM, Marshall JF. Binding of TGF-beta1 latency-associated peptide (LAP) to alpha(v)beta6 integrin modulates behaviour of squamous carcinoma cells. *Br J Cancer* (2002) 87:859–67. doi: 10.1038/sj.bjc.6600545
21. Khan Z, Marshall JF. The role of integrins in TGFβ activation in the tumour stroma. *Cell Tissue Res*. (2016) 365:657–73. doi: 10.1007/s00441-016-2474-y
22. Henderson NC, Arnold TD, Katamura Y, Giacomini MM, Rodriguez JD, McCarty JH, et al. Targeting of αv integrin identifies a core molecular pathway that regulates fibrosis in several organs. *Nat Med*. (2013) 19:1617–24. doi: 10.1038/nm.3282
23. Caja L, Dituri F, Mancarella S, Caballero-Diaz D, Moustakas A, Giannelli G, et al. TGF-β and the tissue microenvironment: relevance in fibrosis and cancer. *Int J Mole Sci*. (2018) 19:1294. doi: 10.3390/ijms19051294
24. Drabsch Y, ten Dijke P. TGF-β signalling and its role in cancer progression and metastasis. *Cancer Metastasis Rev*. (2012) 31:553–68. doi: 10.1007/s10555-012-9375-7
25. Heldin C-H, Vanlandewijck M, Moustakas A. Regulation of EMT by TGFβ in cancer. *FEBS Lett*. (2012) 586:1959–70. doi: 10.1016/j.febslet.2012.02.037
26. Morrison CD, Parvani JG, Schiemann WP. The relevance of the TGF-β Paradox to EMT-MET programs. *Cancer Lett*. (2013) 341:30–40. doi: 10.1016/j.canlet.2013.02.048
27. Bataller R, Brenner DA. Liver fibrosis. *J Clin Invest*. (2005) 115:209–18. doi: 10.1172/JCI24282
28. Schuppan D. Liver fibrosis: common mechanisms and antifibrotic therapies. *Clin Res Hepatol Gastroenterol*. (2015) 39 (Suppl. 1):S51–59. doi: 10.1016/j.clinre.2015.05.005
29. Mallat A, Lotersztajn S. Cellular mechanisms of tissue fibrosis. 5. Novel insights into liver fibrosis. *Am J Physiol Cell Physiol*. (2013) 305:C789–99. doi: 10.1152/ajpcell.00230.2013
30. Cao Q, Mak KM, Lieber CS. DLPC decreases TGF-β1-induced collagen mRNA by inhibiting p38 MAPK in hepatic stellate cells. *Am J Physiol Gastrointestinal Liver Physiol*. (2002) 283:G1051–61. doi: 10.1152/ajpgi.00128.2002
31. Furukawa F, Matsuzaki K, Mori S, Tahashi Y, Yoshida K, Sugano Y, et al. p38 MAPK mediates fibrogenic signal through Smad3 phosphorylation in rat myofibroblasts. *Hepatology* (2003) 38:879–89. doi: 10.1002/hep.1840380414
32. Zeisberg M, Kalluri R. Cellular mechanisms of tissue fibrosis. 1. Common and organ-specific mechanisms associated with tissue fibrosis. *Am. J. Physiol. Cell Physiol*. (2013) 304:C216–25. doi: 10.1152/ajpcell.00328.2012
33. Wynn TA, Barron L. Macrophages: master regulators of inflammation and fibrosis. *Semin Liver Dis*. (2010) 30:245–57. doi: 10.1055/s-0030-1255354
34. Khalil N, Bereznay O, Sporn M, Greenberg AH. Macrophage production of transforming growth factor beta and fibroblast collagen synthesis in chronic pulmonary inflammation. *J Exp Med*. (1989) 170:727–37. doi: 10.1084/jem.170.3.727
35. Koslowski R, Seidel D, Kuhlisch E, Knoch KP. Evidence for the involvement of TGF-beta and PDGF in the regulation of prolyl 4-hydroxylase and lysyloxidase in cultured rat lung fibroblasts. *Exp Toxicol Pathol*. (2003) 55:257–64. doi: 10.1078/0940-2993-00323
36. Leicester KL, Olynyk JK, Brunt EM, Britton RS, Bacon BR. CD14-positive hepatic monocytes/macrophages increase in hereditary hemochromatosis. *Liver Int*. (2004) 24:446–51. doi: 10.1111/j.1478-3231.2004.0943.x
37. Li H, You H, Fan X, Jia J. Hepatic macrophages in liver fibrosis: pathogenesis and potential therapeutic targets. *BMJ Open Gastroenterol*. (2016) 3:e000079. doi: 10.1136/bmjgast-2016-000079
38. Ramm GA, Nair VG, Bridle KR, Shepherd RW, Crawford DH. Contribution of hepatic parenchymal and nonparenchymal cells to hepatic fibrogenesis in biliary atresia. *Am J Pathol*. (1998) 153:527–35. doi: 10.1016/S0002-9440(10)65595-2
39. Heymann F, Trautwein C, Tacke F. Monocytes and macrophages as cellular targets in liver fibrosis. *Inflamm Allergy Drug Targets* (2009) 8:307–18. doi: 10.2174/187152809789352230
40. Schuppan D, Kim YO. Evolving therapies for liver fibrosis. *J Clin Invest*. (2013) 123:1887–901. doi: 10.1172/JCI66028
41. Dey A, Allen J, Hankey-Giblin PA. Ontogeny and polarization of macrophages in inflammation: blood monocytes versus tissue macrophages. *Front Immunol*. (2015) 5:683. doi: 10.3389/fimmu.2014.00683
42. Naito M, Hasegawa G, Ebe Y, Yamamoto T. Differentiation and function of Kupffer cells. *Med Electron Microsc* (2004) 37:16–28. doi: 10.1007/s00795-003-0228-x
43. Sica A, Mantovani A. Macrophage plasticity and polarization: *in vivo* veritas. *J Clin Invest*. (2012) 122:787–95. doi: 10.1172/JCI59643
44. De Minicis S, Seki E, Uchinami H, Kluwe J, Zhang Y, Brenner DA, et al. Gene expression profiles during hepatic stellate cell activation in culture and *in vivo*. *Gastroenterology* (2007) 132:1937–46. doi: 10.1053/j.gastro.2007.02.033
45. Karlmark KR, Weiskirchen R, Zimmermann HW, Gassler N, Ginhoux F, Weber C, et al. Hepatic recruitment of the inflammatory Gr1+ monocyte subset upon liver injury promotes hepatic fibrosis. *Hepatology* (2009) 50:261–74. doi: 10.1002/hep.22950
46. Pradere JP, Kluwe J, De Minicis S, Jiao JJ, Gwak GY, Dapito DH, et al. Hepatic macrophages but not dendritic cells contribute to liver fibrosis by promoting the survival of activated hepatic stellate cells in mice. *Hepatology* (2013) 58:1461–73. doi: 10.1002/hep.26429

47. Sun YY, Li XF, Meng XM, Huang C, Zhang L, Li J. Macrophage phenotype in liver injury and repair. *Scand J Immunol*. (2017) 85:166–74. doi: 10.1111/sji.12468
48. Baeck C, Wehr A, Karlmark KR, Heymann F, Vucur M, Gassler N, et al. Pharmacological inhibition of the chemokine CCL2 (MCP-1) diminishes liver macrophage infiltration and steatohepatitis in chronic hepatic injury. *Gut* (2012) 61:416–26. doi: 10.1136/gutjnl-2011-300304
49. Imamura M, Ogawa T, Sasaguri Y, Chayama K, Ueno H. Suppression of macrophage infiltration inhibits activation of hepatic stellate cells and liver fibrogenesis in rats. *Gastroenterology* (2005) 128:138–46. doi: 10.1053/j.gastro.2004.10.005
50. Braga TT, Agudelo JSH, Camara NOS. Macrophages during the fibrotic process: M2 as friend and foe. *Front Immunol*. (2015) 6:602. doi: 10.3389/fimmu.2015.00602
51. Mills CD, Kincaid K, Alt JM, Heilman MJ, Hill AM. M-1/M-2 macrophages and the Th1/Th2 paradigm. *J Immunol*. (2000) 164:6166–73. doi: 10.4049/jimmunol.164.12.6166
52. Mosser DM, Edwards JP. Exploring the full spectrum of macrophage activation. *Nat Rev Immunol*. (2008) 8:958–69. doi: 10.1038/nri2448
53. Tacke F, Zimmermann HW. Macrophage heterogeneity in liver injury and fibrosis. *J Hepatol*. (2014) 60:1090–6. doi: 10.1016/j.jhep.2013.12.025
54. Koh TJ, DiPietro LA. Inflammation and wound healing: the role of the macrophage. *Expert Rev Mol Med*. (2011) 13:e23. doi: 10.1017/S1462399411001943
55. Zhang F, Wang H, Wang X, Jiang G, Liu H, Zhang G, et al. TGF-β induces M2-like macrophage polarization via SNAIL-mediated suppression of a pro-inflammatory phenotype. *Oncotarget* (2016) 7:52294–306. doi: 10.18632/oncotarget.10561
56. Bai L, Liu X, Zheng Q, Kong M, Zhang X, Hu R, et al. M2-like macrophages in the fibrotic liver protect mice against lethal insults through conferring apoptosis resistance to hepatocytes. *Sci Rep*. (2017) 7:10518. doi: 10.1038/s41598-017-11303-z
57. Murray LA, Chen Q, Kramer MS, Hesson DP, Argentieri RL, Peng X, et al. TGF-beta driven lung fibrosis is macrophage dependent and blocked by Serum amyloid P. *Int J Biochem Cell Biol*. (2011) 43:154–62. doi: 10.1016/j.biocel.2010.10.013
58. Wang S, Meng X-M, Ng Y-Y, Ma FY, Zhou S, Zhang Y, et al. TGF-β/Smad3 signalling regulates the transition of bone marrowderived macrophages into myofibroblasts during tissue fibrosis. *Oncotarget* (2015) 7:8809–22. doi: 10.18632/oncotarget.6604
59. Gong D, Shi W, Yi S, Chen H, Groffen J, Heisterkamp N. TGFβ signaling plays a critical role in promoting alternative macrophage activation. *BMC Immunol*. (2012) 13:31. doi: 10.1186/1471-2172-13-31
60. Wijesundera KK, Izawa T, Tennakoon AH, Murakami H, Golbar HM, Katou-Ichikawa C, et al. M1- and M2-macrophage polarization in rat liver cirrhosis induced by thioacetamide (TAA), focusing on Iba1 and galectin-3. *Exp Mol Pathol*. (2014) 96:382–92. doi: 10.1016/j.yexmp.2014.04.003
61. Bility MT, Nio K, Li F, McGivern DR, Lemon SM, Feeney ER, et al. Chronic hepatitis C infection-induced liver fibrogenesis is associated with M2 macrophage activation. *Sci Rep*. (2016) 6:39520. doi: 10.1038/srep39520
62. Tacke F. Targeting hepatic macrophages to treat liver diseases. *J Hepatol*. (2017) 66:1300–12. doi: 10.1016/j.jhep.2017.02.026
63. Seki E, Brenner DA. Recent advancement of molecular mechanisms of liver fibrosis. *J Hepato-Biliary-Pancreat Sci*. (2015) 22:512–8. doi: 10.1002/jhbp.245
64. Elpek GÖ. Cellular and molecular mechanisms in the pathogenesis of liver fibrosis: an update. *World J Gastroenterol*. (2014) 20:7260–76. doi: 10.3748/wjg.v20.i23.7260
65. Iwaisako K, Jiang C, Zhang M, Cong M, Moore-Morris TJ, Park TJ, et al. Origin of myofibroblasts in the fibrotic liver in mice. *Proc Natl Acad Sci U. S. A*. (2014) 111:E3297–3305. doi: 10.1073/pnas.1400062111
66. Wells RG. Cellular sources of extracellular matrix in hepatic fibrosis. *Clin Liver Dis*. (2008) 12:759–68. doi: 10.1016/j.cld.2008.07.008
67. Tsuchida T, Friedman SL. Mechanisms of hepatic stellate cell activation. *Nat Rev Gastroenterol Hepatol*. (2017) 14:397–411. doi: 10.1038/nrgastro.2017.38
68. Russo FP, Alison MR, Bigger BW, Amofah E, Florou A, Amin F, et al. The bone marrow functionally contributes to liver fibrosis. *Gastroenterology* (2006) 130:1807–21. doi: 10.1053/j.gastro.2006.01.036
69. Del Castillo G, Murillo MM, Alvarez-Barrientos A, Bertran E, Fernández M, Sánchez A, et al. Autocrine production of TGF-beta confers resistance to apoptosis after an epithelial-mesenchymal transition process in hepatocytes: role of EGF receptor ligands. *Exp Cell Res*. (2006) 312:2860–71. doi: 10.1016/j.yexcr.2006.05.017
70. Kaimori A, Potter J, Kaimori J-Y, Wang C, Mezey E, Koteish A. Transforming growth factor-beta1 induces an epithelial-to-mesenchymal transition state in mouse hepatocytes *in vitro*. *J Biol Chem*. (2007) 282:22089–101. doi: 10.1074/jbc.M700998200
71. Valdés F, Alvarez AM, Locascio A, Vega S, Herrera B, Fernández M, et al. The epithelial mesenchymal transition confers resistance to the apoptotic effects of transforming growth factor Beta in fetal rat hepatocytes. *Mol Cancer Res*. (2002) 1:68–78.
72. Maher JJ, McGuire RF. Extracellular matrix gene expression increases preferentially in rat lipocytes and sinusoidal endothelial cells during hepatic fibrosis *in vivo*. *J Clin Invest*. (1990) 86:1641–8. doi: 10.1172/JCI114886
73. Hernandez-Gea V, Friedman SL. Pathogenesis of liver fibrosis. *Annu Rev Pathol*. (2011) 6:425–56. doi: 10.1146/annurev-pathol-011110-130246
74. Fabregat I, Malfettone A, Soukupova J. New insights into the crossroads between EMT and stemness in the context of cancer. *J Clin Med*. (2016) 5:37. doi: 10.3390/jcm5030037
75. Giannelli G, Koudelkova P, Dituri F, Mikulits W. Role of epithelial to mesenchymal transition in hepatocellular carcinoma. *J Hepatol*. (2016) 65:798–808. doi: 10.1016/j.jhep.2016.05.007
76. Thiery JP. Epithelial-mesenchymal transitions in tumour progression. *Nat Rev Cancer* (2002) 2:442–54. doi: 10.1038/nrc822
77. Kalluri R, Weinberg RA. The basics of epithelial-mesenchymal transition. *J Clin Invest*. (2009) 119:1420–8. doi: 10.1172/JCI39104
78. Zeisberg M, Neilson EG. Biomarkers for epithelial-mesenchymal transitions. *J Clin Invest*. (2009) 119:1429–37. doi: 10.1172/JCI36183
79. Walkup MH, Gerber DA. Hepatic stem cells: in search of. *Stem Cells* (2006) 24:1833–40. doi: 10.1634/stemcells.2006-0063
80. Weng HL, Ciuclan L, Liu Y, Hamzavi J, Godoy P, Gaitantzi H, et al. Profibrogenic transforming growth factor-beta/activin receptor-like kinase 5 signaling via connective tissue growth factor expression in hepatocytes. *Hepatology* (2007) 46:1257–70. doi: 10.1002/hep.21806
81. Xie G, Diehl AM. Evidence for and against epithelial-to-mesenchymal transition in the liver. *Am J Physiol Gastrointest Liver Physiol*. (2013) 305:G881–90. doi: 10.1152/ajpgi.00289.2013
82. Zeisberg M, Yang C, Martino M, Duncan MB, Rieder F, Tanjore H, et al. Fibroblasts derive from hepatocytes in liver fibrosis via epithelial to mesenchymal transition. *J Biol Chem*. (2007) 282:23337–47. doi: 10.1074/jbc.M700194200
83. Dooley S, Hamzavi J, Ciuclan L, Godoy P, Ilkavets I, Ehnert S, et al. Hepatocyte-specific Smad7 expression attenuates TGF-beta-mediated fibrogenesis and protects against liver damage. *Gastroenterology* (2008) 135:642–59. doi: 10.1053/j.gastro.2008.04.038
84. Bi WR, Xu GT, Lv LX, Yang CQ. The ratio of transforming growth factor-β1/bone morphogenetic protein-7 in the progression of the epithelial-mesenchymal transition contributes to rat liver fibrosis. *Genet Mol Res*. (2014) 13:1005–14. doi: 10.4238/2014.February.20.2
85. Lazaridis KN, Strazzabosco M, Larusso NF. The cholangiopathies: disorders of biliary epithelia. *Gastroenterology* (2004) 127:1565–77. doi: 10.1053/j.gastro.2004.08.006
86. Yin C, Evason KJ, Asahina K, Stainier DYR. Hepatic stellate cells in liver development, regeneration, and cancer. *J Clin Invest*. (2013) 123:1902–10. doi: 10.1172/JCI66369
87. Barnes JL, Gorin Y. Myofibroblast differentiation during fibrosis: role of NAD(P)H oxidases. *Kidney Int*. (2011) 79:944–56. doi: 10.1038/ki.2010.516
88. Dooley S, Delvoux B, Lahme B, Mangasser-Stephan K, Gressner AM. Modulation of transforming growth factor beta response and signaling during transdifferentiation of rat hepatic stellate cells to myofibroblasts. *Hepatology* (2000) 31:1094–106. doi: 10.1053/he.2000.6126

89. Sancho P, Mainez J, Crosas-Molist E, Roncero C, Fernández-Rodriguez CM, Pinedo F, et al. NADPH oxidase NOX4 mediates stellate cell activation and hepatocyte cell death during liver fibrosis development. *PLoS ONE* (2012) 7:e45285. doi: 10.1371/journal.pone.0045285
90. Ding Z, Jin G, Liang H, Wang W, Chen W, Datta PK, et al. Transforming growth factor β induces expression of connective tissue growth factor in hepatic progenitor cells through Smad independent signaling. *Cell Signal*. (2013) 25:1981–92. doi: 10.1016/j.cellsig.2013.05.027
91. Liu Y, Liu H, Meyer C, Li J, Nadalin S, Königsrainer A, et al. Transforming growth factor-β (TGF-β)-mediated connective tissue growth factor (CTGF) expression in hepatic stellate cells requires Stat3 signaling activation. *J Biol Chem*. (2013) 288:30708–19. doi: 10.1074/jbc.M113.478685
92. Jia D, Duan F, Peng P, Sun L, Liu X, Wang L, et al. Up-regulation of RACK1 by TGF-β1 promotes hepatic fibrosis in mice. *PLoS ONE* (2013) 8:e60115. doi: 10.1371/journal.pone.0060115
93. Liu M, Peng P, Wang J, Wang L, Duan F, Jia D, et al. RACK1-mediated translation control promotes liver fibrogenesis. *Biochem Biophys Res Commun*. (2015) 463:255–61. doi: 10.1016/j.bbrc.2015.05.040
94. Li L, Wang JY, Yang CQ, Jiang W. Effect of RhoA on transforming growth factor β1-induced rat hepatic stellate cell migration. *Liver Int.* (2012) 32:1093–102. doi: 10.1111/j.1478-3231.2012.02809.x
95. Fang L, Huang C, Meng X, Wu B, Ma T, Liu X, et al. TGF-β1-elevated TRPM7 channel regulates collagen expression in hepatic stellate cells via TGF-β1/Smad pathway. *Toxicol Appl Pharmacol*. (2014) 280:335–44. doi: 10.1016/j.taap.2014.08.006
96. Kisseleva T, Cong M, Paik Y, Scholten D, Jiang C, Benner C, et al. Myofibroblasts revert to an inactive phenotype during regression of liver fibrosis. *Proc Natl Acad Sci U. S. A*. (2012) 109:9448–53. doi: 10.1073/pnas.1201840109
97. Liu X, Xu J, Brenner DA, Kisseleva T. Reversibility of liver fibrosis and inactivation of fibrogenic myofibroblasts. *Curr Pathobiol Rep*. (2013) 1:209–14. doi: 10.1007/s40139-013-0018-7
98. Foo N-P, Lin S-H, Lee Y-H, Wu M-J, Wang Y-J. α-Lipoic acid inhibits liver fibrosis through the attenuation of ROS-triggered signaling in hepatic stellate cells activated by PDGF and TGF-β. *Toxicology* (2011) 282:39–46. doi: 10.1016/j.tox.2011.01.009
99. Abhilash PA, Harikrishnan R, Indira M. Ascorbic acid supplementation down-regulates the alcohol induced oxidative stress, hepatic stellate cell activation, cytotoxicity and mRNA levels of selected fibrotic genes in guinea pigs. *Free Radic Res*. (2012) 46:204–13. doi: 10.3109/10715762.2011.647691
100. Torok NJ. Dysregulation of redox pathways in liver fibrosis. *Am J Physiol Gastrointest Liver Physiol*. (2016) 311:G667–74. doi: 10.1152/ajpgi.00050.2016
101. Crosas-Molist E, Fabregat I. Role of NADPH oxidases in the redox biology of liver fibrosis. *Redox Biol*. (2015) 6:106–11. doi: 10.1016/j.redox.2015.07.005
102. Pociask DA, Sime PJ, Brody AR. Asbestos-derived reactive oxygen species activate TGF-beta1. *Lab Invest*. (2004) 84:1013–23. doi: 10.1038/labinvest.3700109
103. Wang L, Clutter S, Benincosa J, Fortney J, Gibson LF. Activation of transforming growth factor-beta1/p38/Smad3 signaling in stromal cells requires reactive oxygen species-mediated MMP-2 activity during bone marrow damage. *Stem Cells* (2005) 23:1122–34. doi: 10.1634/stemcells.2004-0354
104. Jobling MF, Mott JD, Finnegan MT, Jurukovski V, Erickson AC, Walian PJ, et al. Isoform-specific activation of latent transforming growth factor beta (LTGF-beta) by reactive oxygen species. *Radiat Res*. (2006) 166:839–48. doi: 10.1667/RR0695.1
105. Proell V, Carmona-Cuenca I, Murillo MM, Huber H, Fabregat I, Mikulits W. TGF-beta dependent regulation of oxygen radicals during transdifferentiation of activated hepatic stellate cells to myofibroblastoid cells. *Comp Hepatol*. (2007) 6:1. doi: 10.1186/1476-5926-6-1
106. Boudreau HE, Emerson SU, Korzeniowska A, Jendrysik MA, Leto TL. Hepatitis C virus (HCV) proteins induce NADPH oxidase 4 expression in a transforming growth factor beta-dependent manner: a new contributor to HCV-induced oxidative stress. *J Virol*. (2009) 83:12934–46. doi: 10.1128/JVI.01059-09
107. Liang S, Kisseleva T, Brenner DA. The Role of NADPH oxidases (NOXs) in liver fibrosis and the activation of myofibroblasts. *Front Physiol*. (2016) 7:17. doi: 10.3389/fphys.2016.00017
108. Paik YH, Kim J, Aoyama T, De Minicis S, Bataller R, Brenner DA. Role of NADPH oxidases in liver fibrosis. *Antioxid Redox Signal*. (2014) 20:2854–72. doi: 10.1089/ars.2013.5619
109. Paik YH, Iwaisako K, Seki E, Inokuchi S, Schnabl B, Osterreicher CH, et al. The nicotinamide adenine dinucleotide phosphate oxidase (NOX) homologues NOX1 and NOX2/gp91(phox) mediate hepatic fibrosis in mice. *Hepatology* (2011) 53:1730–41. doi: 10.1002/hep.24281
110. Crosas-Molist E, Bertran E, Fabregat I. Cross-Talk Between TGF-β and NADPH Oxidases During Liver Fibrosis and Hepatocarcinogenesis. *Curr Pharm Des*. (2015) 21:5964–76. doi: 10.2174/1381612821666151029112126
111. Cucoranu I, Clempus R, Dikalova A, Phelan PJ, Ariyan S, Dikalov S, et al. NAD(P)H oxidase 4 mediates transforming growth factor-beta1-induced differentiation of cardiac fibroblasts into myofibroblasts. *Circ Res*. (2005) 97:900–7. doi: 10.1161/01.RES.0000187457.24338.3D
112. Hecker L, Vittal R, Jones T, Jagirdar R, Luckhardt TR, Horowitz JC, et al. NADPH oxidase-4 mediates myofibroblast activation and fibrogenic responses to lung injury. *Nat Med*. (2009) 15:1077–81. doi: 10.1038/nm.2005
113. Bondi CD, Manickam N, Lee DY, Block K, Gorin Y, Abboud HE, et al. NAD(P)H oxidase mediates TGF-beta1-induced activation of kidney myofibroblasts. *J Am Soc Nephrol*. (2010) 21:93–102. doi: 10.1681/ASN.2009020146
114. Jiang JX, Chen X, Serizawa N, Szyndralewiez C, Page P, Schröder K, et al. Liver fibrosis and hepatocyte apoptosis are attenuated by GKT137831, a novel NOX4/NOX1 inhibitor in v0ivo. *Free Radic Biol Med*. (2012) 53:289–96. doi: 10.1016/j.freeradbiomed.2012.05.007
115. Jiang JX, Mikami K, Venugopal S, Li Y, Török NJ. Apoptotic body engulfment by hepatic stellate cells promotes their survival by the JAK/STAT and Akt/NF-kappaB-dependent pathways. *J Hepatol*. (2009) 51:139–48. doi: 10.1016/j.jhep.2009.03.024
116. Aoyama T, Paik Y-H, Watanabe S, Laleu B, Gaggini F, Fioraso-Cartier L, et al. Nicotinamide adenine dinucleotide phosphate oxidase in experimental liver fibrosis: GKT137831 as a novel potential therapeutic agent. *Hepatology* (2012) 56:2316–27. doi: 10.1002/hep.25938
117. Lan T, Kisseleva T, Brenner DA. Deficiency of NOX1 or NOX4 prevents liver inflammation and fibrosis in mice through inhibition of hepatic stellate cell activation. *PLoS ONE* (2015) 10:e0129743. doi: 10.1371/journal.pone.0129743
118. European Association For The Study Of The Liver and European Organisation For Research And Treatment Of Cancer. EASL-EORTC clinical practice guidelines: management of hepatocellular carcinoma. *J Hepatol*. (2012) 56:908–43. doi: 10.1016/j.jhep.2011.12.001
119. Naugler WE, Sakurai T, Kim S, Maeda S, Kim K, Elsharkawy AM, et al. Gender disparity in liver cancer due to sex differences in MyD88-dependent IL-6 production. *Science* (2007) 317:121–4. doi: 10.1126/science.1140485
120. Tabrizian P, Roayaie S, Schwartz ME. Current management of hepatocellular carcinoma. *World J Gastroenterol*. (2014) 20:10223–37. doi: 10.3748/wjg.v20.i30.10223
121. Bruix J, Gores GJ, Mazzaferro V. Hepatocellular carcinoma: clinical frontiers and perspectives. *Gut* (2014) 63:844–55. doi: 10.1136/gutjnl-2013-306627
122. Balogh J, Victor D, Asham EH, Burroughs SG, Boktour M, Saharia A, et al. Hepatocellular carcinoma: a review. *J Hepatocell Carcinoma* (2016) 3:41–53. doi: 10.2147/JHC.S61146
123. Forner A, Llovet JM, Bruix J. Hepatocellular carcinoma. *Lancet* (2012) 379:1245–55. doi: 10.1016/S0140-6736(11)61347-0
124. Bruix J, Reig M, Sherman M. Evidence-based diagnosis, staging, and treatment of patients with hepatocellular carcinoma. *Gastroenterology* (2016) 150:835–53. doi: 10.1053/j.gastro.2015.12.041
125. Wallace MC, Friedman SL. Hepatic fibrosis and the microenvironment: fertile soil for hepatocellular carcinoma development. *Gene Expr*. (2014) 16:77–84. doi: 10.3727/105221614X13919976902057
126. Lu L-C, Hsu C-H, Hsu C, Cheng A-L. Tumor heterogeneity in hepatocellular carcinoma: facing the challenges. *Liver Cancer* (2016) 5:128–38. doi: 10.1159/000367754

127. Blagotinsek K, Rozman D. Targeting signalling pathways in hepatocellular carcinoma. *Curr Pharm Des*. (2017) 23:170–5. doi: 10.2174/1381612822666161006160005
128. Moeini A, Cornellà H, Villanueva A. Emerging signaling pathways in hepatocellular carcinoma. *Liver Cancer* (2012) 1:83–93. doi: 10.1159/000342405
129. Hernandez-Gea V, Toffanin S, Friedman SL, Llovet JM. Role of the microenvironment in the pathogenesis and treatment of hepatocellular carcinoma. *Gastroenterology* (2013) 144:512–27. doi: 10.1053/j.gastro.2013.01.002
130. Rani B, Cao Y, Malfettone A, Tomuleasa C, Fabregat I, Giannelli G. Role of the tissue microenvironment as a therapeutic target in hepatocellular carcinoma. *World J Gastroenterol*. (2014) 20:4128–40. doi: 10.3748/wjg.v20.i15.4128
131. Achyut BR, Yang L. Transforming growth factor-β in the gastrointestinal and hepatic tumor microenvironment. *Gastroenterology* (2011) 141:1167–78. doi: 10.1053/j.gastro.2011.07.048
132. Sanchez A, Alvarez AM, Benito M, Fabregat I. Transforming growth factor beta modulates growth and differentiation of fetal hepatocytes in primary culture. *J Cell Physiol*. (1995) 165:398–405. doi: 10.1002/jcp.1041650221
133. Massagué J, Blain SW, Lo RS. TGFbeta signaling in growth control, cancer, and heritable disorders. *Cell* (2000) 103:295–309. doi: 10.1016/S0092-8674(00)00121-5
134. Majumdar A, Curley SA, Wu X, Brown P, Hwang JP, Shetty K, et al. Hepatic stem cells and transforming growth factor β in hepatocellular carcinoma. *Nat Rev Gastroenterol Hepatol*. (2012) 9:530–8. doi: 10.1038/nrgastro.2012.114
135. Bornstein S, White R, Malkoski S, Oka M, Han G, Cleaver T, et al. Smad4 loss in mice causes spontaneous head and neck cancer with increased genomic instability and inflammation. *J Clin Invest*. (2009) 119:3408–19. doi: 10.1172/JCI38854
136. Kitisin K, Ganesan N, Tang Y, Jogunoori W, Volpe EA, Kim SS, et al. Disruption of transforming growth factor-beta signaling through beta-spectrin ELF leads to hepatocellular cancer through cyclin D1 activation. *Oncogene* (2007) 26:7103–10. doi: 10.1038/sj.onc.1210513
137. Khor TO, Huang MT, Prawan A, Liu Y, Hao X, Yu S, et al. Increased susceptibility of Nrf2 knockout mice to colitis-associated colorectal cancer. *Cancer Prev Res.* (2008) 1:187–91. doi: 10.1158/1940-6207.CAPR-08-0028
138. Seoane J. Escaping from the TGFbeta anti-proliferative control. *Carcinogenesis* (2006) 27:2148–56. doi: 10.1093/carcin/bgl068
139. Bertran E, Caja L, Navarro E, Sancho P, Mainez J, Murillo MM, et al. Role of CXCR4/SDF-1 alpha in the migratory phenotype of hepatoma cells that have undergone epithelial-mesenchymal transition in response to the transforming growth factor-beta. *Cell Signal*. (2009) 21:1595–606. doi: 10.1016/j.cellsig.2009.06.006
140. Cepeda EB, Dediulia T, Fernando J, Bertran E, Egea G, Navarro E, et al. Mechanisms regulating cell membrane localization of the chemokine receptor CXCR4 in human hepatocarcinoma cells. *Biochim Biophys Acta* (2015) 1853:1205–18. doi: 10.1016/j.bbamcr.2015.02.012
141. Fabregat I, Herrera B, Fernández M, Alvarez AM, Sánchez A, Roncero C, et al. Epidermal growth factor impairs the cytochrome C/caspase-3 apoptotic pathway induced by transforming growth factor beta in rat fetal hepatocytes via a phosphoinositide 3-kinase-dependent pathway. *Hepatology* (2000) 32:528–35. doi: 10.1053/jhep.2000.9774
142. Caja L, Ortiz C, Bertran E, Murillo MM, Miró-Obradors MJ, Palacios E, et al. Differential intracellular signalling induced by TGF-beta in rat adult hepatocytes and hepatoma cells: implications in liver carcinogenesis. *Cell Signal*. (2007) 19:683–94. doi: 10.1016/j.cellsig.2006.09.002
143. Valdés F, Murillo MM, Valverde AM, Herrera B, Sánchez A, Benito M, et al. Transforming growth factor-beta activates both pro-apoptotic and survival signals in fetal rat hepatocytes. *Exp Cell Res*. (2004) 292:209–18. doi: 10.1016/j.yexcr.2003.08.015
144. Wilkes MC, Mitchell H, Penheiter SG, Doré JJ, Suzuki K, Edens M., et al. Transforming growth factor-beta activation of phosphatidylinositol 3-kinase is independent of Smad2 and Smad3 and regulates fibroblast responses via p21-activated kinase-2. *Cancer Res*. (2005) 65, 10431–10440. doi: 10.1158/0008-5472.CAN-05-1522
145. Song K, Wang H, Krebs TL, Danielpour D. Novel roles of Akt and mTOR in suppressing TGF-beta/ALK5-mediated Smad3 activation. *EMBO J*. (2006) 25:58–69. doi: 10.1038/sj.emboj.7600917
146. Murillo MM, del Castillo G, Sánchez A, Fernández M, Fabregat I. Involvement of EGF receptor and c-Src in the survival signals induced by TGF-beta1 in hepatocytes. *Oncogene* (2005) 24:4580–87. doi: 10.1038/sj.onc.1208664
147. Park SS, Eom YW, Kim EH, Lee JH, Min DS, Kim S, et al. Involvement of c-Src kinase in the regulation of TGF-beta1-induced apoptosis. *Oncogene* (2004) 23:6272–81. doi: 10.1038/sj.onc.1207856
148. Fabregat I, Sánchez A, Alvarez AM, Nakamura T, Benito M. Epidermal growth factor, but not hepatocyte growth factor, suppresses the apoptosis induced by transforming growth factor-beta in fetal hepatocytes in primary culture. *FEBS Lett*. (1996) 384:14–8. doi: 10.1016/0014-5793(96)00266-9
149. Carmona-Cuenca I, Herrera B, Ventura J-J, Roncero C, Fernández M, Fabregat I. EGF blocks NADPH oxidase activation by TGF-beta in fetal rat hepatocytes, impairing oxidative stress, and cell death. *J Cell Physiol*. (2006) 207:322–30. doi: 10.1002/jcp.20568
150. Carmona-Cuenca I, Roncero C, Sancho P, Caja L, Fausto N, Fernández M, et al. Upregulation of the NADPH oxidase NOX4 by TGF-beta in hepatocytes is required for its pro-apoptotic activity. *J Hepatol*. (2008) 49:965–76. doi: 10.1016/j.jhep.2008.07.021
151. Sancho P, Fabregat I. NADPH oxidase NOX1 controls autocrine growth of liver tumor cells through up-regulation of the epidermal growth factor receptor pathway. *J Biol Chem*. (2010) 285:24815–24. doi: 10.1074/jbc.M110.114280
152. Murillo MM, Carmona-Cuenca I, Del Castillo G, Ortiz C, Roncero C, Sánchez A, et al. Activation of NADPH oxidase by transforming growth factor-beta in hepatocytes mediates up-regulation of epidermal growth factor receptor ligands through a nuclear factor-kappaB-dependent mechanism. *Biochem J*. (2007) 405:251–9. doi: 10.1042/BJ20061846
153. Moreno-Càceres J, Mainez J, Mayoral R, Martín-Sanz P, Egea G, Fabregat I. Caveolin-1-dependent activation of the metalloprotease TACE/ADAM17 by TGF-β in hepatocytes requires activation of Src and the NADPH oxidase NOX1. *FEBS J*. (2016) 283:1300–10. doi: 10.1111/febs.13669
154. Moreno-Càceres J, Caballero-Díaz D, Chike Nwosu Z, Meyer C, López-Luque J, Malfettone A, et al. The level of caveolin-1 expression determines response to TGF-β as a tumour suppressor in hepatocellular carcinoma cells. *Cell Death Dis*. (2017) 8:e3098. doi: 10.1038/cddis.2017.469
155. Sancho P, Fabregat I. The NADPH oxidase inhibitor VAS2870 impairs cell growth and enhances TGF-β-induced apoptosis of liver tumor cells. *Biochem Pharmacol*. (2011) 81:917–24. doi: 10.1016/j.bcp.2011.01.007
156. Caja L, Bertran E, Campbell J, Fausto N, Fabregat I. The transforming growth factor-beta (TGF-β) mediates acquisition of a mesenchymal stem cell-like phenotype in human liver cells. *J Cell Physiol*. (2011) 226:1214–23. doi: 10.1002/jcp.22439
157. Sánchez A, Alvarez AM, López Pedrosa JM, Roncero C, Benito M, Fabregat I. Apoptotic response to TGF-beta in fetal hepatocytes depends upon their state of differentiation. *Exp Cell Res*. (1999) 252:281–91. doi: 10.1006/excr.1999.4624
158. Caja L, Sancho P, Bertran E, Iglesias-Serret D, Gil J, Fabregat I. Overactivation of the MEK/ERK pathway in liver tumor cells confers resistance to TGF-{beta}-induced cell death through impairing up-regulation of the NADPH oxidase NOX4. *Cancer Res*. (2009) 69:7595–602. doi: 10.1158/0008-5472.CAN-09-1482
159. Coulouarn C, Factor VM, Thorgeirsson SS. Transforming growth factor-beta gene expression signature in mouse hepatocytes predicts clinical outcome in human cancer. *Hepatology* (2008) 47:2059–67. doi: 10.1002/hep.22283
160. Moustakas A, Heldin CH. Induction of epithelial-mesenchymal transition by transforming growth factor β. *Semin Cancer Biol*. (2012) 22:446–54. doi: 10.1016/j.semcancer.2012.04.002
161. Gonzalez DM, Medici D. Signaling mechanisms of the epithelial-mesenchymal transition. *Sci Signal* (2014) 7:re8. doi: 10.1126/scisignal.2005189
162. Willis BC, Liebler JM, Luby-Phelps K, Nicholson AG, Crandall ED, du Bois RM., et al. Induction of epithelial-mesenchymal transition in alveolar epithelial cells by transforming growth factor-beta1: potential

role in idiopathic pulmonary fibrosis. *Am J Pathol*. (2005) 166:1321–32. doi: 10.1016/S0002-9440(10)62351-6
163. Balli D, Ustiyan V, Zhang Y, Wang I-C, Masino AJ, Ren X, et al. Foxm1 transcription factor is required for lung fibrosis and epithelial-to-mesenchymal transition. *EMBO J*. (2013) 32:231–44. doi: 10.1038/emboj.2012.336
164. Bakin AV, Tomlinson AK, Bhowmick NA, Moses HL, Arteaga CL. Phosphatidylinositol 3-kinase function is required for transforming growth factor beta-mediated epithelial to mesenchymal transition and cell migration. *J Biol Chem*. (2000) 275:36803–10. doi: 10.1074/jbc.M005912200
165. Lamouille S, Derynck R. Cell size and invasion in TGF-beta-induced epithelial to mesenchymal transition is regulated by activation of the mTOR pathway. *J Cell Biol*. (2007) 178:437–51. doi: 10.1083/jcb.200611146
166. Pinzani M. Epithelial-mesenchymal transition in chronic liver disease: fibrogenesis or escape from death? *J Hepatol*. (2011) 55:459–65. doi: 10.1016/j.jhep.2011.02.001
167. Bertran E, Crosas-Molist E, Sancho P, Caja L, Lopez-Luque J, Navarro E, et al. Overactivation of the TGF-β pathway confers a mesenchymal-like phenotype and CXCR4-dependent migratory properties to liver tumor cells. *Hepatology* (2013) 58:2032–44. doi: 10.1002/hep.26597
168. Wang B, Hsu S-H, Majumder S, Kutay H, Huang W, Jacob ST, et al. TGFbeta-mediated upregulation of hepatic miR-181b promotes hepatocarcinogenesis by targeting TIMP3. *Oncogene* (2010) 29:1787–97. doi: 10.1038/onc.2009.468
169. Taylor MA, Sossey-Alaoui K, Thompson CL, Danielpour D, Schiemann WP. TGF-β upregulates miR-181a expression to promote breast cancer metastasis. *J Clin Invest*. (2013) 123:150–63. doi: 10.1172/JCI64946
170. Li L, Xu QH, Dong YH, Li GX, Yang L, Wang LW, et al. MiR-181a upregulation is associated with epithelial-to-mesenchymal transition (EMT) and multidrug resistance (MDR) of ovarian cancer cells. *Eur Rev Med Pharmacol Sci*. (2016) 20:2004–10.
171. Chen C, Lou T. Hypoxia inducible factors in hepatocellular carcinoma. *Oncotarget* (2017) 8:46691–703. doi: 10.18632/oncotarget.17358
172. Jou J, Diehl AM. Epithelial-mesenchymal transitions and hepatocarcinogenesis. *J Clin Invest*. (2010) 120:1031–4. doi: 10.1172/JCI42615
173. Pani G, Galeotti T, Chiarugi P. Metastasis: cancer cell's escape from oxidative stress. *Cancer Metastasis Rev*. (2010) 29:351–78. doi: 10.1007/s10555-010-9225-4
174. Copple BL. Hypoxia stimulates hepatocyte epithelial to mesenchymal transition by hypoxia-inducible factor and transforming growth factor-beta-dependent mechanisms. *Liver Int*. (2010) 30:669–82. doi: 10.1111/j.1478-3231.2010.02205.x
175. Lee J-S, Heo J, Libbrecht L, Chu I-S, Kaposi-Novak P, Calvisi DF, et al. A novel prognostic subtype of human hepatocellular carcinoma derived from hepatic progenitor cells. *Nat Med*. (2006) 12:410–6. doi: 10.1038/nm1377
176. Rao S, Zaidi S, Banerjee J, Jogunoori W, Sebastian R, Mishra B, et al. Transforming growth factor-β in liver cancer stem cells and regeneration. *Hepatol Commun*. (2017) 1:477–93. doi: 10.1002/hep4.1062
177. Malfettone A, Soukupova J, Bertran E, Crosas-Molist E, Lastra R, Fernando J, et al. Transforming growth factor-β-induced plasticity causes a migratory stemness phenotype in hepatocellular carcinoma. *Cancer Lett*. (2017) 392:39–50. doi: 10.1016/j.canlet.2017.01.037
178. del Castillo G, Alvarez-Barrientos A, Carmona-Cuenca I, Fernández M, Sánchez A, Fabregat I. Isolation and characterization of a putative liver progenitor population after treatment of fetal rat hepatocytes with TGF-beta. *J Cell Physiol*. (2008) 215:846–55. doi: 10.1002/jcp.21370
179. Wu K, Ding J, Chen C, Sun W, Ning BF, Wen W., et al. (2012). Hepatic transforming growth factor beta gives rise to tumor-initiating cells and promotes liver cancer development. *Hepatology* 56, 2255–2267. doi: 10.1002/hep.26007
180. Paik J-H, Kollipara R, Chu G, Ji H, Xiao Y, Ding Z, et al. FoxOs are lineage-restricted redundant tumor suppressors and regulate endothelial cell homeostasis. *Cell* (2007) 128:309–23. doi: 10.1016/j.cell.2006.12.029
181. Mima K, Okabe H, Ishimoto T, Hayashi H, Nakagawa S, Kuroki H, et al. CD44s regulates the TGF-β-mediated mesenchymal phenotype and is associated with poor prognosis in patients with hepatocellular carcinoma. *Cancer Res*. (2012) 72:3414–23. doi: 10.1158/0008-5472.CAN-12-0299
182. Nomura A, Banerjee S, Chugh R, Dudeja V, Yamamoto M, Vickers SM, et al. CD133 initiates tumors, induces epithelial-mesenchymal transition and increases metastasis in pancreatic cancer. *Oncotarget* (2015) 6:8313–22. doi: 10.18632/oncotarget.3228
183. Fernando J, Malfettone A, Cepeda EB, Vilarrasa-Blasi R, Bertran E, Raimondi G, et al. A mesenchymal-like phenotype and expression of CD44 predict lack of apoptotic response to sorafenib in liver tumor cells. *Int J Cancer* (2015) 136:E161–172. doi: 10.1002/ijc.29097
184. Hashimoto N, Tsunedomi R, Yoshimura K, Watanabe Y, Hazama S, Oka M. Cancer stem-like sphere cells induced from de-differentiated hepatocellular carcinoma-derived cell lines possess the resistance to anti-cancer drugs. *BMC Cancer* (2014) 14:722. doi: 10.1186/1471-2407-14-722
185. Rani B, Malfettone A, Dituri F, Soukupova J, Lupo L, Mancarella S, et al. Galunisertib suppresses the staminal phenotype in hepatocellular carcinoma by modulating CD44 expression. *Cell Death Dis*. (2018) 9:373. doi: 10.1038/s41419-018-0384-5
186. Bitzer M, Horger M, Giannini EG, Ganten TM, Wörns MA, Siveke JT, et al. Resminostat plus sorafenib as second-line therapy of advanced hepatocellular carcinoma - The SHELTER study. *J Hepatol*. (2016) 65:280–8. doi: 10.1016/j.jhep.2016.02.043
187. Soukupova J, Bertran E, Peñuelas-Haro I, Urdiroz-Urricelqui U, Borgman M, Kohlhof H, et al. Resminostat induces changes in epithelial plasticity of hepatocellular carcinoma cells and sensitizes them to sorafenib-induced apoptosis. *Oncotarget* (2017) 8:110367–79. doi: 10.18632/oncotarget.22775
188. Fransvea E, Mazzocca A, Antonaci S, Giannelli G. Targeting transforming growth factor (TGF)-betaRI inhibits activation of beta1 integrin and blocks vascular invasion in hepatocellular carcinoma. *Hepatology* (2009) 49:839–50. doi: 10.1002/hep.22731
189. Bhowmick NA, Neilson EG, Moses HL. Stromal fibroblasts in cancer initiation and progression. *Nature* (2004) 432:332–7. doi: 10.1038/nature03096
190. Eiró N, Vizoso FJ. Importance of tumor/stroma interactions in prognosis of hepatocellular carcinoma. *Hepatobiliary Surg Nutr*. (2014) 3:98–101. doi: 10.3978/j.issn.2304-3881.2014.02.12
191. Kubo N, Araki K, Kuwano H, Shirabe K. Cancer-associated fibroblasts in hepatocellular carcinoma. *World J Gastroenterol*. (2016) 22:6841–50. doi: 10.3748/wjg.v22.i30.6841
192. Lau EYT, Lo J, Cheng BYL, Ma MKF, Lee JMF, Ng JKY, et al. Cancer-associated fibroblasts regulate tumor-initiating cell plasticity in hepatocellular carcinoma through c-Met/FRA1/HEY1 Signaling. *Cell Rep*. (2016) 15:1175–89. doi: 10.1016/j.celrep.2016.04.019
193. Liu J, Chen S, Wang W, Ning B-F, Chen F, Shen W, et al. Cancer-associated fibroblasts promote hepatocellular carcinoma metastasis through chemokine-activated hedgehog and TGF-β pathways. *Cancer Lett*. (2016) 379:49–59. doi: 10.1016/j.canlet.2016.05.022
194. Kuang D-M, Zhao Q, Peng C, Xu J, Zhang J-P, Wu C, et al. Activated monocytes in peritumoral stroma of hepatocellular carcinoma foster immune privilege and disease progression through PD-L1. *J Exp Med*. (2009) 206:1327–37. doi: 10.1084/jem.20082173
195. Zhang HH, Mei MH, Fei R, Liu F, Wang JH, Liao WJ, et al. Regulatory T cells in chronic hepatitis B patients affect the immunopathogenesis of hepatocellular carcinoma by suppressing the anti-tumour immune responses. *J Viral Hepat*. (2010) 17 (Suppl. 1):34–43. doi: 10.1111/j.1365-2893.2010.01269.x
196. Sprinzl MF, Galle PR. Immune control in hepatocellular carcinoma development and progression: role of stromal cells. *Semin Liver Dis*. (2014) 34:376–88. doi: 10.1055/s-0034-1394138
197. Solinas G, Germano G, Mantovani A, Allavena P. Tumor-associated macrophages (TAM) as major players of the cancer-related inflammation. *J Leukoc Biol*. (2009) 86:1065–73. doi: 10.1189/jlb.0609385
198. Pollard JW. Tumour-educated macrophages promote tumour progression and metastasis. *Nat Rev Cancer* (2004) 4:71–8. doi: 10.1038/nrc1256
199. Qian B-Z, Pollard JW. Macrophage diversity enhances tumor progression and metastasis. *Cell* (2010) 141:39–51. doi: 10.1016/j.cell.2010.03.014
200. Lewis CE, Pollard JW. Distinct role of macrophages in different tumor microenvironments. *Cancer Res*. (2006) 66:605–12. doi: 10.1158/0008-5472.CAN-05-4005

201. Shirabe K, Mano Y, Muto J, Matono R, Motomura T, Toshima T, et al. Role of tumor-associated macrophages in the progression of hepatocellular carcinoma. *Surg Today* (2012) 42:1–7. doi: 10.1007/s00595-011-0058-8
202. Fan Q-M, Jing Y-Y, Yu G-F, Kou X-R, Ye F, Gao L, et al. Tumor-associated macrophages promote cancer stem cell-like properties via transforming growth factor-beta1-induced epithelial-mesenchymal transition in hepatocellular carcinoma. *Cancer Lett*. (2014) 352:160–8. doi: 10.1016/j.canlet.2014.05.008
203. Li T, Yang Y, Hua X, Wang G, Liu W, Jia C, et al. Hepatocellular carcinoma-associated fibroblasts trigger NK cell dysfunction via PGE2 and IDO. *Cancer Lett*. (2012) 318:154–61. doi: 10.1016/j.canlet.2011.12.020
204. Cheng J-T, Deng Y-N, Yi H-M, Wang G-Y, Fu B-S, Chen W-J, et al. Hepatic carcinoma-associated fibroblasts induce IDO-producing regulatory dendritic cells through IL-6-mediated STAT3 activation. *Oncogenesis* (2016) 5:e198. doi: 10.1038/oncsis.2016.7
205. Yang L, Pang Y, Moses HL. TGF-beta and immune cells: an important regulatory axis in the tumor microenvironment and progression. *Trends Immunol*. (2010) 31:220–7. doi: 10.1016/j.it.2010.04.002
206. Francisco LM, Salinas VH, Brown KE, Vanguri VK, Freeman GJ, Kuchroo VK, et al. PD-L1 regulates the development, maintenance, and function of induced regulatory T cells. *J Exp Med*. (2009) 206:3015–29. doi: 10.1084/jem.20090847
207. Grivennikov SI, Greten FR, Karin M. Immunity, inflammation, and cancer. *Cell* (2010) 140:883–99. doi: 10.1016/j.cell.2010.01.025
208. Chen DS, Mellman I. Oncology meets immunology: the cancer-immunity cycle. *Immunity* (2013) 39:1–10. doi: 10.1016/j.immuni.2013.07.012
209. Flavell RA, Sanjabi S, Wrzesinski SH, Licona-Limón P. The polarization of immune cells in the tumour environment by TGFbeta. *Nat Rev Immunol*. (2010) 10:554–67. doi: 10.1038/nri2808
210. Sakaguchi S, Yamaguchi T, Nomura T, Ono M. Regulatory T cells and immune tolerance. *Cell* (2008) 133:775–87. doi: 10.1016/j.cell.2008.05.009
211. Zhou L, Chong MMW, Littman DR. Plasticity of CD4+ T cell lineage differentiation. *Immunity* (2009) 30:646–55. doi: 10.1016/j.immuni.2009.05.001
212. Chen W, Jin W, Hardegen N, Lei K-J, Li L, Marinos N, et al. Conversion of peripheral CD4+CD25- naive T cells to CD4+CD25+ regulatory T cells by TGF-beta induction of transcription factor Foxp3. *J Exp Med*. (2003) 198:1875–86. doi: 10.1084/jem.20030152
213. Shen Y, Wei Y, Wang Z, Jing Y, He H, Yuan J, et al. TGF-β regulates hepatocellular carcinoma progression by inducing treg cell polarization. *CPB* (2015) 35:1623–32. doi: 10.1159/000373976
214. Giannelli G, Mazzocca A, Fransvea E, Lahn M, Antonaci S. Inhibiting TGF-β signaling in hepatocellular carcinoma. *Biochim Biophys Acta* (2011) 1815:214–23. doi: 10.1016/j.bbcan.2010.11.004
215. Zhang S, Sun W-Y, Wu J-J, Wei W. TGF-β signaling pathway as a pharmacological target in liver diseases. *Pharmacol. Res.* (2014) 85:15–22. doi: 10.1016/j.phrs.2014.05.005
216. Mazzocca A, Fransvea E, Dituri F, Lupo L, Antonaci S, Giannelli G. Down-regulation of connective tissue growth factor by inhibition of transforming growth factor beta blocks the tumor-stroma cross-talk and tumor progression in hepatocellular carcinoma. *Hepatology* (2010) 51:523–34. doi: 10.1002/hep.23285
217. Fabregat I, Fernando J, Mainez J, Sancho P. TGF-beta signaling in cancer treatment. *Curr Pharm Des*. (2014) 20:2934–47. doi: 10.2174/13816128113199990591
218. Ezquerro IJ, Lasarte JJ, Dotor J, Castilla-Cortázar I, Bustos M, Peñuelas I., et al. A synthetic peptide from transforming growth factor beta type III receptor inhibits liver fibrogenesis in rats with carbon tetrachloride liver injury. *Cytokine* (2003) 22:12–20. doi: 10.1016/S1043-4666(03)00101-7
219. Dotor J, López-Vázquez AB, Lasarte JJ, Sarobe P, García-Granero M, Riezu-Boj JI., et al. Identification of peptide inhibitors of transforming growth factor beta 1 using a phage-displayed peptide library. *Cytokine* (2007) 39:106–15. doi: 10.1016/j.cyto.2007.06.004
220. Llopiz D, Dotor J, Casares N, Bezunartea J, Díaz-Valdés N, Ruiz M, et al. Peptide inhibitors of transforming growth factor-beta enhance the efficacy of antitumor immunotherapy. *Int J Cancer* (2009) 125:2614–23. doi: 10.1002/ijc.24656
221. Hanafy NAN, Quarta A, Di Corato R, Dini L, Nobile C, Tasco V, et al. Hybrid polymeric-protein nano-carriers (HPPNC) for targeted delivery of TGFβ inhibitors to hepatocellular carcinoma cells. *J Mater Sci Mater Med*. (2017) 28:120. doi: 10.1007/s10856-017-5930-7
222. Dituri F, Mazzocca A, Fernando J, Peidrò FJ, Papappicco P, Fabregat I., et al. Differential inhibition of the TGF-β signaling pathway in HCC Cells Using the Small Molecule Inhibitor LY2157299 and the D10 Monoclonal Antibody against TGF-β Receptor Type II. *PLoS ONE* (2013) 8:e67109. doi: 10.1371/annotation/c943a596-3965-4a5b-a27c-55c16685ea32
223. Serova M, Tijeras-Raballand A, Dos Santos C, Albuquerque M, Paradis V, Neuzillet C, et al. Effects of TGF-beta signalling inhibition with galunisertib (LY2157299) in hepatocellular carcinoma models and in *ex vivo* whole tumor tissue samples from patients. *Oncotarget* (2015) 6:21614–27. doi: 10.18632/oncotarget.4308
224. Liang S, Hu J, Xie Y, Zhou Q, Zhu Y, Yang X. A polyethylenimine-modified carboxyl-poly(styrene/acrylamide) copolymer nanosphere for co-delivering of CpG and TGF-β receptor I inhibitor with remarkable additive tumor regression effect against liver cancer in mice. *Int J Nanomedicine* (2016b) 11:6753–62. doi: 10.2147/IJN.S122047
225. Luangmonkong T, Suriguga S, Bigaeva E, Boersema M, Oosterhuis D, de Jong KP, et al. Evaluating the antifibrotic potency of galunisertib in a human *ex vivo* model of liver fibrosis. *Br J Pharmacol*. (2017) 174:3107–17. doi: 10.1111/bph.13945
226. Hammad S, Cavalcanti E, Werle J, Caruso ML, Dropmann A, Ignazzi A, et al. Galunisertib modifies the liver fibrotic composition in the Abcb4Ko mouse model. *Arch Toxicol*. (2018) 92:2297–309. doi: 10.1007/s00204-018-2231-y
227. Hanafy NAN, Quarta A, Ferraro MM, Dini L, Nobile C, De Giorgi ML, et al. Polymeric Nano-micelles as novel cargo-carriers for LY2157299 liver cancer cells delivery. *Int J Mol Sci* (2018) 19: E748. doi: 10.3390/ijms19030748
228. Fischer ANM, Fuchs E, Mikula M, Huber H, Beug H, Mikulits W. PDGF essentially links TGF-beta signaling to nuclear beta-catenin accumulation in hepatocellular carcinoma progression. *Oncogene* (2007) 26:3395–405. doi: 10.1038/sj.onc.1210121
229. Cao Y, Agarwal R, Dituri F, Lupo L, Trerotoli P, Mancarella S, et al. NGS-based transcriptome profiling reveals biomarkers for companion diagnostics of the TGF-β receptor blocker galunisertib in HCC. *Cell Death Dis*. (2017) 8:e2634. doi: 10.1038/cddis.2017.44

Conflict of Interest Statement: The authors declare that the research was conducted in the absence of any commercial or financial relationships that could be construed as a potential conflict of interest.

frontiers in Oncology

ORIGINAL RESEARCH
published: 05 September 2018
doi: 10.3389/fonc.2018.00337

Phenotypic Basis for Matrix Stiffness-Dependent Chemoresistance of Breast Cancer Cells to Doxorubicin

*M. Hunter Joyce[1], Carolyne Lu[1], Emily R. James[1], Rachel Hegab[2], Shane C. Allen[1], Laura J. Suggs[1,3] and Amy Brock[1,3]**

[1] Department of Biomedical Engineering, University of Texas at Austin, Austin, TX, United States, [2] Department of Biomedical Engineering, Louisiana Tech University, Ruston, LA, United States, [3] Institute for Cellular and Molecular Biology, University of Texas at Austin, Austin, TX, United States

The persistence of drug resistant cell populations following chemotherapeutic treatment is a significant challenge in the clinical management of cancer. Resistant subpopulations arise via both cell intrinsic and extrinsic mechanisms. Extrinsic factors in the microenvironment, including neighboring cells, glycosaminoglycans, and fibrous proteins impact therapy response. Elevated levels of extracellular fibrous proteins are associated with tumor progression and cause the surrounding tissue to stiffen through changes in structure and composition of the extracellular matrix (ECM). We sought to determine how this progressively stiffening microenvironment affects the sensitivity of breast cancer cells to chemotherapeutic treatment. MDA-MB-231 triple negative breast carcinoma cells cultured in a 3D alginate-based hydrogel system displayed a stiffness-dependent response to the chemotherapeutic doxorubicin. MCF7 breast carcinoma cells cultured in the same conditions did not exhibit this stiffness-dependent resistance to the drug. This differential therapeutic response was coordinated with nuclear translocation of YAP, a marker of mesenchymal differentiation. The stiffness-dependent response was lost when cells were transferred from 3D to monolayer cultures, suggesting that endpoint ECM conditions largely govern the response to doxorubicin. To further examine this response, we utilized a platform capable of dynamic ECM stiffness modulation to allow for a change in matrix stiffness over time. We found that MDA-MB-231 cells have a stiffness-dependent resistance to doxorubicin and that duration of exposure to ECM stiffness is sufficient to modulate this response. These results indicate the need for additional tools to integrate mechanical stiffness with therapeutic response and inform decisions for more effective use of chemotherapeutics in the clinic.

Keywords: chemotherapy, resistance, extracellular matrix, tumor microenvironment, 3D cell culture

OPEN ACCESS

Edited by:
Ubaldo Emilio Martinez-Outschoorn, Thomas Jefferson University, United States

Reviewed by:
Hamid Morjani, Université de Reims Champagne Ardenne, France
Saraswati Sukumar, Johns Hopkins University, United States

***Correspondence:**
Amy Brock
amy.brock@utexas.edu

Specialty section:
This article was submitted to Molecular and Cellular Oncology, a section of the journal Frontiers in Oncology

Received: *07 May 2018*
Accepted: *03 August 2018*
Published: *05 September 2018*

Citation:
Joyce MH, Lu C, James ER, Hegab R, Allen SC, Suggs LJ and Brock A (2018) Phenotypic Basis for Matrix Stiffness-Dependent Chemoresistance of Breast Cancer Cells to Doxorubicin. Front. Oncol. 8:337. doi: 10.3389/fonc.2018.00337

INTRODUCTION

Cancer is a complex disease capable of affecting multiple properties of tissue organization and is driven by numerous factors. Hanahan and Weinberg (1, 2) have summarized and defined "hallmarks of cancer" which describe biological conditions characteristic of tumorigenesis. Pickup (3) revisited these hallmarks and described roles that the extracellular matrix (ECM) plays in

each. The ECM includes the non-cellular components of a cell's microenvironment responsible for providing physical scaffolding and facilitating signaling from the surrounding tissue (4). Studies aimed at characterizing the role that physical cues play in tumor development have demonstrated that ligand type, ligand density, substrate composition, and substrate stiffness are important factors in tumor initiation, progression, and metastasis (5–12). Additional studies investigate how cells manipulate the ECM and vice-versa, suggesting a reciprocal nature whereby each shapes the response of the other (7, 8, 13–15).

With cellular remodeling of the ECM, tumors become progressively more rigid than surrounding tissue, a characteristic that informs diagnosis by physical palpitation and imaging (16). These serve as early detection methods for breast cancer (16), the second leading cause of cancer death among women (17). The ECM influences organization (15) and differentiation (18, 19) of mammary cells into functional mammary structures and tissues. It plays a role in tumor suppression through trafficking of intercellular signals (20) and exerting physical forces sensed by cell surface proteins, such as integrins (10, 13, 15). Changes in the ECM composition (15, 18, 19, 21) and stiffness (6–8, 15, 22, 23) have been shown to promote malignant phenotypes. Previous work in the field has investigated the role of ECM in determining cellular response to chemotherapy treatment (9, 24). Rice et al. (25) and Zustiak et al. (26) both demonstrate that ECM stiffness can alter chemotherapeutic response for some cancer cell lines. Shin and Mooney (9) examined the relationship between ECM ligands and cancer cell resistance to chemotherapeutics. Here we utilize a hydrogel platform to examine how ECM stiffness and the dynamic modulation of that microenvironmental stiffness affect the response of two distinct breast carcinoma cell lines to chemotherapeutic treatment.

Hydrogels have served to isolate and model aspects of the ECM for *in vitro* studies of cellular organization (15) and differentiation (18, 26, 27), tumor suppression (10, 13, 15), tumorigenesis (6, 13, 28–30), promotion of malignant phenotypes (6–8, 15, 22, 23), and cellular response to chemotherapy (9, 24, 31). Materials native to mammalian cellular ECM (i.e., scaffolding proteins such as collagens and fibrins) as well as biomimetic materials (such as agar and acrylamide) are used to produce 3D scaffolds for *in vitro* cultures. The mechanical properties of these hydrogel scaffolds are largely determined during the initial preparation; overall stiffness of the hydrogel is determined by the density of protein/polymer or number of cross-links formed. However, with these systems is it not possible to adjust matrix stiffness in a controlled manner after initial formation of the hydrogel. Recent work has shown that the contractile force of MDA-MB-231 cells can cause significant increases in stiffness of their surrounding ECM (32). Microrheology with optical tweezers has been used to measure the stiffness gradient created by cells grown in collagen hydrogels; the linear stiffness of hydrogels adjacent to MDA-MB-231 cells was measured to be up to two orders of magnitude stiffer than areas of unoccupied hydrogel 200 μm away. Similar stiffening was seen for MDA-MB-231 cells in Matrigel cultures and human umbilical vein endothelial cells in fibrin hydrogels, indicating that maintaining hydrogel stiffness within a defined range will be challenging as cells rearrange their ECM over time.

Our studies utilized the alginate-based hydrogel system described by Stowers et al. (33) as a means to predictably modulate hydrogel stiffness. Alginate is bio-inert, and alginate polymers can be cross-linked with calcium ions, providing a means for controlling hydrogel stiffness. Additionally, this system incorporates 1,2-dipalmitoyl-sn-glycero-3-phosphocholine (DPPC) liposomes loaded with calcium and gold nanorods. Irradiation with NIR light causes the gold nanorods to undergo surface plasmon resonance and heat the liposomes. As the liposomes approach the phase transition temperature (41°C), they undergo gel-to-liquid transition causing the encapsulated calcium to leak out and form additional alginate cross-links. This experimental platform allowed us to seed breast cancer cells into hydrogels of an initial stiffness (200 and 2,000 Pa), further stiffen their ECM during the course of the experiment (200 1,600 Pa and 2,000 3,000 Pa), and treat samples with the chemotherapeutic doxorubicin to determine how dynamic changes to the ECM affect chemotherapeutic resistance. Here we show that stiffness of the ECM is sufficient to modulate MDA-MB-231 breast cancer cell resistance to doxorubicin.

MATERIALS AND METHODS

Cell Culture

MDA-MB-231 cells were cultured in Dulbecco's Modified Eagle's Medium (DMEM, Life Technologies, REF: 10569-010, 94%) supplemented with FBS (Life Technologies, REF: 10437-028 5%) and P/S (Life Technologies, REF: 15070-063, 1%). MCF7 cells were cultured in Minimum Essential Media (MEM, Life Technologies, REF: 11095-080, 89%) supplemented with Fetal Bovine Serum (FBS, Life Technologies, REF: 10437-028, 10%) and Penicillin/Streptomycin (P/S, Life Technologies, REF: 15070-063, 1%). All cultures were incubated at 37°C with 5% CO_2.

Hydrogel Preparation

Hydrogels were prepared by mixing the following ingredients in the order described with thorough mixing after addition of each ingredient: 4% alginate (Pronova UP MVG; 40% total volume, 1.6% final concentration), 5–20 mM calcium carbonate (5% total volume), liposomes loaded 500 mM calcium chloride plus AuNRs (20% total volume), cells (8 million cells/mL; 5% total volume), 10–40 mM D-(+)-Gluconic acid δ-lactone (Sigma-Aldrich, G4750; 5% total volume), and Matrigel (VWR International, 47743-715; 25% total volume). Once mixed, 50 μL of the gel solution was pipetted into each well of a 96-well plate and placed in an incubator (37°C, 5% CO_2) for 1 h to promote gelation. After gelation, 100 μL of media was added to each sample and placed back in an incubator.

Liposome Preparation

Liposomes were prepared using the interdigitation-fusion method described by Ahl et al. (34). 1,2-dipalmitoyl-sn-glycero-3-phosphocholine (DPPC, Avanti, 850355P/C) was diluted in chloroform (Fisher Scientific, CAS: 67-66-3) at 25 mg/mL and rotary evaporation (150 mbar vacuum, ∼60 rpm, 55°C, 15 min.)

was used to coat a round-bottom flask with thin layers of lipids. After 15 min. on the rotovap, the newly formed lipid cake was placed in a desiccator overnight to ensure complete evaporation of any residual chloroform. The lipid cake was rehydrated with 2 mL of ultra-pure water and placed on a rotator for 30 min. to ensure hydration of the entire lipid cake. The solution was then sonicated via sonic probe (60% amplitude for 10 min.) to form small unilaminar vesicles. At this point, the lipid solution was passed through a 0.22 μM filter (Millipore, SLGS033SB) and 424 μL of 100% ethanol (Fisher Scientific, CAS: 64-17-5) was added to form interdigitated sheets. Gold nanorods and 500 mM calcium chloride (Sigma-Aldrich, C1016) was added and allowed to incubate at 55°C for 2 h with gentle agitation every 30 min. to ensure encapsulation of cargo into newly forming liposomes. After incubation, a series of washes with 300 mM sodium chloride (Fisher Scientific, 7647-14-5) plus 1 mM HEPES (Sigma-Aldrich, H3375) was done to remove any free-floating nanorods or calcium.

Dynamic Stiffening of Alginate Hydrogels

Prior to exposing samples to near infrared light, all media was removed from each sample to minimize light scattering. A Lasermate (IML808-2500FLAM4A) set at 2.0 W was used to irradiate samples for 45 s each. After irradiating the final sample, 100 μL of fresh culture media was added to each well and the samples were placed back in an incubator (37°C, 5% CO_2).

Rheometry

To determine stiffness of the hydrogels used, gel solutions were prepared and pipetted into PDMS molds, incubated at room temperature for 2 h, and measured on a Physica MCR 101 Rheometer using an 8 mm geometry (Anton Paar, Cat.#: 5681). Rheoplus (v3.40) software was used to take frequency sweep measurements from 0.05 to 500 rad/s with 5% initial strain.

Dosing With Chemotherapeutics

Samples were exposed to doxorubicin (Sigma-Aldrich, Cat.#: D1515) for 48 h. A broad range (1 nM – 200 μM) of doses was used to determine the drug sensitivity.

Isolation of Cells From Hydrogels

To extract the cells cultured in hydrogels for analysis, each 50 μL gel was soaked in 100 μL of 50 mM sodium citrate (Fisher Scientific, Cat#: BP327) for 15 min. at room temperature. Gels were then mechanically disrupted by pipetting until the alginate dissolved to a liquid solution. Each sample was transferred to a microcentrifuge tube and centrifuged at 600 × g for 10 min. to pellet.

Measuring Viability

Viability measures were assessed using acridine orange/propidium iodide (AOPI, Nexcelom, Cat#: CS2-0106) stain. Samples treated with AOPI were pelleted, resuspended in AccuMAX (Innovative Cell Technologies, Cat.#: AM-105), and mixed 1:1 with AOPI stain. A Nexcelom Cellometer Vision was used to count live cells. The data gathered from cell viability assays was fit to a sigmoid function in Microsoft Excel and used to calculate drug sensitivity, as measured by LD50 value.

Staining for EMT Markers

Samples were fixed with a 15 min. exposure to 4% paraformaldehyde at room temperature. Blocking and permeabilization buffer (0.1% Triton X-100 and 1% bovine serum albumin [BSA] diluted in 1 × PBS) was added to each sample and incubated at room temperature for 1 h. Following this, samples were incubated with primary antibody against YAP (Santa Cruz, sc-101199) for 1 h at room temperature. Cell nuclei were stained with 300 nM DAPI (ThermoFisher, D1306) for 30 min. at room temperature before being imaged on a Zeiss confocal or EVOS epifluorescent microscope.

Quantitative Real-Time PCR

Total RNA was extracted using the RNeasy Mini Kit (Qiagen, 74104, Hilden, Germany) and was reverse-transcribed using the High-Capacity cDNA Reverse Transcription Kit (Applied Biosystems, 4368814) according to the manufacturer's instructions. Quantitative PCR was performed using the PowerUp SYBR Green Master Mix (Applied Biosystems, A25743) with 20 ng cDNA input in 20 μl reaction volume run on a ViiA7 Real-Time PCR system (Applied Biosciences). GAPDH (glyceraldehyde 3-phosphate dehydrogenase) expression level was used for normalization as a housekeeping gene. The primers for GAPDH (HK-GAPDH) and CDH1 (VHPS-1738; E-Cadherin) were designed and synthesized by RealTimePrimers.com (www.realtimeprimers.com).

Statistical Analysis

A two-tailed Student's *t*-test assuming unequal variance was used to compare samples, and a *p*-value of less than 0.05 was used to determine statistical significance. Microsoft Excel Solver was used to fit cell viability data to a sigmoidal function to generate LD50 curves.

RESULTS

MDA-MB-231 Cells Exhibit Stiffness-Dependent Resistance to Doxorubicin

Cells were cultured either as a monolayer on tissue culture plastic (2D) or in alginate-Matrigel hydrogels (3D) for six days before treatment with doxorubicin (**Figure 1A**). Oscillatory shear stress rheometry (1% strain, 0.5–50 Hz) was used to measure hydrogel stiffness. The elastic modulus was calculated for each frequency measured within this range (static soft = 228 Pa, $n = 3$; stiffened soft = 1,552, $n = 2$; static stiff = 1,958 Pa, $n = 5$; stiffened stiff = 3,210 Pa, $n = 5$; **Figure 1B**). We observed that chemoresistance of MDA-MB-231 cells to doxorubicin was 3-fold higher in the stiff ECM environment (LD50 = 10 μM in 200 Pa hydrogel cultures vs. LD50 = 32 μM in 2,000 Pa cultures; $p = 0.002$; **Figures 2A,C**). MCF7 cells did not display any significant ($p = 0.134$; **Figures 2B,D**) differences in resistance across substrates of increasing stiffness. When cultured as a monolayer on tissue culture plastic, MDA-MB-231 cells (LD50 = 27 μM; **Figure 2E**) were found to be more resistant ($p = 0.001$)

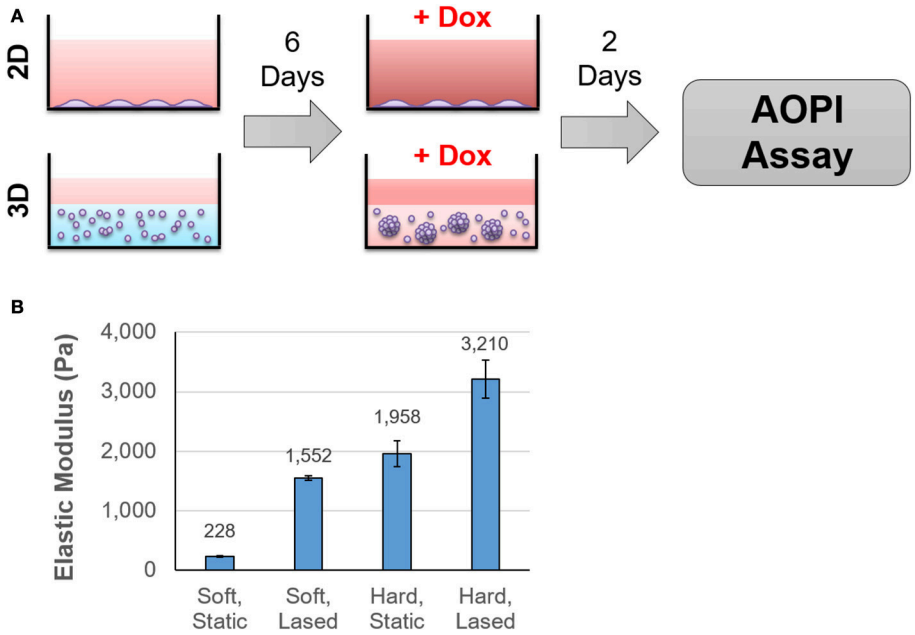

FIGURE 1 | Cells were cultured in hydrogels of varying stiffness before treatment with doxorubicin. The experimental protocol is outlined in **(A)**. Briefly, cells were seeded onto tissue culture plastic or into hydrogels that ranged in stiffness from 200 to 2,000 Pa. After 6 days in culture, samples were exposed to doxorubicin for 48 h and cell viability was determined using AOPI staining. Hydrogel stiffness was determined by calculating Young's modulus from frequency sweep measurements obtained from a rheometer **(B)**.

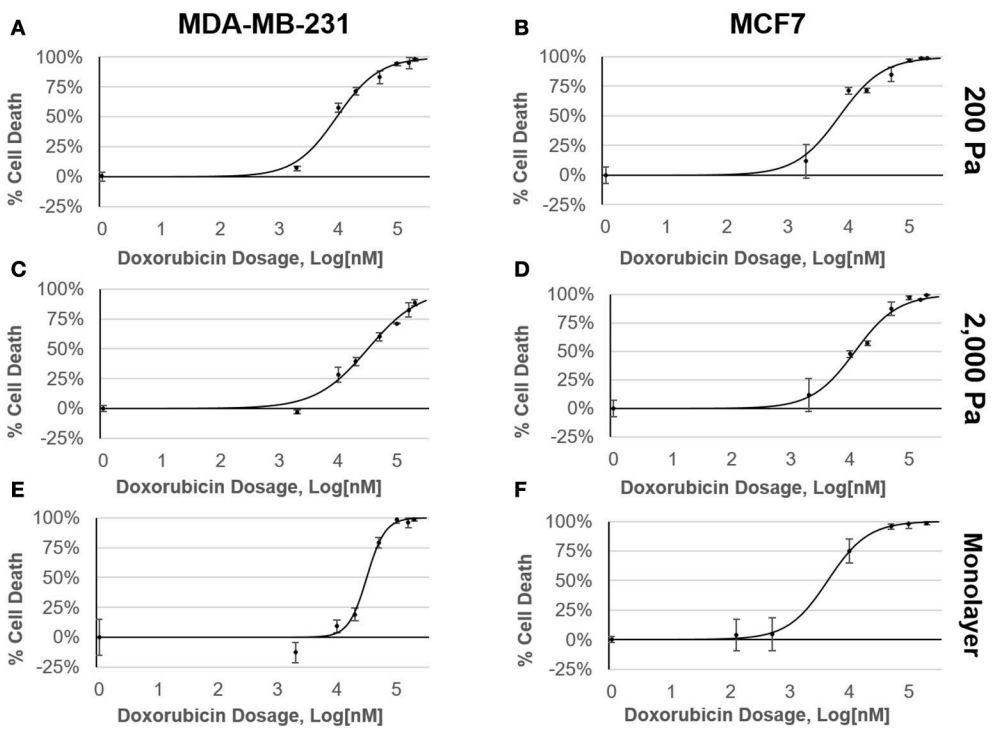

FIGURE 2 | MDA-MB-231 cells have a stiffness-dependent resistance to doxorubicin. Dose response curves of MDA-MB-231 and MCF7 cells cultured in **(A,B)** 200 Pa hydrogel, **(C,D)** 2,000 Pa hydrogel, and **(E,F)** 2D monolayer following 48 h exposure to doxorubicin. Percent cell death was determined by staining samples with AOPI and counting live cells using a Nexcelom Cellometer.

to doxorubicin than similar MCF7 cultures (LD50 = 4 μM; **Figure 2F**).

To further investigate this stiffness-dependence, cells were cultured in an alginate-Matrigel hydrogel platform, as described in Stowers et al. (33), which uses calcium-loaded liposomes to drive cross-linking following exposure to near infrared (NIR) light. Cells were initially cultured in hydrogels, for 3 days to begin formation of micro-structures (**Figure 3A**). Hydrogels were stiffened via NIR triggered cross-linking (**Figures 3B,C**), and cells were cultured for 3 additional days before treatment with doxorubicin for 48 h (**Figure 3A**). NIR light alone was not shown to significantly affect resistance to doxorubicin ($p = 0.06$; **Supplementary Figure 1**). MDA-MB-231 cultures that were grown in dynamically stiffened hydrogels had a significant decrease in sensitivity to doxorubicin for cultures that were stiffened from 200 Pa to 1,600 Pa (LD50 = 10 μM in 200 Pa static cultures vs. LD50 = 80 μM in cultures stiffened from 200 to 1,600 Pa; $p = 0.004$; **Figure 4A**) as well as those stiffened from 2,000 to 3,000 Pa (LD50 = 32 μM in 2,000 Pa static cultures vs. LD50 = 185 μM in cultures stiffened from 2,000 to 3,000 Pa, $p = 0.014$) compared to their static hydrogel counterparts (**Figure 4A**). This relationship was not observed in MCF7 (**Figure 4B**); there was no statistically significant difference in sensitivity to doxorubicin for cultures stiffened from 200 to 1,600 Pa (LD50 = 6 μM in 200 Pa static cultures vs. LD50 = 13 μM in cultures stiffened from 200 to 1,600 Pa; $p = 0.143$) or 2,000 to 3,000 Pa (LD50 = 12 μM in 2,000 Pa static cultures vs. LD50 = 17 μM in cultures stiffened from 2,000 to 3,000 Pa; $p = 0.492$) when compared to static cultures.

Duration of Acclimation Modulates Stiffness-Dependent Resistance

The time between dynamic stiffening of hydrogel cultures and treatment with doxorubicin was varied to determine if cells undergo adaptation to stiffened ECM that may alter drug sensitivity. Cells were cultured in hydrogels for 3 days to allow formation of micro-structures before being exposed to NIR to induce dynamic stiffening. Cultures were then maintained 24, 72, or 120 h in the stiffened ECM before treatment with doxorubicin. Resistance to doxorubicin peaked in MDA-MB-231 cells that were treated 72 h post-stiffening with an LD50 of 80 μM for cultures stiffened from 200 to 1,600 Pa and 185 μM for cultures stiffened from 2,000 to 3,000 Pa (**Figure 4A**). By 120 h post-stiffening, this increase in resistance dropped to 87 μM for cultures stiffened from 200 to 1,600 Pa ($p = 0.323$) and 71 μM for cultures stiffened from 2,000 to 3,000 Pa ($p = 0.021$). We hypothesize that the stiffening from 2,000 to 3,000 Pa elicits an acute response from MDA-MB-231 cells that results in an increased resistance to doxorubicin, which is shown at the 72 h acclimation time-point. However, our data suggests this response equilibrates by the 120 h acclimation time-point. Sensitivity of MDA-MB-231 to doxorubicin was greatest at 24 h post-stiffening with LD50 measures of 5 μM for cultures stiffened from 200 to 1,600 Pa and 3 μM for cultures stiffened from 2,000 to 3,000 Pa.

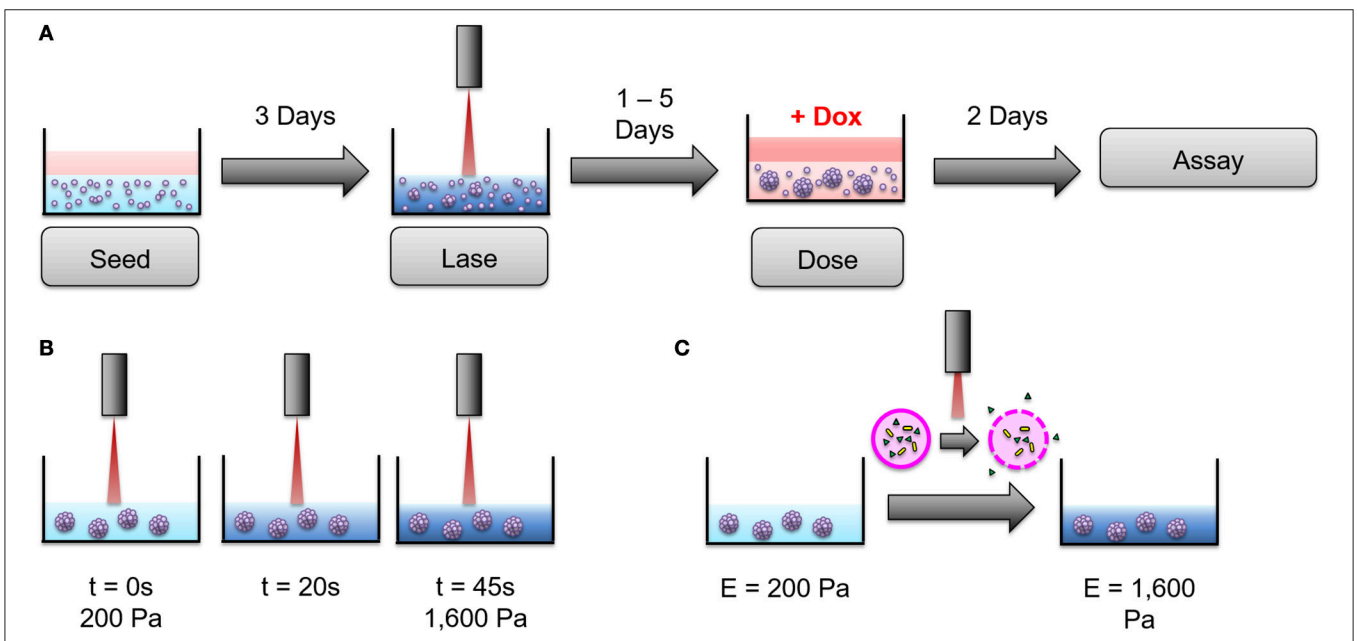

FIGURE 3 | An alginate hydrogel platform was used to dynamically stiffen hydrogels to mimic progressive ECM stiffening. **(A)** Cells were seeded into hydrogels and cultured for 3 days before dynamic stiffening with NIR light. After stiffening, cultures were given 1–5 days to acclimate to the new stiffness of the hydrogel before being exposed to doxorubicin for 2 days (48 h). Following treatment with doxorubicin, viability assays were performed to determine doxorubicin resistance. **(B)** 200 Pa hydrogels were exposed to NIR light for 45 s to achieve ECM stiffness similar to 2,000 Pa static hydrogels. The same technique was used to stiffen 2,000 Pa hydrogels to 3,000 Pa. **(C)** NIR light induces surface plasmon resonance in encapsulated gold nanorods (gold) to heat liposomes (pink) close to their gel-to-liquid transition temperature. This causes calcium (green) to leak from the liposomes and form additional alginate cross-links, thereby stiffening the hydrogel. The above figure was adapted from Joyce et al. (35).

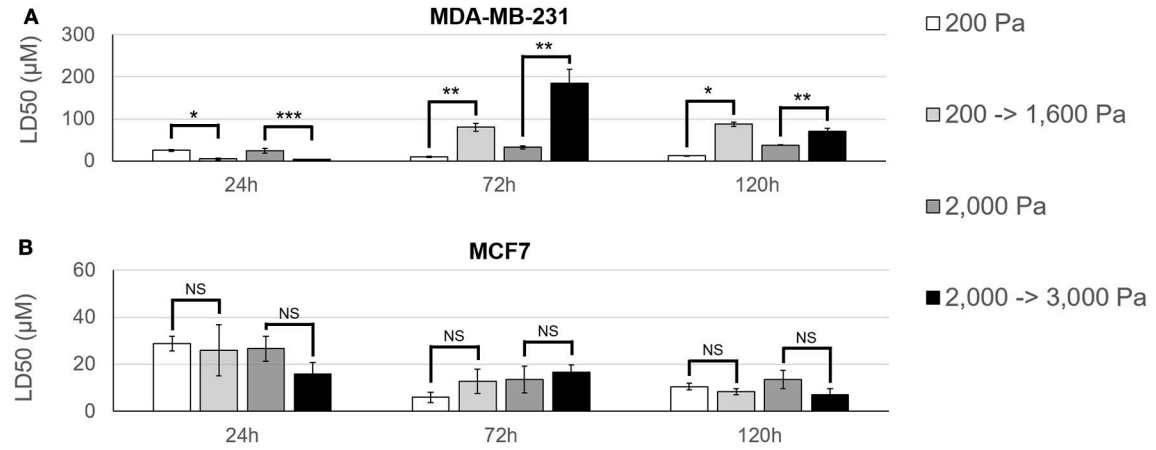

FIGURE 4 | MDA-MB-231 cultures have an acclimation-dependent increase in resistance to doxorubicin. **(A)** MDA-MB-231 and **(B)** MCF7 cells were cultured in hydrogels with an initial stiffness of 200 Pa or 2,000 Pa for 3 days. On day 3, hydrogels either remained static (200 or 2,000 Pa) or were stiffened (200 –>1,600 Pa or 2,000 –>3,000 Pa) using NIR light. Samples were then given 24–120 h to acclimate to the hydrogel stiffness before 48 h treatment with doxorubicin. MDA-MB-231 cells showed a higher resistance to doxorubicin as hydrogel stiffness increased and this stiffness-dependent resistance was found to be partially dependent on duration of exposure to hydrogel stiffness. Comparable MCF7 samples did not show any significant change in resistance to doxorubicin across hydrogel stiffness or acclimation time. *$p < 0.01$; **$p < 0.02$; ***$p < 0.03$; NS, not significant, $p > 0.05$.

MCF7 cultures behaved inversely to their MDA-MB-231 counterparts (**Figure 4B**). Peak resistance for MCF7 cultures was seen at 24 h acclimation with an LD50 of 26 μM for cultures stiffened from 200 to 1,600 Pa and 16 μM for cultures stiffened from 2,000 to 3,000 Pa. Resistance progressively decreased to LD50 values of 13 μM ($p = 0.154$) and 8 μM ($p = 0.104$) for cultures stiffened from 200 to 1,600 Pa and 17 μM ($p = 0.834$) and 7 μM ($p = 0.072$) for cultures stiffened from 2,000 to 3,000 Pa at 72 and 120 h acclimation, respectively. When comparing across acclimation periods, however, these decreases in resistance were not statistically significant.

Dynamic stiffening had a significant difference for every acclimation duration tested with MDA-MB-231 cultures as determined by a Student's *t*-test with $p < 0.05$ denoting significance. This suggests that the duration of exposure to a particular set of ECM microenvironmental stiffness conditions contributes to resistance to doxorubicin in these cells.

MDA-MB-231 Increase Markers of Mesenchymal Phenotypes on Stiff ECM

Samples grown on 200 or 2,000 Pa hydrogels were also stained with YAP antibodies as a marker of mesenchymal phenotype. High levels of YAP nuclear localization confirmed that MDA-MB-231 cultures (**Figure 5A**) exhibited higher markers of mesenchymal phenotype than their MCF7 (**Figure 5B**) counterparts. The mean fluorescent intensity (MFI) of YAP-labeled nuclei was MFI = 930 a.u. in MDA-MB-231 cells cultured in 200 Pa hydrogels ($n = 123$) and MFI = 2,030 a.u. for the same cells cultured in 2000 Pa hydrogels ($n = 119$). Given the MDA-MB-231 cells grown on 2,000 Pa hydrogels showed higher levels of YAP nuclear localization than similar cultures on 200 Pa hydrogels ($p = 1.36E-22$), we believe that a stiffer ECM promotes the mesenchymal phenotype for these cells. Similar findings were observed in MCF7 cultures, but to a much lesser extent ($p = 0.02$) with MFI = 25 a.u. for cells cultured in 200 Pa hydrogels ($n = 72$) and MFI = 31 a.u. for cells cultured in 2,000 Pa hydrogels ($n = 90$). In addition, MCF7 cells cultured in 2,000 Pa hydrogels no longer grew in epithelial patches instead spreading more sparsely through the hydrogel suggesting a decreased propensity to bind to their neighbor cells. Quantitative real-time PCR showed a significant decrease in expression of E-Cadherin for both MDA-MB-231 (**Figure 5A**) and MCF7 (**Figure 5B**) cells cultured in 2,000 Pa hydrogels when compared to similar cultures in 200 Pa hydrogels. Decreased expression of E-Cadherin is a well-known marker of EMT, thus further supporting our findings that the stiffer hydrogels promote transition toward a mesenchymal phenotype.

DISCUSSION

In this current study, we sought to better understand how progressive stiffening of the ECM affects breast cancer response to chemotherapeutic treatment. Using an alginate-based hydrogel system, we observed that hydrogel stiffness and the duration of time that cells are exposed to ECM stiffness are sufficient to modulate resistance to doxorubicin in MDA-MB-231 cells. Hydrogels were prepared to mimic the stiffness of normal mammary tissue (200 Pa) and early stage breast tumors (2,000 Pa). When MDA-MB-231 cells were cultured in these conditions, doxorubicin resistance increased as the stiffness of the hydrogels increased. These findings were further verified when NIR light was used to dynamically stiffen cultures from normal mammary tissue stiffness (200 Pa) to approximately early stage breast tumor stiffness (1,600 Pa) and from early stage breast tumor stiffness (2,000 Pa) to a more advanced breast tumor stiffness (3,000 Pa). This stiffness-dependent resistance was not observed in similar MCF7 cultures, may be due to factors

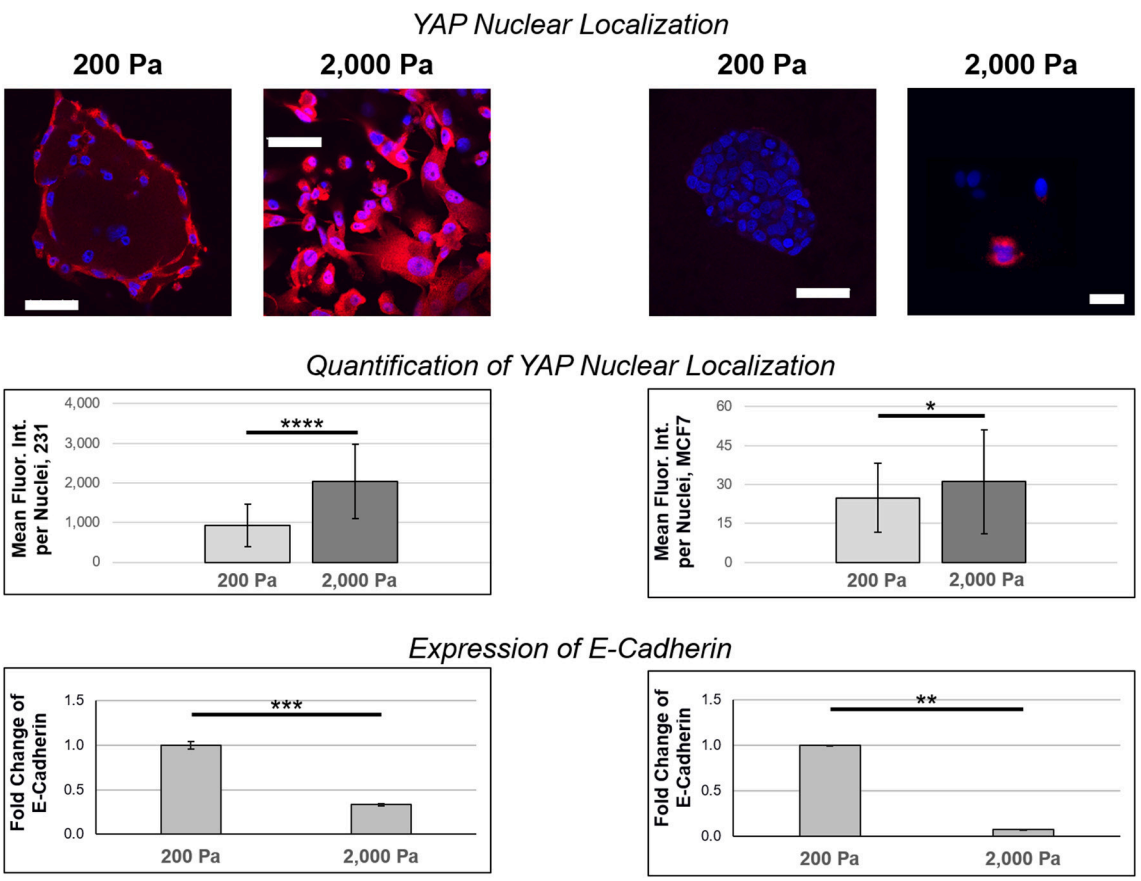

FIGURE 5 | Stiffer ECM increases nuclear localization of YAP and decreases expression of E-Cadherin. **(A)** MDA-MB-231 and **(B)** MCF7 cells were cultured on 200 or 2,000 Pa hydrogels for 3 days before fixation and staining with YAP (red) antibodies and DAPI (blue). Images were captured using confocal microscopy and analysis was done in ImageJ to determine nuclear localization of YAP ($n = 123$ for MDA-MB-231 cells cultured in 200 Pa hydrogels, $n = 119$ for MDA-MB-231 cells cultured in 2,000 Pa hydrogels, $n = 72$ for MCF7 cells cultured in 200 Pa hydrogels, $n = 90$ for MCF7 cells cultured in 2,000 Pa hydrogels). There is a stiffness-dependent increase in nuclear localization of YAP for both 231 ($p = 1.38E-22$) and MCF7 ($p = 0.02$) cultures, though the increase in MCF7 cultures is small. MDA-MB-231 cultures showed significantly higher expression of nuclear YAP compared to similar MCF7 cultures ($p = 2.37E-37$ for 200 Pa and $p = 4.44E-46$ for 2,000 Pa). Quantitative PCR indicates that cells cultured in stiffer hydrogels have decreased expression of E-Cadherin for both MDA-MB-231 ($p = 0.001$) and MCF7 ($p = 0.014$) cultures. Scale bar = 50 μm. *$p < 0.05$; **$p = 0.01$; ***$p = 0.001$; ****$p << 0.001$.

responsible for the phenotypic differences between the two cell lines.

Previous studies have demonstrated that epithelial-to-mesenchymal transition (EMT) is a critical factor in chemotherapeutic resistance across multiple cancer types including breast (36), cervical (37), ovarian (38), lung (39, 40), nasopharyngeal (41), and prostate (42). Rice et al. (25) were able to link ECM stiffness to induction of EMT in pancreatic cancer cells, which resulted in increased resistance to paclitaxel and gemcitabine. Shin and Mooney (9) found that stiffness of the microenvironment and presence of specific ligands was sufficient to increase myeloid leukemia resistance to select chemotherapeutics. These studies support our findings and highlight a role for EMT and microenvironment stiffness in chemotherapeutic resistance.

Yes-associated protein (YAP) is a transcriptional regulator that induces expression of proliferation and anti-apoptotic genes by shuttling between the cytoplasm and nucleus to interact with transcription factors (43). It is directly regulated by ECM and translocation to the nucleus is high in cells cultured on stiff ECM (44–47) which can then trigger EMT (48–51) and increased drug resistance (52). Here we used confocal microscopy to visualize and quantify YAP nuclear localization for both MDA-MB-231 and MCF7 cells grown on 200 and 2,000 Pa hydrogels. MDA-MB-231 cultures showed higher levels of YAP nuclear localization on the stiffer (2,000 Pa) hydrogels, this relationship was much weaker in MCF7 cultures. This data agrees with similar findings from the literature linking YAP nuclear localization to EMT and subsequent increases in drug resistance.

The hydrogel system used here allows dynamic control of stiffening though NIR release of calcium. Here additional stiffening occurs over the course of hours, though breast cancer cells would experience similar microenvironment stiffening over the course of months or years *in vivo*. Our study identifies the

need for an *in vitro* system that could be used to modulate cell microenvironment stiffness over a longer time-frame to more accurately mimic the progressive stiffening breast cancer cells experience *in vivo*.

In conclusion, our work has found that MDA-MB-231 cells have a stiffness-dependent resistance to doxorubicin. The duration of exposure to ECM stiffness is sufficient to modulate this resistance, but MDA-MB-231 cells grown in stiffer hydrogels were more resistance to doxorubicin treatment for all acclimation durations tested after 24 h. MCF7 cultures did not show a stiffness-dependent resistance to doxorubicin, which may be due to factors underlying their epithelial phenotype. Nuclear localization of YAP increased with hydrogel stiffness in MDA-MB-231 but not MCF7 cultures, indicating hydrogel stiffness alone was not sufficient to induce EMT in MCF7 cells but was sufficient to increase expression of the mesenchymal phenotype in MDA-MB-231 cells. This work highlights the importance of microenvironment stiffness in studies of chemotherapeutic resistance and demonstrates that progressive stiffening of the microenvironment can modulate drug resistance.

AUTHOR CONTRIBUTIONS

AB and MJ: planning of the study and writing of the manuscript; CL, EJ, MJ, RH, and SA: conducting of experiments; All authors: analysis of the manuscript.

FUNDING

This work was supported by the National Institutes of Health (R01CA226258 and R21CA212928 to AB), the Texas 4000 Foundation (Cancer Research Seed grant to AB), the Breast Cancer Research Foundation (14-60-26 to AB), the THRUST 2000 Fellowship (University of Texas at Austin fellowship to MJ), the Charles M. Simmons Endowed Presidential Fellowship (University of Texas at Austin fellowship to MJ), the Cancer Prevention & Research Institute of Texas (RP130372 to LS), and the NSF Research Experience for Undergraduates Award (#1757885 to RH).

SUPPLEMENTARY MATERIAL

The Supplementary Material for this article can be found online at: https://www.frontiersin.org/articles/10.3389/fonc.2018.00337/full#supplementary-material

Supplementary Figure 1 | Exposure to Near Infrared (NIR) light does not significantly affect response to doxorubicin. MDA-MB-231 cells were cultured as a monolayer (2D) on tissue culture plastic before being exposed to NIR light for 45 s. Samples were cultured an additional 2 days after lasing prior to treatment with doxorubicin. Staining with acridine orange/propidium iodide (AOPI) was used to quantify the ratio of live/dead cells. **(A)** Cells that were exposed to NIR light did not show a significant difference ($p = 0.064$) in resistance to doxorubicin compared to **(B)** control samples that were not exposed to NIR light. $n = 3$.

REFERENCES

1. Hanahan D, Weinberg RA. The hallmarks of cancer. *Cell* (2000) 100:57–70. doi: 10.1016/S0092-8674(00)81683-9
2. Hanahan D Weinberg RA. Hallmarks of cancer: the next generation. *Cell* (2011) 144:646–74. doi: 10.1016/j.cell.2011.02.013
3. Pickup MW, Mouw JK, Weaver VM. The extracellular matrix modulates the hallmarks of cancer. *EMBO Rep.* (2014) 15:1243–53. doi: 10.15252/embr.201439246
4. Frantz C, Stewart KM, Weaver VM. The extracellular matrix at a glance. *J Cell Sci.* (2010) 123:4195–200. doi: 10.1242/jcs.023820
5. Weaver VM, Petersen OW, Wang F, Larabell CA, Briand P, Damsky C, et al. Reversion of the malignant phenotype of human breast cells in three-dimensional culture and *In Vivo* by integrin blocking antibodies. *J Cell Biol.* (1997) 137:231–45. doi: 10.1083/jcb.137.1.231
6. Provenzano PP, Inman DR, Eliceiri KW, Knittel JG, Yan L, Rueden CT, et al. Collagen density promotes mammary tumor initiation and progression. *BMC Med.* (2008) 6:11. doi: 10.1186/1741-7015-6-11
7. Provenzano PP, Inman DR, Eliceiri KW, Keely PJ. Matrix density-induced mechanoregulation of breast cell phenotype, signaling and gene expression through a FAK-ERK linkage. *Oncogene* (2009) 28:4326–43. doi: 10.1038/onc.2009.299
8. Levental KR, Yu H, Kass L, Lakins JN, Erler JT, Fong SFT, et al. Matrix crosslinking forces tumor progression by enhancing integrin signaling. *Cell* (2010) 139:891–906. doi: 10.1016/j.cell.2009.10.027
9. Shin J, Mooney D. Extracellular matrix stiffness causes systematic variations in proliferation and chemosensitivity in myeloid leukemias. *Proc Natl Acad Sci USA.* (2016) 113:12126–31. doi: 10.1073/pnas.16113 38113
10. Abu-Tayeh H, Weidenfeld K, Zhilin-Roth A, Schif-Zuck S, Thaler S, Cotarelo C, et al. 'Normalizing' the malignant phenotype of luminal breast cancer cells via alpha(v)beta(3)-integrin. *Cell Death Dis.* (2016) 7:e2491. doi: 10.1038/cddis.2016.387
11. Carey SP, Martin KE, Reinhart-King CA. Three-dimensional collagen matrix induces a mechanosensitive invasive epithelial phenotype. *Sci Rep.* (2017) 7:42088. doi: 10.1038/srep42088
12. Gopal S, Veracini L, Grall D, Butori C, Schaub S, Audebert S, et al. Fibronectin-guided migration of carcinoma collectives. *Nat Commun.* (2017) 8:14105. doi: 10.1038/ncomms14105
13. Paszek MJ, Zahir N, Johnson KR, Lakins JN, Rozenberg GI, Gefen A, et al. Tensional homeostasis and the malignant phenotype. *Cancer Cell* (2005) 8:241–54. doi: 10.1016/j.ccr.2005.08.010
14. Yuan TL, Cantley LC. PI3K pathway alterations in cancer: variations on a theme. *Oncogene* (2008) 27:5497–510. doi: 10.1038/onc.2008.245
15. Chaudhuri O, Koshy ST, da Cunhan CB, Shin JW, Verbeke CS, Allison KH, et al. Extracellular matrix stiffness and composition jointly regulate the induction of malignant phenotypes in mammary epithelium. *Nature Mater.* (2014) 13:970–8. doi: 10.1038/nmat4009
16. Sak MA, Littrup PJ, Duric N, Mullooly M, Sherman ME, Gierach GL. Current and future methods for measuring breast density: a brief comparative review. *Breast Cancer Manag.* (2015) 4:209–221. doi: 10.2217/bmt.15.13
17. American Cancer Society. *Cancer Facts & Figures 2017.* Atlanta, GA: American Cancer Society (2017).
18. Bruno RD, Fleming JM, George AL, Boulanger CA, Schedin P, Smith GH. Mammary extracellular matrix directs differentiation of testicular and embryonic stem cells to form functional mammary glands *in vivo*. *Sci Rep.* (2017) 7:40196. doi: 10.1038/srep40196
19. Macias H, Hinck L. Mammary Gland Development. Wiley Interdisciplinary Reviews. *Dev Biol.* (2012) 1:533–57. doi: 10.1002/wdev.35
20. Engelmann I, Bauer G. How can tumor cells escape intercellular induction of apoptosis? *Anticancer Res.* (2000) 20:2297–306
21. Inman JL, Mott JD, Bissell MJ. The extracellular matrix as a multivalent signaling scaffold that orchestrates tissue organization and function. In: MM Muleller, NE Fusenig editors. *Tumor-Associated Fibroblasts and Their Matrix.* Dordrecht; Heidelberg; London; New York, NY: Springer Science+Business Media (2011). pp. 285–300. doi: 10.1007/978-94-007-0659-0_16

22. Lang NR, Skodzek K, Hurst S, Mainka A, Steinwachs J, Schneider J, et al. Biphasic response of cell invasion to matrix stiffness in three-dimensional biopolymer networks. *Acta Biomaterialia* (2015) 13:61–7. doi: 10.1016/j.actbio.2014.11.003
23. Krause S, Maffini MV, Soto AM, Sonnenschein C. The microenvironment determines the breast cancer cells' phenotype: organization of MCF7 cells in 3D cultures. *BMC Cancer* (2010) 10:263. doi: 10.1186/1471-2407-10-263
24. Miroshnikova YA, Mouw JK, Barnes JM, Pickup MW, Lakins JN, Kim Y, et al.Tissue mechanics promote IDH1-dependent HIF1α-tenascin C feedback to regulate glioblastoma aggression. *Nature Cell Biol.* (2016) 18:1336–45. doi: 10.1038/ncb3429
25. Rice AJ, Cortes E, Lachowski D, Cheung BCH, Karim SA, Morton JP, et al. Matrix stiffness induces epithelial-mesenchymal transition and promotes chemoresistance in pancreatic cancer cells. *Oncogenesis* (2017) 6:e352. doi: 10.1038/oncsis.2017.54
26. Zustiak S, Nossal R, Sackett D. Multiwell stiffness assay for the study of cell responsiveness to cytotoxic drugs. *Biotechnol Bioeng.* (2014) 111:396–403. doi: 10.1002/bit.25097
27. Davis C, Naci H, Gurpinar E, Poplavska E, Pinto A, Aggarwal A. Availability of evidence of benefits on overall survival and quality of life of cancer drugs approved by European Medicines Agency: retrospective cohort study of drug approvals 2009–13. *BMJ.* (2017) 359:j4530. doi: 10.1136/bmj.j4530
28. Tschumperlin DJ, Dai G, Maly IV, Kikuchi T, Laiho LH, McVittie AK, et al. Mechanotransduction through growth-factor shedding into the extracellular space. *Nature* (2004) 429:83–86. doi: 10.1038/nature02543
29. Wipff PJ, Rifkin DB, Meister JJ, Hinz B. Myofibroblast contraction activates latent TGF-β1 from the extracellular matrix. *J. Cell Biol.* (2007) 179:1311–23. doi: 10.1083/jcb.200704042
30. Wolfe JN. Risk for breast cancer development determined by mammographic parenchymal pattern. *Cancer* (1976) 37:2486–92. doi: 10.1002/1097-0142(197605)37:5<2486::AID-CNCR2820370542>3.0.CO;2-8
31. Wolfe JN. Breast patterns as an index of risk for developing breast cancer. *AJR Am. J. Roentgenol.* (1976a) 126:1130–7. doi: 10.2214/ajr.126.6.1130
32. Han YL, Ronceray P, Xu G, Malandrino A, Kamm RD, Broedersz CP, et al. Cell contraction induces long-ranged stress stiffening in the extracellular matrix. *Proc Natl Acad Sci USA*. (2018). doi: 10.1073/pnas.1722619115.
33. Stowers R, Allen S, Suggs L. Dynamic phototuning of 3D hydrogel stiffness. *Proc Natl Acad Sci USA*. (2015) 112:1953–8. doi: 10.1073/pnas.1421897112
34. Ahl PL, Chen L, Perkins WR, Minchey SR, Boni LT, Taraschi TF, et al. A new method for producing lipid vesicles of high internal volume. *Biochim Biophys Acta* (1994) 1195:237–44. doi: 10.1016/0005-2736(94)90262-3
35. Joyce MH, Allen S, Suggs L, Brock A. Novel nanomaterials enable biomimetic models of tumor microenvironment. *J Nanotechnol.* (2017) 2017:8 doi: 10.1155/2017/5204163
36. Yang Q, Huang J, Wu Q, Cai Y, Zhu L, Lu X, et al. Acquisition of epithelial-mesenchymal transition is associated with Skp2 expression in paclitaxel-resistant breast cancer cells. *Br J Cancer* (2017) 110:1958–67. doi: 10.1038/bjc.2014.136
37. Shen Y, Zhou J, Li Y, Ye F, Wan X, Lu W, et al. miR-375 Mediated Acquired Chemo-Resistance in Cervical Cancer by Facilitating EMT. *PLoS ONE* (2014) 9:e109299. doi: 10.1371/journal.pone.0109299
38. Wang L, Zhang F, Cui J-Y, Chen L, Chen YT, Liu BW. CAFs enhance paclitaxel resistance by inducing EMT through the IL-6/JAK2/STAT3 pathway. *Oncol Rep.* (2018) 39:2081–90. doi: 10.3892/or.2018.6311
39. Tomono T, Yano K, Ogihara T. Snail-induced epithelial-to-mesenchymal transition enhances P-gp-mediated multidrug resistance in HCC827 Cells. *J Pharmaceut Sci.* (2017) 106:2642–9. doi: 10.1016/j.xphs.2017.03.011
40. Shintani Y, Okimura A, Sato K, Nakagiri T, Kadota Y, Inoue M, et al. Epithelial to mesenchymal transition is a determinant of sensitivity to chemoradiotherapy in non-small cell lung cancer. *Ann Thorac Surg.* (2011) 92:1794–804. doi: 10.1016/j.athoracsur.2011.07.032
41. Hou Y, Zhu Q, Li Z, Peng Y, Yu X, Yuan B, et al. The FOXM1-ABCC5 axis contributes to paclitaxel resistance in nasopharyngeal carcinoma cells. *Cell Death Dis.* (2017) 8:e2659. doi: 10.1038/cddis.2017.53
42. Kim JJ, Yin B, Christudass CS, Terada N, Rajagopalan K, Fabry B, et al. Acquisition of paclitaxel resistance is associated with a more aggressive and invasive phenotype in prostate cancer. *J Cell Biochem.* (2013) 114:1286–93. doi: 10.1002/jcb.24464
43. Mo JS, Park H. W. Guan K. L. The Hippo signaling pathway in stem cell biology and cancer. *EMBO Rep.* (2014) 15:642–56. doi: 10.15252/embr.201438638
44. Calvo F. Ege N, Grande-Garcia A, Hooper S, Jenkins RP, Chaudhry SI, et al. Mechanotransduction and YAP-dependent matrix remodelling is required for the generation and maintenance of cancer-associated fibroblasts. *Nature Cell Biol.* (2013) 15:637–46. doi: 10.1038/ncb2756
45. Aragona M. Panciera T, Manfrin A, Giulitti S, Michielin F, Elvassore N, et al. A mechanical checkpoint controls multicellular growth through YAP/TAZ regulation by actin-processing factors. *Cell* (2013) 154:1047–59. doi: 10.1016/j.cell.2013.07.042
46. Dupont S. Morsut L, Aragona M, Enzo E, Giulitti S, Cordenonsi M, et al. Role of YAP/TAZ in mechanotransduction. *Nature* (2011) 474:179–83. doi: 10.1038/nature10137
47. Tang Y. Rowe RG, Botvinick EL, Kurup A, Putnam AJ, Seiki M, et al. MT1 -MMP-dependent control of skeletal stem cell commitment via a β1 -integrin/YAP/TAZ signaling axis. *Dev. Cell* (2013) 25:402–16. doi: 10.1016/j.devcel.2013.04.011
48. Chen D, Sun Y, Wei Y, Zhang P, Rezaeian AH, Teruya-Feldstein J, et al. LIFR is a breast cancer metastasis suppressor upstream of the Hippo–YAP pathway and a prognostic marker. *Nature Med.* (2012) 18:1511–17. doi: 10.1038/nm.2940
49. Hong J. H. Hwang ES, McManus MT, Amsterdam A, Tian Y, Kalmukova R, et al. TAZ, a transcriptional modulator of mesenchymal stem cell differentiation. *Science* (2005) 309:1074–78. doi: 10.1126/science.1110955
50. Cordenonsi M, Zanconato F, Azzolin L, Forcato M, Rosato A, Frasson C, et al. The Hippo transducer TAZ confers cancer stem cell-related traits on breast cancer cells. *Cell* (2011) 147:759–72. doi: 10.1016/j.cell.2011.09.048
51. Chan SW, Lim CJ, Guo K, Ng CP, Lee I, Hunziker W, et al. A role for TAZ in migration, invasion, and tumorigenesis of breast cancer cells. *Cancer Res.* (2008) 68:2592–8. doi: 10.1158/0008-5472.CAN-07-2696
52. Lin CH, Pelissier FA, Zhang H, Lakins J, Weaver VM, Park C, et al. Microenvironment rigidity modulates responses to the HER2 receptor tyrosine kinase inhibitor lapatinib via YAP and TAZ transcription factors. *Mol Biol Cell* (2015) 26:3946–53. doi: 10.1091/mbc.e15-07-0456

Conflict of Interest Statement: The authors declare that the research was conducted in the absence of any commercial or financial relationships that could be construed as a potential conflict of interest.

frontiers in Oncology

REVIEW
published: 04 September 2018
doi: 10.3389/fonc.2018.00331

Fructose 2,6-Bisphosphate in Cancer Cell Metabolism

Ramon Bartrons[1], Helga Simon-Molas[1], Ana Rodríguez-García[1], Esther Castaño[2], Àurea Navarro-Sabaté[1], Anna Manzano[1] and Ubaldo E. Martinez-Outschoorn[3]*

[1] Unitat de Bioquímica, Departament de Ciències Fisiològiques, Universitat de Barcelona, Institut d'Investigació Biomèdica de Bellvitge (IDIBELL), Catalunya, Spain, [2] Centres Científics i Tecnològics, Universitat de Barcelona, Catalunya, Spain, [3] Department of Medical Oncology, Thomas Jefferson University, Philadelphia, PA, United States

For a long time, pioneers in the field of cancer cell metabolism, such as Otto Warburg, have focused on the idea that tumor cells maintain high glycolytic rates even with adequate oxygen supply, in what is known as aerobic glycolysis or the Warburg effect. Recent studies have reported a more complex situation, where the tumor ecosystem plays a more critical role in cancer progression. Cancer cells display extraordinary plasticity in adapting to changes in their tumor microenvironment, developing strategies to survive and proliferate. The proliferation of cancer cells needs a high rate of energy and metabolic substrates for biosynthesis of biomolecules. These requirements are met by the metabolic reprogramming of cancer cells and others present in the tumor microenvironment, which is essential for tumor survival and spread. Metabolic reprogramming involves a complex interplay between oncogenes, tumor suppressors, growth factors and local factors in the tumor microenvironment. These factors can induce overexpression and increased activity of glycolytic isoenzymes and proteins in stromal and cancer cells which are different from those expressed in normal cells. The fructose-6-phosphate/fructose-1,6-bisphosphate cycle, catalyzed by 6-phosphofructo-1-kinase/fructose 1,6-bisphosphatase (PFK1/FBPase1) isoenzymes, plays a key role in controlling glycolytic rates. PFK1/FBpase1 activities are allosterically regulated by fructose-2,6-bisphosphate, the product of the enzymatic activity of the dual kinase/phosphatase family of enzymes: 6-phosphofructo-2-kinase/fructose 2,6-bisphosphatase (PFKFB1-4) and TP53-induced glycolysis and apoptosis regulator (TIGAR), which show increased expression in a significant number of tumor types. In this review, the function of these isoenzymes in the regulation of metabolism, as well as the regulatory factors modulating their expression and activity in the tumor ecosystem are discussed. Targeting these isoenzymes, either directly or by inhibiting their activating factors, could be a promising approach for treating cancers.

Keywords: fructose 2,6-bisphosphate, cancer metabolism, glycolysis, PFKFB isoenzymes, TIGAR, tumor microenvironment

OPEN ACCESS

Edited by:
Michael Breitenbach, University of Salzburg, Austria

Reviewed by:
Markus Schosserer, Universität für Bodenkultur Wien, Austria
Johannes A. Mayr, Paracelsus Medical University Salzburg, Austria

****Correspondence:***
Ramon Bartrons
rbartrons@ub.edu

Specialty section:
This article was submitted to Molecular and Cellular Oncology, a section of the journal Frontiers in Oncology

Received: *07 June 2018*
Accepted: *01 August 2018*
Published: *04 September 2018*

Citation:
Bartrons R, Simon-Molas H, Rodríguez-García A, Castaño E, Navarro-Sabaté À, Manzano A and Martinez-Outschoorn UE (2018) Fructose 2,6-Bisphosphate in Cancer Cell Metabolism. Front. Oncol. 8:331. doi: 10.3389/fonc.2018.00331

INTRODUCTION

Otto Warburg, using the Warburg manometer to measure the oxygen consumption in cells, demonstrated that tumor cells showed rapid and intense glycolysis, in which glucose was oxidized into lactate, despite the presence of abundant oxygen (1). This "Warburg effect" is characteristic of proliferating and transformed cells. Warburg postulated that cancer was a result of defects in mitochondrial respiration, which forced the cell to adopt an anaerobic form of energy generation,

glycolysis (2). There are different molecular mechanisms that can explain the Warburg effect, including: mitochondrial malfunction (3), oncogenic alterations (4–7), as well as responses to adapt to the tumor microenvironment (TME) (8–10). Even though not all cancer cells have high glycolytic flux (11), the Warburg effect has been observed in most tumor cells and represents an adaptation to support biomass production (10).

At the same time as Otto Warburg, Herbert G. Crabtree studied the heterogeneity of glycolysis in tumors, describing that the magnitude and relationships between respiratory and glycolytic processes were a common feature of uncontrolled proliferation and not specific to malignant tissues (12). He observed considerable variability between respiratory and glycolytic metabolism among different tumors (13). Moreover, he found that glycolytic activity significantly affected the respiration capacity of tumor tissues being respiration and oxidative phosphorylation inhibited by glucose (13). This observation, referred as the "Crabtree effect," might be advantageous to cancer cells, allowing them to adjust their metabolism to heterogeneous microenvironments in malignant cells, through the glucose-dependent accumulation of essential metabolites, such as serine, phosphoribosyl-pyrophosphate, and glycerol-3-phosphate, which can trigger mitogenic events (11, 14, 15). The Crabtree effect on tumor cells can be eliminated by adding an excess of inorganic phosphate (Pi) (15, 16).

The resurgence of the role of bioenergetics in cancer began in the early 1990s when studies using 2-deoxy-D-glucose (2-DG) in positron emission tomography (PET) showed that most tumors displayed increased glucose uptake in about an order of magnitude higher than that of normal tissue (8). The increased glucose uptake largely depends on the rate of glucose phosphorylation by hexokinases and the upregulation of glucose transporters Glut1 and Glut3 and less often Glut4 (17). More than 90% of primary and metastatic tumors have high glucose uptake, which directly correlates with tumor aggressiveness (8, 18).

For a long time, studies on cancer cell metabolism had focused on investigating a single cell type. However, recent studies have reported a more complex situation in which metabolic heterogeneity within tumors plays a critical role in cancer progression (19–21). Cancer cells display extraordinary plasticity in adapting to changes in their TME, developing strategies to survive and proliferate. Interactions between tumor cells and non-malignant cells of the TME influence cancer initiation and progression as well as patient prognosis (22–24). Local differences in the TME, including acidity and hypoxia, affect cancer cells progression. If located close to blood vessels, cancer cells can proliferate at a higher rate because of the abundant supply of nutrients, growth factors and oxygen. By contrast, if the supply of nutrients and oxygen is reduced, cancer cells rely more on glycolysis, forcing them to develop strategies for survival and proliferation. Thus, it is not surprising that these cells in metabolically deprived environments are usually chemoresistant and have higher malignancy grades (25). Stromal cells, especially cancer-associated fibroblasts (CAFs), influence the homeostasis of the TME. The interactions between TME and cancer cells strongly affect tumor metabolism and growth (26–29). A "two-compartment" model, referred to as the "reversed Warburg effect," has been proposed as a new perspective of tumor metabolism in which tumor stroma and adjacent host tissues are catabolic, while cancer cells are anabolic (19–21, 28–30). Energy is transferred from the catabolic to the anabolic compartment via the sharing of nutrients, which promotes tumor growth. Although lactate is generally considered a waste product, it has been demonstrated to fuel oxidative metabolism in cancer cells, favoring a symbiosis between glycolytic and oxidative tumor cells (19–21, 28–30). Metabolic reprogramming of cancer and stromal cells involves a complex interplay between oncogenes, tumor suppressors, growth factors and local factors from the TME. These factors can induce the overexpression and increased activity of isoenzymes and other proteins in cancer cells that are different from those found in non-malignant cells (30).

REPROGRAMMING THE GLYCOLYTIC PHENOTYPE OF CANCER CELLS

Most tumor cells have a markedly modified energy metabolism in comparison to differentiated cells. Their metabolism, previously based on respiration, changes to another eminently glycolytic, recognized as the glycolytic phenotype (7, 31–34). Several glycolytic genes are usually overexpressed in many tumors and give place to this phenotype (35). This occurs because tumor cells reprogram cellular metabolism increasing the transcription and/or alternative splicing of glycolytic genes induced by the Hypoxia Inducible Factor-1α (HIF-1α), oncogenes and inactivated tumor suppressor genes and distinct growth factors (34, 36–39). The glycolytic phenotype is a distinctive characteristic of tumor cells (7, 31, 33), providing advantages

Abbreviations: 2,3-BPG, 2,3-bisphosphoglycerate; 2-DG, 2-deoxy-D-glucose; AML, acute myeloid leukemia; AMPK, AMP-activated protein kinase; APC/C, anaphase-promoting complex; AR, androgen receptor; CAF, cancer-associated fibroblast; CAV1, caveolin-1; CDK1, cyclin-dependent kinase 1; CML, chronic myeloid leukemia; ConA, concanavalin A; CREB, CRE-binding protein; DRAM, damage-regulated autophagy modulator; EC, endothelial cell; ECyd, 1-(3-C-ethynyl-beta-d-ribo-pentofuranosyl)cytosine; ER, estrogen receptor; ERE, estrogen response element; FBPase1, fructose 1,6-bisphosphatase; FBPase-2, fructose 2,6-bisphosphatase; Fru-1,6-P_2, fructose-1,6-bisphosphate; Fru-2,6-P_2, fructose 2,6-bisphosphate; Fru-6-P, fructose-6-phosphate; GASC, glioblastoma-associated stromal cell; GC, glucocorticoid; Glut1, glucose transporter 1; HCC, hepatocellular carcinoma; HIF-1α, hypoxia inducible factor-1α; HK-2, hexokinase-II; IL-6, interleukin-6; LPS, lipopolysaccharide; LUBAC, linear ubiquitination assembly complex; MACC1, metastasis-associated in colon cancer protein 1; MAPK-1, mitogen-activated protein kinase 1; MCT4, metabolic coupling monocarboxylate transporter 4; NFκB, nuclear factor κB; PDK1, pyruvate dehydrogenase kinase; PEP, phosphoenolpyruvate; PEPCK1, phosphoenolpyruvate carboxykinase 1; PET, positron emission tomography; PFK1, 6-phosphofructo-1-kinase; PFK1/FBPase1, 6-phosphofructo-1-kinase/fructose 1,6-bisphosphatase; PFK-2, 6-phosphofructo-2-kinase; PFK-2/FBPase-2, 6-fosfofructo-2-kinase/fructose 2,6-bisphosphatase; PGAM, phosphoglycerate mutase; PKA, cAMP-dependent protein kinase; PKB, protein kinase B; PKM2, pyruvate kinase isoenzyme M2; PP-1, protein phosphatase 1; PPARγ, peroxisome proliferator-activating receptor γ; PPP, pentose phosphate pathway; PR, progesterone receptor; PRE, progesterone response element; RB, retinoblastoma; ROBO1, round about guidance receptor 1; ROS, reactive oxygen species; RSK, p90 ribosomal S6 kinase; SCNC, small cell neuroendocrine carcinoma; SCO2, cytochrome C-oxidase-2; SLIT2, slit guidance ligand 2; SP1, specificity protein 1; SRC-3; steroid receptor coactivator-3; TGF-β1, transforming growth factor beta 1; TIGAR, TP53-induced glycolysis and apoptosis regulator; TME, tumor microenvironment; VEGF, vascular endothelial growth factor.

to proliferating cells and allowing them to metabolize the most plentiful nutrient, glucose, to generate energy and anabolic precursors. Even though the yield of ATP per glucose molecule consumed is low, the percentage of cellular ATP generated from glycolysis can surpass that produced from oxidative phosphorylation if the glycolytic flux is high enough (11, 32, 40). Furthermore, glucose metabolism provides intermediates that are needed for biosynthetic pathways, such as ribose sugars for nucleotide synthesis and hexose sugar derivatives, glycerol and citrate for lipid production, non-essential amino acids (serine, glycine, and cysteine) and NADPH. Therefore, the Warburg effect has a positive impact on bioenergetics, biosynthesis and detoxification of reactive oxygen species (ROS) (10).

There are several checkpoints regulating the acquisition of the glycolytic phenotype. The first point of commitment of glucose-6-phosphate to the glycolytic pathway involves the fructose-6-phosphate/fructose-1,6-bisphosphate cycle (Fru-6-P/Fru-1,6-P_2) (41) (**Figure 1**). The following paragraphs describe the specific isoenzymes regulating this substrate cycle, the main properties of which are summarized in **Table 1**.

6-Phosphofructo-1-Kinase (PFK1)

PFK1 is a tetrameric protein, with three genes encoding the PFK-M (muscle), PFK-L (liver), and PFK-P (platelet) human isoforms, with a molecular weight of their subunits of 82.5, 77, and 86.5 kDa, respectively (42). The different isoforms can form homo- or hetero-tetramers depending on the cell type (38, 42). Lactate induces the dissociation of the tetramers into dimers, reducing enzymatic activity and providing negative feedback in the regulation of the glycolytic rate (43). PFK1 isozymes can be phosphorylated by different kinases but this does not produce significant catalytic effects (41, 44, 45), although the covalent modification can affect their association with other proteins (46–48). Localization to the actin filaments of the cytoskeleton has been shown to increase PFK-M activity (49), which can also bind to and modulate protein phosphatase-1 (50). PFK-L, but not PFK-M and PFK-P, assembles into filaments, with fructose-6-P binding essential for their formation (51). These filaments have been observed to localize in the plasma membrane, where they promote the vessel sprouting of endothelial cells (52). PFK-L forms clusters in human cancer cells and colocalizes with other rate-limiting enzymes in both glycolysis and gluconeogenesis, supporting the formation of multienzyme metabolic complexes for glucose metabolism, integrating PFK-L, FBPase1, the pyruvate kinase isoenzyme M2 (PKM2) and phosphoenolpyruvate carboxykinase 1 (PEPCK1), among others, and forming the "glycosome" (53). PFK1 is also regulated by different allosteric effectors, which provides control of the glycolytic flux and coordination of glucose entry into glycolysis. It is a tightly-regulated enzyme and its kinetic and regulatory characteristics depend on the composition of its different subunits. Its regulation involves a series of negative (citrate, ATP, phosphoenolpyruvate, and [H^+]) and positive effectors (Fru-2,6-P_2, AMP, Fru-1,6-P_2, Glu-1,6-P_2, $NH4^+$, and Pi) (41, 42), which coordinate its response to the energy status of the cell. PFK1 activity increases in response to proliferation signals alongside elevated glycolysis in proliferating and cancer cells (54), although there are exceptions where its activity does not increase (44, 54). The main isoenzymes expressed in tumor cells are PFK-P and PFK-L (54, 55). In human lymphomas and gliomas, PFK1 is less sensitive to inhibition by ATP and citrate, and more sensitive to activation by Fru-2,6-P_2 and AMP (44, 56). PFK1 activity is induced by HIF-1α (57) or the overexpression of the oncogenes RAS and SRC (58). PFK-L and PFK-P can be glycosylated in response to hypoxia, which inhibits PFK1 activity and redirects the glucose flux toward the pentose phosphate pathway (PPP), providing pentose sugars for nucleotide synthesis and NADPH to combat oxidative stress (59). Similarly, the transcription repressor Snail reprograms glucose metabolism by repressing PFK-P, suppressing lactate production and amino acids biosynthesis, while promoting cancer cell survival under metabolic stress (60). Akt can bind to and phosphorylate PFK-P at S386, which inhibits the binding of TRIM21 E3 ligase to PFK-P and its subsequent polyubiquitylation and degradation. This has been shown to increase PFK-P activity, glycolysis, cell proliferation and brain tumor growth (48). Recently, EGFR activation has been reported to elicit lysine acetyl-transferase-5-mediated PFK-P acetylation and subsequent translocation of PFK-P to the plasma membrane, where EGFR phosphorylates PFK-P at Y64. Phosphorylated PFK-P binds to the N-terminal

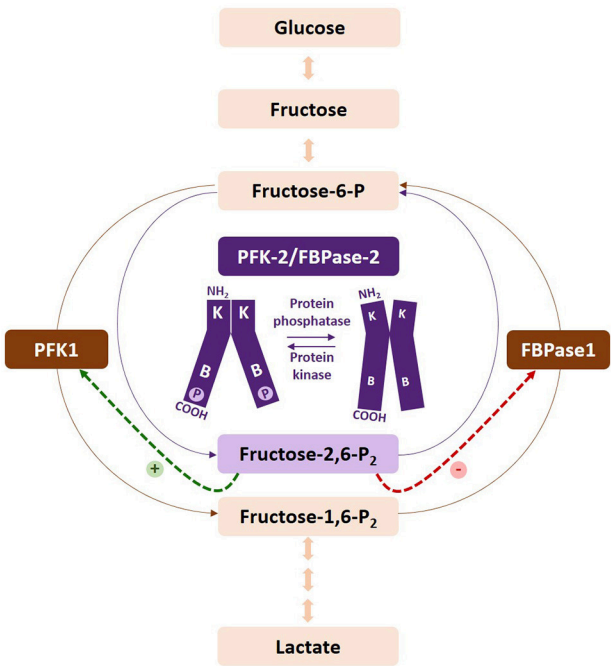

FIGURE 1 | Regulation of the fructose-6-P/fructose-1,6-P_2 substrate cycle. Fructose-2,6-P_2 is synthesized and degraded by PFK-2/FBPase-2, respectively. Increased levels of the metabolite activate PFK-1 and inhibit FBPase1, increasing the glycolytic flux. Phosphorylation of the PFKFB2 and PFKFB3 isoenzymes increases their kinase activity. The kinases and phosphatases responsible for their regulation vary according to the isoenzyme. PFKFB1 is not represented by this figure, as phosphorylation increases the bisphosphatase activity of the enzyme. At present, PFKFB4 has not been found to be regulated by phosphorylation.

TABLE 1 | Properties of the glycolytic enzymes acting on Fru-6-P/Fru-1,6-P_2 substrate cycle.

Protein	Gene	Chromosomal location (human)	Kinase/phosphatase ratio	Isoenzymes	Regulation
6-phosphofructokinase (PFK1)	*PFK-M*	12q13.11	Only kinase	PFK-M (muscle)	PKA, PKC and AMPK in rabbit, rat, and pig, respectively
	PFK-L	21q22.3	Only kinase	PFK-L (liver)	Ras, Src, HIF1α
	PFK-P	10p15.2	Only kinase	PFK-P (platelets)	Akt, EGFR, HIF-1α Glycosylation, Snail
Fructose-1,6-bisphosphatase (FBPase)	*FBPase1*	9q22.32*	Only phosphatase	FBPase1	Snail
	FBPase2	9q22.32*	Only phosphatase	FBPase2	Not described
6-phosphofructo-2-kinase/fructose-2,6-bisphosphatase (PFK-2/FBPase-2)	*PFKFB1*	Xp11.21	2.5 (rat liver) 1.2 (bovine liver) 0.4 (rat muscle)	lPFK-2 (liver) mPFK-2 (muscle) fPFK-2 (fetal)	PKA PP-1
	PFKFB2	1q32.1	1.8 (bovine heart)	hPFK-2 (heart)	AMPK, PKA, Akt, PKC, RSK Glucocorticoids, androgens, RNA LINC00092
	PFKFB3	10p15.1	710 (human placenta) 3.1 (bovine brain)	uPFK-2 (ubiquitous) iPFK-2 (inducible)	AMPK, PKA, Akt, PKC, Smad, RSK, p38-MK2 Estrogens, adenosine, LPS p53, S-glutathionylation, demethylation
	PFKFB4	3p21.31	4.1 (rat testis) 0.9 (human testis)	tPFK-2 (testis)	HIF-1α, P-PPARγ, testosterone p53
TIGAR	*C12orf5*	12p13.32	Only phosphatase	Not described	p53, CREB, HIF-1α, SP1

*Information regarding gene name, chromosomal location, isoenzymes, enzymatic activity, and regulation of the glycolytic enzymes acting on Fru-6-P/Fru-1,6-P2 substrate cycle is shown. Positive and negative regulators are written in green and red, respectively. *Same chromosomal region, different locus.*

domain of p85α and promotes the activation of PI3K and Akt, leading to increased PFKFB2 activity, Fru-2,6-P_2 synthesis and PFK1 activation, which in turn promote cell proliferation and tumorigenesis (61).

Fructose 1,6-Bisphosphatase (FBPase1)

FBPase1, a rate-limiting enzyme that catalyzes the opposite reaction to that of PFK1 in the Fru-6-P/Fru-1,6-P_2 cycle, exists as two isoenzymes in mammals: FBPase1 and FBPase2. Both isozymes are inhibited by Fru-2,6-P_2 synergistically with AMP (41, 62, 63) (**Figure 1**). FBPase1 can be phosphorylated by different kinases, but this leads to non-significant catalytic effects (41). FBPase1 is ubiquitously expressed and has been reported to be lost in several human cancers (64). FBPase1 overexpression suppresses cancer cell growth (65) and its loss correlates with advanced tumor stage and poor prognosis (66). Snail can repress FBPase1 in breast cancer cells (67), thus tightly controlling glucose flux through the PPP, by suppressing both PFK-P and FBPase1. FBPase1 and PFK-L directly interact forming multienzyme complexes that can modulate their activities (53). By contrast, FBPase2 is restricted to muscle cells and participates in the synthesis of glycogen from carbohydrate precursors (62).

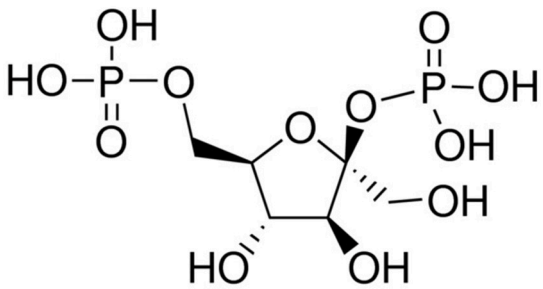

FIGURE 2 | Structure of β-Fructose 2,6-bisphosphate.

6-Phosphofructo-2-Kinase/fructose 2,6-Bisphosphatase (PFK-2/FBPase-2) Isoenzymes

Fru-2,6-P_2 (**Figure 2**), a powerful allosteric modulator of the Fru-6-P/Fru-1,6-P_2 substrate cycle, was discovered in 1980 when its concentration was observed greatly increased in hepatocytes upon incubation with glucose and disappeared in the presence of glucagon, providing a refined regulatory mechanism between

glycolysis and gluconeogenesis (41, 68–71) (**Figure 2**). Fru-2,6-P_2 has a dual function, increasing the affinity of PFK1 for Fru-6-P and releasing the enzyme from ATP-mediated inhibition. It also synergistically increases the affinity of PFK1 for AMP, a positive allosteric effector of the enzyme. By contrast, both Fru-2,6-P_2 and AMP inhibit FBPase1 (41, 68–71). Furthermore, Fru-2,6-P_2 stabilizes PFK1 (68) and promotes its association into tetramers and higher oligomers with enhanced activity (72). Therefore, changes in the concentration of this metabolite regulate the activities of PFK1 and FBPase1, thereby conferring a key role to Fru-2,6-P_2 in the regulation of the Fru-6-P/Fru-1,6-P_2 substrate cycle and the intensity and direction of glycolysis and gluconeogenesis (**Figure 1**). Since Fru-2,6-P_2 does not take part as an intermediary in any metabolic interconversion, and given its lability in acid extracts used to measure phosphoric acid esters in tissues, this metabolite managed to escape discovery until 1980 (41, 70). Fru-2,6-P_2 has been shown to carry out a leading function in regulating glycolysis in other eukaryotic cells (41, 68, 69).

Fru-2,6-P_2 concentration is significantly higher in tumor cells than in normal cells (56, 73, 74) and is regulated by different bifunctional isoenzymes called 6-phosphofructo-2-kinases/fructose 2,6-bisphosphatases (PFK-2/FBPase-2), which catalyze the synthesis and degradation of this metabolite (68–71, 75). The balance between the activity of 6-phosphofructo-2-kinase (PFK-2), which synthesizes Fru-2,6-P_2 from Fru-6-P and ATP, and that of fructose 2,6-bisphosphatase (FBPase-2), which hydrolyzes Fru-2,6-P_2 into Fru-6-P and inorganic phosphate, ultimately determines the concentration of this metabolite (**Figure 1**). PFK-2/FBPase-2 is one of the few homodimeric bifunctional enzymes, composed of two 55-kDa subunits. Each monomer presents both kinase and bisphosphatase domains in the same polypeptide chain, with the kinase domain at the N-terminal end of the protein and the bisphosphatase domain at the C-terminal (68–71, 75, 76) (**Figure 3**). The amino acids located near the N- and C-terminal ends of the PFK-2/FBPase2 isoenzymes protein are responsible for its post-translational regulation as they can be phosphorylated by different protein kinases. The protein is derived from the fusion of two genes that express a kinase domain, evolutionarily related to the family of proteins that link mononucleotides, and a bisphosphatase domain, which is related to the family of phosphoglycerate phosphatases and acid phosphatases (75–77). The regulatory function of Fru-2,6-P_2 in carbohydrate metabolism implies that the modulation of Fru-2,6-P_2 synthesis and degradation must be very well compensated to adapt Fru-2,6-P_2 concentration to the needs of the cell. The degree of complexity involved in regulating Fru-2,6-P_2 levels in each tissue and physiological condition is reflected by the existence of different PFK-2/FBPase-2 isoenzymes that are capable of adapting to different conditions (75, 76, 78). These isoenzymes, encoded by four genes (*PFKFB1-PFKFB4*), display variances in their kinetic properties and distribution, as well as in their responses to allosteric, hormonal, and growth factors (75, 76). The *PFKFB1* gene encodes the isoforms that were originally identified in the liver, muscle and fetal tissue, while the *PFKFB2* gene encodes the isoenzyme occurring in the heart and kidney and in some cancer cells. The *PFKFB3* gene encodes the isoforms present in the brain, placenta and adipose tissue, and is the most expressed *PFKFB* gene in proliferating and cancer cells. Finally, the *PFKFB4* gene encodes the isoenzyme occurring in the testis, although it has also been found in several types of tumor cells (**Table 1**).

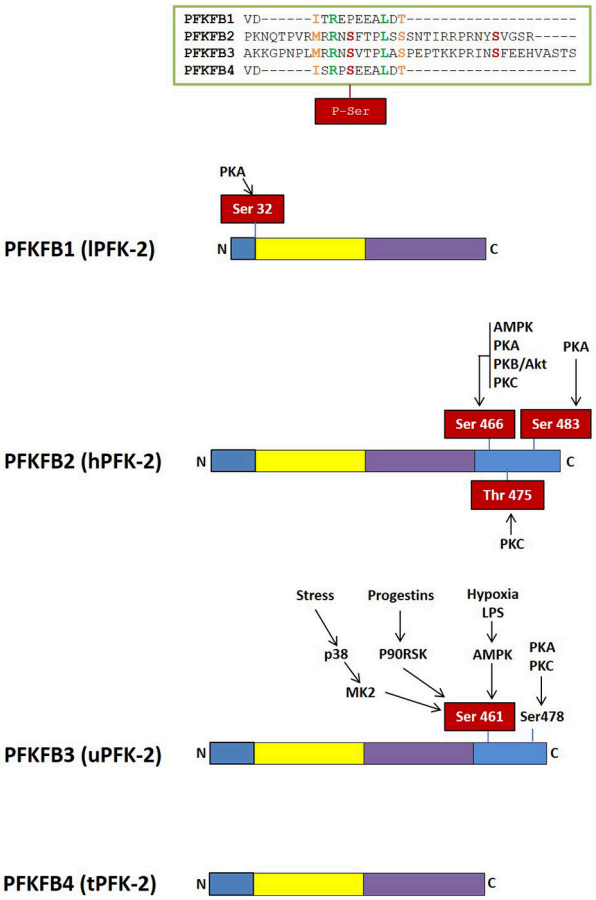

FIGURE 3 | Domain organization of PFK-2/FBPase-2 isoenzymes. The N-terminal PFK-2 domain is shown in yellow and the C-terminal FBPase-2 domain is in purple. Regulatory regions with residues susceptible of phosphorylation by different protein kinases are shown in blue.

PFKFB1

The *PFKFB1* gene was cloned from rat and human liver (71, 79, 80) and is composed of 60,944 bp. It contains 17 exons under the control of different promoters and gives rise to three different transcripts, mRNAs L (liver), M (muscle), and FL (fetal) (68, 70, 75, 81). The muscle and fetal transcripts have the same sequence as that of the liver, except for the exon encoding the N-terminal end containing the S32 residue, that can be phosphorylated by the cAMP-dependent protein kinase (PKA) in response to glucagon and dephosphorylated by protein phosphatase 2A (PP2A), activating the bisphosphatase and inhibiting the kinase activities of the liver isoenzyme, respectively (68, 70, 82) (**Figure 3**). The FL mRNA variant, present in several rat-derived cell lines and

proliferating tissues, contains two non-coding exons (1aF and 1bF) (83). Although the liver, muscle and fetal isoenzymes come from the same gene, they are regulated differently, since glucagon induces glucose synthesis in the liver but not in other tissues. *PFKFB1* has not been found to be overexpressed in cancer cells.

PFKFB2

The human *PFKFB2* gene was cloned from human heart and it contains 15 exons spanning 27,961 bp. This gene generates nine transcripts, four of which encode full-length proteins, two encode truncated proteins and the other three contain an open reading frame without producing any protein (84). PFKFB2 is a homodimeric protein, with isoform A being a 58-kDa protein containing 505 amino acids and isoform B a 54-kDa protein containing 471 amino acids. The sequence of the catalytic site is preserved, but those of the N- and C-terminal regions exhibit more variances (75, 76, 84, 85). *PFKFB2* is mainly expressed in the heart, being also located in other tissues, but in lesser proportion (76, 86). Moreover, it is expressed in cancer cells from different origins (76, 86, 87).

PFKFB2 can undergo multisite phosphorylation, integrating signals from many pathways (**Figure 3**). The C-terminal domain residues S29, S466, T475 and S483 can be phosphorylated by protein kinases such as 3-phosphoinositide-dependent kinase-1 (PDPK-1), AMP-activated protein kinase (AMPK), PKA, protein kinase B (PKB; also known as Akt), mitogen-activated protein kinase 1 (MAPK-1), and p70 ribosomal S6 kinase (S6K1). PFKFB2 phosphorylation at three conserved residues (S466, T475, and S483) results in the activation of the enzyme, decreasing its Km for Fru-6-P and increasing the Vmax of PFK-2 activity (75). PFK-2 activity, however, varies depending on the kinase that activates it (75, 88). Moreover, it has been proposed that the 14-3-3 proteins, which promote cell survival (89), bind to PFKFB2 when it is phosphorylated at S483 by Akt in response to insulin and IGF-1 or when transfected with active forms of Akt, mediating growth factors-induced glycolysis (90). Oncogenic BRAF V600E has also been found to activate p90 ribosomal S6 kinase (RSK), which phosphorylates and activates PFKFB2, that then binds to 14-3-3 to promote glycolysis and melanoma cell growth (91). Furthermore, amino acids increase Fru-2,6-P_2 synthesis and glycolysis in cardiomyocytes and cancer cell lines by PI3K and Akt-mediated phosphorylation of PFKFB2 at S483 (92). Moreover, EGFR activation induces PFK-P phosphorylation (Y64), which binds to the N-terminal SH2 domain of p85α and promotes Akt-dependent PFKFB2 phosphorylation (S483), glycolysis, cell proliferation and brain tumorigenesis (61). Adrenalin promotes PFKFB2 phosphorylation by PKA at S466 and S483, while AMPK activation during ischemia or hypoxia induces PFKFB2 phosphorylation at S466, which increases Fru-2,6-P_2 levels and stimulates glycolysis (75, 88). PFKFB2 is also a substrate of PKC, which phosphorylates S84, S466, and T475 residues (75, 93) (**Figure 3**). Several studies have reported that HIF-1α can regulate PFKFB2 expression *in vivo* but this appears to be cell-specific (86). Citrate, whose concentration is increased by the oxidation of fatty acids and ketone bodies, competitively blocks Fru-6-P binding, down-regulating *PFKFB2* expression and glycolysis through the "glucose-sparing effect" (85).

PFKFB2 is one of the genes increased in lymphoblasts from glucocorticoid (GC)-treated children suffering from acute lymphoblastic leukemia (94). Surprisingly, overexpression of the two *PFKFB2* splice variants seems to have little effect on lactate and ATP production, two metabolites that are reduced after GC treatment, and cell survival, suggesting that this gene is not an essential regulator of the anti-leukemic effects of GC (95). The androgen receptor (AR) is a key regulator of prostate growth, promoting glycolysis and anabolic metabolism, and the principal drug target for the treatment of prostate cancer (96). One of the mechanisms behind this phenotype is the transcriptional upregulation of *PFKFB2*, possibly under the control of the AR-CAMKII-AMPK signaling pathway (96). Androgens have been shown to stimulate glycolysis for *de novo* lipid synthesis. Androgens promote transcriptional up-regulation of *de novo*, mediated by binding of ligand-activated AR to its promoter, and phosphorylation of PFKFB2 generated by the PI3K/Akt signaling pathway. Moreover, blocking *PFKFB2* expression with siRNA or inhibiting PFK-2 activity with LY294002 (PI3K inhibitor) has been observed to reduce glucose uptake and lipogenesis, suggesting that the induction of *de novo* lipid synthesis by androgens requires the transcriptional up-regulation of *PFKFB2* (97). *PFKFB2* expression is also enhanced in human gastric malignant tumors, being associated with increased levels of HIF-1α dependent genes, vascular endothelial growth factor (VEGF) and Glut1, indicating that HIF-1α could be responsible for the induction of *PFKFB2* expression (87). In hepatocellular carcinoma, high expression of metastasis-associated in colon cancer protein 1 (MACC1), a key regulator of the hepatocyte growth factor (HGF)/c-Met pathway, has been noted to correlate with the high expression of *PFKFB2*, this correlation being associated to TNM stage (classification of malignant tumors), overall survival and Edmondson-Steier classification (98). Furthermore, MAPK-activated RSK, which directly phosphorylates PFKFB2, is required to maintain glycolytic metabolism in BRAF-mutated melanoma cells. RSK inhibition reduces PFKFB2 activity and glycolytic flux, suggesting an important role for RSK in BRAF-mediated metabolic rewiring (91).

Another observation highlighting the importance of PFKFB2 in metabolic reprogramming is its contribution to osteosarcoma development. Slit guidance ligand 2 (SLIT2) binds to round about guidance receptor 1 (ROBO1) and plays important roles in various physiological and pathological conditions, such as axon guidance, organ development, and angiogenesis (99). The SLIT2/ROBO1 axis promotes proliferation, inhibits apoptosis and contributes to the Warburg effect in osteosarcoma cells via activation of the SRC/ERK/c-MYC/PFKFB2 pathway (99).

PFKFB2 expression has also been linked to the regulation of non-coding RNAs. In ovarian cancer, the long non-coding RNA LINC00092 has been identified as a nodal driver of CAF-mediated metastasis. The pro-metastatic properties of CAFs have been linked to the elevated expression of both the chemokine *CXCL14* and *PFKFB2*, correlating with poor prognosis. Mechanistic studies have demonstrated that

LINC00092 binds PFKFB2, thereby promoting metastasis by inducing a glycolytic phenotype in these tumors and sustaining the local supportive function of CAFs (100). Similarly, the long non-coding RNA UCA1/miR-182 has been observed to be a nodal driver of metastasis in glioma that is mediated by glioblastoma-associated stromal cells (GASCs) and the GASC-secreted chemokine CXCL14. In clinical specimens, CXCL14 upregulation in GASCs cells was seen to correlate with poor prognosis. Interestingly, GASCs expressing high levels of CXCL14 have been shown to upregulate lncRNA UCA1 and downregulate miR-182, with miR-182 directly binding to PFKFB2 to modulate CXCL14 secretion, glycolysis, and the invasion of glioma cells (101).

PFKFB2 has also important roles in the physiology of human CD3+ T cells. Treatment of activated human CD3+ T cells with the proinflammatory chemokine CCL5 induces the activation of AMPK and PFKFB2 phosphorylation and activation, promoting glycolytic flux and suggesting that both glycolysis and AMPK signaling are required for efficient T cell activation in response to CCL5 (102).

PFKFB3

The *PFKFB3* gene was cloned from a cDNA library of fetal brain and has been found expressed in all the tissues studied (103–107). It spans 109,770 bp and is composed of 19 exons. The variable C-terminal domain can undergo alternative splicing to produce six different isoforms. The two main isoforms are generated by alternative splicing of exon 15 and differ in their C-terminal sequence, the 4,553 bp mRNA variant initially named as ubiquitous PFK-2 (uPFK-2) (107) and the 4,226 bp mRNA inducible PFK-2 (iPFK-2) variant (106). Four additional splice variants have also been described (108). As many proto-oncogenes and pro-inflammatory cytokines, PFKFB3 has multiple copies of the AUUUA sequence in the 3′UTR of its mRNA, which confer instability and enhanced translational activity (106). It has been found that miR-26b and miR-206 interact with the 3′UTR of the PFKFB3 mRNA, decreasing glycolysis in osteosarcoma and breast cancer cells, respectively (109, 110).

PFKFB3 gene expression is induced by different stimuli, such as hypoxia (31, 111, 112), progestin (104, 113), estrogens (114) and stress stimuli (115), through the interactions of HIF-1α, the progesterone receptor (PR), estrogen receptor (ER), and the serum response factor (SRF). These factors bind to specific sequences in PFKFB3 promoter which are the consensus hypoxia response element (HRE), the progesterone response element (PRE), estrogen response element (ERE), and the serum response element (SRE), respectively. *PFKFB3* expression can also be stimulated by growth factors such as insulin (73), pro-inflammatory molecules (106) such as interleukin-6 (IL-6) (116, 117), lipopolysaccharide (LPS) and adenosine (118), mitogenic lectins such as concanavalin A (ConA) (119) and phytohemagglutinin (PHA) (120), and the transforming growth factor beta 1 (TGF-β1) (121).

PFKFB3 gene expresses an isoenzyme that has high kinase and low bisphosphatase activity (K/B = 710), favoring the net synthesis of Fru-2,6-P_2 and eliciting high concentrations of this metabolite in proliferating and tumor cells (122). The presence of a serine instead of an arginine at position 302 in the bisphosphatase active site gives place to the low bisphosphatase activity (123).

Different protein kinases, such as AMPK (124, 125), RSK (113), MK2 (115), PKA, PKB (119), and PKC (125) regulate the PFKFB3 isoenzyme by covalent modification of its C-terminal domain (**Figure 3**). PI3K/Akt also controls the PFKFB3 isoenzyme downstream of growth factors signaling (119, 126, 127). Phosphorylated PFKFB3 has increased Vmax of its kinase activity and decreased Km for fructose-6-P (119, 124). ROS-mediated S-glutathionylation (128) or demethylation (129) also regulate PFKFB3 in cancer cells, decreasing its catalytic activity and redirecting the glycolytic flux to the PPP, increasing NADPH and decreasing ROS levels. Similarly, cell damage-mediated induction of p53 stimulates nucleotide biosynthesis by inhibiting *PFKFB3* expression and enhancing the flux of glucose through the PPP to increase nucleotide production, which promotes DNA repair and cell survival (130) (**Figure 4**).

The PFKFB3 isoenzyme can also be regulated through the ubiquitin-proteasome system (131), as it contains a KEN box that can be ubiquitinated by the E3 ubiquitin ligase of the anaphase-promoting complex (APC/C), which is activated by Cdh1, in a similar way to that of other proteins in the cell cycle. The proliferative response depends on the reduced activity of APC/C-Cdh1 to activate proliferation and glycolysis (132). PFKFB3 silencing prevents cell cycle progression, illustrating that this isoenzyme is essential for cell division (133). The tumor suppressor PTEN promotes APC/C-Cdh1 activity (127, 134) and cells from mice that overexpress PTEN show APC/C-Cdh1-mediated degradation of PFKFB3 and glutaminase, resulting in a decrease of glycolysis and proliferation, and an increase in resistance to oncogenic transformation (127). PFKFB3 isoenzyme levels have also been shown to increase in proliferating cells through the activation of cyclin D and E2F1, two downstream effectors of the PI3K-Akt-mTOR pathway (126), localizing in the nucleus and regulating proliferation through cyclin-dependent kinases (135). The nuclear targeting of PFKFB3 has been shown to increase cyclin-dependent kinase 1 (CDK1) expression among other cell cycle proteins. In particular, Fru-2,6-P_2 stimulates the phosphorylation of the Cip/Kip protein p27 mediated by CDK1, which in turn elicits p27 ubiquitination and proteasomal degradation (136). PFKFB3 also interacts with CDK4, inhibiting its degradation via the ubiquitin proteasome pathway to promote cell cycle progression (137).

PFKFB3 expression is induced by endotoxin in human macrophages (106, 124). Macrophage Toll-4 receptor agonists cooperate with adenosine to increase glycolysis by heightening *PFKFB3* gene expression and Fru-2,6-P_2 synthesis, which increases glycolysis and favors ATP synthesis, developing the long-term defensive and reparative functions of macrophages (118). Macrophage glycolysis and pro-inflammatory activation mainly depend on HIF-1α and its effects on glucose uptake and the expression of hexokinase-II (HK-2) and *PFKFB3* (138) (**Figure 4**). These findings indicate that hypoxia enhances glycolytic flux in macrophages through HIF-1α and PFKFB3 proportionally to the upregulation of pro-inflammatory activities

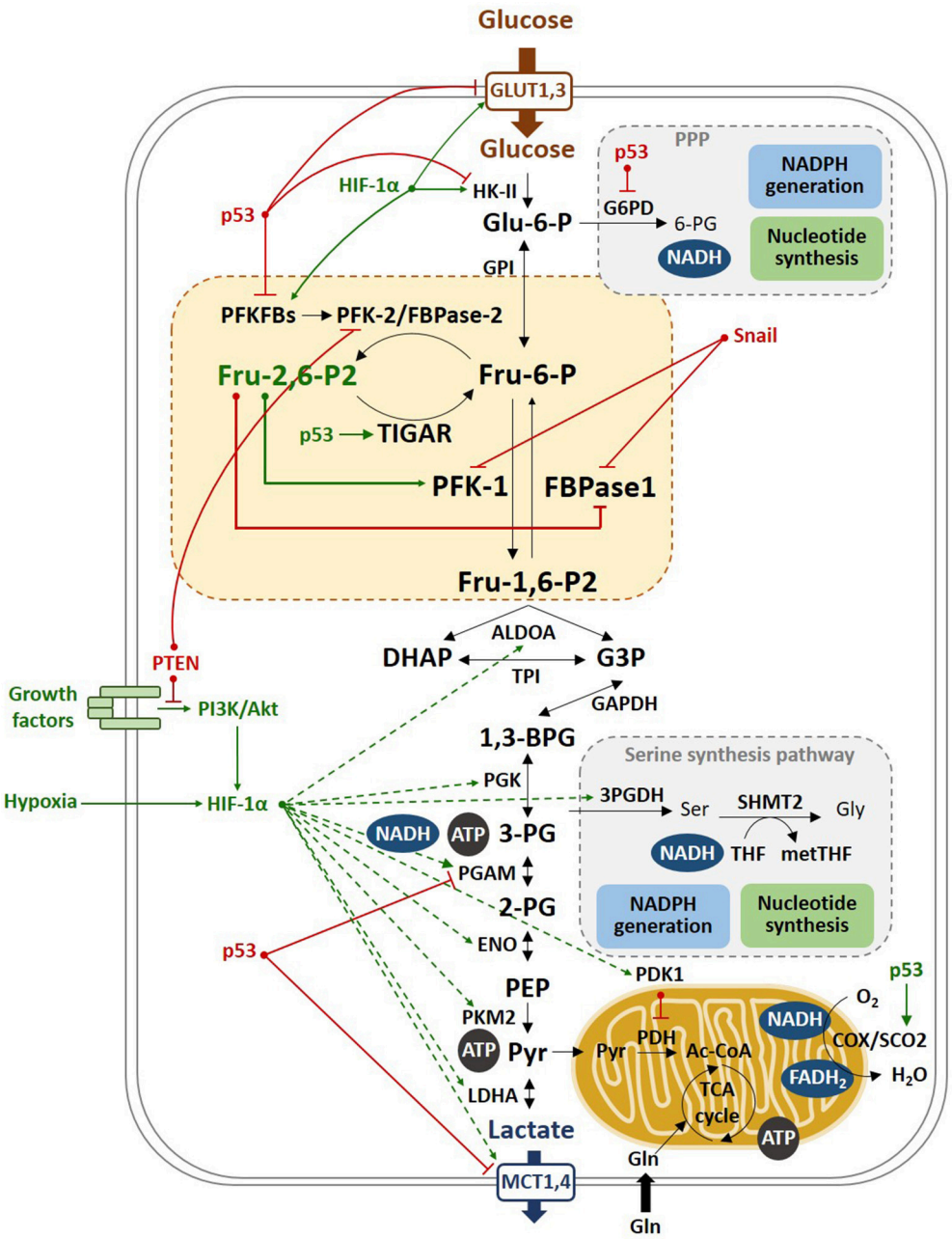

FIGURE 4 | Molecular mechanisms of the Warburg effect. Hypoxia stabilizes HIF-1α, which transactivates most of the glycolytic genes, such as HK-II and PFKFBs, as well as PDK1, which in turn inhibits PDH, that catalyzes the conversion of pyruvate to Ac-CoA. PDH inhibition blocks the entry of pyruvate into the TCA, promoting the oxidation of pyruvate to lactate. Lactate is then excreted through the MCT transporters, which expression is also increased by HIF-1α. p53 inhibits the glycolytic genes PFKFB3, PFKFB4, and PGAM and the lactate transporter MCT1, and induces TIGAR, reducing the glycolytic flux. This results in increased flux of the pentose phosphate shunt to produce NADPH and ribose-5P. Moreover, p53 stimulates respiration by inducing SCO2, a component of cytochrome c oxidase (COX). In tumors, limited access to oxygen and mutations in the p53 gene drive to increased glycolysis, a phenomenon named as the Warburg effect.

in these cells (138). These *in vivo* observations suggest that HIF-1α antagonists or PFKFB3 inhibitors could be used to alleviate inflammatory diseases. Furthermore, cytosolic viral recognition by secondary interferon signaling has been demonstrated to upregulate glycolysis preferentially in macrophages through PFKFB3 induction, promoting the extrinsic antiviral capacity of macrophages and being a crucial component of innate antiviral immunity (139).

PFKFB3 is constitutively overexpressed in different cancer cell lines and in several human leukemias and solid tumors (140, 141), including ovarian and thyroid carcinomas (142), colon adenocarcinoma, breast cancer, gastric tumors and pancreatic

cancer (73, 87, 111, 113, 143), and has been associated with lymph node metastasis and the TNM stage (143). PFKFB3 can also represent a biomarker and an anti-neoplastic target in gastric cancer (144). Furthermore, *PFKFB3* expression is required for cell growth and increased metabolic activity in myeloproliferative neoplasms expressing the oncogenic JAK2V617F kinase, which is a very common mutation in these malignancies. JAK2V617F and active STAT5 overexpress *PFKFB3* and *PFKFB3* silencing reduces cell growth under normoxic and hypoxic conditions and prevents tumor formation (145). In chronic myeloid leukemia (CML), PFKFB3 has been found to be strongly associated with resistance to the BCR-ABL tyrosine kinase inhibitors. *PFKFB3* silencing or pharmacological inhibition of its kinase activity enhances the sensitivity of CML cells to these inhibitors (146). In acute myeloid leukemia (AML), mTOR-mediated up-regulation of PFKFB3 is essential for cell survival, as mTORC1 up-regulates PFKFB3 in a HIF1α-dependent manner, and PFKFB3 silencing suppresses glycolysis and cell proliferation and activates apoptosis (147).

In malignant human colon tumors, PFKFB3 overexpression and phosphorylation of its S461 residue (P-PFKFB3 S461) has been observed (148). The cytokine IL-6 increases glycolysis by inducing *PFKFB3* expression through STAT3 activation (116), suggesting a functional role of PFKFB3 in chronic inflammation and in the development of colorectal cancer (117). Similar results have been reported in TGF-β1-induced lung fibrosis, in which PFKFB3 inhibition attenuates prefibrotic phenotypes and blocks the differentiation of lung fibroblasts (149). Furthermore, we have shown that TGF-β1 overexpresses *PFKFB3* mRNA and protein in glioblastoma cells through the activation of the Smad, p38 MAPK and PI3K/Akt signaling pathways. Inhibiting PFKFB3 expression or activity significantly suppressed the ability of T98G cells to form colonies, which is one of the hallmarks of cell transformation (121).

High-grade astrocytomas also contain increased PFKFB3 protein levels (150). The expression of the PFKFB splice variant UBI2K4 prevents tumor cell growth, acting as a tumor suppressor in astrocytic tumors (151). Besides, loss of heterozygosity in 10p14-p15, which leads to the allelic deletion of UBI2K4, has been detected in 55% of glioblastomas and is associated with poor prognosis (152).

PFKFB3 has also a key role in the interaction between cancer cells and other cells in the TME. Endothelial cells (ECs) depend on glycolysis more than on oxidative phosphorylation for ATP synthesis and loss of PFKFB3 in ECs impairs vessel formation (52). Inhibition of glycolysis by silencing PFKFB3 expression or pharmacologically blocking its kinase activity has been observed to inhibit pathological angiogenesis, such as ocular and inflammatory disease, without causing systemic effects (153). Recently, an article reported that targeting PFKFB3 in ECs significantly impeded metastasis by normalizing tumor vessels and improved the delivery and efficacy of chemotherapy (154). Nuclear factor (erythroid-derived 2)-like 2 (Nrf2) regulates endothelial glycolysis and proliferation through the transcriptional regulation of PFKFB3, *VEGFA*, *FOXO1*, and *MYC* (155), with a positive correlation occurring between Nrf2, HIF-1α, and *PFKFB3* expression in breast cancer cells, and cancer patients with high *PFKFB3* expression showing poorer overall survival (156).

PFKFB3 expression is also linked to hepatocellular carcinoma (HCC) growth. *PFKFB3* overexpression has been associated with a large tumor size and poor survival in patients, while *PFKFB3* knockdown inhibits HCC growth by reducing glucose consumption and impeding DNA repair, which leads to cell cycle arrest at the G2/M phase and apoptosis. Silencing PFKFB3 expression decreases Akt phosphorylation and reduces the expression of ERCC1, a protein involved in DNA repair (157). The combination of aspirin and sorafenib has been shown to perform a synergistic effect against liver cancer. *PFKFB3* overexpression, associated with high glycolytic flux, is frequently observed with sorafenib resistance, which can be overcome by aspirin. By inhibiting PFKFB3, sorafenib plus aspirin induce apoptosis in tumors without eliciting weight loss, hepatotoxicity and inflammation, suggesting that their combination may be an effective treatment for HCC (158).

A large number of studies have reported that increased *PFKFB3* expression promotes proliferation and carcinogenesis, indicating that its inhibition could be crucial for treating inflammation and cancer. Indeed, siRNA suppression of PFKFB3 has been reported to reduce cancer cell viability (159, 160) while small molecule inhibitors of the PFKFB3 isoenzyme have been developed (161).

PFKFB4

PFKFB4, firstly cloned from rat (162) and human testis (163), is a 44,332 bp gene composed of 14 exons. Several splice variants have been reported, with the PFK-2 core domain being conserved among all of them (162, 164). The *PFKFB4* gene encodes an isoenzyme that is expressed in the testis under the regulation of testosterone (165, 166). Moreover, it has been demonstrated that PFKFB4 mRNA and protein levels are regulated by hypoxia and glucose levels in different cancer cell lines from the prostate, liver, colon, bladder, stomach and pancreas (86, 87, 167–171). PFKFB4 is a prognostic marker in invasive bladder cancer (172), where its expression is activated by HIF-1α (171) (**Figure 4**). In hepatic cancer cell lines, sulforaphane-induced apoptosis was shown to decrease PFKFB4 protein expression and glucose consumption whereas HIF-1α induced *PFKFB4* expression under hypoxic conditions (173). *PFKFB4* expression is also controlled by heme-oxygenase-2 in HepG2 cancer cells (174). In HCC, upregulated Peroxisome proliferator-activating receptor γ (PPARγ) induces *PFKFB4* expression through the transcriptional activity of its promoter, regulating glycolysis and cell proliferation (175). High PFKFB4 mRNA and protein expression have been described in three different glioblastoma stem-like cell lines, with shRNA-mediated knockdown of *PFKFB4* promoting apoptosis (176) and no phenotypic effect occurring in PFKFB4-silenced normal neural stem cells. Furthermore, HIF1α-induced PFKFB4 mRNA expression correlates with glioma tumor grade (176).

PFKFB4 is required to balance glycolytic activity and antioxidant production to maintain the cellular redox balance in prostate cancer cells (169). PFKFB4 mRNA expression has been found to be greater in metastatic prostate cancer cells than in primary tumors. PFKFB4 silencing selectively increases Fru-2,6-P_2 concentration in prostate cancer cells, suggesting that it mainly functions as a fructose-2,6-bisphosphatase in these particular cells. The increase in Fru-2,6-P_2 levels should direct

glucose 6-phosphate toward the glycolytic pathway, thereby reducing the activity of the PPP. This would explain why prostate cancer cells show lower NADPH and glutathione levels after PFKFB4 silencing, which results in enhanced oxidative stress and cell death (169). Furthermore, p53 decreases *PFKFB4* gene expression by binding to its promoter to mediate transcriptional repression via histone deacetylases. PFKFB4 depletion also attenuates biosynthetic activity and induced ROS accumulation and cell death in the absence of p53 (177).

In a study investigating the differences in glucose metabolism between two forms of prostate cancer, small cell neuroendocrine carcinoma (SCNC) was found to be more glycolytic than adenocarcinoma, CD44 being a key regulator of glucose metabolism. *PFKFB4* expression in benign prostate tissue was lower than that in the adenocarcinoma, and significantly higher in SCNC. CD44 ablation in SCNC cells reduced both mRNA and protein levels of PFKFB4 (178). Thus, CD44 can modulate the aggressive phenotype of prostate cancer cells by increasing *PFKFB4* expression (179).

PFKFB4 can also regulate autophagy by influencing the redox balance. In PC3 prostate cancer cells, PFKFB4 inhibition was observed to cause p62 accumulation, which is usually associated with the inhibition of autophagy. However, the autophagic flux was increased in these cells. The combination of antioxidants and PFKFB4 inhibition prevented p62 accumulation, which was instead mediated by Nrf2, thus avoiding autophagy. Hence, *PFKFB4* expression is required for appropriate ROS detoxification in these cells (180). It was recently found that epithelial and endothelial tyrosine kinase interacts with PFKFB4 modulating chemoresistance of small-cell lung cancer by regulating autophagy (181).

Solid malignant tumors of the breast present a higher *PFKFB4* expression compared to non-malignant tissue. In several breast cancer cell lines, *PFKFB4* expression increased upon exposure to hypoxia (87). PFKFB4 was recently shown to act as a protein kinase phosphorylating the oncogenic steroid receptor coactivator-3 (SRC-3) and enhancing its transcriptional activity to drive breast cancer (182). PFKFB4 suppression or ectopic expression of a phosphorylation-deficient S857A mutant of SRC-3 abolished SRC-3-mediated transcription. Mechanistically, SRC-3 phosphorylation increases its binding with the ATF4 transcription factor by stabilizing the recruitment of SRC-3 and ATF4 to target gene promoters. Functionally, PFKFB4-induced SRC-3 activation directs the glucose flux toward the PPP and the synthesis of purines by transcriptionally upregulating the expression of transketolase. *PFKFB4* or SRC-3 silencing inhibits breast tumor growth and metastasis (182).

Apart from the importance of PFKFB4 in regulating cancer cell glycolysis, its expression also determines the metabolic adaptation of non-tumor cells. In mitogen-stimulated rat thymocytes, ConA was shown to induce the expression of *PFKFB3* and *PFKFB4* as well as increase glycolysis, cell proliferation and protein synthesis. This supports a role for these two proteins in coupling glycolysis to cell proliferation in lymphoid tissues (119).

TIGAR

The *c12orf5* gene was discovered during a computer-based analysis of microarray data trying to find novel p53-regulated genes that are activated in response to ionizing radiation (183). This gene was cloned and characterized, and named as TP53-Induced Glycolysis and Apoptosis Regulator (*TIGAR*) (184) (**Figure 4**). *TIGAR* is a target of p53 that becomes rapidly activated by low levels of stress. The human *TIGAR* gene consists of six exons spanning about 38,835 bp, coding for a unique mRNA transcript variant of 8.2 kb with a 813 bp coding sequence. *TIGAR* promoter contains two p53 binding sites, one upstream of the first exon and the other within the first intron, the latter being the most efficient (184). *TIGAR* can be induced by Nutlin-3, an antagonist of Mdm2 that increases p53 levels (185), radiotherapy (183, 186), glutamine (29), chemotherapy (187), UV light (187), TNFα, and radiotherapy mimetics (188) or by the Akt signaling pathway in response to the metabolic stress caused by *PFKFB3* knockdown (189). *TIGAR* expression can also be regulated in a p53 independent manner (186, 189) by linking the CRE-binding protein (CREB) to the *TIGAR* promoter (190). Another transcription factor, the specificity protein 1 (SP1), can bind to *TIGAR* promoter and is considered important for its basal activity (191). *TIGAR* can be induced in response to hypoxia in myocytes (192) and some studies have identified HIF-1α as a regulator of cytochrome C-oxidase-2 (*SCO2*) and *TIGAR* gene expression in response to hypoxia (193). SCO2, a metallochaperone that is involved in the biogenesis of cytochrome C oxidase subunit II, participates in the mitochondrial chain, it is also induced by p53 and its blockage leads to the glycolytic phenotype (194).

The human TIGAR protein is composed of 270 amino acids and has a molecular weight of 30 kDa. It contains a bisphosphatase active center in which two histidine residues, H11 and H198, and one glutamic acid, E102, are essential for its activity (184). TIGAR contains a catalytic domain similar to the histidine phosphatase superfamily of proteins with a histidine forming a transient phosphoenzyme during catalysis (195). This domain shares similarity with those of the phosphoglycerate mutase (PGAM) family of enzymes and with the bisphosphatase domain of PFK-2/FBPase-2 isoenzymes (196). TIGAR bisphosphatase activity hydrolyzes Fru-2,6-P_2 into Fru-6-P, which can then enter in the PPP to synthesize NADPH and ribose-5-phosphate, thus reducing ROS and producing nucleotide precursors that are essential for biosynthesis, DNA repair and cell proliferation (184) (**Figure 4**). As TIGAR has no kinase domain, it behaves as a kinase-deficient PFKFB isoform. Thus, cells overexpressing FBPase-2 show similar enhanced PPP flux and resistance to oxidative stress (197). The FBPase catalytic activity of TIGAR is several orders of magnitude lower than that of the FBPase-2 component of PFK-2/FBPase-2 isoenzymes, pointing out that Fru-2,6-P_2 could not be its main physiological substrate (198).

TIGAR mRNA is expressed in all the tissues in which it has been analyzed to date and is overexpressed in several cancer cells. It localizes mainly in the cytoplasm, but has been observed to relocalize to the outer mitochondrial membrane

under hypoxic conditions to form complexes with HK-2, limiting ROS production (199).

TIGAR has also been linked to autophagy. For example, TIGAR overexpression and reduced ROS levels have been observed alongside suppressed autophagy in cells exposed to stress conditions, and TIGAR suppression induced autophagy that subsequently mediates apoptosis by restraining ROS levels (200). The relationship between autophagy and apoptosis is regulated distinctively according to the stimulus and cell type. Thus, treatment of neuroblastoma cells with D-galactose induces necroptosis and autophagy, as reflected in the upregulation of *BMF, BNIP3, ATG5*, and *TIGAR*, without affecting the expression of the genes associated with apoptosis (201). Decreased mRNA levels of TIGAR and reduced levels of the damage-regulated autophagy modulator (DRAM) have been reported in HepG2 cells exposed to high oxidative stress or nutrient starvation (202). Upon disruption of the homeostasis balance of the cell, TIGAR is activated and provides protection through its antioxidant properties rather than by inhibiting autophagy, while other transcriptionally activated targets, such as DRAM, enhance autophagy (203). Some studies have proposed that p53 regulates stress-induced autophagy by balancing TIGAR and DRAM, which have opposite effects (204, 205).

Like the PFKFB isoenzymes, TIGAR can also play a role in cancer. The function of TIGAR in a specific cell type depends on the metabolic state of the cell and PFKFBs activities that determine Fru-2,6-P_2 concentration and glycolytic flux. TIGAR activity could limit glycolysis and produce antioxidant molecules and precursors for nucleotide synthesis, thereby limiting cancer development. However, *TIGAR* overexpression can also promote the growth of tumor cells with high ROS levels. TIGAR has been reported not be necessary for normal growth and development in mice, but plays an important function in intestinal regeneration. The lack of TIGAR causes growth defects which are recovered by ROS scavengers and nucleosides (206). Besides, *TIGAR* deficiency has been reported to reduce tumor growth and improve survival in a mouse intestinal adenoma model, while elevated *TIGAR* expression supported cancer progression (206). *TIGAR* expression is increased in human breast, gastric and lung cancer, inversely correlating with p53 expression levels (207–209). Furthermore, TIGAR downregulation inhibits growth in several cancer cell lines (184). In a model of nasopharyngeal cancer, 1-(3-C-ethynyl-beta-d-ribo-pentofuranosyl)cytosine (ECyd), an RNA-nucleoside anti-metabolite with potent anticancer activity, was shown to downregulate TIGAR and deplete NADPH. *TIGAR* overexpression was able to recover the growth inhibition induced by ECyd (210). In the same model, c-Met protein kinase maintained *TIGAR* expression, whereas c-Met silencing significantly decreased *TIGAR* expression and subsequently depleted intracellular NADPH, which lead to cell death (211). TIGAR silencing induces also apoptosis and autophagy in HepG2 cells (212), while RNAi-mediated knockdown of citrate synthase in human cervical carcinoma cells accelerates cancer cell metastasis and proliferation deregulating the p53/TIGAR pathway (213). In HeLa cervical carcinoma cells, TIGAR can be induced in an Akt-dependent manner in response to the inhibition of glycolysis. PFKFB3 depletion by RNAi increases ROS levels and decreases cell viability, this effect being highly exacerbated when TIGAR is also inhibited. However, TIGAR inhibition alone does not have an impact on HeLa cell survival (189). Furthermore, some studies have reported that TIGAR regulates the cell cycle by de-phosphorylating the retinoblastoma protein (RB) and stabilizing RB-E2F1 complex, thus delaying entry into the S phase (187, 214).

In multiple myeloma cells, inhibition of MUC1-C oncoprotein increases ROS levels and downregulates *TIGAR* expression, resulting in decreased NADPH and glutathione levels and promoting ROS-mediated apoptosis/necrosis (215). Sensitivity to fludarabine and p53-mediated *TIGAR* induction has been described in chronic lymphocytic leukemia. The sensitivity to fludarabine varied despite all patients presented wild-type p53 (216). Glioblastoma cells overexpress *TIGAR* which reduces cell death induced by restricting glucose and oxygen (217). These results indicate the potential therapeutic use of TIGAR as an antitumoral target (186). Similarly, *TIGAR* expression was found decreased with a sonodynamic therapy tested in a neuroblastoma cell model which decreases cell proliferation, possibly through increased ROS levels (218). In glioblastoma-derived cell lines, *TIGAR* abrogation increased radiation-induced cell destruction, providing a new therapeutic strategy that could be used to increase cell death in glial tumors, thus allowing the use of lower doses of radiotherapy. Gliomas are resistant to radiotherapy and to TNFα-induced killing. Radiation-induced TNFα increases radioresistance through nuclear factor κB (NFκB). Thus, the existence of an ATM-NFκB axis regulating TIGAR indicates its involvement in the inflammation and resistance to radiomimetics (188). It was recently reported that TIGAR regulates NF-κB activation by suppressing phosphorylation and activation of the upstream IKKβ, which occurs through a direct binding competition between NEMO and TIGAR for the linear ubiquitination assembly complex (LUBAC), preventing the linear ubiquitination of NEMO required for the activation of IKKβ and other downstream targets. Furthermore, a TIGAR mutant with impaired phosphatase activity was equally effective as wild-type TIGAR in inhibiting the linear ubiquitination of NEMO, IKKβ phosphorylation/activation and NF-κB signaling, indicating that the effect of TIGAR on NF-κB signaling is due to a non-enzymatic molecular function, that directly inhibits the E3 ligase activity of LUBAC (219).

In a co-culture system, oxidative stress-induced autophagy correlated with caveolin-1 (CAV1) downregulation in CAFs and *TIGAR* overexpression in adjacent breast cancer cells (**Figure 5**). Reduced CAV1 expression in fibroblasts reduces mitochondrial function and induces glycolysis through HIF-1α and NF-kB signaling (30). Consequently, autophagic CAFs supply recycled substrates for the cancer cell metabolism and, also, avoid cancer cell death by overexpressing TIGAR, thereby conferring resistance to apoptosis and autophagy (220). Other studies by the same group have shown that the metabolic coupling between cancer cells and fibroblasts contribute to tamoxifen resistance, as CAFs enhanced TIGAR activity in cancer cells, that protected against tamoxifen-induced apoptosis (221). In

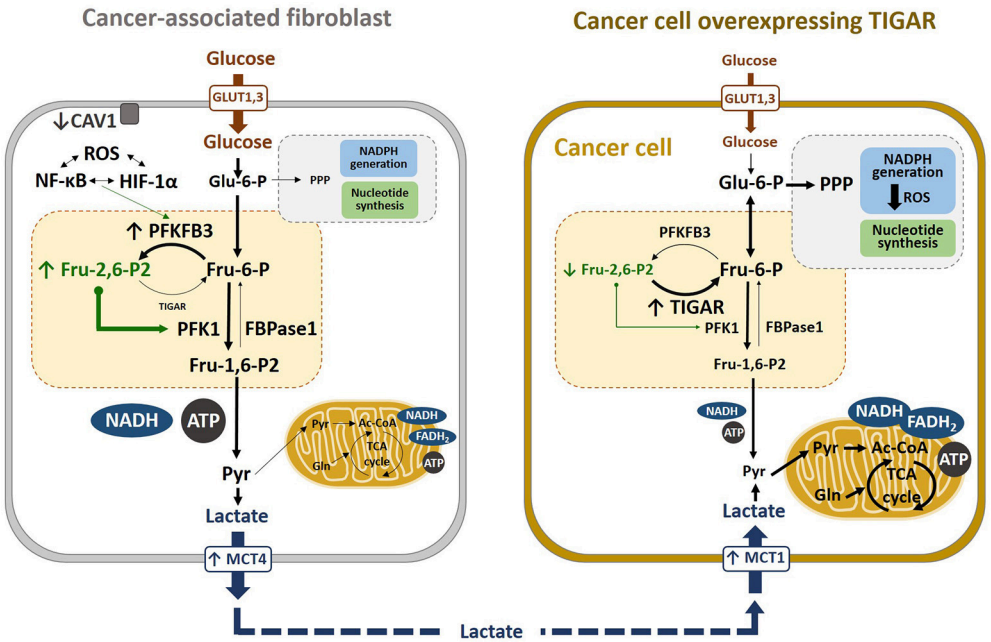

FIGURE 5 | Metabolic reprogramming in cancer cells. Lactate transport is crucial in the crossed-regulation of metabolism between cancer-associated fibroblasts (CAFs) and cancer cells. In the fibroblasts close to carcinoma cells, ROS, HIF-1α, and NF-κB induce glycolysis, downregulating CAV1 and upregulating MCT4, which results in increased lactate secretion in CAFs. Conversely, TIGAR overexpression in carcinoma cells alters their metabolic state, increasing the pentose phosphate pathway (PPP). Lactate released from CAFs is taken by cancer cells via MCT1 and converted to pyruvate, which can enter the TCA cycle. These cancer cells have high mitochondrial OXPHOS and low glycolysis, which is associated with high proliferation and low apoptosis rates, resulting in increased tumor growth.

another study, glutamine was described to increase TIGAR and be needed for CAV1 downregulation in CAFs, decreasing mediators and markers of autophagy in cancer cells. In this model, glutamine from autophagic fibroblasts may serve to fuel cancer cell mitochondrial activity. Thus, a cycle of nutrients between catabolic stromal cells and anabolic tumor cells has been suggested to account for the relationship between cells in the TME (19–21, 28–30, 222). In addition, *TIGAR* overexpression has been shown to reprogram carcinoma and stromal cells in breast cancer (29), as well as to increase oxygen consumption rates and ATP levels in the presence of glutamine and lactate, leading to enhanced ATP synthesis. Moreover, when carcinoma cells overexpress TIGAR in co-cultures with fibroblasts, a glycolytic phenotype is induced in the fibroblasts, inducing HIF-1α expression as well as increasing glucose uptake and the expression of *PFKFB3* and lactate dehydrogenase-A. *TIGAR* overexpression in carcinoma cells increases tumor growth and proliferation rates *in vivo* (29, 30). All these data support a two-compartment model of tumor metabolism (**Figure 5**). The mechanisms by which *TIGAR* overexpression increases mitochondrial activity remain unknown to date (29, 217).

Fru-2,6-P_2 Metabolism and the Regulation of Glycolysis and the Pentose Phosphate Pathway in Cancer Cells

The different PFKFB isoenzymes and TIGAR have important roles in the TME. The genes encoding these isoenzymes are commonly overexpressed in tumors and can be induced in response to cellular stress. These isoenzymes, regulating Fru-2,6-P_2 concentration, have contrary effects on cell metabolism and different studies have dealt with the cross-regulation of these enzymes (**Figure 4**). The contribution of TIGAR to the regulation of Fru-2,6-P_2 levels is expected to vary depending on the expression levels of the PFKFB1–PFKFB4 isoenzymes. *TIGAR* overexpression is associated with decreased survival of patients with acute myeloid leukemia (AML) (223) and other tumors (217, 224). Overexpression of *PFKFB2-4* has similar outcomes (97, 98, 113, 161, 176). However, crosstalk between these genes must exist in cancer cells since it has been observed that when *TIGAR* is eliminated in leukemia cells expressing high levels of *TIGAR*, *PFKFB3* expression increase, and when *TIGAR* is overexpressed in cells with low levels of *TIGAR*, *PFKFB3* expression decrease (223). Moreover, we have reported that *PFKFB3* silencing in HeLa cells elevates ROS levels and overexpresses *TIGAR* through Akt signaling, preserving against DNA damage and apoptosis (189). These results indicate that cancer cells sustain high glycolytic flux in order to fuel biosynthetic pathways under basal conditions. Nevertheless, if glycolysis is impeded, for example by ROS-induced S-glutathionylation or demethylation of PFKFB3 (128, 129), *PFKFB3* interference, or PFKFB3 inhibitors (189), cancer cells divert the flow toward the PPP. Cancer cells can also inhibit glycolysis to decrease ROS in response to DNA damage. In this respect, following DNA damage, the function of p53 reducing the mRNA and protein levels of PFKFB3 (130) and PFKFB4 (177) as

well as the glycolytic flux, while increasing TIGAR expression and the levels of NADPH and nucleotides through the PPP (184, 186), enhances DNA repair and cell survival. In this sense, in p53-deficient cells exposed to UV radiation, glycolysis is not impeded supporting that p53 is required for this regulatory role (130, 177).

The FBPase catalytic efficiency of TIGAR has been reported to be several orders of magnitude lower than that of the FBPase-2 activity of PFKFBs (195, 198), thus challenging the concept that TIGAR acts primarily on Fru-2,6-P_2. TIGAR could also exert its effects by directly increasing flux through the terminal part of glycolysis, given that it was found to act as the phosphoglycolate-independent 2,3-bisphosphoglycerate phosphatase (225), with 2,3-bisphosphoglycerate (2,3-BPG), 2-phosphoglycerate (2-PG) and phosphoenolpyruvate (PEP) being better substrates than Fru-2,6-P_2 (198). These effects could also be enhanced by the presence of PKM2 in cancer cells, which has low affinity for PEP and provides a large amount of metabolic precursors for biosynthesis (14, 226). The concentration of 2,3-BPG in cells is three orders of magnitude lower than that in erythrocytes (227) and very little is known about its function, apart from the fact that it is an essential cofactor for the phosphoglycerate mutase. This adds a novel layer of complexity to the function of TIGAR that should be taken into account in future studies.

PFKFB4 expression is essential for prostate and p53-null colon cancer cell survival, maintaining the balance between the use of glucose for energy generation and the synthesis of antioxidants (177). PFKFB4 silencing increases Fru-2,6-P_2 levels in prostate cancer cells, suggesting that it mainly functions as a fructose-2,6-bisphosphatase in these particular cells, diverting glucose 6-phosphate toward the PPP (169). By contrast, *PFKFB4* that is expressed in other types of transformed cells and tumors synthesizes Fru-2,6-P_2 and is required for the glycolytic reprogramming of cancer cells (170). Specific analyses of the enzymatic activity and regulation of PFKFB4 are needed to characterize its potential role as a FBPase-2 proposed in some studies (169, 177).

PFKFB4 has been shown to act as a protein kinase of SRC-3 resulting in the upregulation of transketolase (182). This finding could explain the effect of *PFKFB4* overexpression in some cancer cells, such as the transcription of a key non-oxidative enzyme of the PPP and the redirection of glycolytic intermediates to the non-oxidative arm of PPP.

Other inhibitory glycolytic effects that contribute to cancer development, such as the glycosylation of PFK1 in response to hypoxia (59) and the Snail repression of PFK-P (60), redirect glucose flux through the PPP, thereby conferring a selective growth advantage to cancer cells. Furthermore, FBPase1 overexpression suppresses cancer cell growth (65), its loss correlating with advanced tumor stage and poor prognosis (66). Snail can also repress FBPase1 in breast cancer cells (67), regulating glucose flux toward glycolysis or the PPP by suppressing either FBPase1 or PFK-P, respectively.

Finally, FBPase1 and PFK-L are part of the "glycosome," a complex that modulates the activities of these enzymes and integrates them with others such as PKM2 and PEPCK1. Quantitative high-content imaging assays indicate that the direction of glucose flux between glycolysis, the PPP and serine biosynthesis seems to be spatially regulated by these multienzyme complexes in a cluster size-dependent manner, providing new mechanistic insight into how a cell regulates the direction of glucose flux between energy metabolism and anabolic biosynthesis (53).

TARGETING THE TUMOR METABOLIC ECOSYSTEM

The ability to selectively modulate the metabolism of cancer cells could have high therapeutic potential. Tumor cells expressing active oncogenes and/or defects in their tumor suppressors enter apoptosis when glucose oxidation is limited. Peculiarly, these same cells often show resistance to other forms of apoptotic stimuli (radiation and chemotherapy) and the use of glycolytic inhibitors sensitizes cells to these stimuli and promotes their death (21, 228, 229).

The dependence of cancer cells on glucose consumption led to the development of different therapeutic approaches. Pharmacological inhibition of glycolysis has emerged as a novel strategy since high glycolytic activity is considered a metabolic hallmark of cancer (6, 21, 31, 34). HIF-1α overexpression and the induction of glycolytic isoenzymes, present in many tumors, have been shown to generate resistance to chemotherapy and radiation (39, 230, 231). Therefore, inhibiting HIF-1α could be an important component of cancer therapy (232, 233).

One of the most studied inhibitors has been 2-DG, a glucose molecule in which the 2-hydroxyl group has been replaced by hydrogen. 2-DG can be phosphorylated by hexokinase, but it cannot be metabolized by phosphohexose-isomerase. Therefore, its intracellular accumulation produces a competitive inhibition of hexokinases. 2-DG has cytotoxic effects on different types of cancer cells, especially those overexpressing HIF-1α and with mitochondrial defects (229, 234). Accordingly, 2-DG significantly increases the response to treatment with adriamycin and paclitaxel in human osteosarcoma-bearing mice and of small cell lung cancer (234). However, the high doses needed to compete with glucose can induce toxicity (21, 235). Inhibition of other glycolytic enzymes has been shown to successfully suppress tumor cell growth, although systemic toxicity and lack of therapeutic benefit has precluded further development in numerous preclinical studies (21).

The fact that the *PFKFB2-4* genes are overexpressed in different tumors and are activated by hypoxia and/or oncogenes indicates that their role is necessary in the development of the glycolytic phenotype, facilitating the adaptation and survival of tumor cells in hypoxic micro-environments. Thus, small molecule inhibitors of PFKFBs could be used to improve the efficiency and specificity of cancer treatment (161, 236).

The expression of more than one PFKFB isoenzyme in some cells suggests the use of less specific PFKFB kinase inhibitors to effectively reduce Fru-2,6-P_2 concentrations. In this sense, targeting of both PFKFB3 and PFKFB4 isoenzymes has been proposed to be advantageous due to their high expression in some cancer cells (173). PFKFB isoenzyme inhibitors could also be used in combination with agents that mimic hypoxic conditions,

increasing cellular dependence on the upregulation of glycolysis and PFKFBs. The use of chemotherapeutic drugs together with PFKFB3 inhibitors may improve response rates as well as progression-free survival in cancer patients. This is corroborated by recent data demonstrating that sorafenib resistance in HCC can be overcome by aspirin, through PFKFB3 inhibition (158). This type of anti-glycolytic approach substantially differs from previous cancer treatments that attempted to block glycolysis entirely and in a permanent way, causing significant adverse effects. Given that Fru-2,6-P_2 is not part of a main metabolic pathway, and is not a biosynthetic precursor or intermediate in energy production, its concentration can be independently controlled, making PFKFB isoenzymes more specific targets.

TIGAR has important functions in the regulation of cell processes such as apoptosis, autophagy, DNA repair, and the control of oxidative stress. The elevated levels of *TIGAR* expression in some types of tumors (207, 217) and the action of different therapeutic agents associated with decreased *TIGAR* expression, highlight the importance of *TIGAR* in tumor cell survival. TIGAR can support tumorigenesis by reducing ROS production and generating precursors for biosynthesis. These data indicate that the inhibition of TIGAR might confer advantages in cancer treatments (29, 186, 206, 221). Moreover, TIGAR silencing has been shown to increase sensitivity of glioblastoma cells to radiotherapy (186, 237) and increase cell death mediated by PFKFB3 inhibition (189).

The current results show that the metabolic phenotype of tumor cells is heterogeneous and that metabolic coupling occurs between different cell populations of the TME with complementary metabolic profiles. The metabolic differences between tumor and non-tumor cells can potentially be exploited therapeutically. There are currently no glycolytic inhibitors that have been approved as anticancer agents (21) and little is known about the degree of glycolysis inhibition in tumor vs. non-tumor tissues that can be achieved with glycolytic inhibitors, but the preclinical results obtained with these molecules look promising.

The targeting of mitochondrial oxidative metabolism and antioxidant effectors also hold promise as anticancer strategies. Arsenic trioxide, an inhibitor of the mitochondrial oxidative metabolism, has been approved for the treatment of acute promyelocytic leukemia (238). Metformin, an inhibitor of complex I of oxidative phosphorylation (239), has been shown to increase lactate levels and induce apoptosis in a clinical trial in head and neck squamous cell cancer (240). In the same clinical trial, metformin was shown to induce CAV1 expression in CAFs, preventing the metabolic coupling between stromal and cancer cells (240, 241). Another example of effective anti-metabolic cancer therapies is the use of N-acetyl cysteine (NAC), whose antioxidant potential reduced both the proliferation of cancer cells and the expression of the metabolic coupling monocarboxylate transporter 4 (MCT4) in stromal cells in a clinical trial in breast cancer (242). In summary, inhibiting oxidative metabolism or altering the redox state of tumors appear as promising approaches for the treatment of cancer.

CONCLUSIONS

In this review, we summarize current knowledge on the enzymes regulating the Fru-6-P/Fru-1,6-P_2 cycle and their role in cancer and TME cells. PFKFB and TIGAR enzymes control this cycle and are overexpressed in cancer cells, acting as prognostic markers. Small molecule inhibitors of PFKFB2-4 in combination with other drugs could increase the efficiency of cancer treatment. Further preclinical data on PFKFBs inhibitors are required to confirm their potential clinical use.

In summary, glycolysis in tumor cells is a complex phenomenon in which this and other metabolic pathways are reprogrammed to increase energy production and biomolecular synthesis required for cell proliferation. Understanding the regulation of genes and glycolytic isoenzymes in cancer cells and other cells of the TME will have implications for cancer diagnosis and prognosis and for the development of more selective therapies.

AUTHOR CONTRIBUTIONS

All authors jointly developed the structure and arguments of the paper, prepared the manuscript, reviewed it and approved the final version. RB supervised each of the tasks.

FUNDING

The authors are supported by the Instituto de Salud Carlos III–Fondo de Investigaciones Sanitarias (grants PI13/0096 and PI17/00412) and the Fondo Europeo de Desarrollo Regional (FEDER).

ACKNOWLEDGMENTS

We would like to thank E. Adanero for her helpful assistance and T. Evans for English correction. AR-G and HS-M were recipients of a fellowship from the University of Barcelona and the Generalitat de Catalunya, respectively.

REFERENCES

1. Otto Warburg B, Wind F, Negelein N. The metabolism of tumors in the body. *J Gen Physiol*. (1926) 309:397–519.
2. Warburg O. On the origin of cancer cells. *Science*. (1956) 123:309–14. doi: 10.1126/science.123.3191.309
3. Wallace DC. Mitochondria and cancer: Warburg addressed. *Cold Spring Harb Symp Quant Biol*. (2005) 70:363–74. doi: 10.1101/sqb.2005.70.035
4. Dang CV, Semenza GL. Oncogenic alterations of metabolism. *Trends Biochem Sci*. (1999) 24:68–72. doi: 10.1016/S0968-0004(98)01344-9
5. Hanahan D, Weinberg RA. The hallmarks of cancer. *Cell* (2000) 100:57–70. doi: 10.1016/S0092-8674(00)81683-9
6. Hanahan D, Weinberg RA. Hallmarks of cancer: the next generation. *Cell* (2011) 144:646–74. doi: 10.1016/j.cell.2011.02.013
7. Vander Heiden MG, Cantley LC, Thompson CB. Understanding the Warburg effect: the metabolic requirements of cell

proliferation. *Science* (2009) 324:1029–33. doi: 10.1126/science.1160809
8. Gatenby RA, Gillies RJ. Why do cancers have high aerobic glycolysis? *Nat Rev Cancer* (2004) 4:891–9. doi: 10.1038/nrc1478
9. Tennant DA, Durán RV, Gottlieb E. Targeting metabolic transformation for cancer therapy. *Nat Rev Cancer* (2010) 10:267–77. doi: 10.1038/nrc2817
10. Liberti M V, Locasale JW. The Warburg effect: how does it benefit cancer cells? *Trends Biochem Sci*. (2016) 41:211–8. doi: 10.1016/j.tibs.2015.12.001
11. Guppy M, Greiner E, Brand K. The role of the Crabtree effect and an endogenous fuel in the energy metabolism of resting and proliferating thymocytes. *Eur J Biochem*. (1993) 212:95–9. doi: 10.1111/j.1432-1033.1993.tb17637.x
12. Crabtree HG. The carbohydrate metabolism of certain pathological overgrowths. *Biochem J*. (1928) 22:1289–98. doi: 10.1042/bj0221289
13. Crabtree HG. Observations on the carbohydrate metabolism of tumours. *Biochem J*. (1929) 23:536–45. doi: 10.1042/bj0230536
14. Eigenbrodt E, Gerbracht U, Mazurek S, Presek P, Friis R. Carbohydrate metabolism and neoplasia: new perspectives for diagnosis and therapy. In: *Biochemical and Molecular Aspects of Selected Cancers, Vol. 2*. Boston, MA: Academic Press (1994) p. 311–85.
15. Diaz-Ruiz R, Rigoulet M, Devin A. The Warburg and Crabtree effects: on the origin of cancer cell energy metabolism and of yeast glucose repression. *Biochim Biophys Acta Bioenerg*. (2011) 1807:568–76. doi: 10.1016/j.bbabio.2010.08.010
16. Koobs DH. Phosphate mediation of the Crabtree and Pasteur effects. *Science* (1972) 178:127–33. doi: 10.1126/science.178.4057.127
17. Szablewski L. Expression of glucose transporters in cancers. *Biochim Biophys Acta Rev Cancer* (2013) 1835:164–9. doi: 10.1016/j.bbcan.2012.12.004
18. Smallbone K, Gatenby RA, Gillies RJ, Maini PK, Gavaghan DJ. Metabolic changes during carcinogenesis: potential impact on invasiveness. *J Theor Biol*. (2007) 244:703–13. doi: 10.1016/j.jtbi.2006.09.010
19. Sonveaux P, Végran F, Schroeder T, Wergin MC, Verrax J, Rabbani ZN, et al. Targeting lactate-fueled respiration selectively kills hypoxic tumor cells in mice. *J Clin Invest*. (2008) 118:3930–42. doi: 10.1172/JCI36843
20. Martinez-Outschoorn U, Sotgia F, Lisanti MP. Tumor microenvironment and metabolic synergy in breast cancers: critical importance of mitochondrial fuels and function. *Semin Oncol*. (2014) 41:195–216. doi: 10.1053/j.seminoncol.2014.03.002
21. Martinez-Outschoorn UE, Peiris-Pagés M, Pestell RG, Sotgia F, Lisanti MP. Cancer metabolism: a therapeutic perspective. *Nat Rev Clin Oncol*. (2017) 14:113. doi: 10.1038/nrclinonc.2017.1
22. Hanahan D, Coussens LM, Bissell MJ, Lindblom P, Betsholtz C, Gerhardt H, et al. Accessories to the crime: functions of cells recruited to the tumor microenvironment. *Cancer Cell* (2012) 21:309–22. doi: 10.1016/j.ccr.2012.02.022
23. Balkwill FR, Capasso M, Hagemann T. The tumor microenvironment at a glance. *J Cell Sci*. (2012) 125:5591–6. doi: 10.1242/jcs.116392
24. Quail DF, Joyce JA. Microenvironmental regulation of tumor progression and metastasis. *Nat Med*. (2013) 19:1423–37. doi: 10.1038/nm.3394
25. Icard P, Kafara P, Steyaert J-M, Schwartz L, Lincet H. The metabolic cooperation between cells in solid cancer tumors. *Biochim Biophys Acta* (2014) 1846:216–25. doi: 10.1016/j.bbcan.2014.06.002
26. Orimo A, Gupta PB, Sgroi DC, Arenzana-Seisdedos F, Delaunay T, Naeem R, et al. Stromal fibroblasts present in invasive human breast carcinomas promote tumor growth and angiogenesis through elevated SDF-1/CXCL12 secretion. *Cell* (2005) 121:335–48. doi: 10.1016/j.cell.2005.02.034
27. Sotgia F, Martinez-Outschoorn UE, Howell A, Pestell RG, Pavlides S, Lisanti MP. Caveolin-1 and cancer metabolism in the tumor microenvironment: markers, models, and mechanisms. *Annu Rev Pathol Mech Dis*. (2012) 7:423–67. doi: 10.1146/annurev-pathol-011811-120856
28. Martinez-Outschoorn UE, Lisanti MP, Sotgia F. Catabolic cancer-associated fibroblasts transfer energy and biomass to anabolic cancer cells, fueling tumor growth. *Semin Cancer Biol*. (2014) 25:47–60. doi: 10.1016/j.semcancer.2014.01.005
29. Ko Y-H, Domingo-Vidal M, Roche M, Lin Z, Whitaker-Menezes D, Seifert E, et al. TP53-inducible glycolysis and apoptosis regulator (TIGAR) metabolically reprograms carcinoma and stromal cells in breast cancer. *J Biol Chem*. (2016) 291:26291–303. doi: 10.1074/jbc.M116.740209
30. Wilde L, Roche M, Domingo-Vidal M, Tanson K, Philp N, Curry J, et al. Metabolic coupling and the Reverse Warburg effect in cancer: implications for novel biomarker and anticancer agent development. *Semin Oncol*. (2017) 44:198–203. doi: 10.1053/j.seminoncol.2017.10.004
31. Bartrons R, Caro J. Hypoxia, glucose metabolism and the Warburg's effect. *J Bioenerg Biomembr*. (2007) 39:223–9. doi: 10.1007/s10863-007-9080-3
32. DeBerardinis RJ, Lum JJ, Hatzivassiliou G, Thompson CB. The biology of cancer: metabolic reprogramming fuels cell growth and proliferation. *Cell Metab*. (2008) 7:11–20. doi: 10.1016/j.cmet.2007.10.002
33. Koppenol WH, Bounds PL, Dang CV. Otto Warburg's contributions to current concepts of cancer metabolism. *Nat Rev Cancer* (2011) 11:325–37. doi: 10.1038/nrc3038
34. Pavlova NN, Thompson CB. The Emerging hallmarks of cancer metabolism. *Cell Metab*. (2016) 23:27–47. doi: 10.1016/j.cmet.2015.12.006
35. Cuezva JM, Krajewska M, de Heredia ML, Krajewski S, Santamaría G, Kim H, et al. The bioenergetic signature of cancer: a marker of tumor progression. *Cancer Res*. (2002) 62:6674–81.
36. Ward PS, Thompson CB. Metabolic reprogramming: a cancer hallmark even warburg did not anticipate. *Cancer Cell* (2012) 21:297–308. doi: 10.1016/j.ccr.2012.02.014
37. Flöter J, Kaymak I, Schulze A. Regulation of metabolic activity by p53. *Metabolites* (2017) 7:21. doi: 10.3390/metabo7020021
38. Marín-Hernández A, Gallardo-Pérez JC, Ralph SJ, Rodríguez-Enríquez S, Moreno-Sánchez R. HIF-1alpha modulates energy metabolism in cancer cells by inducing over-expression of specific glycolytic isoforms. *Mini Rev Med Chem*. (2009) 9:1084–101. doi: 10.2174/138955709788922610
39. Semenza GL. Hypoxia-inducible factors: coupling glucose metabolism and redox regulation with induction of the breast cancer stem cell phenotype. *EMBO J*. (2017) 36:252–9. doi: 10.15252/embj.201695204
40. Pfeiffer T, Schuster S, Bonhoeffer S. Cooperation and competition in the evolution of ATP-producing pathways. *Science* (2001) 292:504–7. doi: 10.1126/science.1058079
41. Hers HG, Van Schaftingen E. Fructose 2,6-bisphosphate 2 years after its discovery. *Biochem J*. (1982) 206:1–12. doi: 10.1042/bj2060001
42. Dunaway GA, Kasten TP, Sebo T, Trapp R. Analysis of the phosphofructokinase subunits and isoenzymes in human tissues. *Biochem J*. (1988) 251:677–83. doi: 10.1042/bj2510677
43. Costa Leite T, Da Silva D, Guimarães Coelho R, Zancan P, Sola-Penna M. Lactate favours the dissociation of skeletal muscle 6-phosphofructo-1-kinase tetramers down-regulating the enzyme and muscle glycolysis. *Biochem J*. (2007) 408:123–30. doi: 10.1042/BJ20070687
44. Staal GE, Kalff A, Heesbeen EC, van Veelen CW, Rijksen G. Subunit composition, regulatory properties, and phosphorylation of phosphofructokinase from human gliomas. *Cancer Res*. (1987) 47:5047–51.
45. Foe LG, Kemp RG. Isozyme composition and phosphorylation of brain phosphofructokinase. *Arch Biochem Biophys*. (1984) 228:503–11. doi: 10.1016/0003-9861(84)90016-X
46. Campanella ME, Chu H, Low PS. Assembly and regulation of a glycolytic enzyme complex on the human erythrocyte membrane. *Proc Natl Acad Sci USA*. (2005) 102:2402–7. doi: 10.1073/pnas.0409741102
47. Deng H, Yu F, Chen J, Zhao Y, Xiang J, Lin A. Phosphorylation of bad at Thr-201 by JNK1 promotes glycolysis through activation of phosphofructokinase. *J Biol Chem*. (2008) 283:20754–60. doi: 10.1074/jbc.M800024200
48. Lee J-H, Liu R, Li J, Zhang C, Wang Y, Cai Q, et al. Stabilization of phosphofructokinase 1 platelet isoform by AKT promotes tumorigenesis. *Nat Commun*. (2017) 8:949. doi: 10.1038/s41467-017-00906-9
49. Real-Hohn A, Zancan P, Da Silva D, Martins ER, Salgado LT, Mermelstein CS, et al. Filamentous actin and its associated binding proteins are the stimulatory site for 6-phosphofructo-1-kinase association within the membrane of human erythrocytes. *Biochimie* (2010) 92:538–44. doi: 10.1016/j.biochi.2010.01.023
50. Zhao S, Lee EYC. Targeting of the catalytic subunit of protein phosphatase-1 to the glycolytic enzyme phosphofructokinase. *Biochemistry* (1997) 36:8318–24. doi: 10.1021/bi962814r
51. Webb BA, Dosey AM, Wittmann T, Kollman JM, Barber DL. The glycolytic enzyme phosphofructokinase-1 assembles into filaments. *J Cell Biol*. (2017) 216:2305–13. doi: 10.1083/jcb.201701084

52. De Bock K, Georgiadou M, Schoors S, Kuchnio A, Wong BWW, Cantelmo ARR, et al. Role of PFKFB3-driven glycolysis in vessel sprouting. *Cell* (2013) 154:651–63. doi: 10.1016/j.cell.2013.06.037
53. Kohnhorst CL, Kyoung M, Jeon M, Schmitt DL, Kennedy EL, Ramirez J, et al. Identification of a multienzyme complex for glucose metabolism in living cells. *J Biol Chem*. (2017) 292:9191–203. doi: 10.1074/jbc.M117.783050
54. Vora S, Halper JP, Knowles DM. Alterations in the activity and isozymic profile of human phosphofructokinase during malignant transformation *in vivo* and *in vitro*: transformation- and progression-linked discriminants of malignancy. *Cancer Res*. (1985) 45:2993–3001.
55. Moon J-S, Kim HE, Koh E, Park SH, Jin W-J, Park B-W, et al. Krüppel-like factor 4 (KLF4) activates the transcription of the gene for the platelet isoform of phosphofructokinase (PFKP) in breast cancer. *J Biol Chem*. (2011) 286:23808–16. doi: 10.1074/jbc.M111.236737
56. Colomer D, Vives-Corrons JL, Pujades A, Bartrons R. Control of phosphofructokinase by fructose 2,6-bisphosphate in B-lymphocytes and B-chronic lymphocytic leukemia cells. *Cancer Res*. (1987) 47:1859–62.
57. Semenza GL, Roth PH, Fang HM, Wang GL. Transcriptional regulation of genes encoding glycolytic enzymes by hypoxia-inducible factor 1. *J Biol Chem*. (1994) 269:23757–63.
58. Kole HK, Resnick RJ, Van Doren M, Racker E. Regulation of 6-phosphofructo-1-kinase activity in ras-transformed rat-1 fibroblasts. *Arch Biochem Biophys*. (1991) 286:586–90. doi: 10.1016/0003-9861(91)90084-V
59. Yi W, Clark PM, Mason DE, Keenan MC, Hill C, Goddard WA, et al. Phosphofructokinase 1 glycosylation regulates cell growth and metabolism. *Science* (2012) 337:975–80. doi: 10.1126/science.1222278
60. Kim NH, Cha YH, Lee J, Lee S-H, Yang JH, Yun JS, et al. Snail reprograms glucose metabolism by repressing phosphofructokinase PFKP allowing cancer cell survival under metabolic stress. *Nat Commun*. (2017) 8:14374. doi: 10.1038/ncomms14374
61. Lee J-H, Liu R, Li J, Wang Y, Tan L, Li X-J, et al. EGFR-phosphorylated platelet isoform of phosphofructokinase 1 promotes PI3K activation. *Mol Cell* (2018) 70:197–210.e7. doi: 10.1016/j.molcel.2018.03.018
62. Dzugaj A. Localization and regulation of muscle fructose-1,6-bisphosphatase, the key enzyme of glyconeogenesis. *Adv Enzyme Regul*. (2006) 46:51–71. doi: 10.1016/j.advenzreg.2006.01.021
63. Gizak A, Maciaszczyk E, Dzugaj A, Eschrich K, Rakus D. Evolutionary conserved N-terminal region of human muscle fructose 1,6-bisphosphatase regulates its activity and the interaction with aldolase. *Proteins Struct Funct Bioinforma*. (2008) 72:209–16. doi: 10.1002/prot.21909
64. Dai J, Ji Y, Wang W, Kim D, Fai LY, Wang L, et al. Loss of fructose-1,6-bisphosphatase induces glycolysis and promotes apoptosis resistance of cancer stem-like cells: an important role in hexavalent chromium-induced carcinogenesis. *Toxicol Appl Pharmacol*. (2017) 331:164–73. doi: 10.1016/j.taap.2017.06.014
65. Li B, Qiu B, Lee DSM, Walton ZE, Ochocki JD, Mathew LK, et al. Fructose-1,6-bisphosphatase opposes renal carcinoma progression. *Nature* (2014) 513:251–5. doi: 10.1038/nature13557
66. Zhang J, Wang J, Xing H, Li Q, Zhao Q, Li J. Down-regulation of FBP1 by ZEB1-mediated repression confers to growth and invasion in lung cancer cells. *Mol Cell Biochem*. (2016) 411:331–40. doi: 10.1007/s11010-015-2595-8
67. Dong C, Yuan T, Wu Y, Wang Y, Fan TWM, Miriyala S, et al. Loss of FBP1 by Snail-mediated repression provides metabolic advantages in basal-like breast cancer. *Cancer Cell* (2013) 23:316–31. doi: 10.1016/j.ccr.2013.01.022
68. Van Schaftingen E. Fructose 2,6-bisphosphate. *Adv Enzymol Relat Areas Mol Biol*. (1987) 59:315–95. doi: 10.1002/9780470123058.ch7
69. Hue L, Rider MH. Role of fructose 2,6-bisphosphate in the control of glycolysis in mammalian tissues. *Biochem J*. (1987) 245:313–24. doi: 10.1042/bj2450313
70. Rider MH, Bartrons R. Fructose 2,6-bisphosphate: the last milestone of the 20th century in metabolic control? *Biochem J*. (2010) 32:1–5. doi: 10.1042/BJ20091921
71. Pilkis SJ, Claus TH, Kurland IJ, Lange AJ. 6-Phosphofructo-2-kinase/fructose-2,6-bisphosphatase: a metabolic signaling enzyme. *Annu Rev Biochem*. (1995) 64:799–835. doi: 10.1146/annurev.bi.64.070195.004055
72. Sola-Penna M, Da Silva D, Coelho WS, Marinho-Carvalho MM, Zancan P. Regulation of mammalian muscle type 6-phosphofructo-1-kinase and its implication for the control of the metabolism. *IUBMB Life* (2010) 62:791–6. doi: 10.1002/iub.393
73. Riera L, Manzano A, Navarro-Sabaté A, Perales JC, Bartrons R. Insulin induces PFKFB3 gene expression in HT29 human colon adenocarcinoma cells. *Biochim Biophys Acta* (2002) 1589:89–92. doi: 10.1016/S0167-4889(02)00169-6
74. Rousseau GG, Hue L. Mammalian 6-phosphofructo-2-kinase/fructose-2,6-bisphosphatase: a bifunctional enzyme that controls glycolysis. *Prog Nucleic Acid Res Mol Biol*. (1993) 45:99–127. doi: 10.1016/S0079-6603(08)60868-5
75. Rider MH, Bertrand L, Vertommen D, Michels PA, Rousseau GG, Hue L. 6-Phosphofructo-2-kinase/fructose-2,6-bisphosphatase: head-to-head with a bifunctional enzyme that controls glycolysis. *Biochem J*. (2004) 381:561–79. doi: 10.1042/BJ20040752
76. Okar DA, Manzano A, Navarro-Sabatè A, Riera L, Bartrons R, Lange AJ. PFK-2/FBPase-2: maker and breaker of the essential biofactor fructose-2,6-bisphosphate. *Trends Biochem Sci*. (2001) 26:30–5. doi: 10.1016/S0968-0004(00)01699-6
77. Jedrzejas MJ. Structure, function, and evolution of phosphoglycerate mutases: comparison with fructose-2,6-bisphosphatase, acid phosphatase, and alkaline phosphatase. *Prog Biophys Mol Biol*. (2000) 73:263–87. doi: 10.1016/S0079-6107(00)00007-9
78. Goren N, Manzano A, Riera L, Ambrosio S, Ventura F, Bartrons R. 6-Phosphofructo-2-kinase/fructose-2,6-bisphosphatase expression in rat brain during development. *Brain Res Mol Brain Res*. (2000) 75:138–42. doi: 10.1016/S0169-328X(99)00319-8
79. Darville MI, Crepin KM, Vandekerckhove J, Van Damme J, Octave JN, Rider MH, et al. Complete nucleotide sequence coding for rat liver 6-phosphofructo-2-kinase/fructose-2,6-bisphosphatase derived from a cDNA clone. *FEBS Lett*. (1987) 224:317–21. doi: 10.1016/0014-5793(87)80476-3
80. Algaier J, Uyeda K. Molecular cloning, sequence analysis, and expression of a human liver cDNA coding for fructose-6-P,2-kinase:fructose-2,6-bisphosphatase. *Biochem Biophys Res Commun*. (1988) 153:328–33. doi: 10.1016/S0006-291X(88)81226-9
81. Lee Y-H, Li Y, Uyeda K, Hasemann CA. Tissue-specific structure/function differentiation of the liver isoform of 6-phosphofructo-2-kinase/fructose-2,6-bisphosphatase. *J Biol Chem*. (2003) 278:523–30. doi: 10.1074/jbc.M209105200
82. Bartrons R, Hue L, Van Schaftingen E, Hers HG. Hormonal control of fructose 2,6-bisphosphate concentration in isolated rat hepatocytes. *Biochem J*. (1983) 214:829–37. doi: 10.1042/bj2140829
83. Cosin-Roger J, Vernia S, Alvarez MS, Cucarella C, Boscá L, Martin-Sanz P, et al. Identification of a novel Pfkfb1 mRNA variant in rat fetal liver. *Biochem Biophys Res Commun*. (2013) 431:36–40. doi: 10.1016/j.bbrc.2012.12.109
84. Heine-Suñer D, Díaz-Guillén MA, Lange AJ, Rodríguez de Córdoba S. Sequence and structure of the human 6-phosphofructo-2-kinase/fructose-2,6-bisphosphatase heart isoform gene (PFKFB2). *Eur J Biochem*. (1998) 254:103–10.
85. Crochet RB, Kim J-D, Lee H, Yim Y-S, Kim S-G, Neau D, et al. Crystal structure of heart 6-phosphofructo-2-kinase/fructose-2,6-bisphosphatase (PFKFB2) and the inhibitory influence of citrate on substrate binding. *Proteins* (2017) 85:117–24. doi: 10.1002/prot.25204
86. Minchenko O, Opentanova I, Caro J. Hypoxic regulation of the 6-phosphofructo-2-kinase/fructose-2,6-bisphosphatase gene family (PFKFB-1-4) expression *in vivo*. *FEBS Lett*. (2003) 554:264–70. doi: 10.1016/S0014-5793(03)01179-7
87. Bobarykina AY, Minchenko DO, Opentanova IL, Moenner M, Caro J, Esumi H, et al. Hypoxic regulation of PFKFB-3 and PFKFB-4 gene expression in gastric and pancreatic cancer cell lines and expression of PFKFB genes in gastric cancers. *Acta Biochim Pol*. (2006) 53:789–99.
88. Marsin AS, Bertrand L, Rider MH, Deprez J, Beauloye C, Vincent MF, et al. Phosphorylation and activation of heart PFK-2 by AMPK has a role in the stimulation of glycolysis during ischaemia. *Curr Biol*. (2000) 10:1247–55. doi: 10.1016/S0960-9822(00)00742-9
89. Masters SC, Subramanian RR, Truong A, Yang H, Fujii K, Zhang H, et al. Survival-promoting functions of 14-3-3 proteins. *Biochem Soc Trans*. (2002) 30:360–5. doi: 10.1042/bst0300360
90. Pozuelo Rubio M, Peggie M, Wong BHC, Morrice N, MacKintosh C. 14-3-3s regulate fructose-2,6-bisphosphate levels by binding to PKB-phosphorylated

cardiac fructose-2,6-bisphosphate kinase/phosphatase. *EMBO J*. (2003) 22:3514–23. doi: 10.1093/emboj/cdg363

91. Houles T, Gravel S-P, Lavoie G, Shin S, Savall M, Méant A, et al. RSK regulates PFK-2 activity to promote metabolic rewiring in melanoma. *Cancer Res*. (2018) 78:2191–204. doi: 10.1158/0008-5472.CAN-17-2215
92. Novellasdemunt L, Tato I, Navarro-Sabate A, Ruiz-Meana M, Méndez-Lucas A, Perales JC, et al. Akt-dependent activation of the heart 6-phosphofructo-2-kinase/fructose-2,6-bisphosphatase (PFKFB2) isoenzyme by amino acids. *J Biol Chem*. (2013) 288:10640–51. doi: 10.1074/jbc.M113.455998
93. Kitamura K, Kangawa K, Matsuo H, Uyeda K. Phosphorylation of myocardial fructose-6-phosphate,2-kinase: fructose-2,6-bisphosphatase by cAMP-dependent protein kinase and protein kinase C. Activation by phosphorylation and amino acid sequences of the phosphorylation sites. *J Biol Chem*. (1988) 263:16796–801.
94. Schmidt S, Rainer J, Riml S, Ploner C, Jesacher S, Achmüller C, et al. Identification of glucocorticoid-response genes in children with acute lymphoblastic leukemia. *Blood*. (2006) 107:2061–9. doi: 10.1182/blood-2005-07-2853
95. Carlet M, Janjetovic K, Rainer J, Schmidt S, Panzer-Grümayer R, Mann G, et al. Expression, regulation and function of phosphofructo-kinase/fructose-biphosphatases (PFKFBs) in glucocorticoid-induced apoptosis of acute lymphoblastic leukemia cells. *BMC Cancer* (2010) 10:638. doi: 10.1186/1471-2407-10-638
96. Massie CE, Lynch A, Ramos-Montoya A, Boren J, Stark R, Fazli L, et al. The androgen receptor fuels prostate cancer by regulating central metabolism and biosynthesis. *EMBO J*. (2011) 30:2719–33. doi: 10.1038/emboj.2011.158
97. Moon J-S, Jin W-J, Kwak J-H, Kim H-J, Yun M-J, Kim J-W, et al. Androgen stimulates glycolysis for de novo lipid synthesis by increasing the activities of hexokinase 2 and 6-phosphofructo-2-kinase/fructose-2,6-bisphosphatase 2 in prostate cancer cells. *Biochem J*. (2011) 433:225–33. doi: 10.1042/BJ20101104
98. Ji D, Lu Z-T, Li Y-Q, Liang Z-Y, Zhang P-F, Li C, et al. MACC1 expression correlates with PFKFB2 and survival in hepatocellular carcinoma. *Asian Pac J Cancer Prev*. (2014) 15:999–1003. doi: 10.7314/APJCP.2014.15.2.999
99. Zhao S-J, Shen Y-F, Li Q, He Y-J, Zhang Y-K, Hu L-P, et al. SLIT2/ROBO1 axis contributes to the Warburg effect in osteosarcoma through activation of SRC/ERK/c-MYC/PFKFB2 pathway. *Cell Death Dis*. (2018) 9:390. doi: 10.1038/s41419-018-0419-y
100. Zhao L, Ji G, Le X, Wang C, Xu L, Feng M, et al. Long noncoding RNA LINC00092 acts in cancer-associated fibroblasts to drive glycolysis and progression of ovarian cancer. *Cancer Res*. (2017) 77:1369–82. doi: 10.1158/0008-5472.CAN-16-1615
101. He Z, You C, Zhao D. Long non-coding RNA UCA1/miR-182/PFKFB2 axis modulates glioblastoma-associated stromal cells-mediated glycolysis and invasion of glioma cells. *Biochem Biophys Res Commun*. (2018) 500:569–76. doi: 10.1016/j.bbrc.2018.04.091
102. Chan O, Burke JD, Gao DF, Fish EN. The chemokine CCL5 regulates glucose uptake and AMP kinase signaling in activated T cells to facilitate chemotaxis. *J Biol Chem*. (2012) 287:29406–16. doi: 10.1074/jbc.M112.348946
103. Ventura F, Ambrosio S, Bartrons R, El-Maghrabi MR, Lange AJ, Pilkis SJ. Cloning and expression of a catalytic core bovine brain 6-phosphofructo-2-kinase/fructose-2,6-bisphosphatase. *Biochem Biophys Res Commun*. (1995) 209:1140–8. doi: 10.1006/bbrc.1995.1616
104. Hamilton JA, Callaghan MJ, Sutherland RL, Watts CK. Identification of PRG1, a novel progestin-responsive gene with sequence homology to 6-phosphofructo-2-kinase/fructose-2,6-bisphosphatase. *Mol Endocrinol*. (1997) 11:490–502. doi: 10.1210/mend.11.4.9909
105. Manzano A, Rosa JL, Ventura F, Pérez JX, Nadal M, Estivill X, et al. Molecular cloning, expression, and chromosomal localization of a ubiquitously expressed human 6-phosphofructo-2-kinase/fructose-2, 6-bisphosphatase gene (PFKFB3). *Cytogenet Cell Genet*. (1998) 83(3–4):214–7.
106. Chesney J, Mitchell R, Benigni F, Bacher M, Spiegel L, Al-Abed Y, et al. An inducible gene product for 6-phosphofructo-2-kinase with an AU-rich instability element: role in tumor cell glycolysis and the Warburg effect. *Proc Natl Acad Sci USA*. (1999) 96:3047–52. doi: 10.1073/pnas.96.6.3047
107. Navarro-Sabaté A, Manzano A, Riera L, Rosa JL, Ventura F, Bartrons R. The human ubiquitous 6-phosphofructo-2-kinase/fructose-2,6-bisphosphatase gene (PFKFB3): promoter characterization and genomic structure. *Gene* (2001) 264:131–8. doi: 10.1016/S0378-1119(00)00591-6
108. Kessler R, Eschrich K. Splice isoforms of ubiquitous 6-phosphofructo-2-kinase/fructose-2,6-bisphosphatase in human brain. *Brain Res Mol Brain Res*. (2001) 87:190–5. doi: 10.1016/S0169-328X(01)00014-6
109. Ge X, Lyu P, Cao Z, Li J, Guo G, Xia W, et al. Overexpression of miR-206 suppresses glycolysis, proliferation and migration in breast cancer cells via PFKFB3 targeting. *Biochem Biophys Res Commun*. (2015) 463:1115–21. doi: 10.1016/j.bbrc.2015.06.068
110. Du J-Y, Wang L-F, Wang Q, Yu L-D. miR-26b inhibits proliferation, migration, invasion and apoptosis induction via the downregulation of 6-phosphofructo-2-kinase/fructose-2,6-bisphosphatase-3 driven glycolysis in osteosarcoma cells. *Oncol Rep*. (2015) 33:1890–8. doi: 10.3892/or.2015.3797
111. Obach M, Navarro-Sabaté A, Caro J, Kong X, Duran J, Gómez M, et al. 6-Phosphofructo-2-kinase (pfkfb3) gene promoter contains hypoxia-inducible factor-1 binding sites necessary for transactivation in response to hypoxia. *J Biol Chem*. (2004) 279:53562–70. doi: 10.1074/jbc.M406096200
112. Minchenko A, Leshchinsky I, Opentanova I, Sang N, Srinivas V, Armstead V, et al. Hypoxia-inducible factor-1-mediated expression of the 6-phosphofructo-2-kinase/fructose-2,6-bisphosphatase-3 (PFKFB3) gene. Its possible role in the Warburg effect. *J Biol Chem*. (2002) 277:6183–7. doi: 10.1074/jbc.M110978200
113. Novellasdemunt L, Obach M, Millán-Ariño L, Manzano A, Ventura F, Rosa JL, et al. Progestins activate 6-phosphofructo-2-kinase/fructose-2,6-bisphosphatase 3 (PFKFB3) in breast cancer cells. *Biochem J*. (2012) 442:345–56. doi: 10.1042/BJ20111418
114. Imbert-Fernandez Y, Clem BF, O'Neal J, Kerr DA, Spaulding R, Lanceta L, et al. Estradiol stimulates glucose metabolism via 6-phosphofructo-2-kinase (PFKFB3). *J Biol Chem*. (2014) 289:9440–8. doi: 10.1074/jbc.M113.529990
115. Novellasdemunt L, Bultot L, Manzano A, Ventura F, Rosa JLL, Vertommen D, et al. PFKFB3 activation in cancer cells by the p38/MK2 pathway in response to stress stimuli. *Biochem J*. (2013) 452:531–43. doi: 10.1042/BJ20121886
116. Ando M, Uehara I, Kogure K, Asano Y, Nakajima W, Abe Y, et al. Interleukin 6 enhances glycolysis through expression of the glycolytic enzymes hexokinase 2 and 6-phosphofructo-2-kinase/fructose-2,6-bisphosphatase-3. *J Nippon Med Sch*. (2010) 77:97–105. doi: 10.1272/jnms.77.97
117. Han J, Meng Q, Xi Q, Zhang Y, Zhuang Q, Han Y, et al. Interleukin-6 stimulates aerobic glycolysis by regulating PFKFB3 at early stage of colorectal cancer. *Int J Oncol*. (2015) 48:215–24. doi: 10.3892/ijo.2015.3225
118. Ruiz-Garcia A, Monsalve E, Novellasdemunt L, Navarro-Sabate A, Manzano A, Rivero S, et al. Cooperation of adenosine with macrophage toll-4 receptor agonists leads to increased glycolytic flux through the enhanced expression of PFKFB3 gene. *J Biol Chem*. (2011) 286:19247–58. doi: 10.1074/jbc.M110.190298
119. Houddane A, Bultot L, Novellasdemunt L, Johanns M, Gueuning M-A, Vertommen D, et al. Role of Akt/PKB and PFKFB isoenzymes in the control of glycolysis, cell proliferation and protein synthesis in mitogen-stimulated thymocytes. *Cell Signal* (2017) 34:23–37. doi: 10.1016/j.cellsig.2017.02.019
120. Simon-Molas H, Arnedo-Pac C, Fontova P, Vidal-Alabró A, Castaño E, Rodríguez-García A, et al. PI3K-Akt signaling controls PFKFB3 expression during human T-lymphocyte activation. *Mol Cell Biochem*. (2018) [Epub ahead of print]. doi: 10.1007/s11010-018-3325-9
121. Rodríguez-García A, Samsó P, Fontova P, Simon-Molas H, Manzano A, Castaño E, et al. TGF-β1 targets Smad, p38 MAPK, and PI3K/Akt signaling pathways to induce PFKFB3 gene expression and glycolysis in glioblastoma cells. *FEBS J*. (2017) 284:3437–54. doi: 10.1111/febs.14201
122. Sakakibara R, Uemura M, Hirata T, Okamura N, Kato M. Human placental fructose-6-phosphate,2-kinase/fructose-2,6-bisphosphatase: its isozymic form, expression and characterization. *Biosci Biotechnol Biochem*. (1997) 61:1949–52. doi: 10.1271/bbb.61.1949
123. Cavalier MC, Kim S-G, Neau D, Lee Y-H. Molecular basis of the fructose-2,6-bisphosphatase reaction of PFKFB3: transition state and the C-terminal function. *Proteins* (2012) 80:1143–53. doi: 10.1002/prot.24015
124. Marsin A-S, Bouzin C, Bertrand L, Hue L. The stimulation of glycolysis by hypoxia in activated monocytes is mediated by AMP-activated protein kinase and inducible 6-phosphofructo-2-kinase. *J Biol Chem*. (2002) 277:30778–83. doi: 10.1074/jbc.M205213200

125. Okamura N, Sakakibara R. A common phosphorylation site for cyclic AMP-dependent protein kinase and protein kinase C in human placental 6-phosphofructo-2-kinase/fructose-2,6-bisphosphatase. *Biosci Biotechnol Biochem*. (1998) 62:2039–42. doi: 10.1271/bbb.62.2039
126. Duran J, Obach M, Navarro-Sabate A, Manzano A, Gómez M, Rosa JL, et al. Pfkfb3 is transcriptionally upregulated in diabetic mouse liver through proliferative signals. *FEBS J*. (2009) 276:4555–68. doi: 10.1111/j.1742-4658.2009.07161.x
127. Garcia-Cao I, Song MS, Hobbs RM, Laurent G, Giorgi C, de Boer VCJ, et al. Systemic elevation of PTEN induces a tumor-suppressive metabolic state. *Cell* (2012) 149:49–62. doi: 10.1016/j.cell.2012.02.030
128. Seo M, Lee Y-H. PFKFB3 regulates oxidative stress homeostasis via its S-glutathionylation in cancer. *J Mol Biol*. (2014) 426:830–42. doi: 10.1016/j.jmb.2013.11.021
129. Yamamoto T, Takano N, Ishiwata K, Ohmura M, Nagahata Y, Matsuura T, et al. Reduced methylation of PFKFB3 in cancer cells shunts glucose towards the pentose phosphate pathway. *Nat Commun*. (2014) 5:3480. doi: 10.1038/ncomms4480
130. Franklin DA, He Y, Leslie PL, Tikunov AP, Fenger N, Macdonald JM, et al. p53 coordinates DNA repair with nucleotide synthesis by suppressing PFKFB3 expression and promoting the pentose phosphate pathway. *Sci Rep*. (2016) 6:38067. doi: 10.1038/srep38067
131. Riera L, Obach M, Navarro-Sabaté A, Duran J, Perales JC, Viñals F, et al. Regulation of ubiquitous 6-phosphofructo-2-kinase by the ubiquitin-proteasome proteolytic pathway during myogenic C2C12 cell differentiation. *FEBS Lett*. (2003) 550:23–9. doi: 10.1016/S0014-5793(03)00808-1
132. Almeida A, Bolaños JP, Moncada S. E3 ubiquitin ligase APC/C-Cdh1 accounts for the Warburg effect by linking glycolysis to cell proliferation. *Proc Natl Acad Sci USA*. (2010) 107:738–41. doi: 10.1073/pnas.0913668107
133. Tudzarova S, Colombo SL, Stoeber K, Carcamo S, Williams GH, Moncada S. Molecular architecture of the DNA replication origin activation checkpoint. *EMBO J*. (2011) 108:3381–94. doi: 10.1073/pnas.1102247108
134. Song MS, Carracedo A, Salmena L, Song SJ, Egia A, Malumbres M, et al. Nuclear PTEN regulates the APC-CDH1 tumor-suppressive complex in a phosphatase-independent manner. *Cell*. (2011) 144:187–99. doi: 10.1016/j.cell.2010.12.020
135. Yalcin A, Telang S, Clem B, Chesney J. Regulation of glucose metabolism by 6-phosphofructo-2-kinase/fructose-2,6-bisphosphatases in cancer. *Exp Mol Pathol*. (2009) 86:174–9. doi: 10.1016/j.yexmp.2009.01.003
136. Yalcin A, Clem BF, Imbert-Fernandez Y, Ozcan SC, Peker S, O'Neal J, et al. 6-Phosphofructo-2-kinase (PFKFB3) promotes cell cycle progression and suppresses apoptosis via Cdk1-mediated phosphorylation of p27. *Cell Death Dis*. (2014) 5:e1337. doi: 10.1038/cddis.2014.292
137. Jia W, Zhao X, Zhao L, Yan H, Li J, Yang H, et al. Non-canonical roles of PFKFB3 in regulation of cell cycle through binding to CDK4. *Oncogene* (2018) 37:1685–98. doi: 10.1038/s41388-017-0072-4
138. Tawakol A, Singh P, Mojena M, Pimentel-Santillana M, Emami H, MacNabb M, et al. HIF-1α and PFKFB3 mediate a tight relationship between proinflammatory activation and anerobic metabolism in atherosclerotic macrophages. *Arterioscler Thromb Vasc Biol*. (2015) 35:1463–71. doi: 10.1161/ATVBAHA.115.305551
139. Zou Y, Zeng S, Huang M, Qiu Q, Xiao Y, Shi M, et al. Inhibition of 6-phosphofructo-2-kinase suppresses fibroblast-like synoviocytes-mediated synovial inflammation and joint destruction in rheumatoid arthritis. *Br J Pharmacol*. (2017) 174:893–908. doi: 10.1111/bph.13762
140. Chesney J. 6-Phosphofructo-2-kinase/fructose-2,6-bisphosphatase and tumor cell glycolysis. *Curr Opin Clin Nutr Metab Care*. (2006) 9:535–9. doi: 10.1097/01.mco.0000241661.15514.fb
141. Novellasdemunt L, Navarro-Sabaté À, Manzano A, Rodríguez-García A, Bartrons R. PFKFB3 (6-phosphofructo-2-kinase/fructose-2,6-biphosphatase 3). *Atlas Genet Cytogenet Oncol Haematol*. (2013) 17:609–22.
142. Atsumi T, Chesney J, Metz C, Leng L, Donnelly S, Makita Z, et al. High expression of inducible 6-phosphofructo-2-kinase/fructose-2,6-bisphosphatase (iPFK-2; PFKFB3) in human cancers. *Cancer Res*. (2002) 62:5881–7.
143. Marotta LLC, Almendro V, Marusyk A, Shipitsin M, Schemme J, Walker SR, et al. The JAK2/STAT3 signaling pathway is required for growth of $CD44^+CD24^-$ stem cell-like breast cancer cells in human tumors. *J Clin Invest*. (2011) 121:2723–35. doi: 10.1172/JCI44745
144. Han J, Meng Q, Xi Q, Wang H, Wu G. PFKFB3 was overexpressed in gastric cancer patients and promoted the proliferation and migration of gastric cancer cells. *Cancer Biomarkers* (2017) 18:249–56. doi: 10.3233/CBM-160143
145. Reddy MM, Fernandes MS, Deshpande A, Weisberg E, Inguilizian HV, Abdel-Wahab O, et al. The JAK2V617F oncogene requires expression of inducible phosphofructokinase/fructose-bisphosphatase 3 for cell growth and increased metabolic activity. *Leukemia*. (2012) 26:481–9. doi: 10.1038/leu.2011.225
146. Zhu Y, Lu L, Qiao C, Shan Y, Li H, Qian S, et al. Targeting PFKFB3 sensitizes chronic myelogenous leukemia cells to tyrosine kinase inhibitor. *Oncogene* (2018) 37:2837–49. doi: 10.1038/s41388-018-0157-8
147. Feng Y, Wu L. mTOR up-regulation of PFKFB3 is essential for acute myeloid leukemia cell survival. *Biochem Biophys Res Commun*. (2017) 483:897–903. doi: 10.1016/j.bbrc.2017.01.031
148. Bando H, Atsumi T, Nishio T, Niwa H, Mishima S, Shimizu C, et al. Phosphorylation of the 6-phosphofructo-2-kinase/fructose 2,6-bisphosphatase/PFKFB3 family of glycolytic regulators in human cancer. *Clin Cancer Res*. (2005) 11:5784–92. doi: 10.1158/1078-0432.CCR-05-0149
149. Xie N, Tan Z, Banerjee S, Cui H, Ge J, Liu R-M, et al. Glycolytic reprogramming in myofibroblast differentiation and lung fibrosis. *Am J Respir Crit Care Med*. (2015) 192:1462–74. doi: 10.1164/rccm.201504-0780OC
150. Kessler R, Bleichert F, Warnke J-P, Eschrich K. 6-Phosphofructo-2-kinase/fructose-2,6-bisphosphatase (PFKFB3) is up-regulated in high-grade astrocytomas. *J Neurooncol*. (2008) 86:257–64. doi: 10.1007/s11060-007-9471-7
151. Zscharnack K, Kessler R, Bleichert F, Warnke JP, Eschrich K. The PFKFB3 splice variant UBI2K4 is downregulated in high-grade astrocytomas and impedes the growth of U87 glioblastoma cells. *Neuropathol Appl Neurobiol*. (2009) 35:566–78. doi: 10.1111/j.1365-2990.2009.01027.x
152. Fleischer M, Kessler R, Klammer A, Warnke J-P, Eschrich K. LOH on 10p14-p15 targets the PFKFB3 gene locus in human glioblastomas. *Genes Chromosom Cancer* (2011) 50:1010–20. doi: 10.1002/gcc.20914
153. Schoors S, De Bock K, Cantelmo ARR, Georgiadou M, Ghesquière B, Cauwenberghs S, et al. Partial and transient reduction of glycolysis by PFKFB3 blockade reduces pathological angiogenesis. *Cell Metab*. (2014) 19:37–48. doi: 10.1016/j.cmet.2013.11.008
154. Cantelmo AR, Conradi L-C, Brajic A, Goveia J, Kalucka J, Pircher A, et al. Inhibition of the glycolytic activator PFKFB3 in endothelium induces tumor vessel normalization, impairs metastasis, and improves chemotherapy. *Cancer Cell* (2016) 30:968–85. doi: 10.1016/j.ccell.2016.10.006
155. Kuosmanen SM, Kansanen E, Kaikkonen MU, Sihvola V, Pulkkinen K, Jyrkkänen H-K, et al. NRF2 regulates endothelial glycolysis and proliferation with miR-93 and mediates the effects of oxidized phospholipids on endothelial activation. *Nucleic Acids Res*. (2018) 46:1124–38. doi: 10.1093/nar/gkx1155
156. Zhang H-S, Du G-Y, Zhang Z-G, Zhou Z, Sun H-L, Yu X-Y, et al. NRF2 facilitates breast cancer cell growth via HIF1α-mediated metabolic reprogramming. *Int J Biochem Cell Biol*. (2018) 95:85–92. doi: 10.1016/j.biocel.2017.12.016
157. Shi W-K, Zhu X-D, Wang C-H, Zhang Y-Y, Cai H, Li X-L, et al. PFKFB3 blockade inhibits hepatocellular carcinoma growth by impairing DNA repair through AKT. *Cell Death Dis*. (2018) 9:428. doi: 10.1038/s41419-018-0435-y
158. Li S, Dai W, Mo W, Li J, Feng J, Wu L, et al. By inhibiting PFKFB3, aspirin overcomes sorafenib resistance in hepatocellular carcinoma. *Int J Cancer* (2017) 141:2571–84. doi: 10.1002/ijc.31022
159. Calvo MN, Bartrons R, Castaño E, Perales JC, Navarro-Sabaté A, Manzano A. PFKFB3 gene silencing decreases glycolysis, induces cell-cycle delay and inhibits anchorage-independent growth in HeLa cells. *FEBS Lett*. (2006) 580:3308–14. doi: 10.1016/j.febslet.2006.04.093
160. Telang S, Yalcin A, Clem AL, Bucala R, Lane AN, Eaton JW, et al. Ras transformation requires metabolic control by 6-phosphofructo-2-kinase. *Oncogene* (2006) 25:7225–34. doi: 10.1038/sj.onc.1209709
161. Clem BF, O'Neal J, Tapolsky G, Clem AL, Imbert-Fernandez Y, Kerr DA, et al. Targeting 6-phosphofructo-2-kinase (PFKFB3) as a

therapeutic strategy against cancer. *Mol Cancer Ther*. (2013) 12:1461–70. doi: 10.1158/1535-7163.MCT-13-0097
162. Sakata J, Abe Y, Uyeda K. Molecular cloning of the DNA and expression and characterization of rat testes fructose-6-phosphate,2-kinase:fructose-2,6-bisphosphatase. *J Biol Chem*. (1991) 266:15764–70.
163. Manzano A, Pérez JX, Nadal M, Estivill X, Lange A, Bartrons R. Cloning, expression and chromosomal localization of a human testis 6-phosphofructo-2-kinase/fructose-2,6-bisphosphatase gene. *Gene* (1999) 229:83–9.
164. Minchenko DO, Mykhalchenko VG, Tsuchihara K, Kanehara S, Yavorovsky OP, Zavgorodny IV, et al. Alternative splice variants of rat 6-phosphofructo-2-kinase/ fructose-2,6-bisphosphatase-4 mRNA. *Ukr Biokhim Zh (1999)* (2008) 80:66–73.
165. Gómez M, Manzano A, Navarro-Sabaté A, Duran J, Obach M, Perales JC, et al. Specific expression of pfkfb4 gene in spermatogonia germ cells and analysis of its 5′-flanking region. *FEBS Lett*. (2005) 579:357–62. doi: 10.1016/j.febslet.2004.11.096
166. Gómez M, Manzano A, Figueras A, Viñals F, Ventura F, Rosa JL, et al. Sertoli-secreted FGF-2 induces PFKFB4 isozyme expression in mouse spermatogenic cells by activation of the MEK/ERK/CREB pathway. *Am J Physiol Endocrinol Metab*. (2012) 303:E695–707. doi: 10.1152/ajpendo.00381.2011
167. Minchenko O, Opentanova I, Minchenko D, Ogura T, Esumi H. Hypoxia induces transcription of 6-phosphofructo-2-kinase/fructose-2,6-biphosphatase-4 gene via hypoxia-inducible factor-1α activation. *FEBS Lett*. (2004) 576:14–20. doi: 10.1016/j.febslet.2004.08.053
168. Minchenko OH, Tsuchihara K, Minchenko DO, Bikfalvi A, Esumi H. Mechanisms of regulation of PFKFB expression in pancreatic and gastric cancer cells. *World J Gastroenterol*. (2014) 20:13705. doi: 10.3748/wjg.v20.i38.13705
169. Ros S, Santos CR, Moco S, Baenke F, Kelly G, Howell M, et al. Functional metabolic screen identifies 6-phosphofructo-2-kinase/fructose-2,6-biphosphatase 4 as an important regulator of prostate cancer cell survival. *Cancer Discov*. (2012) 2:328–43. doi: 10.1158/2159-8290.CD-11-0234
170. Chesney J, Clark J, Klarer AC, Imbert-Fernandez Y, Lane AN, Telang S. Fructose-2,6-bisphosphate synthesis by 6-phosphofructo-2-kinase/fructose-2,6-bisphosphatase 4 (PFKFB4) is required for the glycolytic response to hypoxia and tumor growth. *Oncotarget* (2014) 5:6670–86. doi: 10.18632/oncotarget.2213
171. Zhang H, Lu C, Fang M, Yan W, Chen M, Ji Y, et al. HIF-1α activates hypoxia-induced PFKFB4 expression in human bladder cancer cells. *Biochem Biophys Res Commun*. (2016) 476:146–52. doi: 10.1016/j.bbrc.2016.05.026
172. Yun SJ, Jo S-W, Ha Y-S, Lee O-J, Kim WT, Kim Y-J, et al. PFKFB4 as a prognostic marker in non-muscle-invasive bladder cancer. *Urol Oncol*. (2012) 30:893–9. doi: 10.1016/j.urolonc.2010.08.018
173. Jeon YK, Yoo DR, Jang YH, Jang SY, Nam MJ. Sulforaphane induces apoptosis in human hepatic cancer cells through inhibition of 6-phosphofructo-2-kinase/fructose-2,6-biphosphatase4, mediated by hypoxia inducible factor-1-dependent pathway. *Biochim Biophys Acta* (2011) 1814:1340–8. doi: 10.1016/j.bbapap.2011.05.015
174. Li B, Takeda K, Ishikawa K, Yoshizawa M, Sato M, Shibahara S, et al. Coordinated expression of 6-phosphofructo-2-kinase/fructose-2,6-bisphosphatase 4 and heme oxygenase 2: evidence for a regulatory link between glycolysis and heme catabolism. *Tohoku J Exp Med*. (2012) 228:27–41. doi: 10.1620/tjem.228.27
175. Shu Y, Lu Y, Pang X, Zheng W, Huang Y, Li J, et al. Phosphorylation of PPARγ at Ser84 promotes glycolysis and cell proliferation in hepatocellular carcinoma by targeting PFKFB4. *Oncotarget* (2016) 7:76984–94. doi: 10.18632/oncotarget.12764
176. Goidts V, Bageritz J, Puccio L, Nakata S, Zapatka M, Barbus S, et al. RNAi screening in glioma stem-like cells identifies PFKFB4 as a key molecule important for cancer cell survival. *Oncogene* (2012) 31:3235–43. doi: 10.1038/onc.2011.490
177. Ros S, Flöter J, Kaymak I, Da Costa C, Houddane A, Dubuis S, et al. 6-Phosphofructo-2-kinase/fructose-2,6-biphosphatase 4 is essential for p53-null cancer cells. *Oncogene* (2017) 36:3287–99. doi: 10.1038/onc.2016.477
178. Li W, Cohen A, Sun Y, Squires J, Braas D, Graeber TG, et al. The role of CD44 in glucose metabolism in prostatic small cell neuroendocrine carcinoma. *Mol Cancer Res*. (2016) 14:344–53. doi: 10.1158/1541-7786.MCR-15-0466
179. Li W, Qian L, Lin J, Huang G, Hao N, Wei X, et al. CD44 regulates prostate cancer proliferation, invasion and migration via PDK1 and PFKFB4. *Oncotarget* (2017) 8:65143–51. doi: 10.18632/oncotarget.17821
180. Strohecker AM, Joshi S, Possemato R, Abraham RT, Sabatini DM, White E. Identification of 6-phosphofructo-2-kinase/fructose-2,6-bisphosphatase as a novel autophagy regulator by high content shRNA screening. *Oncogene* (2015) 34:5662–76. doi: 10.1038/onc.2015.23
181. Wang Q, Zeng F, Sun Y, Qiu Q, Zhang J, Huang W, et al. Etk interaction with PFKFB4 modulates chemoresistance of small-cell lung cancer by regulating autophagy. *Clin Cancer Res*. (2018) 24:950–62. doi: 10.1158/1078-0432.CCR-17-1475
182. Dasgupta S, Rajapakshe K, Zhu B, Nikolai BC, Yi P, Putluri N, et al. Metabolic enzyme PFKFB4 activates transcriptional coactivator SRC-3 to drive breast cancer. *Nature* (2018) 556:249–54. doi: 10.1038/s41586-018-0018-1
183. Jen K-Y, Cheung VG. Identification of novel p53 target genes in ionizing radiation response. *Cancer Res*. (2005) 65:7666–73. doi: 10.1158/0008-5472.CAN-05-1039
184. Bensaad K, Tsuruta A, Selak MA, Vidal MNC, Nakano K, Bartrons R, et al. TIGAR, a p53-inducible regulator of glycolysis and apoptosis. *Cell* (2006) 126:107–20. doi: 10.1016/j.cell.2006.05.036
185. Hasegawa H, Yamada Y, Iha H, Tsukasaki K, Nagai K, Atogami S, et al. Activation of p53 by Nutlin-3a, an antagonist of MDM2, induces apoptosis and cellular senescence in adult T-cell leukemia cells. *Leukemia* (2009) 23:2090–101. doi: 10.1038/leu.2009.171
186. Peña-Rico MA, Calvo-Vidal MN, Villalonga-Planells R, Martínez-Soler F, Giménez-Bonafé P, Navarro-Sabaté À, et al. TP53 induced glycolysis and apoptosis regulator (TIGAR) knockdown results in radiosensitization of glioma cells. *Radiother Oncol*. (2011) 101:132–9. doi: 10.1016/j.radonc.2011.07.002
187. Madan E, Gogna R, Bhatt M, Pati U, Kuppusamy P, Mahdi AA. Regulation of glucose metabolism by p53: emerging new roles for the tumor suppressor. *Oncotarget* (2011) 2:948–57. doi: 10.18632/oncotarget.389
188. Sinha S, Ghildiyal R, Mehta VS, Sen E. ATM-NFκB axis-driven TIGAR regulates sensitivity of glioma cells to radiomimetics in the presence of TNFα. *Cell Death Dis*. (2013) 4:e615. doi: 10.1038/cddis.2013.128
189. Simon-Molas H, Calvo-Vidal MN, Castaño E, Rodríguez-García A, Navarro-Sabaté À, Bartrons R, et al. Akt mediates TIGAR induction in HeLa cells following PFKFB3 inhibition. *FEBS Lett*. (2016) 590:2915–26. doi: 10.1002/1873-3468.12338
190. Zou S, Wang X, Deng L, Wang Y, Huang B, Zhang N, et al. CREB, another culprit for TIGAR promoter activity and expression. *Biochem Biophys Res Commun*. (2013) 439:481–6. doi: 10.1016/j.bbrc.2013.08.098
191. Zou S, Gu Z, Ni P, Liu X, Wang J, Fan Q. SP1 plays a pivotal role for basal activity of TIGAR promoter in liver cancer cell lines. *Mol Cell Biochem*. (2012) 359:17–23. doi: 10.1007/s11010-011-0993-0
192. Kimata M, Matoba S, Iwai-Kanai E, Nakamura H, Hoshino A, Nakaoka M, et al. p53 and TIGAR regulate cardiac myocyte energy homeostasis under hypoxic stress. *Am J Physiol Heart Circ Physiol*. (2010) 299:H1908–16. doi: 10.1152/ajpheart.00250.2010
193. Rajendran R, Garva R, Ashour H, Leung T, Stratford I, Krstic-Demonacos M, et al. Acetylation mediated by the p300/CBP-associated factor determines cellular energy metabolic pathways in cancer. *Int J Oncol*. (2013) 42:1961–72. doi: 10.3892/ijo.2013.1907
194. Matoba S, Kang J-G, Patino WD, Wragg A, Boehm M, Gavrilova O, et al. p53 Regulates mitochondrial respiration. *Science* (2006) 312:1650–3. doi: 10.1126/science.1126863
195. Li H, Jogl G. Structural and biochemical studies of TIGAR (TP53-induced glycolysis and apoptosis regulator). *J Biol Chem*. (2009) 284:1748–54. doi: 10.1074/jbc.M807821200
196. Rigden DJ. The histidine phosphatase superfamily: structure and function. *Biochem J*. (2008) 409:333–48. doi: 10.1042/BJ20071097
197. Boada J, Roig T, Perez X, Gamez A, Bartrons R, Cascante M, et al. Cells overexpressing fructose-2,6-bisphosphatase showed enhanced pentose phosphate pathway flux and resistance to oxidative stress. *FEBS Lett*. (2000) 480:261–4. doi: 10.1016/S0014-5793(00)01950-5

198. Gerin I, Noël G, Bolsée J, Haumont O, Van Schaftingen E, Bommer GT. Identification of TP53-induced glycolysis and apoptosis regulator (TIGAR) as the phosphoglycolate-independent 2,3-bisphosphoglycerate phosphatase. *Biochem J*. (2014) 458:439–48. doi: 10.1042/BJ20130841
199. Cheung EC, Ludwig RL, Vousden KH. Mitochondrial localization of TIGAR under hypoxia stimulates HK2 and lowers ROS and cell death. *Proc Natl Acad Sci USA*. (2012) 109:20491–6. doi: 10.1073/pnas.1206530109
200. Bensaad K, Cheung EC, Vousden KH. Modulation of intracellular ROS levels by TIGAR controls autophagy. *EMBO J*. (2009) 28:3015–26. doi: 10.1038/emboj.2009.242
201. Li N, He Y, Wang L, Mo C, Zhang J, Zhang W, et al. D-galactose induces necroptotic cell death in neuroblastoma cell lines. *J Cell Biochem*. (2011) 112:3834–44. doi: 10.1002/jcb.23314
202. Kim S-J, Jung H-J, Lim C-J. Reactive oxygen species-dependent down-regulation of tumor suppressor genes PTEN, USP28, DRAM, TIGAR, and CYLD under oxidative stress. *Biochem Genet*. (2013) 51:901–15. doi: 10.1007/s10528-013-9616-7
203. Pietrocola F, Izzo V, Niso-Santano M, Vacchelli E, Galluzzi L, Maiuri MC, et al. Regulation of autophagy by stress-responsive transcription factors. *Semin Cancer Biol*. (2013) 23:310–22. doi: 10.1016/j.semcancer.2013.05.008
204. Zhang X, Qin Z, Wang J. The role of p53 in cell metabolism. *Acta Pharmacol Sin*. (2010) 31:1208–12. doi: 10.1038/aps.2010.151
205. Cui L, Song Z, Liang B, Jia L, Ma S, Liu X. Radiation induces autophagic cell death via the p53/DRAM signaling pathway in breast cancer cells. *Oncol Rep*. (2016) 35:3639–47. doi: 10.3892/or.2016.4752
206. Cheung EC, Athineos D, Lee P, Ridgway RA, Lambie W, Nixon C, et al. TIGAR is required for efficient intestinal regeneration and tumorigenesis. *Dev Cell*. (2013) 25:463–77. doi: 10.1016/j.devcel.2013.05.001
207. Won KY, Lim S-J, Kim GY, Kim YW, Han S-A, Song JY, et al. Regulatory role of p53 in cancer metabolism via SCO2 and TIGAR in human breast cancer. *Hum Pathol*. (2012) 43:221–8. doi: 10.1016/j.humpath.2011.04.021
208. Liu J, Lu F, Gong Y, Zhao C, Pan Q, Ballantyne S, et al. High expression of synthesis of cytochrome c oxidase 2 and TP53-induced glycolysis and apoptosis regulator can predict poor prognosis in human lung adenocarcinoma. *Hum Pathol*. (2018) 77:54–62. doi: 10.1016/j.humpath.2017.12.029
209. Kim SH, Choi SI, Won KY, Lim S-J. Distinctive interrelation of p53 with SCO2, COX, and TIGAR in human gastric cancer. *Pathol Res Pract*. (2016) 212:904–10. doi: 10.1016/j.prp.2016.07.014
210. Lui VWY, Lau CPY, Cheung CSF, Ho K, Ng MHL, Cheng SH, et al. An RNA-directed nucleoside anti-metabolite, 1-(3-C-ethynyl-beta-d-ribo-pentofuranosyl)cytosine (ECyd), elicits antitumor effect via TP53-induced glycolysis and apoptosis regulator (TIGAR) downregulation. *Biochem Pharmacol*. (2010) 79:1772–80. doi: 10.1016/j.bcp.2010.02.012
211. Lui VWY, Wong EYL, Ho K, Ng PKS, Lau CPY, Tsui SKW, et al. Inhibition of c-Met downregulates TIGAR expression and reduces NADPH production leading to cell death. *Oncogene* (2011) 30:1127–34. doi: 10.1038/onc.2010.490
212. Ye L, Zhao X, Lu J, Qian G, Zheng JC, Ge S. Knockdown of TIGAR by RNA interference induces apoptosis and autophagy in HepG2 hepatocellular carcinoma cells. *Biochem Biophys Res Commun*. (2013) 437:300–6. doi: 10.1016/j.bbrc.2013.06.072
213. Lin C-C, Cheng T-L, Tsai W-H, Tsai H-J, Hu K-H, Chang H-C, et al. Loss of the respiratory enzyme citrate synthase directly links the Warburg effect to tumor malignancy. *Sci Rep*. (2012) 2:785. doi: 10.1038/srep00785
214. Madan E, Gogna R, Kuppusamy P, Bhatt M, Pati U, Mahdi AA. TIGAR induces p53-mediated cell-cycle arrest by regulation of RB-E2F1 complex. *Br J Cancer* (2012) 107:516–26. doi: 10.1038/bjc.2012.260
215. Yin L, Kosugi M, Kufe D. Inhibition of the MUC1-C oncoprotein induces multiple myeloma cell death by down-regulating TIGAR expression and depleting NADPH. *Blood* (2012) 119:810–6. doi: 10.1182/blood-2011-07-369686
216. López-Guerra M, Trigueros-Motos L, Molina-Arcas M, Villamor N, Casado FJ, Montserrat E, et al. Identification of TIGAR in the equilibrative nucleoside transporter 2-mediated response to fludarabine in chronic lymphocytic leukemia cells. *Haematologica* (2008) 93:1843–51. doi: 10.3324/haematol.13186
217. Wanka C, Steinbach JP, Rieger J. Tp53-induced glycolysis and apoptosis regulator (TIGAR) protects glioma cells from starvation-induced cell death by up-regulating respiration and improving cellular redox homeostasis. *J Biol Chem*. (2012) 287:33436–46. doi: 10.1074/jbc.M112.384578
218. Canaparo R, Varchi G, Ballestri M, Foglietta F, Sotgiu G, Guerrini A, et al. Polymeric nanoparticles enhance the sonodynamic activity of meso-tetrakis (4-sulfonatophenyl) porphyrin in an *in vitro* neuroblastoma model. *Int J Nanomed.* (2013) 8:4247–63. doi: 10.2147/IJN.S51070
219. Tang Y, Kwon H, Neel BA, Kasher-Meron M, Pessin J, Yamada E, et al. The fructose-2,6-bisphosphatase TIGAR suppresses NF-κB signaling by directly inhibiting the linear ubiquitin assembly complex LUBAC. *J Biol Chem*. (2018) 293:7578–91. doi: 10.1074/jbc.RA118.002727
220. Martinez-Outschoorn UE, Trimmer C, Lin Z, Whitaker-Menezes D, Chiavarina B, Zhou J, et al. Autophagy in cancer associated fibroblasts promotes tumor cell survival: role of hypoxia, HIF1 induction and NFκB activation in the tumor stromal microenvironment. *Cell Cycle* (2010) 9:3515–33. doi: 10.4161/cc.9.17.12928
221. Martinez-Outschoorn UE, Pavlides S, Howell A, Pestell RG, Tanowitz HB, Sotgia F, et al. Stromal-epithelial metabolic coupling in cancer: integrating autophagy and metabolism in the tumor microenvironment. *Int J Biochem Cell Biol*. (2011) 43:1045–51. doi: 10.1016/j.biocel.2011.01.023
222. Ko Y-H, Lin Z, Flomenberg N, Pestell RG, Howell A, Sotgia F, et al. Glutamine fuels a vicious cycle of autophagy in the tumor stroma and oxidative mitochondrial metabolism in epithelial cancer cells. *Cancer Biol Ther*. (2011) 12:1085–97. doi: 10.4161/cbt.12.12.18671
223. Qian S, Li J, Hong M, Zhu Y, Zhao H, Xie Y, et al. TIGAR cooperated with glycolysis to inhibit the apoptosis of leukemia cells and associated with poor prognosis in patients with cytogenetically normal acute myeloid leukemia. *J Hematol Oncol*. (2016) 9:128. doi: 10.1186/s13045-016-0360-4
224. Zhou X, Xie W, Li Q, Zhang Y, Zhang J, Zhao X, et al. TIGAR is correlated with maximal standardized uptake value on FDG-PET and survival in non-small cell lung cancer. *PLoS ONE* (2013) 8:e80576. doi: 10.1371/journal.pone.0080576
225. Pons G, Carreras J. Functional characterization of the enzymes with 2,3-bisphosphoglycerate phosphatase activity from pig skeletal muscle. *Comp Biochem Physiol B* (1986) 85:879–85. doi: 10.1016/0305-0491(86)90191-4
226. Mazurek S. Pyruvate kinase type M2: a key regulator of the metabolic budget system in tumor cells. *Int J Biochem Cell Biol*. (2011) 43:969–80. doi: 10.1016/j.biocel.2010.02.005
227. Tauler A, Gil J, Bartrons R, Carreras J. Levels of glycerate 2,3-P2, 2,3-bisphosphoglycerate synthase and 2,3-bisphosphoglycerate phosphatase activities in rat tissues. A method to quantify blood contamination of tissue extracts. *Comp Biochem Physiol B* (1987) 86:11–3. doi: 10.1016/0305-0491(87)90167-2
228. Scatena R, Bottoni P, Pontoglio A, Mastrototaro L, Giardina B. Glycolytic enzyme inhibitors in cancer treatment. *Expert Opin Investig Drugs* (2008) 17:1533–45. doi: 10.1517/13543784.17.10.1533
229. El Mjiyad N, Caro-Maldonado A, Ramírez-Peinado S, Muñoz-Pinedo C. Sugar-free approaches to cancer cell killing. *Oncogene* (2011) 30:253–64. doi: 10.1038/onc.2010.466
230. Semenza G. Signal transduction to hypoxia-inducible factor 1. *Biochem Pharmacol*. (2002) 64:993–8. doi: 10.1016/S0006-2952(02)01168-1
231. Semenza GL. Molecular mechanisms mediating metastasis of hypoxic breast cancer cells. *Trends Mol Med*. (2012) 18:534–43. doi: 10.1016/j.molmed.2012.08.001
232. Semenza GL. Targeting HIF-1 for cancer therapy. *Nat Rev Cancer* (2003) 3:721–32. doi: 10.1038/nrc1187
233. Hu Y, Liu J, Huang H. Recent agents targeting HIF-1α for cancer therapy. *J Cell Biochem*. (2013) 114:498–509. doi: 10.1002/jcb.24390
234. Pelicano H, Martin DS, Xu R-H, Huang P. Glycolysis inhibition for anticancer treatment. *Oncogene* (2006) 25:4633–46. doi: 10.1038/sj.onc.1209597
235. Raez LE, Papadopoulos K, Ricart AD, Chiorean EG, DiPaola RS, Stein MN, et al. A phase I dose-escalation trial of 2-deoxy-d-glucose alone or combined with docetaxel in patients with advanced solid tumors. *Cancer Chemother Pharmacol*. (2013) 71:523–30. doi: 10.1007/s00280-012-2045-1
236. Chesney J, Clark J, Lanceta L, Trent JO, Telang S. Targeting the sugar metabolism of tumors with a first-in-class 6-phosphofructo-2-kinase (PFKFB4) inhibitor. *Oncotarget*. (2015) 6:18001–11. doi: 10.18632/oncotarget.4534

237. Zhang Y, Chen F, Tai G, Wang J, Shang J, Zhang B, et al. TIGAR knockdown radiosensitizes TrxR1-overexpressing glioma *in vitro* and *in vivo* via inhibiting Trx1 nuclear transport. *Sci Rep*. (2017) 7:42928. doi: 10.1038/srep42928
238. Lo-Coco F, Avvisati G, Vignetti M, Thiede C, Orlando SM, Iacobelli S, et al., Study Alliance Leukemia. Retinoic acid and arsenic trioxide for acute promyelocytic leukemia. *N Engl J Med*. (2013) 369:111–21. doi: 10.1056/NEJMoa1300874
239. El-Mir MY, Nogueira V, Fontaine E, Avéret N, Rigoulet M, Leverve X. Dimethylbiguanide inhibits cell respiration via an indirect effect targeted on the respiratory chain complex I. *J Biol Chem*. (2000) 275:223–8. doi: 10.1074/jbc.275.1.223
240. Curry J, Johnson J, Tassone P, Vidal MD, Menezes DW, Sprandio J, et al. Metformin effects on head and neck squamous carcinoma microenvironment: window of opportunity trial. *Laryngoscope* (2017) 127:1808–15. doi: 10.1002/lary.26489
241. Martinez-Outschoorn UE, Sotgia F, Lisanti MP. Caveolae and signalling in cancer. *Nat Rev Cancer* (2015) 15:225–37. doi: 10.1038/nrc3915
242. Monti D, Sotgia F, Whitaker-Menezes D, Tuluc M, Birbe R, Berger A, et al. Pilot study demonstrating metabolic and anti-proliferative effects of *in vivo* anti-oxidant supplementation with N-acetylcysteine in breast cancer. *Semin Oncol*. (2017) 44:226–32. doi: 10.1053/j.seminoncol.2017.10.001

Conflict of Interest Statement: The authors declare that the research was conducted in the absence of any commercial or financial relationships that could be construed as a potential conflict of interest.

frontiers in Oncology

ORIGINAL RESEARCH
published: 28 August 2018
doi: 10.3389/fonc.2018.00324

Monocarboxylate Transporter 4 (MCT4) Knockout Mice Have Attenuated 4NQO Induced Carcinogenesis; A Role for MCT4 in Driving Oral Squamous Cell Cancer

Sara Bisetto[1†], Diana Whitaker-Menezes[2†], Nicole A. Wilski[3], Madalina Tuluc[1], Joseph Curry[4], Tingting Zhan[5], Christopher M. Snyder[3], Ubaldo E. Martinez-Outschoorn[2] and Nancy J. Philp[1*]*

[1] Department of Pathology, Anatomy and Cell Biology, Sydney Kimmel Cancer Center, Thomas Jefferson University, Philadelphia, PA, United States, [2] Department of Medical Oncology, Sydney Kimmel Cancer Center, Thomas Jefferson University, Philadelphia, PA, United States, [3] Department of Microbiology and Immunology, Sydney Kimmel Cancer Center, Thomas Jefferson University, Philadelphia, PA, United States, [4] Department of Otolaryngology–Head and Neck Surgery, Sydney Kimmel Cancer Center, Thomas Jefferson University, Philadelphia, PA, United States, [5] Division of Biostatistics, Department of Pharmacology and Experimental Therapeutics, Sydney Kimmel Cancer Center, Thomas Jefferson University, Philadelphia, PA, United States

OPEN ACCESS

Edited by:
Jacques Pouyssegur, Université Côte d'Azur, France

Reviewed by:
Margaret Ashcroft, University of Cambridge, United Kingdom
Paolo E. Porporato, Università degli Studi di Torino, Italy

***Correspondence:**
Ubaldo E. Martinez-Outschoorn Ubaldo.Martinez-Outschoorn@jefferson.edu
Nancy J. Philp nancy.philp@jefferson.edu

[†]These authors have contributed equally to this work

Specialty section:
This article was submitted to Molecular and Cellular Oncology, a section of the journal Frontiers in Oncology

Received: *18 June 2018*
Accepted: *30 July 2018*
Published: *28 August 2018*

Citation:
Bisetto S, Whitaker-Menezes D, Wilski NA, Tuluc M, Curry J, Zhan T, Snyder CM, Martinez-Outschoorn UE and Philp NJ (2018) Monocarboxylate Transporter 4 (MCT4) Knockout Mice Have Attenuated 4NQO Induced Carcinogenesis; A Role for MCT4 in Driving Oral Squamous Cell Cancer. Front. Oncol. 8:324. doi: 10.3389/fonc.2018.00324

Head and neck squamous cell carcinoma (HNSCC) is the 6th most common human cancer and affects approximately 50,000 new patients every year in the US. The major risk factors for HNSCC are tobacco and alcohol consumption as well as oncogenic HPV infections. Despite advances in therapy, the overall survival rate for all-comers is only 50%. Understanding the biology of HNSCC is crucial to identifying new biomarkers, implementing early diagnostic approaches and developing novel therapies. As in several other cancers, HNSCC expresses elevated levels of MCT4, a member of the SLC16 family of monocarboxylate transporters. MCT4 is a H^+-linked lactate transporter which functions to facilitate lactate efflux from highly glycolytic cells. High MCT4 levels in HNSCC have been associated with poor prognosis, but the role of MCT4 in the development and progression of this cancer is still poorly understood. In this study, we used 4-nitroquinoline-1-oxide (4NQO) to induce oral cancer in $MCT4^{-/-}$ and wild type littermates, recapitulating the disease progression in humans. Histological analysis of mouse tongues after 23 weeks of 4NQO treatment showed that $MCT4^{-/-}$ mice developed significantly fewer and less extended invasive lesions than wild type. In mice, as in human samples, MCT4 was not expressed in normal oral mucosa but was detected in the transformed epithelium. In the 4NQO treated mice we detected MCT4 in foci of the basal layer undergoing transformation, and progressively in areas of carcinoma *in situ* and invasive carcinomas. Moreover, we found MCT4 positive macrophages within the tumor and in the stroma surrounding the lesions in both human samples of HNSCC and in the 4NQO treated animals. The results of our studies showed that MCT4 could be used as an early diagnostic biomarker of HNSCC. Our finding with the $MCT4^{-/-}$ mice suggest MCT4 is a driver of progression to oral squamous cell cancer and MCT4 inhibitors could have clinical benefits for preventing invasive HNSCC.

Keywords: MCT4, 4NQO, oral squamous cell carcinoma, tumor microenvironment, metabolism

INTRODUCTION

Head and neck squamous cell carcinoma (HNSCC) is the 6th most common human cancer with almost 50,000 new cases diagnosed in the United States each year (1, 2). Among the different subtypes of HNSCC, oral squamous cell carcinoma (OSCC), especially of the tongue, is the most common. Risk factors for OSCC are tobacco use and alcohol consumption (3, 4). The high mortality with HNSCC and OSCC in particular, with a 5-year survival rate of only 50%, creates an urgent need for better understanding of disease biology as well as prognostic and predictive biomarkers and novel therapies.

Recent studies have shown that, similar to other types of cancer, an increase in monocarboxylate transporter 4 (MCT4) expression in patients with OSCC correlates with a poor outcome (5–8). MCT4 is a member of the SLC16 family of solute transporters and functions as a proton-coupled lactate transporter (9). MCT4 is primarily expressed in glycolytic cells including fast twitch muscle, neural retina and activated macrophages where it facilitates the efflux of lactate (10–12). Warburg was the first to show that cancer cells often exhibit a high rate of aerobic glycolysis producing large amounts of lactate. In tumors, high levels of lactate are generated by a subset of highly glycolytic cancer and stromal cells. It is then taken up and oxidized by other tumor cells expressing high levels of monocarboxylate transporter 1 (MCT1), another member of the SLC16 family (13). Lactate is metabolized through oxidative phosphorylation to produce ATP and intermediates that support tumor growth. In addition to its role as metabolic substrate, lactate is also a signaling molecule with important roles in angiogenesis, tumor migration and invasion, as well as modulation of the immune system (14).

The experimental models currently available for understanding the contribution of MCTs and lactate to the progression of cancer are based on the manipulation of gene expression in cancer cell lines for *in vitro* and *in vivo* studies (15–17). These studies have contributed to a greater understanding of the role of lactate in tumor progression and survival, highlighting the therapeutic potential of targeting MCT1 and MCT4. However, the importance of epithelial and stromal MCT4 in driving cancer progression remains poorly understood.

In this study we investigated the role of MCT4 in the progression of OSCC in a well-established model of oral squamous cell carcinoma using the carcinogen 4-nitroquinoline-1-oxide (4NQO) (18) in wild type ($MCT4^{+/+}$) and MCT4 knockout ($MCT4^{-/-}$) mice. After exposure to 4NQO, MCT4 knockout animals developed significantly fewer and less extensive invasive SCC lesions compared to wild type mice. Importantly, MCT4, which is typically absent in normal tongue epithelium, was expressed early in regions of dysplastic epithelium and later in areas of *in situ* carcinomas (CIS) and invasive squamous cell carcinomas (SCC). In addition, MCT4 was detected in macrophages within the lesion and adjacent stroma after 4NQO exposure, similar to what is observed in human OSCC samples. Our results suggest that MCT4 is critical for the progression from dysplastic lesions to invasive cancer and is therefore a relevant therapeutic target for the treatment of OSCC.

MATERIALS AND METHODS

Human Study

This study was approved by the institutional review board (IRB) at Thomas Jefferson University. Samples of primary tumors from 9 patients with head and neck cancer were obtained from archived paraffin-embedded tissue blocks for histological analysis. Patient data were collected, including: age, sex, tobacco use, stage of disease, location of tumor, and histological features.

Animals

$MCT4^{+/-}$ mice were purchased from Taconic Bioscience. The animals were backcrossed for 10 generations to C57Bl/6N (Taconic) mice and $MCT4^{+/-}$ mice were used for breeding to obtain knock out and wild type littermates. Genotype was confirmed by PCR. Mice were kept in a 12:12 light/dark cycle and provided with *ad libitum* food and drinking water.

Mouse Oral Carcinogenesis Induction

$MCT4^{-/-}$ and wild type mice ($n = 15$–16) 12 weeks of age, were treated with 4-nitroquinoline-1-oxide (4NQO; cat # N8141, Sigma-Aldrich) in the drinking water at a concentration of 50 μg/ml. The animals were treated for 16 weeks with the 4NQO and then for an additional 7 weeks with water only. Fresh 4NQO/water was supplied every week. Animals were sacrificed after 14 weeks of treatment and at 23 weeks or when body weight loss was >20% of original weight. Oral cavities were inspected weekly for signs of lesions, and body weight was monitored as a sign of distress. All the experiments were conducted in accordance and with the approval of the Institutional Animal Care and Use Committee (IACUC) at Thomas Jefferson University.

Antibodies

The following antibodies were used: MCT4 (SLC16A3) 19-mer peptide sequence CKAEPEKNGEVVHTPETSV-cooh affinity purified rabbit antibody and MCT1 (SLC16A1) 19-mer peptide sequence CSPDQKDTEGGPKEEESPV-cooh affinity purified rabbit antibodies were generated by YenZym Antibodies, South San Francisco, CA. (11). Mouse anti-human MCT4 (D-1) antibody was from Santa Cruz Biotechnology. Rabbit anti human- CD163 was from Abcam. Rat anti-mouse F4/80 (CI-A3-1) was from Novus Biologicals. CD45.2 (clone 104), PD-L1 (clone 10F.9G2), Ly6C (clone HK1.4), Ly6G (clone 1A8), CD11b (clone M1/70) were from BioLegend.

Analysis of Human Dual Labeling for CD163-Positive Macrophages and MCT4

Paraffin sections of human HNSCC were dual labeled by immunohistochemistry as detailed below with CD163 (Abcam) developed in red/pink and MCT4 (Santa Cruz Biotechnology) developed in brown. Slides were scanned at low power (4x) and 3 areas containing cancer cells and identifiable macrophages (stained in red/pink) that were within tumor nests or in the

immediate adjacent stroma were selected and then scored at high power (40x). Each 40x field was scored as positive when >80% macrophages were also MCT4 positive. The same method was used to evaluate normal, non-tumor areas within the same section. These areas were located in stroma underlying normal squamous epithelium or in areas of non-involved muscle.

Macroscopic Photography and Lesional Area Quantification

Tongues were harvested and placed on ice in phosphate buffered saline (PBS). Immediately prior to photography, individual tongues were incubated for one minute in a solution of 10% acetic acid and 4% ethanol followed by two PBS rinses [modified from Mashberg et al. (19)]. This treatment accentuated lesional areas from relatively unaffected areas. Images were captured with AxioVision LE software using a 5megapixel Zeiss AxioCam Erc5s color camera coupled to a Stemi 2000C Zeiss stereomicroscope at 0.65x magnification. ImageJ was used for the quantification of the affected areas on the dorsal surface of the tongue. Briefly, lesional areas which were identified as white opaque raised regions, were measured and the average percentage lesional area was calculated for wild type versus MCT4$^{-/-}$ tongues. The images were evaluated in a blinded manner by 2 independent observers.

Tissue Collection and Histopathological Analysis

Tongue samples were fixed in 10% formalin and then cut lengthwise into 3 pieces and embedded separately in paraffin. Four micron sections were cut from all blocks and stained with hematoxylin and eosin (H&E) for histopathological evaluation by an expert in oral cancer pathology, to determine presence of carcinoma-*in-situ* and invasive carcinoma. In other experiments, tongues samples were cut lengthwise and either flash frozen in liquid nitrogen or embedded in OCT compound for frozen sectioning.

Immunohistochemistry of Paraffin and Frozen Sections

A 3-step avidin-biotin horseradish peroxidase method was used for single antibody labeling on paraffin sections as previously described (20). Briefly after deparaffinization and rehydration of the sections, antigen retrieval was performed in 0.01M citrate buffer, pH 6.0 using an electric pressure cooker. An avidin-biotin kit (Biocare Medical) was used to block endogenous biotin and the sections were blocked with 10% goat serum (Vector Labs) in PBS at 4°C. Primary antibody was incubated for 1 hour followed by biotinylated species-specific secondary antibody (Vector Labs) and avidin-biotin-horseradish peroxidase complex (ABC Elite Kit, Vector Labs) with washing in PBS between steps. Antibody binding was detected with 3,3′ diaminobenzidine (DAB liquid substrate kit, Agilent Technologies). A similar procedure was used for frozen sections that were fixed in acetone. For dual antibody labeling, a 2-step procedure was used as described in (21). Briefly, after antigen retrieval and blocking in 5% BSA, sections were incubated simultaneously with primary antibodies followed species-specific secondary antibodies conjugated with alkaline phosphatase or peroxidase (Jackson ImmunoResearch). Antibody binding was detected using DAB liquid substrate kit and ImmPACT Vector Red substrate kit (Vector) containing 1.25 mM levamisole (Sigma-Aldrich). Light microscopy images were captured using cellSens Entry software and the Olympus DP22 camera attached to an Olympus CX41 microscope (Olympus Scientific Solutions Americas).

Dual Labeling by Immunofluorescence

For mouse samples double labeling immunofluorescence was performed using frozen sections after fixation in acetone and blocking in 5% BSA. Primary antibodies were incubated together for one hour at RT, washed and detected with AlexaFluor 488 conjugated donkey anti-rat IgG and AlexaFluor 568 conjugated goat anti-rabbit IgG (ThermoFisher Scientific). Nuclei were stained with DAPI and sections were mounted with ProLong Gold anti-fade (ThermoFisher Scientific). All immunofluorescent labeling images were captured on the Nikon A1R confocal microscope with a 40x oil objective lens with or without 2x zoom.

Macrophage Quantification in 4NQO-Treated Mice

Macrophages were identified by immunohistochemistry using the F4/80 antibody in frozen tissue sections at 14 and 23 weeks. Areas of involved and non-involved epithelia were identified by a pathologist with expertise in head and neck pathology, and 3–5 digital images were taken at 20× magnification and analyzed with Image J software calibrated for magnification. The subepithelial stromal area for each image was measured and the number of F4/80 positive cells was counted within each area. The number of F4/80 positive cells per cubic micron was calculated and adjusted per mm^3 and the average number for involved and non-involved areas were generated for wild type and knockout samples.

Implantable Tumor Models

TC-1 cells (kindly provided by Dr. Ulrich Rodeck) were maintained in RPMI (Corning Life Science) with 1% PenStrep (Gemini Bio-Products) and 10% fetal bovine serum (Benchmark serum, Gemini Bio-Products). TC-1 cells are HPV transformed C57Bl/6 lung epithelium cells (22). For the transplantable tumor model, TC-1 cells were implanted subcutaneously in the shaved right flank of 10-12 week old MCT4$^{-/-}$ and control littermates. 1×10^5 TC-1 cells were injected in 100uL PBS. Tumor area was calculated using the length and width of the tumor (in mm^2), which was measured using digital calipers. For growth curve studies, animals were sacrificed after 25 days from implantation when the tumor was growing exponentially.

Blood Collection and Flow Cytometry

Approximately 80 μL of blood was collected in a tube containing 12 μL heparin from the retro-orbital sinus. 40 uL of the collected blood was stained using Zombie Aqua Fixable Viability Kit (BioLegend) and antibodies specific for the monocyte population. Following staining, red blood cell lysis buffer (150 mmol/l NH_4Cl, 10 mmol/l NaHCO) was added to the samples to isolate leukocytes. CountBright absolute counting

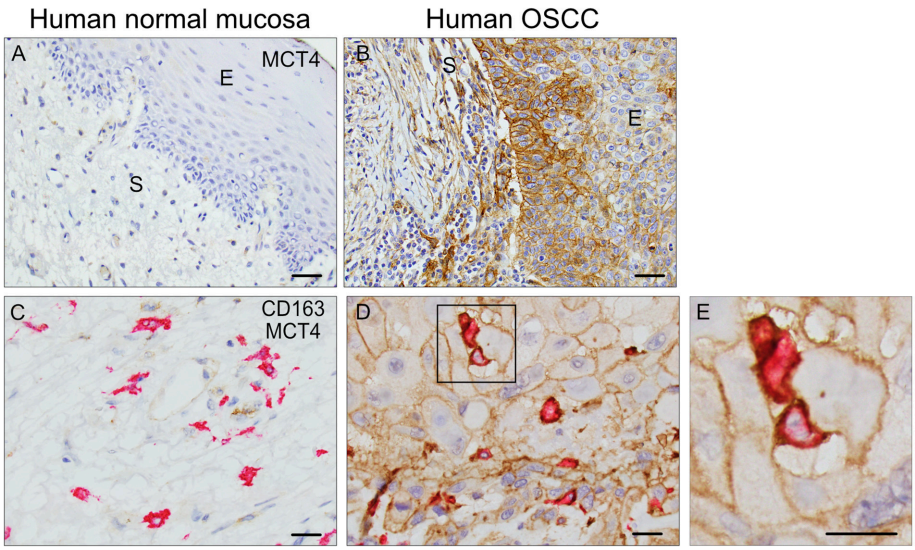

FIGURE 1 | MCT4 is expressed in Human OSCC: Single MCT4 **(A,B)** and dual MCT4/CD163 **(C–E)** immunostaining in paraffin embedded samples of human OSCC. Area of adjacent normal epithelium in OSCC sample #1 **(A)**, area of squamous cell carcinoma within the same sample #1 **(B)**. MCT4 negative/CD163 positive macrophages in adjacent normal area of oral mucosa in sample #2 **(C)**. MCT4 positive/CD163 positive macrophages in areas of cancer cells within same sample #2 **(D)**. Boxed region in D is showed at higher magnification in E (2.5X). Scale bar: 20 μm. S, stroma; E, epithelium.

beads (ThermoFisher Scientific) were added to the samples immediately prior to analysis. Samples were run on the BD LSRFortessa flow cytometer (BD Biosciences) and data was analyzed using FlowJo Version 10.1 (Treestar).

Western Blot Analysis

Cells and tissues were lysed in RIPA buffer (ThermoFisher Scientific) containing protease inhibitor cocktail (ThermoFisher Scientific). Samples were centrifuged and supernatant collected for protein analysis. After protein quantification with the BCA method, samples were separated using Bis-Tris NuPage precast gels (ThermoFisher Scientific) and transferred to PVDF membranes. After blocking with 5% nonfat milk for 1 hour, primary antibodies were incubated overnight at 4°C. Membranes were washed in TBS-tween buffer and incubated in HRP conjugated secondary antibodies for 1h at room temperature. Blots were developed using SuperSignal West Dura ECL substrate (ThermoFisher Scientific) and imaged using FluorChem M ProteinSimple imager.

Data Analysis

All data are presented as mean ± standard error. Data were analyzed with GraphPad Prism v7 (GraphPad software) or R v3.5.0 (R-project.org). Unless specified differently, two-tailed-t test or ANOVA were performed to analyze the mean difference between groups. For correlation analysis Fisher's exact test was used. Data reported in **Figure 6M** data were analyzed using a robust linear mixed effect model with random effect of mice and fixed effect of time, genotype and area. Statistical significance was defined as p-value < 0.05.

RESULTS

MCT4 Expression in Human Oral Squamous Cell Carcinoma

MCT4 is expressed in both cancer cell and stromal compartments in human OSCC and is typically not present in normal squamous epithelia (**Figures 1A,B**). In the present study, MCT4 expression was further evaluated in macrophages identified by the marker CD163 in nine cases of HNSCC. The demographic and pathological characteristics of these cases are summarized in **Table 1**. Paraffin sections were labeled with antibodies to CD163 and MCT4 simultaneously (**Figures 1C–E**) and the percentage of macrophages positive for MCT4 was evaluated in a blinded fashion by two independent observers (**Table 2**). CD163-positive macrophages within cancer cell nests or in the immediate adjacent stroma were evaluated at high power and compared to macrophages in normal or non-involved or control areas distant from cancer cell sites. MCT4 staining in macrophages was scored as positive in fields that contained 80% or greater double positive cells. Six of nine cases had macrophages positive for CD163 that were also positive for MCT4 (66.7%). When CD163-positive macrophages were evaluated in non-involved or control areas that were distant and free from the presence of cancer cells, all cases were negative ($p < 0.01$).

MCT4$^{-/-}$ Mouse Model for Oral Carcinoma Development

Based on the strong correlation between MCT4 expression and poor outcomes in OSCC we wanted to develop an *in vivo* animal model to test whether MCT4 was a marker or a driver of aggressive cancer. MCT4$^{+/-}$ mice were purchased from Taconic

TABLE 1 | Demographics and Pathologic characteristics.

Mean age (range)	64.9 (50–82)
Gender	6 male/3 females
Tobacco use (>10 pack/year)	6 (67%)
p16 positive	1 (11%)
SUBSITE	
Oral cavity	7 (78%)
Oral tongue	2
Floor of mouth	3
Gingiva	2
Oropharynx	2 (22%)
Base of tongue	1
Tonsil	1
T STAGE	
T1	1 (1%)
T2	3 (33%)
T4a	5 (56%)
N STAGE	
N0	5 (56%)
N2b	3 (33%)
N2c	1 (11%)
PATHOLOGICAL MARKERS	
ECE	2 (22%)
Positive margins	2 (22%)
PNI	4 (44%)
LVI	2 (22%)
DIFFERENTIATION	
Well	0
Moderate	8 (89%)
Poor	1 (11%)

TABLE 2 | HNSCC MCT4 Expression in CD163-positive macrophages.

Site	MCT-4 Positive	MCT-4 Negative	Total
Tumor	6	3	9
Control	0	8	8
Total	6	11	17

Number of samples with CD163 stained macrophages positive or negative for MCT4 in human HNSCC (n = 9). Tumor site is intra-tumoral or immediate peri-tumoral area; Control is adjacent non-tumor i.e., subepithelial stroma or non-involved muscle; Positive is >80% dual positive within field.

Biosciences and backcrossed to homozygosity, on a C57BL6/N background. No changes in breeding or growth were observed in these mice. **Figure 2A** is a representative Western blot showing that MCT4 was detected in lysates from retina, skeletal muscle and activated macrophages from wild type but not in MCT4$^{-/-}$ mice (**Figure 2A**). Frozen sections of wild type and MCT4$^{-/-}$ tongues from animals not exposed to 4NQO were labeled with MCT4 antibody. MCT4 was not present in the mucosa but was detected in the sarcolemma of the skeletal muscle fibers (**Figures 2B,C**). This pattern of MCT4 expression was identical to that of human oral mucosa (**Figure 1A**).

Administration of 4NQO Induces More Aggressive Oral Squamous Carcinoma in Wild Type Animals

Treatment of mice with 4NQO in the drinking water is a well-established model for induction of OSCC (23). To understand the contribution of MCT4 to the development and progression of oral squamous cell carcinoma (OSCC), MCT4$^{-/-}$ mice and control littermates were treated for 16 weeks with 50 μg/ml 4NQO in the drinking water, followed by 7 weeks of pure water (**Figure 3A**). After 23 weeks of treatment, the animals were euthanized and the tongues excised and assessed for cancerous lesions as described in materials and methods. As reported in other studies using 4NQO, during the treatment with the carcinogen the mice lost up to 20% of the initial body weight, but the change was not significantly different between the wild type and the MCT4$^{-/-}$ group. Macroscopic examination of the tongues showed that wild type animals developed more prominent and numerous lesions compared to MCT4$^{-/-}$ animals (**Figures 3B,C**). Quantification of the area occupied by the white lesions on the dorsal surface of the tongues showed that the wild type animals had 39% of the surface covered by lesions while the MCT4$^{-/-}$ animals had only 25% ($p < 0.05$) (**Figure 3D**). The tongues of the 23 week 4NQO treated wild type and MCT4$^{-/-}$ mice were paraffin embedded and sectioned. Microscopic observation of H&E-stained sections revealed epithelial changes that ranged from mild to severe dysplasia and carcinoma *in situ* (CIS; **Figures 3E,F,I,J**) to invasive oral squamous cell carcinoma (OSCC; **Figures 3G,H,K,L**). There was nuclear enlargement and hyperchromasia that was restricted to the basal layer in areas of mild dysplasia as well as cytologic atypia that involved the entire epithelial thickness, with associated acanthosis and hyperparakeratosis in areas of severe dysplasia and CIS (**Figure 3**). All animals showed evidence of CIS, however, in MCT4$^{-/-}$ the pathological features of CIS were qualitatively less pronounced, with fewer areas of epithelial involvement (**Figures 3E,F,I,J**). MCT4$^{-/-}$ mice had fewer invasive lesions (>1 mm depth of invasion), with 2 of 12 knockout mice (16.7%) having invasive SCC compared to 8 of 13 wild type animals with invasive SCC (61.5%; $p < 0.05$) (**Figures 3G,H,K,L**). However, MCT4$^{-/-}$ mice did show limited micro-invasive features with involvement of less than 1mm depth in 4 of 12 animals (33.3%), compared to 2 of 13 wild type animals (15.4%) but this was not statistically significantly different. The number of CIS, invasive SCC and micro-invasive SCC are summarized in **Table 3**.

MCT4 Is Expressed at an Early Stage of Disease

4NQO treated animals developed a complex range of changes in the epithelium that allowed us to study changes in MCT4 expression during the tumorigenic process. To understand the importance of MCT4 in the development of oral cancer, we sacrificed the animals after 14 weeks of 4NQO treatment when early visible changes could be identified on the surface of the tongues (24). Immunohistochemistry of frozen section of the tongues was performed with MCT4 antibody. Focal expression

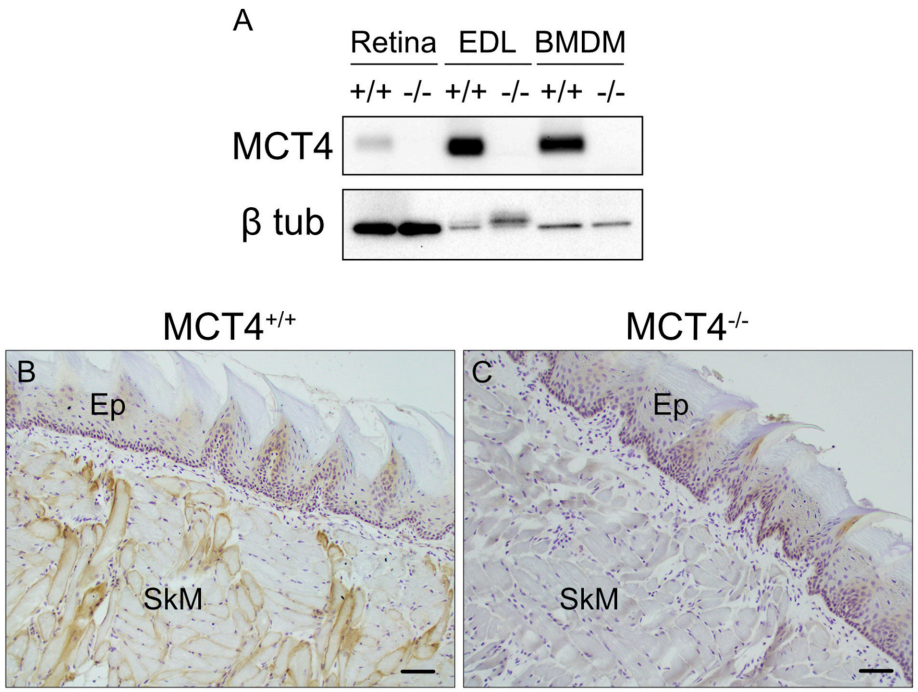

FIGURE 2 | Characterization of MCT4$^{-/-}$ animals. Western blot of detergent lysates prepared from retinas, extensor digitorum longus (EDL) muscle, and LPS activated bone marrow derived macrophages (BMDM) from wild type (+/+) and MCT4 knock out (-/-) mice **(A)**. Frozen sections of mouse tongue from MCT4 $^{(+/+)}$ **(B)** and MCT4$^{-/-}$ **(C)** mice labeled with MCT4 antibody. Ep, epithelium; SkM, skeletal muscle. Scale bar, 50 μm.

of MCT4 was detected in the epithelial cells of the stratum basalis as well as in small foci extending into the stratum spinosum (**Figures 4A–D**). Additionally, in areas where there was epithelial MCT4 expression, we also detected an increase in MCT4 positive cells in the adjacent stroma (**Figure 4B**). Immunostaining of frozen sections of tongue tissues after 23 weeks showed that with progression of OSCC, the expression of MCT4 persisted and was primarily detected in foci within the upper layers of the epithelium (**Figures 4E,F**) and often in CIS lesions having a papillary morphology (papillary carcinoma *in-situ*). In regions of invasive cancer, MCT4 was detected in a more widespread pattern throughout the tumor (**Figures 4G,H**) and was present on transformed epithelial cells and also in adjacent stromal cells within lesional areas.

Increased Expression of MCT1 in OSCC in Wild Type and MCT4 Knock Out Mice

We investigated the expression of MCT1 in wild type and MCT4$^{-/-}$ mice. In tongues from wild type and MCT4$^{-/-}$ untreated mice, MCT1 was primarily restricted to the stratum basalis with faint labeling in the lower layers of the stratum spinosum (**Figures 5A,E**). This pattern of expression also parallels the MCT1 expression observed in normal human oral squamous epithelium (5, 25). Note that skeletal muscle fibers stain positively for MCT1 as shown in the figure and serve as a positive control. After 4NQO treatment, the expression of MCT1 increased in focal dysplastic areas of the tongues of both wild type and MCT4$^{-/-}$ animals and could be detected in the upper layers of the epithelium (**Figures 5B,F**). However, in the more aggressive invasive SCC lesions, MCT1 expression became irregular and was confined to groups of cells with an epithelial morphology (**Figures 5C,D,G,H**). Overall the changes in MCT1 expression patterns were similar in both wild type and MCT4$^{-/-}$ tongues and was not consistent with any compensatory expression due to the absence of MCT4 in MCT4$^{-/-}$ mice.

MCT4 Positive Macrophages Are Present in the Stroma

In the human OSCC, MCT4 positive macrophages were found within the lesions and in the adjacent stroma. Therefore, we investigated the presence of MCT4 positive macrophages in the 4NQO treated animals. Macrophages identified by F4/80 were positive for MCT4 in wild type mice at both 14 weeks (data not shown) and 23 weeks (**Figures 6A–C**). While F4/80 positive cells were detected in the mucosa of MCT4$^{-/-}$ mice, they were not co-labeled with MCT4 (**Figures 6D–F**). To determine whether there was a difference in macrophage number between wild type and MCT4$^{-/-}$ mice, tongue sections from untreated, and 14 and 23 week 4NQO-treated mice were stained with F4/80 by immunohistochemistry (**Figures 6G–L**) and the number of positive cells was quantified as described in Materials and Methods. In normal untreated wild type and MCT4$^{-/-}$ tongues

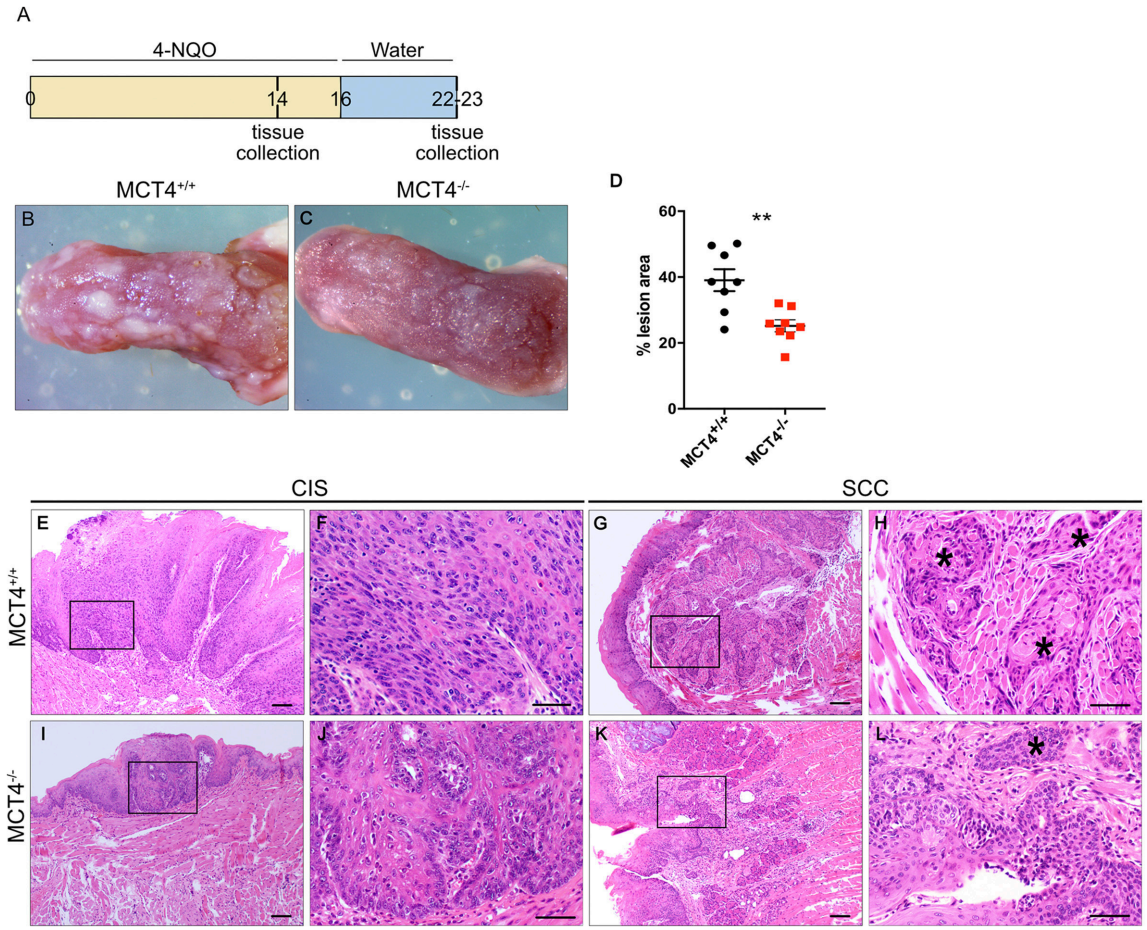

FIGURE 3 | Reduced invasive oral squamous cell carcinoma in MCT4$^{-/-}$ mice after 4NQO: Study design: 12 week old mice were treated for 16 weeks with 4NQO (50μg/ml) in the drinking water, followed by 7 weeks of plain water. Mice were sacrificed after 14 weeks of treatment or at 23 weeks **(A)**. Photographs of wild type **(B)** and MCT4$^{-/-}$ **(C)** tongues after 23 weeks of treatment. Quantification of superficial lesions expressed as percentage of total dorsal tongue surface area ($n = 8$ per group), $^{**}p < 0.01$ **(D)**. Representative H&E stained paraffin sections of tongues from wild type and MCT4$^{-/-}$ animals treated with 4NQO and sacrificed at 23 weeks **(E–L)** CIS, carcinoma-*in-situ*; SCC, invasive squamous cell carcinoma. F, H, J and L are higher magnifications of E, G, I and K respectively. *Indicates invasive SCC. Scale bar: 100μm **(F,H,J, L)** or 50μm **(E,G,I,K)**.

the numbers of F4/80 positive macrophages were not significantly different (**Figure 6M**), with both groups having similar baseline numbers of macrophages. After 14 weeks of 4NQO treatment the number of macrophages present in the involved regions (perilesional areas) of wild type animals was 23% greater than in the MCT4$^{-/-}$ animals ($p < 0.05$). By 23 weeks, the number of macrophages in the MCT4$^{-/-}$ affected areas was similar to the wild type. We also evaluated the number of macrophages in non-involved areas, (not lesional) and they were similar in both wild type and MCT4$^{-/-}$ animals exposed to 4NQO, although the numbers in the lesional areas were significantly increased compared to the non-involved areas (average difference 35.3, $p < 0.03$). This indicates that the increase in macrophages is due to the presence of cancer cells and not because of a general inflammatory response to the 4NQO.

We also analyzed the levels of circulating monocytes in the 4NQO treated animals to determine if the differences in macrophage number in the lesion was due to a defect in recruitment and mobilization. The total number of monocytes in circulation was higher in the untreated MCT4$^{-/-}$ animals, but the difference was not statistically significant. At 23 weeks after 4NQO treatment, the number of circulating monocytes in the MCT4$^{-/-}$ animals was 2.6 times higher than the wild type

TABLE 3 | Histological findings in 23 weeks 4NQO treated wild type and MCT4$^{-/-}$ tongues.

	wild type	MCT4$^{-/-}$
CIS	13	12
Micro invasive SCC	2	4
Invasive SCC	8	2

CIS, carcinoma in situ; SCC, squamous cell carcinoma.

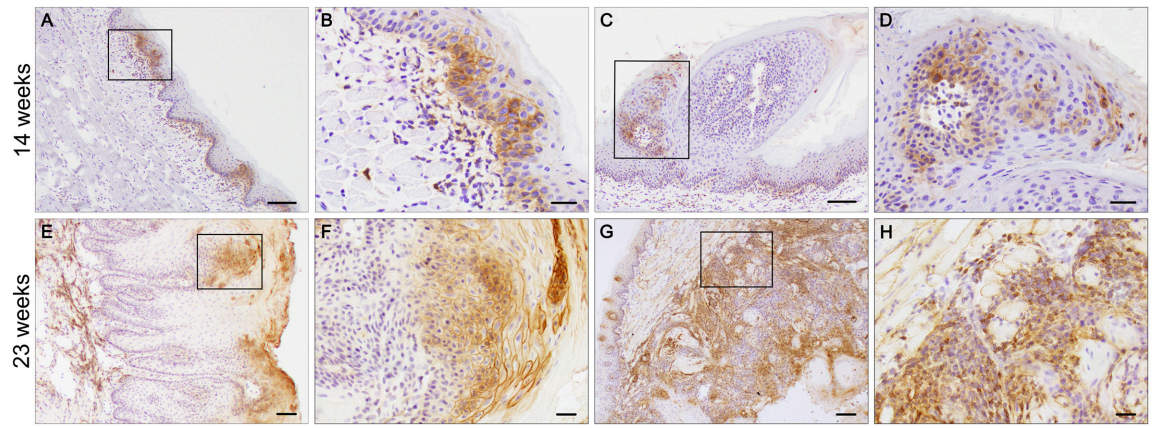

FIGURE 4 | MCT4 is expressed at different stages of oral cancer. Frozen sections of tongues from 4NQO treated wild type mice. MCT4 staining is detected in the basal and suprabasal epithelial layers and in the stroma (**A**, magnified in **B**), in papilloma (**C**, magnified in **D**) after 14 weeks of treatment; and in the upper squamous epithelium of carcinoma *in situ* (**E**, magnified in **F**) and in both the epithelium and stroma of invasive cancer (**G**, magnified in **H**) at the 23 weeks timepoint. Scale bar: 100 μm **(A**,**C**,**E**,**G)** or 20 μm **(B**,**D**,**F**,**H)**.

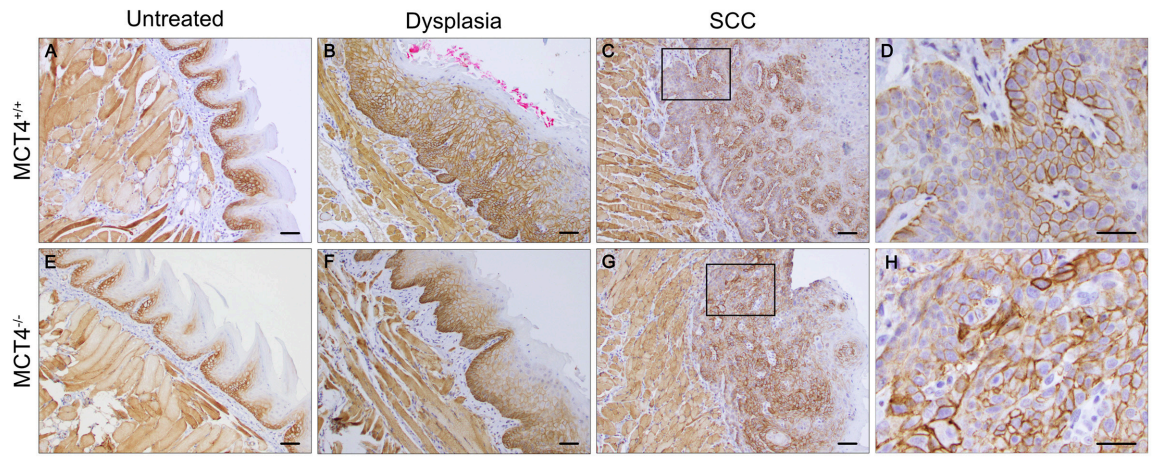

FIGURE 5 | MCT1 expression is altered in 4NQO treated wild type and MCT4$^{-/-}$ animals. IHC staining of paraffin sections of tongues from untreated and 23 weeks 4NQO treated wild type and MCT4$^{-/-}$ mice. MCT1 expression in normal tongue tissue is restricted to the basal cell layer of the epithelium in both wild type and MCT4$^{-/-}$ mice **(A**,**E)**. After 4NQO treatment, MCT1 extends into the suprabasal region of dysplastic lesions **(B,F)**, and is irregularly expressed in areas at the leading edge of invasive cancer **(C,D,G,H)**. Scale bar: 50μm or 20 μm **(D,H)**.

($p < 0.05$), suggesting a defect in the recruitment of macrophages to the tumors.

MCT4 in Syngeneic Tumors Is Sufficient to Drive Cancer Growth

To investigate the contribution of MCT4 expressed in tumor stroma to the development and progression of the OSCC, TC-1 cells, derived from C57Bl/6 lung carcinoma were implanted into the flanks of MCT4$^{-/-}$ mice and control littermates. Surprisingly the tumor growth was independent of the host genotype with similar tumor sizes in wild type and MCT4$^{-/-}$ animals (**Figures 7A–B**). Additionally, there was no difference in the number of circulating monocytes between wild type and MCT4$^{-/-}$ mice (**Figure 7C**). Since we were perplexed by this finding we examined the expression of MCT1 and MCT4 in TC-1 cells cultured *in vitro* and from the syngeneic tumors. We found that the level of MCT4 in TC-1 tumors was increased significantly compared to the basal expression levels detected in lysates of cultured TC-1 cells (**Figures 7D**). The result suggests that MCT4 expression by the epithelial cells is sufficient to support tumor growth in this syngeneic model.

DISCUSSION

MCT4 expression in cancers such as HNSCC, breast cancer, melanoma, and hepatocellular carcinoma has been associated with a poor prognosis (5, 26–28). In patient tumors, MCT4

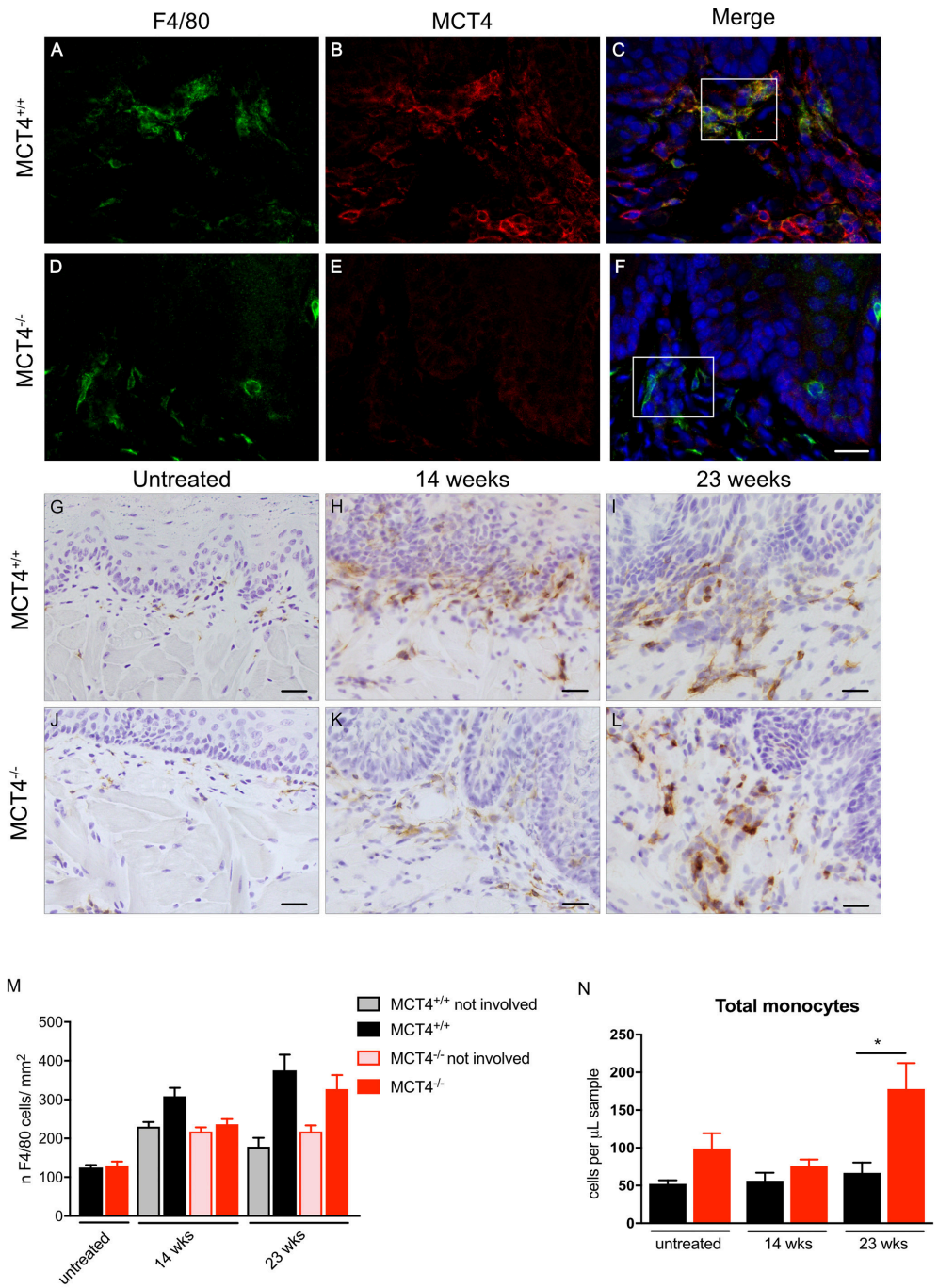

FIGURE 6 | Evaluation of peri-lesional macrophages in wild type and MCT4$^{-/-}$ tumors. Immunofluorescence staining for F4/80 (green) and MCT4 (red) and dapi nuclear staining (blue) in wild type and MCT4$^{-/-}$ tongue frozen sections at 23 weeks of 4NQO treatment **(A–F)** scale bar: 20µm. F4/80 staining of frozen sections in untreated tongues and at 14 and 23 weeks 4NQO treatment in wild type and MCT4$^{-/-}$ animals **(G–L)** Scale bar: 20 µm. Quantification of F4/80 positive macrophages in tongue sections. Involved areas represent regions identified by nuclear atypia and/or other signs of epithelial transformation, whereas non-involved areas did not display these features within the same section (n = 3 for untreated, n= 8 for 14 weeks, n= 4 for 23 weeks per group) **(M).** Quantification of total monocytes **(N)** in peripheral blood (n= 5–6 per group). *P < 0.05.

has been detected in cancer cells, cancer associated fibroblasts (CAFs) as well as tumor associated macrophages (TAMs) where it supports tumor growth (17), angiogenesis (29), and metastasis (30) (**Figure 1**). In the current study, we used the well-established 4NQO model of carcinogenesis to induce OSCC in wild type and MCT4$^{-/-}$ mice, with the goal of determining whether MCT4

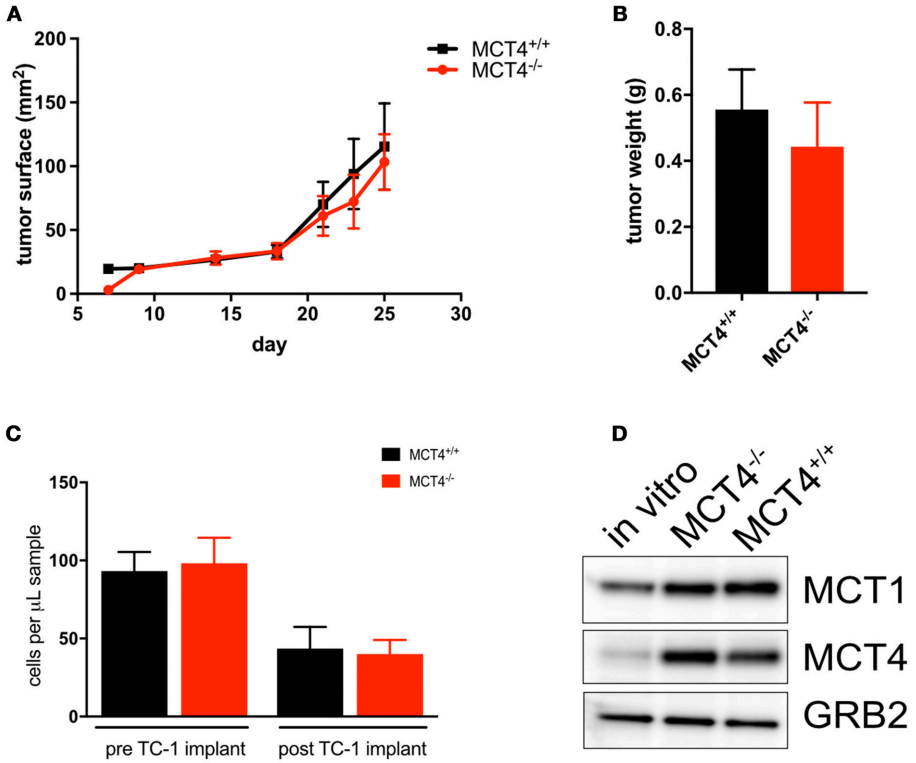

FIGURE 7 | MCT4 expression in syngeneic tumor cells is sufficient for tumor growth. Growth curve of TC-1 tumors in MCT4$^{-/-}$ and wild type mice ($n = 10$ per group) **(A)** and average tumor weight at sacrifice **(B)**. Quantification of total monocytes in peripheral blood of wild type and MCT4$^{-/-}$ animals before and after transplantation ($n = 5$ per group) **(C)**. Western blot analysis of lysates prepared from TC-1 cancer cells *in vitro* and TC-1 tumors grown in MCT4$^{-/-}$ and wild type mice for MCT1 and MCT4 using GRB2 as a loading control **(D)**.

is a driver or marker of OSCC progression. Our findings show that in the absence of MCT4, tumor burden, and invasiveness is reduced.

Growth and metastasis of cancer cells is supported by CAFs and TAMs present in the tumor ecosystem. The use of 4NQO in the drinking water to induce OSCC has several advantages over syngeneic models. Chemical induction of OSCC results in tumor formation in the normal ecosystem so the development and progression to invasive cancer more closely mimics what is seen in human patients (23). Models using transplantable OSCC cell lines do not recapitulate the epithelial and stromal interactions since the cells are injected into the flank of the mouse between the hypodermis and skeletal muscles. This region lacks the capillary bed and stroma found in the lamina propria of epithelial tumors. The 4NQO model recapitulates histological features and metabolic reprogramming observed in patient samples of OSCC and thus provides a valuable model to investigate *in vivo* the contribution of MCT4 to the development and progression of OSCC.

In 4NQO treated animals, the cancer originates from the highly proliferative cells found in the basal cell layer of the stratified squamous epithelium covering the tongue (31). 4NQO treatment causes mutagenesis and oxidative stress in these cells, which in turn translates in the dysregulation of key transcription factors such as NF-kB (32) and Hif1α (33). The cross-talk between the two transcription factors leads to the activation of glycolysis (34, 35) through transcription of glycolytic genes including MCT4 (36), glucose transporter 1 (GLUT1), hexokinase (HK), lactate dehydrogenase A (LDHA), and genes regulating cell proliferative pathways. In the current study, MCT4 was not detected in epithelium or stroma of the untreated tongue but was detected focally in the basal and suprabasal layers of the epithelium in tongues of wild type mice treated with 4NQO (**Figures 4A,B**). The MCT4$^{-/-}$ mice treated with 4NQO also developed dysplastic lesions and carcinomas *in situ* (CIS) similarly to the wild type mice, demonstrating that MCT4 is not necessary for the induction of non-invasive OSCC. Our findings indicate that the early increase in MCT4 expression results from a global reprogramming of the epithelial cells undergoing oncogenic transformation. When we analyzed MCT4 expression in more severe and extensive lesions such as carcinomas *in situ*, we found that MCT4 was often expressed in a central compartment of the lesions (**Figures 4E,F**), which may correspond with hypoxic areas. This centralized pattern of expression replicates what has been documented in human OSCC (5). Future studies will be needed to confirm if this pattern correlates with regions of hypoxia. Large *in situ* lesions were not found in tongues from MCT4$^{-/-}$ mice treated with 4NQO since these epithelial cells cannot shift their metabolism toward a hyperglycolytic state. It has been shown that inhibition of the lactate transport has a negative effect on cell proliferation (17, 37). The intracellular accumulation of lactate slows the glycolytic

flux by directly inhibiting hexokinase and phosphofructokinase (38) and by decreasing the NAD^+/NADH ratio. In addition, the decrease in glycolytic intermediates affects the production of other metabolites necessary for cell proliferation. The inhibition of MCT4 also leads to the acidification of the cytosol, which can inhibit cell proliferation through the mTOR pathway (39). In sum, future studies will need to be conducted to determine the mechanism by which loss of MCT4 reduces tumor aggressiveness.

The current study showed that $MCT4^{-/-}$ mice developed fewer and smaller invasive carcinomas, more often they developed micro-invasive lesions. Additional studies are required to establish the contribution of MCT4 to microinvasive oral squamous cell tumors. The data suggest that the lack of MCT4 prevents the progression of early microinvasive lesions to full invasive, arresting the tumors in a less aggressive form. In the wild type invasive lesions, MCT4 was expressed in both epithelial cells and in stroma (**Figures 4G,H**). In wild type mice expression of MCT4 facilitates lactate efflux and acidification of the microenvironment promoting invasiveness and metastasis. We and others have previously shown that MCT4 is important for cancer cell migration through interaction with beta 1 integrin (6, 40, 41) and it has been shown that lactate in the microenvironment induce angiogenesis (42), contributing to the progression of the disease.

We have shown that in human samples of HNSCC, CD163 positive macrophages also express MCT4 (**Figures 1D,E**). In the 4NQO treated animals we found macrophages in the peri-lesional areas as early as 14 weeks of treatment and these F4/80 positive cells expressed MCT4 (**Figures 6A–C**). In the $MCT4^{-/-}$ animals, the number of macrophages noted in the tumor microenvironment is lower compared to the wild type (**Figure 6M**) suggesting that MCT4 in either one of the compartments, or in both of them, has an effect on the macrophage population. MCT4 is usually associated with a higher glycolytic flux, therefore TAMs may have a glycolytic metabolism as suggested by Liu et al. (43). It has also been reported that bone marrow derived macrophages (BMDM) knock down of MCT4 reduced the production of cytokines after LPS stimulation (12), indicating that the F4/80 cells in the tumor microenvironment of the $MCT4^{-/-}$ animals may be compromised. Macrophages are recruited to the tumor invasive edge by chemoattractants released by the cancer cells. The recruited immune cells promote the migration and invasion of the cancer by secreting factors for the remodeling of the extracellular matrix (44). The observation that fewer macrophages were present in the stroma of the $MCT4^{-/-}$ tongues suggest that there was a failure of the tumor to release sufficient levels of chemokines and cytokines required to recruit monocytes from circulation. This conclusion was supported by our analysis of the peripheral blood from 4NQO treated $MCT4^{-/-}$ mice which showed an increase in total monocytes in circulation (**Figure 6N**). The circulating monocytes were the same in wild type and $MCT4^{-/-}$ mice after TC-1 syngeneic tumors implantation and the tumors expressed MCT4 independently of the genotype of the host. This supports the idea that MCT4 expression in the epithelium is necessary for the recruitment of macrophages to the tumor microenvironment from the circulation (**Figure 7**) but future studies will need to determine the contribution of MCT4 expression in TC-1 cells to syngeneic tumor growth.

MCT1 and MCT4 require the accessory protein CD147 for maturation and trafficking to the plasma membrane. CD147 is constitutively expressed and is stabilized through its interaction with MCT1 and MCT4 (45). Consistently, we and others have used *in vitro* and *in vivo* techniques to show that ablation of any of these proteins (MCTs or CD147) causes the degradation of the entire complex. Conversely, the increase in MCT1 and/or MCT4 in OSCC results in the obligatory increase in CD147. In 4NQO-treated wild type and $MCT4^{-/-}$ mice, MCT1 expression increased in dysplastic areas. The invasive lesions also showed persistent expression of MCT1 (**Figure 5**). It has been reported that increased expression of CD147 (also known as EMMPRIN and basigin) is associated with poor outcomes in OSCC (8). The use of drugs targeting CD147 in cancer has been explored (39) and the use of anti-CD147 antibodies resulted in reduced growth of OSCC xenografts (40). Silencing CD147 or using drugs that target CD147 impact the expression or activity of MCT1 and MCT4, supporting the idea that targeting these transporters in patients with OSCC could slow the development and progression of the disease.

This study showed that MCT4 is an early marker of OSCC and that $MCT4^{-/-}$ mice had fewer lesions and less invasive cancer. MCT4 could provide a viable target for drug therapy to slow progression and aggressiveness in OSCC.

ETHICS STATEMENT

Human study: The study was carried in accordance with the recommendation of Institutional review board (IRB) at Thomas Jefferson University, with written informed consent from all subjects. All subjects gave written informed consent in accordance with the Declaration of Helsinki. The protocol was approved by the IRB at Thomas Jefferson University.

Animal study: The study was carried out in accordance with the recommendations of the IACUC of Thomas Jefferson University. The protocol was approved by The IACUC at Thomas Jefferson University.

AUTHOR CONTRIBUTIONS

SB contributed to the design of the experiments, performed all animal experiments, contributed to histological staining and analysis of tissue, analysis of data, and writing the manuscript. DW-M contributed to the design of the experiments, performed immunohistochemistry and immunofluorescence, performed animal experiments, analyzed tissue, writing of manuscript. NW performed the syngeneic tumor injections and analysis of peripheral blood. MT performed histopathological analysis. JC collected human samples, contributed to discussion. TZ

performed data analysis. CS contributed to experimental design and discussion. UM-O contributed to experimental design, data analysis and writing the manuscript. NP contributed to experimental design, data analysis, and writing the manuscript.

FUNDING

This work was supported by the following grants: R01-EY012042 (NP); NCI K08-CA175193 and NCI 5 P30 CA-56036 (UM-O); RSG-15-184-01-MPC (CS).

REFERENCES

1. Siegel RL, Miller KD, Jemal A. Cancer statistics, 2017. *CA Cancer J Clin*. (2017) 67:7–30. doi: 10.3322/caac.21387
2. Bar-Ad V, Palmer J, Yang H, Cognetti D, Curry J, Luginbuhl A, et al. Current management of locally advanced head and neck cancer: the combination of chemotherapy with locoregional treatments. *Semin Oncol*. (2014) 41:798–806. doi: 10.1053/j.seminoncol.2014.09.018
3. Brunin F, Mosseri V, Jaulerry C, Point D, Cosset JM, Rodriguez J. Cancer of the base of the tongue: past and future. *Head Neck* (1999) 21:751–9.
4. Sano D, Myers JN. Metastasis of squamous cell carcinoma of the oral tongue. *Cancer Metastasis Rev*. (2007) 26:645–62. doi: 10.1007/s10555-007-9082-y
5. Curry JM, Tuluc M, Whitaker-Menezes D, Ames JA, Anantharaman A, Butera A, et al. Cancer metabolism, stemness and tumor recurrence: MCT1 and MCT4 are functional biomarkers of metabolic symbiosis in head and neck cancer. *Cell Cycle* (2013) 12:1371–84. doi: 10.4161/cc.24092
6. Zhu J, Wu YN, Zhang W, Zhang XM, Ding X, Li HQ, et al. Monocarboxylate transporter 4 facilitates cell proliferation and migration and is associated with poor prognosis in oral squamous cell carcinoma patients. *PLoS ONE* (2014) 9:e87904. doi: 10.1371/journal.pone.0087904
7. Simões-Sousa S, Granja S, Pinheiro C, Fernandes D, Longatto-Filho A, Laus AC, et al. Prognostic significance of monocarboxylate transporter expression in oral cavity tumors. *Cell Cycle* (2016) 15:1865–73. doi: 10.1080/15384101.2016.1188239
8. Bovenzi CD, Hamilton J, Tassone P, Johnson J, Cognetti DM, Luginbuhl A, et al. Prognostic indications of elevated MCT4 and CD147 across cancer types: a meta-analysis. *Biomed Res Int*. (2015) 2015:242437. doi: 10.1155/2015/242437
9. Adijanto J, Philp NJ. The SLC16A family of monocarboxylate transporters (MCTs)–physiology and function in cellular metabolism, pH homeostasis, and fluid transport. *Curr Top Membr*. (2012) 70:275–311. doi: 10.1016/B978-0-12-394316-3.00009-0
10. Bonen A. The expression of lactate transporters (MCT1 and MCT4) in heart and muscle. *Eur J Appl Physiol*. (2001) 86:6–11. doi: 10.1007/s004210100516
11. Philp NJ, Ochrietor JD, Rudoy C, Muramatsu T, Linser PJ. Loss of MCT1, MCT3, and MCT4 expression in the retinal pigment epithelium and neural retina of the 5A11/basigin-null mouse. *Invest Ophthalmol Vis Sci*. (2003) 44:1305–11. doi: 10.1167/iovs.02-0552
12. Tan Z, Xie N, Banerjee S, Cui H, Fu M, Thannickal VJ, et al. The monocarboxylate transporter 4 is required for glycolytic reprogramming and inflammatory response in macrophages. *J Biol Chem*. (2015) 290:46–55. doi: 10.1074/jbc.M114.603589
13. Wilde L, Roche M, Domingo-Vidal M, Tanson K, Philp N, Curry J, et al. Metabolic coupling and the reverse Warburg effect in cancer: implications for novel biomarker and anticancer agent development. *Semin Oncol*. (2017) 44:198–203. doi: 10.1053/j.seminoncol.2017.10.004
14. San-Mill a n INI, Brooks GA. Reexamining cancer metabolism: lactate production for carcinogenesis could be the purpose and explanation of the Warburg Effect. *Carcinogenesis* (2017) 38:119–33. doi: 10.1093/carcin/bgw127
15. Doherty JR, Cleveland JL. Targeting lactate metabolism for cancer therapeutics. *J Clin Invest*. (2013) 123:3685–92. doi: 10.1172/JCI69741
16. Doherty JR, Yang C, Scott KEN, Cameron MD, Fallahi M, Li W, et al. Blocking lactate export by inhibiting the Myc target MCT1 Disables glycolysis and glutathione synthesis. *Cancer Res*. (2014) 74:908–20. doi: 10.1158/0008-5472.CAN-13-2034
17. Marchiq I, Le Floch R, Roux D, Simon MP, Pouyssegur J. Genetic disruption of lactate/H+ symporters (MCTs) and their subunit CD147/BASIGIN sensitizes glycolytic tumor cells to phenformin. *Cancer Res*. (2015) 75:171–80. doi: 10.1158/0008-5472.CAN-14-2260
18. Tang XH, Knudsen B, Bemis D, Tickoo S, Gudas LJ. Oral cavity and esophageal carcinogenesis modeled in carcinogen-treated mice. *Clin Cancer Res*. (2004) 10:301–13. doi: 10.1158/1078-0432.CCR-0999-3
19. Mashberg A. Tolonium (toluidine blue) rinse–a screening method for recognition of squamous carcinoma. Continuing study of oral cancer IV. *J Am Med Assoc*. (1981) 245:2408–10. doi: 10.1001/jama.1981.03310480024019
20. Ko YH, Domingo-Vidal M, Roche M, Lin Z, Whitaker-Menezes D, Seifert E, et al. TP53-inducible glycolysis and apoptosis regulator (TIGAR) metabolically reprograms carcinoma and stromal cells in breast cancer. *J Biol Chem*. (2016) 291:26291–303. doi: 10.1074/jbc.M116.740209
21. Gooptu M, Whitaker-Menezes D, Sprandio J, Domingo-Vidal M, Lin Z, Uppal G, et al. Mitochondrial and glycolytic metabolic compartmentalization in diffuse large B-cell lymphoma. *Semin Oncol*. (2017) 44:204–17. doi: 10.1053/j.seminoncol.2017.10.002
22. Lin KY, Guarnieri FG, Staveley-O'Carroll KF, Levitsky HI, August JT, Pardoll DM, et al. Treatment of established tumors with a novel vaccine that enhances major histocompatibility class II presentation of tumor antigen. *Cancer Res*. (1996) 56:21–26.
23. Kanojia D, Vaidya MM. 4-nitroquinoline-1-oxide induced experimental oral carcinogenesis. *Oral Oncol*. (2006) 42:655–67. doi: 10.1016/j.oraloncology.2005.10.013
24. Miki K, Orita Y, Gion Y, Takao S, Ohno K, Takeuchi M, et al. Regulatory T cells function at the early stage of tumor progression in a mouse model of tongue squamous cell carcinoma. *Cancer Immunol Immunother*. (2016) 65:1401–10. doi: 10.1007/s00262-016-1902-x
25. Jensen DH, Therkildsen MH, Dabelsteen E. A reverse Warburg metabolism in oral squamous cell carcinoma is not dependent upon myofibroblasts. *J Oral Pathol Med*. (2015) 44:714–21. doi: 10.1111/jop.12297
26. Baenke F, Dubuis S, Brault C, Weigelt B, Dankworth B, Griffiths B, et al. Functional screening identifies MCT4 as a key regulator of breast cancer cell metabolism and survival. *J Pathol*. (2015) 237:152–65. doi: 10.1002/path.4562
27. Pinheiro C, Miranda-Gonçalves V, Longatto-Filho A, Vicente ALSA, Berardinelli GN, Scapulatempo-Neto C, et al. The metabolic microenvironment of melanomas: Prognostic value of MCT1 and MCT4. *Cell Cycle* (2016) 15:1462–70. doi: 10.1080/15384101.2016.1175258
28. Doyen J, Trastour C, Ettore F, Peyrottes I, Toussant N, Gal J, et al. Expression of the hypoxia-inducible monocarboxylate transporter MCT4 is increased in triple negative breast cancer and correlates independently with clinical outcome. *Biochem Biophys Res Commun*. (2014) 451:54–61. doi: 10.1016/j.bbrc.2014.07.050
29. Kumar VBS, Viji RI, Kiran MS, Sudhakaran PR. Endothelial cell response to lactate: Implication of PAR modification of VEGF. *J Cell Physiol*. (2007) 211:477–85. doi: 10.1002/jcp.20955
30. Goetze K, Walenta S, Ksiazkiewicz M, Kunz-Schughart LA, Mueller-Klieser W. Lactate enhances motility of tumor cells and inhibits monocyte migration and cytokine release. *Int J Oncol*. (2011) 39:453–63. doi: 10.3892/ijo.2011.1055
31. Osei-Sarfo K, Tang X-H, Urvalek AM, Scognamiglio T, Gudas LJ. The molecular features of tongue epithelium treated with the carcinogen 4-nitroquinoline-1-oxide and alcohol as a model for HNSCC. *Carcinogenesis* (2013) 34:2673–81. doi: 10.1093/carcin/bgt223
32. Chen Z, Yan B, Van Waes C. The role of the NF-kappaB Transcriptome and proteome as biomarkers in human head and neck squamous cell carcinomas. *Biomark Med*. (2008) 2:409–426. doi: 10.2217/17520363.2.4.409
33. Eckert AW, Schutze A, Lautner MHW, Taubert H, Schubert J, Bilkenroth U. HIF-1alpha is a prognostic marker in oral squamous cell carcinomas. *Int J Biol Markers* (2010) 25:87–92. doi: 10.1177/172460081002500205

34. Görlach A, Bonello S. The cross-talk between NF-kappaB and HIF-1: further evidence for a significant liaison. *Biochem J*. (2008) 412:e17–9. doi: 10.1042/BJ20080920
35. van Uden P, Kenneth NS, Rocha S. Regulation of hypoxia-inducible factor-1alpha by NF-kappaB. *Biochem J*. (2008) 412:477–84. doi: 10.1042/BJ20080476
36. Ullah MS, Davies AJ, Halestrap AP. The plasma membrane lactate transporter MCT4, but not MCT1, is up-regulated by hypoxia through a HIF-1alpha-dependent mechanism. *J Biol Chem*. (2006) 281:9030–37. doi: 10.1074/jbc.M511397200
37. Kim HK, Lee I, Bang H, Kim HC, Lee WY, Yun SH, et al. MCT4 Expression Is a potential therapeutic target in colorectal cancer with peritoneal carcinomatosis. *Mole Cancer Ther*. (2018) 17:838–48. doi: 10.1158/1535-7163.MCT-17-0535
38. Leite TC, Coelho RG, Da Silva D, Coelho WS, Marinho-Carvalho MM, Sola-Penna M. Lactate downregulates the glycolytic enzymes hexokinase and phosphofructokinase in diverse tissues from mice. *FEBS Lett*. (2011) 585:92–8. doi: 10.1016/j.febslet.2010.11.009
39. Balgi AD, Diering GH, Donohue E, Lam KKY, Fonseca BD, Zimmerman C, et al. Regulation of mTORC1 signaling by pH. *PLoS ONE* (2011) 6:e21549. doi: 10.1371/journal.pone.0021549
40. Gallagher SM, Castorino JJ, Wang D, Philp NJ. Monocarboxylate transporter 4 regulates maturation and trafficking of CD147 to the plasma membrane in the metastatic breast cancer cell line MDA-MB-231. *Cancer Res*. (2007) 67:4182–4189. doi: 10.1158/0008-5472.CAN-06-3184
41. Kong SC, N-Nielsen A, Zeeberg K, Reshkin SJ, Hoffmann EK, Novak I, et al. Monocarboxylate transporters MCT1 and MCT4 regulate migration and invasion of pancreatic ductal adenocarcinoma cells. *Pancreas* (2016) 45:1036–47. doi: 10.1097/MPA.0000000000000571
42. Polet F, Feron O. Endothelial cell metabolism and tumour angiogenesis: glucose and glutamine as essential fuels and lactate as the driving force. *J Int Med*. (2013) 273:156–65. doi: 10.1111/joim.12016
43. Liu D, Chang C, Lu N, Wang X, Lu Q, Ren X, et al. Comprehensive proteomics analysis reveals metabolic reprogramming of tumor-associated macrophages stimulated by the tumor microenvironment. *J Proteome Res*. (2016) 16:288–97. doi: 10.1021/acs.jproteome.6b00604
44. Noy R, Pollard JW. Tumor-associated macrophages: from mechanisms to therapy. *Immunity* (2014) 41:866. doi: 10.1016/j.immuni.2014.09.021
45. Kirk P, Wilson MC, Heddle C, Brown MH, Barclay AN, Halestrap AP. CD147 is tightly associated with lactate transporters MCT1 and MCT4 and facilitates their cell surface expression. *EMBO J*. (2000) 19:3896–904. doi: 10.1093/emboj/19.15.3896

Conflict of Interest Statement: The authors declare that the research was conducted in the absence of any commercial or financial relationships that could be construed as a potential conflict of interest.

frontiers in Oncology

REVIEW
published: 28 August 2018
doi: 10.3389/fonc.2018.00344

Intercellular Communication in Tumor Biology: A Role for Mitochondrial Transfer

Patries M. Herst[1,2], *Rebecca H. Dawson*[1,3] *and Michael V. Berridge*[1*]

[1] Malaghan Institute of Medical Research, Wellington, New Zealand, [2] Department of Radiation Therapy, University of Otago, Wellington, New Zealand, [3] School of Biological Sciences, Victoria University of Wellington, Wellington, New Zealand

Intercellular communication between cancer cells and other cells in the tumor microenvironment plays a defining role in tumor development. Tumors contain infiltrates of stromal cells and immune cells that can either promote or inhibit tumor growth, depending on the cytokine/chemokine milieu of the tumor microenvironment and their effect on cell activation status. Recent research has shown that stromal cells can also affect tumor growth through the donation of mitochondria to respiration-deficient tumor cells, restoring normal respiration. Nuclear and mitochondrial DNA mutations affecting mitochondrial respiration lead to some level of respiratory incompetence, forcing cells to generate more energy by glycolysis. Highly glycolytic cancer cells tend to be very aggressive and invasive with poor patient prognosis. However, purely glycolytic cancer cells devoid of mitochondrial DNA cannot form tumors unless they acquire mitochondrial DNA from adjacent cells. This perspective article will address this apparent conundrum of highly glycolytic cells and cover aspects of intercellular communication between tumor cells and cells of the microenvironment with particular emphasis on intercellular mitochondrial transfer.

Keywords: cancer, mitochondria, intercellular transfer, stress, damage, treatment-resistance

OPEN ACCESS

Edited by:
Ubaldo Emilio Martinez-Outschoorn, Thomas Jefferson University, United States

Reviewed by:
Sergio Giannattasio, Consiglio Nazionale delle Ricerche, Istituto di Biomembrane, Bioenergetica e Biotecnologie Molecolari (IBIOM), Italy
Carlos Villalobos, Consejo Superior de Investigaciones Científicas (CSIC), Spain

***Correspondence:**
Michael V. Berridge
mberridge@malaghan.org.nz

Specialty section:
This article was submitted to Molecular and Cellular Oncology, a section of the journal Frontiers in Oncology

Received: *07 June 2018*
Accepted: *06 August 2018*
Published: *28 August 2018*

Citation:
Herst PM, Dawson RH and Berridge MV (2018) Intercellular Communication in Tumor Biology: A Role for Mitochondrial Transfer. Front. Oncol. 8:344. doi: 10.3389/fonc.2018.00344

INTRODUCTION

Tumor development depends critically on the intimate interplay between individual neoplastic cells, normal cells from the tissue of origin, and their abiotic environment. This concept, originally proposed by Paget (1) in his "seed and soil" analogy, is now well-established. In the last few decades, the focus has been on cumulative driver mutations and loss of suppressor gene function in cancer cells. However, it is the microenvironment of the developing tumor that acts as the natural selector, resulting in expansion of the best adapted ("fittest") clones over time (2–5). Tumors can therefore be seen as evolving clones of cancer cells within an increasingly disorganized tissue microenvironment that compete for resources and are characterized by an evolving set of hallmarks (6). Individual tumors are made up of cancer stem cells with self-renewal and multiple differentiation properties, and proliferating progenitors with limited differentiating potential alongside normal tissue cells (7). The tumor microenvironment consists of cells from the tissue of origin, activated fibroblasts, invading immune cells and vascular cells, embedded in an extracellular matrix (ECM) that contains various connective tissue structures as well as growth factors, cytokines and chemokines, metabolites and nutrients, electrolytes, oxygen, etc. [reviewed by Kalluri (8)]. Infiltration of

the tumor by stromal cells and immune cells can either promote or inhibit tumor growth, depending on the cytokine/chemokine milieu of the tumor microenvironment and its effect on cell activation status. Recent research has shown that stromal cells can donate healthy mitochondria to respiration-deficient tumor cells, restoring normal respiration as well as their ability to form tumors in mice. This perspective article will cover aspects of intercellular communication between tumor cells and cells from the tumor microenvironment with particular emphasis on intercellular mitochondrial transfer.

CELLS IN THE TUMOR MICROENVIRONMENT

Within the developing tumor, activated fibroblasts generate connective tissue that structurally supports the tumor as it grows first at its primary site and later during metastasis. Fibroblasts are extremely resistant to various stressors, including cancer treatments like radiation, and chemotherapy. Normal tissue stroma contains few fibroblasts that are in a resting state with basal metabolic activity. Following tissue injury, resting fibroblasts become activated, contractile, highly proliferative, and migratory. They produce growth factors and cytokines that recruit immune cells, promote angiogenesis, and remodel the extracellular matrix by altering connective tissue components. In the context of acute injury, activated fibroblasts facilitate wound healing, and tissue regeneration and return to their resting state after repair is complete. The presence of cancer cells within a tissue ecosystem results in fibrosis, a chronic wound healing response mediated by stromal cells in the developing tumor [see Kalluri (8)]. These activated fibroblasts called cancer- or tumor-associated fibroblasts, referred to here as CAFs, can also be recruited to the tumor by growth factors released by cancer cells and infiltrating immune cells. Several recent reviews cover various aspects of the rapidly expanding CAF literature, including their origin, activation, recruitment, interactions with tumor cells and immune cells, and role in treatment resistance (9–12). CAF precursors include resident tissue fibroblasts, bone marrow-derived mesenchymal stem cells, hematopoietic stem cells, epithelial cells (via mesenchymal-epithelial transition), and endothelial cells (via mesenchymal-endothelial transition). Most CAFs express α-smooth muscle actin (α-SMA), fibroblast activation protein (FAP), and platelet-derived growth factor receptor (PDGFR)-α and -β. CAFs promote tumorigenesis in various ways, e.g., though secretion of growth factors and cytokines, and the degradation of ECM proteins. Activation into CAFs is accomplished through epigenetic alterations, changes in the expression of non-coding miRNAs and long non-coding RNAs and the aberrant activation of several signaling pathways such as NFκB, IL-6/STAT3, FGF-2/FGFR1, and TGF-β/SMAD (10, 12, 13).

Immune cells including T cells, macrophages and dendritic cells recruited by IL-1α and the epithelial chemokine TSLP (14), infiltrate the developing tumor through the highly permeant vasculature and via migratory processes, and promote or inhibit tumor progression by generating pro- and anti-inflammatory responses or mediating immune attack, depending on the mutational load of the tumor and other factors (15, 16). Some CAFs are highly immunosuppressive and can protect the tumor from immune attack. Costa et al. (11) very recently demonstrated that only myofibroblast CAFs that express FAP (CAF-S1) were strongly immunosuppressive and these cells were found to be particularly enriched in triple negative breast cancers. In contrast, a low α-SMA-expressing subpopulation of CAFs in mouse and human pancreatic ductal adenocarcinoma were highly pro-inflammatory, producing high levels of IL-6 which stimulated tumor growth via STAT3 activation (17).

Other cells that assist tumor progression are recruited by growth factors such as vascular endothelial growth factor A (VEGFA), cytokines, and chemokines secreted by cancer cells and CAFs. Recruited endothelial cells are highly proliferative and develop leaky vascular structures that provide nutrients and oxygen to the developing tumor (8). These structures are also centrally involved in tumor metastasis that involves breaking constraints on tissue boundaries, basement membrane penetration, intravasation, circulation, extravasation, and seeding in tissues of distant organs. **Figure 1** depicts the different cell types in the tumor microenvironment and their effect on tumorigenesis.

ENERGY METABOLISM IN THE TUMOR MICROENVIRONMENT

The TME of most if not all solid cancers is characterized by strongly fluctuating oxygen levels with very steep and transient oxygen gradients caused by highly compromised tumor microvasculature. This challenging environment favors cells that can easily shift the balance between mitochondrial and glycolytic energy metabolism. This metabolic shift is controlled by hypoxia-inducible factor 1α (HIF-1α) which is highly expressed in most solid tumors [reviewed in Courtnay et al. (18)]. Most, but not all, highly aggressive tumors bias their energy metabolism toward glycolysis irrespective of oxygen levels, a phenomenon referred to as the *Warburg effect* (19). The balance between mitochondrial and glycolytic energy could be viewed as a "rheostat" rather than an "on/off" switch as both are essential for life in physiological situations. A rheostat strategy allows cells to finely balance their energy requirements according to oxygen and nutrient supply with glycolytic intermediates available for anabolic processes. It would also allow fast proliferating cells to escape the detrimental effects of high levels of reactive oxygen species (ROS) generated during mitochondrial electron transport whilst retaining adequate ROS levels for signaling and mitogenic purposes [reviewed in Idelchik et al. (20)]. Mutations in mtDNA, changes in mtDNA copy number and epigenetic changes to mtDNA affecting mtDNA gene expression, are very common in a large variety of different types of cancer (21) leading to a re-balancing of mitochondrial and glycolytic energy metabolism to favor glycolysis. Highly glycolytic phenotypes have been associated with increased invasive and metastatic potential and chemoresistance to cancer treatments [reviewed by Guerra et al. (22)]. In most instances

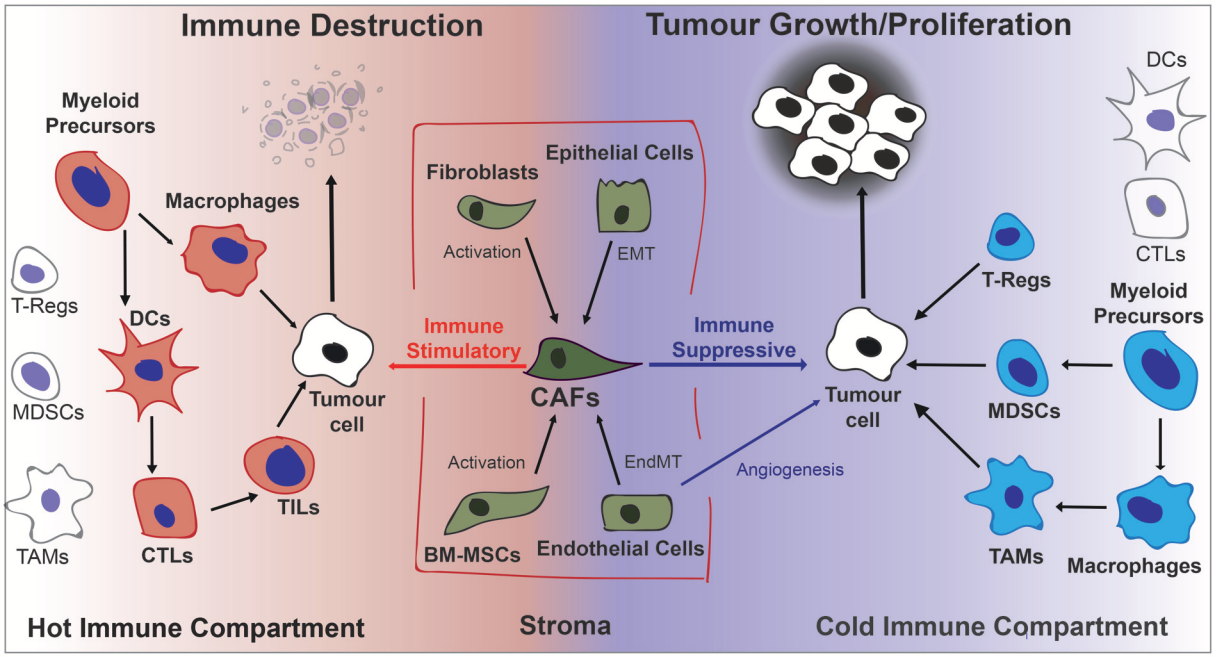

FIGURE 1 | Diagrammatic overview of cells contributing to the fate of the developing tumor in the tumor microenvironment. Activated stromal cells that become CAFs and immune cells can either stimulate or inhibit tumor growth depending on the cytokine/chemokine environment. Generally a pro-inflammatory "hot" microenvironment will favor immune destruction and an anti-inflammatory "cold" microenvironment will favor tumor progression. BM-MSCs, Bone Marrow-derived Stromal Cells; CAFs, Cancer-Associated Fibroblasts; DCs, Dendritic Cells; EndMT, Endothelial-to-Mesenchymal Transition; EMT, Epithelial-to-Mesenchymal Transition; MDSCs, Myeloid Derived Suppressor Cells; TAMs, Tumor Associate macrophages; TILs, Tumor Infiltrating Lymphocytes; Tregs, regulatory T lymphocytes.

cells with mutated mtDNA or reduced mtDNA copy number retain some level of functional mitochondrial electron transport. Tumor cells without any mtDNA such as ρ^0 cells completely lack functional mitochondrial electron transport and survive *in vitro* only when supplemented with uridine and often pyruvate (23).

Based on the aggressive nature and poor patient prognosis of many highly glycolytic tumors we expected that our metastatic murine breast (4T1) and melanoma (B16) ρ^0 cells would generate tumors at the same rate or faster than the parental cells. However, tumor cells without mtDNA produced tumors only after a long lag period compared with parental cells (24, 25). Surprisingly, these cells had taken up mtDNA (25) and therefore mitochondria (26) from cells in the tumor microenvironment of the host mouse, and had recovered respiratory capacity. These findings led us to hypothesize that purely glycolytic ρ^0 cells cannot form tumors unless they acquire mtDNA from elsewhere. This apparent conundrum between aggressive highly glycolytic tumors and purely glycolytic ρ^0 tumor cells that cannot form tumors needs further consideration. The explanation we believe lies in the detail: highly glycolytic cells likely have some respiratory capacity, even though they may not use it or depend on it. Purely glycolytic ρ^0 tumor cells have no functional respiratory complexes and therefore no mitochondrial electron transport, explaining their auxotrophy for uridine. This is because respiratory capacity is required for the activity of dihydroorotate dehydrogenase (DHODH), a flavoprotein found on the outer surface of the inner mitochondrial membrane. DHODH catalyzes the ubiquinone-mediated fourth step in pyrimidine biosynthesis, the oxidation of dihydroorotate to orotate. Electrons from this oxidation are used to reduce coenzyme Q (CoQ) just prior to complex III in the electron transport chain (23). In the absence of functional mitochondrial electron transport, DHODH is unable to oxidize dihydroorotate, thus blocking pyrimidine biosynthesis. Adding uridine to the growth medium bypasses the block in pyrimidine biosynthesis and thus DNA replication and is therefore required for the maintenance of ρ^0 cells in culture (23). Other substrates such as pyruvate are needed with some ρ^0 cells. In a nutshell, ρ^0 cells cannot synthesize DNA and are unable to divide and therefore cannot form tumors in mice as the tumor microenvironment does not have enough uridine to support DNA synthesis. In contrast, cells with mutated mtDNA or decreased mtDNA copy number have reduced ability to use the electron transport chain and may rely on glycolytic energy production, but they are still able to synthesize pyrimidines and thus are able to form tumors *in vivo*. Some authors (22) have attributed slower tumor development of injected ρ^0 tumor cells to their slower growth rate *in vitro*. However, most of these studies have not checked the ρ^0 tumors for the presence of mtDNA or respiration recovery. Kulawiec et al reported that the complete absence of mtDNA conferred tumorigenicity to non-tumorigenic human breast epithelial MCF12A cells and increased the tumorigenic potential of human breast cancer MDA-MB-435 cells in a

SCID mouse model (27). MDA-MB-435ρ° cells demonstrated increased invasive and clonogenic potential when cultured in the presence of uridine. Interestingly, MDA-MB-435ρ° cells started developing tumors in the flank of mice 3 weeks after injection without the lag phase we have seen in our ρ° tumor models. It would have been interesting to see whether or not the resulting MCF7ρ° and MDA-MB-435ρ° tumors had acquired mouse mtDNA from the tumor microenvironment and regained respiratory capacity as shown for syngeneic mouse models.

INTERCELLULAR MITOCHONDRIAL TRANSPORT

Intercellular mitochondrial transfer involving horizontal transfer of the entire mitochondrial genome is an emerging concept in tumor biology that challenges well-established concepts (28). Successful mitochondrial transfer depends on communication between donor and recipient cells, even though at this stage these signals have not been clearly identified. In the next part of this perspective article, we will focus on mitochondrial transfer between stromal cells and mitochondrially incompetent cancer cells without functional respiration.

MITOCHONDRIAL ACQUISITION BY CANCER CELLS

Mouse Tumor Models Lacking mtDNA

Initial experiments investigating whether or not B16ρ° melanoma cells would grow as tumors in syngeneic mice focussed on tumor growth and not on mitochondrial acquisition (24). A 20-day lag to tumor growth was observed with B16ρ° cells injected into C57BL/6 mice subcutaneously, and a longer lag period was seen in NOD/SCID mice. In contrast, when B16ρ° cells were injected intravenously, no lung metastases were observed in these models. We used tumor-derived cell lines, PCR primers specific for the mitochondrial gene, *Cytb,* and antibodies against mitochondrially-encoded proteins to determine whether B16ρ° cells had adapted to growth in response to support from stromal cells in the tissue microenvironment, or had re-expressed latent mtDNA or perhaps even acquired mtDNA from other cells (25). Rigorous confirmation of the presence of host mouse mtDNA in this model, and in the 4T1ρ° mouse breast cancer model in Balb/c mice, involved the presence of stable mtDNA polymorphisms that occur between each of these tumors and the mouse from which they were derived. In both cases the mtDNA in the tumors that grew from ρ° cells contained the mtDNA polymorphisms of the recipient mouse and not the tumor, "proving" that mtDNA had transferred from recipient mouse cells. This mtDNA transfer was later shown to involve transfer of intact mitochondria from BM-MSCs by prior co-culture with these cells (26). Intercellular mitochondrial transfer was shown to be responsible for tumor growth and respiration recovery. Possible contribution of contaminating stromal cells to the acquired mitochondrial genotype was excluded by long-term culture of B16ρ°-derived cells. Stromal cells do not divide in the culture media used to grow the tumor cells, resulting in the dilution of stromal cells over time. In the case of 6-thioguanine-resistant 4T1ρ°-derived cell lines, stromal cells sensitive to this drug were eliminated in culture medium containing 6-thioguanine. In each model, cell lines were derived from subcutaneous tumors, from circulating tumor cells and from lung metastases, and in the case of 4T1ρ°-derived cell lines, from the orthotopic mammary gland site. These mouse models clearly demonstrate that mitochondrial transfer occurs subcutaneously and orthotopically in extreme models of mtDNA damage and show that the transferred mitochondria rescue respiration and facilitate tumor growth. The nature of the stromal cells donating mitochondria in these models was not addressed.

Xenotransplantation

The ability of human osteosarcoma 143B cells without mtDNA (143Bρ° cells) to grow subcutaneously as tumors in immunocompromised Balb/c nude mice was investigated recently (29). Tumors grew slowly in 60% of mice inoculated with 10^6 cells. After FACS-sorting to remove contaminating mouse stromal cells, tumors were found to contain low levels of mouse mtDNA, but no human mtDNA. FACS-sorted tumors cells were re-injected and were found to grow as small tumors with higher levels of mtDNA than the those in the original tumors, but 4 out of 5 of these tumors arrested at 200–300 mm^3 and regressed because human nDNA replication factors do not recognize murine mtDNA promotors, resulting in dilution of mouse mtDNA in the human 143B cells.

Cells devoid of mtDNA are not the only cells that benefit from acquiring mitochondria. Human primary acute myeloid leukemia (AML) cells contain mtDNA but have greatly increased mitochondrial content when isolated from bone marrow. Mitochondrial transfer from bone marrow-derived stromal cells (BMSCs) to primary human AML blasts and MOLM-14 AML cells via endocytosis was demonstrated in xenografts in NOD/SCID/gamma (NSG) immunodeficient mice (30). In this study, the mouse mtDNA gene*, mt-Co2,* was present in four primary AML patient samples and in MOLM-14 cells FACS-purified from mouse bone marrow following transplantation. Treatment with cytarabine, etoposide, and doxorubicin increased mitochondrial transfer and tumorigenicity of AML cells. Similarly, Marlein et al. (31) reported NOX2-driven transfer of mitochondria from BMSCs to primary human AML cells injected into NSG mice via AML-derived tunneling nanotubes (TNTs). Mitochondrial transfer was enhanced by treatments that increase ROS levels in BMSC such as hypoxia, hydrogen peroxide, daunorubicin, and cobalt chloride. Inhibition of NOX2 by diphenyleneiodonium (DPI) or by NADPH oxidase-2-depleted AML cells inhibited mitochondrial transfer and increased mouse survival (31).

Cells Used as Mitochondrial Donors in Co-culture Approaches

The primary donor cell types used in co-cultures to investigate mitochondrial transfer to cancer cells have been bone marrow-derived mesenchymal stem or stromal cells (BM-MSCs),

although MSCs can be derived from many different tissues. Because MSCs can give rise to CAFs (32), resting fibroblasts can be considered to be MSCs that become CAFs when stimulated (8). MSCs and CAFs share many important characteristics; they contain cells that are pluripotent and can differentiate into osteoblasts, chondrocytes and adipocytes and possibly also myocytes and neurons. Both MSCs and CAFs are highly migratory, and travel to inflamed and injured regions to facilitate repair (10, 12, 32). In tumors, MSCs increase the proliferation, invasion and metastatic potential of many solid tumors by inducing the epithelial-to-mesenchymal transition (EMT) in primary tumor cells (reviewed in Ridge et al. (32). BM-MSCs are able to donate mitochondria to both cancerous and non-cancerous cells (28, 33–37). However, these cells are functionally different from MSCs isolated from other tissues, which may affect their ability to donate mitochondria. Differences in tissue types and growth conditions can favor certain subpopulations and future research should characterize the MSCs used in mitochondrial transfer experiments.

The first demonstration of mitochondrial transfer to tumor cells involved co-culture of human A549 lung adenocarcinoma cells without mtDNA (ρ° cells) with human BM-MSCs (38). This seminal study showed that auxotrophy for uridine and pyruvate was lost and respiration restored in clones that had acquired mtDNA, and that the mitochondrial genotype was that of the donor BM-MSCs. Furthermore, whole mitochondria were transferred as shown by using donor cells with a DsRed2 construct containing a mitochondrial import sequence. Cell fusion was excluded as a plausible explanation of mitochondrial transfer in cell lines derived from A549ρ° cells and neither platelets nor isolated mitochondria, used by others in mitochondrial transplantation (39, 40), were able to act as mitochondrial donors in this system. Mitochondrial transfer from BM-MSC to human 143Bρ° osteosarcoma cells and cells depleted of mtDNA with rhodamine 6G has been reported, but surprisingly, no transfer was detected to 143Bρ° cybrids harboring pathogenic mtDNA mutations (41). Others have reported mitochondrial transfer from BM-MSCs to murine B16ρ° melanoma cells (26), human ovarian cancer cell lines (42), breast cancer cell lines (39, 42), human lung adenocarcinoma A549 cells and mouse LA-4 lung adenocarcinoma cells (43), and to primary human AML cells and several AML cell lines (30, 31). MSC's derived from umbilical cord Wharton's jelly (WJ-MSC) were shown to transfer mitochondria to 143Bρ° cells. Cells surviving selection in the absence of uridine and pyruvate and in the presence of BrdU to remove WJ-MSC contained mtDNA polymorphisms of the WJ-MSCs and not the 143Bρ° cells, and respiration was restored (44).

In addition to MSCs, skin fibroblasts (31, 38) and embryonic mouse 3T3 fibroblasts (43) have been used in co-culture studies as mitochondrial donors. Endothelial cells (ECs) have also been used as mitochondrial donors in co-culture with ovarian and breast cancer cell lines. Endothelial cells are abundant in the vasculature of developing tumors where they form the inner lining of newly-formed blood vessels. Combining BM-MSCs and ECs with MCF7 breast cancer cells in co-culture showed preferential transfer of mitochondria by ECs (42). **Table 1** summarizes the donor and recipient cells used in the studies described above.

MITOCHONDRIAL TRANSFER BETWEEN TUMOR CELLS

Although not strictly related to mitochondrial transfer between host stromal cells and tumor cells, a number of studies have demonstrated intercellular mitochondrial transfer between tumor cells that are worth mentioning here. Of particular interest are reports that astrocytic brain tumors including glioblastomas form an interconnected network that protects from cell death and damage caused by radiation and chemotherapy (47, 48). These tunneling nanotube (TNT) and tumor microtube networks, visualized by confocal microscopy, were shown to transfer mitochondria and other organelles, vesicles, and small molecule messengers including calcium and siRNAs. A number of studies have also described intercellular mitochondrial transfer in a range of different cancer co-culture systems (42, 49–54).

MECHANISM OF MITOCHONDRIAL TRANSFER BETWEEN CELLS

The mechanisms of mitochondrial transfer between cells have been reviewed recently (37, 55–58). In cell co-culture approaches most focus has been on direct cell-cell connections referred to as TNTs, where a cell under stress or with mitochondrial damage signals for help from a potentially supportive donor stromal cell. These TNTs, and membrane conduits of larger dimensions, are characterized by cellular junctions containing connexin43 and by actin or microtubular structures that contain supporting mitochondrial transport adaptor and ATP-dependent motor proteins, similar to those described in axons of neurons [reviewed by Vignais et al. (59)]. In addition to TNTs, other vesicular structures have been described that contain whole mitochondria or mitochondrial fragments, often of poor quality with disorganized cristae and swollen organelles reminiscent of mitochondria destined for "transmitophagy," a term coined to describe packaging of damaged or spent mitochondria in the optic nerve head and elsewhere in the brain that are destined for recycling in adjacent astrocytes (60). Jurkat cells subjected to chemotherapy offload their damaged mitochondria to BM-MSCs via ICAM-1-mediated cell adhesion (45) and similar transfer to BM-MSCs has been observed by others (39). Dysfunctional mitochondria in neurons in neurodegenerative diseases may also be able to manage faulty mtDNA by intercellular transfer of and therefore, transmitophagy of these mitochondria (60, 61). Cell-cell contact has also been implicated as a mechanism of mitochondrial transfer between stromal cells and AML cells (30) where an endocytic pathway was involved.

Except for astrocytoma growth in the brain of mice (47) where intravital confocal microscopy was employed to visualize mitochondrial transport between tumor cells, the mechanism of mitochondrial transfer between tumor and stromal cells has not been elucidated in tumor models *in vivo*. Isolated mitochondria have been shown to be taken up by some cell types (40). McCully

TABLE 1 | Mitochondrial transfer to and from cancer cells *in vitro*.

Donor cell type	h/m*	Recipient cell type	References
MESENCHYMAL ORIGIN (MSC)			
Bone marrow (BM)	h	hA549rho0 lung adenocarcinoma	(38)
	h	h143Brho0 osteosarcoma	(41)
	h	h multiple ovarian and breast cancer lines	(42)
	h	hMDA-MB-231 breast cancer	(39)
	h	hAML blasts, CD34+ peripheral blood progenitors	(31)
	m	mB16rho0 melanoma	(26)
	h	hAML blasts and cell lines ± chemotherapy	(30)
(MS-5 cell line)	m	hAML blasts and cell lines ± chemotherapy	(30)
	m	mLA-4 lung adenoma	(43)
	h	hA549 lung adenocarcinoma	(43)
Wharton's jelly (WJ)	h	h143Brho0 osteosarcoma	(44)
FIBROBLAST ORIGIN			
Skin	h	hA549rho0 lung adenocarcinoma	(38)
	h	hAML blasts, CD34+ peripheral blood progenitors	(31)
3T3	h	hA549 lung adenocarcinoma	(43)
ENDOTHELIAL ORIGIN			
	h	h multiple ovarian and breast cancer lines	(42)
OTHER			
Jurkat T-ALL	h	hBM-MSC	(45)
hMDA-MB-231	h	hBM-MSC	(46)

**h, human; m, mouse.*

et al describes transfer of isolated mitochondria into cardiac muscle cells as *mitochondrial transplantation*. Cardiomyocytes sustain mtDNA damage after ischaemic injury and decrease their ATP production leading to loss of function. Mitochondria isolated from skeletal muscle cells injected intravenously or directly into the heart muscle of the same animal, result in cardiomyocyte recovery and improved function in animal studies and in an early human study with very young pediatric patients (40).

VISUALISING MITOCHONDRIAL TRANSFER

Visualising and measuring mitochondrial transfer can be challenging (62). Mitochondria-targeting fluorescent dyes (MitoTracker) can be used for short-term *in vitro* studies under defined conditions as they require a mitochondrial membrane potential, tend to leak out of mitochondria over time and can be toxic when used at concentrations exceeding manufacturer's recommendations. Mitochondrially-imported fluorescent proteins such as mitoGFP, mitoRFP, mitoYFP, and mitoDsRed are a less toxic. However, the exact location of newly acquired mitochondria within recipient cells needs to be confirmed by high resolution confocal Z-stack imaging with appropriate deconvolution strategies to exclude the possibility that mitochondria are attached to the outside of the recipient cell. Genetic approaches that use the presence of unique mtDNA polymorphisms between co-cultured cells or in tumor models provide the most convincing evidence of mitochondrial transfer. Different mtDNA polymorphisms can be quantified using qPCR or other mtDNA polymorphism amplification methodologies. Genetic approaches can also be used to study the long-term consequences of mitochondrial transfer such as in bone marrow and organ transplantation and in tumor biology where inherent mitochondrial damage is often a key feature. Combining mitochondrial genetic markers with fluorescent visualization strategies that assess mitochondrial network morphology as well as functional evaluation of the respiratory capacity of recipient cells provides the best evidence for mitochondrial trafficking between cells (62).

TARGETING CELLULAR INTERACTIONS

Combining therapies that target tumor cell-stromal cell interactions with treatments that specifically target cancer cell mutations may well be an approach of future anticancer regimens. Blocking the immunosuppressive effects of FAP-expressing CAFs increases effector T cell recruitment and function and reduces tumor growth in mice (63), and are well-tolerated in patients with advanced/refractory mesothelioma (64). Similarly, preventing mitochondrial transfer between tumor cells and donor cells within the TME that restore the tumor's respiratory ability would also augment more traditional therapies and/or restore sensitivity to radiation and chemotherapy. For example, blocking TNT formation by Cytochalasin B decreased

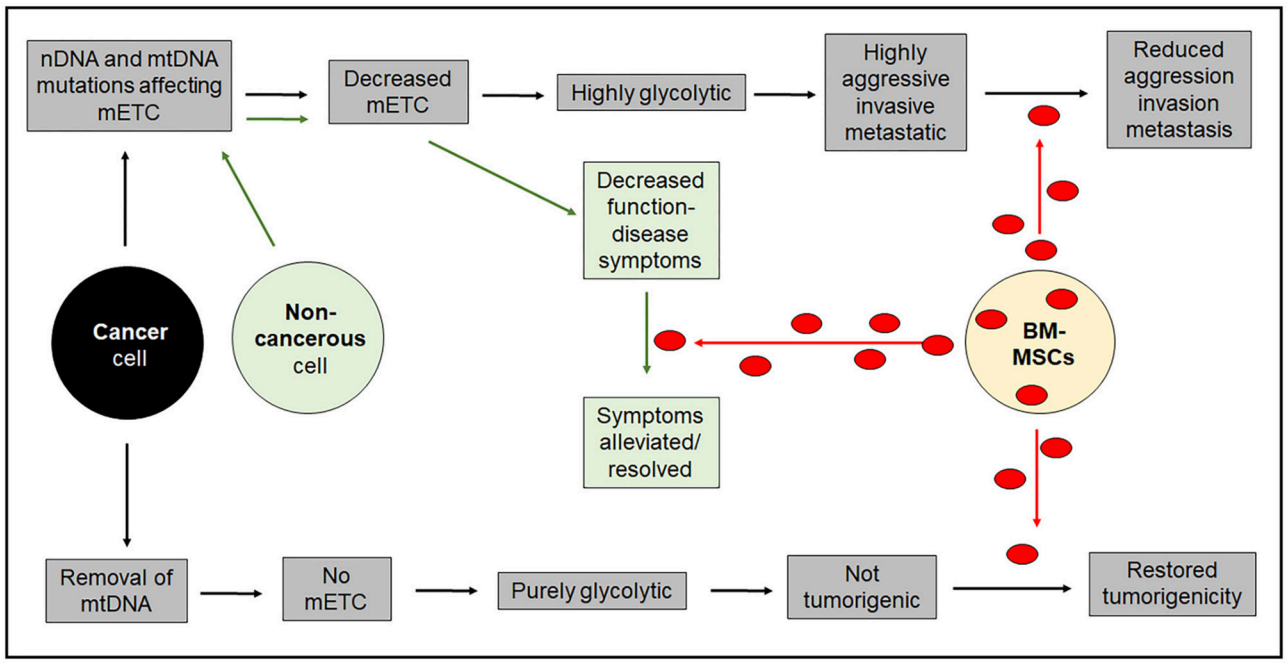

FIGURE 2 | Diagrammatic representation of the long-term outcomes of intercellular mitochondrial transfer. Acquisition of mitochondria in non-cancerous cells that have defects in mitochondrial respiration are likely to benefit from acquisition of healthy mitochondria. The situation for cancer cells is more complicated and will depend on their ability to synthesize DNA. Highly aggressive cancer cells with diminished respiratory capacity will not benefit from acquiring healthy mitochondria that will impose a less aggressive phenotype. On the other hand purely glycolytic cancer cells that cannot synthesize DNA because of a block in pyrimidine biosynthesis in the complete absence of mitochondrial respiration will not be able to form tumors unless they acquire healthy mitochondria from the host. mETC = mitochondrial electron transport chain.

but did not fully inhibit mitochondrial transfer from MSCs to macrophages to improve their phagocytic and bacterial clearance ability in ARDS (34), or to lung endothelial cells to attenuate cigarette smoke induced damage in COPD (35). Blocking the formation of new TNTs by Cytochalasin B did little to destabilize or destroy existing TNTs which facilitate mitochondrial transfer between rat pheochromocytoma (PC12) cells (49). Inhibition of NOX2-mediated mitochondrial transfer by diphenyleneiodonium (DPI) and antioxidants such as N-acetyl cysteine and glutathione was shown to decrease mitochondrial transfer between mouse BMSCs and human primary AML cells and increase mouse survival significantly (31).

CONCLUDING REMARKS

Intercellular mitochondrial transfer is a relatively new concept in tumor biology allowing replacement of mutated or treatment-damaged mitochondria in cancerous and non-cancerous cells. Harnessing the mitochondrial donating properties of cells in the body or following transplantation has the potential to be a game-changer in many diseases involving compromised mitochondrial function, including neurological and neuromuscular disorders and in aging, potentially leading to a lessening or even a reversal of disease symptoms. However, whether or not mitochondrial transfer could be an anti-cancer treatment remains to be seen. Highly aggressive cancer cells with mtDNA mutations that have acquired a highly aggressive invasive and metastatic phenotype would be ill-served by acquiring undamaged mitochondria from their environment. In those situations, mitochondrial transfer would be expected to decrease invasiveness and metastatic potential, and could be seen as a possible anti-cancer strategy. However, tumor cells without functional mtDNA due to severe deletions, that are unable to provide a source of oxidized ubiquinone for DHODH activity and are thus unable to synthesize pyrimidines to make DNA, need to acquire mitochondria from elsewhere to become established perhaps as secondary metastatic tumors. **Figure 2** depicts the differential effects of intercellular mitochondrial transfer in different scenarios.

Although we can speculate about the benefits of mitochondrial transfer as a treatment option for cancer, we do not know the extent to which this is a physiological occurrence *in vivo*, nor do we know much about cells that have the potential to donate mitochondria in the body. Although BM-MSCs are the most widely used cell type to be used in mitochondrial transfer studies *in vitro*, skin fibroblasts and endothelial cell are also able to donate mitochondria under certain conditions. While directly correcting detrimental mitochondrial mutations may be an insurmountable treatment barrier with current technologies, exploiting mitochondrial movement between cells for health gain is a more tangible goal that could see translation into the clinic in the forseeable future. Although not all intercellular mitochondrial transfer will be compatible with nuclear genetics, even within a species, these challenges are potentially surmountable and could lead to a new wave of regenerative applications in the health and medical sciences.

AUTHOR CONTRIBUTIONS

This invited review was conceived by MB and PH contributing equally to the writing. RD provided text in her areas of expertise. RD generated **Figure 1** and PH generated **Figure 2**.

FUNDING

This article was supported by funding from the Health Research Council of New Zealand, the Cancer Society of New Zealand, the Marsden Fund and support from the Malaghan Institute of Medical Research.

REFERENCES

1. Paget S. The distribution of secondary growths in cancer of the breast. *Lancet* (1889) 133:571–3. doi: 10.1016/S0140-6736(00)49915-0
2. Nowell PC. The clonal evolution of tumor cell populations. *Science* (1976) 194:23–8. doi: 10.1126/science.959840
3. Maley CC, AktipisA, Graham TA, Sottoriva A, Boddy AM, Janiszewska M, et al. Classifying the evolutionary and ecological features of neoplasms. *Nat Rev Cancer* (2017) 17:605–19. doi: 10.1038/nrc.2017.69
4. Vineis P. Cancer as an evolutionary process at the cell level: an epidemiological perspective. *Carcinogenesis* (2003) 24:1–6. doi: 10.1093/carcin/24.1.1
5. Merlo LMF, Pepper JW, Reid BJ, Maley CC. Cancer as an evolutionary and ecological process. *Nat Rev Cancer* (2006) 6:924–35. doi: 10.1038/nrc2013
6. Hanahan D, Weinberg RA. Hallmarks of cancer: the next generation. *Cell* (2011) 144:646–74. doi: 10.1016/j.cell.2011.02.013
7. Berridge MV, Herst PM. Tumor cell complexity and metabolic flexibility in tumorigenesis and metastasis. In: Mazurek S, Shoshan M, editors. *Tumor Cell Metabolism* (2015). p. 23–43. doi: 10.1007/978-3-7091-1824-5
8. Kalluri R. The biology and function of fibroblasts in cancer. *Nat Rev Cancer* (2016) 16:582–98. doi: 10.1038/nrc.2016.73
9. Su S, Chen J, Yao H, Liu J, Yu S, Lao L, et al. CD10+GPR77+cancer-associated fibroblasts promote cancer formation and chemoresistance by sustaining cancer stemness. *Cell* (2018) 172:841–56.e16. doi: 10.1016/j.cell.2018.01.009
10. LeBleu VS, Kalluri R. A peek into cancer-associated fibroblasts: origins, functions and translational impact. *Dis Models Mech.* (2018) 11:dmm029447. doi: 10.1242/dmm.029447
11. Costa A, KiefferY, Scholer-Dahirel A, Pelon F, Bourachot B, Cardon M, et al. Fibroblast heterogeneity and immunosuppressive environment in human breast cancer. *Cancer Cell* (2018) 33:463–79.e10. doi: 10.1016/j.ccell.2018.01.011
12. Liao Z, Tan ZW, Zhu P, Tan NS. Cancer-associated fibroblasts in tumor microenvironment - accomplices in tumor malignancy. *Cell Immunol.* (2018). doi: 10.1016/j.cellimm.2017.12.003. [Epub ahead of print].
13. Gascard P, Tlsty TD. Carcinoma-associated fibroblasts: orchestrating the composition of malignancy. *Genes Dev.* (2016) 30:1002–19. doi: 10.1101/gad.279737.116
14. Kuan EL, Ziegler SF. A tumor–myeloid cell axis, mediated via the cytokines IL-1α and TSLP, promotes the progression of breast cancer. *Nat Immunol.* (2018) 19:366–74. doi: 10.1038/s41590-018-0066-6
15. Barnes TA, Amir E. HYPE od HOPE: the prognostic value of infiltrating immune cells in cancer *Br J Cancer* (2013) 117:451–60. doi: 10.1038/bjc.2017.220
16. Alexandrov LBS, Nik-Zainal DC, Wedge SA, Aparicio S, Behjati AV, Biankin GR, et al. Signatures of mutational processes in human cancers. *Nature* (2013) 500:415–21. doi: 10.1038/nature12477
17. Öhlund D, Handly-Santana G, Biffi E, Elyada AS, Almeida M, Ponz-Sarvise V, et al. Distinct populations of inflammatory fibroblasts and myofibroblasts in pancreatic cancer. *J Exp Med.* (2017) 214:579–96. doi: 10.1084/jem.20162024
18. Courtnay R, Ngo DC, Malik N, Ververis K, Tortorella SM, Karagiannis TC. Cancer metabolism and the warburg effect: the role of HIF-1 and PI3K. *Mol Biol Rep.* (2015) 42:841–51. doi: 10.1007/s11033-015-3858-x
19. Warburg O. On the origin of cancer Ells. *Nature* (1956) 123:309–314.
20. Idelchik MDPS, Begley U, Begley TJ, Melendez JA. Mitochondrial ROS control of cancer. *Semin Cancer Biol.* (2017) 47:57–66. doi: 10.1016/j.semcancer.2017.04.005
21. Singh B, Modica-Napolitano JS, Singh KK. Defining the momiome: promiscuous information transfer by mobile mitochondria and the mitochondrial genome. *Semin Cancer Biol.* 47:1–17. doi: 10.1016/j.semcancer.2017.05.004
22. Guerra F, Arbini AA, Moro L. Mitochondria and cancer chemoresistance. *Biochim Biophys Acta Bioenerget.* (2017) 1858:686–99. doi: 10.1016/j.bbabio.2017.01.012
23. King MP, Attardi G. Human cells lacking MtDNA: repopulation with exogenous mitochondria by complementation. *Science* (1989) 246:500–3. doi: 10.1126/science.2814477
24. Berridge MV, Tan AS. Effects of mitochondrial gene deletion on tumorigenicity of metastatic melanoma: reassessing the warburg effect. *Rejuvenation Res.* (2010) 13:139–41. doi: 10.1089/rej.2009.0948
25. Tan AS, Baty JW, Dong LF, Bezawork-Geleta A, Endaya B, Goodwin J, et al. Mitochondrial genome acquisition restores respiratory function and tumorigenic potential of cancer cells without mitochondrial DNA. *Cell Metabol.* (2015) 21:81–94. doi: 10.1016/j.cmet.2014.12.003
26. Dong LF, Kovarova J, Bajzikova M, Bezawork-Geleta A, Svec D, Endaya B, et al. Horizontal transfer of whole mitochondria restores tumorigenic potential in mitochondrial DNA-deficient cancer cells. *ELife* (2017) 6:e22187. doi: 10.7554/eLife.22187
27. Kulawiec, M, SafinaAF, Desouki MM, Still I, Matsui SI, Bakin A, et al. Tumorigenic transformation of human breast epithelial cells induced by mitochondrial DNA depletion. *Cancer Biol Ther.* (2008) 7:1732–43. doi: 10.4161/cbt.7.11.6729
28. Herst PM, RoweMR, Carson GM, Berridge MV. Functional mitochondria in health and disease. *Front Endocrinol.* (2017) 8:296. doi: 10.3389/fendo.2017.00296
29. Lee WT, Cain JE, Cuddihy A, Johnson J, Dickinson A, Yeung KY, et al. Mitochondrial DNA plasticity is an essential inducer of tumorigenesis. *Cell Death Discov.* (2016) 2:16016. doi: 10.1038/cddiscovery.2016.16
30. Moschoi R, Imbert V, Nebout M, Chiche J, Mary D, Prebet T, et al. Protective mitochondrial transfer from bone marrow stromal cells to acute myeloid leukemic cells during chemotherapy. *Blood* (2016) 128:253–64. doi: 10.1182/blood-2015-07-655860
31. Marlein CR, Zaitseva L, Piddock RE, Robinson SD, Edwards DR, Shafat MS, et al. NADPH Oxidase-2 derived superoxide drives mitochondrial transfer from bone marrow stromal cells to leukemic blasts. *Blood* (2017) 130:1649–60. doi: 10.1182/blood-2017-03-772939
32. Ridge SM, Sullivan FJ, Glynn SA. Mesenchymal stem cells: key players in cancer progression. *Mol Cancer* (2017) 16:31. doi: 10.1186/s12943-017-0597-8
33. Babenko VA, Silachev DN, Zorova LD, Pevzner IB, Khutornenko AA, Plotnikov EY, et al. Improving the post-stroke therapeutic potency of mesenchymal multipotent stromal cells by cocultivation with cortical neurons: the role of crosstalk between cells. *Stem Cells Transl Med.* (2015) 4:1011–20. doi: 10.5966/sctm.2015-0010
34. Jackson MV, Morrison TJ, Doherty DF, McAuley DF, Matthay MA, Kissenpfennig A, et al. Mitochondrial transfer via Tunneling Nanotubes (TNT) is an important mechanism by which mesenchymal stem cells enhance macrophage phagocytosis in the *in vitro* and *in vivo* models of ARDS. *Stem Cells* (2016) 2014:2210–23. doi: 10.1002/stem.2372
35. Li X, Zhang Y, Yeung SC, Liang Y, Liang X, Ding Y, et al. Mitochondrial transfer of induced pluripotent stem cell-derived mesenchymal stem cells to airway epithelial cells attenuates cigarette smoke-induced damage. *Am J Respir Cell Mol Biol.* (2014) 51:455–65. doi: 10.1165/rcmb.2013-0529OC
36. Sinclair KA, Yerkovich ST, Hopkins PMA, Chambers DC. Characterization of intercellular communication and mitochondrial donation by mesenchymal stromal cells derived from the human lung. *Stem Cell Res Ther.* (2016) 7:91. doi: 10.1186/s13287-016-0354-8

37. Sinha P, Islam MN, Bhattacharya S, Bhattacharya J. Intercellular mitochondrial transfer: bioenergetic crosstalk between cells. *Curr Opin Genet Dev.* (2016) 38:97–101. doi: 10.1016/j.gde.2016.05.002
38. Spees JL, Olson SD, Whitney MJ, Prockop DJ. Mitochondrial transfer between cells can rescue aerobic respiration. *Proc Natl Acad SciUSA.* (2006) 103:1283–8. doi: 10.1073/pnas.0510511103
39. Caicedo A, Fritz V, Brondello JM, Ayala M, Dennemont I, Abdellaoui N, et al. MitoCeption as a new tool to assess the effects of mesenchymal stem/stromal cell mitochondria on cancer cell metabolism and function. *Sci Rep.* (2015) 5:9073. doi: 10.1038/srep09073
40. McCully JD, Cowan DB, Emani SM, Del Nido PJ. Mitochondrial transplantation: from animal models to clinical use in humans. *Mitochondrion* (2017) 34:127–34. doi: 10.1016/j.mito.2017.03.004
41. Cho YM, Kim JH, Kim M, Park SJ, Koh SH, Ahn HS, et al. Mesenchymal stem cells transfer mitochondria to the cells with virtually no mitochondrial function but not with pathogenic mtdna mutations. *PLoS ONE* (2012) 7:e32778. doi: 10.1371/journal.pone.0032778
42. Pasquier J, Guerrouahen BS, Al Thawadi H, Ghiabi P, Maleki M, Abu-Kaoud N, et al. Preferential transfer of mitochondria from endothelial to cancer cells through tunneling nanotubes modulates chemoresistance. *J Transl Med.* (2013) 11:94. doi: 10.1186/1479-5876-11-94
43. Ahmad T, Mukherjee S, Pattnaik B, Kumar M, Singh S, Kumar M, et al. Miro1 regulates intercellular mitochondrial transport & enhances mesenchymal stem cell rescue efficacy. *EMBO J.* (2014) 33:994–1010. doi: 10.1002/embj.201386030
44. Lin HY, Liou CW, Chen SD, Hsu TY, Chuang JH, Wang PW, et al. Mitochondrial transfer from wharton's jelly-derived mesenchymal stem cells to mitochondria-defective cells recaptures impaired mitochondrial function. *Mitochondrion* (2015) 22:31–44. doi: 10.1016/j.mito.2015.02.006
45. Wang, J, Liu X, Qiu Y, Shi Y, Cai J, Wang B, et al. Cell adhesion-mediated mitochondria transfer contributes to mesenchymal stem cell-induced chemoresistance on T cell acute lymphoblastic leukemia cells. *J Hematol Oncol.* (2018) 11:11. doi: 10.1186/s13045-018-0554-z
46. Caicedo A, Aponte PM, Cabrera F, Hidalgo C, Khoury M. Artificial mitochondria transfer: current challenges, advances, and future applications. *Stem Cells Int.* (2017) 2017:7610414. doi: 10.1155/2017/7610414
47. Osswald M, Solecki G, Wick W, Winkler F. A malignant cellular network in gliomas: potential clinical implications. *Neuro Oncol.* (2016) 18:479–85. doi: 10.1093/neuonc/now014
48. Weil S, Osswald M, Solecki G, Grosch J, Jung E, Lemke D, et al. Tumor microtubes convey resistance to surgical lesions and chemotherapy in gliomas. *Neuro Oncol.* (2017) 19:1316–26. doi: 10.1093/neuonc/nox070
49. Bukoreshtliev NV, Wang X, Hodneland E, Gurke S, Barroso JF, Gerdes HH. Selective block of tunneling nanotube (TNT) formation inhibits intercellular organelle transfer between pc12 cells. *FEBS Lett.* (2009) 583:1481–88. doi: 10.1016/j.febslet.2009.03.065
50. Antanavičiute I, RysevaiteK, Liutkevičius V, Marandykina A, Rimkute L, Sveikatiene R, et al. (2014). Long-distance communication between laryngeal carcinoma cells. *PLoS ONE* 9:e99196. doi: 10.1371/journal.pone.0099196
51. Wang X, Gerdes HH. Transfer of mitochondria via tunneling nanotubes rescues apoptotic PC12 Cells. *Cell Death Differ.* (2015) 22:1181–91. doi: 10.1038/cdd.2014.211
52. Lu J, Zheng X, Li F, Yu Y, Chen Z, Liu Z, et al. Tunneling nanotubes promote intercellular mitochondria transfer followed by increased invasiveness in bladder cancer cells. *Oncotarget* (2017) 8:15539–52. doi: 10.18632/oncotarget.14695
53. Thayanithy V, Dickson EL, Steer C, Subramanian S, Lou E. Tumor-stromal cross talk: direct cell-to-cell transfer of oncogenic microRNAs via tunneling nanotubes. *Transl Res.* (2014) 164:359–65. doi: 10.1016/j.trsl.2014.05.011
54. Ady JW, Desir S, Thayanithy V, Vogel RI, Moreira AL, Downey RJ, et al. Intercellular communication in malignant pleural mesothelioma: properties of tunneling nanotubes. *Front Physiol.* (2014) 5:400. doi: 10.3389/fphys.2014.00400
55. Plotnikov EY, Babenko VA, Silachev DN, Zorova LD, Khryapenkova TG, Savchenko ES, et al. Intercellular transfer of mitochondria. *Biochemistry* (2015) 80:542–8. doi: 10.1134/S00062979150 50041
56. Torralba D, Baixauli F, Sánchez-MadridF. Mitochondria know no boundaries: mechanisms and functions of intercellular mitochondrial transfer. *Front Cell Dev Biol.* (2016) 4:107. doi: 10.3389/fcell.2016. 00107
57. Nawaz M, Fatima F. Extracellular vesicles, tunneling nanotubes, and cellular interplay: synergies and missing links. *Front Mol Biosci.* (2017) 4:50. doi: 10.3389/fmolb.2017.00050
58. Rodriguez AM, Nakhle J, Griessinger E, Vignais ML. Intercellular mitochondria trafficking highlighting the dual role of mesenchymal stem cells as both sensors and rescuers of tissue injury. *Cell Cycle* (2018) 17:712–21. doi: 10.1080/15384101.2018.1445906
59. Vignais ML, Caicedo A, Brondello JM, Jorgensen C. Cell connections by tunneling nanotubes: effects of mitochondrial trafficking on target cell metabolism, homeostasis, and response to therapy. *Stem Cells Int.* (2017) 2017:6917941. doi: 10.1155/2017/6917941
60. Davis CO, Kim KY, Bushong EA, Mills EA, Boassa D, Shih T. et al. Transcellular degradation of axonal mitochondria. *Proc Natl Acad Sci USA.* (2014) 111:9633–8. doi: 10.1073/pnas.1404651111
61. Phinney, DG, Di Giuseppe M, Njah J, Sala E, Shiva S, St Croix CM, et al. Mesenchymal stem cells use extracellular vesicles to outsource mitophagy and shuttle microRNAs. *Nat Commun.* (2015) 6:8472. doi: 10.1038/ncomms9472
62. Berridge MV, Herst PM, Rowe MR, Schneider R, McConnell MJ. Mitochondrial transfer between cells: methodological constraints in cell culture and animal models. *Anal Biochem.* (2018) 552:75–80. doi: 10.1016/j.ab.2017.11.008
63. Barreira Da Silva R, Laird ME, Yatim N, Fiette L, Ingersoll MA, Albert ML. Dipeptidylpeptidase 4 inhibition enhances lymphocyte trafficking, improving both naturally occurring tumor immunity and immunotherapy. *Nat Immunol.* (2015) 16:850–8. doi: 10.1038/ni.3201
64. Angevin E, Isambert N, Trillet-Lenoir V, You B, Alexandre J, Zalcman G. et al. First-in-human phase 1 of YS110, a monoclonal antibody directed against CD26 in advanced CD26-expressing cancers. *Br J Cancer* (2017) 116:1126–34. doi: 10.1038/bjc.2017.62

Conflict of Interest Statement: The authors declare that the research was conducted in the absence of any commercial or financial relationships that could be construed as a potential conflict of interest.

frontiers in Oncology

REVIEW
published: 28 August 2018
doi: 10.3389/fonc.2018.00341

Metformin as a Therapeutic Target in Endometrial Cancers

*Teresa Y. Lee[1], Ubaldo E. Martinez-Outschoorn[1], Russell J. Schilder[1], Christine H. Kim[2], Scott D. Richard[2], Norman G. Rosenblum[2] and Jennifer M. Johnson[1]**

[1] *Department of Medical Oncology, Thomas Jefferson University, Philadelphia, PA, United States,* [2] *Department of Obstetrics and Gynecology, Thomas Jefferson University, Philadelphia, PA, United States*

Endometrial cancer is the most common gynecologic malignancy in developed countries. Its increasing incidence is thought to be related in part to the rise of metabolic syndrome, which has been shown to be a risk factor for the development of hyperestrogenic and hyperinsulinemic states. This has consequently lead to an increase in other hormone-responsive cancers as well e.g., breast and ovarian cancer. The correlation between obesity, hyperglycemia, and endometrial cancer has highlighted the important role of metabolism in cancer establishment and persistence. Tumor-mediated reprogramming of the microenvironment and macroenvironment can range from induction of cytokines and growth factors to stimulation of surrounding stromal cells to produce energy-rich catabolites, fueling the growth, and survival of cancer cells. Such mechanisms raise the prospect of the metabolic microenvironment itself as a viable target for treatment of malignancies. Metformin is a biguanide drug that is a first-line treatment for type 2 diabetes that has beneficial effects on various markers of the metabolic syndrome. Many studies suggest that metformin shows potential as an adjuvant treatment for uterine and other cancers. Here, we review the evidence for metformin as a treatment for cancers of the endometrium. We discuss the available clinical data and the molecular mechanisms by which it may exert its effects, with a focus on how it may alter the tumor microenvironment. The pleiotropic effects of metformin on cellular energy production and usage as well as intercellular and hormone-based interactions make it a promising candidate for reprogramming of the cancer ecosystem. This, along with other treatments aimed at targeting tumor metabolic pathways, may lead to novel treatment strategies for endometrial cancer.

Keywords: tumor microenvironment, metabolism, metformin, endometrial cancer, reverse Warburg

OPEN ACCESS

Edited by:
Simona Pisanti,
Università degli Studi di Salerno, Italy

Reviewed by:
Ronca Roberto,
Università degli Studi di Brescia, Italy
Raquel Aloyz,
Lady Davis Institute (LDI), Canada

****Correspondence:***
Jennifer M. Johnson
jennifer.m.johnson@jefferson.edu

Specialty section:
This article was submitted to Molecular and Cellular Oncology, a section of the journal Frontiers in Oncology

Received: *31 May 2018*
Accepted: *06 August 2018*
Published: *28 August 2018*

Citation:
Lee TY, Martinez-Outschoorn UE, Schilder RJ, Kim CH, Richard SD, Rosenblum NG and Johnson JM (2018) Metformin as a Therapeutic Target in Endometrial Cancers. Front. Oncol. 8:341. doi: 10.3389/fonc.2018.00341

ENDOMETRIAL CANCER

Cancer of the endometrium is the fifth most common malignancy in women worldwide, with 455,000 new cases diagnosed worldwide in 2015 (1). The incidence is rising, and is noted to be much higher in developed than developing countries (1, 2). The American Cancer Society estimates that 63,230 new cases will be diagnosed in the United States in 2018 (representing 7% of cancer diagnoses in women), with 11,350 predicted deaths (3). The majority of cases arise in the post-menopausal period, but up to 14% of cases occur in women age 40 or younger (4). The principal risk factor for development of endometrial cancer is exposure to endogenous and exogenous estrogens, which is influenced by factors such as age at menarche and menopause, parity,

use of unopposed estrogen therapy or other hormonal therapies (e.g., tamoxifen), and a host of metabolic factors including obesity. 5–25% of cases are also associated with high risk germline mutations, particularly those affecting DNA mismatch repair pathways, leading to early onset of disease (5).

The most common classification system divides endometrial cancers into two subtypes (6). Type I cancers are low-grade, diploid, endometrioid, and hormone-receptor positive, carrying a better prognosis. They frequently display mutations in phosphate and tensin homolog (*PTEN*). Type II cancers (which include the serous, clear cell, mixed cell, undifferentiated, and carcinosarcoma histologies) are high grade, non-endometrioid, aneuploid, and hormone-negative, with higher rates of metastasis and worse prognosis. They tend to occur in older patients and are more likely to have mutations in the tumor suppressor p53. Type II cancers make up only 10% of endometrial cancers but account for almost 50% of relapses and deaths (7), suggesting a fundamental biologic difference between the two subsets.

Most cases are diagnosed at an early stage due to the early detection sign of abnormal bleeding. Standard treatment for apparent stage I endometrial cancer consists of surgical resection (primary hysterectomy with bilateral salpingo-oophorectomy with possible lymph node mapping). Disease that is confirmed to be uterine-confined with low risk features, can be treated with surgery only and has a >90% relapse-free survival rate at 5 years (8). Radiation decreases local relapse rates but does not affect relapse at distant sites or increase overall survival (9, 10). Trials of adjuvant chemotherapy alone with cyclophosphamide, doxorubicin, and cisplatin demonstrated no significant improvement in progression-free survival, overall survival, or relapse (11). Combined adjuvant chemoradiation has shown a slight increase in progression-free survival but not overall survival (11).

For metastatic or recurrent disease, management may include surgery or radiation (if localized to a single site); those with unresectable disease may sometimes receive primary chemotherapy followed by cytoreductive surgery. For disease not amenable to local therapy, a carboplatin-paclitaxel combination is increasingly used as a first-line alternative to the traditional cisplatin, paclitaxel, and doxorubicin (7). With respect to hormonal therapy in advanced disease, a 33% response rate was noted after alternating tamoxifen and medroxyprogesterone (11–13). In recurrent or metastatic disease, progestogens, tamoxifen alternated with megestrol, gonadotropin-releasing hormone analogues, selective estrogen receptor modulators, and aromatase inhibitors have been used with response rates ranging from 11 to 56% (13, 14). Ultimately, the response rates for recurrent advanced disease are low, and there are no standard second line therapies (13, 15).

This lack of effective treatment for advanced stage endometrial cancer has led to exploration of alternative therapeutic modalities. In particular, numerous studies have examined the effectiveness of targeted therapies acting on the phosphoinositide 3-Kinase (PI3K)/Protein kinase B (Akt)/mammalian target of rapamycin (mTOR) pathway, epidermal growth factor receptor (EGFR), human epidermal growth factor receptor 2 (HER2), and vascular endothelial growth factor (VEGF), reviewed elsewhere (11). The results of single-agent mTOR inhibitor treatment, or EGFR and HER2 inhibitors have been disappointing, with response rates of 0–12%. Anti-angiogenic drugs such as bevacizumab, sunitinib, brivanib, and lenvatinib have resulted in slightly higher objective response rates of 14–19%. Studies of additional targets, including fibroblast growth factor receptor (FGFR), luteinizing hormone releasing hormone (LHRH), poly ADP-ribose polymerase (PARP), and Programmed Death-1/Programmed Death Ligand-1 (PD-1/PD-L1) are underway. At this point, no targeted therapies have been approved. Therefore, further interest has been focused on other factors that could contribute to development and progression of endometrial cancer.

ASSOCIATIONS WITH METABOLIC SYNDROME, OBESITY, AND METABOLISM

Among the risk factors associated with endometrial cancer, metabolic syndrome (a constellation of obesity, hyperglycemia, hypertension, and hyperlipidemia) has attracted a large amount of interest in recent years. Multiple associative studies have suggested that the metabolic syndrome is a risk factor for development of many different types of cancers (16–18), including endometrial cancer (19–24). A meta-analysis of 6 studies from North America, Europe, and China estimated a relative risk (RR) for endometrial cancer of 1.89 in patients with metabolic syndrome (95% confidence interval [CI] 1.34–2.67, $p = 0.001$) (25). Another meta-analysis of 7 European cohorts reported a 56% increase in endometrial cancer risk per increase of one standard deviation in a composite metabolic risk score derived from sex- and cohort-specific means in body mass index (BMI), blood pressure, plasma cholesterol, triglycerides, and glucose (18). Apart from incidence, Ni and colleagues reported increased endometrial cancer stage, grade, vascular invasion, tumor size, and lymphatic metastasis in patients with metabolic syndrome, as well as decreased overall survival (26).

The individual components of the metabolic syndrome have also been studied in relation to endometrial cancer risk, but it is unknown if their contribution is additive or synergistic. In particular, obesity has been noted to be strongly associated with risk of endometrial cancer in several case-control studies and meta-analyses (21–25, 27, 28). Multiple measures of adiposity, including BMI, waist circumference, waist-to-hip-ratio, and hip circumference, have been found to be directly associated with endometrial cancer incidence. Increased waist circumference and BMI have also been shown to be significantly associated with increased risk of overall mortality from endometrial cancer (29, 30). Other studies have demonstrated positive albeit less robust association between endometrial cancer and the other components of the metabolic syndrome: hypertension (21–24), hyperlipidemia (21–24), and hyperglycemia or diabetes mellitus (19, 21–25, 31, 32). The association between diabetes and endometrial cancer appears to be partially confounded by co-existing overweight/obesity (33, 34). However, elevated risk of endometrial cancer in patients with diabetes has been reported even after adjustment for BMI, with one meta-analysis including

29 cohort studies reporting a summary relative risk of 1.89 [95% CI, 1.46–2.45, $p < 0.001$] (32). This study also noted a small increased risk of disease-specific mortality in diabetic patients with endometrial cancer (RR 1.32, 95% CI, 1.10–1.60; $p = 0.003$).

The major driver of increased risk of endometrial and other hormone-responsive cancers in obesity is thought to be the generation of a hyper-estrogenic state caused by the presence of the aromatase enzyme in adipose tissue (35). This enzyme catalyzes conversion of androgens to estrogens, making adipose tissue a key source of estrogens in post-menopausal women. In addition, adiposity has been associated with other factors that may drive tumorigenesis in general, including increased inflammation, depressed immune function, and chronic insulin resistance and hyperinsulinemia. Endometrial cancer patients have been shown to have increased markers of insulin resistance, including higher fasting insulin levels and elevated non-fasting and fasting C-peptide levels (36, 37). Supporting this link between abnormal glucose metabolism and cancer risk is the observation that better diabetic control is associated with decreased endometrial cancer risk (21). Ultimately, these data suggest that abnormal metabolism, including insulin resistance and hyperglycemia, may play a role in the development of endometrial cancer and thus represent a possible therapeutic target.

METFORMIN REPURPOSING AND EPIDEMIOLOGIC DATA FROM ENDOMETRIAL CANCER

In recent years there has been growing interest in drug repurposing or repositioning, a process which seeks to identify new pharmacologic properties (e.g., anti-tumorigenic) of existing medications for use as primary or adjuvant treatments for other conditions (38, 39). These drugs are already well-studied in terms of tolerability and side effects, often inexpensive, and amenable to retrospective and associative studies as many patients are already taking them for other indications. The association between obesity, diabetes, hyperinsulinemia, and endometrial cancer has led to the hypothesis that medications which target glucose metabolism such as metformin may be effective in preventing or treating such malignancies. One drug that has received a significant amount of attention in this arena has been metformin [1,1-dimethylbiguanide] which is a first line oral antihyperglycemic agent used in the treatment of type 2 diabetes (40). Broadly, its effects include lowering of blood glucose concentrations, increasing insulin sensitization, and reducing plasma fasting insulin levels. Furthermore, unlike with some oral hypoglycemic medications and insulin, metformin users show a tendency toward sustained weight loss (41). The low toxicity of metformin makes it especially interesting as a potential adjunctive therapy, or even as monotherapy for patients with contraindications to chemotherapy or considerations such as the desire to preserve fertility.

Many investigators have sought to examine the effect of metformin exposure on the development of endometrial cancer (**Table 1**). Multiple epidemiologic studies have reported lower overall cancer incidence in metformin users, reviewed by several groups (47–53). Studies evaluating the relationship between metformin use and endometrial cancer incidence specifically have yielded more conflicting results. Three cohort studies and two case-control studies found no decrease in the risk of endometrial cancer in metformin users compared to nonusers (34, 42, 43, 45, 46). However, these studies show considerable heterogeneity in factors such as study size, indication for metformin use, and duration and method of measurement of metformin exposure (e.g., prescriptions vs. self-report). Notably, a large study of 478,921 Taiwanese women with diabetes showed a significantly decreased incidence of endometrial cancer (hazard ratio [HR] 0.675, 95% CI 0.614–0.742) in metformin users compared to never users (44). When stratified by duration of use or cumulative doses, the decrease in incidence demonstrated a dose-response effect. Additionally, a meta-analysis by Tang and colleagues found that metformin use was associated with a decreased risk of endometrial cancer incidence (RR 0.87, 95% CI 0.80–0.95) (54).

Other associative studies have focused instead on the relationship between metformin exposure and endometrial cancer outcomes (**Table 2**). Metformin use in diabetic patients with endometrial cancer was associated with improved overall survival compared to those not taking metformin in two separate studies, including one involving patients with stage III–IV or recurrent endometrial cancer receiving chemotherapy (56, 59). The study by Ko also found improved recurrence-free survival in patients taking metformin. In contrast, some did not find any effect of metformin exposure on survival parameters (57, 58, 61). Still others have reported effects only on certain subgroups of patients. For example, Nevadunsky found increased survival for metformin users only among patients with non-endometrioid but not endometrioid forms of endometrial cancer (55), while Hall reported a significantly lower recurrence rate of only endometrioid endometrial cancers among metformin users (60). As with the incidence research, these studies are limited by heterogeneity and sample size. However, a 2017 meta-analysis including 6 of the above studies supports a higher overall survival rate in metformin-users with endometrial cancer compared to non-metformin users and non-diabetic patients (HR 0.82, 95% CI 0.70–0.95, $I^2 = 40\%$) (62). Finally, a meta-analysis of 28 studies reported that metformin use was associated with decreased all-cause mortality in patients with concurrent diabetes for several cancer types, including endometrial (RR 0.49, 95% CI 0.32, 0.73, $p < 0.001$) (63).

CELLULAR AND MOLECULAR MECHANISMS OF METFORMIN INHIBITION OF ENDOMETRIAL CANCER

Metabolic alterations in endometrial cancer have been described not only on a systemic but also on a cellular and molecular level. For example, Byrne and colleagues examined microarray data from women with women with type I endometrial cancer and demonstrated that tumor-derived endometrium showed enrichment of genes related to glycolysis and lipogenesis

TABLE 1 | Studies of metformin use and incidence of endometrial cancer.

References	Design	Results
(42) (UK)	Case-control 2,554 cases, 15,324 controls	• Ever-use of metformin not associated with risk of endometrial cancer (OR 0.86, 95% CI 0.63–1.18) • Long-term use of metformin (>25 prescriptions) not associated with risk of endometrial cancer (OR 0.79, 95% CI 0.54–1.17)
(34) (USA)	Retrospective cohort 88,107 postmenopausal women (age 50–79)	• Self-reported metformin use at study baseline not associated with risk of endometrial cancer (HR 1.64, 95% CI 0.92–2.91)
(43) (USA)	Retrospective cohort 541,128 women (new prescription of metformin or sulfonylurea, any indication)	• Metformin use not associated with endometrial cancer risk compared to sulfonylurea use (HR 1.09, 95% CI 0.88–1.35)
(44) (Taiwan)	Retrospective cohort 478,921 women (new diagnosis of type 2 diabetes)	• Ever-use of metformin associated with decreased incidence of endometrial cancer (HR 0.675, 95% CI 0.614–0.742) • Dose-response was observed when adjusted for duration of metformin use or cumulative metformin doses
(45) (Italy)	Case-control 376 cases, 7,485 controls	• Ever-use of metformin use not associated with endometrial cancer risk (OR 1.07, 95% CI 0.82–1.41)
(46) (Finland)	Retrospective cohort 92,366 women (new diagnosis of type 2 diabetes) Nested case-control 590 cases (endometrioid), 11,792 controls	• Metformin ever-use associated with increased risk of endometrial cancer in full cohort (OR 1.23, 95% CI 1.03–1.48). • Metformin use associated with increased risk of endometrial cancer in nested case-control (OR 1.24, 95% CI 1.02–1.51)

OR, odds ratio; CI, confidence interval; HR, hazard ratio.

compared to normal endometrium (64). They also reported that multiple human endometrial cancer cell lines showed strong upregulation of the glucose transporter GLUT6 as well as activation of AKT compared to nonmalignant cells. *In vitro* metabolic profiling demonstrated that these changes were associated with upregulation of glycolysis, decreased glucose oxidation, and increased *de novo* lipogenesis. Finally, the authors demonstrated that endometrial cancer cell cultures experience cytotoxicity when exposed to a variety of inhibitors targeting metabolic pathways, including the glycolysis inhibitors 2-deoxy-D-glucose [2-DG] and 3-bromopyruvate (BrPA), the lipogenesis inhibitor 5-(tetradecyloxy)-2-furoic acid (TOFA), the fatty acid oxidation inhibitor etomixir, and the pleiotropic metabolic inhibitor metformin. Further support for the importance of glucose metabolism on endometrial cancer cell growth comes from Han and colleagues, who studied the growth of two endometrial cancer cell lines (ECC-1 and Ishikawa cells) under low, normal, or high glucose conditions (65). High glucose conditions (corresponding to physiologic hyperglycemia) led to increased cell proliferation, *in vitro colony* formation, and increased expression of the GLUT1 glucose transporter along with increased glucose uptake. High glucose also increased phosphorylation of lactate dehydrogenase A (LDHA) and decreased levels of pyruvate dehydrogenase (PDH), suggesting an increase in glycolytic activity. Conversely, low glucose conditions led to increased cell apoptosis, cell cycle arrest, decreased adhesion, and invasion. All of these data support the idea that the metabolic vulnerabilities of endometrial cancer may make it susceptible to therapies such as metformin.

Multiple studies have demonstrated the ability of metformin to inhibit proliferation of both type I and type II human endometrial cancer cell lines in culture (66–73). Metformin treatment of endometrial cancer cell lines upregulates markers of cell cycle arrest (66, 68, 69, 74), apoptosis (66, 67, 69, 72, 73, 75, 76), and autophagy (69, 77), while decreasing markers associated with senescence (66, 74) and inhibiting cell migration (68, 71, 76). The anticancer effects of metformin treatment may not be limited to direct effects on endometrial cancer cells, but may also result from changes to the systemic milieu. Polycystic ovary syndrome (PCOS) is a condition which is associated with endometrial hyperplasia and predisposition to endometrial cancer (78). Endometrial cancer cell lines incubated with sera from PCOS patients showed increased migration and markers of invasiveness such as activity of matrix metalloproteinases (MMP)−2 and −9 compared to cells incubated with sera from healthy controls. In contrast, sera from PCOS patients treated with metformin for 6 months showed attenuation of this effect, with decreased migration and MMP-2/9 activity compared to cells treated with sera from PCOS patients not on metformin (79).

The molecular mechanisms of metformin's effects in endometrial cancer cells are diverse and continue to be an active area of investigation (**Figure 1**). Its general mechanisms are complex and multifactorial and are reviewed in detail elsewhere (80). Multiple groups have demonstrated that metformin's ability to inhibit oxidative phosphorylation (OXPHOS) at the mitochondrial level is an important mediator of its biologic activity (81, 82). The end result is a decrease in proton gradient across the inner mitochondrial membrane, ultimately leading to reduction in proton-driven synthesis of adenosine triphosphate (ATP) and an increase in the ratio of cellular adenosine monophosphate (AMP) to ATP, caused by imbalance in the rate of ATP production vs. consumption. The decrease in ATP is theorized to be responsible for a key effect of metformin treatment, namely, phosphorylation and activation of the serine/threonine AMP-activated protein kinase (AMPK), a regulatory protein which plays a role in sensing and energy status of the cell and regulating cellular function under conditions of energy restriction (83, 84). This leads to AMP binding to AMPK and a conformational change that allows for phosphorylation/activation of AMPK by liver kinase B1 (LKB1) (85). Activation of AMPK switches cells to a catabolic state via AMPK-mediated phosphorylation and inhibition of key enzymes and transcription factors involved

TABLE 2 | Observational studies of metformin exposure in endometrial cancer.

	Number				
		DM		No DM	
References	Total	MFM	No MFM	No MFM	Results
(55) (USA)	985	114	136	735	• Non-endometrioid endometrioid cancer patients had greater OS in metformin vs. non-metformin users (HR 0.54, 95% CI 0.30–0.97) • No association between metformin use and endometrioid endometrial cancer (HR 0.79, 95% CI 0.31–2.0)
(56) (USA)	1,495	196	167	1,132	• RFS 1.8 times worse in patients not on metformin compared to metformin users (95% CI 1.1–2.9) • OS 2.3 times worse in patients not on metformin compared to metformin users (95% CI 1.3–4.2) • TTR not associated with metformin use (HR 1.12, 95% CI 0.6–2.2)
(57) (Poland)	107	30	38	39	• No difference in OS between metformin users vs. non-users ($p = 0.86$)
(58) (USA)	1,303	116	161	1,026	• OS not significantly different between diabetic metformin-users and diabetic non-metformin users (HR 0.61; 95% CI 0.30–1.23) or non-diabetic patients (HR 1.03; 95% CI 0.57–1.85). • PFS not significantly different between diabetic metformin-users compared to diabetic non-metformin users (HR 1.06; 95% CI 0.34–3.30) or non-diabetic patients (HR 1.14; 95% CI 0.46–2.62)
(59) (USA)	349	31	27	291	• OS greater in diabetic metformin-users compared to diabetic patients not taking metformin (HR 0.42, 95% CI 0.23–0.78) but not compared to non-diabetic patients (HR 0.65, 95% CI 0.41–1.05)
(60) (USA)	351	64	287		• Recurrence rate for all metformin-users vs. non-metformin users not statistically different, but recurrence of type I endometrial cancers was significantly lower for metformin users (1.9%) compared to non-metformin users (10.3%), $p = 0.05$
(61) (Austria)	465	46	41	378	• Metformin use not associated with OS (HR 0.9, 95% CI 0.69–1.2) or RFS (HR 1.2, 95% CI 0.8–1.70)

MFM, metformin; OS, overall survival; HR, hazard ratio; CI, confidence interval; RFS, recurrence-free survival; TTR, time to regression; PFS, progression-free survival.

in ATP-consuming synthetic pathways (e.g., glucose, lipid and protein).

Among the known downstream effects of AMPK activation is decreased protein synthesis due to inhibition of the mTOR pathway, resulting in the inhibition of translation by the eukaryotic initiation factor 4E-binding protein-1 [4E-BP1] complex and decreased activity of the S6 kinase 1 (S6K1) responsible for phosphorylation of the ribosomal S6 protein (rpS6) (86, 87). Metformin inhibition of mTOR signaling in endometrial cancer cells has been confirmed by multiple groups (66, 74, 88–90). Other well-described effects of AMPK activation include phosphorylation and inactivation of Acetyl-CoA carboxylase (ACC) leading to downregulation of fatty acid synthesis (83, 91) as well as inhibition of signaling via the insulin-like growth factor-1 receptor (IGF-1R). Metformin inhibition of ACC has not been reported in endometrial cancer cell lines, but Wallbillich did observe decreased expression of fatty acid synthetase (FAS) in metformin-treated tumor tissue from a xenograft model (73). In endometrial cancer cell cultures, metformin treatment lowers secretion of insulin-like growth factor (IGF-1) (70), downregulates expression of insulin receptor (68) and IGF-1R (70, 75), inhibits phosphorylation of IGF-1R (68), and increases expression of insulin-like growth factor-binding protein 1 (IGFBP-1) (75). In other cancer types, this is associated with inhibitory phosphorylation of the signaling adapter, insulin receptor substrate-1 (IRS-1) and inhibition of the downstream PI3K/Akt/mTOR and mitogen-activated protein-kinase/extracellular signal-regulated kinase (MAPK/ERK) pathways (92–94). Inhibition of PI3K/Akt signaling has been observed in metformin-treated endometrial cancer cells (70), and both Akt and ERK1/2 are inhibited in endometrial cancer cells incubated with serum from women with PCOS who are receiving metformin treatment (79). The cumulative result is inhibition of individual cell growth and proliferation, decreased synthesis of proteins and fatty acids, as well as decreased paracrine and endocrine release of pro-proliferative systemic factors.

In addition to IGF-1-related signaling pathways, metformin treatment of endometrial cancer cells has been reported to affect the activity of the transcription factor signal transducer and activator of transcription 3 (STAT3), which is usually activated via signaling by various growth factors and cytokines to dimerize, translocate to the nucleus, and induce transcription of multiple pro-survival and pro-proliferative genes (95). STAT3 levels are elevated in endometrial cancer cells, in particular the serine-phosphorylated form, phospho-STAT3 Ser727 (96). High glucose concentrations induces transcription of STAT3 as well as its upstream regulators Janus kinases 1 and 2 (JAK1/2), while metformin treatment reduces total STAT3 protein as well as phospho-STAT3 Ser727 (73). This is associated with significantly decreased expression of multiple pro-survival downstream targets of STAT3, including c-Myc and B-cell lymphoma (Bcl)-2 and –XL, providing another possible mechanism for metformin's anti-cancer activity. The authors also examined the effect of

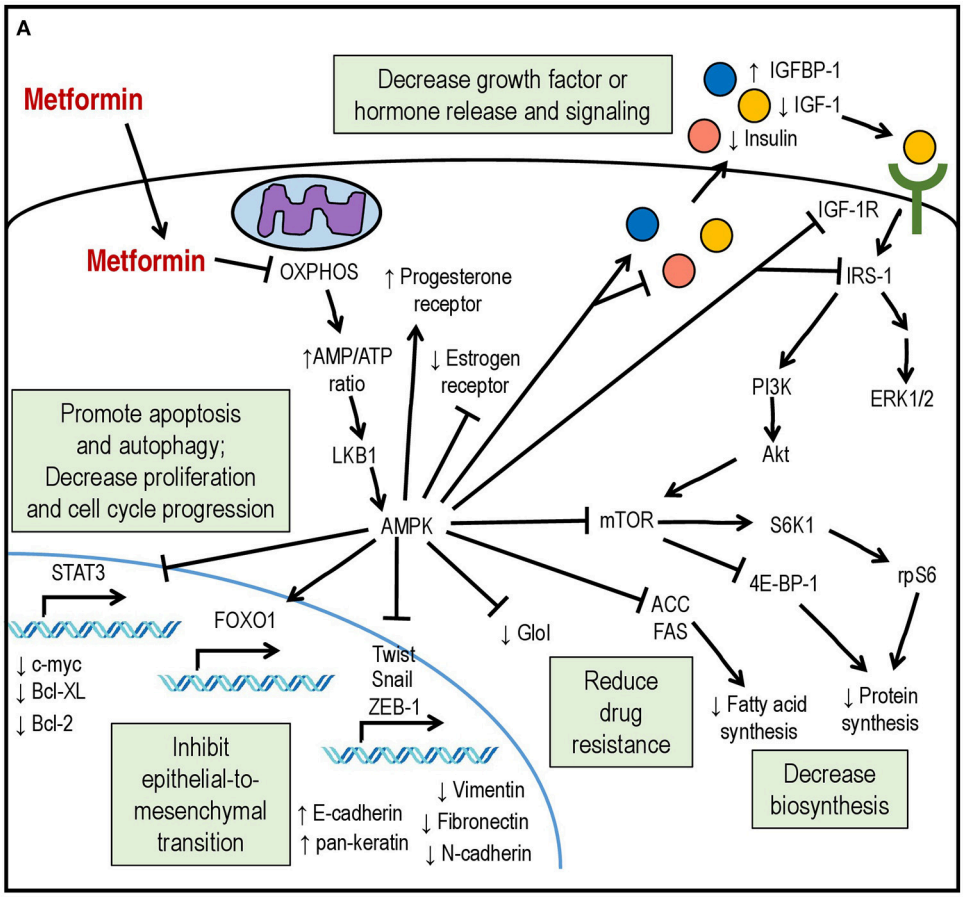

FIGURE 1 | (A) Mechanisms of action of metformin within the endometrial cancer cell. **(B)** Downstream molecular targets of metformin showing differential expression or activity in endometrial cancer.

metformin in a xenograft model of endometrioid endometrial cancer cells. While not statistically significant, metformin exposure was associated with a trend toward decreased tumor size, and analysis of tumor tissues demonstrated decreased expression of STAT3 and its targets (73).

Another recently-reported target of metformin in endometrial cancer is the transcription factor forkhead box protein 1 (FOXO1), which plays numerous roles in cellular function, including regulation of gluconeogenesis, adipogenesis, protection from oxidative stress, and tumor suppression (97). FOXO1 is negatively regulated via inhibitory phosphorylation by Akt, which causes it to translocate out of the nucleus to the cytoplasm where it is degraded (98). Conversely, AMPK activation leads to FOXO1 nuclear localization and activation (99). Zou demonstrated that endometrial cancer cells show decreased levels of phospho-AMPK and total FOXO1 protein, and endometrial cancer tissues show significantly less staining of activated AMPK and higher levels of phospho-Akt compared to controls (72). This is associated with a shift toward cytoplasmic (inactive) rather than nuclear (active) FOXO1 staining. *In vitro*,

they reported that metformin treatment increased FOXO1 protein levels, decreased inhibitory FOXO1 phosphorylation, and increased FOXO1 nuclear accumulation in an AMPK-dependent manner, resulting in inhibition of endometrial cancer cell proliferation. Conversely, knockdown of FOXO1 expression using siRNA partially attenuates the antiproliferative effect of metformin on endometrial cancer cells. Metformin treatment inhibited growth of tumors in a xenograft mouse model, and tumor staining also showed increased phospho-AMPK and nuclear localization of FOXO1 as well as decreased staining of the proliferative marker Ki-67 (72). Decreased FOXO1 expression during metformin treatment has been reported by others as well (68).

Metformin treatment has also been shown to inhibit epithelial-to-mesenchymal transition (EMT) in endometrial cancer cell lines. Metformin increases epithelial markers such as E-cadherin and pan-keratin in endometrial cancer cells *in vitro* (76, 100) and decreases mesenchymal markers (e.g., N-cadherin, fibronectin, vimentin) (76, 100) and transcriptional drivers of EMT (e.g., Twist-1, snail-1, zinc finger E-box-binding homeobox-1 [ZEB-1]) (100). In cultured cells, metformin was able to attenuate the molecular and morphologic changes induced by EMT-inducing stimuli such as 17β-estradiol and transforming-growth factor-β (TGF-β) (76). Correspondingly, histologic staining for E-cadherin was significantly higher in endometrial carcinomas taken from patients with a history of metformin use (100).

Metformin has demonstrated the ability to synergize with other endometrial cancer therapies *in vitro*, leading to enhanced apoptosis of cultured endometrial cell lines in the presence of paclitaxel (74, 101), cisplatin (101, 102), or progestin (89). For the latter two, this effect is dependent on downregulation of glycoxylase I (GloI), a mediator of chemotherapy resistance (89, 101). Metformin treatment was also able to increase expression of the progesterone receptor in endometrial cancer cells (88) and sensitize progestin-resistant endometrial carcinoma cells to medroxyprogesterone-induced apoptosis (89). Conversely, metformin alters expression of the estrogen receptor (ER) in endometrial cancer cells, decreasing the ERα isoform while increasing expression of ERβ, with overall inhibition of estradiol-induced proliferation (90). In endometrial cancer patients with type 2 diabetes, metformin leads to decreased expression of the estrogen receptor in tumor tissue compared to insulin treatment (103).

Possible mutation-specific effects of metformin have also been explored in preclinical *in vivo* models of endometrial cancer. Oral metformin is capable of reducing *in vitro* cell proliferation as well as tumor size in xenograft models of multiple human and mouse endometrial cancer cell lines. (67). This effect occurred only in cell lines with activating *K-Ras* mutations but not wild-type *K-Ras* and could be partially attenuated by siRNA-based inhibition of K-Ras expression. Moreover, metformin treatment was shown to cause mislocalization of K-Ras to the cytoplasm in a protein kinase C (PKC)-dependent manner. No association was seen between metformin-responsiveness and *PTEN* mutations. Another study utilized a primary endometrioid endometrial carcinoma xenograft model using cells taken directly from patient biopsies for culture and inoculation into nude mice. The authors noted that one sample contained a *K-Ras* mutation while the other was wild-type; neither tumor was inhibited by metformin treatment, either alone or in combination with cisplatin (104). It should be noted that the dosage of metformin used in this study was lower than in the study by Iglesias (250 mg/kg/day for 21 days vs. 1 g/kg/day for 29-64 days). However, in both these studies, the tumors that displayed no susceptibility to metformin treatment also showed no changes in levels of activated AMPK or downstream mediators, emphasizing the likely importance of this pathway for mediating metformin-induced tumor suppression. Several studies have now shown that higher doses of metformin are required in mice to have antitumor effects than those administered in clinical trials and this may be a reflection of pharmacokinetic differences between rodents and humans (86, 105, 106).

Attention is now also being paid to the impact of metformin on other cellular components of the tumor microenvironment (TME) beyond the cancer cells themselves as described in Rivadeneira and Delgoffe (107). Metformin is capable of decreasing the rate of tumor cell oxygen consumption and thus is able to reduce hypoxia levels within the tumor. The reduction of hypoxia can enhance the activity of agents aimed at stimulating anti-tumor T-cells (108). Further effects of metformin on the immune microenvironment are hypothesized to be mediated through tumor-associated macrophage reprogramming from an M2 to M1-like phenotype (109). A review on the effects of metformin on other tumor cells is beyond the scope of this work. In sum, the pre-clinical data provide sufficient evidence for continued evaluation of metformin's antineoplastic potential. Nonetheless, they also highlight the likely complex interaction between tumor- and patient-specific factors dictating the efficacy of metformin as an anticancer treatment and underscore the need for ongoing human studies.

METFORMIN IN PRESURGICAL AND OTHER CLINICAL TRIALS IN ENDOMETRIAL CANCER

The preponderance of preclinical data has prompted several early phase clinical trials of metformin in human endometrial cancers (**Table 3**). Many groups have utilized the pre-surgical window approach, in which patients with a biopsy-based histologic diagnosis of endometrial cancer receive metformin treatment during the period prior to hysterectomy. Compared to baseline levels or control patients, patients receiving metformin (between 850 and 2,250 mg daily) showed a post-treatment reduction in markers of DNA replication (topoisomerase IIα) (112) and cellular proliferation (Ki-67) (111, 114, 115, 119). No change in Ki-67 staining was observed by Soliman and colleagues, though notably the dose and duration of metformin exposure was the lowest among these studies (117). Metformin treatment was associated with histologic evidence for inhibition of key signaling pathways including PI3K/Akt/mTOR (111, 112, 114, 116, 117, 119) and MAPK/ERK (112, 117). Tumor immunohistochemistry in one trial also revealed decreased expression of estrogen

TABLE 3 | Clinical trials of metformin in endometrial cancer.

References	Design	Assessment	Treatment	No MFM	MFM	Results
(110) (Iran)	Non-blinded randomized controlled trial	Endometrial histology after metformin vs. progesterone treatment for dysfunctional uterine bleeding	Metformin 500 mg twice daily or megestrol 40 mg daily for 3 months	21	22	• Metformin induced endometrial atrophy in 95.5% (21/22) of patients (including 2 with low grade EEC) compared to 61.9% (13/21) receiving megestrol
(111) (Canada)	Single arm	Effect of metformin on serum and tumor biomarkers during window from biopsy-proven EC diagnosis to resection in non-diabetic patients	Metformin 500 mg three times daily from enrollment to surgery (21–50 days, mean 36.6 days, median 38 days)	10 (banked tissues)	11 (8 EEC, 3 NEEC)	• Metformin reduced plasma insulin, IGF-1 and IGFBP-7 and decreased tumor Ki-67 and phospho-rpS6. • Metformin treatment led to non-significant increase in plasma IGFBP-1
(112) (Japan)	Single arm	Effect of metformin on serum and tumor biomarkers during window from biopsy-proven EC diagnosis to surgical resection in non-diabetic patients	Metformin starting dose 750 mg daily, increased weekly as tolerated to 1,500–2,250 mg daily (divided) from enrollment to surgery (4–6 weeks)	10 (banked tissues)	31	• Metformin reduced tumor topoisomerase IIα, Ki-67, phospho-rpS6, and phospho-ERK1/2 and increased tumor phospho-AMPK • Metformin decreased serum insulin, glucose, and IGF-1 • metformin decreased ability of sera to stimulate DNA synthesis in cultured cells
(113) (China)	Single arm	Effect of metformin plus estrogen/progesterone combination on early stage EC (Ia) in women with PCOS	Cyproterone acetate 2 mg daily, ethinyl estradiol 35 μg daily, and metformin 1,000 mg daily for 6 months	N/A	5	• Estrogen/progesterone treatment combined with metformin led to reversion to normal endometrial epithelium in all patients
(114) (USA)	Single arm	Effect of metformin on tumor biomarkers during window from biopsy-proven EEC diagnosis to surgical resection in obese women	Metformin 850 mg daily from enrollment to surgery (7–28 days, mean 14.65 days)	N/A	20	• Metformin decreased tumor Ki-67, phospho-AMPK, phospho-Akt, phospho-rpS6, phospho-4E-BP-1 and ER but did not change PR level • Responders had increased serum free fatty acids and tumor staining for markers of fatty acid oxidation and glycogen synthesis
(115) (UK)	Non-randomized controlled trial	Effect of metformin on tumor biomarkers during window from biopsy-proven diagnosis of AEH or EEC to surgical resection	Metformin 850 mg twice daily from enrollment to surgery (7–34 days, median 20 days) vs. no treatment	12 (2 AEH, 10 EEC)	28 (0 AEH, 28 EEC)	• Metformin decreased tumor Ki-67 and phospho-4E-BP1 but did not change levels of phospho-Akt, phospho-ACC, phospho-rpS6, ER, PR, or caspase-3
(116) (China)	Non-randomized controlled trial	Effect of metformin on serum and tumor biomarkers during window from biopsy-proven diagnosis of EC and surgical resection in non-diabetic women	Metformin 500 mg three times daily from enrollment to surgery (3–4 weeks) vs. no treatment	30	30	• EC patients had higher serum IGF-1, lower tumor phospho-AMPK, and higher tumor phospho-mTOR at baseline than non-EC patients • Metformin led to lower serum IGF-1, higher tumor phospho-AMPK and lower tumor phospho-mTOR in EC patients
(117) (USA)	Single arm	Effect of metformin on serum and tumor biomarkers during window from biopsy-proven diagnosis of EC to surgical resection	Metformin 850 mg daily from enrollment to surgery (7–24 days, median 9.5 days)	N/A	20	• Metformin decreased serum IGF-1, omentin, insulin, C-peptide, and leptin • Metformin decreased tumor phospho-Akt, phospho-rpS6, phospho-ERK1/2 but did not change levels of Ki-67, phospho-ACC or caspase-3
(118) (Japan)	Single arm	Efficacy of metformin in preventing recurrence after progestin therapy for AEH or early stage EC (stage Ia)	Metformin starting dose 750 mg daily, increased weekly as tolerated to 2,250 mg daily (divided, concurrent with medroxyprogesterone acetate-based protocol for 24–36 weeks, continued alone in complete responders until conception or recurrence)	N/A	16 AEH, 13 EC	• Metformin maintenance associated with 3-year recurrence-free survival of 89%, compared to expected baseline of 52% recurrence-free survival at 2 years
(119) (China)	Non-randomized controlled trial	Effect of metformin on tumor biomarkers during window from biopsy-proven diagnosis of EC to surgical resection	Metformin 500 mg three times daily for 3–4 weeks	32	33	• EC patients had higher tumor Ki-67, PI3K, phospho-Akt, phospho-S6K1, and phospho-4E-BP1 at baseline than non-EC patients • Metformin decreased tumor Ki-67, PI3K, phospho-Akt, phospho-S6K1, and phospho-4E-BP1 in EC patients

MFM, metformin; EC, endometrial cancer; EEC, endometrioid endometrial cancer; NEEC, non-endometrioid endometrial cancer; IGF-1, insulin-like growth factor-1; IGFBP-1/7, insulin-like growth factor binding protein-1/7; rpS6, ribosomal protein S6; ERK1/2, extracellular signal-regulated kinase-1/2; AMPK, AMP-activated kinase; PCOS, polycystic ovary syndrome; Akt, protein kinase B; 4E-BP1, eukaryotic initiation factor 4E-binding protein-1; ER, estrogen receptor; PR, progesterone receptor; AEH, atypical endometrial hyperplasia; ACC, acetyl-CoA carboxylase; mTOR, mammalian target of rapamycin; PI3K, phosphoinositide 3-kinase; S6K1, S6 kinase 1.

receptor after metformin treatment (114). Plasma measures of a hyperinsulinemic state, including insulin, IGF-1, glucose, and leptin were significantly reduced post-metformin (111, 112, 116, 117). Furthermore, serum from metformin-treated patients showed decreased ability to stimulate DNA synthesis in cultured endometrial cancer cells (112), suggesting that systemic effects of metformin also play a role in its antiproliferative activity.

In terms of clinical outcomes, a randomized study by Tabrizi examined the ability of metformin to reverse endometrial hyperplasia or disordered proliferative endometrium in patients with abnormal uterine bleeding compared to megestrol. Metformin was able to induce endometrial atrophy/restore endometrial histology in 95.5% of patients compared to 61.9% in the megestrol group. Significantly, this study included two patients with low grade endometrial carcinomas (stage Ia) who received metformin. After 3 months of treatment, repeat biopsy showed conversion to atrophic endometrium (110). A study of 5 PCOS patients with early stage endometrial carcinoma showed that co-treatment with the oral contraceptive Diane-35 (cyproterone and ethinyl estradiol) and metformin for 6 months led to reversion to normal epithelia on repeat biopsy in all patients (113). This included three patients who had previously been on megestrol treatment for 3 months with documented progesterone resistance. Mitsuhashi also used a combination approach of metformin with medroxyprogesterone to induce remission in patients with atypical endometrial hyperplasia (AEH) or early stage endometrial cancer, and further studied the use of maintenance metformin to prevent relapse. Metformin treatment led to a relapse-free survival of 89% at 3 years, which was higher than their projected baseline of 52% (118). These studies were also notable for their stated goal of fertility preservation, an important consideration for some endometrial cancer patients.

Larger trials are underway, including a phase 3 trial of metformin monotherapy as chemoprevention for endometrial cancer compared to placebo and lifestyle interventions in non-diabetic obese women (NCT01697566) and a phase 2/3 trial by the Gynecologic Oncology Group for advanced (stage III, IVA, IVB) or recurrent endometrial cancer that will compare the addition of metformin vs. placebo to combination paclitaxel/carboplatin as first-line therapy (NCT02065687). Several phase 2 or earlier studies will utilize metformin in combination with hormonal treatments such as megestrol acetate (NCT01968317) or levonorgestrel (as an intrauterine device) for early stage endometrial cancer or complex atypical hyperplasia in young women with the goal of fertility preservation or contraindications to surgery (NCT02990728, NCT02035787, NCT01686126). Also ongoing are a phase 2 study of metformin combined with letrozole and everolimus for advanced or recurrent endometrial cancer (NCT01797523) and a phase 1/2 study of metformin plus metronomic cyclophosphamide and olaparib for advanced or recurrent endometrial cancer (NCT02755844). These efforts will give valuable insight into the preventative and therapeutic value of metformin in endometrial malignancy.

THE METABOLIC MICROENVIRONMENT AS A THERAPEUTIC TARGET IN ENDOMETRIAL CANCER

The role of glucose metabolism in endometrial cancer is also still being explored. Malignant tissues in general have been known to have high levels of glycolytic metabolism, even in the presence of oxygen, a phenomenon known as the Warburg effect after its discoverer, Otto Warburg (120). One theory was that cancer cells are less dependent on oxidative phosphorylation, allowing them to survive in the often relatively hypoxic tumor microenvironment. However, in recent years, a more nuanced model has emerged for some tumor types, known as the reverse Warburg theory (121). This is based on the recognition of heterogeneity in tumor composition; malignant tissues are composed of cancer cells surrounded by diverse types of stromal cells and adipocytes, each of which make contributions to the tumor microenvironment (122, 123). Our research in breast and prostate cancer cell models among others have demonstrated that glycolysis occurs not in the tumor cells themselves, but in the surrounding stromal cells (124–127). This relationship is thought to occur via oxidative stress in the cancer associated stroma (CAS), driven by tumor cell generation of reactive oxygen species and stromal cell loss of caveolin-1 (CAV1), an inhibitor of nitric oxide production (124–129). CAS cells undergo metabolic reprogramming associated with mitophagy (selective degradation of mitochondria by autophagy) and cell autophagy, and they generate high levels of energy-rich metabolites (including lactate and ketones) through glycolysis, which is then shuttled to cancer cells as substrates for oxidative phosphorylation. We have reported that lactate shuttling to tumor epithelial cells is dependent on transporters of the monocarboxylate transporter (MCT) family, with MCT4 being important for lactate efflux from stromal cells and MCT1 for lactate uptake in tumor epithelial cells in a breast cancer cell co-culture system (130). Others have observed similar lactate shuttling in prostate cancer and sarcoma models and have reported that lactate upload promotes tumor cell proliferation and angiogenesis (131, 132). Aside from lactate, Sousa and colleagues have described a similar two-compartment metabolic system in pancreatic ductal adenocarcinoma in which stroma-associated pancreatic stellate cells are stimulated by contact with pancreatic cancer cells to undergo autophagy and secrete primarily alanine which fuels the tricarboxylic acid (TCA) cycle and biosynthesis in the cancer cells themselves (133).

In this model, metformin treatment may play an important part in disrupting cancer cell metabolism via its direct inhibition of mitochondrial respiration in the cancer cells. In agreement with this, our previous results suggest that metformin treatment of cultured breast cancer cells inhibits their ability to induce loss of CAV1 (a marker of tumor-stromal metabolic coupling) in co-cultured fibroblasts (126). We have also observed that a short course of metformin was also able to increase stromal CAV1 expression *in vivo* in patients with head and neck squamous cell carcinoma in a presurgical window of opportunity trial (106).

The existence of such symbiotic metabolic reprogramming has not yet been investigated closely in endometrial cancer, but supportive evidence comes from a study by Latif et al. that showed differential histologic localization for MCT1 (tumor) vs. MCT4 (stroma) for some though not all endometrial cancer samples analyzed (134). High MCT1 expression was also a poor prognostic indicator for recurrence-free, cancer-free, and overall survival in the same study. Moreover, Zhao studied endometrial stromal-epithelial cell interactions in a non-cancer primary cell culture model and showed that epithelial cell proliferation and migration was enhanced when cultured with conditioned media from CAV1 depleted stromal cells (135). A phase 2 study currently underway at our institution utilizes a combination of metformin and doxycycline for the treatment of breast and uterine cancers, with outcomes including the measurement of biomarkers of tumor-stromal metabolic compartmentalization, such as stromal CAV1 and MCT4 and tumor MCT1 (NCT02874430). This will provide new insight into the effects of metformin treatment on the metabolic microenvironment in endometrial cancer.

The Reverse Warburg framework also opens up the possibility of multi-targeted therapies that simultaneously act on aberrant glucose metabolism in both cancer and stromal cells, such as metformin combined with inhibitors of glycolysis, autophagy, or transport of lactate and other energetic substrates. Combined metformin and glycolytic inhibitors have been utilized in xenograft models of breast cancer, gastric cancer, and glioblastoma with synergistic inhibition of tumor growth or prolongation of survival occurring at doses where each agent is ineffective alone (136, 137). Such approaches would exploit the vulnerabilities of tumor-stroma metabolic reprogramming that typically allow for cancer cell survival under a variety of energetic conditions. Overall, the metabolic microenvironment of endometrial cancer represents a promising therapeutic target, one which metformin and other biguanides may be uniquely poised to act upon.

CONCLUSIONS

Endometrial cancer is a disease with few effective treatments for advanced and metastatic disease. In addition, the need for fertility-sparing options for patients with early stage disease means there is a need for more primary or adjunctive treatment approaches. A large body of evidence links endometrial cancer incidence to metabolic conditions such as obesity and hyperglycemic states. Increasing rates of the latter has been mirrored by a rise in the former, particularly in developing countries, highlighting the need for a better understanding of the contribution of the metabolic microenvironment to endometrial cancer tumorigenesis. There is substantial evidence that the mechanisms of nutrient utilization and synthesis are significantly dysregulated in malignancy on both an intracellular and intercellular level. Models such as the reverse Warburg effect especially emphasize the importance of considering the interplay between cancer epithelial cells and their surrounding stroma. Dysregulation of metabolic pathways may represent adaptations that facilitate survival and proliferation in some scenarios (e.g., the idea of the parasitic cancer cell), but can also become liabilities for cancer cells particularly in times of nutrient or energy deprivation. Drugs such as metformin may be uniquely poised to exploit these defects, possibly in conjunction with other therapies that target glucose utilization. Indeed, preclinical and early clinical studies have shown promise for metformin as an adjunctive treatment for endometrial cancer, with effects on both cancer-specific as well as patient-specific metrics. Further study is needed to elucidate the role of metformin as a therapy for endometrial cancer, and several clinical trials are underway that will greatly expand our understanding of its potential benefits.

AUTHOR CONTRIBUTIONS

JJ and UM-O contributed to the conception and design of the manuscript. TL wrote the first draft of the manuscript. UM-O, RS, CK, SR, NR, and JJ contributed to manuscript revision. All authors read and approved the submitted version.

REFERENCES

1. Global Burden of Disease Cancer, Fitzmaurice C, Allen C, Barber RM, Barregard L, Bhutta Z A, et al. Global, regional, and national cancer incidence, mortality, years of life lost, years lived with disability, and disability-adjusted life-years for 32 cancer groups, 1990 to 2015: a systematic analysis for the global burden of disease study. *JAMA Oncol* (2017) 3:524–48. doi: 10.1001/jamaoncol.2016.5688
2. Global Burden of Disease Cancer, Fitzmaurice C, Dicker D, Pain A, Hamavid H, Moradi-Lakeh M, et al. The global burden of cancer 2013. *JAMA Oncol* (2015) 1:505–27. doi: 10.1001/jamaoncol.2015.0735
3. American Cancer Society. *Cancer Facts & Figures 2018*. Atlanta, GA: American Cancer Society (2018).
4. Duska LR, Garrett A, Rueda BR, Haas J, Chang Y, Fuller AF. Endometrial cancer in women 40 years old or younger. *Gynecol Oncol.* (2001) 83:388–93. doi: 10.1006/gyno.2001.6434
5. Moir-Meyer GL, Pearson JF, Lose F, Scott RJ, Mcevoy M, Attia J, et al. Rare germline copy number deletions of likely functional importance are implicated in endometrial cancer predisposition. *Hum Genet.* (2015) 134:269–78. doi: 10.1007/s00439-014-1507-4
6. Bokhman JV. Two pathogenetic types of endometrial carcinoma. *Gynecol Oncol.* (1983) 15:10–7. doi: 10.1016/0090-8258(83)90111-7
7. Del Carmen MG, Birrer M, Schorge JO. Uterine papillary serous cancer: a review of the literature. *Gynecol Oncol.* (2012) 127:651–61. doi: 10.1016/j.ygyno.2012.09.012
8. Kilgore LC, Partridge EE, Alvarez RD, Austin JM, Shingleton HM, Noojin F III, et al. Adenocarcinoma of the endometrium: survival comparisons of patients with and without pelvic node sampling. *Gynecol Oncol.* (1995) 56:29–33. doi: 10.1006/gyno.1995.1005
9. Nout RA, Smit VT, Putter H, Jurgenliemk-Schulz IM, Jobsen JJ, Lutgens LC, et al. Vaginal brachytherapy versus pelvic external beam radiotherapy for patients with endometrial cancer of high-intermediate risk (PORTEC-2): an open-label, non-inferiority, randomised trial. *Lancet* (2010) 375:816–23. doi: 10.1016/S0140-6736(09)62163-2
10. Kong A, Johnson N, Kitchener HC, Lawrie TA. Adjuvant radiotherapy for stage I endometrial cancer: an updated Cochrane systematic

review and meta-analysis. *J Natl Cancer Inst.* (2012) 104:1625–34. doi: 10.1093/jnci/djs374
11. Morice P, Leary A, Creutzberg C, Abu-Rustum N, Darai E. Endometrial cancer. *Lancet* (2016) 387:1094–108. doi: 10.1016/S0140-6736(15)00130-0
12. Quinn MA. Hormonal treatment of endometrial cancer. *Hematol Oncol Clin North Am.* (1999) 13:163–87.ix. doi: 10.1016/S0889-8588(05)70159-3
13. Network NCC. *Uterine Neoplasms Version 1.2018* (2018) Available online at: https://www.nccn.org/professionals/physician_gls/pdf/uterine.pdf (Accessed April 30, 2018).
14. Moore TD, Phillips PH, Nerenstone SR, Cheson BD. Systemic treatment of advanced and recurrent endometrial carcinoma: current status and future directions. *J Clin Oncol.* (1991) 9:1071–88. doi: 10.1200/JCO.1991.9.6.1071
15. Humber CE, Tierney JF, Symonds RP, Collingwood M, Kirwan J, Williams C, et al. Chemotherapy for advanced, recurrent or metastatic endometrial cancer: a systematic review of Cochrane collaboration. *Ann Oncol.* (2007) 18:409–20. doi: 10.1093/annonc/mdl417
16. Russo A, Autelitano M, Bisanti L. Metabolic syndrome and cancer risk. *Eur J Cancer* (2008) 44:293–7. doi: 10.1016/j.ejca.2007.11.005
17. Esposito K, Chiodini P, Colao A, Lenzi A, Giugliano D. Metabolic syndrome and risk of cancer: a systematic review and meta-analysis. *Diabetes Care* (2012) 35:2402–11. doi: 10.2337/dc12-0336
18. Stocks T, Bjorge T, Ulmer H, Manjer J, Haggstrom C, Nagel G, et al. Metabolic risk score and cancer risk: pooled analysis of seven cohorts. *Int J Epidemiol.* (2015) 44:1353–63. doi: 10.1093/ije/dyv001
19. Cust AE, Kaaks R, Friedenreich C, Bonnet F, Laville M, Tjonneland A, et al. Metabolic syndrome, plasma lipid, lipoprotein and glucose levels, and endometrial cancer risk in the European Prospective Investigation into Cancer and Nutrition (EPIC). *Endocr Relat Cancer* (2007) 14:755–67. doi: 10.1677/ERC-07-0132
20. Bjorge T, Stocks T, Lukanova A, Tretli S, Selmer R, Manjer J, et al. Metabolic syndrome and endometrial carcinoma. *Am J Epidemiol.* (2010) 171:892–902. doi: 10.1093/aje/kwq006
21. Zhang Y, Liu Z, Yu X, Zhang X, Lu S, Chen X, et al. The association between metabolic abnormality and endometrial cancer: a large case-control study in China. *Gynecol Oncol.* (2010) 117:41–6. doi: 10.1016/j.ygyno.2009.12.029
22. Friedenreich CM, Biel RK, Lau DC, Csizmadi I, Courneya KS, Magliocco AM, et al. Case-control study of the metabolic syndrome and metabolic risk factors for endometrial cancer. *Cancer Epidemiol Biomarkers Prev.* (2011) 20:2384–95. doi: 10.1158/1055-9965.EPI-11-0715
23. Rosato V, Zucchetto A, Bosetti C, Dal Maso L, Montella M, Pelucchi C, et al. Metabolic syndrome and endometrial cancer risk. *Ann Oncol.* (2011) 22:884–9. doi: 10.1093/annonc/mdq464
24. Trabert B, Wentzensen N, Felix AS, Yang HP, Sherman ME, Brinton LA. Metabolic syndrome and risk of endometrial cancer in the united states: a study in the SEER-medicare linked database. *Cancer Epidemiol Biomarkers Prev.* (2015) 24:261–7. doi: 10.1158/1055-9965.EPI-14-0923
25. Esposito K, Chiodini P, Capuano A, Bellastella G, Maiorino MI, Giugliano D. Metabolic syndrome and endometrial cancer: a meta-analysis. *Endocrine* (2014) 45:28–36. doi: 10.1007/s12020-013-9973-3
26. Ni J, Zhu T, Zhao L, Che F, Chen Y, Shou H, et al. Metabolic syndrome is an independent prognostic factor for endometrial adenocarcinoma. *Clin Transl Oncol.* (2015) 17:835–9. doi: 10.1007/s12094-015-1309-8
27. Aune D, Navarro Rosenblatt DA, Chan DS, Vingeliene S, Abar L, Vieira AR, et al. Anthropometric factors and endometrial cancer risk: a systematic review and dose-response meta-analysis of prospective studies. *Ann Oncol.* (2015) 26:1635–48. doi: 10.1093/annonc/mdv142
28. Wise MR, Jordan V, Lagas A, Showell M, Wong N, Lensen S, et al. Obesity and endometrial hyperplasia and cancer in premenopausal women: a systematic review. *Am J Obstet Gynecol.* (2016) 214:689.e1–689.e17. doi: 10.1016/j.ajog.2016.01.175
29. Calle EE, Rodriguez C, Walker-Thurmond K, Thun MJ. Overweight, obesity, and mortality from cancer in a prospectively studied cohort of U.S. adults. *N Engl J Med.* (2003) 348:1625–38. doi: 10.1056/NEJMoa021423
30. Secord AA, Hasselblad V, Von Gruenigen VE, Gehrig PA, Modesitt SC, Bae-Jump V, et al. Body mass index and mortality in endometrial cancer: a systematic review and meta-analysis. *Gynecol Oncol.* (2016) 140:184–90. doi: 10.1016/j.ygyno.2015.10.020
31. Friberg E, Orsini N, Mantzoros CS, Wolk A. Diabetes mellitus and risk of endometrial cancer: a meta-analysis. *Diabetologia* (2007) 50:1365–74. doi: 10.1007/s00125-007-0681-5
32. Liao C, Zhang D, Mungo C, Tompkins DA, Zeidan AM. Is diabetes mellitus associated with increased incidence and disease-specific mortality in endometrial cancer? A systematic review and meta-analysis of cohort studies. *Gynecol Oncol.* (2014) 135:163–71. doi: 10.1016/j.ygyno.2014.07.095
33. Anderson KE, Anderson E, Mink PJ, Hong CP, Kushi LH, Sellers TA, et al. Diabetes and endometrial cancer in the Iowa women's health study. *Cancer Epidemiol Biomarkers Prev* (2001) 10:611–6. Available online at: http://cebp.aacrjournals.org/content/10/6/611.long
34. Luo J, Beresford S, Chen C, Chlebowski R, Garcia L, Kuller L, et al. Association between diabetes, diabetes treatment and risk of developing endometrial cancer. *Br J Cancer* (2014) 111:1432–9. doi: 10.1038/bjc.2014.407
35. Byers T, Sedjo RL. Body fatness as a cause of cancer: epidemiologic clues to biologic mechanisms. *Endocr Relat Cancer* (2015) 22:R125–34. doi: 10.1530/ERC-14-0580
36. Dossus L, Lukanova A, Rinaldi S, Allen N, Cust AE, Becker S, et al. Hormonal, metabolic, and inflammatory profiles and endometrial cancer risk within the EPIC cohort–a factor analysis. *Am J Epidemiol.* (2013) 177:787–99. doi: 10.1093/aje/kws309
37. Hernandez AV, Pasupuleti V, Benites-Zapata VA, Thota P, Deshpande A, Perez-Lopez FR. Insulin resistance and endometrial cancer risk: a systematic review and meta-analysis. *Eur J Cancer* (2015) 51:2747–58. doi: 10.1016/j.ejca.2015.08.031
38. Gupta SC, Sung B, Prasad S, Webb LJ, Aggarwal BB. Cancer drug discovery by repurposing: teaching new tricks to old dogs. *Trends Pharmacol Sci.* (2013) 34:508–17. doi: 10.1016/j.tips.2013.06.005
39. Wurth R, Thellung S, Bajetto A, Mazzanti M, Florio T, Barbieri F. Drug-repositioning opportunities for cancer therapy: novel molecular targets for known compounds. *Drug Discov Today* (2016) 21:190–9. doi: 10.1016/j.drudis.2015.09.017
40. Pryor R, Cabreiro F. Repurposing metformin: an old drug with new tricks in its binding pockets. *Biochem J* (2015) 471:307–22. doi: 10.1042/BJ20150497
41. Diabetes Prevention Program Research G, Knowler WC, Fowler SE, Hamman RF, Christophi CA, Hoffman HJ, et al. 10-year follow-up of diabetes incidence and weight loss in the diabetes prevention program outcomes study. *Lancet* (2009) 374:1677–86. doi: 10.1016/S0140-6736(09)61457-4
42. Becker C, Jick SS, Meier CR, Bodmer M. Metformin and the risk of endometrial cancer: a case-control analysis. *Gynecol Oncol.* (2013) 129:565–9. doi: 10.1016/j.ygyno.2013.03.009
43. Ko EM, Sturmer T, Hong JL, Castillo WC, Bae-Jump V, Funk MJ. Metformin and the risk of endometrial cancer: a population-based cohort study. *Gynecol Oncol.* (2015) 136:341–7. doi: 10.1016/j.ygyno.2014.12.001
44. Tseng CH. Metformin and endometrial cancer risk in Chinese women with type 2 diabetes mellitus in Taiwan. *Gynecol Oncol.* (2015) 138:147–53. doi: 10.1016/j.ygyno.2015.03.059
45. Franchi M, Asciutto R, Nicotra F, Merlino L, La Vecchia C, Corrao G, et al. Metformin, other antidiabetic drugs, and endometrial cancer risk: a nested case-control study within Italian healthcare utilization databases. *Eur J Cancer Prev.* (2016) 26:225–31. doi: 10.1097/CEJ.0000000000000235
46. Arima R, Hautakoski A, Marttila M, Arffman M, Sund R, Ilanne-Parikka P, et al. Cause-specific mortality in endometrioid endometrial cancer patients with type 2 diabetes using metformin or other types of antidiabetic medication. *Gynecol Oncol.* (2017) 147:678–83. doi: 10.1016/j.ygyno.2017.10.014
47. Pierotti MA, Berrino F, Gariboldi M, Melani C, Mogavero A, Negri T, et al. Targeting metabolism for cancer treatment and prevention: metformin, an old drug with multi-faceted effects. *Oncogene* (2013) 32:1475–87. doi: 10.1038/onc.2012.181
48. Febbraro T, Lengyel E, Romero IL. Old drug, new trick: repurposing metformin for gynecologic cancers? *Gynecol Oncol.* (2014) 135:614–21. doi: 10.1016/j.ygyno.2014.10.011
49. Coperchini F, Leporati P, Rotondi M, Chiovato L. Expanding the therapeutic spectrum of metformin: from diabetes to cancer. *J Endocrinol Invest.* (2015) 38:1047–55. doi: 10.1007/s40618-015-0370-z

50. Imai A, Ichigo S, Matsunami K, Takagi H, Yasuda K. Clinical benefits of metformin in gynecologic oncology. *Oncol Lett.* (2015) 10:577–82. doi: 10.3892/ol.2015.3262
51. Chae YK, Arya A, Malecek MK, Shin DS, Carneiro B, Chandra S, et al. Repurposing metformin for cancer treatment: current clinical studies. *Oncotarget* (2016) 7:40767–80. doi: 10.18632/oncotarget.8194
52. Gong J, Kelekar G, Shen J, Shen J, Kaur S, Mita M. The expanding role of metformin in cancer: an update on antitumor mechanisms and clinical development. *Target Oncol.* (2016) 11:447–67. doi: 10.1007/s11523-016-0423-z
53. Irie H, Banno K, Yanokura M, Iida M, Adachi M, Nakamura K, et al. Metformin: a candidate for the treatment of gynecological tumors based on drug repositioning. *Oncol Lett.* (2016) 11:1287–93. doi: 10.3892/ol.2016.4075
54. Tang YL, Zhu LY, Li Y, Yu J, Wang J, Zeng XX, et al. Metformin use is associated with reduced incidence and improved survival of endometrial cancer: a meta-analysis. *Biomed Res Int.* (2017) 2017:5905384. doi: 10.1155/2017/5905384
55. Nevadunsky NS, Van Arsdale A, Strickler HD, Moadel A, Kaur G, Frimer M, et al. Metformin use and endometrial cancer survival. *Gynecol Oncol.* (2014) 132:236–40. doi: 10.1016/j.ygyno.2013.10.026
56. Ko EM, Walter P, Jackson A, Clark L, Franasiak J, Bolac C, et al. Metformin is associated with improved survival in endometrial cancer. *Gynecol Oncol.* (2014) 132:438–42. doi: 10.1016/j.ygyno.2013.11.021
57. Lemanska A, Zaborowski M, Spaczynski M, Nowak-Markwitz E. Do endometrial cancer patients benefit from metformin intake? *Ginekol Pol.* (2015) 86:419–23. doi: 10.17772/gp/2397
58. Al Hilli MM, Bakkum-Gamez JN, Mariani A, Cliby WA, Mc Gree ME, Weaver AL, et al. The effect of diabetes and metformin on clinical outcomes is negligible in risk-adjusted endometrial cancer cohorts. *Gynecol Oncol.* (2016) 140:270–6. doi: 10.1016/j.ygyno.2015.11.019
59. Ezewuiro O, Grushko TA, Kocherginsky M, Habis M, Hurteau JA, Mills KA, et al. Association of metformin use with outcomes in advanced endometrial cancer treated with chemotherapy. *PLoS ONE* (2016) 11:e0147145. doi: 10.1371/journal.pone.0147145
60. Hall C, Stone RL, Gehlot A, Zorn KK, Burnett AF. Use of metformin in obese women with type I endometrial cancer is associated with a reduced incidence of cancer recurrence. *Int J Gynecol Cancer* (2016) 26:313–7. doi: 10.1097/IGC.0000000000000603
61. Seebacher V, Bergmeister B, Grimm C, Koelbl H, Reinthaller A, Polterauer S. The prognostic role of metformin in patients with endometrial cancer: a retrospective study. *Eur J Obstet Gynecol Reprod Biol.* (2016) 203:291–6. doi: 10.1016/j.ejogrb.2016.06.013
62. Meireles CG, Pereira SA, Valadares LP, Rego DF, Simeoni LA, Guerra ENS, et al. Effects of metformin on endometrial cancer: systematic review and meta-analysis. *Gynecol Oncol.* (2017) 147:167–80. doi: 10.1016/j.ygyno.2017.07.120
63. Zhang ZJ, Li S. The prognostic value of metformin for cancer patients with concurrent diabetes: a systematic review and meta-analysis. *Diabetes Obes Metab.* (2014) 16:707–10. doi: 10.1111/dom.12267
64. Byrne FL, Poon IK, Modesitt SC, Tomsig JL, Chow JD, Healy ME, et al. Metabolic vulnerabilities in endometrial cancer. *Cancer Res.* (2014) 74:5832–45. doi: 10.1158/0008-5472.CAN-14-0254
65. Han J, Zhang L, Guo H, Wysham WZ, Roque DR, Willson AK, et al. Glucose promotes cell proliferation, glucose uptake and invasion in endometrial cancer cells via AMPK/mTOR/S6 and MAPK signaling. *Gynecol Oncol.* (2015) 138:668–75. doi: 10.1016/j.ygyno.2015.06.036
66. Cantrell LA, Zhou C, Mendivil A, Malloy KM, Gehrig PA, Bae-Jump VL. Metformin is a potent inhibitor of endometrial cancer cell proliferation–implications for a novel treatment strategy. *Gynecol Oncol.* (2010) 116:92–8. doi: 10.1016/j.ygyno.2009.09.024
67. Iglesias DA, Yates MS, Van Der Hoeven D, Rodkey TL, Zhang Q, Co NN, et al. Another surprise from Metformin: novel mechanism of action via K-Ras influences endometrial cancer response to therapy. *Mol Cancer Ther.* (2013) 12:2847–56. doi: 10.1158/1535-7163.MCT-13-0439
68. Sarfstein R, Friedman Y, Attias-Geva Z, Fishman A, Bruchim I, Werner H. Metformin downregulates the insulin/IGF-I signaling pathway and inhibits different uterine serous carcinoma (USC) cells proliferation and migration in p53-dependent or -independent manners. *PLoS ONE* (2013) 8:e61537. doi: 10.1371/journal.pone.0061537
69. Takahashi A, Kimura F, Yamanaka A, Takebayashi A, Kita N, Takahashi K, et al. Metformin impairs growth of endometrial cancer cells via cell cycle arrest and concomitant autophagy and apoptosis. *Cancer Cell Int.* (2014) 14:53. doi: 10.1186/1475-2867-14-53
70. Zhang Y, Li MX, Wang H, Zeng Z, Li XM. Metformin down-regulates endometrial carcinoma cell secretion of IGF-1 and expression of IGF-1R. *Asian Pac J Cancer Prev.* (2015) 16:221–5. doi: 10.7314/APJCP.2015.16.1.221
71. De Barros Machado A, Dos Reis V, Weber S, Jauckus J, Brum IS, Von Eye Corleta H, et al. Proliferation and metastatic potential of endometrial cancer cells in response to metformin treatment in a high versus normal glucose environment. *Oncol Lett.* (2016) 12:3626–32. doi: 10.3892/ol.2016.5041
72. Zou J, Hong L, Luo C, Li Z, Zhu Y, Huang T, et al. Metformin inhibits estrogen-dependent endometrial cancer cell growth by activating the AMPK-FOXO1 signal pathway. *Cancer Sci.* (2016) 107:1806–17. doi: 10.1111/cas.13083
73. Wallbillich JJ, Josyula S, Saini U, Zingarelli RA, Dorayappan KD, Riley MK, et al. High Glucose-mediated STAT3 activation in endometrial cancer is inhibited by metformin: therapeutic implications for endometrial cancer. *PLoS ONE* (2017) 12:e0170318. doi: 10.1371/journal.pone.0170318
74. Hanna RK, Zhou C, Malloy KM, Sun L, Zhong Y, Gehrig PA, et al. Metformin potentiates the effects of paclitaxel in endometrial cancer cells through inhibition of cell proliferation and modulation of the mTOR pathway. *Gynecol Oncol.* (2012) 125:458–69. doi: 10.1016/j.ygyno.2012.01.009
75. Xie Y, Wang JL, Ji M, Yuan ZF, Peng Z, Zhang Y, et al. Regulation of insulin-like growth factor signaling by metformin in endometrial cancer cells. *Oncol Lett.* (2014) 8:1993–9. doi: 10.3892/ol.2014.2466
76. Liu Z, Qi S, Zhao X, Li M, Ding S, Lu J, et al. Metformin inhibits 17beta-estradiol-induced epithelial-to-mesenchymal transition via betaKlotho-related ERK1/2 signaling and AMPKalpha signaling in endometrial adenocarcinoma cells. *Oncotarget* (2016) 7:21315–31. doi: 10.18632/oncotarget.7040
77. Zhuo Z, Wang A, Yu H. Metformin targeting autophagy overcomes progesterone resistance in endometrial carcinoma. *Arch Gynecol Obstet.* (2016) 294:1055–61. doi: 10.1007/s00404-016-4148-0
78. Barry JA, Azizia MM, Hardiman PJ. Risk of endometrial, ovarian and breast cancer in women with polycystic ovary syndrome: a systematic review and meta-analysis. *Hum Reprod Update* (2014) 20:748–58. doi: 10.1093/humupd/dmu012
79. Tan BK, Adya R, Chen J, Lehnert H, Sant Cassia LJ, Randeva HS. Metformin treatment exerts antiinvasive and antimetastatic effects in human endometrial carcinoma cells. *J Clin Endocrinol Metab.* (2011) 96:808–16. doi: 10.1210/jc.2010-1803
80. Viollet B, Guigas B, Sanz Garcia N, Leclerc J, Foretz M, Andreelli F. Cellular and molecular mechanisms of metformin: an overview. *Clin Sci.* (2012) 122:253–70. doi: 10.1042/CS20110386
81. El-Mir MY, Nogueira V, Fontaine E, Averet N, Rigoulet M, Leverve X. Dimethylbiguanide inhibits cell respiration via an indirect effect targeted on the respiratory chain complex I. *J Biol Chem.* (2000) 275:223–8. doi: 10.1074/jbc.275.1.223
82. Owen MR, Doran E, Halestrap AP. Evidence that metformin exerts its anti-diabetic effects through inhibition of complex 1 of the mitochondrial respiratory chain. *Biochem J.* (2000) 348(Pt. 3):607–14. doi: 10.1042/bj3480607
83. Zhou G, Myers R, Li Y, Chen Y, Shen X, Fenyk-Melody J, et al. Role of AMP-activated protein kinase in mechanism of metformin action. *J Clin Invest.* (2001) 108:1167–74. doi: 10.1172/JCI13505
84. Stephenne X, Foretz M, Taleux N, Van Der Zon GC, Sokal E, Hue L, et al. Metformin activates AMP-activated protein kinase in primary human hepatocytes by decreasing cellular energy status. *Diabetologia* (2011) 54:3101–10. doi: 10.1007/s00125-011-2311-5
85. Shaw RJ, Lamia KA, Vasquez D, Koo SH, Bardeesy N, Depinho RA, et al. The kinase LKB1 mediates glucose homeostasis in liver and therapeutic effects of metformin. *Science* (2005) 310:1642–6. doi: 10.1126/science.1120781
86. Dowling RJ, Zakikhani M, Fantus IG, Pollak M, Sonenberg N. Metformin inhibits mammalian target of rapamycin-dependent translation

initiation in breast cancer cells. *Cancer Res.* (2007) 67:10804–12. doi: 10.1158/0008-5472.CAN-07-2310
87. Wang Y, Xu W, Yan Z, Zhao W, Mi J, Li J, et al. Metformin induces autophagy and G0/G1 phase cell cycle arrest in myeloma by targeting the AMPK/mTORC1 and mTORC2 pathways. *J Exp Clin Cancer Res.* (2018) 37:63. doi: 10.1186/s13046-018-0731-5
88. Xie Y, Wang YL, Yu L, Hu Q, Ji L, Zhang Y, et al. Metformin promotes progesterone receptor expression via inhibition of mammalian target of rapamycin (mTOR) in endometrial cancer cells. *J Steroid Biochem Mol Biol.* (2011) 126:113–20. doi: 10.1016/j.jsbmb.2010.12.006
89. Zhang Z, Dong L, Sui L, Yang Y, Liu X, Yu Y, et al. Metformin reverses progestin resistance in endometrial cancer cells by downregulating GloI expression. *Int J Gynecol Cancer* (2011) 21:213–21. doi: 10.1097/IGC.0b013e318207dac7
90. Zhang J, Xu H, Zhou X, Li Y, Liu T, Yin X, et al. Role of metformin in inhibiting estrogen-induced proliferation and regulating ERalpha and ERbeta expression in human endometrial cancer cells. *Oncol Lett.* (2017) 14:4949–56. doi: 10.3892/ol.2017.6877
91. Harwood HJJr, Petras SF, Shelly LD, Zaccaro LM, Perry DA, Makowski MR, et al. Isozyme-nonselective N-substituted bipiperidylcarboxamide acetyl-CoA carboxylase inhibitors reduce tissue malonyl-CoA concentrations, inhibit fatty acid synthesis, and increase fatty acid oxidation in cultured cells and in experimental animals. *J Biol Chem.* (2003) 278:37099–111. doi: 10.1074/jbc.M304481200
92. Ning J, Clemmons DR. AMP-activated protein kinase inhibits IGF-I signaling and protein synthesis in vascular smooth muscle cells via stimulation of insulin receptor substrate 1 S794 and tuberous sclerosis 2 S1345 phosphorylation. *Mol Endocrinol.* (2010) 24:1218–29. doi: 10.1210/me.2009-0474
93. Karnevi E, Said K, Andersson R, Rosendahl AH. Metformin-mediated growth inhibition involves suppression of the IGF-I receptor signalling pathway in human pancreatic cancer cells. *BMC Cancer* (2013) 13:235. doi: 10.1186/1471-2407-13-235
94. Quinn BJ, Dallos M, Kitagawa H, Kunnumakkara AB, Memmott RM, Hollander MC, et al. Inhibition of lung tumorigenesis by metformin is associated with decreased plasma IGF-I and diminished receptor tyrosine kinase signaling. *Cancer Prev Res.* (2013) 6:801–10. doi: 10.1158/1940-6207.CAPR-13-0058-T
95. Yuan J, Zhang F, Niu R. Multiple regulation pathways and pivotal biological functions of STAT3 in cancer. *Sci Rep.* (2015) 5:17663. doi: 10.1038/srep17663
96. Tierney BJ, Mccann GA, Naidu S, Rath KS, Saini U, Wanner R, et al. Aberrantly activated pSTAT3-Ser727 in human endometrial cancer is suppressed by HO-3867, a novel STAT3 inhibitor. *Gynecol Oncol.* (2014) 135:133–41. doi: 10.1016/j.ygyno.2014.07.087
97. Accili D, Arden KC. FoxOs at the crossroads of cellular metabolism, differentiation, and transformation. *Cell* (2004) 117:421–6. doi: 10.1016/S0092-8674(04)00452-0
98. Matsuzaki H, Daitoku H, Hatta M, Tanaka K, Fukamizu A. Insulin-induced phosphorylation of FKHR (Foxo1) targets to proteasomal degradation. *Proc Natl Acad Sci USA.* (2003) 100:11285–90. doi: 10.1073/pnas.1934283100
99. Yun H, Park S, Kim MJ, Yang WK, Im DU, Yang KR, et al. AMP-activated protein kinase mediates the antioxidant effects of resveratrol through regulation of the transcription factor FoxO1. *FEBS J.* (2014) 281:4421–38. doi: 10.1111/febs.12949
100. Laskov I, Abou-Nader P, Amin O, Philip CA, Beauchamp MC, Yasmeen A, et al. Metformin increases E-cadherin in tumors of diabetic patients with endometrial cancer and suppresses epithelial-mesenchymal transition in endometrial cancer cell lines. *Int J Gynecol Cancer* (2016) 26:1213–21. doi: 10.1097/IGC.0000000000000761
101. Dong L, Zhou Q, Zhang Z, Zhu Y, Duan T, Feng Y. Metformin sensitizes endometrial cancer cells to chemotherapy by repressing glyoxalase I expression. *J Obstet Gynaecol Res.* (2012) 38:1077–85. doi: 10.1111/j.1447-0756.2011.01839.x
102. Uehara T, Mitsuhashi A, Tsuruoka N, Shozu M. Metformin potentiates the anticancer effects of cisplatin under normoxic conditions *in vitro*. *Oncol Rep.* (2015) 33:744–50. doi: 10.3892/or.2014.3611
103. Markowska A, Pawalowska M, Filas V, Korski K, Grybos M, Sajdak S, et al. Does Metformin affect ER, PR, IGF-1R, beta-catenin and PAX-2 expression in women with diabetes mellitus and endometrial cancer? *Diabetol Metab Syndr.* (2013) 5:76. doi: 10.1186/1758-5996-5-76
104. Schrauwen S, Coenegrachts L, Cattaneo A, Hermans E, Lambrechts D, Amant F. The antitumor effect of metformin with and without carboplatin on primary endometrioid endometrial carcinoma *in vivo*. *Gynecol Oncol.* (2015) 138:378–82. doi: 10.1016/j.ygyno.2015.06.006
105. Chandel NS, Avizonis D, Reczek CR, Weinberg SE, Menz S, Neuhaus R, et al. Are metformin doses used in murine cancer models clinically relevant? *Cell Metab.* (2016) 23:569–70. doi: 10.1016/j.cmet.2016.03.010
106. Curry J, Johnson J, Tassone P, Vidal MD, Menezes DW, Sprandio J, et al. Metformin effects on head and neck squamous carcinoma microenvironment: window of opportunity trial. *Laryngoscope* (2017) 127:1808–15. doi: 10.1002/lary.26489
107. Rivadeneira DB, Delgoffe GM. Antitumor T-cell reconditioning: improving the metabolic fitness for optimal cancer immunotherapy. *Clin Cancer Res.* (2018) 24:2473–81. doi: 10.1158/1078-0432.CCR-17-0894
108. Sharping NE, Menk AV, Whetstone RD, Zeng X, Delgoffe GM. Efficacy of PD-1 blockake is potentiated by metformin-induced reduction of tumor hypoxia. *Cancer Immunol Res.* (2017) 5:9–16. doi: 10.1158/2326-6066.CIR-16-0103
109. Wang JC, Sun X, Ma Q, Fu GF, Cong LL, Zhang H, et al. Metformin's antitumor and anti-angiogenic activities are mediated by skewing macrophage polarization. *J Cell Mol Med.* (2018) 22:3825–936. doi: 10.1111/jcmm.13655
110. Tabrizi AD, Melli MS, Foroughi M, Ghojazadeh M, Bidadi S. Antiproliferative effect of metformin on the endometrium–a clinical trial. *Asian Pac J Cancer Prev.* (2014) 15:10067–70. doi: 10.7314/APJCP.2014.15.23.10067
111. Laskov I, Drudi L, Beauchamp MC, Yasmeen A, Ferenczy A, Pollak M, et al. Anti-diabetic doses of metformin decrease proliferation markers in tumors of patients with endometrial cancer. *Gynecol Oncol.* (2014) 134:607–14. doi: 10.1016/j.ygyno.2014.06.014
112. Mitsuhashi A, Kiyokawa T, Sato Y, Shozu M. Effects of metformin on endometrial cancer cell growth *in vivo*: a preoperative prospective trial. *Cancer* (2014) 120:2986–95. doi: 10.1002/cncr.28853
113. Li X, Guo YR, Lin JF, Feng Y, Billig H, Shao R. Combination of diane-35 and metformin to treat early endometrial carcinoma in PCOS women with insulin resistance. *J Cancer* (2014) 5:173–81. doi: 10.7150/jca.8009
114. Schuler KM, Rambally BS, Difurio MJ, Sampey BP, Gehrig PA, Makowski L, et al. Antiproliferative and metabolic effects of metformin in a preoperative window clinical trial for endometrial cancer. *Cancer Med.* (2015) 4:161–73. doi: 10.1002/cam4.353
115. Sivalingam VN, Kitson S, Mcvey R, Roberts C, Pemberton P, Gilmour K, et al. Measuring the biological effect of presurgical metformin treatment in endometrial cancer. *Br J Cancer* (2016) 114:281–9. doi: 10.1038/bjc.2015.453
116. Cai D, Sun H, Qi Y, Zhao X, Feng M, Wu X. Insulin-like growth factor 1/mammalian target of rapamycin and AMP-activated protein kinase signaling involved in the effects of metformin in the human endometrial cancer. *Int J Gynecol Cancer* (2016) 26:1667–72. doi: 10.1097/IGC.0000000000000818
117. Soliman PT, Zhang Q, Broaddus RR, Westin SN, Iglesias D, Munsell MF, et al. Prospective evaluation of the molecular effects of metformin on the endometrium in women with newly diagnosed endometrial cancer: a window of opportunity study. *Gynecol Oncol.* (2016) 143:466–71. doi: 10.1016/j.ygyno.2016.10.011
118. Mitsuhashi A, Sato Y, Kiyokawa T, Koshizaka M, Hanaoka H, Shozu M. Phase II study of medroxyprogesterone acetate plus metformin as a fertility-sparing treatment for atypical endometrial hyperplasia and endometrial cancer. *Ann Oncol.* (2016) 27:262–6. doi: 10.1093/annonc/mdv539
119. Zhao Y, Sun H, Feng M, Zhao J, Zhao X, Wan Q, et al. Metformin is associated with reduced cell proliferation in human endometrial cancer by inbibiting PI3K/AKT/mTOR signaling. *Gynecol Endocrinol.* (2018) 34:428–32. doi: 10.1080/09513590.2017.1409714
120. Warburg O, Wind F, Negelein E. The metabolism of tumors in the body. *J Gen Physiol.* (1927) 8:519–30. doi: 10.1085/jgp.8.6.519

121. Fu Y, Liu S, Yin S, Niu W, Xiong W, Tan M, et al. The reverse Warburg effect is likely to be an Achilles' heel of cancer that can be exploited for cancer therapy. *Oncotarget* (2017) 8:57813–25. doi: 10.18632/oncotarget.18175
122. Nieman KM, Kenny HA, Penicka CV, Ladanyi A, Buell-Gutbrod R, Zillhardt MR, et al. Adipocytes promote ovarian cancer metastasis and provide energy for rapid tumor growth. *Nat Med.* (2011) 17:1498–503. doi: 10.1038/nm.2492
123. Romero IL, Mukherjee A, Kenny HA, Litchfield LM, Lengyel E. Molecular pathways: trafficking of metabolic resources in the tumor microenvironment. *Clin Cancer Res.* (2015) 21:680–6. doi: 10.1158/1078-0432.CCR-14-2198
124. Pavlides S, Whitaker-Menezes D, Castello-Cros R, Flomenberg N, Witkiewicz AK, Frank PG, et al. The reverse Warburg effect: aerobic glycolysis in cancer associated fibroblasts and the tumor stroma. *Cell Cycle* (2009) 8:3984–4001. doi: 10.4161/cc.8.23.10238
125. Chiavarina B, Whitaker-Menezes D, Migneco G, Martinez-Outschoorn UE, Pavlides S, Howell A, et al. HIF1-alpha functions as a tumor promoter in cancer associated fibroblasts, and as a tumor suppressor in breast cancer cells: autophagy drives compartment-specific oncogenesis. *Cell Cycle* (2010) 9:3534–51. doi: 10.4161/cc.9.17.12908
126. Martinez-Outschoorn UE, Balliet RM, Rivadeneira DB, Chiavarina B, Pavlides S, Wang C, et al. Oxidative stress in cancer associated fibroblasts drives tumor-stroma co-evolution: a new paradigm for understanding tumor metabolism, the field effect and genomic instability in cancer cells. *Cell Cycle* (2010) 9:3256–76. doi: 10.4161/cc.9.16.12553
127. Pavlides S, Tsirigos A, Vera I, Flomenberg N, Frank PG, Casimiro MC, et al. Transcriptional evidence for the "Reverse Warburg Effect" in human breast cancer tumor stroma and metastasis: similarities with oxidative stress, inflammation, Alzheimer's disease, and "Neuron-Glia Metabolic Coupling". *Aging* (2010) 2:185–99. doi: 10.18632/aging.100134
128. Bonuccelli G, Whitaker-Menezes D, Castello-Cros R, Pavlides S, Pestell RG, Fatatis A, et al. The reverse Warburg effect: glycolysis inhibitors prevent the tumor promoting effects of caveolin-1 deficient cancer associated fibroblasts. *Cell Cycle* (2010) 9:1960–71. doi: 10.4161/cc.9.10.11601
129. Ko YH, Lin Z, Flomenberg N, Pestell RG, Howell A, Sotgia F, et al. Glutamine fuels a vicious cycle of autophagy in the tumor stroma and oxidative mitochondrial metabolism in epithelial cancer cells: implications for preventing chemotherapy resistance. *Cancer Biol Ther.* (2011) 12:1085–97. doi: 10.4161/cbt.12.12.18671
130. Whitaker-Menezes D, Martinez-Outschoorn UE, Lin Z, Ertel A, Flomenberg N, Witkiewicz AK, et al. Evidence for a stromal-epithelial "lactate shuttle" in human tumors: MCT4 is a marker of oxidative stress in cancer-associated fibroblasts. *Cell Cycle* (2011) 10:1772–83. doi: 10.4161/cc.10.11.15659
131. Fiaschi T, Marini A, Giannoni E, Taddei ML, Gandellini P, De Donatis A, et al. Reciprocal metabolic reprogramming through lactate shuttle coordinately influences tumor-stroma interplay. *Cancer Res.* (2012) 72:5130–40. doi: 10.1158/0008-5472.CAN-12-1949
132. Goodwin ML, Jin H, Straessler K, Smith-Fry K, Zhu JF, Monument MJ, et al. Modeling alveolar soft part sarcomagenesis in the mouse: a role for lactate in the tumor microenvironment. *Cancer Cell* (2014) 26:851–62. doi: 10.1016/j.ccell.2014.10.003
133. Sousa CM, Biancur DE, Wang X, Halbrook CJ, Sherman MH, Zhang L, et al. Pancreatic stellate cells support tumour metabolism through autophagic alanine secretion. *Nature* (2016) 536:479–83. doi: 10.1038/nature19084
134. Latif A, Chadwick AL, Kitson SJ, Gregson HJ, Sivalingam VN, Bolton J, et al. Monocarboxylate transporter 1 (MCT1) is an independent prognostic biomarker in endometrial cancer. *BMC Clin Pathol.* (2017) 17:27. doi: 10.1186/s12907-017-0067-7
135. Zhao L, Zhou S, Zou L, Zhao X. The expression and functionality of stromal caveolin 1 in human adenomyosis. *Hum Reprod.* (2013) 28:1324–38. doi: 10.1093/humrep/det042
136. Cheong JH, Park ES, Liang J, Dennison JB, Tsavachidou D, Nguyen-Charles C, et al. Dual inhibition of tumor energy pathway by 2-deoxyglucose and metformin is effective against a broad spectrum of preclinical cancer models. *Mol Cancer Ther.* (2011) 10:2350–62. doi: 10.1158/1535-7163.MCT-11-0497
137. Kim EH, Lee JH, Oh Y, Koh I, Shim JK, Park J, et al. Inhibition of glioblastoma tumorspheres by combined treatment with 2-deoxyglucose and metformin. *Neuro Oncol.* (2017) 19:197–207. doi: 10.1093/neuonc/now174

Conflict of Interest Statement: The authors declare that the research was conducted in the absence of any commercial or financial relationships that could be construed as a potential conflict of interest.

frontiers in Oncology

ORIGINAL RESEARCH
published: 23 August 2018
doi: 10.3389/fonc.2018.00328

Benzylamine and Thenylamine Derived Drugs Induce Apoptosis and Reduce Proliferation, Migration and Metastasis Formation in Melanoma Cells

Marina Mojena[1†], Adrián Povo-Retana[1†], Silvia González-Ramos[1,2†], Victoria Fernández-García[1], Javier Regadera[3], Arturo Zazpe[4], Inés Artaiz[4], Paloma Martín-Sanz[1,2], Francisco Ledo[4] and Lisardo Boscá[1,2*]*

[1] Instituto de Investigaciones Biomédicas Alberto Sols (CSIC-UAM), Madrid, Spain, [2] Centro de Investigación Biomédica en Red de Enfermedades Cardiovasculares y Hepáticas y Digestivas, ISC III, Madrid, Spain, [3] Departamento de Anatomía, Histología y Neurociencia, Facultad de Medicina, Universidad Autónoma de Madrid, Madrid, Spain, [4] R&D+i Department Faes-Farma, Avda Autonomía, Leioa, Spain

Melanomas are heterogeneous and aggressive tumors, and one of the worse in prognosis. Melanoma subtypes follow distinct pathways until terminal oncogenic transformation. Here, we have evaluated a series of molecules that exhibit potent cytotoxic effects over the murine and human melanoma cell lines B16F10 and MalMe-3M, respectively, both *ex vivo* and in animals carrying these melanoma cells. *Ex vivo* mechanistic studies on molecular targets involved in melanoma growth, migration and viability were evaluated in cultured cells treated with these drugs which exhibited potent proapoptotic and cytotoxic effects and reduced cell migration. These drugs altered the Wnt/β-catenin pathway, which is important for the oncogenic phenotype of melanoma cells. In *in vivo* experiments, male C57BL/6 or nude mice were injected with melanoma cells that rapidly expanded in these animals and, in some cases were able to form metastasis in lungs. Treatment with anti-tumor drugs derived from benzylamine and 2-thiophenemethylamine (F10503LO1 and related compounds) significantly attenuated tumor growth, impaired cell migration, and reduced the metastatic activity. Several protocols of administration were applied, all of them leading to significant reduction in the tumor size and enhanced animal survival. Tumor cells carrying a luciferase transgene allowed a time-dependent study on the progression of the tumor. Molecular analysis of the pathways modified by F10503LO1 and related compounds defined the main relevant targets for tumor regression: the activation of pro-apoptotic and anti-proliferative routes. These data might provide the proof-of-principle and rationale for its further clinical evaluation.

Keywords: melanoma, cytotoxicity, chemotherapy, cellular lines, animal models, metastasis, apoptosis

OPEN ACCESS

Edited by:
Ramon Bartrons, University of Barcelona, Spain

Reviewed by:
Pedro A. Lazo, Instituto de Biología Molecular y Celular del Cancer (IBMCC), Spain
Ahmed Lasfar, Rutgers University, The State University of New Jersey, United States

****Correspondence:***
Francisco Ledo
fledo@gesgenericos.com
Lisardo Boscá
lbosca@iib.uam.es

[†] These authors have contributed equally to the work

Specialty section:
This article was submitted to Molecular and Cellular Oncology, a section of the journal Frontiers in Oncology

Received: *05 May 2018*
Accepted: *31 July 2018*
Published: *23 August 2018*

Citation:
Mojena M, Povo-Retana A, González-Ramos S, Fernández-García V, Regadera J, Zazpe A, Artaiz I, Martín-Sanz P, Ledo F and Boscá L (2018) Benzylamine and Thenylamine Derived Drugs Induce Apoptosis and Reduce Proliferation, Migration and Metastasis Formation in Melanoma Cells. Front. Oncol. 8:328. doi: 10.3389/fonc.2018.00328

INTRODUCTION

Metastatic melanoma is one of the most therapeutically difficult cancers to be treated, mainly at advanced stages of diagnosis. The incidence of metastatic melanoma has been increasing around the World over the past decades, and death rates rose faster than for other cancers, being melanoma one of the worse in prognosis (1–3). In fact, the mean overall survival of melanoma patients with unresectable distant metastases remains to be less than 1 year (4). Clinical management of melanoma patients also represents a clinical challenge because the lack of contrasted protocols (5–7). This is in addition to the absence of reliable biomarkers identifying groups of patients who could benefit from more specific treatments (8). Many patients are excluded from novel therapies only because of fast high-speed progression of the disease before a clinical positive response can be expected (9, 10). Taken these facts together, consensus exists in the field suggesting that significant improvements of the overall survival rates of melanoma cohorts require an initial fast response to treatment as an inclusion condition (11). Long-term survival could then be achieved by an increased rate of complete responses or long-term stabilization of partial responses in what is defined in the melanoma field as *consolidation phase* (2, 7, 12). The discovery of the frequent BRAF(V600E) mutation in human melanoma tumors offered the first opportunity to develop an oncogene-directed therapy for these patients profiting the use of selective inhibitors of constitutive BRAF activity (11, 13–16). The fact that melanoma cells express activating mutations in BRAF, but not in A-RAF or C-RAF, allowed the development of the small-molecule drug PLX4032, an orally available and well-tolerated selective BRAF inhibitor. Clinical trials demonstrated its therapeutic value for melanomas carrying the activating BRAF mutation. Due to the RAS/RAF/MEK/ERK pathway deregulation in ca. 90% of malignant melanomas, MEK is a current target in drug development and in clinical trials (11, 13, 17–19). However, dose-limiting side effects are observed, and MEK inhibitors that reduce ERK activation in patients show a low clinical response, probably because MEK inhibition promotes an imbalanced compensatory cell signaling that reduces the therapeutic value of these drugs. Several groups have found that BRAF inhibitor-resistant melanoma cell lines can recover ERK phosphorylation independently of the presence of BRAF inhibitors, and the same remains true for the classic chemotherapeutic drug dacarbazine (DTIC) (11, 13, 17, 18, 20–24). For these reasons, the development of novel small molecules that could counteract resistance mechanisms constitutes a first line of research in the melanoma field. Progress in molecular-targeted melanoma therapies have shown significant successful responses in the reduction of tumor size and increased survival in patients (4, 11, 13, 18, 20, 22, 24–27).

In this work, we analyzed the effect of a series of benzylamine/2-thiophenemethylamine (thenylamine)-derived compounds, being F10503LO1 the lead molecule, which exhibited antitumoral activity over a panel of melanoma tumors (NCI-60 human tumor cell lines screen). These drugs have been assayed in different human and rodent cell lines, from hepatoma to leukemia, with consistent results on growth arrest and induction of apoptosis/necrosis in tumor cells. The target of choice was the very aggressive murine melanoma B16F10 and the human melanoma MalMe-3M cell line. Interestingly, both tumor cell lines express the wild type forms of BRAF and p53, offering the possibility to be used as targets for alternative drugs for the treatment of melanoma cells with activating mutations of the BRAF and Ras oncogenes. Our data indicate that these molecules exhibit a potent cytotoxic/antiproliferative activity *in vitro* and in animal models bearing the melanoma cells. These results provide the basis for a meticulous study on the dissection of pathways involved in the mechanism of action of these compounds. Indeed, our studies suggest that the metastatic capacity of both aggressive tumors can be impaired after administration of F10503LO1, providing novel strategies in preventing the dissemination of melanoma cells.

MATERIALS AND METHODS

Materials

Reagents were from Sigma-Aldrich-Merck (St Louis, MO, USA) or Roche (Darmstadt, Germany). Murine cytokines and TNFα, IL6, and PGE_2 ELISA kits were obtained from PeproTech (London, UK) and Cayman Chem. (Ann Arbor, MI). Antibodies were from Abcam (Cambridge, UK) or Cell Signaling (Danvers, MA, USA). Dacarbazine (DTIC) was from TEVA (Petaj Tikva, IL). Reagents for electrophoresis were from Bio-Rad (Hercules, CA, USA). Tissue culture dishes were from Falcon (Lincoln Park, NJ, USA), and serum and culture media were from Invitrogen (ThermoFisher, Madrid, Spain).

Animal Care and Preparation of Macrophages

Male C57BL/6 and athymic nude mice 12 ± 4-week-old were used and housed under 12 h light/dark cycle and food and water was provided *ad libitum*. Animals were treated following directive 2010/63/EU of the European Parliament. Bone marrow derived macrophages (MF) were obtained from male C57BL/6 mice by flushing pelvises, femurs, and tibiae with DMEM. Bone marrow mononuclear phagocytic precursor cells were propagated in suspension by culturing in DMEM containing 10% FBS, 100 U/ml penicillin, 100 mg/l streptomycin, and 0.2 nM recombinant murine M-CSF (PeproTech) in tissue-culture plates. Precursor cells became adherent within 7 days of culture. MF cells were maintained in RPMI 1640 medium supplemented with 10% FBS for 14 h prior to use.

Preparation of Chemotherapeutic Molecules (F10503LO1, F21010RS1–benzylamines-and F60472RS1−2-Thiophenemethylamine or Thenylamine-)

Solid samples (**Table 1**) were stored in a silica gel container at 4°C, and dissolved in DMSO to prepare 10 mM stock solutions maintained at −20°C. Further dilutions were prepared in PBS and the equivalent amount of DMSO was used as control for administration to the cells (*in vitro* assays) or to the animals.

TABLE 1 | Chemical structure of the drugs.

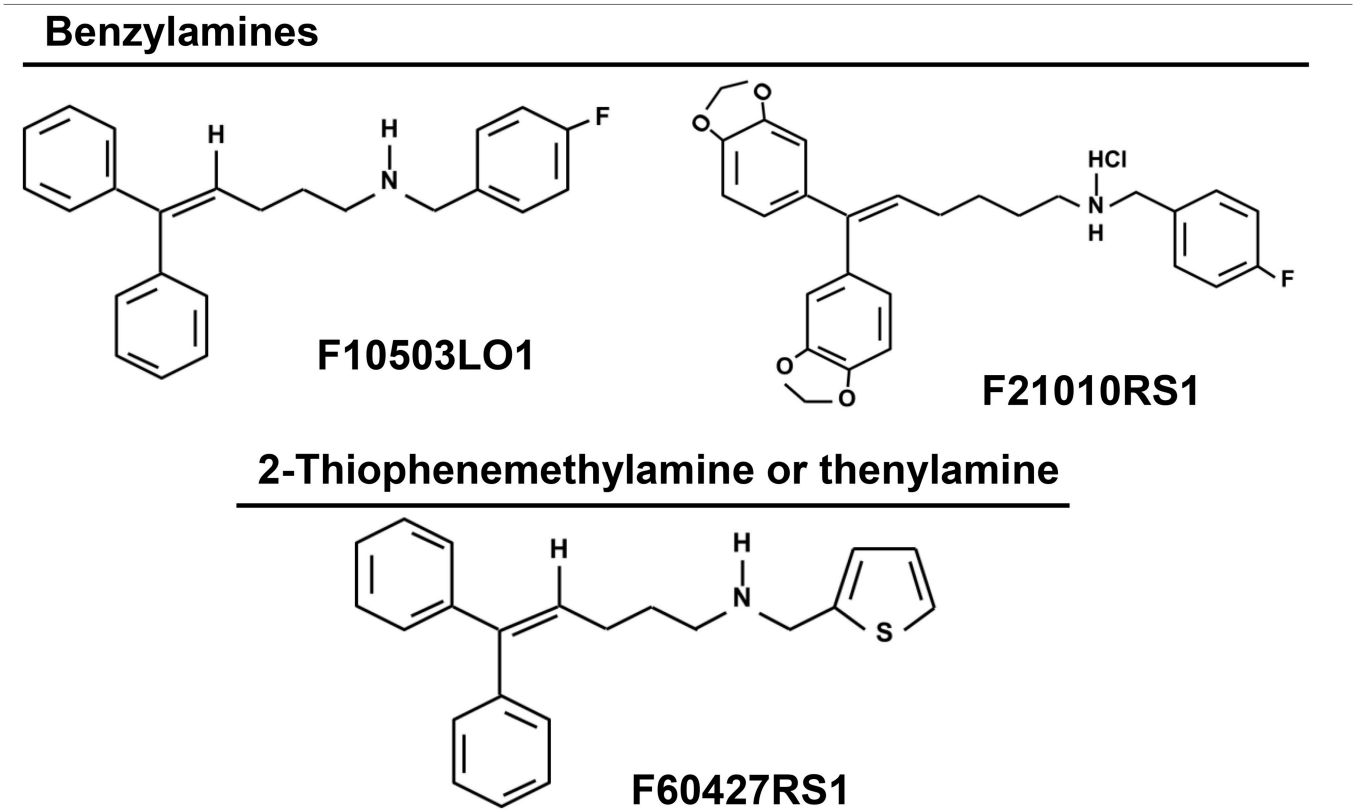

The benzylamine derivatives F10503LO1 and F21010RS1 and the 2-thiophenemethylamine derivative (thenylamine) F60427RS1 are represented.

When F10503LO1 was dissolved in N,N′-dimethyl acetamide (DMA) solution (5% vol:vol of DMA in saline-glucose 5% w:vol), this was prepared on a daily basis in pure DMA and then adding the glucose solution until the final volume was reached. Control animals received the maximal amount of DMA solution lacking F10503LO1.

In vivo Administration of Melanoma Cells

Mice (12 ± 4 weeks-old) were injected 10^6 cells (200 µl) from the B16F10 melanoma cell line, carrying a luciferase transgene. At the indicated days, F10503LO1 or vehicle (DMSO in PBS as for the drug, or DMA in saline-glucose) were i.p. or i.v. administered. Dacarbazine (DTIC), an alkylating chemotherapeutic agent, was used as reference compound for melanoma treatment and was administered i.p. at 30 mg/kg. For measurement of the tumor growth, animals received i.p. 300 µl of 15 mg/ml luciferine. Luminescence was measured in an IVIS Lumina *in vivo* imaging system (Perkin Elmer, Madrid, ES) under deep anesthesia (isofluorane). Luminescence was recorded each 4 min, with a 1 min capture, repeating the cycle 10 times. The software of the program provides the total area of the luminescence and its quantification.

Measurement of Serum Markers

The starting experiments were carried out in male C57/BL6 mice (12 ± 4-wks-old), and an evaluation of the effect of i.p. administration of F10503LO1 on the main biochemical markers of injury was carried out. Animals were challenged with DMSO/PBS (DMSO at the concentration prevailing in the drug administration), or F10503LO1 i.p. at 30 mg/kg at day 1; days 1 to 4; days 1 to 6. Serum was obtained at days 7 and 14 by retroortibal punction. The serum levels of transaminases (GOT and GPT), gamma-glutamyltransferase (GGT), glucose, lactate, triglycerides, cholesterol, uric acid, creatinine and hemoglobin were determined using specific analyte strips (Reflotron; Roche) and measuring the enzyme kinetics in a spectrophotometer. The levels of cholesterol (<100 mg/dl), uric acid (<2 mg/dl), creatinine (<5 mg/dl) and triglycerides (<35 mg/dl) remained indistinguishable between both animal groups at days 7 and 14. These data show a modest impact of F10503LO1 (30 mg/kg; i.p.) on hepatic markers, with an excellent recovery after 1 week without treatment. In addition to this, the absence of changes in creatinine levels, marker of kidney injury, suggested negligible kidney toxicity.

Evaluation of Drug Toxicity Over Myeloid Cells

Animals received two consecutive doses of F10503LO1 (30 mg/kg) or vehicle, and the distribution of myeloid cells was determined in blood, bone marrow and spleen on the third day. To analyze leukocyte subpopulations, after euthanizing mice,

blood was collected, and spleens and femurs were harvested. All single cell suspensions were subjected to red-blood-cell lysis, incubated with proper dye-conjugated antibodies against CD45, CD115, Ly6G, CD11b, Ly6C, and F4/80 and analyzed in a FACSCanto II flowcytometer (BD). For cell counting, absolute counting beads were used.

Evaluation of Cell Viability by Flow-Cell Cytometry

To quantify apoptosis cells were harvested and washed in ice-cold PBS. After centrifugation at 4°C for 5 min, cells were resuspended in annexin V-binding buffer (10 mM HEPES; pH 7.4, 140 mM NaCl, 2.5 mM $CaCl_2$). Cells were labeled with annexin V-FITC solution (BD Biosciences, San Jose, CA) and/or propidium iodide (PI; 10 μg/ml) for 15 min at room temperature in the dark. PI is impermeable to living and apoptotic cells, but stains necrotic and apoptotic dying cells with impaired membrane integrity, in contrast to annexin V, which stains early apoptotic cells. Quantification of positive cells was done in a FACSCanto II flowcytometer (BD). Z-VAD-FMK (carbobenzoxy-valyl-alanyl-aspartyl-O-methyl-fluoromethylketone) was used at 20 μM to inhibit caspases.

Measurement of Caspase Activity

Cell extracts were prepared at the indicated times and the activity of caspase 3 and caspase 9 were determined using specific commercial fluorimetric kits (Sigma-Aldrich-Merck).

Measurement of Mitochondrial Inner Membrane Potential

To measure the mitochondrial inner membrane potential, cells were incubated at 37°C for 15 min in the presence of 30 nM chloromethyl X-rosamine (CMXRos; ThermoFisher), followed by immediate analysis of fluorochrome incorporation in a FACScanto II flow cytometer. Incubation of the cells with 200 nM of staurosporine was used as a control to induce full mitochondrial-dependent apoptosis as described (28).

Measurement of Accumulation of Cytokines, Prostaglandin and NO in the Cell Culture Medium

The accumulation of TNF-α, IL-6, and PGE_2 in the culture medium was measured per triplicate using commercial kits, following the indications of the supplier. Nitric oxide accumulation in the culture medium was measured as nitrite plus nitrate, as previously described (29).

Histological Examination of Fixed Sections

Anatomopathological analyses were performed using 3 to 5 tumors from each experimental group. Tissue samples were fixed in 10% buffered formalin and embedded in paraffin, and 4-μm sections were prepared. Hematoxylin/eosin stain was used for analysis to assess morphological changes, using a light microscope (Zeiss x20 and x40 images). Examinations of the slides were performed in a blinded fashion.

Infiltration of B16F10 in Tissues

To evaluate metastatic/migratory B16F10 melanoma cells, tissues (lung in particular) were homogenized with 20 mM Hepes, pH 7.4; 100 mM KCl, 5 mM $MgCl_2$, 2 mM DTT and luciferease activity was measured in a luminometer using the luciferase assay kit from Promega (WI, USA), following the instructions of the supplier. Usually, 10 μg of protein were assayed in 0.5 ml of reaction mixture.

Preparation of Protein Cell Extracts

Macrophages total protein extracts were prepared after homogenization in a buffer containing 10 mM Tris-HCl, pH 7.5; 1 mM $MgCl_2$, 1 mM EGTA, 10% glycerol, 0.5% CHAPS, 1 mM β-mercaptoethanol and a protease and phosphatase inhibitor cocktail (Sigma). The extracts were vortexed for 30 min at 4°C and after centrifuging for 20 min at 13,000 g, the supernatants were stored at −20°C. When cytosolic and nuclear extracts were prepared, cells were homogenized and processed as previously described (30). Protein levels were determined using Bradford reagent (Bio-Rad).

Western Blotting

Protein extracts were boiled in loading buffer (250 mM Tris-HCl; pH 6.8, 2% SDS, 10% glycerol, and 2% β-mercaptoethanol) and 30 μg of protein were subjected to 8–10% SDS-PAGE electrophoresis gels. Proteins were transferred into polyvinylidene difluoride membranes (GE Healthcare). Membranes were incubated for 1 h with low-fat milk powder (5%) in PBS containing 0.1% Tween-20. Blots were incubated for 2 h or overnight at 4°C with primary antibodies at the dilutions recommended by the suppliers. The blots were developed with ECL Advance protocol (GE Healthcare) and different exposure times were performed for each blot in an ImageQuant analyzer (LAS 500, GE Healthcare) to ensure the linearity of the band intensities. Blots were normalized for lane charge using antibodies against GAPDH.

RNA Isolation and qRT-PCR Analysis

RNA was extracted with TRIzol Reagent (ThermoFisher) and reverse transcribed using Transcriptor First Strand cDNA Synthesis Kit for RT-PCR following the indications of the manufacturer (Thermo-Fisher). Real-time PCR was conducted with SYBR Green Master on a MyiQ Real-Time PCR System (Bio-Rad). Primer oligonucleotide sequences are available on request. Validation of amplification efficiency was performed for each pair of primers (29). PCR thermocycling parameters were 95°C for 10 min, 40 cycles of 95°C for 15 s, and 60°C for 1 min. Each sample was run in duplicate and was normalized vs. 36B4. The fold induction (FI) was determined in a ΔΔCt based fold-change calculation.

Statistical Analysis

Unless otherwise stated, data are the mean ± standard deviation. To compare means between two independent samples Mann-Whitney rank sum test was used. Data were analyzed by SPSS for Windows statistical package version v21. Analysis of statistical

significance of Kaplan-Meier curves was performed using the Mantel-Cox test. The results were considered significant at $p < 0.05$.

RESULTS

Specific Effects of New Benzylamine- and Thenylamine-Derived Anti-tumor Drugs on Melanoma Cells

The compounds under study were initially characterized by their capacity to interact with adaptor molecules of the NF-κB pathway, a transcription factor involved in oncogenic processes (31), and were tested in the NCI-60 cell line panel that contained 8 melanoma cell lines. Most of these cells were sensitive to the lead drugs used in this study. For this reason, several assays were performed to evaluate the action of the drugs shown in **Table 1**, on early NF-κB signaling and on cell viability. As **Figure 1A** shows, the benzylamines F10503LO1 and F21010RS1 failed to modify IκBα levels or the LPS-dependent IκBα degradation in macrophages. Moreover, in murine macrophages stimulated with LPS these drugs minimally altered the accumulation of nitrate plus nitrite (**Figure 1B**), PGE_2, TNFα, and IL6 (**Figure 1C**) or lactate in the culture medium, including the inhibition of the PFKFB3 with the selective inhibitor 3PO (**Figure 1D**) in LPS stimulated cells. Together, the data indicate that these drugs did not affect the transcription dependent on NF-κB activity. Interestingly, these drugs promoted a loss in viability of human (MalMe-3M) and murine (B16F10) melanoma cell lines, but not in other cells such as resting macrophages (**Figure 1E**) or resting T and B cells (not shown). Indeed, incubation of melanoma cell lines with F10503LO1 induced a dose-dependent loss in viability, with $I_{0.5}$ *ca.* 500 nM (**Figure 1F**). This cell death was accompanied by a dose-dependent decrease in the mitochondrial inner membrane potential (**Figure 1G**), and was partially prevented by the broad caspase inhibitor z-VAD, as deduced by a reduction in the percentage of annexin V-positive cells (**Figure 1H**). The time course of melanoma apoptotic death is shown in **Figure 1I**.

In vitro Analysis of the Effect of Benzylamine and Thenylamine Chemotherapeutic Drugs on Murine Melanoma B16F10 Cells

B16F10 melanoma cells constitutively exhibit AKT phosphorylation. Treatment with F10503LO1 or F60427RS1 decreased pAKT levels and promoted PARP and caspase 3 activation (**Figure 2A**). Moreover, measurement of caspase 3 and caspase 9 activities in the cell extracts showed a time-dependent increase in B16F10 cells treated with benzylamine or thenylamine drugs (**Figure 2B**). These data support the induction of apoptosis in these cells after treatment with these compounds. Indeed, the levels of anti-apoptotic proteins, such as Bcl-xL and to a lesser extent Bcl2, declined and a rise in pro-apoptotic proteins, such as Bax, was observed (**Figure 2C**). A time-dependent cleavage of PARP was evidenced, with minimal changes in p53 that usually increase in apoptotic cells (**Figure 2C**). In addition to this, treatment of B16F10 cells with F10503LO1 or F60427RS1 induced a degradation of β-catenin that was also reflected in a downregulation in the corresponding mRNA levels (**Figures 2D,E**). These changes were accompanied by a decrease in the nuclear content of β-catenin and in the mRNA levels of *Ctnnb1* (**Figure 2E**). This drop in *Ctnnb1* was quite selective since the mRNA levels of other genes involved in inflammation remained minimally affected (**Figure 2F**, upper panel). Interestingly, *Myc* and *Bcl2* exhibited a decrease at 1 and 18 h, whereas classic stemness genes, such as *Nanog*, *Oct4* or *Sox2* increased in cells treated with F60427RS1 (**Figure 2F**, lower panel), suggesting the existence of specific responses that differentiate the action of benzylamine and thenylamine drugs.

Melanoma Cell Migration Is Inhibited by F10503LO1

In addition to the effects observed on cell viability, 200 nM of F10503LO1, F21010RS1 or F60427RS1 significantly inhibited B16F10 and MalMe-3M cell migration in a transwell assay (**Figure 3A**). Moreover, melanoma cell motion was also rapidly blocked in a dose-dependent manner suggesting that even doses that are only moderately toxic for these cells decreased their capacity to migrate (**Figure 3B**, **Supplementary Videos v1_B16F10**, **v2_MalMe-3M**).

In vivo Effects of F10503LO1

To gain insight on the *in vivo* effects of these drugs, a series of experiments were done in C57BL/6 and in nude mice. As **Figure 4A** shows, pre-treatment of B16F10 cells for 1 h with 5 μM of F10503 followed by administration in the right flank of mice resulted in a significant inhibition of tumor growth vs. the administration of untreated cells in the contralateral flank, as reflected by *in vivo* luciferase imaging and by the size of the tumors. Subsequently, animals received 2×10^5 B16F10 cells in each flank and 5 h later were i.p. administered 30 mg/kg of F10503LO1 in 200 μl or vehicle. F10503LO1 was provided on a daily basis for 14 days and the *in vivo* luciferase activity was measured at days 3 and 7. At the end of the experiment, tumors were removed, weighted and used for anatomopathological analysis and biochemical processing (**Figure 4B**). One important point is the evaluation of the broad toxicity of the therapeutic drugs. As **Figure 5A** shows, F10503LO1 administration during the indicated periods exhibited a moderate rise in serum transaminase levels, and normalization was observed at day 14, suggesting a moderate liver toxicity. The glucose, cholesterol, triglycerides, hemoglobin, creatinine and uric acid concentrations were not affected by the drug (not shown). In addition to this, in animals carrying B16F10 cells and treated i.p. with F10503LO1, the classic chemotherapeutic drug DTIC or combinations of these, the drugs affected moderately transaminases, and other markers, such as gamma-glutamyltranspeptidase (bile duct injury), and alkaline phosphatase (liver and gallbladder injury), but not α-amylase (pancreas injury), glucose and blood lipid levels (cholesterol and triglycerides; not shown) or creatinine (kidney

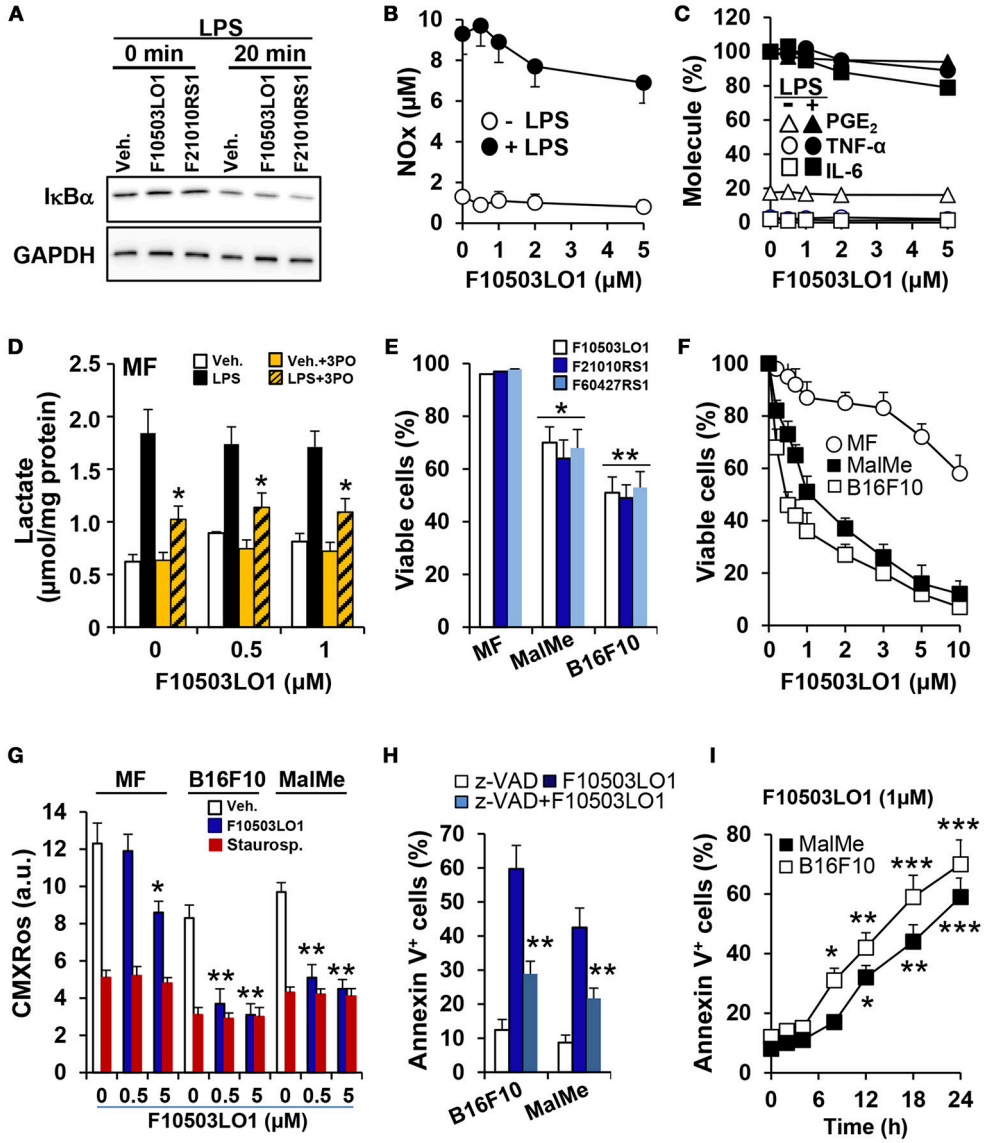

FIGURE 1 | Effect of benzylamine- and thenylamine-derived drugs on cell viability and function. **(A)** Bone marrow derived macrophages (MF) were incubated for 30 min with 1 μM of the indicated molecules or vehicle, followed by challenge with 200 ng/ml of LPS. The degradation of IκBα was evaluated by immunoblot. **(B–D)** The dose-dependent effect vs. F10503LO1 on the accumulation in the culture medium of nitrates and nitrites (in μM), IL6, TNFα, PGE_2 (expressed as percentage of F10503LO1-untreated cells; 100% corresponds to 12.2, 18.7, and 1.25 ng/ml for IL6, TNFα and PGE_2, respectively) and lactate were determined after 18 h of treatment with 200 ng/ml of LPS and the PFKFB3 inhibitor 3PO (10 μM). **(E)** The effect of 500 nM of the indicated molecules on the viability of MF and the melanoma cell lines B16F10 and MalMe-3M was determined after 24 h of treatment. **(F)** The dose-dependent effect of F10503LO1 on the viability of MF, B16F10, and MalMe-3M cells was determined at 24 h. **(G)** The mitochondrial inner membrane potential was evaluated after 5 h of treatment with 500 nM F10503LO1 or 200 nM staurosporine (as an inducer of mitochondrial-dependent apoptosis) and measuring the fluorescence (in arbitrary units; a.u.) of 30 nM CMXRos. **(H)** The effect of 10 μM of z-VAD on the apoptosis induced by 500 nM F10503LO1 was determined at 18 h. **(I)** The time-course of the apoptosis induced by 1 μM F10503LO1 was determined at the indicated times. Results show a representative blot **(A)**, or the mean ± SD of three experiments. $^{*}P < 0.05$; $^{**}P < 0.01$; $^{***}P < 0.005$ vs. the corresponding control, untreated cells or macrophages.

injury; not shown), suggesting a low toxicity of F10503LO1 at the doses used (**Figure 5B**). In line with these results, the analysis of pro-inflammatory cell markers in blood by flow cytometry showed a tendency to reduce circulating leukocyte populations (**Supplementary Figure S1**). Of note, an emerging role for the spleen in the pharmacokinetics of drugs has been highlighted recently (32). However, the analysis of pro-inflammatory cells in the spleen also revealed a tendency to low content of monocyte, macrophage and neutrophil cell populations (**Supplementary Figure S1**), thus excluding the involvement of systemic pro-inflammatory profiles in drug response. Furthermore, the analysis of activated

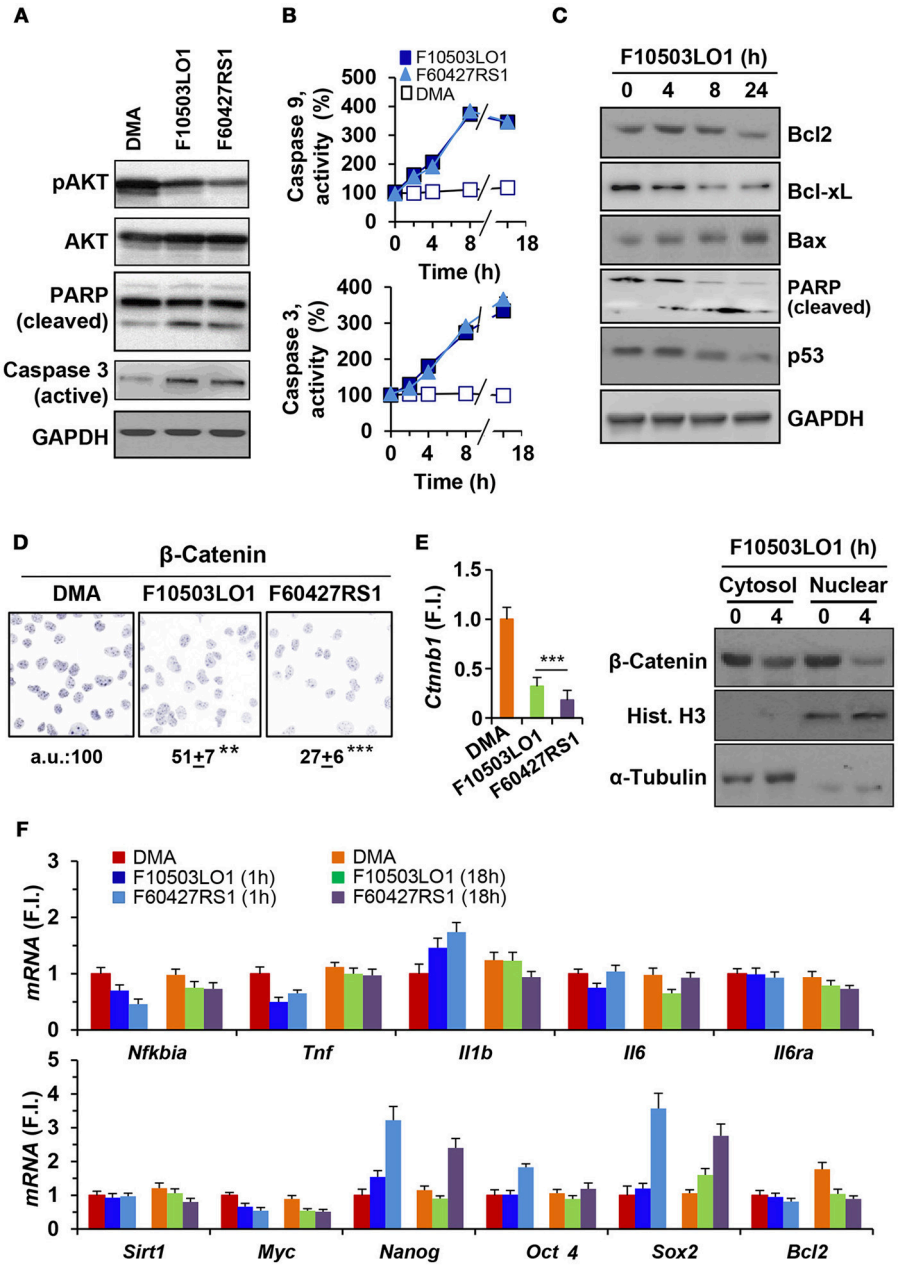

FIGURE 2 | Effect of F10503LO1 and F60427RS1 on apoptosis related proteins, β-catenin and genes related to cell survival. **(A)** B16F10 melanoma cells exhibit constitutive activation of AKT that was inhibited by F10503LO1 and F60427RS1 (1 μM) after 8 h of incubation. PARP and caspase 3 processing were evaluated under these conditions. **(B)** The time course of caspase 9 and caspase 3 activities were determined in cell extracts, using selective fluorescent substrates. **(C)** Time-course of the protein levels of pro-apoptotic and anti-apoptotic genes from B16F10 cells treated with 1 μM of F10503LO1. **(D)** Immunostaining of β-catenin levels in cells treated for 4 h with 200 nM of F10503LO1 and F60427RS1. The intensity of the labeling was referred to the value of untreated cells and expressed in percentage. **(E)** The β-catenin protein levels in the cytosolic and nuclear fractions were determined by immunoblot, as well as the corresponding mRNA levels (*Ctnnb1*) that were determined at 4 h. **(F)** The mRNA levels of the indicated genes were determined at 1 and 18 h after treatment with 200 nM of F10503LO1 and F60427RS1, and expressed as fold-induction (F.I.) vs. cells treated with DMA at 1 h. Results show a representative blot, out of three **(A,C)**. The mean ± SD for the caspases activities **(B)**. A representative staining of β-catenin and the mean±SD of three experiments **(D)**. $^{**}P < 0.01$; $^{***}P < 0.005$ vs. DMA condition **(C)**.

inflammatory cells suggests that F10503LO1 may increase the number of $CD11b^{+}$ lymphocytes (**Supplementary Figure S1**), highly susceptible of infiltrating in tumors and improve its prognosis (33).

In addition to this, fixed samples of experimental melanomas and normal skin were analyzed. Histological studies showed a higher proliferative activity, with an elevated number of mitosis, of the B16F10 melanoma cells. In all cases, an evident

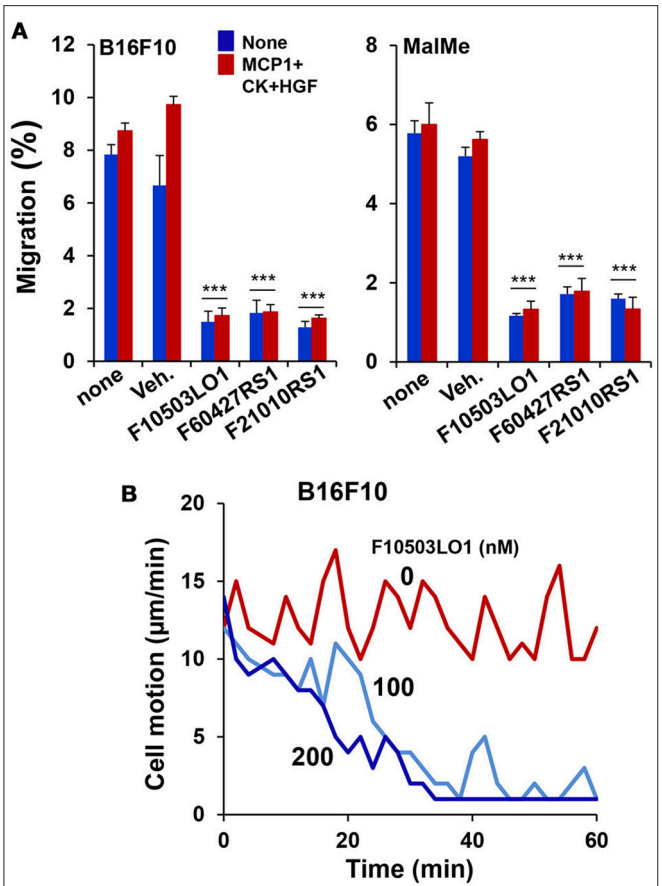

FIGURE 3 | F10503LO1 reduces cell migration and motion. **(A)** B16F10 and MalMe-3M cells were seeded in transwells (uncoated 8 μm porous transwells) according to the manufacturer's instructions. 5×10^4 cells were seeded in the upper chamber and allowed to attach for 2 h in DMEM containing 2%FCS and antibiotics. Non-attached cells were removed after washing with PBS. The lower side of the membrane was cleaned and the transwells were transferred to dishes containing fresh DMEM medium supplemented with 200 nM of the indicated drugs and stimuli (10 ng/ml of MCP1 and HGF). After 3 h, the number of cells present in the lower part of the chamber (including the membrane) were counted and expressed as percentage vs. the total number of cells in the well. **(B)** The motion of the cells was evaluated in a Cell Observer microscope and the corresponding images (**Supplementary Videos v1_B16F10**, **v2_MalMe-3M**) were recorded and analyzed. Results show the mean±SD of three experiments per duplicate **(A)**, or a representative experiment of cell motion (**B**, **Supplementary Videos**). ***$P < 0.005$ vs. the corresponding untreated cells.

invasive capacity of melanoma cells was demonstrated, with invasion of peritumoral adipose tissue and destruction of adjacent muscular striated cells, located in the hypodermis (**Figures 6A–D**). In the group of melanoma tumors that received administration of F10503LO1, a restricted tumor growth was found. In these treated cases, the infiltrative capacity of tumor cells is low, and the integrity of many skin muscle fascicles are preserved; additionally, apoptotic activity of tumor cells with extends areas of cytolysis and necrosis were observed in melanoma treated tumors (**Figures 6E–H**).

In vivo Studies of F10503LO1 in Melanoma-Carrying Nude Mice: Comparison With Combinations With the Chemotherapeutic Drug DTIC

Nude mice carrying the B16F10 melanoma bilaterally injected were treated i.p. with F10503LO1 or DTIC at the same doses. Drugs were given i.p. at 10 or 30 mg/kg at days 3 to 7 and 10 to 14. After this period, drug administration ceased and animals were kept until death. The tumors were resected and weighed, and several tissues (lung and liver) were excised off and frozen. *In vivo* luminescence was measured at days 7 and 15. As **Figures 7A,B** shows, both F10503LO1 and DTIC at 30 mg/kg, and F10503LO1 at 10 mg/kg significantly inhibited tumor growth. Animal survival was determined (**Figure 7C**) and, after animal death, the tumor mass was quantified (**Figure 7B**). To note that after suppression of drug treatment, tumors expanded in all cases; however, the tumor mass in animals treated with F10503LO1 was significantly lower than in DMA or DTIC-treated animals. In addition to this, samples of liver and lung were homogenized and the luciferase activity was determined as an index of infiltration of B16F10 cells. In the liver, the luminescence was undetectable. However, the lungs exhibited a significant luciferase activity (**Figure 7D**). Interestingly, animals treated with F10503LO1 that exhibited the maximal survival, showed minimal infiltration in the lung; however, no metastases were evident upon anatomopathological observation (not shown). Tissues obtained at day 12 of treatment were analyzed for the presence of pAKT, pAMPK, VEGF, and p53. As **Figure 7E** shows, treatment with F10503LO1 decreased AKT and AMPK phosphorylation and p53 and VEGF levels; again, this drug was more efficient than DTIC on the attenuation of these survival, proliferation and angiogenic markers.

An additional set of experiments was carried out using 3 different doses of F10503LO1 administered i.v. and in combination with DTIC, given i.p. at 30 mg/kg. F10503LO1 was administered i.v. through the tail vein at 0.25; 0.5, and 1 mg/kg bodyweight at days 1, 4, 7, 10, 14, 17, 21, 24, and 28, following B16F10 bilateral administration. A combination of i.p. DTIC and i.v. 0.5 mg/kg F10503LO1 was included. Luminescence lectures were taken at days 4, 11, and 16. **Figure 8A** shows the luminescence records for 8–10 tumors (4–5 animals) per each condition, and the Kaplan Meier plot of animal survival (**Figure 8B**). **Figure 8C** shows the luminescence associated to the tumors at day 16, including a series of three animals treated i.v. 2.5 mg/kg F10503LO1. Animals treated with 1 mg/kg F10503LO1 exhibited lesser tumor mass at the time of death. **Figure 8D** shows the increased half-life of the animals vs. the dose of F10503LO1 administered. After animal death, the tumors were excised off and weighted (**Figure 8E**). These data indicate that F10503LO1 significantly reduced tumor growth; however, the possibility of tumor evasion and metastatic development cannot be excluded as a cause of death. Finally, and supporting previous data, the effect of DTIC on tumor growth was less effective than F10503LO1, and there was a lack of synergism between both drugs under these experimental conditions.

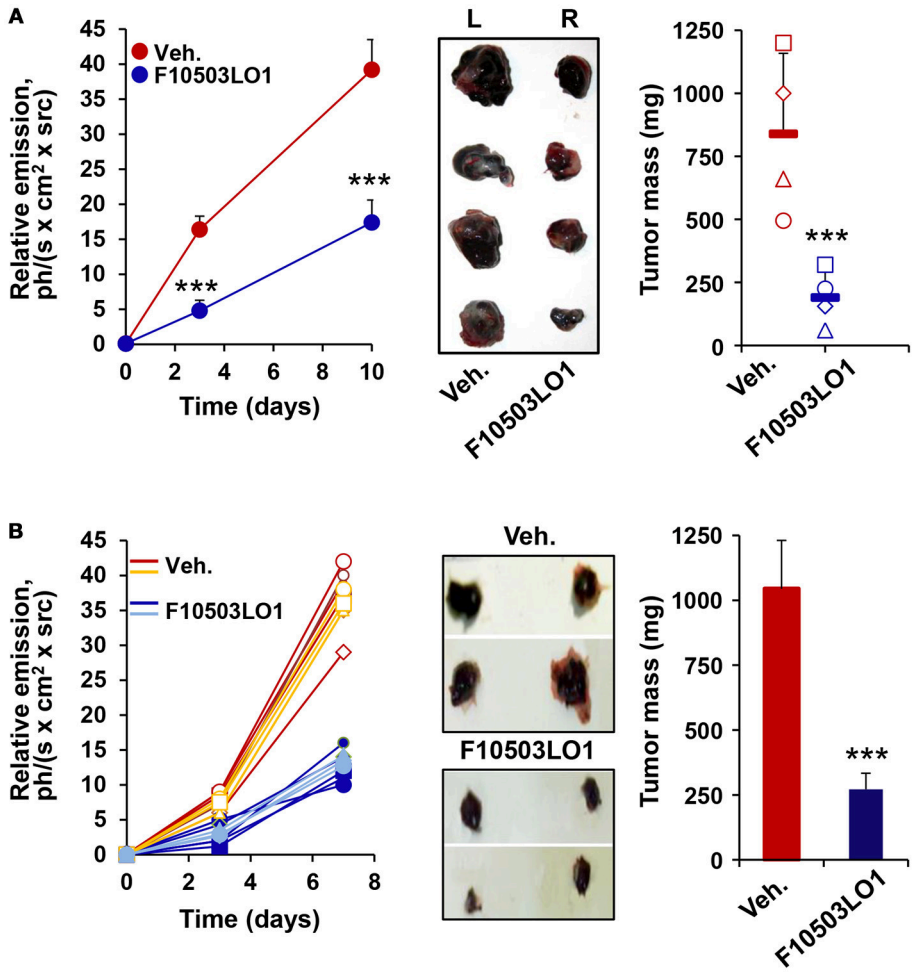

FIGURE 4 | F10503LO1 reduces melanoma tumor growth in mice. **(A)** B16F10 cells carrying a luciferase transgene were treated for 1 h *in vitro* with vehicle (DMSO) or 5 μM F10503LO1. After washing the dishes, 1×10^6 cells were administered to opposite flanks of C57BL/6 mice ($n = 4$). Tumor growth was recorded by the luciferase activity of the B16F10 cells. Tumors were excised off (central panel) and the tumor mass was determined at day 15th. **(B)** B16F10 cells were bilaterally injected (2×10^5 per flank) in nude mice ($n = 7$ per condition), and following 14 days of i.p. treatment with F10503LO1 (30 mg/kg) or vehicle. The luminescence of the tumors was recorded at days 3 and 7 and the tumors were extracted at day 15th (central panel) and weighed. Results show the individual luminescence values **(B)**, and the mean ± SD of the corresponding values. ***$P < 0.005$ vs. the vehicle condition.

DISCUSSION

Melanocyte tumorigenesis involves different types of lesions, from benign nevi to malignant melanomas. Because melanocytes are derived from the neural crest and are present in several tissues, a diversity of melanoma phenotypes account for these tumors, which also carry distinct mutations (1, 3, 10, 20, 34). The most common mutated genes are BRAF, p53, NRAS, and KIT, and these mutations use to accumulate in the course of malignization (11, 14, 18, 35). In fact, these mutations occur in different combinations and temporal sequences affecting the activity of genes that regulate key signaling pathways: DNA damage repair, proliferation, cell cycle regulation, cell-specific metabolism, resistance to apoptosis and replicative lifespan among other. In this regard, the area of the discovery and assessment of new biomarkers for melanoma progression is under continuous development (36). Additionally, other factors, such as an enhanced reactive oxygen production appears to be critical in the success for the treatment of melanoma cells that acquired resistance to the BRAF chemotherapy (37). This is one of the main reasons why melanomas have to be attacked combining several chemotherapeutic drugs (3, 18, 23, 38). Indeed, novel drugs are on the pipeline of the pharmaceutical industry. In this work we investigated a series of lead molecules that blocked the interaction between the signaling adaptor p62 and the NF-κB pathway related to tumorigenesis (39), followed by screening on the NCI-60 panel of cancer cells (40). Under these premises, benzylamine and thenylamine-derived molecules emerged as lead candidates for the study of their action on melanoma cells. Interestingly, these drugs, did not affect NF-κB activity in cells such as macrophages, but compromised the viability of human and

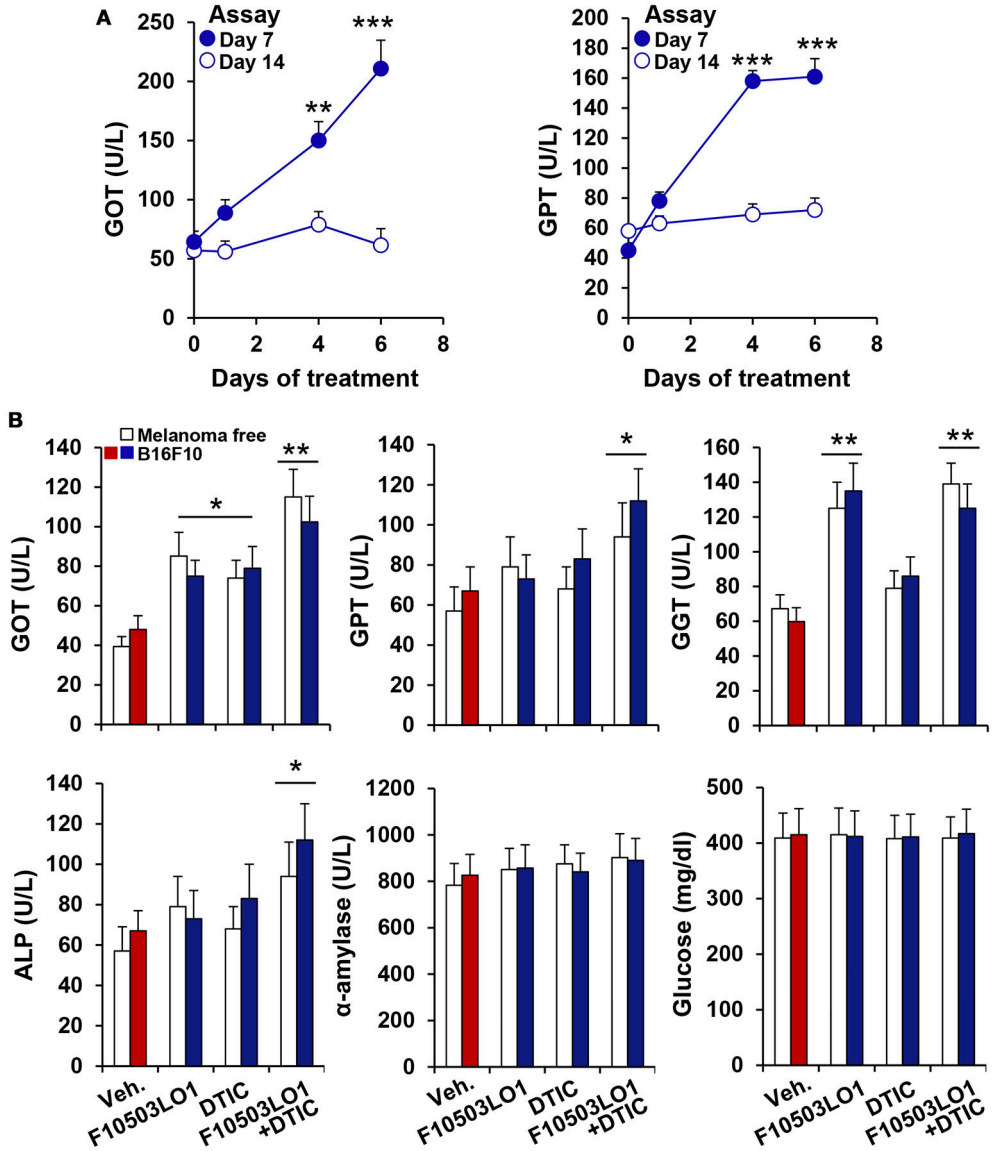

FIGURE 5 | Evaluation of F10503LO1 toxicity in mice. **(A)** Serum levels of GOT and GPT in animals treated i.p. for the indicated periods with 30 mg/kg F10503LO1 (3 for each time: 0, 1, 4, and 6 consecutive days of drug administration). Blood was collected by retroorbital punction at days 7 and 14, and the enzyme activities were measured. **(B)** Animals were injected 1×10^6 B16F10 cells in each flank and F10503LO1 (30 mg/kg), DTIC (30 mg/kg) or both were i.p. administered at days 1 to 5 and 8 to 12. Serum levels of injury markers were determined at day 14. Data are expressed as mean±SD. $^*P < 0.05$; $^{**}P < 0.01$; $^{***}P < 0.005$ vs. the corresponding control.

murine melanoma cells by promoting apoptosis and inhibiting survival pathways and cell migration when used in the 0.5–1 μM range.

Among the assayed molecules, F10503LO1 proved to exhibit a reduced systemic toxicity as reflected by the minor impact on myeloid cell generation in the bone marrow. Administration of F10503LO1 *via* i.p. or i.v. induced only a minor hepatic injury, but did not show alterations in other classic injury-markers associated to kidney, gallbladder and pancreas, nor did it in blood lipid and metabolic markers in C57BL/6 and nude mice. Interestingly enough, control animals recovered normal serum levels of altered injury markers in less than 1 week of cessation of F10503LO1 administration.

In vitro effects of F10503LO1 on melanoma cells suggested a potential efficacy in *in vivo* models of melanoma tumorigenesis. In fact, not only did F10503LO1 exhibit cytotoxicity (apoptosis) on B16F10 cells, but it impaired melanoma infiltration and metastases in distal organs (liver, lung) as well. From a molecular point of view, F10503LO1 decreased the content of phospho-AKT, and phospho-AMPK, impaired angiogenesis through a decrease in the intratumor content of VEGF and decreased p53 levels suggesting a specific mechanism leading to a reduced

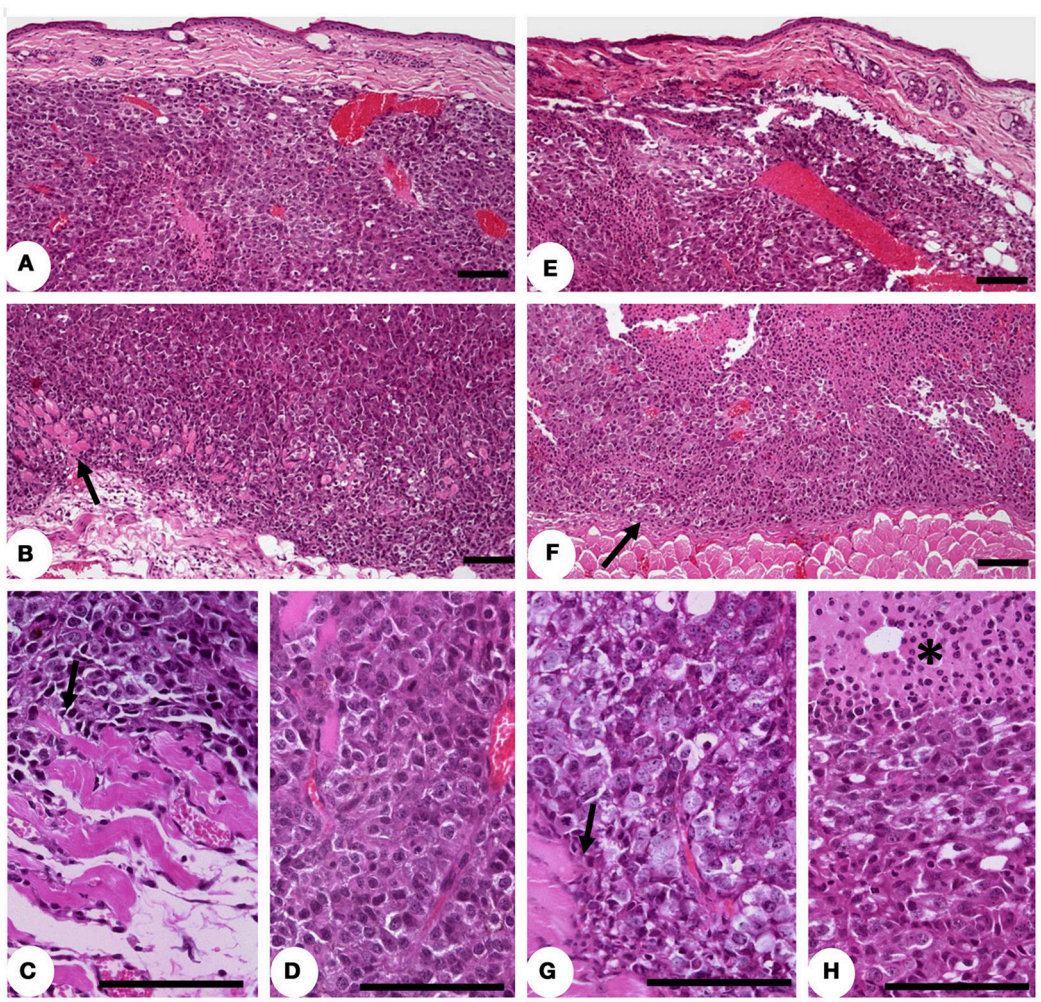

FIGURE 6 | Immunohistochemistry of tumors. Mounted fixed sections of B16F10 melanoma tumors from mice at day 7 and 15 (from **Figure 4B**). Animals were treated i.p. from day 1 to 6 with vehicle (DMSO) or with 30 mg/kg of F10503LO1. Representative sections of the tumors after hematoxylin-eosin staining. **(A)** diffuse melanoma in dermis reticular; **(B)** infiltration of hypodermis and invasion and destruction of subcutaneous muscular layer (arrow) by melanoma cells; **(C)** the melanoma infiltrating cells produce evident lesions of myocytolysis (arrow); **(D)** pleomorphic melanoma cells with higher mitotic activity in infiltrating tumor; **(E)** F10503 treated melanoma tumor, characterizes by extent invasion of dermis and hypodermis; **(F)** multiple and extends areas of necrosis is seen in treated tumor, and the tumor cells push the muscular striated layer of skin (arrow), but no evident infiltration are observed; **(G)** in detail, the muscular cells sited in the vicinity of melanoma cells not showed apparent myofibril destruction (arrow); **(H)** the melanoma cells showed a clear vacuolated cytoplasm with evident necrotic changes, associated to multiples areas of apoptosis (asterisk). Bar= 100 μm.

in vivo viability of B16F10 cells and tumor dissemination. In addition, the observation that AMPK is dephosphorylated in samples of tumors treated with the drug probably contributes to cancer cell death due to the inability to provide energy substrates to the growing tumor (41). Interestingly, DTIC did not reproduce these effects, nor did it exhibit a significant synergism with F10503LO1 in terms of signaling or tumor growth arrest, prevailing the action of the benzylamine derivative over the DTIC treatment (5, 21). Complementary to these studies, the *in vitro* effects of F10503LO1 and F60427RS1 on melanoma cells well supported the *in vivo* data on tumorigenesis. Both F10503LO1 and F21010RS1 decreased the content of phospho-AKT, at the time that activate PARP and caspase 9 and 3, all mechanisms compatible with the observed loss of viability of the melanoma cells. Interestingly enough, the thenylamine F60427RS1 was as effective as the benzylamines in promoting AKT dephosphorylation, caspase 3/9 activation and inducing apoptosis, but included a rise in acetyl-CoA carboxylase phosphorylation that is frequently associated to an elevation of cytoplasmic calcium. In addition to this, treatment with F10503LO1 or F60427RS1 rapidly downregulate β-catenin levels both in B16F10 and MalMe-3M cells; however, the impact of this pathway in melanoma pathology remains to be controversial (38, 42–44). Regarding the potent effect

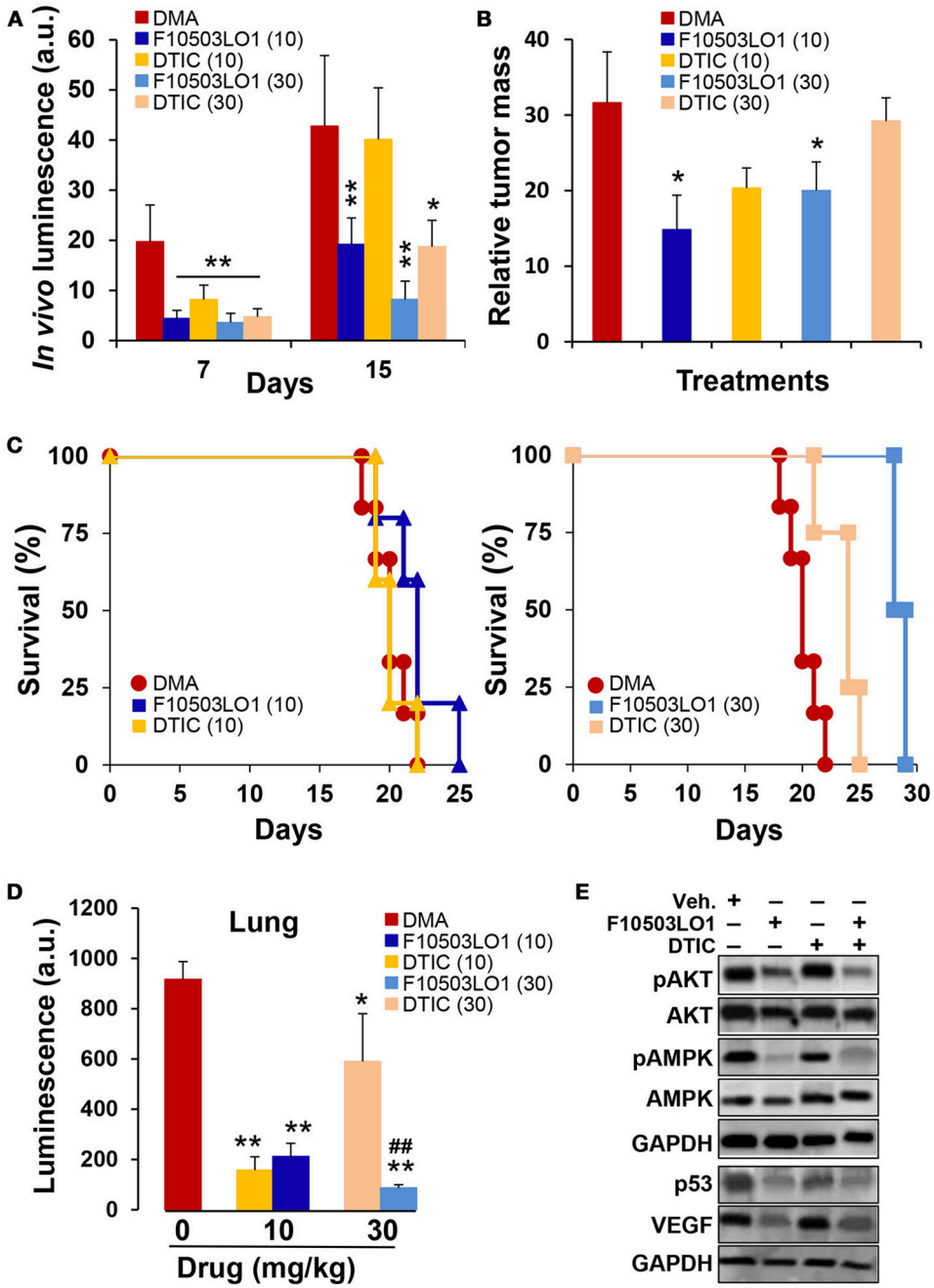

FIGURE 7 | Intraperitoneal administration of F10503LO1 enhances survival of mice-bearing melanoma tumors. **(A)** Nude mice (5 animals for each treatment) received B16F10 cells bilaterally (1×10^6 per flank) and were treated i.p. with the indicated doses of F10503LO1, DTIC (in mg/kg) or vehicle (DMA) at days 4 to 8 and 10 to 15. *In vivo* luminescence lectures were obtained at days 7 and 15 **(A)**. After day 15, animals were maintained untreated and survival was determined. **(B)** Relative tumor mass in dying mice (mg/days of survival). **(C)** Kaplan-Meier plot of animal survival; $P = 0.0097$ (30 mg/kg DTIC vs. DMA); $P = 0.0022$ (30 mg/kg F10503LO1 vs. DMA); $P = 0.042$ (10 mg/kg F10503LO1 vs. DMA). DTIC at 10 mg/kg was not statistically significant vs. DMA. **(D)** Samples of lung from tumor-bearing mice were homogenized and the luciferase activity measured. **(E)** Tumor samples ($n = 6$) were obtained at day 12 and extracts were prepared for Western blot analysis. Data are expressed as mean±SD. $^*P < 0.05$; $^{**}P < 0.01$ vs. DMA controls; $^{\#\#}P < 0.01$ vs. DTIC at 30 mg/kg.

of the drugs on the Wnt/β-catenin pathway, it should be mentioned that two types of cell surface receptors appear to be involved in its activation: the low density lipoprotein receptor–related proteins 5/6, and the GPCR-coupled Frizzled receptors (44). Indeed, this pathway is activated in many cancer cells leading to dysregulated cell growth and tumorigenesis, at the time that it is mutated in several oncogenic processes, such as melanoma (45). However, due to the diversity in

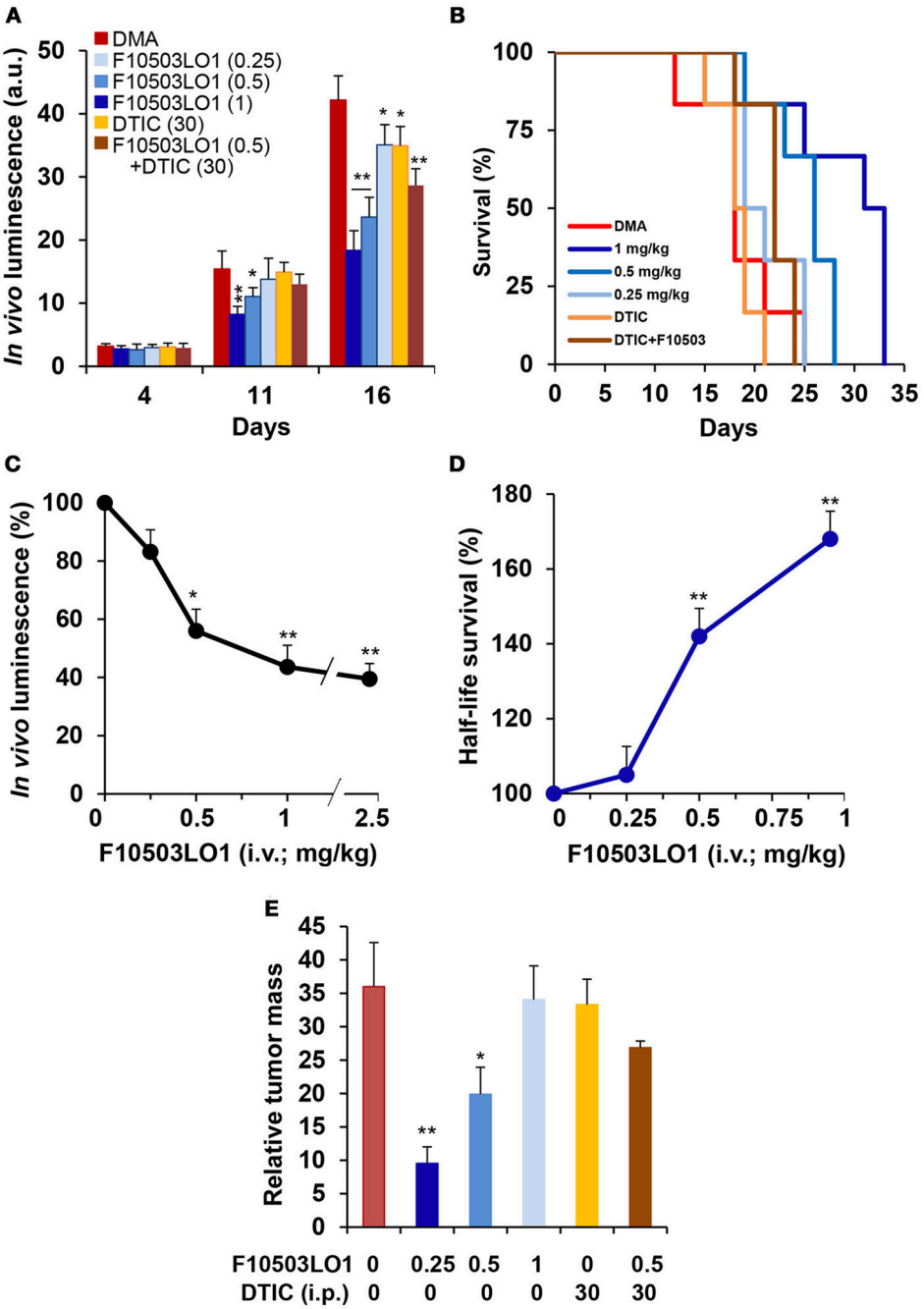

FIGURE 8 | Intravenous administration of F10503LO1 enhances survival in mice-bearing melanoma tumors. **(A)** B16F10 melanoma tumor growth in nude mice treated i.v. with 1, 0.5, 0.25 mg/kg of F10503LO1, i.p. 30 mg/kg DTIC, or i.v. 0.5 mg/kg F10503LO1 and i.p. 30 mg/kg DTIC at days 1, 4, 7, 10, 14, 17, 21, 24, and 28. Each treatment involves 6 mice injected bilaterally with 1×10^6 B16F10 cells. **(B)** Kaplan-Meier survival curves. The statistical significance was; $P = 0.0091$ (0.5 mg/kg vs. DMA); $P = 0.0089$ (1 mg/kg vs. DMA); $P = 0.379$ (DTIC vs. DMA); $P = 0.9647$ (DTIC+F10503LO1 vs. DMA). **(C)** Dose-dependent luminescence curve at day 16. **(D)** Half-life survival curve after F10503LO1 administration. **(E)** Relative tumor mass of the different treatments (mass of the tumor/days of survival). Data are expressed as mean ± SD. $^*P < 0.05$; $^{**}P < 0.01$ vs. DMA condition.

the origins of melanoma, conflictive and opposite views have been proposed regarding the possibility to target the Wnt (more than 19 proteins in this family) and the β-catenin pathways (acting as a coactivator of transcription factors involved in chromatin remodeling). Whereas some authors described that activation of the Wnt/β-catenin pathway is involved in a better prognostic on melanoma metastasis other groups reported opposite results, probably due to the fact that the

mutations present in melanoma cells determine the onset of the pathway and the possibility of the effectiveness of immune-regulatory responses in animal models (43, 45–47). This aspect is under study, due to the rapid degradation observed in the β-catenin levels, but we do not know if the β-catenin-dependent transcriptional activity has been fully expressed prior to degradation.

The growth of the melanoma cell line B16F10 implanted in nude mice was reduced after i.v. or i.p. treatment with F10503LO1. In agreement with this, F10503LO1 was able to expand animal survival significantly vs. animals treated with vehicle. This antitumoral activity was dose-dependent and it was observed in almost all the applied administration protocols. F10503LO1 impairs tumor growth at concentrations in the range 0.25–1 mg/kg when administered i.v. twice a week. Administration of 1 mg/kg of F10503LO1 under this protocol extended survival from 25 days in vehicle-treated animals to 33 days in F10503LO1LO1-treated mice. In addition to this, significant reduction in tumor growth was observed in C57/BL6 mice after i.p. treatment, suggesting efficacy for these drugs in the different ways of administration tested. Comparison of the effect of F10503LO1 (i.p. at 30 mg/kg or i.v. at 1 mg/kg) with the reference drug DTIC—an alkylating chemotherapeutic compound—at 30 mg/kg showed a greater effect of F10503LO1 in terms of tumor growth arrest and survival. However, both drugs failed to show any significant synergism under the experimental conditions used in this report.

Anatomopathological analysis of samples of tumors from animals treated with F10503LO1 showed wide areas of cytolysis, necrosis and lesser number of mitotic cells. Advanced tumors from untreated animals exhibited infiltration of the melanoma cells in muscle, adipose tissue and skin at the subcutaneous level, tissues that were more preserved when F10503LO1 was administered. Although no anatomopathological evidence of lung or liver metastases was observed in the different analyzed sections, in whole lung extracts luciferase activity was detected suggesting that some foci were present within the tissue; however, F10503LO1 prevented significantly this metastatic activity as evidenced in the tissue extracts from all analyzed animals. In addition to this, the luciferase activity in lung (indicative of potential metastasis) was significantly lower in animals treated with F10503LO1 when compared to the DTIC counterparts at the highest survival periods.

In summary, the benzylamine and thenylamine derived drugs assayed in this work can be envisaged as an interesting novel molecules for the treatment of melanoma in terms of the efficacy in counteracting the *in vivo* tumor growth of the aggressive murine and human melanoma cell lines assayed, and would provide the proof-of-principle and rationale for further clinical evaluation. Extension of these studies to other human-derived melanoma cells will support this idea, in particular in view of the clear benefits over the action of the classic DTIC treatment. Moreover, the provision additional molecular mechanisms of action for these drugs might help to unravel their relevant targets in the inhibition of tumor growth and promotion of melanoma cell death, alone or in combination with other well established strategies in the field.

AUTHOR CONTRIBUTIONS

MM, AP-R, and SG-R performed part of the experiments and contributed to the conception, and progress of the work. VF-G performed part of the experiments on flowcytometry. JR performed the immunohistochemistry analysis and discussed the experimental protocols. MM, AZ and IA contributed additional confirmatory experiments and discussed the results. PM-S revised and discussed the manuscript. FL and LB contributed to the conception, design and analysis of the manuscript. AP-R and LB wrote the first draft of the manuscript. All authors contributed to manuscript revision.

FUNDING

This work was supported by grants CENIT-Pharma, SAF2017-82436R and SAF2016-75004R from MINEICO, S2017/BMD-3686 from Comunidad de Madrid, CIVP18A3864 from Fundación Ramón Areces and Cibercv and Ciberehd (funded by the Instituto de Salud Carlos III) and Fondos FEDER.

ACKNOWLEDGMENTS

We acknowledge Ms Verónica Terrón for valuable help in the manipulation of the animals. We acknowledge support of the publication fee by the CSIC Open Access Publication Support Initiative through its Unit of Information Resources for Research (URICI).

SUPPLEMENTARY MATERIAL

The Supplementary Material for this article can be found online at: https://www.frontiersin.org/articles/10.3389/fonc.2018.00328/full#supplementary-material

REFERENCES

1. Curtin JA, Fridlyand J, Kageshita T, Patel HN, Busam KJ, Kutzner H, et al. Distinct sets of genetic alterations in melanoma. *N Engl J Med.* (2005) 353:2135–47. doi: 10.1056/NEJMoa050092
2. Eggermont AM, Robert C. Melanoma in 2011: a new paradigm tumor for drug development. *Nat Rev Clin Oncol.* (2011) 9:74–6. doi: 10.1038/nrclinonc.2011.201
3. Mattia G, Puglisi R, Ascione B, Malorni W, Care A, Matarrese P. Cell death-based treatments of melanoma:conventional treatments and new therapeutic strategies. *Cell Death Dis.* (2018) 9:e112. doi: 10.1038/s41419-017-0059-7
4. Mellman I, Coukos G, Dranoff G. Cancer immunotherapy comes of age. *Nature* (2011) 80:480–9. doi: 10.1038/nature10673
5. Eisen T, Marais R, Affolter A, Lorigan P, Robert C, Corrie P, et al. Sorafenib and dacarbazine as first-line therapy for advanced melanoma: phase I and open-label phase II studies. *Br J Cancer* (2011) 105:353–9. doi: 10.1038/bjc.2011.257

6. McQuade JL, Daniel CR, Hess KR, Mak C, Wang DY, Rai RR, et al. Association of body-mass index and outcomes in patients with metastatic melanoma treated with targeted therapy, immunotherapy, or chemotherapy: a retrospective, multicohort analysis. *Lancet Oncol.* (2018) 19:310–22. doi: 10.1016/S1470-2045(18)30078-0
7. Valero T, Steele S, Neumuller K, Bracher A, Niederleithner H, Pehamberger H, et al. Combination of dacarbazine and dimethylfumarate efficiently reduces melanoma lymph node metastasis. *J Invest Dermatol.* (2010) 130:1087–94. doi: 10.1038/jid.2009.368
8. Eggermont AM. Therapeutic cancer vaccine development: will it ride the wave of new immunomodulatory agents? *Cancer J.* (2011) 17:276. doi: 10.1097/PPO.0b013e31823436bf
9. Hodi FS, O'Day SJ, McDermott DF, Weber RW, Sosman JA, Haanen JB, et al. Improved survival with ipilimumab in patients with metastatic melanoma. *N Engl J Med.* (2010) 363:711–23. doi: 10.1056/NEJMoa1003466
10. Jessurun CAC, Vos JAM, Limpens J, Luiten RM. Biomarkers for response of melanoma patients to immune checkpoint inhibitors: a systematic review. *Front Oncol.* (2017) 7:e233. doi: 10.3389/fonc.2017.00233
11. Chen P, Chen F, Zhou B. Therapeutic efficacy and safety of combined BRAF and MEK inhibition in patients with malignant melanoma: a meta-analysis. *Onco Targets Ther.* (2017) 10:5391–403. doi: 10.2147/OTT.S147438
12. Kondo E, Maeda Y. Immune checkpoint inhibitors and allogeneic hematopoietic stem cell transplantation. *Rinsho Ketsueki* (2017) 58:506–13. doi: 10.11406/rinketsu.58.506
13. Amaria RN, Prieto PA, Tetzlaff MT, Reuben A, Andrews MC, Ross MI, et al. Neoadjuvant plus adjuvant dabrafenib and trametinib versus standard of care in patients with high-risk, surgically resectable melanoma: a single-centre, open-label, randomised, phase 2 trial. *Lancet Oncol.* (2018) 19:181–93. doi: 10.1016/S1470-2045(18)30015-9
14. Chapman PB, Hauschild A, Robert C, Haanen JB, Ascierto P, Larkin J, et al. Improved survival with vemurafenib in melanoma with BRAF V600E mutation. *N Engl J Med.* (2011) 364:2507–16. doi: 10.1056/NEJMoa1103782
15. Davies H, Bignell GR, Cox C, Stephens P, Edkins S, Clegg S, et al. Mutations of the BRAF gene in human cancer. *Nature* (2002) 417:949–54. doi: 10.1038/nature00766
16. Dong J, Phelps RG, Qiao R, Yao S, Benard O, Ronai Z, et al. BRAF oncogenic mutations correlate with progression rather than initiation of human melanoma. *Cancer Res.* (2003) 63:3883–5.
17. Arnault JP, Mateus C, Escudier B, Tomasic G, Wechsler J, Hollville E, et al. Skin tumors induced by sorafenib; paradoxic RAS-RAF pathway activation and oncogenic mutations of HRAS, TP53, and TGFBR1. *Clin Cancer Res.* (2012) 18:263–72. doi: 10.1158/1078-0432.CCR-11-1344
18. Lu H, Liu S, Zhang G, Bin W, Zhu Y, Frederick DT, et al. PAK signalling drives acquired drug resistance to MAPK inhibitors in BRAF-mutant melanomas. *Nature* (2017) 550:133–6. doi: 10.1038/nature24040
19. Wang R, He G, Nelman-Gonzalez M, Ashorn CL, Gallick GE, Stukenberg PT, et al. Regulation of Cdc25C by ERK-MAP kinases during the G2/M transition. *Cell* (2007) 128:1119–32. doi: 10.1016/j.cell.2006.11.053
20. Axelrod ML, Johnson DB, Balko JM. Emerging biomarkers for cancer immunotherapy in melanoma. *Semin Cancer Biol.* (2017) 17:30121–9. doi: 10.1016/j.semcancer.2017.09.004
21. Hafeez A, Kazmi I. Dacarbazine nanoparticle topical delivery system for the treatment of melanoma. *Sci Rep.* (2017) 7:16517. doi: 10.1038/s41598-017-16878-1
22. Ratnikov BI, Scott DA, Osterman AL, Smith JW, Ronai ZA. Metabolic rewiring in melanoma. *Oncogene* (2017) 36:147–57. doi: 10.1038/onc.2016.198
23. Soengas MS, Lowe SW. Apoptosis and melanoma chemoresistance. *Oncogene* (2003) 22:3138–51. doi: 10.1038/sj.onc.1206454
24. Zambon A, Niculescu-Duvaz I, Niculescu-Duvaz D, Marais R, Springer CJ. Small molecule inhibitors of BRAF in clinical trials. *Bioorg Med Chem Lett.* (2012) 22:789–92. doi: 10.1016/j.bmcl.2011.11.060
25. Denkert C, Siegert A, Leclere A, Turzynski A, Hauptmann S. An inhibitor of stress-activated MAP-kinases reduces invasion and MMP-2 expression of malignant melanoma cells. *Clin Exp Metastasis* (2002) 19:79–85. doi: 10.1023/A:1013857325012
26. Lev DC, Onn A, Melinkova VO, Miller C, Stone V, Ruiz M, et al. Exposure of melanoma cells to dacarbazine results in enhanced tumor growth and metastasis *in vivo*. *J Clin Oncol.* (2004) 22:2092–100. doi: 10.1200/JCO.2004.11.070
27. Turajlic S, Furney SJ, Lambros MB, Mitsopoulos C, Kozarewa I, Geyer FC, et al. Whole genome sequencing of matched primary and metastatic acral melanomas. *Genome Res.* (2012) 22:196–207. doi: 10.1101/gr.125591.111
28. Hortelano S, Alvarez AM, Bosca L. Nitric oxide induces tyrosine nitration and release of cytochrome c preceding an increase of mitochondrial transmembrane potential in macrophages. *FASEB J.* (1999) 13:2311–7. doi: 10.1096/fasebj.13.15.2311
29. Rodriguez-Prados JC, Traves PG, Cuenca J, Rico D, Aragones J, Martin-Sanz P, et al. Substrate fate in activated macrophages: a comparison between innate, classic, and alternative activation. *J Immunol.* (2010) 185:605–14. doi: 10.4049/jimmunol.0901698
30. Diaz-Guerra MJ, Castrillo A, Martin-Sanz P, Bosca L. Negative regulation by phosphatidylinositol 3-kinase of inducible nitric oxide synthase expression in macrophages. *J Immunol.* (1999) 162:6184–90.
31. Castrillo A, Traves PG, Martin-Sanz P, Parkinson S, Parker PJ, Bosca L. Potentiation of protein kinase C zeta activity by 15-deoxy-Δ(12,14)-prostaglandin J(2) induces an imbalance between mitogen-activated protein kinases and NF-κB that promotes apoptosis in macrophages. *Mol Cell Biol.* (2003) 23:1196–208. doi: 10.1128/MCB.23.4.1196-1208.2003
32. Cataldi M, Vigliotti C, Mosca T, Cammarota M, Capone D. Emerging role of the spleen in the pharmacokinetics of monoclonal antibodies, nanoparticles and exosomes. *Int J Mol Sci.* (2017) 18:e1249. doi: 10.3390/ijms18061249
33. Burton AL, Roach BA, Mays MP, Chen AF, Ginter BA, Vierling AM, et al. Prognostic significance of tumor infiltrating lymphocytes in melanoma. *Am Surg.* (2011) 77:188–92.
34. O'Day S, Boasberg P. Management of metastatic melanoma 2005. *Surg Oncol Clin N Am.* (2006) 15:419–37. doi: 10.1016/j.soc.2005.12.002
35. Hatzivassiliou G, Haling JR, Chen H, Song K, Price S, Heald R, et al. Mechanism of MEK inhibition determines efficacy in mutant KRAS- versus BRAF-driven cancers. *Nature* (2013) 501:232–6. doi: 10.1038/nature12441
36. Buder-Bakhaya K, Hassel JC. Biomarkers for clinical benefit of immune checkpoint inhibitor treatment-a review from the melanoma perspective and beyond. *Front Immunol.* (2018) 9:1474. doi: 10.3389/fimmu.2018.01474
37. Wang L, Leite de Oliveira R, Huijberts S, Bosdriesz E, Pencheva N, Brunen D, et al. An acquired vulnerability of drug-resistant melanoma with therapeutic potential. *Cell* (2018) 173:1413–25. doi: 10.1016/j.cell.2018.04.012
38. Chien AJ, Haydu LE, Biechele TL, Kulikauskas RM, Rizos H, Kefford RF, et al. Targeted BRAF inhibition impacts survival in melanoma patients with high levels of Wnt/beta-catenin signaling. *PLoS ONE* (2014) 9:e94748. doi: 10.1371/journal.pone.0094748
39. Duran A, Linares JF, Galvez AS, Wikenheiser K, Flores JM, Diaz-Meco MT, et al. The signaling adaptor p62 is an important NF-kappaB mediator in tumorigenesis. *Cancer Cell* (2008) 13:343–54. doi: 10.1016/j.ccr.2008.02.001
40. Abaan OD, Polley EC, Davis SR, Zhu YJ, Bilke S, Walker RL, et al. The exomes of the NCI-60 panel: a genomic resource for cancer biology and systems pharmacology. *Cancer Res.* (2013) 73:4372–82. doi: 10.1158/0008-5472.CAN-12-3342
41. Kfoury A, Armaro M, Collodet C, Sordet-Dessimoz J, Giner MP, Christen S, et al. AMPK promotes survival of c-Myc-positive melanoma cells by suppressing oxidative stress. *EMBO J.* (2018) 37:e97673. doi: 10.15252/embj.201797673
42. Chien AJ, Moore EC, Lonsdorf AS, Kulikauskas RM, Rothberg BG, Berger AJ, et al. Activated Wnt/β-catenin signaling in melanoma is associated with decreased proliferation in patient tumors and a murine melanoma model. *Proc Natl Acad Sci USA.* (2009) 106:1193–8. doi: 10.1073/pnas.0811902106
43. Valenta T, Hausmann G, Basler K. The many faces and functions of beta-catenin. *EMBO J.* (2012) 31:2714–36. doi: 10.1038/emboj.2012.150
44. Xiao Q, Wu J, Wang WJ, Chen S, Zheng Y, Yu X, et al. DKK2 imparts tumor immunity evasion through beta-catenin-independent suppression

of cytotoxic immune-cell activation. *Nat Med.* (2018) 24:262–70. doi: 10.1038/nm.4496

45. Kovacs D, Migliano E, Muscardin L, Silipo V, Catricala C, Picardo M, et al. The role of Wnt/beta-catenin signaling pathway in melanoma epithelial-to-mesenchymal-like switching: evidences from patients-derived cell lines. *Oncotarget* (2016) 7:43295–314. doi: 10.18632/oncotarget.9232
46. Katoh M. Canonical and non-canonical WNT signaling in cancer stem cells and their niches: cellular heterogeneity, omics reprogramming, targeted therapy and tumor plasticity (Review). *Int J Oncol.* (2017) 51:1357–69. doi: 10.3892/ijo.2017.4129
47. Zimmerman ZF, Kulikauskas RM, Bomsztyk K, Moon RT, Chien AJ. Activation of Wnt/β-catenin signaling increases apoptosis in melanoma cells treated with trail. *PLoS ONE* (2013) 8:e69593. doi: 10.1371/journal.pone.0069593

Conflict of Interest Statement: AZ, IA, and FL were employed by company FAES-FARMA, Spain.

The remaining authors declare that the research was conducted in the absence of any commercial or financial relationships that could be construed as a potential conflict of interest.

frontiers in Oncology

REVIEW
published: 06 August 2018
doi: 10.3389/fonc.2018.00299

The Guanylate Cyclase C—cGMP Signaling Axis Opposes Intestinal Epithelial Injury and Neoplasia

*Jeffrey A. Rappaport and Scott A. Waldman**

Department of Pharmacology and Experimental Therapeutics, Thomas Jefferson University, Philadelphia, PA, United States

Guanylate cyclase C (GUCY2C) is a transmembrane receptor expressed on the luminal aspect of the intestinal epithelium. Its ligands include bacterial heat-stable enterotoxins responsible for traveler's diarrhea, the endogenous peptide hormones uroguanylin and guanylin, and the synthetic agents, linaclotide, plecanatide, and dolcanatide. Ligand-activated GUCY2C catalyzes the synthesis of intracellular cyclic GMP (cGMP), initiating signaling cascades underlying homeostasis of the intestinal epithelium. Mouse models of GUCY2C ablation, and recently, human populations harboring GUCY2C mutations, have revealed the diverse contributions of this signaling axis to epithelial health, including regulating fluid secretion, microbiome composition, intestinal barrier integrity, epithelial renewal, cell cycle progression, responses to DNA damage, epithelial-mesenchymal cross-talk, cell migration, and cellular metabolic status. Because of these wide-ranging roles, dysregulation of the GUCY2C-cGMP signaling axis has been implicated in the pathogenesis of bowel transit disorders, inflammatory bowel disease, and colorectal cancer. This review explores the current understanding of cGMP signaling in the intestinal epithelium and mechanisms by which it opposes intestinal injury. Particular focus will be applied to its emerging role in tumor suppression. In colorectal tumors, endogenous GUCY2C ligand expression is lost by a yet undefined mechanism conserved in mice and humans. Further, reconstitution of GUCY2C signaling through genetic or oral ligand replacement opposes tumorigenesis in mice. Taken together, these findings suggest an intriguing hypothesis that colorectal cancer arises in a microenvironment of functional GUCY2C inactivation, which can be repaired by oral ligand replacement. Hence, the GUCY2C signaling axis represents a novel therapeutic target for preventing colorectal cancer.

Keywords: guanylate cyclase C, cGMP, intestinal epithelium, colorectal cancer, microbiome, DNA repair, inflammation, cancer prevention

OPEN ACCESS

Edited by:
Ramon Bartrons, University of Barcelona, Spain

Reviewed by:
Bruno A. Cisterna, Universidad Andrés Bello, Chile
William Farias Porto, Universidade Católica Dom Bosco, Brazil

****Correspondence:***
Scott A. Waldman
scott.waldman@jefferson.edu

Specialty section:
This article was submitted to Molecular and Cellular Oncology, a section of the journal Frontiers in Oncology

Received: *02 May 2018*
Accepted: *17 July 2018*
Published: *06 August 2018*

Citation:
Rappaport JA and Waldman SA (2018) The Guanylate Cyclase C—cGMP Signaling Axis Opposes Intestinal Epithelial Injury and Neoplasia. Front. Oncol. 8:299. doi: 10.3389/fonc.2018.00299

INTRODUCTION

Constituting the largest interface with non-sterile material from the outside world, the intestinal epithelium regulates fluid and nutrient transport, hosts commensal flora, and protects against infiltration by toxins and pathogenic organisms that pass through the digestive tract (1). These functions are accomplished by a single-cell layer of columnar epithelial cells, which form a

mechanical barrier dividing the systemic compartment from the turbulent gut lumen. Insults from the lumen induce continuous epithelial cell turnover, requiring tremendous regenerative capacity, with as many as 10^{11} gut epithelial cells replaced each day (2). This proliferative status predisposes the epithelium to neoplastic transformation, arising from corruption of circuits that normally maintain epithelial homeostasis.

The healthy epithelium exhibits a highly organized structure (**Figure 1**). Epithelial cells are polarized such that their apical surface faces the intestinal lumen, engaging in nutrient absorption and fluid secretion. The basolateral surface rests on a basement membrane and interfaces with the supportive stroma, vasculature, and mesenchymal cells of the underlying lamina propria. A network of junctional complexes stiches adjacent epithelial cells together, restricting paracellular transport between the mucosal surface, and subepithelial tissue (3). To increase absorptive surface area, the small intestinal epithelium is organized vertically with invaginations into the mucosa, called crypts, and projections into the lumen, called villi. In contrast, the surface of the large intestine is relatively smooth (lacking villi), with deep mucus-secreting crypts, enabling fluid absorption and stool transit.

This crypt-villus axis is a physiologically unique structure, characterized by continuous cell proliferation and turnover. At the base of the crypt, long-lived stem cells give rise to rapidly proliferating daughter cells, which differentiate into specialized epithelial cell subtypes (4). These cells migrate upwards from crypt to villus, differentiating into nutrient-absorbing enterocytes (the majority of the epithelial population), mucus-secreting goblet cells, and hormone secreting enteroendocrine cells (2). Another cell type, Paneth cells, migrate downward into the crypt, where they nourish the stem cells and secrete antimicrobial compounds into the lumen (5, 6). Terminally differentiated villus cells persist only 3–5 days, over which time they migrate to the tip of the villus, undergo apoptosis, and slough off into the fecal stream (2).

Tight homeostatic control of the circuits regulating cell division, differentiation, migration, and apoptosis, are critical to maintain the barrier integrity, secretory, and absorptive activity of the intestinal mucosa. The intestinal epithelial receptor, guanylate cyclase C (GUCY2C), and its cyclic nucleotide second messenger, cyclic guanosine monophosphate (cGMP), play a critical role in the maintenance of mucosal homeostasis, with GUCY2C being considered an emerging guardian of intestinal integrity. Identified nearly 30 years ago as a signaling network hijacked by diarrheagenic bacteria to stimulate intestinal secretion (7), cGMP signaling in the intestine is now recognized to underlie many homeostatic functions required for epithelial health. As such, dysregulation of cGMP signaling contributes to intestinal diseases including bowel transit disorders, inflammatory bowel disease, and cancer (8–11). We will briefly discuss the key players responsible for the generation, effector function, and degradation of cGMP in the intestine, followed by their contribution to intestinal physiology and disease. Finally, we will conclude with current approaches to targeting this axis for cancer prevention.

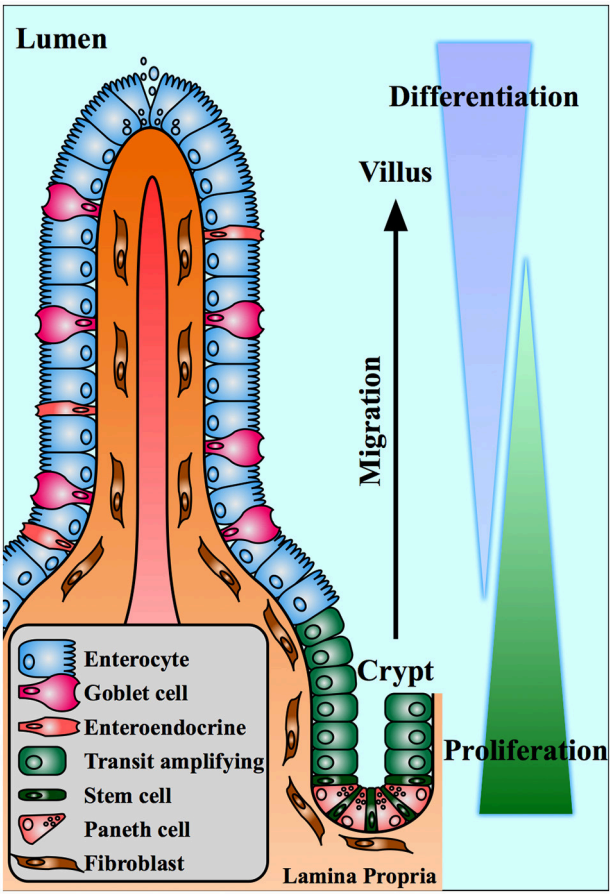

FIGURE 1 | The intestinal crypt-villus axis. The small intestinal epithelium is organized into villus projections into the gut lumen and crypt invaginations into the lamina propria. Stem cells at the base of the crypt produce proliferative daughter cells that give rise to differentiated cells of the villus. Epithelial cells migrate from the proliferating compartment toward the tip of the villus where they undergo apoptosis.

COMPONENTS OF THE INTESTINAL CGMP SIGNALING AXIS

Guanylate cyclases are a ubiquitous class of enzymes that catalyze the cyclization of the purine nucleotide guanosine triphosphate (GTP) to the second messenger, cGMP (12, 13). They are broadly classified by intracellular localization, residing in either the particulate (membrane-bound) or soluble (cytosolic) fractions of the cell. Depending on the isoform, guanylate cyclases are activated by an array of signals including peptide ligands, Ca^{2+} transients, and nitric oxide. In turn, cGMP effectors include cGMP-dependent protein kinases (PKGs), cGMP-gated ion channels, and phosphodiesterases (PDEs). The spatiotemporal parameters of intracellular cGMP transients are a function of synthesis by guanylate cyclases and degradation by phosphodiesterases. In the spirit of brevity, we refer readers to thorough reviews of guanylate cyclase signaling (12, 14). Here, we will focus on the key elements of cGMP signaling in the intestinal epithelium and their canonical role in fluid secretion (**Figure 2**).

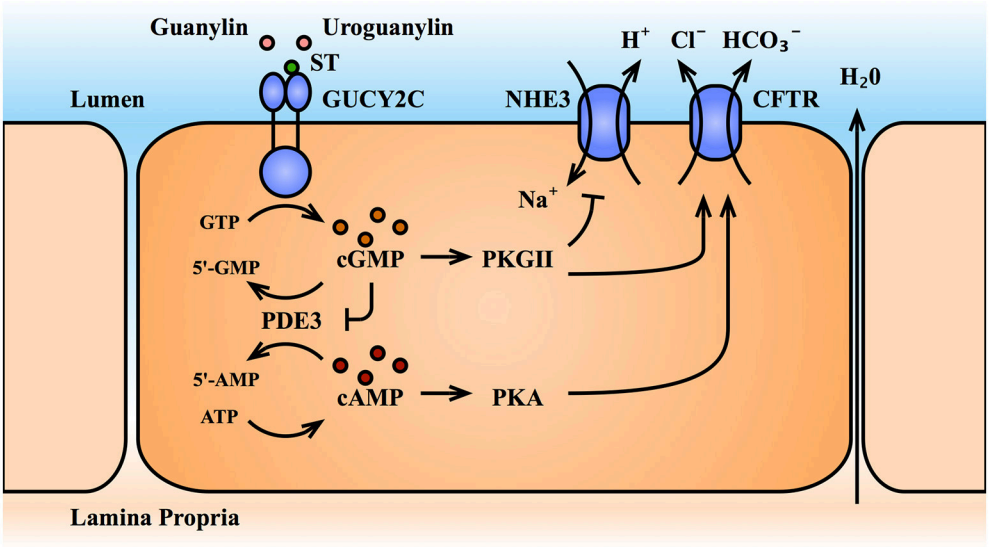

FIGURE 2 | The GUCY2C-cGMP signaling axis and intestinal fluid secretion. Activation of the receptor GUCY2C by its ligands increases intracellular cGMP levels. The cGMP effector, PKGII, inhibits sodium ion absorption by the NHE3 transporter, and promotes anion secretion by the CFTR transporter, producing an electrolyte and fluid gradient into the gut lumen. Through inhibition of the dual-specificity phosphodiesterases, PDE3, cGMP accumulation also cross-activates cAMP/PKA signaling, which further potentiates CFTR. ATP, adenosine triphosphate; cAMP, cyclic adenosine monophosphate; CFTR, cystic fibrosis transmembrane conductance regulator; cGMP, cyclic guanosine monophosphate; GTP, guanosine triphosphate; GUCY2C, guanylate cyclase C; NHE3, Na^+/H^+ exchanger III; PDE3, phosphodiesterases III; PKA, protein kinase A; PKGII, protein kinase G II; ST, bacterial heat-stable enterotoxin; 5′-AMP, 5′-adenosine monophosphate; 5′-GMP, 5′-guanosine monophosphate.

Guanylate Cyclase C (GUCY2C)

The GUCY2C isoform belongs to the particulate family of guanylate cyclases. While other cyclases (including soluble guanylate cyclase and the particulate guanylate cyclases A and B) have a widespread tissue distribution, GUCY2C is largely restricted to the intestinal tract (15, 16). It is expressed as a homodimer on the apical brush border of intestinal epithelial cells from the duodenum to the rectum, with its ligand-binding extracellular domain facing the intestinal lumen and its intracellular catalytic domain facing the cytosol (12, 14). GUCY2C was initially characterized as the receptor for the bacterial heat-stable enterotoxin, ST, the causative agent of traveler's diarrhea (7, 17). Extracellular ST binding activates the catalytic domain, generating intracellular cGMP. In turn, cGMP signaling canonically drives phosphorylation and translocation of the cystic fibrosis transmembrane conductance regulator (CFTR) to the cell surface, triggering Cl^- and HCO_3^- efflux into the intestinal lumen (18–20). Additionally, cGMP signaling inhibits the apical Na^+/H^+ exchanger 3 (NHE3), preventing Na^+ absorption from the lumen (18–20). The combined electrolyte efflux and retention in the lumen produces an osmotic gradient that drives fluid secretion and, in the pathological scenario, secretory diarrhea. Given this secretory function, GUCY2C has emerged as an attractive target for the treatment of constipation syndromes (21, 22). Two GUCY2C agonists recently received FDA-approval for the treatment of chronic idiopathic constipation and constipation-predominant irritable bowel syndrome: linaclotide (*Linzess*^{TM}) (23–25) an ST analog, and plecanatide *(Trulance*^{TM}*)* (26, 27) an analog of the endogenous GUYC2C ligand, uroguanylin (discussed below). Efficacy and tolerability of these agents was recently summarized (28).

GUCY2C Ligands

Ligands of GUCY2C include the aforementioned ST, of bacterial origin, and the two endogenous peptides, uroguanylin and guanylin, secreted by the epithelium of the human small and large bowel, respectively (**Figure 3**) (29, 30). Two additional guanylin species of non-human origin, lymphoguanylin and renoguanylin, have been isolated from the American opossum (*D. virginiana*) and the European eel (*A. japonica*), respectively (31–33). The human intestinal guanylins are synthesized as propeptides by epithelial cells of secretory lineages (34–37), and processed to their mature, biologically-active, 16-mer (uroguanylin), or 15-mer (guanylin) forms. The propeptide sequence is thought to shield the site of ligand receptor interaction, although a precise role for the pro-sequence and the steps in peptide maturation remains unresolved (38). Structurally, these peptides are characterized by disulfide bridges (three for ST and two for the guanylins), which confer stability and resistance to denaturation (hence the name "heat-stable" enterotoxin) (14, 39, 40). Although the peptides share a high degree of sequence similarity, uroguanylin is more potent at acidic pH. In uroguanylin, two N-terminal aspartic acid residues were shown to act as an acidic switch, altering the protein conformation and enhancing ligand-receptor affinity 100-fold at pH 5 vs. pH 8 (40, 41). However, recent molecular dynamics simulations of lymphoguanylin suggest that the hydrophobic core, rather than

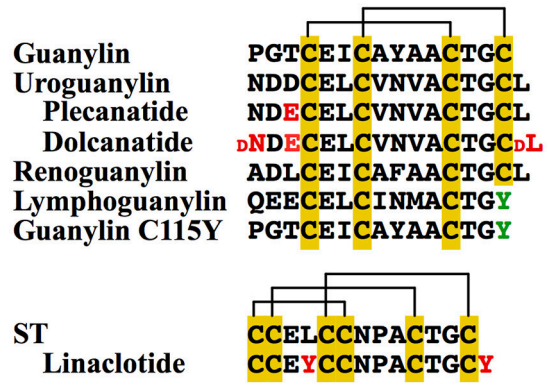

FIGURE 3 | GUCY2C Ligands. The four members of the guanylin protein family are guanylin and uroguanylin, found in humans, and renoguanylin and lymphoguanylin, found in other species. While the first three have a structural conformation characterized by two disulfide bonds (yellow), lymphoguanylin lacks the C-terminal cysteine (green), and therefore has only one disulfide bond. A mutant guanylin (C115Y) similarly has only one disulfide bond and lower potency of GUCY2C activation. In contrast, bacterial ST is characterized by a rigid structure with three disulfide bonds. Synthetic GUCY2C agonists include plecanatide and dolcanatide (uroguanylin analogs), and linaclotide (ST analog). Amino acid differences between these analogs and the parent compound are shown in red.

the acidic N-terminal residues, controls peptide conformation (42). Despite our evolving understanding of the molecular behavior of these peptides, it is clear that differences in pH sensitivity of the ligands parallel their expression profiles along the intestinal axis, with uroguanylin expressed in the acidic environment of the duodenum, and guanylin expressed in the neutral environment of the colorectum (22).

Guanylin peptides have gained increasing attention as drug templates for the treatment of gastrointestinal disorders. In addition to the aforementioned linaclotide and plecanatide, both already FDA-approved, a second uroguanylin analog, dolcanatide has shown promise in ameliorating intestinal inflammation in rodent models (43, 44). From a production perspective, guanylin peptide analogs can be challenging to synthesize due to the presence of multiple cysteine bonds. Interestingly, lymphoguanylin and a recently-identified mutant form of human guanylin (C115Y) harbor a C-terminal tyrosine residue in place of the typical cysteine, eliminating one disulfide bridge in these species and lowering their potency to activate GUCY2C (**Figure 3**) (45). Recent single nucleotide polymorphism and structural analyses of guanylin peptide variants have lent insights into features that can be exploited to develop new compounds in this growing class of pharmaceutics (42, 45, 46).

cGMP-Dependent Protein Kinases

The primary effectors of cGMP are the cGMP-dependent protein kinases (PKGs), PKGI, and PKGII. PKGs belong to the serine/threonine class of protein kinases and consist of three domains: (1) an N-terminal domain necessary for homodimerization, autoinhibition, and subcellular localization, (2) a regulatory domain consisting of two cGMP binding pockets, and (3) a catalytic domain containing the ATP and substrate-binding pockets (47). cGMP binding drives a conformation change that releases the catalytic domain from the inhibitory N-terminal domain, enabling kinase activity. Both PKG isoforms are expressed in tissues throughout the body, including the intestine. PKGI is present in smooth muscle cells, where it regulates intestinal contractility (48), while PKGII is the predominant cGMP effector in the intestinal epithelium, where it regulates luminal fluid secretion (47, 49, 50). Tethered to the apical plasma membrane, cGMP-activated PKGII canonically phosphorylates CFTR and NHE3 to promote fluid and electrolyte efflux (51, 52).

Phosphodiesterases

The cyclic nucleotides cGMP and cAMP are degraded to 5′-GMP and 5′-AMP by a family of enzymes called phosphodiesterases (PDEs). Eleven PDEs have been identified, each with varying tissue distribution, subcellular localization, and affinity for cGMP and cAMP. For example, PDE-4,−7, and−8 have higher affinity for cAMP, PDE-5,−6, and−9 for cGMP, and PDE-1,−2,−3,−10, and−11 hydrolyze both (53–55). PDEs that are expressed by the intestinal epithelium and contribute to cGMP hydrolysis include PDE-1,−2,−3,−5,−9 (53, 56, 57), and recently PDE10 (58). The extent to which epithelial-expressed PDEs with higher cAMP affinity [such as PDE4 (57)] modulate cGMP signaling remains unclear. However, cAMP and cGMP effectors converge on several physiological endpoints, including CFTR phosphorylation and fluid secretion. cGMP elevation indirectly potentiates cAMP effectors by occupying dual-specificity PDEs, thereby slowing degradation of cAMP. Additionally, some PDEs contain regulatory binding sites for cGMP that potentiate (PDE2 and 5) or inhibit (PDE3) cyclic nucleotide degradation. Hence, PDEs contribute a level of complexity to cyclic nucleotide signaling, particularly through cAMP-cGMP cross talk. These interactions remain to be comprehensively evaluated in the intestine, and are an area of significant interest.

CGMP SIGNALING AND INTESTINAL HOMEOSTASIS

The most apparent role of cGMP signaling in the intestine can be appreciated from human populations harboring mutations in GUCY2C, resulting in hyper- or hypo-secretion syndromes. In the recently described familial GUCY2C diarrhea syndrome (FGDS), a single missense mutation in the catalytic domain of GUCY2C produces hyperactivation of the receptor in response to ligand (9, 59, 60). This rare autosomal dominant disorder (initially reported in 32 members of a Norwegian family) is clinically characterized by loose stools, inflammation resembling irritable bowel disease with diarrhea (IBS-D), a doubling of intestinal transit time, and elevated intestinal pH. GUCY2C-deactivating mutations have also been reported, including missense mutations in the ligand-binding and catalytic domains, and nonsense mutations eliminating the catalytic domain entirely (10, 61). These autosomal recessive disorders, reported in Bedoin and Lebanese families, produce meconium ileus (neonatal

intestinal obstruction) due to GUCY2C insensitivity to its ligands, diminished epithelial cGMP, and diminished CFTR-mediated intestinal secretion.

These findings in humans mimic secretory defects observed in mice lacking components of the cGMP signaling axis. For example, GUCY2C$^{-/-}$ (62, 63) and PKGII$^{-/-}$ mice (50) are insensitive to ST-mediated intestinal fluid secretion. Guanylin deficient mice also have altered colonic electrolyte transport (64). Given the small population of humans harboring GUCY2C mutations, knockout mice have proven invaluable to the identification of the more subtle functions of cGMP in intestinal homeostasis, to be described below.

cGMP, Epithelial Proliferation, and Differentiation Along the Crypt-Villus Axis

Intestinal epithelial renewal requires a continuous supply of new cells produced by proliferation in the crypt. This renewal is regulated by a signaling cascade controlled by the extracellular ligand, Wnt, and its downstream transcriptional effector, β-catenin (65). In the differentiated villus, extracellular Wnt expression is low. In this context, cytosolic β-catenin enters a multi-protein complex stabilized by the scaffold proteins, adenomatous polyposis coli (APC) and axin. There, serine/threonine kinases, casein kinase 1a and glycogen synthase kinase 3, phosphorylate β-catenin, marking it for poly-ubiquitination by the β-TrCP E3 ubiquitin ligase and degradation by the proteasome. The presence of extracellular Wnt blocks this process. Wnt binds to its cell surface receptor, Frizzled, and co-receptor, LRP, which recruit axin to the plasma membrane to destabilize the destruction complex. This allows β-catenin to accumulate, translocate to the nucleus, associate with the T-cell factor (TCF) family of nuclear transcription factors, and activate a transcriptional program driving proliferation (66–69). Wnt hormones are secreted at the base of the intestinal crypt, providing a local niche conducive to stem cell renewal and epithelial proliferation (5, 65). The intestinal stem cell, identified only 10 years ago as the LGR5^{+} crypt base columnar cell (4), gives rise to daughter cells that populate the transit amplifying zone of the crypt. As these cells proliferate, migrate up the crypt, and leave the stem cell niche, Wnt tone diminishes and is replaced by Hedgehog and bone morphogenic protein (BMP) cascades, which support senescence and differentiation into the various specialized cells of the mature villus (70–72).

The balance of signaling promoting and opposing intestinal Wnt signaling is essential for life. Elimination of Wnt signaling in mice through disruption of β-catenin, TCF, its downstream target c-myc, or overexpression of the Wnt inhibitor dickkopf, results in crypt loss and fatal intestinal damage (73–76). Conversely, uncontrolled Wnt signaling underlies the majority of colorectal cancers. Spontaneous mutations inactivating the tumor suppressor, APC, or stabilizing oncogenic β-catenin represent the most common (>80%) driving mutations of sporadic colon cancer (77). APC is a prototypical tumor suppressor, where an initial spontaneous mutation produces allelic heterozygosity and cancer susceptibility. Loss of the remaining allele (loss of heterozygosity) eliminates APC from the β-catenin destruction complex, enabling uncontrolled β-catenin-driven transcription and tumorigenesis. This paradigm is most dramatic in patients with the hereditary cancer syndrome familial adenomatous polyposis (FAP), who harbor a germline mutation in one allele of APC and develop hundreds of adenomas throughout the colorectum by age 40 (77). This effect is mimicked in the widely-studied APC$^{min/+}$ mouse, the first mouse model of intestinal cancer, which harbors a truncating germline mutation in one allele of APC and develops multiple intestinal polyps (78, 79).

cGMP signaling opposes intestinal proliferation and promotes differentiation. Genetic elimination of GUCY2C, its ligand guanylin, or the cGMP effector PKGII results in intestinal crypt hyperplasia, characterized by increased crypt length and expansion of the proliferating compartment of transit-amplifying cells (measured by the number of PCNA and Ki67-positive cells) (80–82). In turn, differentiated cells of the secretory lineage, including goblet, Paneth, and enteroendocrine cells, are lost (81, 82). Interestingly elimination of GUCY2C also changes the stem cell compartment, producing endoplasmic reticulum stress in the crypt and shifting the balance of stem cells from canonical LGR5^{+} cells, to reserve BMI1^{+} cells, which normally remain in a quiescent state and repopulate the crypt upon injury (83). Corresponding with these changes, silencing GUCY2C increases tumorigenesis in APC$^{min/+}$ mice and mice exposed to the mutagens, azoxymethane or N-nitroso-N-methylamine, reflecting loss of epithelial cGMP (84, 85). These findings suggest that cGMP signaling opposes the events required for transformation by restricting proliferation and promoting differentiation along the crypt-villus axis. Interestingly, the absence of cGMP signaling is insufficient to induce tumorigenesis, but may instead create a selective advantage for transformed cells to proliferate and develop tumors.

Several studies demonstrate that cGMP opposes proliferation by arresting the cell cycle. This was observed nearly two decades ago in colorectal cancer cell lines treated with the GUCY2C ligands, ST and uroguanylin, 8-Br-cGMP (a cell permeable cGMP), or the PDE inhibitor, zaprinast (86). Subsequently, inactivation of GUCY2C in mice was shown to accelerate epithelial cell cycle progression, specifically by releasing a block at the G1/S transition (81). These mice over-express epithelial cell cycle drivers (e.g., pRb, CDK4, cyclinD1, β-catenin) and under-express cell cycle suppressors (e.g., p27) (87). In turn, cGMP elevating agents, including ST, 8-Br-cGMP, and the PDE inhibitor, exisulind, increase transcription of the cyclin dependent kinase inhibitors, p21 and p27, which control this G1/S transition (85, 87, 88). PKGII-mediated phosphorylation and activation of the transcription factor, SP1, initiates transcription at the p21/p27 promoters (88).

In addition to cell cycle arrest, cGMP signaling modulates other pathways involved in cell proliferation (**Figure 4**). For example, extracellular Ca^{2+} opposes proliferation through activation of plasma membrane-bound calcium-sensing receptors (CaRs), and entry through cyclic-nucleotide-gated ion channels. Stimulation of GUCY2C with ST recruits

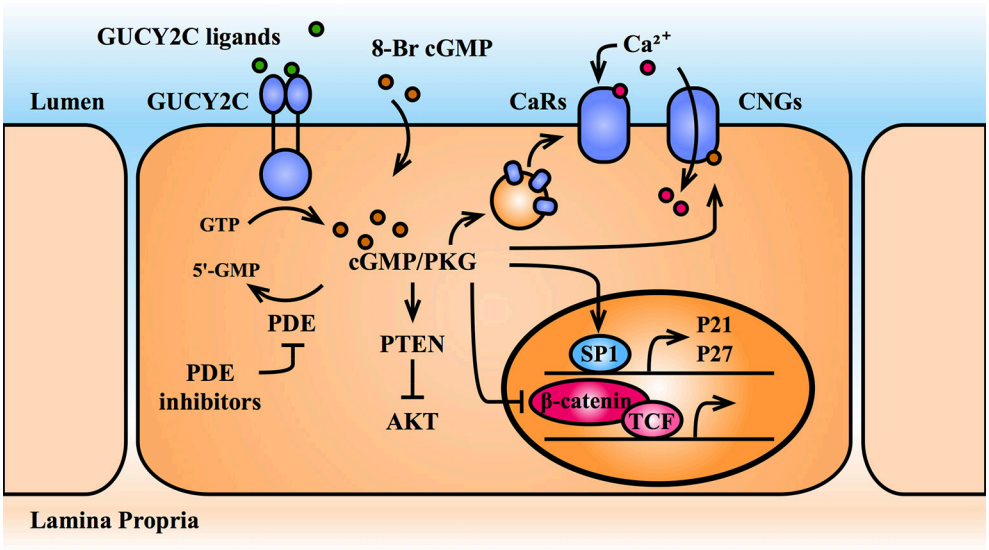

FIGURE 4 | cGMP opposes cellular proliferation. cGMP elevating agents include GUCY2C agonists, PDE inhibitors, and cell-permeable 8-Br-cGMP. cGMP and its effector, PKG, oppose intestinal epithelial cell proliferation by upregulating nuclear transcription of cell cycle inhibitors (p21 and p27) and by opposing pro-proliferative transcription mediated by the β-catenin/TCF and Akt pathways. Further, cGMP recruits calcium-sensing G-protein coupled receptors (CaRs) to the plasma membrane and directly activates cGMP-gated calcium channels (CNGs), promoting Ca^{2+}-mediated cytostasis. Akt, protein kinase B; CaR, calcium-sensing receptor; cGMP, cyclic guanosine monophosphate; CNG, cGMP-gated calcium channel; GTP, guanosine triphosphate; GUCY2C, guanylate cyclase C; p21, cyclin dependent kinase inhibitor 1A; p27, cyclin-dependent kinase inhibitor 1B; PDE, phosphodiesterase; PKG, protein kinase G; PTEN, phosphatase, and tensin homolog; SP1, specificity protein 1; TCF, T-cell factor; 5′-GMP, 5′-guanosine monophosphate; 8-Br-cGMP, 8-bromo-cGMP.

CaRs to the cell surface and activates cGMP-gated channels, resulting in Ca^{2+}-mediated cytostasis (89). In addition, transcriptomic profiling of GUCY2C$^{+/+}$ and GUCY2C$^{-/-}$ mouse intestinal epithelia revealed activation of pro-proliferative circuits downstream of the serine/threonine kinase, AKT, including metabolic reprogramming to a neoplastic, glycolytic phenotype (87). Reconstitution of cGMP signaling mobilizes the phosphatase, PTEN, the canonical inhibitor of AKT, reversing this phenotype (87). Reports also suggest that cGMP directly opposes the proliferative transcriptional program of β-catenin/TCF (90). cGMP elevation through PDE5 and PDE10 inhibition reduced β-catenin accumulation, nuclear translocation, and downstream transcriptional activity by an unknown mechanism in multiple cancer cell lines (91, 92). It has been proposed that PKGII suppresses β-catenin/TCF transcription through activation of cJun N-terminal kinase (JNK) and the downstream forkhead box O transcription factor 4 (FOXO4) (93). In this model, activated-FOXO4 binds and recruits β-catenin to alternative DNA-binding sites, preventing its association with TCF and reducing TCF-mediated transcriptional output. However, it was later shown by the same group that PKGII suppresses JNK in mice (94). Furthermore, although there have been reports of TCF-independent recruitment of β-catenin to DNA, including by the FOXO family, a recent comprehensive analysis of β-catenin DNA-binding sites in mouse intestinal crypts revealed that TCF family members are universally required for β-catenin recruitment (95). Hence, the mechanisms by which cGMP signaling opposes proliferation remain debated and likely involve with several pathways.

cGMP, Genetic Instability, and DNA Damage Repair

The intestinal epithelium is continuously exposed to DNA damaging agents. These include exogenous agents, such as radiation, microorganisms, and mutagenic substances in the lumen, as well as endogenous agents, such as reactive oxidative species (ROS) generated by metabolically-active crypt cells (96). Cells detect and respond to DNA damage by several mechanisms. The best-characterized guardian of genomic integrity, p53, activates a transcriptional program in response to DNA damage (97). Canonically, this begins with transcription of p21 to suspend the cell cycle and DNA replication, followed by activation of genes encoding DNA repair machinery, or if the damage is beyond repair, pro-apoptotic Bcl-2 proteins. Genetic instability, the corruption of normal DNA repair mechanisms and accumulation of mutations, is a hallmark of cancer and plays a central role in colorectal tumor progression (77, 98). Most sporadic colorectal tumors arise through a specific series of mutations, termed the adenoma-carcinoma sequence, beginning with APC, and followed by mutations in tumor suppressors such as p53 (60–70%) or oncogenes such as KRAS (40%) that enable transformation (77). Interestingly, only 10% of preneoplastic lesions progress to carcinoma over a 10 year period, as the accumulation of mutations required for tumorigenesis is slow (77). Genetic instability and disrupted damage sensing mechanisms accelerate the rate

of mutation and provide a survival advantage to malignant cells.

Loss of APC predisposes for colorectal cancer partly because it suppresses oncogenic β-catenin/TCF-driven transcription, but also because APC regulates DNA repair and chromosomal stability (99, 100). APC shuttles between the cytoplasm, where it regulates the β-catenin destruction complex, and the nucleus, where it modulates the DNA base excision repair, double strand break repair, and replication fork dynamics (101–104). Furthermore, through interactions with EB1, a microtubule-binding protein, APC associates with the kinetochore in mitotic cells, regulating spindle assembly, orientation, and chromosome segregation (105). Cells harboring truncated APC mutants have defects in chromosome segregation (106) and $APC^{min/+}$ mice exhibit tetraploidy (107). Indeed, a recent report highlighted the central importance of APC in intestinal tumor suppression using a doxycycline-inducible APC shRNA, enabling toggling of wild type APC. Elimination of APC in the context of p53 and KRAS mutations produced tumors, but removal of the shRNA, reconstituting APC in established tumors, rapidly reversed transformation and restored normal crypt-villus architecture (108).

cGMP signaling promotes DNA damage repair and opposes chromosomal instability in healthy tissue and in the context of APC defects. Elimination of GUCY2C from wild type and $APC^{min/+}$ mice produces DNA double strand breaks (quantified by the marker phospho-γH2AX) and DNA oxidation (84, 109). This underlying environment of DNA damage in the absence of cGMP signaling predisposes to further accumulation of mutations. Indeed, tumors from $APC^{min/+}$ mice lacking GUCY2C have a higher frequency of APC loss of heterozygosity than those with GUCY2C, reflecting genomic instability (84). Although the mechanism has yet to be fully defined, cGMP signaling contributes to genomic stability at least in part through metabolic reprogramming from glycolysis to oxidative phosphorylation (characteristic of proliferating vs. quiescent cells), decreasing ROS production and oxidative DNA damage in mice and cancer cell lines (87). Interestingly, deletion of CDX2, the intestinal transcription factor responsible for GUCY2C expression (110, 111), similarly potentiates tumor burden, chromosomal aberrations, and APC loss of heterozygosity (112). This reflects stimulation of mTOR, a downstream effector of AKT (112). Furthermore, it was recently reported that GUCY2C contributes to DNA integrity in part through a mechanism mediated by p53 (113). Elimination of GUCY2C from mice increased, while oral administration of the GUCY2C ligand, ST, reduced radiation-induced gastrointestinal toxicity in mice. cGMP signaling potentiated p53 activation in response to radiation injury, reducing DNA double strand breaks, abnormal mitotic orientation, and aneuploidy (characteristics of chromosomal instability). In summary, cGMP signaling potentiates DNA damage response mechanisms and promotes cellular quiescence, reducing susceptibility to chromosomal instability underlying tumor progression.

cGMP, Intestinal Inflammation, and Epithelial Barrier Integrity

The intestinal epithelium serves as both a selective conduit and a barrier between the luminal and systemic compartments. Transport between these compartments occurs by the transcellular route (via selective amino acid, electrolyte, and other nutrient transporters on the apical and basolateral surfaces of the enterocyte) or by the paracellular route, which is regulated by junctional complexes that bind the lateral walls of epithelial cells together (114). These junctional complexes are divided into three categories: desmosomes, adherens junctions, and tight junctions, the latter of which seals the paracellular space and is responsible for selective transport between cells. Numerous factors regulate junction complex integrity, particularly regulators of the inflammatory response (115–117). Endogenous anti-inflammatory cytokines, such as interleukin-10 (IL-10), promote barrier integrity (118). Others, such as tumor necrosis factor alpha (TNFα) and interferon gamma (IFNγ), key mediators of inflammation, increase barrier permeability through myosin light chain kinase (MLCK)-mediated phosphorylation of myosin light chain (MLC), leading to tight junction disassembly (119). Exogenous factors, such as alcohol and pathogenic microorganisms, also increase membrane permeability (114). Dysfunction of the epithelial barrier contributes to the pathology of numerous diseases, including inflammatory bowel disease (IBD), irritable bowel syndrome (IBS), sepsis, and autoimmune disease like celiac disease and type I diabetes (114, 117). Severe intestinal inflammation, such as IBD, also increases colorectal cancer risk (120).

Aside from the overt phenotype of intestinal secretory dysfunction, individuals harboring mutations in GUCY2C suffer from IBD (9, 10), suggesting that cGMP signaling regulates intestinal inflammation. Indeed, elimination of GUCY2C from mice produces an inflammatory phenotype associated with increased circulating and epithelial cytokines (109, 121, 122). In one study, intraperitoneal lipopolysaccharide injection (a bacterial endotoxin that provokes the immune response), produced greater proinflammatory gene expression (including TNFα and IFNγ) in colonocytes of $GUCY2C^{-/-}$ relative to wild type littermates (122). Additionally, elimination of GUCY2C from the intestine of a genetic intestinal colitis model ($IL10^{-/-}$) accelerated the onset of the disease (122). This suggests that homeostatic cGMP signaling reduces sensitivity to inflammatory stimuli. For example, mice exposed to dextran-sodium sulfate (DSS; a chemical model of intestinal inflammation mimicking IBD) and treated with plecanatide (a GUCY2C agonist) or sildenafil (a PDE5 inhibitor), were protected from inflammation compared to untreated mice (43, 123, 124). This effect was measured by epithelial histologic scoring, immune cell recruitment, expression of inflammatory cytokines, and inflammation-driven tumorigenesis (43, 123, 124).

cGMP signaling opposes intestinal inflammation at least in part through protection of epithelial barrier integrity. Elimination of GUCY2C in mice produces a phenotype of increased intestinal permeability, driven by MLC-mediated tight

junction disassembly and increased basal levels of epithelial IFNγ, a canonical driver of intestinal permeability (121). Subsequent transcriptomic profiling of GUCY2C$^{-/-}$ mouse epithelium also revealed decreased expression of 74 tight junction genes, including occludin, claudin-2, claudin-4, and JAM-A, contributing to loss of barrier integrity and susceptibility DSS-induced colitis (109). These changes were mediated by aberrant AKT signaling, which is opposed by cGMP signaling. A complementary mechanism was recently proposed, examining the role of reactive oxygen species in disrupting barrier integrity. Wang et al. suggest that cGMP signaling enhances barrier integrity through activation of the transcription factor, FOXO3a and its downstream antioxidant transcriptional targets (125). FOXO3a is phosphorylated and inactivated by AKT. Treatment of colon cancer cells, human biopsy specimens, and mice with 8Br-cGMP or the PDE5 inhibitor, vardenafil, suppressed AKT signaling, activated FOXO3a-mediated transcription of antioxidant species, and enhanced barrier integrity in the DSS-colitis model. These effects were abolished in PKGII$^{-/-}$ animals, confirming the role of cGMP. Collectively, several laboratories have confirmed that cGMP signaling promotes intestinal barrier integrity and opposes intestinal inflammation. The extent to which these effects are mediated changes in cytokine expression, regulators of tight junction assembly, expression of junction components, or potentiation of antioxidant species remains an open-ended question.

cGMP and the Intestinal Microbiome

Beyond its role in regulating fluid transport and nutrient absorption, the human intestine serves as a host for the densest population of microorganisms in the body, over 10^{11} microbes/mL by intestinal volume (126). The gut microbiome consists of over 1,000 species, varying in proportion from individual to individual depending on age, diet, geographic location, genetics, and other factors, which we have only begun to dissect since in the advent of large scale sequencing techniques (127, 128). Commensal bacteria, predominantly of the *bacteroidetes* and *firmicutes* phyla, thrive in the nutrient-rich environment provided by the intestinal epithelium. In turn, they complement gaps in host metabolic pathways, such as the fermentation of indigestible carbohydrates and synthesis of short chain fatty acids, a key energy source and signaling molecule for the epithelium (126, 128, 129). Beyond metabolic commensalism, gut bacteria defend against colonization by pathogenic species. These bacterial defense mechanisms occur indirectly through stimulation of the host immune response, and directly through nutrient competition and release of bactericidal small molecules (126, 130). For example, bacterial synthesis of short chain fatty acids opposes infection by enteropathogenic *E. coli* and virulence gene expression by *S. Typhimurium* in the colon (131, 132).

Alterations in diversity and composition of the intestinal flora, termed dysbiosis, characterize several intestinal diseases, including IBD and colorectal cancer. Whether these changes are a cause or consequence of disease remains an active area of research. However, mice treated with antibiotics, or housed in germ-free environments, exhibit intestinal mucus thinning, susceptibility to colitis, and acceleration of tumorigenesis, indicating that bacterial factors play a driving role (133–136). Chronic inflammation (e.g., IBD) is a risk factor for colorectal cancer, and bacterial species may contribute to tumorigenesis by producing an inflammatory state. Enrichment of specific bacterial species in the intestines of colorectal cancer patients, such as pro-inflammatory *Fusobacterium* and *Enterococcaceae*, and loss of anti-inflammatory butyrate-producing strains, such *Roseburia* and *F. prausnitzii*, alter the epithelial microenvironment and increase tumor susceptibility (137). Further, pro-carcinogenic species, including strains of *E. faecalis,* and *E. coli*, produce ROS and genotoxic virulence factors that drive mutations underlying transformation (137). Indeed, it was recently reported that patients with the hereditary colon cancer syndrome, FAP, harbor patches of *E. coli-,* and *B. Fragilis*-enriched biofilms, which are absent in normal individuals (138). These species secrete the toxins colibactin and B. fragilis toxin, respectively, which increase levels of inflammatory cytokines, DNA damage, and tumor onset in mice (138).

Epithelial cGMP has recently emerged as a regulator of microbiome composition, particularly through modulation of epithelial mucus properties. The colonic mucus is comprised two layers – (1) a sterile inner layer, rich in secreted immunoglobulin A and bioactive molecules (e.g., trefoil factor peptides, restin-like molecule b), that protects the epithelium from direct bacterial contact, and (2) an outer layer home to bacterial flora (126, 139). The mucus matrix is organized around the glycoprotein, mucin 2, secreted by epithelial goblet cells, which provides attachment sites and nutrition to commensal bacteria in the outer layer (139). It has been hypothesized that cGMP-mediated regulation of mucus hydration and pH through apical CFTR and NHE3 channels regulates bacterial colonization of the epithelial surface (140, 141). Indeed, elimination of GUCY2C from mice alters the composition of bacterial flora detected in the stool (140). Further, compromised barrier integrity in these mice increased susceptibility to systemic dissemination of the murine enteric pathogen, *C. rodentium* (140). Mice lacking GUCY2C also were more susceptible to a bacterial species that actively invades enterocytes, *S. enterica*, due to thinning of the protective mucus layer (141). In turn, administration of a GUCY2C agonist reduced bacterial adhesion and invasion. These findings support the notion that cGMP-mediated modulation of mucus hydration regulates bacterial colonization, and in turn, the relative proportions of commensal vs. pathogenic species.

cGMP signaling, microbiome composition, and colorectal cancer intersect in the long-recognized inverse relationship between colonization with diarrheagenic *E. coli* and incidence of colorectal cancer. Geographic regions with endemic enterotoxgenic *E. coli* (ETEC, responsible for Traveler's diarrhea), which produce the virulence factor and GUYC2C agonist, ST, have far lower rates of colon cancer (142). ST stimulation of GUCY2C arrests cell proliferation (86, 89, 142), suggesting an intriguing hypothesis that chronic ETEC colonization confers tumor resistance. Our group recently confirmed a role for chronic ST-exposure in tumor prevention. Mice colonized

for 18 weeks with ST-producing *E. coli*, mimicking chronic ST exposure in endemic regions of the world, developed a 50% lower tumor burden in response to the carcinogen, azoxymethane, than mice colonized with ST-negative *E. coli* (143). This finding reinforces the role of the GUCY2C-cGMP signaling axis, as well as the role of microbiome composition, in tumor susceptibility.

cGMP and Epithelial-Mesenchymal Cross Talk

Intestinal development and homeostasis rely on reciprocal signaling between the epithelium and underlying lamina propria. Derived from embryonic mesoderm, the lamina propria consists of acellular (extracellular matrix) and cellular [fibroblasts, pericytes, stromal stem cells, smooth muscle cells; (144)] elements that provide structural support and paracrine cues to the epithelium. Mesenchymal cells regulate epithelial proliferation and senescence, maintain and restrict the stem cell niche, and remodel the extracellular matrix (145). Under normal conditions, stromal fibroblasts remain in a quiescent state, secreting extracellular matrix proteins, matrix-modulating enzymes, and soluble growth and differentiation factors that maintain the underlying stroma architecture and promote epithelial differentiation. For example, fibroblasts surrounding the crypt base secrete Wnt molecules (Wnt2b, 4, 5a, 5b) and BMP antagonists (gremlin-1, gremlin-2, chordin-like 1) that have receptors on the epithelium and drive proliferation in the crypt (65, 146–148). They also restrict the stem cell niche in a vertical gradient through secretion of BMPs and Wnt antagonists to prevent β-catenin signaling outside of the normal proliferating zone (65, 72, 146, 147, 149). Fibroblasts also respond to epithelial injury (including mechanical stress, reactive oxidative species, inflammatory cytokines, or growth factors), converting to metabolically active myofibroblasts, which engage in matrix remodeling necessary for wound repair (144, 147). The primary stimulus driving the conversion of fibroblasts to myofibroblasts is transforming growth factor beta (TGFβ), secreted by the overlying epithelium. Resolution of injury repair and decline of TGFβ secretion results in myofibroblast apoptosis and/or reversion to a quiescent phenotype.

Pathological conditions, including chronic inflammation and neoplastic transformation, promote the recruitment of activated fibroblasts in a mutually reinforcing feedback loop. Secretion of TGFβ by injured, inflamed, or neoplastic epithelium activates fibroblasts, inducing changes in their proliferation, migration, adhesion, secretory, and matrix remodeling properties (145, 150–152). In turn, activated fibroblasts produce a stromal environment rich in extracellular matrix and secreted growth factors that are conducive to tumor growth, termed desmoplasia. Desmoplastic stroma has unique properties that promotes tumor invasion and metastasis, including remodeling of the normal Wnt and BMP gradients that define crypt architecture (145, 153, 154). Cancer-associated fibroblasts also directly promote tumorigenesis through the secretion of inflammatory cytokines and growth factors, such as hepatocyte growth factor (HGF), which is recognized by epithelial MET proto-oncogene receptor tyrosine kinase (c-MET) and promotes proliferation and invasion (145, 153).

cGMP signaling opposes epithelial-mesenchymal interactions underlying tumorigenesis. Several studies have described mechanisms by which intestinal cGMP signaling inhibits cancer cell migration, invasion, and microenvironment remodeling (155–159). cGMP suppresses the release of matrix metalloproteinases (MMPs; enzymes that cleave extracellular matrix components) by colon cancer cells, and was shown to prevent metastatic seeding of these cancer cells in mice (156). Further, loss of cGMP signaling in colon cancer cells promotes the assembly of actin-based motility organelles (filopodea) and invasion organelles (invadopodia) involved in tumor cell migration (157). PKG-mediated phosphorylation of vasodilator-stimulated protein (VASP), an actin-binding protein, opposes this cytoskeletal remodeling (157). Finally, silencing GUCY2C in mice and human cancer cells drives AKT-dependent secretion of TGFβ by the epithelium, producing fibroblast activation and a desmoplastic phenotype characteristic of early transformation (158). In turn, activated fibroblasts secrete HGF, reciprocally driving epithelial proliferation. Collectively, cGMP signaling opposes matrix remodeling and a cellular-invasion phenotype.

Beyond its role as an intracellular second messenger, cGMP also acts as a paracrine signaling molecule in the intestine. Activation of GUCY2C produces intracellular cGMP accumulation, as well as cGMP release into the extracellular environment (160–162). This extrusion is mediated by the membrane anion channel, multi-drug resistance protein 4 (MRP4), expressed on the apical and basolateral membranes of the epithelium (162, 163). Extracellular cGMP promotes analgesia by acting on visceral nociceptive neurons, and as such, the GUCY2C signaling axis has been targeted for the treatment of pain in constipation-predominant irritable bowel syndrome (IBS-C) (160, 161, 164). Other roles for cGMP in the intestinal stroma are unknown. It is tempting to speculate that given the various tumor-suppressive roles of cGMP signaling, pathological conditions that diminish extracellular cGMP could create a local microenvironment susceptible to transformation. However, its role as a paracrine tumor suppressor remains purely hypothetical because a cGMP receptor or cGMP uptake transporter have yet to be identified, and its extracellular mechanisms of action remain elusive.

cGMP DYSREGULATION IN COLORECTAL CANCER AND THERAPEUTIC IMPLICATIONS

Colorectal cancer remains the second leading cause of cancer death and fourth most incident cancer in the United States (165). Genetic alterations underlying tumorigenesis have been well defined; namely, the driving mutations in APC and β-catenin, which lift a block on proliferation along the crypt-villus axis (77). Furthermore, certain risk factors such as chronic inflammation (i.e., IBD), smoking, and obesity predispose patients to the development of tumors. Yet, the underlying changes in the intestinal epithelial microenvironment

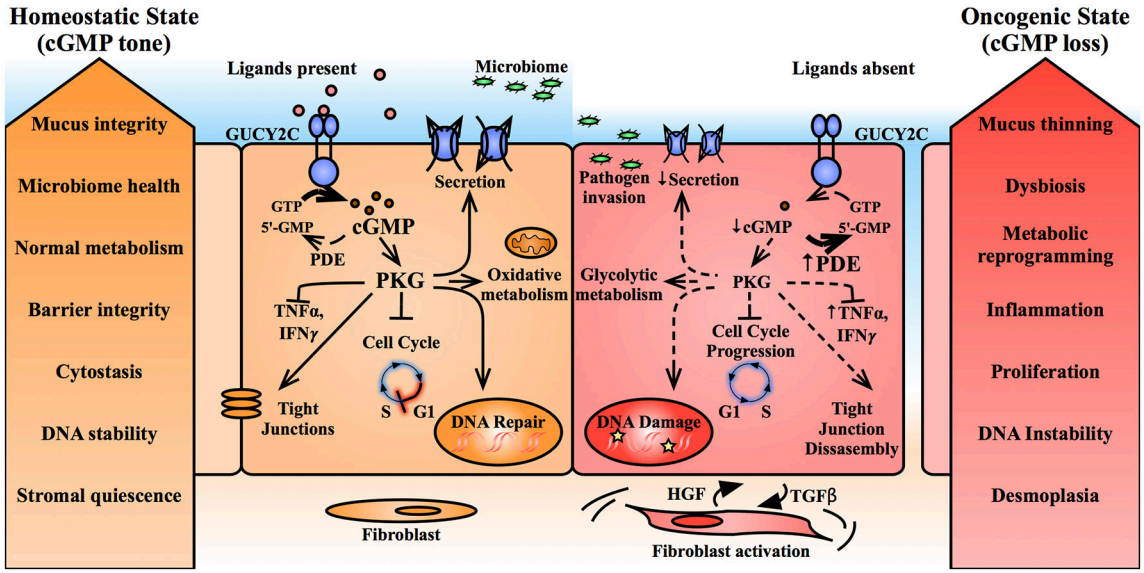

FIGURE 5 | Suppression of cGMP signaling promotes epithelial transformation. Basal cGMP tone in the intestinal epithelium promotes epithelial homeostasis. cGMP, through its effector, PKG, regulates several downstream mechanisms including mucus hydration, metabolism, inflammation, barrier integrity, DNA damage sensing, and cell cycle progression. In contrast, intestinal transformation is characterized by upregulation of phosphodiesterases and suppression of GUCY2C paracrine ligands, reducing intracellular cGMP and producing an epithelial phenotype predisposed to cancer progression. cGMP, cyclic guanosine monophosphate; GTP, guanosine triphosphate; GUCY2C, guanylate cyclase C; HGF, hepatocyte growth factor; IFNγ interferon gamma; PDE, phosphodiesterase; PKG, protein kinase G; TGFβ, transforming growth factor beta; TNFα tumor necrosis factor alpha; 5′-AMP, 5′-adenosine monophosphate; 5′-GMP, 5′-guanosine monophosphate.

that tip the homeostatic balance in favor of tumorigenesis remain poorly understood. Genetic mutations represent an irreversible phenomenon, and the standard of care remains surgical and chemotherapeutic approaches to eliminate transformed tissue. Hence, the identification of reversible factors contributing to the earliest stages of transformation are needed.

Cell-Autonomous Suppression of cGMP Signaling in Colorectal Cancer

cGMP has emerged as a key regulator of intestinal circuits that oppose tumorigenesis (**Figure 5**). As such, suppression of cGMP signaling is a common thread in colorectal cancers and may be necessary for tumorigenesis. Indeed, a recent analysis of mRNA and long non-coding RNA expression in tumor vs. normal tissue samples on the TCGA database identified the PKG-cGMP pathway among the top regulated gene networks (166). One mechanism of cGMP suppression is altered intracellular expression of cGMP axis elements, resulting in loss of cGMP signaling in cancer cells. For example, upregulation of PDEs accelerates hydrolysis of cyclic nucleotides. PDE5 elevation has been observed in human colon cancer cell lines and tumor samples compared to normal tissue, and PDE10 elevation has been observed in human cell lines, biopsy specimens, and tumors from $APC^{min/+}$ mice (58, 90, 124, 167). Another study found that expression of PDE4B (which preferentially degrades cAMP) was elevated in histologically normal-appearing intestinal epithelium from colorectal cancer patients, suggesting that cyclic nucleotide dysregulation occurs early in transformation, preceding other histologic markers (57). Suppression of the cGMP effector, PKGI, has also been observed in colon tumor specimens compared to normal tissue, contributing to angiogenesis in tumor xenografts (168, 169).

TABLE 1 | PDE inhibitors shown to oppose tumorigenic cell circuits.

	Specificity	Functions Regulated	Models
Sulindac sulfone (Exisulind)	PDE5	Apoptosis, (181) cell proliferation, (88) polyp multiplicity (182–184)	cells, mice, humans
Sulindac benzylamine	PDE5	Cell proliferation and apoptosis (167)	cells
Sulindac sulfide	PDE5	Cell proliferation and apoptosis (185)	cells
Sildenafil	PDE5	Polyp multiplicity, (186) colitis, (124) inflammation-induced polyps (124, 187)	mice
Vardenafil	PDE5	Cell proliferation (94), colitis (94), redox stress (125)	cells, mice
Zaprinast	PDE5, 6, 9, 11	Cell proliferation (86)	cells
ADT-094	PDE5, 10	Cell proliferation (91)	cells
Papaverine	PDE10	Cell proliferation (58, 91)	cells
PQ-10	PDE10	Cell proliferation (58)	cells
Pf-2545920	PDE10	Cell proliferation (58, 92)	cells

Inhibition, rather than changes in expression of cGMP signaling elements also contributes to silencing of the signaling axis. C-src, a tyrosine kinase overexpressed in colorectal cancer, phosphorylates tyrosine 820 on the catalytic domain of GUCY2C, inhibiting receptor activation (170). An alternative mechanism of receptor silencing may involve removal from the cell surface and sequestration in subcellular compartments, which was recently observed by immunohistological staining of multiple gastrointestinal malignancies (171). Whether changes in localization regulate cGMP generation remains unknown. Hence, through various mechanisms, silencing the tumor-suppressive properties of cGMP signaling appears to be a common feature of colorectal cancer.

GUCY2C Paracrine Hormone Loss in Colorectal Cancer

The aforementioned examples focus on cell-autonomous mechanisms of modulating of intracellular cGMP signaling in tumorigenesis. Another intriguing paradigm recognizes the role of cGMP signaling in intercellular communication via the secretion of GUCY2C ligands that act in an autocrine and paracrine fashion. The GUCY2C ligands, guanylin, and uroguanylin, are among the most commonly lost gene products in colorectal cancers, and this loss is conserved between mice and humans (172–176). For example, in a study of 300 patient tumor samples, >85% exhibited loss of guanylin (the colonic hormone) mRNA and protein expression compared to matched normal adjacent tissue (176). Ligand loss is also observed in the context of diet-induced obesity and intestinal inflammation, conditions which predispose to the development of colorectal cancer, and may represent a mechanistic link between these risk factors and tumorigenesis (122, 177, 178). Elimination of guanylin from mice results in loss of epithelial cGMP, producing crypt hyperplasia (80), and ligand reconstitution through oral administration or by transgenic expression opposes tumorigenesis (174, 177). Importantly, the receptor, GUCY2C, is retained in transformed tissue, despite the loss of its ligands (16, 171, 174, 179). Collectively, these findings underlie the *paracrine hormone hypothesis* of colorectal cancer (180), which suggests that guanylin insufficiency silences the tumor suppressive properties of the GUCY2C-cGMP axis, producing a microenvironment conducive to transformation.

Colorectal Cancer Prevention by Restoring the cGMP Axis

Activation of cGMP signaling, thereby promoting epithelial homeostasis and restoring its tumor suppressive function represents an enticing approach to cancer prevention, potentially overcoming irreversible genetic mutations in APC or β-catenin. The enzymes responsible for cGMP generation and degradation can be targeted for pharmacological regulation, for example with GUCY2C agonists or PDE inhibitors. Among the earliest demonstrations of the efficacy of targeting the GUCY2C-cGMP axis for tumor prevention, Shailubhai et. al. observed a reduction of tumor burden in $APC^{min/+}$ mice fed uroguanylin in the diet (174). Since then, cGMP-elevating agents, including PDE inhibitors (**Table 1**) and GUCY2C agonists (**Table 2**) have been shown to oppose cellular proliferation, genomic instability, barrier dysfunction, inflammation, dysbiosis, desmoplasia, and other factors discussed above that contribute to tumorigenesis.

TABLE 2 | GUCY2C agonists shown to oppose tumorigenic cell circuits.

	Structural Analog	Functions Regulated	Models
ST		Ca^{2+} conductance, (89, 142) cell proliferation, (85, 89) matrix remodeling and invasion, (156, 157) DNA damage sensing, (113) fibroblast activation, (158) tumor metabolism, (87) colitis and barrier permeability, (109) pathogen defense, (141) carcinogen-induced tumorigenesis, (143)	cells, mice
Guanylin		matrix remodeling and invasion, (156) colitis and barrier permeability, (109) obesity-induced tumorigenesis (177)	mice
Uroguanylin		Cell proliferation, (86) matrix remodeling and invasion, (156) polyp multiplicity (174)	mice
Linaclotide	ST	Polyp multiplicity, (186) cGMP efflux, (162) intestinal pain (160)	cells, mice, humans
Plecanatide	Uroguanylin	Colitis, (43) inflammation-induced dysplasia (123)	mice
Dolcanatide	Uroguanylin	Colitis (43)	mice

Supporting the feasibility of targeting the cGMP axis for tumor prevention, several cGMP elevating agents have been shown to oppose colorectal tumorigenesis in clinical and pre-clinical models. Early trials tested the PDE5 inhibitor, exisulind, in patients with FAP and sporadic colorectal adenomas (182–184). Exisulind, the sulfonated derivative of the NSAID, sulindac, produces intracellular cGMP accumulation, driving caspase-mediated apoptosis in cancer cells (181, 188). In patients, exisulind treatment produced tumor cell apoptosis and polyp regression, but significant hepatic toxicity at therapeutic doses proved insurmountable (182–184). Further, the antineoplastic mechanism of action has been questioned (189), leading to interest in alternate cGMP elevating agents with more desirable safety profiles. Recent studies have turned to agents already FDA-approved for other disorders. These include the PDE5 inhibitor, sildenafil, approved for the treatment of erectile dysfunction and pulmonary hypertension (53), and the synthetic GUCY2C ligands, plecanatide and linaclotide, which target the secretory function of GUCY2C to treat chronic idiopathic constipation and constipation-predominant irritable bowel syndrome (28). Recent reports showed that sildenafil and linaclotide administered orally in water reduced tumor multiplicity in the $APC^{min/+}$ mouse

(186). Furthermore, in mouse models of carcinogen-driven (azoxymethane) and inflammation-driven (DSS) tumorigenesis, sildenafil and plecanatide reduced the incidence of polyps and dysplastic lesions (123, 124, 187). These promising preclinical reports support approaching tumor prevention through reconstitution of the silenced GUCY2C-cGMP signaling axis.

While clinical translation of cGMP-elevating agents for tumor prevention is a logical next step, several questions remain to be answered regarding the mechanism of tumor suppression by the GUCY2C-cGMP axis. One area of debate is the nature of colorectal cancer inception, and where along the transformation continuum cGMP exerts its effects. It remains unclear if cGMP elevating agents oppose the initial drivers of tumorigenesis, for example by opposing genetic instability and therefore avoiding the sequential accumulation of mutations beginning with APC loss. Alternatively, healthy cGMP tone may promote a homeostatic microenvironment that suppresses proliferative signaling, inflammation, and desmoplasia, thereby preventing cancer progression in spite of APC/β-catenin mutations. Another open debate is the nature of the GUCY2C-cGMP axis suppression in cancer, and its implications for therapeutic reconstitution of cGMP signaling. PDEs are overexpressed in transformed tissue, albeit by an unknown mechanism, suggesting that cGMP loss is a cell-autonomous result of transforming mutations. In turn, PDE inhibitors would effectively elevate epithelial cGMP and oppose tumor progression. An alternative view recognizes that endogenous GUCY2C ligands are suppressed early in transformation (again, by a mechanism yet to be defined), suggesting that a paracrine field of GUCY2C silencing is responsible for cGMP loss and tumor susceptibility. This latter paradigm supports the reconstitution of cGMP signaling with exogenous ligand replacement, and forms the basis for clinical trials exploring oral GUCY2C agonists as a chemopreventative strategy in humans (190). The relationship between the GUCY2C-cGMP axis and colorectal cancer inception will undoubtedly become clearer in the coming years, and these molecular insights will ultimately provide a mechanistic framework for tumor prevention.

CONCLUSION

The GUCY2C-cGMP signaling axis has emerged as a key regulator of epithelial homeostasis in the intestine. Initially described as a the regulator of fluid and electrolyte secretion, cGMP is now recognized for its roles in modulating epithelial proliferation, DNA integrity, barrier function, microbiome composition, epithelial-mesenchymal cross talk, and other aspects of epithelial function. Dysregulation of these circuits underlies intestinal transformation, and perhaps unsurprisingly, loss cGMP signaling has emerged as a common feature of colorectal tumors. The precise role of cGMP signaling in the pathophysiology of colorectal cancer remains an open-ended question, but its tumor-suppressive properties are diverse. As such, suppression of cGMP signaling may be a necessary step in tumorigenesis because it lifts a block on proliferation, microenvironment remodeling, and the accrual of DNA mutations necessary for transformation. Supporting this notion, endogenous GUCY2C activating ligands are lost in early in transformation, and also from chronically inflamed epithelium, suggesting a mechanistic basis for this recognized risk factor for colorectal cancer. Preclinical data from several laboratories demonstrates that re-activation of cGMP signaling opposes tumor formation, and the availability of FDA-approved cGMP-elevating agents underscores the tractability of this approach. Given these observations, the GUCY2C-cGMP axis represents a logical, mechanism-based target for colorectal cancer prevention.

AUTHOR CONTRIBUTIONS

JR wrote the manuscript with input, critical feedback, and revisions by SW.

FUNDING

SW was funded by Targeted Diagnostics and Therapeutics, Inc and National Institutes of Health (R01 CA204481, CA206026; P30 CA56036). JR was supported by a Ruth Kirschstein Individual Fellowship Award (F30 CA232469) and a pre-doctoral fellowship from the PhRMA Foundation.

REFERENCES

1. Marchiando AM, Graham WV, Turner JR. Epithelial barriers in homeostasis and disease. *Annu Rev Pathol.* (2010) 5:119–44. doi: 10.1146/annurev.pathol.4.110807.092135
2. Barker N. Adult intestinal stem cells: critical drivers of epithelial homeostasis and regeneration. *Nat Rev Mol Cell Biol.* (2014) 15:19–33. doi: 10.1038/nrm3721
3. Odenwald MA, Turner JR. The intestinal epithelial barrier: a therapeutic target? *Nat Rev Gastroenterol Hepatol.* (2017) 14:9–21. doi: 10.1038/nrgastro.2016.169
4. Barker N, Van Es JH, Kuipers J, Kujala P, Van Den Born M, Cozijnsen M, et al. Identification of stem cells in small intestine and colon by marker gene Lgr5. *Nature* (2007) 449:1003–7. doi: 10.1038/nature06196
5. Farin HF, Jordens I, Mosa MH, Basak O, Korving J, Tauriello DV, et al. Visualization of a short-range Wnt gradient in the intestinal stem-cell niche. *Nature* (2016) 530:340–3. doi: 10.1038/nature16937
6. Gassler N. Paneth cells in intestinal physiology and pathophysiology. *World J Gastrointest Pathophysiol.* (2017) 8:150–60. doi: 10.4291/wjgp.v8.i4.150
7. Schulz S, Green CK, Yuen PS, Garbers DL. Guanylyl cyclase is a heat-stable enterotoxin receptor. *Cell* (1990) 63:941–8. doi: 10.1016/0092-8674(90)90497-3
8. Arshad N, Visweswariah SS. The multiple and enigmatic roles of guanylyl cyclase C in intestinal homeostasis. *FEBS Lett.* (2012) 586:2835–40. doi: 10.1016/j.febslet.2012.07.028
9. Fiskerstrand T, Arshad N, Haukanes BI, Tronstad RR, Pham KD, Johansson S, et al. Familial diarrhea syndrome caused by an activating GUCY2C mutation. *N Engl J Med.* (2012) 366:1586–95. doi: 10.1056/NEJMoa1110132
10. Romi H, Cohen I, Landau D, Alkrinawi S, Yerushalmi B, Hershkovitz R, et al. Meconium ileus caused by mutations in GUCY2C, encoding the CFTR-activating guanylate cyclase 2C. *Am J Hum Genet.* (2012) 90:893–9. doi: 10.1016/j.ajhg.2012.03.022

11. Pattison AM, Merlino DJ, Blomain ES, Waldman SA. Guanylyl cyclase C signaling axis and colon cancer prevention. *World J Gastroenterol.* (2016) 22:8070–7. doi: 10.3748/wjg.v22.i36.8070
12. Lucas KA, Pitari GM, Kazerounian S, Ruiz-Stewart I, Park J, Schulz S, et al. Guanylyl cyclases and signaling by cyclic GMP. *Pharmacol Rev.* (2000) 52:375–414.
13. Potter LR. Guanylyl cyclase structure, function and regulation. *Cell Signal* (2011) 23:1921–6. doi: 10.1016/j.cellsig.2011.09.001
14. Kuhn M. Molecular physiology of membrane guanylyl cyclase receptors. *Physiol Rev.* (2016) 96:751–804. doi: 10.1152/physrev.00022.2015
15. Krause WJ, Cullingford GL, Freeman RH, Eber SL, Richardson KC, Fok KF, et al. Distribution of heat-stable enterotoxin/guanylin receptors in the intestinal tract of man and other mammals. *J Anat.* (1994) 184:407–17.
16. Carrithers SL, Barber MT, Biswas S, Parkinson SJ, Park PK, Goldstein SD, et al. Guanylyl cyclase C is a selective marker for metastatic colorectal tumors in human extraintestinal tissues. *Proc Natl Acad Sci USA.* (1996) 93:14827–32. doi: 10.1073/pnas.93.25.14827
17. Ozaki H, Sato T, Kubota H, Hata Y, Katsube Y, Shimonishi Y. Molecular structure of the toxin domain of heat-stable enterotoxin produced by a pathogenic strain of Escherichia coli. A putative binding site for a binding protein on rat intestinal epithelial cell membranes. *J Biol Chem.* (1991) 266:5934–41.
18. Foulke-Abel J, In J, Yin J, Zachos NC, Kovbasnjuk O, Estes MK, et al. Human enteroids as a model of upper small intestinal ion transport physiology and pathophysiology. *Gastroenterology* (2016) 150:638–49.e638. doi: 10.1053/j.gastro.2015.11.047
19. Pattison AM, Blomain ES, Merlino DJ, Wang F, Crissey MA, Kraft CL, et al. Intestinal enteroids model guanylate cyclase C-dependent secretion induced by heat-stable enterotoxins. *Infect Immun.* (2016) 84:3083–91. doi: 10.1128/IAI.00639-16
20. Ahsan MK, Tchernychev B, Kessler MM, Solinga RM, Arthur D, Linde CI, et al. Linaclotide activates guanylate cyclase-C/cGMP/protein kinase-II-dependent trafficking of CFTR in the intestine. *Physiol Rep.* (2017) 5. doi: 10.14814/phy2.13299
21. Uranga JA, Castro M, Abalo R. Guanylate cyclase C: a current hot target, from physiology to pathology. *Curr Med Chem.* (2018) 25:1879–908. doi: 10.2174/0929867325666171205150310
22. Waldman SA, Camilleri M. Guanylate cyclase-C as a therapeutic target in gastrointestinal disorders. *Gut* (2018) 67:1543–52. doi: 10.1136/gutjnl-2018-316029
23. Lembo AJ, Schneier HA, Shiff SJ, Kurtz CB, Macdougall JE, Jia XD, et al. Two randomized trials of linaclotide for chronic constipation. *N Engl J Med.* (2011) 365:527–36. doi: 10.1056/NEJMoa1010863
24. Chey WD, Lembo AJ, Lavins BJ, Shiff SJ, Kurtz CB, Currie MG, et al. Linaclotide for irritable bowel syndrome with constipation: a 26-week, randomized, double-blind, placebo-controlled trial to evaluate efficacy and safety. *Am J Gastroenterol.* (2012) 107:1702–12. doi: 10.1038/ajg.2012.254
25. Rao S, Lembo AJ, Shiff SJ, Lavins BJ, Currie MG, Jia XD, et al. A 12-week, randomized, controlled trial with a 4-week randomized withdrawal period to evaluate the efficacy and safety of linaclotide in irritable bowel syndrome with constipation. *Am J Gastroenterol.* (2012) 107:1714–24. doi: 10.1038/ajg.2012.255
26. Al-Salama ZT, Syed YY. Plecanatide: first global approval. *Drugs* (2017) 77:593–8. doi: 10.1007/s40265-017-0718-0
27. Brenner DM, Fogel R, Dorn SD, Krause R, Eng P, Kirshoff R, et al. Efficacy, safety, and tolerability of plecanatide in patients with irritable bowel syndrome with constipation: results of two phase 3 randomized clinical trials. *Am J Gastroenterol.* (2018) 113:735–45. doi: 10.1038/s41395-018-0026-7
28. Shah ED, Kim HM, Schoenfeld P. Efficacy and tolerability of guanylate cyclase-C agonists for irritable bowel syndrome with constipation and chronic idiopathic constipation: a systematic review and meta-analysis. *Am J Gastroenterol.* (2018) 113:329–38. doi: 10.1038/ajg.2017.495
29. Currie MG, Fok KF, Kato J, Moore RJ, Hamra FK, Duffin KL, et al. Guanylin: an endogenous activator of intestinal guanylate cyclase. *Proc Natl Acad Sci USA.* (1992) 89:947–51. doi: 10.1073/pnas.89.3.947
30. Hamra FK, Forte LR, Eber SL, Pidhorodeckyj NV, Krause WJ, Freeman RH, et al. Uroguanylin: structure and activity of a second endogenous peptide that stimulates intestinal guanylate cyclase. *Proc Natl Acad Sci USA* (1993) 90:10464–8. doi: 10.1073/pnas.90.22.10464
31. Forte LR, Eber SL, Fan X, London RM, Wang Y, Rowland LM, et al. Lymphoguanylin: cloning and characterization of a unique member of the guanylin peptide family. *Endocrinology* (1999) 140:1800–6. doi: 10.1210/endo.140.4.6630
32. Fonteles MC, Carrithers SL, Monteiro HS, Carvalho AF, Coelho GR, Greenberg RN, et al. Renal effects of serine-7 analog of lymphoguanylin in *ex vivo* rat kidney. *Am J Physiol Renal Physiol.* (2001) 280:F207–213. doi: 10.1152/ajprenal.2001.280.2.F207
33. Yuge S, Inoue K, Hyodo S, Takei Y. A novel guanylin family (guanylin, uroguanylin, and renoguanylin) in eels: possible osmoregulatory hormones in intestine and kidney. *J Biol Chem.* (2003) 278:22726–33. doi: 10.1074/jbc.M303111200
34. Cohen MB, Witte DP, Hawkins JA, Currie MG. Immunohistochemical localization of guanylin in the rat small intestine and colon. *Biochem Biophys Res Commun.* (1995) 209:803–8. doi: 10.1006/bbrc.1995.1571
35. Perkins A, Goy MF, Li Z. Uroguanylin is expressed by enterochromaffin cells in the rat gastrointestinal tract. *Gastroenterology* (1997) 113:1007–14. doi: 10.1016/S0016-5085(97)70198-7
36. Brenna O, Furnes MW, Munkvold B, Kidd M, Sandvik AK, Gustafsson BI. Cellular localization of guanylin and uroguanylin mRNAs in human and rat duodenal and colonic mucosa. *Cell Tissue Res.* (2016) 365:331–41. doi: 10.1007/s00441-016-2393-y
37. Ikpa PT, Sleddens HF, Steinbrecher KA, Peppelenbosch MP, De Jonge HR, Smits R, et al. Guanylin and uroguanylin are produced by mouse intestinal epithelial cells of columnar and secretory lineage. *Histochem Cell Biol.* (2016) 146:445–55. doi: 10.1007/s00418-016-1453-4
38. Lauber T, Neudecker P, Rosch P, Marx UC. Solution structure of human proguanylin: the role of a hormone prosequence. *J Biol Chem.* (2003) 278:24118–24. doi: 10.1074/jbc.M300370200
39. Skelton NJ, Garcia KC, Goeddel DV, Quan C, Burnier JP. Determination of the solution structure of the peptide hormone guanylin: observation of a novel form of topological stereoisomerism. *Biochemistry* (1994) 33:13581–92. doi: 10.1021/bi00250a010
40. Marx UC, Klodt J, Meyer M, Gerlach H, Rosch P, Forssmann WG, et al. One peptide, two topologies: structure and interconversion dynamics of human uroguanylin isomers. *J Pept Res.* (1998) 52:229–40. doi: 10.1111/j.1399-3011.1998.tb01480.x
41. Hamra FK, Eber SL, Chin DT, Currie MG, Forte LR. Regulation of intestinal uroguanylin/guanylin receptor-mediated responses by mucosal acidity. *Proc Natl Acad Sci USA.* (1997) 94:2705–10. doi: 10.1073/pnas.94.6.2705
42. Pires AS, Porto WF, Castro PO, Franco OL, Alencar SA. Theoretical structural characterization of lymphoguanylin: a potential candidate for the development of drugs to treat gastrointestinal disorders. *J Theor Biol.* (2017) 419:193–200. doi: 10.1016/j.jtbi.2017.02.016
43. Shailubhai K, Palejwala V, Arjunan KP, Saykhedkar S, Nefsky B, Foss JA, et al. Plecanatide and dolcanatide, novel guanylate cyclase-C agonists, ameliorate gastrointestinal inflammation in experimental models of murine colitis. *World J Gastrointest Pharmacol Ther.* (2015) 6:213–22. doi: 10.4292/wjgpt.v6.i4.213
44. Boulete IM, Thadi A, Beaufrand C, Patwa V, Joshi A, Foss JA, et al. Oral treatment with plecanatide or dolcanatide attenuates visceral hypersensitivity via activation of guanylate cyclase-C in rat models. *World J Gastroenterol.* (2018) 24:1888–900. doi: 10.3748/wjg.v24.i17.1888
45. Porto WF, Franco OL, Alencar SA. Computational analyses and prediction of guanylin deleterious SNPs. *Peptides* (2015) 69:92–102. doi: 10.1016/j.peptides.2015.04.013
46. Marcolino AC, Porto WF, Pires AS, Franco OL, Alencar SA. Structural impact analysis of missense SNPs present in the uroguanylin gene by long-term molecular dynamics simulations. *J Theor Biol.* (2016) 410:9–17. doi: 10.1016/j.jtbi.2016.09.008
47. Hofmann F, Ammendola A, Schlossmann J. Rising behind NO: cGMP-dependent protein kinases. *J Cell Sci.* (2000) 113:1671–6.
48. Pfeifer A, Klatt P, Massberg S, Ny L, Sausbier M, Hirneiss C, et al. Defective smooth muscle regulation in cGMP kinase I-deficient mice. *Embo J.* (1998) 17:3045–51. doi: 10.1093/emboj/17.11.3045

49. Markert T, Vaandrager AB, Gambaryan S, Pohler D, Hausler C, Walter U, et al. Endogenous expression of type II cGMP-dependent protein kinase mRNA and protein in rat intestine. Implications for cystic fibrosis transmembrane conductance regulator. *J Clin Invest.* (1995) 96:822–30. doi: 10.1172/JCI118128
50. Pfeifer A, Aszodi A, Seidler U, Ruth P, Hofmann F, Fassler R. Intestinal secretory defects and dwarfism in mice lacking cGMP-dependent protein kinase II. *Science* (1996) 274:2082–6. doi: 10.1126/science.274.5295.2082
51. Vaandrager AB. Structure and function of the heat-stable enterotoxin receptor/guanylyl cyclase C. *Mol Cell Biochem.* (2002) 230:73–83. doi: 10.1023/A:1014231722696
52. Chen T, Kocinsky HS, Cha B, Murtazina R, Yang J, Tse CM, et al. Cyclic GMP kinase II (cGKII) inhibits NHE3 by altering its trafficking and phosphorylating NHE3 at three required sites: identification of a multifunctional phosphorylation site. *J Biol Chem.* (2015) 290:1952–65. doi: 10.1074/jbc.M114.590174
53. Bender AT, Beavo JA. Cyclic nucleotide phosphodiesterases: molecular regulation to clinical use. *Pharmacol Rev.* (2006) 58:488–520. doi: 10.1124/pr.58.3.5
54. Francis SH, Busch JL, Corbin JD, Sibley D. cGMP-dependent protein kinases and cGMP phosphodiesterases in nitric oxide and cGMP action. *Pharmacol Rev.* (2010) 62:525–63. doi: 10.1124/pr.110.002907
55. Maurice DH, Ke H, Ahmad F, Wang Y, Chung J, Manganiello VC. Advances in targeting cyclic nucleotide phosphodiesterases. *Nat Rev Drug Discov.* (2014) 13:290–314. doi: 10.1038/nrd4228
56. Arshad N, Visweswariah SS. Cyclic nucleotide signaling in intestinal epithelia: getting to the gut of the matter. *Wiley Interdiscip Rev Syst Biol Med.* (2013) 5:409–24. doi: 10.1002/wsbm.1223
57. Mahmood B, Damm MM, Jensen TS, Backe MB, Dahllof MS, Poulsen SS, et al. Phosphodiesterases in non-neoplastic appearing colonic mucosa from patients with colorectal neoplasia. *BMC Cancer* (2016) 16:938. doi: 10.1186/s12885-016-2980-z
58. Li N, Lee K, Xi Y, Zhu B, Gary BD, Ramirez-Alcantara V, et al. Phosphodiesterase 10A: a novel target for selective inhibition of colon tumor cell growth and beta-catenin-dependent TCF transcriptional activity. *Oncogene* (2015b) 34:1499–509. doi: 10.1038/onc.2014.94
59. Von Volkmann HL, Nylund K, Tronstad RR, Hovdenak N, Hausken T, Fiskerstrand T, et al. An activating gucy2c mutation causes impaired contractility and fluid stagnation in the small bowel. *Scand J Gastroenterol.* (2016) 51:1308–15. doi: 10.1080/00365521.2016.1200139
60. Von Volkmann HL, Bronstad I, Gilja OH, R RT, Sangnes DA, Nortvedt R, et al. Prolonged intestinal transit and diarrhea in patients with an activating GUCY2C mutation. *PLoS ONE* (2017) 12:e0185496. doi: 10.1371/journal.pone.0185496
61. Smith A, Bulman DE, Goldsmith C, Bareke E, Majewski J, Boycott KM, et al. Meconium ileus in a Lebanese family secondary to mutations in the GUCY2C gene. *Eur J Hum Genet.* (2015) 23:990–2. doi: 10.1038/ejhg.2014.236
62. Mann EA, Jump ML, Wu J, Yee E, Giannella RA. Mice lacking the guanylyl cyclase C receptor are resistant to STa-induced intestinal secretion. *Biochem Biophys Res Commun.* (1997) 239:463–6. doi: 10.1006/bbrc.1997.7487
63. Schulz S, Lopez MJ, Kuhn M, Garbers DL. Disruption of the guanylyl cyclase-C gene leads to a paradoxical phenotype of viable but heat-stable enterotoxin-resistant mice. *J Clin Invest.* (1997) 100:1590–5. doi: 10.1172/JCI119683
64. Charney AN, Egnor RW, Steinbrecher KA, Cohen MB. Effect of secretagogues and pH on intestinal transport in guanylin-deficient mice. *Biochim Biophys Acta* (2004) 1671:79–86. doi: 10.1016/j.bbagen.2004.01.007
65. Krausova M, Korinek V. Wnt signaling in adult intestinal stem cells and cancer. *Cell Signal* (2014) 26:570–9. doi: 10.1016/j.cellsig.2013.11.032
66. Van Der Flier LG, Sabates-Bellver J, Oving I, Haegebarth A, De Palo M, Anti M, et al. The intestinal Wnt/TCF signature. *Gastroenterology* (2007) 132:628–32. doi: 10.1053/j.gastro.2006.08.039
67. Hatzis P, Van Der Flier LG, Van Driel MA, Guryev V, Nielsen F, Denissov S, et al. Genome-wide pattern of TCF7L2/TCF4 chromatin occupancy in colorectal cancer cells. *Mol Cell Biol.* (2008) 28:2732–44. doi: 10.1128/MCB.02175-07
68. Hodar C, Assar R, Colombres M, Aravena A, Pavez L, Gonzalez M, et al. Genome-wide identification of new Wnt/beta-catenin target genes in the human genome using CART method. *BMC Genomics* (2010) 11:348. doi: 10.1186/1471-2164-11-348
69. Herbst A, Jurinovic V, Krebs S, Thieme SE, Blum H, Goke B, et al. Comprehensive analysis of beta-catenin target genes in colorectal carcinoma cell lines with deregulated Wnt/beta-catenin signaling. *BMC Genomics* (2014) 15:74. doi: 10.1186/1471-2164-15-74
70. He XC, Zhang J, Tong WG, Tawfik O, Ross J, Scoville DH, et al. BMP signaling inhibits intestinal stem cell self-renewal through suppression of Wnt-beta-catenin signaling. *Nat Genet.* (2004) 36:1117–21. doi: 10.1038/ng1430
71. Van Dop WA, Uhmann A, Wijgerde M, Sleddens-Linkels E, Heijmans J, Offerhaus GJ, et al. Depletion of the colonic epithelial precursor cell compartment upon conditional activation of the hedgehog pathway. *Gastroenterology* (2009) 136:2195–203.e2191–2197. doi: 10.1053/j.gastro.2009.02.068
72. Qi Z, Li Y, Zhao B, Xu C, Liu Y, Li H, et al. BMP restricts stemness of intestinal Lgr5(+) stem cells by directly suppressing their signature genes. *Nat Commun.* (2017) 8:13824. doi: 10.1038/ncomms13824
73. Korinek V, Barker N, Moerer P, Van Donselaar E, Huls G, Peters PJ, et al. Depletion of epithelial stem-cell compartments in the small intestine of mice lacking Tcf-4. *Nat Genet.* (1998) 19:379–83. doi: 10.1038/1270
74. Pinto D, Gregorieff A, Begthel H, Clevers H. Canonical Wnt signals are essential for homeostasis of the intestinal epithelium. *Genes Dev.* (2003) 17:1709–13. doi: 10.1101/gad.267103
75. Muncan V, Sansom OJ, Tertoolen L, Phesse TJ, Begthel H, Sancho E, et al. Rapid loss of intestinal crypts upon conditional deletion of the Wnt/Tcf-4 target gene c-Myc. *Mol Cell Biol.* (2006) 26:8418–26. doi: 10.1128/MCB.00821-06
76. Fevr T, Robine S, Louvard D, Huelsken J. Wnt/beta-catenin is essential for intestinal homeostasis and maintenance of intestinal stem cells. *Mol Cell Biol.* (2007) 27:7551–9. doi: 10.1128/MCB.01034-07
77. Fearon ER. Molecular genetics of colorectal cancer. *Annu Rev Pathol.* (2011) 6:479–507. doi: 10.1146/annurev-pathol-011110-130235
78. Moser AR, Pitot HC, Dove WF. A dominant mutation that predisposes to multiple intestinal neoplasia in the mouse. *Science* (1990) 247:322–4. doi: 10.1126/science.2296722
79. Fodde R, Edelmann W, Yang K, Van Leeuwen C, Carlson C, Renault B, et al. A targeted chain-termination mutation in the mouse Apc gene results in multiple intestinal tumors. *Proc Natl Acad Sci USA* (1994) 91:8969–73. doi: 10.1073/pnas.91.19.8969
80. Steinbrecher KA, Wowk SA, Rudolph JA, Witte DP, Cohen MB. Targeted inactivation of the mouse guanylin gene results in altered dynamics of colonic epithelial proliferation. *Am J Pathol.* (2002) 161:2169–78. doi: 10.1016/S0002-9440(10)64494-X
81. Li P, Lin JE, Chervoneva I, Schulz S, Waldman SA, Pitari GM. Homeostatic control of the crypt-villus axis by the bacterial enterotoxin receptor guanylyl cyclase C restricts the proliferating compartment in intestine. *Am J Pathol.* (2007) 171:1847–58. doi: 10.2353/ajpath.2007.070198
82. Wang R, Kwon IK, Thangaraju M, Singh N, Liu K, Jay P, et al. Type 2 cGMP-dependent protein kinase regulates proliferation and differentiation in the colonic mucosa. *Am J Physiol Gastrointest Liver Physiol.* (2012) 303:G209–219. doi: 10.1152/ajpgi.00500.2011
83. Kraft CL, Rappaport JA, Snook AE, Pattison AM, Lynch JP, Waldman SA. GUCY2C maintains intestinal LGR5(+) stem cells by opposing ER stress. *Oncotarget* (2017) 8:102923–33. doi: 10.18632/oncotarget.22084
84. Li P, Schulz S, Bombonati A, Palazzo JP, Hyslop TM, Xu Y, et al. Guanylyl cyclase C suppresses intestinal tumorigenesis by restricting proliferation and maintaining genomic integrity. *Gastroenterology* (2007) 133:599–607. doi: 10.1053/j.gastro.2007.05.052
85. Basu N, Saha S, Khan I, Ramachandra SG, Visweswariah SS. Intestinal cell proliferation and senescence are regulated by receptor guanylyl cyclase C and p21. *J Biol Chem.* (2014) 289:581–93. doi: 10.1074/jbc.M113.511311
86. Pitari GM, Di Guglielmo MD, Park J, Schulz S, Waldman SA. Guanylyl cyclase C agonists regulate progression through the cell cycle of human colon carcinoma cells. *Proc Natl Acad Sci USA.* (2001) 98:7846–51. doi: 10.1073/pnas.141124698

87. Lin JE, Li P, Snook AE, Schulz S, Dasgupta A, Hyslop TM, et al. The hormone receptor GUCY2C suppresses intestinal tumor formation by inhibiting AKT signaling. *Gastroenterology* (2010) 138:241–54. doi: 10.1053/j.gastro.2009.08.064
88. Cen B, Deguchi A, Weinstein IB. Activation of protein kinase G Increases the expression of p21CIP1, p27KIP1, and histidine triad protein 1 through Sp1. *Cancer Res.* (2008) 68:5355–62. doi: 10.1158/0008-5472.CAN-07-6869
89. Pitari GM, Lin JE, Shah FJ, Lubbe WJ, Zuzga DS, Li P, et al. Enterotoxin preconditioning restores calcium-sensing receptor-mediated cytostasis in colon cancer cells. *Carcinogenesis* (2008) 29:1601–7. doi: 10.1093/carcin/bgn148
90. Lee K, A Piazza G. The interaction between the Wnt/beta-catenin signaling cascade and PKG activation in cancer. *J Biomed Res.* (2017) 31, 189–196. doi: 10.7555/JBR.31.20160133
91. Li N, Chen X, Zhu B, Ramirez-Alcantara V, Canzoneri JC, Lee K, et al. Suppression of beta-catenin/TCF transcriptional activity and colon tumor cell growth by dual inhibition of PDE5 and 10. *Oncotarget* (2015) 6:27403–15. doi: 10.18632/oncotarget.4741
92. Lee K, Lindsey AS, Li N, Gary B, Andrews J, Keeton AB, et al. beta-catenin nuclear translocation in colorectal cancer cells is suppressed by PDE10A inhibition, cGMP elevation, and activation of PKG. *Oncotarget* (2016) 7:5353–65. doi: 10.1158/1538-7445.AM2016-331
93. Kwon IK, Wang R, Thangaraju M, Shuang H, Liu K, Dashwood R, et al. PKG inhibits TCF signaling in colon cancer cells by blocking beta-catenin expression and activating FOXO4. *Oncogene* (2010) 29:3423–34. doi: 10.1038/onc.2010.91
94. Wang R, Kwon IK, Singh N, Islam B, Liu K, Sridhar S, et al. Type 2 cGMP-dependent protein kinase regulates homeostasis by blocking c-Jun N-terminal kinase in the colon epithelium. *Cell Death Differ.* (2014) 21:427–37. doi: 10.1038/cdd.2013.163
95. Schuijers J, Mokry M, Hatzis P, Cuppen E, Clevers H. Wnt-induced transcriptional activation is exclusively mediated by TCF/LEF. *Embo J* (2014) 33:146–56. doi: 10.1002/embj.201385358
96. Lin S, Li Y, Zamyatnin AAJr, Werner J, Bazhin AV. Reactive oxygen species and colorectal cancer. *J Cell Physiol.* (2018) 233:5119–32. doi: 10.1002/jcp.26356
97. Kastenhuber ER, Lowe SW. Putting p53 in context. *Cell* (2017) 170:1062–78. doi: 10.1016/j.cell.2017.08.028
98. Hanahan D, Weinberg RA. Hallmarks of cancer: the next generation. *Cell* (2011) 144:646–74. doi: 10.1016/j.cell.2011.02.013
99. Powell SM, Zilz N, Beazer-Barclay Y, Bryan TM, Hamilton SR, Thibodeau SN, et al. APC mutations occur early during colorectal tumorigenesis. *Nature* (1992) 359:235–7. doi: 10.1038/359235a0
100. Zhang L, Shay JW. Multiple roles of APC and its therapeutic implications in colorectal cancer. *J Natl Cancer Inst.* (2017) 109:djw332. doi: 10.1093/jnci/djw332
101. Henderson BR. Nuclear-cytoplasmic shuttling of APC regulates beta-catenin subcellular localization and turnover. *Nat Cell Biol.* (2000) 2:653–60. doi: 10.1038/35023605
102. Kouzmenko AP, Takeyama K, Kawasaki Y, Akiyama T, Kato S. Truncation mutations abolish chromatin-associated activities of adenomatous polyposis coli. *Oncogene* (2008) 27:4888–99. doi: 10.1038/onc.2008.127
103. Brocardo MG, Borowiec JA, Henderson BR. Adenomatous polyposis coli protein regulates the cellular response to DNA replication stress. *Int J Biochem Cell Biol.* (2011) 43:1354–64. doi: 10.1016/j.biocel.2011.05.013
104. Jaiswal AS, Narayan S. Assembly of the base excision repair complex on abasic DNA and role of adenomatous polyposis coli on its functional activity. *Biochemistry* (2011) 50:1901–9. doi: 10.1021/bi102000q
105. Caldwell CM, Kaplan KB. The role of APC in mitosis and in chromosome instability. *Adv Exp Med Biol.* (2009) 656:51–64. doi: 10.1007/978-1-4419-1145-2_5
106. Kaplan KB, Burds AA, Swedlow JR, Bekir SS, Sorger PK, Nathke IS. A role for the adenomatous polyposis coli protein in chromosome segregation. *Nat Cell Biol.* (2001) 3:429–32. doi: 10.1038/35070123
107. Caldwell CM, Green RA, Kaplan KB. APC mutations lead to cytokinetic failures *in vitro* and tetraploid genotypes in Min mice. *J Cell Biol.* (2007) 178:1109–20. doi: 10.1083/jcb.200703186
108. Dow LE, O'rourke KP, Simon J, Tschaharganeh DF, Van Es JH, Clevers H, et al. Apc restoration promotes cellular differentiation and reestablishes crypt homeostasis in colorectal cancer. *Cell* (2015) 161:1539–52. doi: 10.1016/j.cell.2015.05.033
109. Lin JE, Snook AE, Li P, Stoecker BA, Kim GW, Magee MS, et al. GUCY2C opposes systemic genotoxic tumorigenesis by regulating AKT-dependent intestinal barrier integrity. *PLoS ONE* (2012) 7:e31686. doi: 10.1371/journal.pone.0031686
110. Park J, Schulz S, Waldman SA. Intestine-specific activity of the human guanylyl cyclase C promoter is regulated by Cdx2. *Gastroenterology* (2000) 119:89–96. doi: 10.1053/gast.2000.8520
111. Di Guglielmo MD, Park J, Schulz S, Waldman SA. Nucleotide requirements for CDX2 binding to the cis promoter element mediating intestine-specific expression of guanylyl cyclase C. *FEBS Lett.* (2001) 507:128–32. doi: 10.1016/S0014-5793(01)02952-0
112. Aoki K, Tamai Y, Horiike S, Oshima M, Taketo MM. Colonic polyposis caused by mTOR-mediated chromosomal instability in Apc+/Delta716 Cdx2+/- compound mutant mice. *Nat Genet.* (2003) 35:323–30. doi: 10.1038/ng1265
113. Li P, Wuthrick E, Rappaport JA, Kraft C, Lin JE, Marszalowicz G, et al. GUCY2C signaling opposes the acute radiation-induced GI syndrome. *Cancer Res.* (2017) 77:5095–106. doi: 10.1158/0008-5472.CAN-17-0859
114. Groschwitz KR, Hogan SP. Intestinal barrier function: molecular regulation and disease pathogenesis. *J Allergy Clin Immunol.* (2009) 124:3–20. doi: 10.1016/j.jaci.2009.05.038
115. Ye D, Ma I, Ma TY. Molecular mechanism of tumor necrosis factor-alpha modulation of intestinal epithelial tight junction barrier. *Am J Physiol Gastrointest Liver Physiol.* (2006) 290:G496–504. doi: 10.1152/ajpgi.00318.2005
116. Boirivant M, Amendola A, Butera A, Sanchez M, Xu L, Marinaro M, et al. A transient breach in the epithelial barrier leads to regulatory T-cell generation and resistance to experimental colitis. *Gastroenterology* (2008) 135:1612–23.e1615. doi: 10.1053/j.gastro.2008.07.028
117. Turner JR. Intestinal mucosal barrier function in health and disease. *Nat Rev Immunol.* (2009) 9:799–809. doi: 10.1038/nri2653
118. Kuhn R, Lohler J, Rennick D, Rajewsky K, Muller W. Interleukin-10-deficient mice develop chronic enterocolitis. *Cell* (1993) 75:263–74. doi: 10.1016/0092-8674(93)80068-P
119. Zolotarevsky Y, Hecht G, Koutsouris A, Gonzalez DE, Quan C, Tom J, et al. A membrane-permeant peptide that inhibits MLC kinase restores barrier function *in vitro* models of intestinal disease. *Gastroenterology* (2002) 123:163–72. doi: 10.1053/gast.2002.34235
120. Kinugasa T, Akagi Y. Status of colitis-associated cancer in ulcerative colitis. *World J Gastrointest Oncol.* (2016) 8:351–7. doi: 10.4251/wjgo.v8.i4.351
121. Han X, Mann E, Gilbert S, Guan Y, Steinbrecher KA, Montrose MH, et al. Loss of guanylyl cyclase C (GCC) signaling leads to dysfunctional intestinal barrier. *PLoS ONE* (2011) 6:e16139. doi: 10.1371/journal.pone.0016139
122. Harmel-Laws E, Mann EA, Cohen MB, Steinbrecher KA. Guanylate cyclase C deficiency causes severe inflammation in a murine model of spontaneous colitis. *PLoS ONE* (2013) 8:e79180. doi: 10.1371/journal.pone.0079180
123. Chang WL, Masih S, Thadi A, Patwa V, Joshi A, Cooper HS, et al. Plecanatide-mediated activation of guanylate cyclase-C suppresses inflammation-induced colorectal carcinogenesis in Apc+/Min-FCCC mice. *World J Gastrointest Pharmacol Ther.* (2017) 8:47–59. doi: 10.4292/wjgpt.v8.i1.47
124. Lin S, Wang J, Wang L, Wen J, Guo Y, Qiao W, et al. Phosphodiesterase-5 inhibition suppresses colonic inflammation-induced tumorigenesis via blocking the recruitment of MDSC. *Am J Cancer Res.* (2017) 7:41–52.
125. Wang R, Islam BN, Bridges A, Sharman SK, Hu M, Hou Y, et al. cGMP signaling increases antioxidant gene expression by activating forkhead box O3A in the colon epithelium. *Am J Pathol.* (2017) 187:377–89. doi: 10.1016/j.ajpath.2016.10.016
126. Coleman OI, Haller D. Bacterial signaling at the intestinal epithelial interface in inflammation and cancer. *Front Immunol.* (2017) 8:1927. doi: 10.3389/fimmu.2017.01927
127. Tomasello G, Tralongo P, Damiani P, Sinagra E, Di Trapani B, Zeenny MN, et al. Dismicrobism in inflammatory bowel disease and colorectal cancer:

changes in response of colocytes. *World J Gastroenterol.* (2014) 20:18121–30. doi: 10.3748/wjg.v20.i48.18121
128. Shreiner AB, Kao JY, Young VB. The gut microbiome in health and in disease. *Curr Opin Gastroenterol.* (2015) 31:69–75. doi: 10.1097/MOG.0000000000000139
129. Kasubuchi M, Hasegawa S, Hiramatsu T, Ichimura A, Kimura I. Dietary gut microbial metabolites, short-chain fatty acids, and host metabolic regulation. *Nutrients* (2015) 7:2839–49. doi: 10.3390/nu7042839
130. Ubeda C, Djukovic A, Isaac S. Roles of the intestinal microbiota in pathogen protection. *Clin Transl Immunol.* (2017) 6:e128. doi: 10.1038/cti.2017.2
131. Lawhon SD, Maurer R, Suyemoto M, Altier C. Intestinal short-chain fatty acids alter Salmonella typhimurium invasion gene expression and virulence through BarA/SirA. *Mol Microbiol.* (2002) 46:1451–64. doi: 10.1046/j.1365-2958.2002.03268.x
132. Fukuda S, Toh H, Hase K, Oshima K, Nakanishi Y, Yoshimura K, et al. Bifidobacteria can protect from enteropathogenic infection through production of acetate. *Nature* (2011) 469:543–7. doi: 10.1038/nature09646
133. Sellon RK, Tonkonogy S, Schultz M, Dieleman LA, Grenther W, Balish E, et al. Resident enteric bacteria are necessary for development of spontaneous colitis and immune system activation in interleukin-10-deficient mice. *Infect Immun.* (1998) 66:5224–31.
134. Uronis JM, Muhlbauer M, Herfarth HH, Rubinas TC, Jones GS, Jobin C. Modulation of the intestinal microbiota alters colitis-associated colorectal cancer susceptibility. *PLoS ONE* (2009) 4:e6026. doi: 10.1371/journal.pone.0006026
135. Petersson J, Schreiber O, Hansson GC, Gendler SJ, Velcich A, Lundberg JO, et al. Importance and regulation of the colonic mucus barrier in a mouse model of colitis. *Am J Physiol Gastrointest Liver Physiol.* (2011) 300:G327–333. doi: 10.1152/ajpgi.00422.2010
136. Li Y, Kundu P, Seow SW, De Matos CT, Aronsson L, Chin KC, et al. Gut microbiota accelerate tumor growth via c-jun and STAT3 phosphorylation in APCMin/+ mice. *Carcinogenesis* (2012) 33:1231–8. doi: 10.1093/carcin/bgs137
137. Candela M, Turroni S, Biagi E, Carbonero F, Rampelli S, Fiorentini C, et al. Inflammation and colorectal cancer, when microbiota-host mutualism breaks. *World J Gastroenterol.* (2014) 20:908–22. doi: 10.3748/wjg.v20.i4.908
138. Dejea CM, Fathi P, Craig JM, Boleij A, Taddese R, Geis AL, et al. Patients with familial adenomatous polyposis harbor colonic biofilms containing tumorigenic bacteria. *Science* (2018) 359:592–7. doi: 10.1126/science.aah3648
139. Johansson ME, Larsson JM, Hansson GC. The two mucus layers of colon are organized by the MUC2 mucin, whereas the outer layer is a legislator of host-microbial interactions. *Proc Natl Acad Sci USA* (2011) 108 (Suppl. 1):4659–65. doi: 10.1073/pnas.1006451107
140. Mann EA, Harmel-Laws E, Cohen MB, Steinbrecher KA. Guanylate cyclase C limits systemic dissemination of a murine enteric pathogen. *BMC Gastroenterol.* (2013) 13:135. doi: 10.1186/1471-230X-13-135
141. Amarachintha S, Harmel-Laws E, Steinbrecher KA. Guanylate cyclase C reduces invasion of intestinal epithelial cells by bacterial pathogens. *Sci Rep.* (2018) 8:1521. doi: 10.1038/s41598-018-19868-z
142. Pitari GM, Zingman LV, Hodgson DM, Alekseev AE, Kazerounian S, Bienengraeber M, et al. Bacterial enterotoxins are associated with resistance to colon cancer. *Proc Natl Acad Sci USA*. (2003) 100:2695–9. doi: 10.1073/pnas.0434905100
143. Li P, Lin JE, Snook AE, Waldman SA. ST-producing *E. coli* oppose carcinogen-induced colorectal tumorigenesis in mice. *Toxins* (2017) 9:E279. doi: 10.3390/toxins9090279
144. Powell DW, Pinchuk IV, Saada JI, Chen X, Mifflin RC. Mesenchymal cells of the intestinal lamina propria. *Annu Rev Physiol.* (2011) 73:213–37. doi: 10.1146/annurev.physiol.70.113006.100646
145. Koliaraki V, Pallangyo CK, Greten FR, Kollias G. Mesenchymal cells in colon cancer. *Gastroenterology* (2017) 152:964–97. doi: 10.1053/j.gastro.2016.11.049
146. Kosinski C, Li VS, Chan AS, Zhang J, Ho C, Tsui WY, et al. Gene expression patterns of human colon tops and basal crypts and BMP antagonists as intestinal stem cell niche factors. *Proc Natl Acad Sci USA* (2007) 104:15418–23. doi: 10.1073/pnas.0707210104
147. Pinchuk IV, Mifflin RC, Saada JI, Powell DW. Intestinal mesenchymal cells. *Curr Gastroenterol Rep.* (2010) 12:310–8. doi: 10.1007/s11894-010-0135-y
148. Valenta T, Degirmenci B, Moor AE, Herr P, Zimmerli D, Moor MB, et al. Wnt ligands secreted by subepithelial mesenchymal cells are essential for the survival of intestinal stem cells and gut homeostasis. *Cell Rep.* (2016) 15:911–8. doi: 10.1016/j.celrep.2016.03.088
149. Allaire JM, Roy SA, Ouellet C, Lemieux E, Jones C, Paquet M, et al. Bmp signaling in colonic mesenchyme regulates stromal microenvironment and protects from polyposis initiation. *Int J Cancer* (2016) 138:2700–12. doi: 10.1002/ijc.30001
150. De Boeck A, Hendrix A, Maynard D, Van Bockstal M, Daniels A, Pauwels P, et al. Differential secretome analysis of cancer-associated fibroblasts and bone marrow-derived precursors to identify microenvironmental regulators of colon cancer progression. *Proteomics* (2013) 13:379–88. doi: 10.1002/pmic.201200179
151. Torres S, Bartolome RA, Mendes M, Barderas R, Fernandez-Acenero MJ, Pelaez-Garcia A, et al. Proteome profiling of cancer-associated fibroblasts identifies novel proinflammatory signatures and prognostic markers for colorectal cancer. *Clin Cancer Res.* (2013) 19:6006–19. doi: 10.1158/1078-0432.CCR-13-1130
152. Calon A, Tauriello DV, Batlle E. TGF-beta in CAF-mediated tumor growth and metastasis. *Semin Cancer Biol.* (2014) 25:15–22. doi: 10.1016/j.semcancer.2013.12.008
153. Vermeulen L, De Sousa EMF, Van Der Heijden M, Cameron K, De Jong JH, Borovski T, et al. Wnt activity defines colon cancer stem cells and is regulated by the microenvironment. *Nat Cell Biol.* (2010) 12:468–76. doi: 10.1038/ncb2048
154. Karagiannis GS, Treacy A, Messenger D, Grin A, Kirsch R, Riddell RH, et al. Expression patterns of bone morphogenetic protein antagonists in colorectal cancer desmoplastic invasion fronts. *Mol Oncol.* (2014) 8:1240–52. doi: 10.1016/j.molonc.2014.04.004
155. Deguchi A, Thompson WJ, Weinstein IB. Activation of protein kinase G is sufficient to induce apoptosis and inhibit cell migration in colon cancer cells. *Cancer Res.* (2004) 64:3966–73. doi: 10.1158/0008-5472.CAN-03-3740
156. Lubbe WJ, Zuzga DS, Zhou Z, Fu W, Pelta-Heller J, Muschel RJ, et al. Guanylyl cyclase C prevents colon cancer metastasis by regulating tumor epithelial cell matrix metalloproteinase-9. *Cancer Res.* (2009) 69:3529–36. doi: 10.1158/0008-5472.CAN-09-0067
157. Zuzga DS, Pelta-Heller J, Li P, Bombonati A, Waldman SA, Pitari GM. Phosphorylation of vasodilator-stimulated phosphoprotein Ser239 suppresses filopodia and invadopodia in colon cancer. *Int J Cancer* (2012) 130:2539–48. doi: 10.1002/ijc.26257
158. Gibbons AV, Lin JE, Kim GW, Marszalowicz GP, Li P, Stoecker BA, et al. Intestinal GUCY2C prevents TGF-beta secretion coordinating desmoplasia and hyperproliferation in colorectal cancer. *Cancer Res.* (2013) 73:6654–66. doi: 10.1158/0008-5472.CAN-13-0887
159. Wu M, Wu Y, Qian H, Tao Y, Pang J, Wang Y, et al. Type II cGMP-dependent protein kinase inhibits the migration, invasion and proliferation of several types of human cancer cells. *Mol Med Rep.* (2017) 16:5729–37. doi: 10.3892/mmr.2017.7290
160. Castro J, Harrington AM, Hughes PA, Martin CM, Ge P, Shea CM, et al. Linaclotide inhibits colonic nociceptors and relieves abdominal pain via guanylate cyclase-C and extracellular cyclic guanosine 3′,5′-monophosphate. *Gastroenterology* (2013) 145:1334–46.e1331–e1311. doi: 10.1053/j.gastro.2013.08.017
161. Silos-Santiago I, Hannig G, Eutamene H, Ustinova EE, Bernier SG, Ge P, et al. Gastrointestinal pain: unraveling a novel endogenous pathway through uroguanylin/guanylate cyclase-C/cGMP activation. *Pain* (2013) 154:1820–30. doi: 10.1016/j.pain.2013.05.044
162. Tchernychev B, Ge P, Kessler MM, Solinga RM, Wachtel D, Tobin JV, et al. MRP4 modulation of the guanylate cyclase-C/cGMP pathway: effects on linaclotide-induced electrolyte secretion and cGMP efflux. *J Pharmacol Exp Ther.* (2015) 355:48–56. doi: 10.1124/jpet.115.224329
163. Van Aubel RA, Smeets PH, Peters JG, Bindels RJ, Russel FG. The MRP4/ABCC4 gene encodes a novel apical organic anion transporter in human kidney proximal tubules: putative efflux pump for urinary cAMP and cGMP. *J Am Soc Nephrol.* (2002) 13:595–603.

164. Chandar AK. Diagnosis and treatment of irritable bowel syndrome with predominant constipation in the primary-care setting: focus on linaclotide. *Int J Gen Med.* (2017) 10:385–93. doi: 10.2147/IJGM.S126581
165. Siegel RL, Miller KD, Jemal A. Cancer statistics, 2018. *CA Cancer J Clin.* (2018) 68:7–30. doi: 10.3322/caac.21442
166. Xing Y, Zhao Z, Zhu Y, Zhao L, Zhu A, Piao D. Comprehensive analysis of differential expression profiles of mRNAs and lncRNAs and identification of a 14-lncRNA prognostic signature for patients with colon adenocarcinoma. *Oncol Rep.* (2018) 39:2365–75. doi: 10.3892/or.2018.6324
167. Whitt JD, Li N, Tinsley HN, Chen X, Zhang W, Li Y, et al. A novel sulindac derivative that potently suppresses colon tumor cell growth by inhibiting cGMP phosphodiesterase and beta-catenin transcriptional activity. *Cancer Prev Res.* (2012) 5:822–33. doi: 10.1158/1940-6207.CAPR-11-0559
168. Hou Y, Gupta N, Schoenlein P, Wong E, Martindale R, Ganapathy V, et al. An anti-tumor role for cGMP-dependent protein kinase. *Cancer Lett.* (2006) 240:60–8. doi: 10.1016/j.canlet.2005.08.035
169. Kwon IK, Schoenlein PV, Delk J, Liu K, Thangaraju M, Dulin NO, et al. Expression of cyclic guanosine monophosphate-dependent protein kinase in metastatic colon carcinoma cells blocks tumor angiogenesis. *Cancer* (2008) 112:1462–70. doi: 10.1002/cncr.23334
170. Basu N, Bhandari R, Natarajan VT, Visweswariah SS. Cross talk between receptor guanylyl cyclase C and c-src tyrosine kinase regulates colon cancer cell cytostasis. *Mol Cell Biol.* (2009) 29:5277–89. doi: 10.1128/MCB.00001-09
171. Danaee H, Kalebic T, Wyant T, Fassan M, Mescoli C, Gao F, et al. Consistent expression of guanylyl cyclase-C in primary and metastatic gastrointestinal cancers. *PLoS ONE* (2017) 12:e0189953. doi: 10.1371/journal.pone.0189953
172. Zhang L, Zhou W, Velculescu VE, Kern SE, Hruban RH, Hamilton SR, et al. Gene expression profiles in normal and cancer cells. *Science* (1997) 276:1268–72. doi: 10.1126/science.276.5316.1268
173. Cohen MB, Hawkins JA, Witte DP. Guanylin mRNA expression in human intestine and colorectal adenocarcinoma. *Lab Invest.* (1998) 78:101–8.
174. Shailubhai K, Yu HH, Karunanandaa K, Wang JY, Eber SL, Wang Y, et al. Uroguanylin treatment suppresses polyp formation in the Apc(Min/+) mouse and induces apoptosis in human colon adenocarcinoma cells via cyclic GMP. *Cancer Res.* (2000) 60:5151–7.
175. Steinbrecher KA, Tuohy TM, Heppner Goss K, Scott MC, Witte DP, Groden J, et al. Expression of guanylin is downregulated in mouse and human intestinal adenomas. *Biochem Biophys Res Commun.* (2000) 273:225–30. doi: 10.1006/bbrc.2000.2917
176. Wilson C, Lin JE, Li P, Snook AE, Gong J, Sato T, et al. The paracrine hormone for the GUCY2C tumor suppressor, guanylin, is universally lost in colorectal cancer. *Cancer Epidemiol Biomarkers Prev.* (2014) 23:2328–37. doi: 10.1158/1055-9965.EPI-14-0440
177. Lin JE, Colon-Gonzalez F, Blomain E, Kim GW, Aing A, Stoecker B, et al. Obesity-induced colorectal cancer is driven by caloric silencing of the guanylin-GUCY2C paracrine signaling axis. *Cancer Res.* (2016) 76:339–46. doi: 10.1158/0008-5472.CAN-15-1467-T
178. Di Guglielmo MD, Perdue L, Adeyemi A, Van Golen KL, Corao DU. Immunohistochemical staining for uroguanylin, a satiety hormone, is decreased in intestinal tissue specimens from female adolescents with obesity. *Pediatr Dev Pathol.* (2017) 21:285–95. doi: 10.1177/1093526617722912
179. Cagir B, Gelmann A, Park J, Fava T, Tankelevitch A, Bittner EW, et al. Guanylyl cyclase C messenger RNA is a biomarker for recurrent stage II colorectal cancer. *Ann Intern Med.* (1999) 131:805–12. doi: 10.7326/0003-4819-131-11-199912070-00002
180. Pitari GM, Li P, Lin JE, Zuzga D, Gibbons AV, Snook AE, et al. The paracrine hormone hypothesis of colorectal cancer. *Clin Pharmacol Ther.* (2007) 82:441–7. doi: 10.1038/sj.clpt.6100325
181. Thompson WJ, Piazza GA, Li H, Liu L, Fetter J, Zhu B, et al. Exisulind induction of apoptosis involves guanosine 3′,5′-cyclic monophosphate phosphodiesterase inhibition, protein kinase G activation, and attenuated beta-catenin. *Cancer Res.* (2000) 60:3338–42.
182. Stoner GD, Budd GT, Ganapathi R, Deyoung B, Kresty LA, Nitert M, et al. Sulindac sulfone induced regression of rectal polyps in patients with familial adenomatous polyposis. *Adv Exp Med Biol.* (1999) 470:45–53. doi: 10.1007/978-1-4615-4149-3_5
183. Van Stolk R, Stoner G, Hayton WL, Chan K, Deyoung B, Kresty L, et al. Phase I trial of exisulind (sulindac sulfone, FGN-1) as a chemopreventive agent in patients with familial adenomatous polyposis. *Clin Cancer Res.* (2000) 6:78–89.
184. Arber N, Kuwada S, Leshno M, Sjodahl R, Hultcrantz R, Rex D. Sporadic adenomatous polyp regression with exisulind is effective but toxic: a randomised, double blind, placebo controlled, dose-response study. *Gut* (2006) 55:367–73. doi: 10.1136/gut.2004.061432
185. Li N, Xi Y, Tinsley HN, Gurpinar E, Gary BD, Zhu B, et al. Sulindac selectively inhibits colon tumor cell growth by activating the cGMP/PKG pathway to suppress Wnt/beta-catenin signaling. *Mol Cancer Ther.* (2013) 12:1848–59. doi: 10.1158/1535-7163.MCT-13-0048
186. Sharman SK, Islam BN, Hou Y, Singh N, Berger FG, Sridhar S, et al. Cyclic-GMP-elevating agents suppress polyposis in Apc(Min) mice by targeting the preneoplastic epithelium. *Cancer Prev Res.* (2018) 11:81–92. doi: 10.1158/1940-6207.CAPR-17-0267
187. Islam BN, Sharman SK, Hou Y, Bridges AE, Singh N, Kim S, et al. Sildenafil suppresses inflammation-driven colorectal cancer in mice. *Cancer Prev Res.* (2017) 10:377–88. doi: 10.1158/1940-6207.CAPR-17-0015
188. Haanen C. Sulindac and its derivatives: a novel class of anticancer agents. *Curr Opin Investig Drugs* (2001) 2:677–83.
189. Pitari GM, Li T, Baksh RI, Waldman SA. Exisulind and guanylyl cyclase C induce distinct antineoplastic signaling mechanisms in human colon cancer cells. *Mol Cancer Ther.* (2006) 5:1190–6. doi: 10.1158/1535-7163.MCT-05-0415
190. Weinberg DS, Lin JE, Foster NR, Della'zanna G, Umar A, Seisler D, et al. Bioactivity of oral linaclotide in human colorectum for cancer chemoprevention. *Cancer Prev Res.* (2017) 10:345–54. doi: 10.1158/1940-6207.CAPR-16-0286

Conflict of Interest Statement: SW is the Chair (uncompensated) of the Scientific Advisory Board and a member of the Board of Directors of Targeted Diagnostics & Therapeutics, Inc., which has a license to commercialize inventions arising from his work. Also, he receives research funding from, and has been a compensated speaker for, Synergy Pharmaceuticals, Inc. Further, he is Chair of the Board of Directors of Feelux Company, Ltd. The authors have no other relevant affiliations or financial involvement with any organization or entity with a financial interest in or financial conflict with the subject matter or materials discussed in the manuscript apart from those disclosed.

frontiers in Oncology

REVIEW
published: 02 July 2018
doi: 10.3389/fonc.2018.00248

Unraveling the Role of Angiogenesis in Cancer Ecosystems

*Iratxe Zuazo-Gaztelu and Oriol Casanovas**

Tumor Angiogenesis Group, ProCURE, Catalan Institute of Oncology – IDIBELL, Barcelona, Spain

Activation of the tumor and stromal cell-driven angiogenic program is one of the first requirements in the tumor ecosystem for growth and dissemination. The understanding of the dynamic angiogenic tumor ecosystem has rapidly evolved over the last decades. Beginning with the canonical sprouting angiogenesis, followed by vasculogenesis and intussusception, and finishing with vasculogenic mimicry, the need for different neovascularization mechanisms is further explored. In addition, an overview of the orchestration of angiogenesis within the tumor ecosystem cellular and molecular components is provided. Clinical evidence has demonstrated the effectiveness of traditional vessel-directed antiangiogenics, stressing on the important role of angiogenesis in tumor establishment, dissemination, and growth. Particular focus is placed on the interaction between tumor cells and their surrounding ecosystem, which is now regarded as a promising target for the development of new antiangiogenics.

Keywords: angiogenesis, angiogenic tumor ecosystem, sprouting angiogenesis, vasculogenesis, vasculogenic mimicry, intussusception, antiangiogenics

OPEN ACCESS

Edited by:
Ubaldo Emilio Martinez-Outschoorn, Thomas Jefferson University, United States

Reviewed by:
Ronca Roberto, University of Brescia, Italy
Anca Maria Cimpean, University of Medicine and Pharmacy, Timisoara, Romania
Miguel Ángel Medina, Universidad de Málaga, Spain

***Correspondence:**
Oriol Casanovas
ocasanovas@iconcologia.net

Specialty section:
This article was submitted to Molecular and Cellular Oncology, a section of the journal Frontiers in Oncology

Received: *09 May 2018*
Accepted: *19 June 2018*
Published: *02 July 2018*

Citation:
Zuazo-Gaztelu I and Casanovas O (2018) Unraveling the Role of Angiogenesis in Cancer Ecosystems. Front. Oncol. 8:248. doi: 10.3389/fonc.2018.00248

FOUNDATIONS OF THE TUMOR STROMAL ECOSYSTEM

The simplistic view of a tumor as a conundrum of just mutant cells engaged in clonal expansion is currently evolving into a more holistic approach where tumors are regarded as organ-like structures (1, 2). Genetic deletion, overexpression, mutation, and translocation events certainly lead to the transformation of a normal cell into a malignant cell which will then undergo sustained proliferation. However, for neoplastic cell expansion and growth, the ability to handle the surrounding stroma to create a favorable ecosystem becomes imperative (3). Hence, the information enclosed in the rich and ever-changing tumor microenvironment is crucial for the understanding of antitumor drug sensitivity.

The tumor microenvironment is formed by a tangled combination of both tumor and stromal cells, extracellular matrix (ECM), and secreted factors, thus perfectly fitting in the definition of an ecosystem (4, 5). Alteration of the gene expression of tumor cells provokes a disruption in the normal tissue homeostasis, favoring the secretion of certain molecules (cytokines, growth factors, etc.) that recruit stromal cells. Cells composing the tumor stroma are cancer-associated fibroblasts (CAFs), endothelial cells, pericytes, adipocytes, and immune cells, including monocytes, macrophages, lymphocytes, and dendritic cells (DCs), among others (**Figure 1**). These cells are enclosed in heterogeneously deposited ECMs and are affected by changing biophysical parameters including oxygenation and pH (6–9).

The insight into the dynamic action of the tumor ecosystem has improved exponentially over the last years, regarding the stroma as an integral part of tumor initiation, progression, and malignization. Stromal elements hold the key for prognostic and response predictive information. As such, therapeutic targeting of stroma-related processes are continually described. Tumor cells

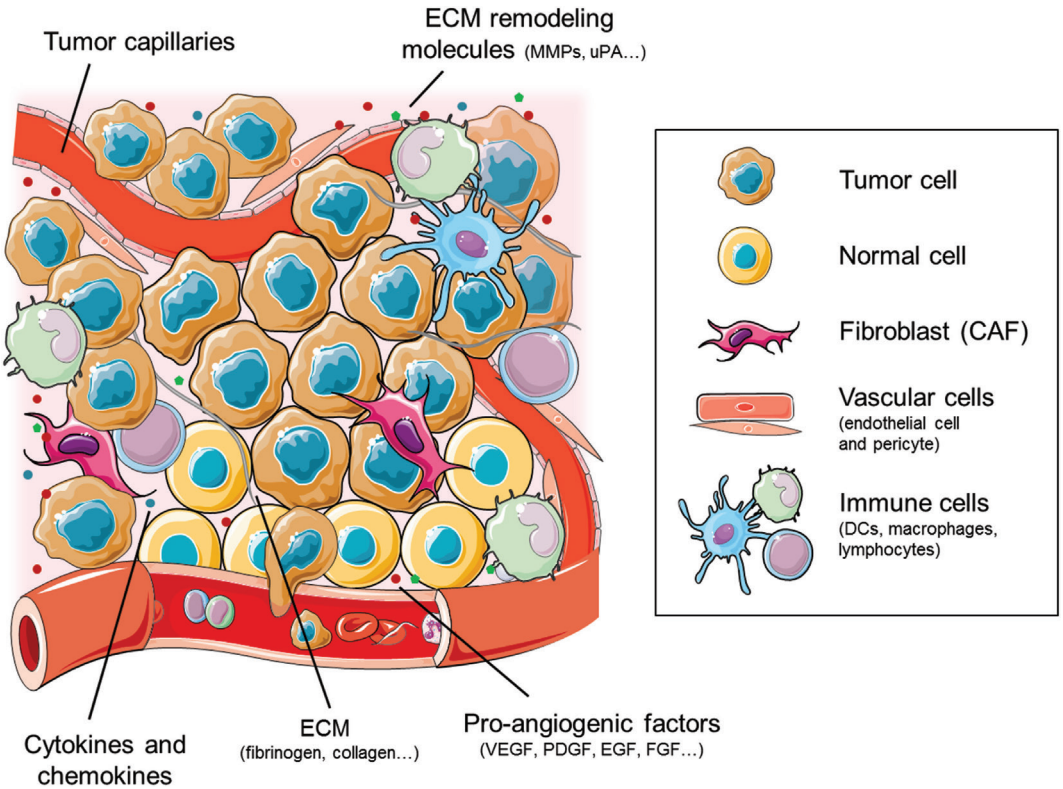

FIGURE 1 | Cellular and molecular components of the tumor ecosystem that shape the tumor angiogenic landscape. The cellular components primarily consist of tumor and normal cells, together with the vascular endothelial and pericyte cells and the stromal fibroblasts [cancer-associated fibroblasts (CAFs)]. The immune cell compartment comprises mainly tumor-infiltrating macrophages, dendritic cells (DCs), and lymphocytes. Figure was created using Servier Medical Art according to a Creative Commons Attribution 3.0 Unported License guidelines 3.0 (https://creativecommons.org/licenses/by/3.0/). Simplification and color changes were made to the original cartoons.

dwell in symbiosis with the rest of the body, mimicking and coopting several normal physiological processes on behalf of their surrounding stroma. Together with sustained proliferation and recruitment of immune cells, angiogenesis is one of the acknowledged promoters of tumor growth and survival (6, 10). In fact, tumor-associated vessels also contribute to dissemination of tumor cells by abetting their entry into the circulatory system and aiding in the generation of the pre-metastatic niche. In this review, we will further explore the role of angiogenesis as a key modulator inside the tumor ecosystem. To do so, we will first describe the different mechanisms responsible for tumor angiogenesis and we will focus later on the action of antiangiogenic drugs upon the stroma.

INSIGHT INTO THE ANGIOGENIC TUMOR ECOSYSTEM

To grow beyond a limited size, all solid tissues require a proper vasculature that grants oxygen, nutrients, and waste disposal. Since neoplasms are no exception to this rule, early activation of angiogenic processes is mandatory to sustain the deregulated proliferation of tumor cells. Apart from serving as nutrient, oxygen, and waste transport providers, vessels also facilitate dissemination of tumor cells to distant sites, promoting metastasis. Tumor angiogenesis is thus defined as the process of blood vessel creation, penetration, and growth in the tumor ecosystem.

The angiogenic program is switched on in response to hypoxia, which, together with the lack of nutrients, bolsters the expression of inflammatory signals and cytokines that recruit vascular cells for the tumor vessel plexus formation (11, 12). Early during tumor progression, hypoxia triggers the transcription of several genes that are key mediators of the angiogenic process, such as VEGF and PDGF (13). Mechanistically, activation of the angiogenic process involves the breakdown of the vascular ECM at different levels for subsequent endothelial cell invasion and tube formation (14). Apart from the role of tumor cells as principal secretors of endothelial cell promoters, the interplay with other stromal cells such as pericytes is also needed for neovessel stability.

For studying tumor angiogenesis, different approaches exist. A compilation of the currently used *in vivo*, *ex vivo*, and *in vitro* bioassays has been recently published as a collaborative work of some of the main experts in the angiogenesis field (15). Briefly, *in vivo* experimental models allow the study of mechanisms, kinetics, and dynamics in the context of a complex organism. The chorioallantoic membrane of a chicken embryo is used without

graft rejection, making it easy and low cost to complete a drug testing assay (16, 17). However, vessel formation is difficult to assess in this model. Besides, zebrafish embryo model also has the translationality for tumor angiogenesis study. Due to its transparency, it allows easy imaging of the tumor angiogenic process (18). Among the existing animal models, mouse models are the ones that better mimic the complexity of human cancer as an evolutionary process while, at the same time, allow easy and cheap monitoring of the process. Even though subcutaneous xenograft induced angiogenesis is easy to visualize, orthotopic transplantation is better regarded as it considers the role of the tumor ecosystem. Currently used mouse models for are reviewed in Gengenbacher et al. (19).

Recently, outstanding advances in the *in vitro* and *in silico* development of tumor angiogenesis models have been made. *In vitro* approaches include the use of microfluidic cancer vasculature on-chip systems, whereas *in silico* models comprise mathematical processes that address tumor growth dynamics. Their progress and challenges are extensively reviewed by Soleimani and colleagues (20).

MECHANISMS INVOLVED IN TUMOR VESSEL GENERATION

Nearly 40 years after the studies that laid the foundations in the field (21), research in tumor angiogenesis has extensively matured, permitting the gathering of detailed knowledge over the processes that govern pathological vessel proliferation. Vessels are ordered tubular networks that permit transportation of nutrients, cells, and gases. Apart from providing nutrients, vessels function as carriers of instructive trophic signals needed for organ morphogenesis (22). Different types of vessels, including arteries, veins, and capillaries, are formed by a luminal side surrounded by a monolayer of endothelial cells. On the outside, following the basement membrane, vessels are covered by a layer of mural accessory cells composed of pericytes and vascular smooth muscle cells.

Archetypal mechanisms for neovascularization include vasculogenesis and sprouting angiogenesis (**Figures 2A,B**). Critical for the formation and remodeling of vessels during development, both mechanisms are reactivated during tumor progression. Vasculogenesis is defined as the *de novo* formation of blood vessels as a consequence of vascular progenitor cell differentiation, whereas sprouting angiogenesis stands for the formation of new vascular structures from a preexisting vessel network. Recently, the role of other less frequent vascular formation mechanisms during tumor growth has been described, including vasculogenic mimicry (VM) and intussusception (**Figures 2C,D**). Usually, neither of the mechanisms are mutually exclusive and even seem to act simultaneously in pathological neovascularization.

Sprouting Angiogenesis

By far, sprouting angiogenesis is the best known angiogenesis-promoting mechanism used by tumor cells to induce their own vascularization from preexisting host capillaries (**Figure 2A**). A thorough interplay between ECM components, cells, and soluble

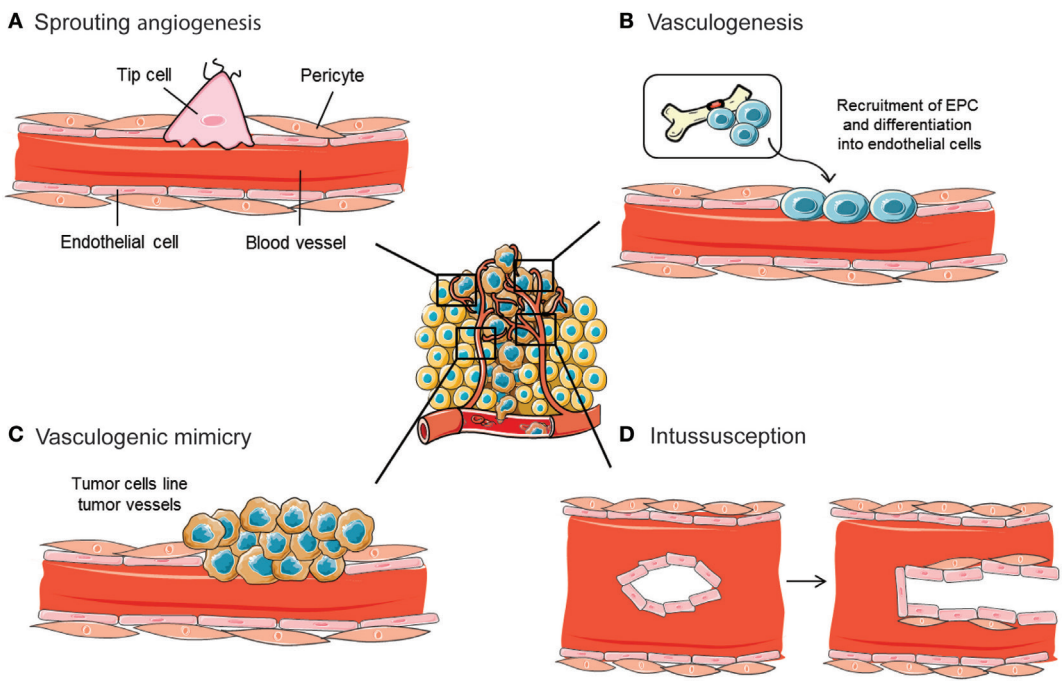

FIGURE 2 | Mechanisms implicated in blood vessel formation. In the tumor ecosystem, blood vessels grow by sprouting angiogenesis **(A)**. In addition, less frequent neovascularization mechanisms include recruitment of bone marrow-derived endothelial progenitor cells (EPCs) **(B)**, intussusceptive microvascular growth **(C)**, and vasculogenic mimicry **(D)**. Figure was created using Servier Medical Art according to a Creative Commons Attribution 3.0 Unported License guidelines 3.0 (https://creativecommons.org/licenses/by/3.0/). Simplification and color changes were made to the original cartoons.

factors, together with a sequence of well-defined steps, define sprouting angiogenesis (23). Destabilization of the endothelial–pericyte contacts, crucial for vessel integrity and maintenance of quiescence, initiates the process. Once the basement membrane that protects endothelial cells is destabilized, these cells undergo an endothelial–mesenchymal transition that triggers their proliferative, migratory, and invasive capabilities. Such activation further enhances the release of several proteases that induce ECM and basement membrane degradation, leading to guided migration and proliferation of vascular cells. The polarization of the moving endothelial cells eventually constitutes the vessel lumen, forming an immature blood vessel (24). An opposite mesenchymal–endothelial transition program is then activated to reverse the endothelial cells to their previous quiescent state. This latter step, known as vessel maturation, is characterized by the absence of angiogenesis, the recruitment of pericyte and mural cells, and the synthesis of a new basement membrane (25).

To engage the angiogenic process, endothelial cells need to follow a multistep specialization, which involves their plasticity in the angiogenic sprout and their following vascular guidance cue, that control the extension of the nascent vessel. The initiation of these morphogenetic events is marked by VEGF and Notch signaling pathways (26). Upon proangiogenic stimuli, sprouting endothelial cells change their phenotype toward an invasive and motile behavior, while activating protease secretion, cell–cell contact remodeling, and polarity reversal. The leading endothelial cells during the sprouting process are known as "tip cells." Their response to VEGF signaling includes extending large filopodia that will allow guidance and sensing of the newly formed vessel, as well as the release of molecular signals that recruit stromal cells for vessel stabilization. On the other hand, endothelial cells can also evolve into highly proliferative cells located at the stalk of the angiogenic sprout. These "stalk cells" are responsible for tube and branch formation, thus assuring the expansion of the vascular structure in response to VEGF-A (27). Stalk cells also collaborate in the basement membrane deposition and establish junctions with adjacent cells to strengthen the integrity of the novel sprout (28).

By anastomosing with cells form adjoining sprouts, tips cells interconnect in vessel loops until their leading phenotype is switched off. The process ends with the reestablishment of quiescence, when proangiogenic signals decrease, a new basement membrane is formed, and VEGF levels dampen (29). During the transition between both states, endothelial cells gain a "phalanx"-like phenotype, becoming non-proliferative and immobile (30). Vessel stabilization and maturity are accomplished with lumen generation and pericyte recruitment along the new basement membrane, which leads to blood flow and perfusion initiation.

The functionality, correct extension, and morphology of the new vessels depend on the balance between stalk cell proliferation and tip cell guidance. Phenotypic specialization of endothelial cells in each of those types depends, in turn, on the balance between proangiogenic factors and endothelial proliferation suppressors (31). Inside the tumor ecosystem, this balance is shifted in favor of a proangiogenic milieu, thus generating a sustained sprouting angiogenic process that produces abnormal vascular structures.

Vasculogenesis

The term "vasculogenesis" was conceived by Werner Risau, to define the physiological formation of the vascular plexus from the mesoderm as a consequence of angioblast differentiation (32). During tumor vasculogenesis, endothelial progenitor cells (EPCs) are mobilized and recruited in response to several chemokines, cytokines, and growth factors produced by tumor and stromal cells (**Figure 2B**). In particular, tumor cells produce a plethora of cytokines and proangiogenic factors, such as VEGF, that recruit bone marrow-derived DCs and induce their proliferation and differentiation (33). In hypoxic conditions, HIF is able to activate the transcription of VEGF, PDGF, stromal-derived factor 1 (SDF-1), and C-X-C chemokine receptor type 4 (CXCR4) (34). Studies with loss of function of HIF demonstrated an inhibition of EPC proliferation and differentiation. The contribution of vasculogenesis to tumor progression has also been demonstrated by knockout studies where some initiator molecules, such as inhibitors of differentiation factors, were genetically ablated. This approach provoked a disruption of tumor vascularization, angiogenesis blockade, and tumor growth impairment that was rescued by the restoration of the mobilization factors after bone marrow transplantation (35).

The first step of EPCs mobilization starts with the proangiogenic factor-mediated activation of the matrix metalloprotease 9 (MMP9) in the osteoblastic zone. Activated MMP9 proteolytically processes the membrane bound Kit ligand to its active soluble conformation. Kit is a stem cell-active migratory cytokine that induces migration and release of EPCs into the circulatory system (36). Once homed, EPCs are either incorporated into angiogenic sprouts or into the endothelial cell monolayer, aided by selectins and integrins (37). Endothelial cell maturation is substantially mediated by VEGF, which also contributes to vessel size establishment. Besides, EPCs share a paracrine mechanism that also triggers tumor angiogenesis by the release of proangiogenic molecules at the sites of neovascularization (38).

Depending on the experimental cancer model and the type of the tumor, vasculogenesis contributes to tumor vessel formation processes ranging from 0.1 to 50% of all vessels. As an example, the tumor ecosystem of hematopoietic and lymphoid tissues is more dependent on EPCs. Besides its role in primary tumor growth, vasculogenesis is also involved in dissemination and metastasis. SDF-1 produced by immune cells might attract EPCs to distant sites and once there spontaneously induce SDF-1 production, generating a gradient of this molecule that will serve as a chemoattractant of tumor cells. The interaction between SDF-1, secreted by EPCs, and its CXCR4 receptor, mainly expressed by tumor cells, would promote extravasation and development of the pre-metastatic niche (39). Moreover, the activation of MMP9 by EPCs is also related to an increase in tumor cell migration and invasion, confirming the role of vasculogenesis in metastatic niche formation (40).

Vasculogenic Mimicry

Vasculogenic mimicry refers to the ability of some malignant cells to start the dedifferentiation process to adopt multiple cellular phenotypes, including endothelial-like properties (41)

(**Figure 2C**). Those cells finally converge in *de novo* vasculogenic-like networks composed of red blood cells that are able to contribute to circulation (42). In this way, cells undergoing VM are able to reproduce the pattern of an early embryonic vascular plexus, providing the tumor ecosystem with an additional circulatory system independent of angiogenesis.

The process of VM was observed in highly invasive melanoma cells, whose phenotype reverted to an embryonic-like state and increased cell plasticity, including expression of endothelium-associated genes such as Ephrin-A2 and VE-cadherin (43). Release of ECM components, hypoxia, and activation of transmembrane metalloproteinases has been described as VM promoters (44). Although the occurrence of VM is relatively infrequent within tumors, it has been related to aggressive tumors, an increased risk of metastasis and poor prognosis (45).

Intussusception

Vessel intussusception or intussusceptive microvascular growth (IMG) is defined as a developmental intravascular growth mechanism consisting of the splitting of preexisting vessels into two new vascular structures. This was first described in postnatal remodeling of lung capillaries (46) (**Figure 2D**). During intussusception, endothelial cell proliferation is not required, which ultimately makes it a rapid process that occurs within hours or minutes if compared with sprouting angiogenesis. Furthermore, IMG does not rely on endothelial cell proliferation, but it is rather a remodeling process of the endothelial cells that happens as a consequence of both their narrowing and volume increase. IMG is described to occur after sprouting angiogenesis or vasculogenesis, as a mean of expanding the capillary plexus without the need of a high-metabolic demand (47).

The "touching spot" between endothelial cells from opposite walls initiates the IMG process. To reinforce the transendothelial cell bridge, the endothelial bilayer is formed with cell–cell junctions and the interstitial pillar is formed. Pericytes and other mural cells are recruited to cover the interstitial wall, which is later widened, allowing endothelial cell retraction and the creation of two independent vessels (47). By using this mechanism, a large vessel is able to split into many smaller functional vessels. Although the precise mechanism underlying IMG is not fully described, alterations in blood flow dynamics, wall stress over pericytes, changes in shear stress on endothelial cells sensed by absence of CD31 and VEGF are some of the possible events that result in IMG initiation (48).

Intussusceptive microvascular growth has been reported in mammary, colorectal, and melanoma tumors (49). In human melanomas, a correlation between VEGF and intussusceptive angiogenesis was found, together with a higher number of intraluminal tissue folds (50). This scenario suggests that sprouting angiogenesis inhibition could stimulate IMG. Taking into account that intussusceptive angiogenesis only occurs in preexisting vascular structures, its most important contribution to tumor malignization is its ability to augment the number and complexity of tumor microvessel networks already created by other angiogenic mechanisms. Ultimately, the creation of new vessel structures also provides additional surface for further activation of sprouting angiogenesis.

ROLE OF TUMOR ECOSYSTEM IN PROMOTING ANGIOGENESIS

Inside the tumor ecosystem, tumor cells are the main producers of the proangiogenic molecules that switch on the angiogenic program. Among the molecules that regulate this process, PDGF, HGF, FGF, and, particularly, VEGF and its cognate receptors (VEGFRs) are the driving force, owing to their specific expression on tumor and endothelial cells. Nevertheless, other cells composing the tumor ecosystem also contribute to tumor angiogenesis and their role must be considered throughout an integrative approach (**Figure 1**).

Cancer-Associated Fibroblasts

Cancer-associated fibroblasts normally originate from tumor or resident stroma, even though they can also differentiate from bone marrow precursors. While CAF-mediated secretion of proteases contributes to ECM degradation, CAFs also produce and deposit ECM, remarking a dual role for these cells in ECM remodeling. Besides, CAFs also secrete multiple angiogenic cues, participating in tumor growth and progression (51). Due to their primary localization at the leading edge of the tumor, where expanded vessel supply is demanded, the contribution to angiogenesis by stromal fibroblasts becomes crucial (52, 53).

One of the most important molecules secreted by stromal CAFs is VEGF-A, which was found to be induced in the stroma of both spontaneously arising and implanted tumors of genetically engineered mice with a reporter for VEGF-A (54). Actually, in ovarian carcinomas, most angiogenic growth factors are provided by CAFs rather than by malignant cells (55). CAFs also supply other factors such as angiopoietin-1 and -2, which are needed for neovascular stabilization (56).

Immune Cells

The tumor ecosystem constitutes a crucible of heterogenous immune cell populations, resulting in tangled interactions between tumor cells and stroma. Immune cells have a remarkable role during the regulation of different aspects of tumor growth, such as modulation of angiogenesis and immune system evasion (57). Particularly, the contribution of macrophages, DCs, and mast cells is further explored in this section.

Tumor-associated macrophages (TAMs) represent one of the most abundant leukocyte population in the tumor ecosystem and their presence correlates with a reduction in survival in most tumor types (58). Regarding their phenotype, macrophages can be classified into the classically activated M1 and alternative activated M2 subsets. Whereas M2 macrophages show a proangiogenic phenotype, M1 macrophages have been described as antitumor effectors (59). TAMs often shift toward the M2 phenotype, becoming an important supplier of angiogenic cytokines and ECM remodeling molecules (60–62). Indeed, in different types of tumors, macrophage presence has been correlated with high vascularity (63, 64). Apart from the canonical signaling pathways, alternative proangiogenic molecules such as semaphorins and plexins have been also described as mediators of the macrophage–endothelial cell cross talk (65).

Dendritic cells, due to their potent antigen-presenting ability, are considered a critical factor in antitumor immunity (66). Nevertheless, defective myelopoiesis inside the tumor ecosystems renders DCs incompetent (67). A role for DCs in tumor angiogenesis has been described after the finding that immature DCs increased neovascularization in implanted tumor models, while depletion of DCs revoked angiogenesis (68).

Mast cells were found more than 30 years ago to be accumulated in tumors before the onset of angiogenesis, residing in close proximity to blood vessels (69). Those granulocytes participate in tumor rejection by IL1, IL4, IL6, and TNF-α production. However, mast cells also promote tumor growth by increasing the angiogenic supply, degradation of the ECM and immunosuppression (70). In detail, mast cells release angiogenic cytokines, such as VEGF, FGF-2, and TGF-β, among others (71).

Vascular-Associated Components

Even though endothelial cells are the main players of the angiogenic tumor ecosystem, other components of the vascular system, such as platelets and pericytes, are also necessary for the proangiogenic switch. For instance, platelets, best known for their role in assisting the blood clotting process, have also been described as proangiogenic cells. Upon interaction with tumor cells, platelets are able to release VEGF from α granules (72, 73).

The contractile cells that surround the basement membrane of vessels are known as pericytes. In absence of angiogenesis, pericytes commonly express proteins such as PDGFRβ, NG2, and desmin and lack expression of α-SMA. Upon the activation of angiogenic signaling *via* PDGF, TGF-β, angiopoietin, and Notch, tumor pericytes loosen their attachment to the vessel, leading to a higher permeability of blood vessels (74, 75). Particularly, the recruitment of pericytes to the tumors highly depends on PDGF-B ligand production by endothelial cells (76, 77).

Nevertheless, the ultimate outcome of pericyte-derived signaling remains to be fully elucidated, since it seems to be context dependent. On the one hand, ectopic expression of PDGF-B in a mouse melanoma model increased tumor growth, indicating that a more stable and functional neovasculature was achieved through pericytes (78, 79). On the other hand, PDGF-B transfection into colorectal and pancreatic tumor cell lines inhibited tumor growth as a consequence of the angiostatic effect of recruited pericytes (80). Pericytes are also involved in the control of the metastatic spread of tumor cells (81). In fact, an increased rate of metastasis was described in a pancreatic neuroendocrine tumor mouse model genetically designed to be pericyte-poor. It remains to be elucidated whether their protective effect against metastasis is due to their active participation or as a consequence of their passive role as a physical barrier to extravasation.

ECM and the Vascular ECM

The organization and composition of the matrix that supports the cells of the tumor ecosystem is essential for the regulation of angiogenesis. In fact, mice bearing alterations in ECM molecules such as collagen, laminin, and fibronectin exhibit vascular abnormalities (82). Vessel ECM is constituted by the basement membrane BM, which is mainly composed of collagen IV and laminin (83) and provides a broad binding surface for other ECM proteins, integrin receptors, and growth factors. Those interactions lead to the activation of many signaling pathways, such as PI3K, AKT, and MAPK, which are involved in adhesion, migration, invasion, and proliferation, thus contributing to tumor angiogenesis (84).

The interstitial matrix that surrounds the BM, which comprises collagen I, II, and III, as well as fibronectin and fibrinogen, also contributes to tumor angiogenesis. It primarily functions as a reservoir of regulatory molecules, such as angiogenic growth factors, cytokines, and proteolytic enzymes (85). Moreover, binding of VEGF to fibronectin has been found to enhance the activity of VEGF. Concomitantly, tumor and stromal cells produce proteolytic enzymes, such as MMPs, that release fragments with promigratory and proangiogenic properties (86), besides the activation of ECM-sequestered growth factors (87).

THE ANGIOGENIC SWITCH IN TUMORIGENESIS

In the absence of new vasculature, during the avascular phase, tumor growth is normally limited to no more than 1–2 mm^3. Tumors obtain nutrients and oxygen from nearby blood vessels and angiogenic processes are not observed. The avascular tumors reach a stable state characterized by a balance between proliferation and apoptosis. To grow beyond the restricted size and sustain unlimited proliferation, tumors require their vascular network to be extended. This transition from this avascular state to the angiogenic phase is commonly known as "angiogenic switch" and occurs early during tumor progression (88). In pursuance of angiogenic activation, tumor cells need to undergo numerous genetic and epigenetic rearrangements that grant them the angiogenic potential for both tumor growth and latter metastasis. Indeed, a plethora of experiments have shown that the lack of a functional vascular network leads to tumor apoptosis or necrosis, reinforcing the importance of tumor vasculature for tumor thriving (89).

The angiogenic switch depends on a dynamic balance between positive (proangiogenic) and negative (antiangiogenic) factors controlling vascular homeostasis (90). Under physiological conditions, this balance is shifted toward negative regulation of angiogenic processes, thus maintaining the quiescence of the vasculature. Once tumor progression is started, different mechanisms, such as the loss of tumor suppressor genes and oncogene upregulation, revert this balance. During the first steps of tumorigenesis, high levels of strong angiogenic inducers, such as VEGF and FGF, are released to the tumor ecosystem. VEGF is regarded as the canonical angiogenesis initiator and has been found to be expressed in most types of cancer in response to different stimuli. Besides hypoxia, hypoglycemia, and growth factors, overexpression of the oncogene Myc produces a 10-fold increase in VEGF levels (91). Apart from VEGF, other proangiogenic molecules upregulated for the engagement of tumor angiogenesis are PDGF, EGF, TGF-β, FGF, MMPs, and angiopoietins.

Aiming at evading the ECM-associated endogenous inhibitors, tumor cells are able to further upregulate proangiogenic factors and even lose the expression of tumor suppressor genes such as p53 (92, 93). Moreover, tumor cell metabolism shifts

and becomes highly acidic, as a consequence of the Warburg effect (94). The net increase in glucose consumption produces an abnormal lactic acid release that turns lowers extracellular pH (95). High levels of lactate have been correlated with EMT, dissemination, and metastases of several types of human cancer, such as melanoma and Lewis lung carcinoma (96–98). In detail, acidification further promotes angiogenesis through the increased expression of VEGF (99).

The Hypoxic Tumor Ecosystem

Lack of oxygen inside the tumor occurs as an inevitable consequence of the rapid expansion of the tumor mass. Neoplasms have been generally described as highly hypoxic structures, bearing distorted, and abnormal vascular networks, inefficient in oxygen transportation (100). Hypoxia is known to upregulate proangiogenic inducers and endothelial–pericyte destabilizing molecules (Ang-2) and downregulate inhibitors. Furthermore, mobilization of bone marrow-derived precursor cells and recruitment of immune cells to the tumor ecosystem is also positively controlled by hypoxia (101). By changing the cytokine milieu, hypoxia can also induce an immunosuppressive microenvironment, allowing immune system evasion by cancer cells (102).

Hypoxia also produces a metabolic switch to apoptosis inhibition, anaerobic metabolism, increased invasiveness, EMT, and metastasis (103). A stem-like phenotype is induced concomitantly with the release of cytokines like IL-6. Consistently, hypoxia-driven expression of VEGF, MMPs, and ANGPTL4 is crucial for intravasation (104). In detail, ANGPTL4 expression disrupts vascular endothelial tight junctions and augments permeability, thereby altering transendothelial barriers (105).

CONTRIBUTION OF ANGIOGENESIS TO METASTASIS AND INVASION

Aside from the role in primary tumor ecosystem maintenance, tumor angiogenesis enables tumor cell invasion and dissemination and favors the creation of new secondary tumor ecosystems at metastasized sites. VEGF-mediated stimulation of blood and lymphatic endothelial cells provides a wide vascular area for intravasation of tumor cells, apart from increasing vascular permeability. In tumor endothelial cells, VEGF upregulates protease secretion, contributing to basement membrane degradation, and increasing the expression of molecules that mediate in tumor–endothelial cell interactions (106).

Other stromal cells also participate in the angiogenic-driven metastasis process. Pericytes covering tumor vessels are more loosely attached to endothelial cells, affecting endothelial cell survival, and increasing the number of intercellular gaps that permit easy access for tumor cell intravasation (81, 107). As a consequence of the increased vascular leakiness, passive escape of tumor cells is highly induced (108).

BLOCKING VESSELS IN THE ECOSYSTEM

Fighting neovascularization to halt tumor progression has become a critical step of the long-established theory of angiogenic activation for tumor growth. In fact, more than 40 years have passed since tumor angiogenesis inhibition was first introduced as a potential therapeutic strategy (21, 109). Since then, many drugs targeting tumor vascularization have proven successful in the treatment of different tumors. Such is the case for the first FDA-approved angiogenesis inhibitors sunitinib (Sutent®) and bevacizumab (Avastin®), which demonstrated promising results in the treatment of kidney and colorectal cancers (110, 111).

Currently, using standard chemotherapy alone for cancer treatment has proven inefficient due to low selectivity of tumor cells, producing toxicity in normal tissues with high-proliferation rates (e.g., bone marrow, hair follicles, and gastrointestinal tract). Besides, tumor cells become resistant, whereas the abnormality of tumor vasculature impairs efficient drug delivery (112). On the contrary, with thousands of people being treated with VEGF inhibitors around the world, antiangiogenic targeting surely serves as an example of specific tumor ecosystem disruption for efficient cancer treatment.

There are different reasons underlying the success of tumor vascular targeting, involving both tumor and stromal cell interplay. First, the concept that tumors are dependent on multiple factors extrinsic to themselves, so rendering them without a functional vasculature that delivers oxygen and nutrients should kill them. Second, stromal cells, unlike neoplastic cells, are genetically more stable, being less likely to develop resistance to therapy. This makes angiogenesis a really attractive target for drug development. Third, tumors have always been described as highly vascular structures, meaning that anti-vascular targeting could be aimed at the treatment of a wide range of solid tumors (113, 114).

Taking into account the abundance of mechanisms involved in tumor angiogenesis, blood vessel formation processes can be inhibited at many different levels (**Figure 3**). Actually, distinct types of compounds, such as antibodies and small molecules, have been developed as antiangiogenic drugs. Production of antibodies presents some disadvantages for the pharma companies regarding the expensive requirement of mammalian cell production systems, dependence on disulfide bonds for stability, overcoming the tendency to aggregation, and low expression yields. Consequently, other promising molecules such as small globular proteins, aptamers, and peptides are currently being investigated (115). Noteworthy, not all antiangiogenic compounds have the same cellular effects nor the same therapeutic relevance. The main effects of angiogenic inhibitors can be classified according to their effects on: inhibition, regression, or normalization of tumor blood vessels. In this section, some of the main mechanisms to inhibit vascular malignization will be highlighted.

Direct Vessel Signaling Inhibition

Endothelial cell activation is commonly initiated upon stimulation of tyrosine kinase (TK) receptors by growth factors. As previously stated, VEGF is the most important growth factor involved in tumor angiogenesis, and its inhibition influences endothelial cell survival, growth, migration, blood flow, and stromal cell recruitment (116, 117). Some of the VEGF-inhibiting approaches imply neutralization of the ligand or the receptor by specific antibodies, soluble receptors, small-molecule inhibitors

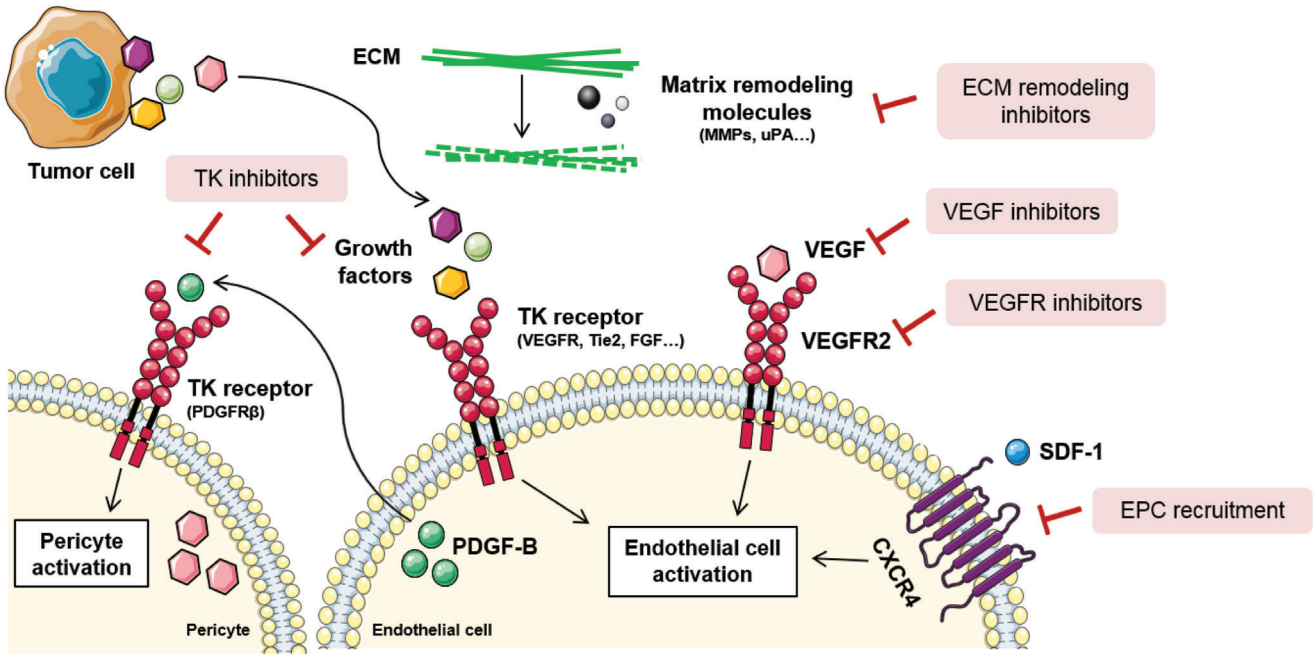

FIGURE 3 | Tumor angiogenesis inhibition strategies. Due to the complexity of tumor angiogenesis, it can be inhibited at different levels. Direct vessel signaling inhibition approaches include VEGF ligand inhibitors, VEGFR receptor inhibitors, and other growth factors inhibitors released by stromal or tumor cells. Other examples are tyrosine kinase (TK) inhibitors, that block endothelial and pericyte cell activation, thus blocking their proliferation, migration, and survival. Novel antiangiogenic strategies are directed toward endothelial progenitor cell (EPC) recruitment inhibition, *via* stromal-derived factor 1 (SDF-1)/C-X-C chemokine receptor type 4 (CXCR4) signaling blockade, and extracellular matrix (ECM) remodeling inhibition. Figure was created using Servier Medical Art according to a Creative Commons Attribution 3.0 Unported License guidelines 3.0 (https://creativecommons.org/licenses/by/3.0/). Simplification and color changes were made to the original cartoons.

of TK phosphorylation, and the direct inhibition of its intracellular signaling pathway (**Figure 3**). Thus far, 10 molecules that target VEGF or VEGFR have been approved for the treatment of various malignancies (118).

Since TK receptors are expressed both in tumor and vascular cells, TK inhibitors (TKIs) are regarded as a useful drugging strategy for their potentially dual effect (**Figure 3**). They are capable of blocking tumor cell proliferation and proangiogenic signaling simultaneously (119). However, the efficacy of TKIs varies depending on the different expression levels of the targeted ligands and effectors depending on the tumor type. Some strategies include compounds that block the binding site of the ATP in the TK receptor, causing the blockade of the receptor. Other TKIs aim at preventing the binding of the TK ligand with antibodies that block the growth factor or the binding site of the receptor (120).

The best known TKIs that block VEGFR and PDGF signaling are sorafenib, sunitinib, and pazopanib. Sorafenib is a synthetic compound that inhibits both Raf signaling, involved in cell division and proliferation, and VEGFR-2 and PDGFRβ signaling, modulators of angiogenesis (121). Its use is approved in the treatment of hepatocellular, thyroid, and renal cell carcinomas. Similarly, sunitinib is a TKI that, apart from blocking VEGFR-2 and PDGFRβ, is able to inhibit c-kit. The FDA approved the use of sunitinib for the treatment of imatinib-resistant gastrointestinal stromal tumor and renal cell carcinoma (122). Recently, anti-VEGFR2 antibody ramucirumab has received the FDA approval for second-line gastric cancer treatment (123). Another example includes pazopanib, a VEGFR-1, -2, -3, c-kit, and PDGFR inhibitor, approved for renal cell carcinoma and soft tissue sarcoma (124).

Novel Antiangiogenic Approaches

Vascular Ecosystem Inhibition

Considering the contribution of EPCs to tumor angiogenesis and metastasis, blocking of EPC recruitment is a recently explored strategy for new blood vessel and metastatic niche abrogation (125) (**Figure 3**). To achieve so, specific targeting of molecules involved in EPC homing and recruitment from the bone marrow is an interesting approach. SDF-1/CXCR4 signaling axis is the main regulator of EPC mobilization and, as such, antagonists and antibodies against CXCR4 have been proposed (126). The action of these compounds is based on their ability to prevent the chemokine gradient that permits the homing of EPCs to the tumor ecosystem. Besides, VEGF is also a key modulator of EPC recruitment and preclinical studies have shown that VEGF blockade negatively modulates EPC-driven vasculogenesis (127).

Given that interactions between cells composing the tumor ecosystem and their surrounding ECM are crucial for angiogenesis

regulation, modifying the structural and biochemical properties of the stroma should also impair vessel growth (128) (**Figure 3**). Among all the molecules that compose the ECM, MMPs are critically relevant for angiogenesis and tumor invasion, as demonstrated by genetic ablation studies where their absence impeded angiogenic tumor growth (129). In this context, tissue inhibitors of MMPs, together with synthetic inhibitors of serine proteases, such as urokinase type plasminogen activator, are regarded as potential antiangiogenics (130). Importantly, there are many endogenous angiogenesis inhibitors composing the ECM that are inactivated during the angiogenic switch. Many laboratories are trying to reproduce these natural angiogenesis inhibitors that act through binding αvβ3 and β1 integrins in endothelial cells. Some examples include arrestin, canstatin, and tumstatin (131).

Since the combination of immune checkpoint inhibitors with VEGF targeted agents shows a strong preclinical rationale, several undergoing studies are exploring its potential clinical exploitance [as reviewed in Ref. (132)]. As an example, a study combining bevacizumab with anti-CTLA4 in melanoma patients showed an increased infiltration of immune cells and extensive morphological changes of CD31 + endothelial cells (133). In a recent study, the use of axitinib, a multireceptor inhibitor that targets VEGFR, PDGF, and c-kit, demonstrated a depletion of mast cells together with an improved T-cell response, pivotal for the therapeutic efficacy (134).

Vessel Normalization

In comparison with physiologic tissue vasculature, tumor vasculature is characterized by aberrant, dilated, disorganized, and tortuous blood vessels. Lack of pericyte association and vascular immaturity produce excessive permeability, increased hypoxia, and poor perfusion, resulting in decreased antitumor treatment efficacy. For instance, chemotherapeutic drugs and immunotherapies are not able to reach all regions of the tumor (135, 136). To overcome this challenge, combination of antitumor treatments and low doses of vascular targeting agents are used. Careful dosage of antiangiogenics are able to restore normal levels of angiogenic signals in different types of tumors, provoking decreased permeability by recruiting pericytes and tightening cell–cell junctions (137). This phenomenon is known as "vascular normalization."

Benefits of vascular normalization have been observed in different types of tumors. The combination of bevacizumab, together with chemotherapy, produced a positive outcome in a subset of breast cancer patients (138). Furthermore, combined inhibition of VEGFR and angiopoietin-2 improves survival of mouse glioblastoma tumor models, by increasing vessel normalization and reprogramming TAMs (139). Another example of the benefits of vessel normalization include the use of trebananib, a fusion protein that inhibits angiogenesis by blocking binding of angiopoietin-1 and -2 to Tie 2 receptor. In a recent study, combination of trebananib and chemotherapy demonstrated benefits in progression-free survival in epithelial ovarian cancer patients (140).

CONCLUSION

Far ahead from the traditional idea that neoplasms are merely characterized by the tumor cells, tumors are now regarded as a heterogeneous association of both tumor and stromal cells that contribute in an interconnected fashion to malignant progression. The tumor ecosystem remains a bustling interchange of tumor cells, secreted molecules, and native tissue elements that, acting together, control the balance toward a proangiogenic program activation. In this way, the correct interaction between the components of the tumor ecosystem is critical for the success of the malignant lesion. Tumor stroma acts as a co-director for the development of vascularized growing mass, becoming the rationale driving the development of new antitumor therapies with antiangiogenic drugs.

Several years after the establishment of tumor angiogenesis as a cancer hallmark, the clinical exploitation of antiangiogenic therapies has reached a certain level of maturity (6). From the archetypal sprouting angiogenesis to describing less known mechanisms such as VM, the understanding of angiogenic mechanisms has become imperative for successful therapeutic targeting. The focus on the importance of these processes and the achievements in the clinical setting are reflected in the increasing number of drugs available to target angiogenesis mediators.

Undoubtedly, the normalization of the tumor ecosystem is an important new aspect for cancer treatment. Even though the tumor microenvironment holds many different cell types and components, the severity of the disease can be reduced by using a single effective drug, as demonstrated with antiangiogenics. Based on this observation, the combination of different therapies targeting different stromal components, together with traditional antitumor agents, could hold the key to impair cancer progression. Despite the rapid progress achieved in tumor ecosystem targeting, only a modest clinical success has been so far observed (141). Ongoing studies in the field which focus on studying the tumor ecosystem from an integrative point of view bear the potential to significantly control tumor angiogenesis and broaden the spectrum of current anticancer treatments.

AUTHOR CONTRIBUTIONS

Both IZ-G and OC have written, revised, and compiled this review.

FUNDING

The authors' work is supported by research grants from EU-FP7-ERC (STROMALIGN ERC-StG-281830), MinEco Spain (SAF2016-79347-R), ISCIII Spain (AES, DTS17/00194), and AGAUR-Generalitat de Catalunya (2017SGR771). Some of these include European Development Regional Funds (ERDF "a way to achieve Europe").

REFERENCES

1. Bissell MJ, Radisky D. Putting tumours in context. *Nat Rev Cancer* (2001) 1:46–54. doi:10.1038/35094059
2. Radisky D, Hagios C, Bissell MJ. Tumors are unique organs defined by abnormal signaling and context. *Semin Cancer Biol* (2001) 11:87–95. doi:10.1006/scbi.2000.0360
3. Rak JW, St Croix BD, Kerbel RS. Consequences of angiogenesis for tumor progression, metastasis and cancer therapy. *Anticancer Drugs* (1995) 6:3–18. doi:10.1097/00001813-199502000-00001
4. Liotta LA, Kohn EC. The microenvironment of the tumour-host interface. *Nature* (2001) 411:375–9. doi:10.1038/35077241
5. Shojaei F, Ferrara N. Role of the microenvironment in tumor growth and in refractoriness/resistance to anti-angiogenic therapies. *Drug Resist Updat* (2008) 11:219–30. doi:10.1016/j.drup.2008.09.001
6. Hanahan D, Weinberg RA. Hallmarks of cancer: the next generation. *Cell* (2011) 144:646–74. doi:10.1016/j.cell.2011.02.013
7. Polyak K, Haviv I, Campbell IG. Co-evolution of tumor cells and their microenvironment. *Trends Genet* (2009) 25:30–8. doi:10.1016/j.tig.2008.10.012
8. Polyak K, Weinberg RA. Transitions between epithelial and mesenchymal states: acquisition of malignant and stem cell traits. *Nat Rev Cancer* (2009) 9:265–73. doi:10.1038/nrc2620
9. Quail DF, Joyce JA. Microenvironmental regulation of tumor progression and metastasis. *Nat Med* (2013) 19:1423–37. doi:10.1038/nm.3394
10. Mittal K, Ebos J, Rini B. Angiogenesis and the tumor microenvironment: vascular endothelial growth factor and beyond. *Semin Oncol* (2014) 41:235–51. doi:10.1053/j.seminoncol.2014.02.007
11. ElShamy WM, Sinha A, Said N. Aggressiveness niche: can it be the foster ground for cancer metastasis precursors? *Stem Cells Int* (2016) 2016:1–7. doi:10.1155/2016/4829106
12. Muz B, de la Puente P, Azab F, Azab AK. The role of hypoxia in cancer progression, angiogenesis, metastasis, and resistance to therapy. *Hypoxia (Auckl)* (2015) 3:83. doi:10.2147/HP.S93413
13. Yang Y, Sun M, Wang L, Jiao B. HIFs, angiogenesis, and cancer. *J Cell Biochem* (2013) 114:967–74. doi:10.1002/jcb.24438
14. Vandekeere S, Dewerchin M, Carmeliet P. Angiogenesis revisited: an overlooked role of endothelial cell metabolism in vessel sprouting. *Microcirculation* (2015) 22:509–17. doi:10.1111/micc.12229
15. Nowak-Sliwinska P, Alitalo K, Allen E, Anisimov A, Aplin AC, Auerbach R, et al. Consensus guidelines for the use and interpretation of angiogenesis assays. *Angiogenesis* (2018):1–108. doi:10.1007/s10456-018-9613-x
16. Ribatti D. The chick embryo chorioallantoic membrane as a model for tumor biology. *Exp Cell Res* (2014) 328:314–24. doi:10.1016/j.yexcr.2014.06.010
17. Vogel HB, Berry RG. Chorioallantoic membrane heterotransplantation of human brain tumors. *Int J Cancer* (1975) 15:401–8. doi:10.1002/ijc.2910150306
18. Tulotta C, He S, van der Ent W, Chen L, Groenewoud A, Spaink HP, et al. *Imaging Cancer Angiogenesis and Metastasis in a Zebrafish Embryo Model*. Cham: Springer (2016). p. 239–63.
19. Gengenbacher N, Singhal M, Augustin HG. Preclinical mouse solid tumour models: status quo, challenges and perspectives. *Nat Rev Cancer* (2017) 17:751–65. doi:10.1038/nrc.2017.92
20. Soleimani S, Shamsi M, Ghazani MA, Modarres HP, Valente KP, Saghafian M, et al. Translational models of tumor angiogenesis: a nexus of in silico and in vitro models. *Biotechnol Adv* (2018) 36:880–93. doi:10.1016/j.biotechadv.2018.01.013
21. Sherwood LM, Parris EE, Folkman J. Tumor angiogenesis: therapeutic implications. *N Engl J Med* (1971) 285:1182–6. doi:10.1056/NEJM197111182852108
22. Carmeliet P, Jain RK. Molecular mechanisms and clinical applications of angiogenesis. *Nature* (2011) 473:298–307. doi:10.1038/nature10144
23. Paku S, Paweletz N. First steps of tumor-related angiogenesis. *Lab Invest* (1991) 65:334–46.
24. Ferrara N, Gerber H-P, LeCouter J. The biology of VEGF and its receptors. *Nat Med* (2003) 9:669–76. doi:10.1038/nm0603-669
25. Jain RK. Molecular regulation of vessel maturation. *Nat Med* (2003) 9:685–93. doi:10.1038/nm0603-685
26. Iruela-Arispe ML, Dvorak HF. Angiogenesis: a dynamic balance of stimulators and inhibitors. *Thromb Haemost* (1997) 78:672–7.
27. Gerhardt H, Golding M, Fruttiger M, Ruhrberg C, Lundkvist A, Abramsson A, et al. VEGF guides angiogenic sprouting utilizing endothelial tip cell filopodia. *J Cell Biol* (2003) 161:1163–77. doi:10.1083/jcb.200302047
28. Dejana E, Orsenigo F, Molendini C, Baluk P, McDonald DM. Organization and signaling of endothelial cell-to-cell junctions in various regions of the blood and lymphatic vascular trees. *Cell Tissue Res* (2009) 335:17–25. doi:10.1007/s00441-008-0694-5
29. Leslie JD, Ariza-McNaughton L, Bermange AL, McAdow R, Johnson SL, Lewis J. Endothelial signalling by the notch ligand delta-like 4 restricts angiogenesis. *Development* (2007) 134:839–44. doi:10.1242/dev.003244
30. Bautch VL. Endothelial cells form a phalanx to block tumor metastasis. *Cell* (2009) 136:810–2. doi:10.1016/j.cell.2009.02.021
31. Geudens I, Gerhardt H. Coordinating cell behaviour during blood vessel formation. *Development* (2011) 138:4569–83. doi:10.1242/dev.062323
32. Risau W. Mechanisms of angiogenesis. *Nature* (1997) 386:671–4. doi:10.1038/386671a0
33. Rafii DC, Psaila B, Butler J, Jin DK, Lyden D. Regulation of vasculogenesis by platelet-mediated recruitment of bone marrow-derived cells. *Arterioscler Thromb Vasc Biol* (2008) 28:217–22. doi:10.1161/ATVBAHA.107.151159
34. Brown JM. Vasculogenesis: a crucial player in the resistance of solid tumours to radiotherapy. *Br J Radiol* (2014) 87:20130686. doi:10.1259/bjr.20130686
35. Benezra R, Rafii S, Lyden D. The Id proteins and angiogenesis. *Oncogene* (2001) 20:8334–41. doi:10.1038/sj.onc.1205160
36. Heissig B, Hattori K, Dias S, Friedrich M, Ferris B, Hackett NR, et al. Recruitment of stem and progenitor cells from the bone marrow niche requires MMP-9 mediated release of kit-ligand. *Cell* (2002) 109:625–37. doi:10.1016/S0092-8674(02)00754-7
37. Deb A, Skelding KA, Wang S, Reeder M, Simper D, Caplice NM. Integrin profile and in vivo homing of human smooth muscle progenitor cells. *Circulation* (2004) 110:2673–7. doi:10.1161/01.CIR.0000139842.15651.B2
38. Urbich C, Dimmeler S. Endothelial progenitor cells. *Trends Cardiovasc Med* (2004) 14:318–22. doi:10.1016/j.tcm.2004.10.001
39. Jin F, Brockmeier U, Otterbach F, Metzen E. New insight into the SDF-1/CXCR4 axis in a breast carcinoma model: hypoxia-induced endothelial SDF-1 and tumor cell CXCR4 are required for tumor cell intravasation. *Mol Cancer Res* (2012) 10:1021–31. doi:10.1158/1541-7786.MCR-11-0498
40. Kopp H-G, Hooper AT, Broekman MJ, Avecilla ST, Petit I, Luo M, et al. Thrombospondins deployed by thrombopoietic cells determine angiogenic switch and extent of revascularization. *J Clin Invest* (2006) 116:3277–91. doi:10.1172/JCI29314
41. Maniotis AJ, Folberg R, Hess A, Seftor EA, Gardner LMG, Pe'er J, et al. Vascular channel formation by human melanoma cells in vivo and in vitro: vasculogenic mimicry. *Am J Pathol* (1999) 155:739–52. doi:10.1016/S0002-9440(10)65173-5
42. Frenkel S, Barzel I, Levy J, Lin AY, Bartsch D-U, Majumdar D, et al. Demonstrating circulation in vasculogenic mimicry patterns of uveal melanoma by confocal indocyanine green angiography. *Eye* (2008) 22:948–52. doi:10.1038/sj.eye.6702783
43. Hendrix MJC, Seftor EA, Hess AR, Seftor REB. Angiogenesis: vasculogenic mimicry and tumour-cell plasticity: lessons from melanoma. *Nat Rev Cancer* (2003) 3:411–21. doi:10.1038/nrc1092
44. Seftor EA, Brown KM, Chin L, Kirschmann DA, Wheaton WW, Protopopov A, et al. Epigenetic transdifferentiation of normal melanocytes by a metastatic melanoma microenvironment. *Cancer Res* (2005) 65:10164–9. doi:10.1158/0008-5472.CAN-05-2497
45. Sun B, Zhang S, Zhang D, Du J, Guo H, Zhao X, et al. Vasculogenic mimicry is associated with high tumor grade, invasion and metastasis, and short survival in patients with hepatocellular carcinoma. *Oncol Rep* (2006) 16:693–8. doi:10.3892/or.16.4.693
46. Caduff JH, Fischer LC, Burri PH. Scanning electron microscope study of the developing microvasculature in the postnatal rat lung. *Anat Rec* (1986) 216:154–64. doi:10.1002/ar.1092160207
47. Burri PH, Hlushchuk R, Djonov V. Intussusceptive angiogenesis: its emergence, its characteristics, and its significance. *Dev Dyn* (2004) 231:474–88. doi:10.1002/dvdy.20184
48. Djonov V, Makanya AN. New insights into intussusceptive angiogenesis. *EXS* (2005) 94:17–33. doi:10.1007/3-7643-7311-3_2
49. Dome F, Taziaux P, Boniver J, Fridman V, Delbecque K. [Ileum intussusception in an adult: a case report]. *Rev Med Liege* (2007) 62:498–500.

50. Ribatti D, Nico B, Floris C, Mangieri D, Piras F, Ennas MG, et al. Microvascular density, vascular endothelial growth factor immunoreactivity in tumor cells, vessel diameter and intussusceptive microvascular growth in primary melanoma. *Oncol Rep* (2005) 14:81–4. doi:10.3892/or.14.1.81
51. Watnick RS. The role of the tumor microenvironment in regulating angiogenesis. *Cold Spring Harb Perspect Med* (2012) 2:a006676. doi:10.1101/cshperspect.a006676
52. Gaggioli C, Hooper S, Hidalgo-Carcedo C, Grosse R, Marshall JF, Harrington K, et al. Fibroblast-led collective invasion of carcinoma cells with differing roles for RhoGTPases in leading and following cells. *Nat Cell Biol* (2007) 9:1392–400. doi:10.1038/ncb1658
53. Granot D, Addadi Y, Kalchenko V, Harmelin A, Kunz-Schughart LA, Neeman M. In vivo imaging of the systemic recruitment of fibroblasts to the angiogenic rim of ovarian carcinoma tumors. *Cancer Res* (2007) 67:9180–9. doi:10.1158/0008-5472.CAN-07-0684
54. Fukumura D, Xavier R, Sugiura T, Chen Y, Park EC, Lu N, et al. Tumor induction of VEGF promoter activity in stromal cells. *Cell* (1998) 94:715–25. doi:10.1016/S0092-8674(00)81731-6
55. Thijssen VLJL, Brandwijk RJMGE, Dings RPM, Griffioen AW. Angiogenesis gene expression profiling in xenograft models to study cellular interactions. *Exp Cell Res* (2004) 299:286–93. doi:10.1016/j.yexcr.2004.06.014
56. Gilad AA, Israely T, Dafni H, Meir G, Cohen B, Neeman M. Functional and molecular mapping of uncoupling between vascular permeability and loss of vascular maturation in ovarian carcinoma xenografts: the role of stroma cells in tumor angiogenesis. *Int J Cancer* (2005) 117:202–11. doi:10.1002/ijc.21179
57. Albini A, Bruno A, Noonan DM, Mortara L. Contribution to tumor angiogenesis from innate immune cells within the tumor microenvironment: implications for immunotherapy. *Front Immunol* (2018) 9:527. doi:10.3389/fimmu.2018.00527
58. Petty AJ, Yang Y. Tumor-associated macrophages: implications in cancer immunotherapy. *Immunotherapy* (2017) 9:289–302. doi:10.2217/imt-2016-0135
59. Schmid MC, Varner JA. Myeloid cells in the tumor microenvironment: modulation of tumor angiogenesis and tumor inflammation. *J Oncol* (2010) 2010:1–10. doi:10.1155/2010/201026
60. Giraudo E, Inoue M, Hanahan D. An amino-bisphosphonate targets MMP-9-expressing macrophages and angiogenesis to impair cervical carcinogenesis. *J Clin Invest* (2004) 114:623–33. doi:10.1172/JCI200422087
61. Hildenbrand R, Dilger I, Hörlin A, Stutte HJ. Urokinase and macrophages in tumour angiogenesis. *Br J Cancer* (1995) 72:818–23. doi:10.1038/bjc.1995.419
62. Sunderkötter C, Steinbrink K, Goebeler M, Bhardwaj R, Sorg C. Macrophages and angiogenesis. *J Leukoc Biol* (1994) 55:410–22. doi:10.1002/jlb.55.3.410
63. Leek RD, Harris AL. Tumor-associated macrophages in breast cancer. *J Mammary Gland Biol Neoplasia* (2002) 7:177–89. doi:10.1023/A:1020304003704
64. Nishie A, Ono M, Shono T, Fukushi J, Otsubo M, Onoue H, et al. Macrophage infiltration and heme oxygenase-1 expression correlate with angiogenesis in human gliomas. *Clin Cancer Res* (1999) 5:1107–13.
65. Sierra JR, Corso S, Caione L, Cepero V, Conrotto P, Cignetti A, et al. Tumor angiogenesis and progression are enhanced by Sema4D produced by tumor-associated macrophages. *J Exp Med* (2008) 205:1673–85. doi:10.1084/jem.20072602
66. Veglia F, Gabrilovich DI. Dendritic cells in cancer: the role revisited. *Curr Opin Immunol* (2017) 45:43–51. doi:10.1016/j.coi.2017.01.002
67. Gabrilovich D. Mechanisms and functional significance of tumour-induced dendritic-cell defects. *Nat Rev Immunol* (2004) 4:941–52. doi:10.1038/nri1498
68. Fainaru O, Almog N, Yung CW, Nakai K, Montoya-Zavala M, Abdollahi A, et al. Tumor growth and angiogenesis are dependent on the presence of immature dendritic cells. *FASEB J* (2010) 24:1411–8. doi:10.1096/fj.09-147025
69. Kessler DA, Langer RS, Pless NA, Folkman J. Mast cells and tumor angiogenesis. *Int J Cancer* (1976) 18:703–9. doi:10.1002/ijc.2910180520
70. Wroblewski M, Bauer R, Cubas Córdova M, Udonta F, Ben-Batalla I, Legler K, et al. Mast cells decrease efficacy of anti-angiogenic therapy by secreting matrix-degrading granzyme B. *Nat Commun* (2017) 8:269. doi:10.1038/s41467-017-00327-8
71. Cimpean AM, Tamma R, Ruggieri S, Nico B, Toma A, Ribatti D. Mast cells in breast cancer angiogenesis. *Crit Rev Oncol Hematol* (2017) 115:23–6. doi:10.1016/j.critrevonc.2017.04.009
72. Battinelli EM, Markens BA, Italiano JE. Release of angiogenesis regulatory proteins from platelet alpha granules: modulation of physiologic and pathologic angiogenesis. *Blood* (2011) 118:1359–69. doi:10.1182/blood-2011-02-334524
73. Italiano JE, Richardson JL, Patel-Hett S, Battinelli E, Zaslavsky A, Short S, et al. Angiogenesis is regulated by a novel mechanism: pro- and antiangiogenic proteins are organized into separate platelet alpha granules and differentially released. *Blood* (2008) 111:1227–33. doi:10.1182/blood-2007-09-113837
74. Gaengel K, Genové G, Armulik A, Betsholtz C. Endothelial-mural cell signaling in vascular development and angiogenesis. *Arterioscler Thromb Vasc Biol* (2009) 29:630–8. doi:10.1161/ATVBAHA.107.161521
75. Morikawa S, Baluk P, Kaidoh T, Haskell A, Jain RK, McDonald DM. Abnormalities in pericytes on blood vessels and endothelial sprouts in tumors. *Am J Pathol* (2002) 160:985–1000. doi:10.1016/S0002-9440(10)64920-6
76. Abramsson A, Lindblom P, Betsholtz C. Endothelial and nonendothelial sources of PDGF-B regulate pericyte recruitment and influence vascular pattern formation in tumors. *J Clin Invest* (2003) 112:1142–51. doi:10.1172/JCI200318549
77. Song S, Ewald AJ, Stallcup W, Werb Z, Bergers G. PDGFRbeta+ perivascular progenitor cells in tumours regulate pericyte differentiation and vascular survival. *Nat Cell Biol* (2005) 7:870–9. doi:10.1038/ncb1288
78. Furuhashi M, Sjöblom T, Abramsson A, Ellingsen J, Micke P, Li H, et al. Platelet-derived growth factor production by B16 melanoma cells leads to increased pericyte abundance in tumors and an associated increase in tumor growth rate. *Cancer Res* (2004) 64:2725–33. doi:10.1158/0008-5472.CAN-03-1489
79. Robinson SP, Ludwig C, Paulsson J, Östman A. The effects of tumor-derived platelet-derived growth factor on vascular morphology and function in vivo revealed by susceptibility MRI. *Int J Cancer* (2007) 122:1548–56. doi:10.1002/ijc.23279
80. McCarty MF, Somcio RJ, Stoeltzing O, Wey J, Fan F, Liu W, et al. Overexpression of PDGF-BB decreases colorectal and pancreatic cancer growth by increasing tumor pericyte content. *J Clin Invest* (2007) 117:2114–22. doi:10.1172/JCI31334
81. Xian X, Håkansson J, Ståhlberg A, Lindblom P, Betsholtz C, Gerhardt H, et al. Pericytes limit tumor cell metastasis. *J Clin Invest* (2006) 116:642–51. doi:10.1172/JCI25705
82. Hirsch E, Brancaccio M, Altruda F. Tissue-specific KO of ECM proteins. *Methods Mol Biol* (2000) 139:147–78. doi:10.1385/1-59259-063-2:147
83. Kalluri R. Angiogenesis: basement membranes: structure, assembly and role in tumour angiogenesis. *Nat Rev Cancer* (2003) 3:422–33. doi:10.1038/nrc1094
84. Chen CS, Tan J, Tien J. Mechanotransduction at cell-matrix and cell-cell contacts. *Annu Rev Biomed Eng* (2004) 6:275–302. doi:10.1146/annurev.bioeng.6.040803.140040
85. Mott JD, Werb Z. Regulation of matrix biology by matrix metalloproteinases. *Curr Opin Cell Biol* (2004) 16:558–64. doi:10.1016/j.ceb.2004.07.010
86. Chambers AF, Matrisian LM. Changing views of the role of matrix metalloproteinases in metastasis. *J Natl Cancer Inst* (1997) 89:1260–70. doi:10.1093/jnci/89.17.1260
87. Egeblad M, Werb Z. New functions for the matrix metalloproteinases in cancer progression. *Nat Rev Cancer* (2002) 2:161–74. doi:10.1038/nrc745
88. Folkman J. What is the evidence that tumors are angiogenesis dependent? *J Natl Cancer Inst* (1990) 82:4–6. doi:10.1093/jnci/82.1.4
89. Holmgren L, O'Reilly MS, Folkman J. Dormancy of micrometastases: balanced proliferation and apoptosis in the presence of angiogenesis suppression. *Nat Med* (1995) 1:149–53. doi:10.1038/nm0295-149
90. Hanahan D, Folkman J. Patterns and emerging mechanisms of the angiogenic switch during tumorigenesis. *Cell* (1996) 86:353–64. doi:10.1016/S0092-8674(00)80108-7
91. Mezquita P, Parghi SS, Brandvold KA, Ruddell A. Myc regulates VEGF production in B cells by stimulating initiation of VEGF mRNA translation. *Oncogene* (2005) 24:889–901. doi:10.1038/sj.onc.1208251

92. Fernando NT, Koch M, Rothrock C, Gollogly LK, D'Amore PA, Ryeom S, et al. Tumor escape from endogenous, extracellular matrix-associated angiogenesis inhibitors by up-regulation of multiple proangiogenic factors. *Clin Cancer Res* (2008) 14:1529–39. doi:10.1158/1078-0432.CCR-07-4126
93. Volpert OV, Alani RM. Wiring the angiogenic switch: Ras, Myc, and thrombospondin-1. *Cancer Cell* (2003) 3:199–200. doi:10.1016/S1535-6108(03)00056-4
94. Warburg O, Wind F, Negelein E. The metabolism of tumors in the body. *J Gen Physiol* (1927) 8:519–30. doi:10.1085/jgp.8.6.519
95. Payen VL, Porporato PE, Baselet B, Sonveaux P. Metabolic changes associated with tumor metastasis, part 1: tumor pH, glycolysis and the pentose phosphate pathway. *Cell Mol Life Sci* (2016) 73:1333–48. doi:10.1007/s00018-015-2098-5
96. Peppicelli S, Bianchini F, Calorini L. Extracellular acidity, a "reappreciated" trait of tumor environment driving malignancy: perspectives in diagnosis and therapy. *Cancer Metastasis Rev* (2014) 33:823–32. doi:10.1007/s10555-014-9506-4
97. Suzuki A, Maeda T, Baba Y, Shimamura K, Kato Y. Acidic extracellular pH promotes epithelial mesenchymal transition in Lewis lung carcinoma model. *Cancer Cell Int* (2014) 14:129. doi:10.1186/s12935-014-0129-1
98. Walenta S, Mueller-Klieser WF. Lactate: mirror and motor of tumor malignancy. *Semin Radiat Oncol* (2004) 14:267–74. doi:10.1016/j.semradonc.2004.04.004
99. Shi Q, Le X, Wang B, Abbruzzese JL, Xiong Q, He Y, et al. Regulation of vascular endothelial growth factor expression by acidosis in human cancer cells. *Oncogene* (2001) 20:3751–6. doi:10.1038/sj.onc.1204500
100. Vaupel P. The role of hypoxia-induced factors in tumor progression. *Oncologist* (2004) 9:10–7. doi:10.1634/theoncologist.9-90005-10
101. Blouw B, Song H, Tihan T, Bosze J, Ferrara N, Gerber HP, et al. The hypoxic response of tumors is dependent on their microenvironment. *Cancer Cell* (2003) 4:133–46. doi:10.1016/S1535-6108(03)00194-6
102. Mohme M, Riethdorf S, Pantel K. Circulating and disseminated tumour cells – mechanisms of immune surveillance and escape. *Nat Rev Clin Oncol* (2017) 14:155–67. doi:10.1038/nrclinonc.2016.144
103. Mimeault M, Batra SK. Hypoxia-inducing factors as master regulators of stemness properties and altered metabolism of cancer- and metastasis-initiating cells. *J Cell Mol Med* (2013) 17:30–54. doi:10.1111/jcmm.12004
104. Lu X, Kang Y. Hypoxia and hypoxia-inducible factors: master regulators of metastasis. *Clin Cancer Res* (2010) 16:5928–35. doi:10.1158/1078-0432.CCR-10-1360
105. Padua D, Zhang XH-F, Wang Q, Nadal C, Gerald WL, Gomis RR, et al. TGFbeta primes breast tumors for lung metastasis seeding through angiopoietin-like 4. *Cell* (2008) 133:66–77. doi:10.1016/j.cell.2008.01.046
106. Carmeliet P. VEGF as a key mediator of angiogenesis in cancer. *Oncology* (2005) 69:4–10. doi:10.1159/000088478
107. Gerhardt H, Semb H. Pericytes: gatekeepers in tumour cell metastasis? *J Mol Med* (2008) 86:135–44. doi:10.1007/s00109-007-0258-2
108. Jain RK. Normalization of tumor vasculature: an emerging concept in antiangiogenic therapy. *Science* (2005) 307:58–62. doi:10.1126/science.1104819
109. Yang JC, Haworth L, Sherry RM, Hwu P, Schwartzentruber DJ, Topalian SL, et al. A randomized trial of bevacizumab, an anti-vascular endothelial growth factor antibody, for metastatic renal cancer. *N Engl J Med* (2003) 349:427–34. doi:10.1056/NEJMoa021491
110. Motzer RJ, Rini BI, Bukowski RM, Curti BD, George DJ, Hudes GR, et al. Sunitinib in patients with metastatic renal cell carcinoma. *JAMA* (2006) 295:2516. doi:10.1001/jama.295.21.2516
111. Salgaller ML. Technology evaluation: bevacizumab, Genentech/Roche. *Curr Opin Mol Ther* (2003) 5:657–67.
112. Bosslet K, Straub R, Blumrich M, Czech J, Gerken M, Sperker B, et al. Elucidation of the mechanism enabling tumor selective prodrug monotherapy. *Cancer Res* (1998) 58:1195–201.
113. Algire GH, Chalkley HW, Earle WE, Legallais FY, Park HD, Shelton E, et al. Vascular reactions of normal and malignant tissues in vivo. III. Vascular reactions' of mice to fibroblasts treated in vitro with methylcholanthrene. *J Natl Cancer Inst* (1950) 11:555–80.
114. Folkman J, Long DM, Becker FF. Growth and metastasis of tumor in organ culture. *Cancer* (1963) 16:453–67. doi:10.1002/1097-0142(196304)16:4<453::AID-CNCR2820160407>3.0.CO;2-Y
115. Hey T, Fiedler E, Rudolph R, Fiedler M. Artificial, non-antibody binding proteins for pharmaceutical and industrial applications. *Trends Biotechnol* (2005) 23:514–22. doi:10.1016/j.tibtech.2005.07.007
116. Ferrara N. Role of vascular endothelial growth factor in the regulation of angiogenesis. *Kidney Int* (1999) 56:794–814. doi:10.1046/j.1523-1755.1999.00610.x
117. Kamba T, McDonald DM. Mechanisms of adverse effects of anti-VEGF therapy for cancer. *Br J Cancer* (2007) 96:1788–95. doi:10.1038/sj.bjc.6603813
118. Jain RK. Antiangiogenesis strategies revisited: from starving tumors to alleviating hypoxia. *Cancer Cell* (2014) 26:605–22. doi:10.1016/j.ccell.2014.10.006
119. Krause DS, Van Etten RA. Tyrosine kinases as targets for cancer therapy. *N Engl J Med* (2005) 353:172–87. doi:10.1056/NEJMra044389
120. Hartmann JT, Haap M, Kopp H-G, Lipp H-P. Tyrosine kinase inhibitors – a review on pharmacology, metabolism and side effects. *Curr Drug Metab* (2009) 10:470–81. doi:10.2174/138920009788897975
121. Kelly RJ, Darnell C, Rixe O. Target inhibition in antiangiogenic therapy a wide spectrum of selectivity and specificity. *Cancer J* (2010) 16:635–42. doi:10.1097/PPO.0b013e3181ff37cf
122. Gan HK, Seruga B, Knox JJ. Sunitinib in solid tumors. *Expert Opin Investig Drugs* (2009) 18:821–34. doi:10.1517/13543780902980171
123. Fuchs CS, Tomasek J, Yong CJ, Dumitru F, Passalacqua R, Goswami C, et al. Ramucirumab monotherapy for previously treated advanced gastric or gastro-oesophageal junction adenocarcinoma (REGARD): an international, randomised, multicentre, placebo-controlled, phase 3 trial. *Lancet* (2014) 383:31–9. doi:10.1016/S0140-6736(13)61719-5
124. Verweij J, Sleijfer S. Pazopanib, a new therapy for metastatic soft tissue sarcoma. *Expert Opin Pharmacother* (2013) 14:929–35. doi:10.1517/14656566.2013.780030
125. Moccia F, Zuccolo E, Poletto V, Cinelli M, Bonetti E, Guerra G, et al. Endothelial progenitor cells support tumour growth and metastatisation: implications for the resistance to anti-angiogenic therapy. *Tumour Biol* (2015) 36:6603–14. doi:10.1007/s13277-015-3823-2
126. Burger JA, Peled A. CXCR4 antagonists: targeting the microenvironment in leukemia and other cancers. *Leukemia* (2009) 23:43–52. doi:10.1038/leu.2008.299
127. Kerbel R, Folkman J. Clinical translation of angiogenesis inhibitors. *Nat Rev Cancer* (2002) 2:727–39. doi:10.1038/nrc905
128. Seiki M, Yana I. Roles of pericellular proteolysis by membrane type-1 matrix metalloproteinase in cancer invasion and angiogenesis. *Cancer Sci* (2003) 94:569–74. doi:10.1111/j.1349-7006.2003.tb01484.x
129. Masson V, de la Ballina LR, Munaut C, Wielockx B, Jost M, Maillard C, et al. Contribution of host MMP-2 and MMP-9 to promote tumor vascularization and invasion of malignant keratinocytes. *FASEB J* (2005) 19:234–6. doi:10.1096/fj.04-2140fje
130. Noel A, Maillard C, Rocks N, Jost M, Chabottaux V, Sounni NE, et al. Membrane associated proteases and their inhibitors in tumour angiogenesis. *J Clin Pathol* (2004) 57:577–84. doi:10.1136/jcp.2003.014472
131. Petitclerc E, Boutaud A, Prestayko A, Xu J, Sado Y, Ninomiya Y, et al. New functions for non-collagenous domains of human collagen type IV. Novel integrin ligands inhibiting angiogenesis and tumor growth in vivo. *J Biol Chem* (2000) 275:8051–61. doi:10.1074/jbc.275.11.8051
132. Hegde PS, Wallin JJ, Mancao C. Predictive markers of anti-VEGF and emerging role of angiogenesis inhibitors as immunotherapeutics. *Semin Cancer Biol* (2017). doi:10.1016/j.semcancer.2017.12.002
133. Hodi FS, Lawrence D, Lezcano C, Wu X, Zhou J, Sasada T, et al. Bevacizumab plus ipilimumab in patients with metastatic melanoma. *Cancer Immunol Res* (2014) 2:632–42. doi:10.1158/2326-6066.CIR-14-0053
134. Läubli H, Müller P, D'Amico L, Buchi M, Kashyap AS, Zippelius A. The multi-receptor inhibitor axitinib reverses tumor-induced immunosuppression and potentiates treatment with immune-modulatory antibodies in preclinical murine models. *Cancer Immunol Immunother* (2018) 67:815–24. doi:10.1007/s00262-018-2136-x
135. Huang Y, Goel S, Duda DG, Fukumura D, Jain RK. Vascular normalization as an emerging strategy to enhance cancer immunotherapy. *Cancer Res* (2013) 73:2943–8. doi:10.1158/0008-5472.CAN-12-4354
136. Jain RK, Martin JD, Stylianopoulos T. The role of mechanical forces in tumor growth and therapy. *Annu Rev Biomed Eng* (2014) 16:321–46. doi:10.1146/annurev-bioeng-071813-105259

137. Viallard C, Larrivée B. Tumor angiogenesis and vascular normalization: alternative therapeutic targets. *Angiogenesis* (2017) 20:409–26. doi:10.1007/s10456-017-9562-9
138. Tolaney SM, Boucher Y, Duda DG, Martin JD, Seano G, Ancukiewicz M, et al. Role of vascular density and normalization in response to neoadjuvant bevacizumab and chemotherapy in breast cancer patients. *Proc Natl Acad Sci U S A* (2015) 112:14325–30. doi:10.1073/pnas.1518808112
139. Kloepper J, Riedemann L, Amoozgar Z, Seano G, Susek K, Yu V, et al. Ang-2/VEGF bispecific antibody reprograms macrophages and resident microglia to anti-tumor phenotype and prolongs glioblastoma survival. *Proc Natl Acad Sci U S A* (2016) 113:4476–81. doi:10.1073/pnas.1525360113
140. Monk BJ, Poveda A, Vergote I, Raspagliesi F, Fujiwara K, Bae D-S, et al. Final results of a phase 3 study of trebananib plus weekly paclitaxel in recurrent ovarian cancer (TRINOVA-1): long-term survival, impact of ascites, and progression-free survival-2. *Gynecol Oncol* (2016) 143:27–34. doi:10.1016/j.ygyno.2016.07.112
141. De Palma M, Biziato D, Petrova TV. Microenvironmental regulation of tumour angiogenesis. *Nat Rev Cancer* (2017) 17:457–74. doi:10.1038/nrc.2017.51

Conflict of Interest Statement: OC declares that has been economically compensated with his assistance to advisory boards and conferences from Novartis, Pfizer, Ipsen, and Teva. Apart from this, there is no conflict of interest that could be perceived as prejudicing the impartiality of the research reported.

Advantages of publishing in Frontiers

OPEN ACCESS
Articles are free to read for greatest visibility and readership

FAST PUBLICATION
Around 90 days from submission to decision

HIGH QUALITY PEER-REVIEW
Rigorous, collaborative, and constructive peer-review

TRANSPARENT PEER-REVIEW
Editors and reviewers acknowledged by name on published articles

Frontiers
Avenue du Tribunal-Fédéral 34
1005 Lausanne | Switzerland

Visit us: www.frontiersin.org
Contact us: info@frontiersin.org | +41 21 510 17 00

REPRODUCIBILITY OF RESEARCH
Support open data and methods to enhance research reproducibility

DIGITAL PUBLISHING
Articles designed for optimal readership across devices

FOLLOW US
@frontiersin

IMPACT METRICS
Advanced article metrics track visibility across digital media

EXTENSIVE PROMOTION
Marketing and promotion of impactful research

LOOP RESEARCH NETWORK
Our network increases your article's readership